

**AN INVESTIGATION INTO THE
RELATIONSHIP BETWEEN ROCKER SOLE
DESIGNS AND ALTERATION TO LOWER LIMB
KINETICS, KINEMATICS AND MUSCLE
FUNCTION DURING ADULT GAIT**

ANDREY AKSENOV

Ph.D. Thesis

2014

**AN INVESTIGATION INTO THE
RELATIONSHIP BETWEEN ROCKER SOLE
DESIGNS AND ALTERATION TO LOWER LIMB
KINETICS, KINEMATICS AND MUSCLE
FUNCTION DURING ADULT GAIT**

Andrey Aksenov

**Centre for Health Research
School of Health Sciences
University of Salford
Salford UK**

**Submitted in fulfilment of the requirements of the Degree of Doctor of
Philosophy, February 2014**

I	TABLE OF CONTENTS	I
II	LIST OF FIGURES	VIII
III	LIST OF TABLES	XVIII
IV	ACKNOWLEDGMENTS	XXVIII
V	ABSTRACT	XXIX
VI	LIST OF ABBREVIATIONS	XXXI

CHAPTER 1	1
1 INTRODUCTION	1
1.1	Rocker-soled shoes	1
1.2	Thesis content	7
CHAPTER 2	9
2 INTERMITTENT CLAUDICATION (IC)	9
2.1	Chapter overview	9
2.2	Intermittent Claudication (IC)	9
2.3	Treatment regimes	11
2.3.1	Walking exercise therapy in the treatment of IC	11
2.3.2	Progressive resistance training (PRT)	15
2.4	Drug therapy	16
2.5	Discussion	16
2.6	Orthotic intervention	17
2.6.1	Rocker-soled shoes	17
2.6.2	Raised heels	18
2.6.3	Specifically-designed rocker profiles	19
2.6.4	Chapter summary	21
CHAPTER 3	23
3 ABLE-BODIED ADULT GAIT AND CLAUDICANT PATHOLOGICAL GAIT	23
3.1	Phases of able-bodied adult gait	23
3.2	Muscles of lower limb	24
3.3	The role of the ankle plantarflexor muscles	25

3.4	The effect of IC on gait parameters and muscle strength in older people - a review of the literature regarding its effect and possible treatment regimes	26
3.4.1	The effect of PAD severity and ABPI values on gait parameters and ambulatory function.	26
3.4.2	The effect of increasing age and PAD.....	26
3.4.3	The effects of a PAD-IC	27
3.4.4	The effect of exercise, drug therapy on claudicant gait parameters	30
3.4.5	Overall analysis regarding gait parameters associated with PAD-IC.....	31
3.5	The effect of walking with shoes adapted with rocker sole profiles.....	32
3.5.1	Reduction of plantar foot pressures.....	32
3.6	Alteration to lower limb joint kinetics and kinematics.....	34
3.6.1	Joint Rotation.....	34
3.7	Alteration to externally-applied sagittal plane lower limb joint moments.....	37
3.7.1	Sagittal plane knee joint moments.....	37
3.7.2	Sagittal plane ankle powers.....	38
3.7.3	Alteration to EMG activity	38
3.8	Comment	39
3.9	Alteration to oxygen consumption	40
3.10	Overall chapter analysis.....	40
CHAPTER 4.....		42
4 MUSCLE PHYSIOLOGY AND RELATED BIOMECHANICS		42
4.1	Chapter overview.....	42
4.2	Basic terminology used in this thesis for muscle biomechanics and gait analysis	42
4.2.1	Planes and axes	42
4.2.2	Lower limb skeletal structure and joint motions	44
4.3	Muscle anatomy	48
4.3.1	Skeletal muscle structure	51
4.3.2	Tendons	53
4.3.3	Force generation	54
4.3.4	Muscle fibre types	55
4.3.5	The pennation angle of muscles.....	58
4.3.6	Muscle contraction.....	61
4.3.7	Force-length relationships of muscle fibres	62
4.3.8	Force-length relationships (for the entire muscle)	64

4.4	Comment	67
4.4.1	Force-velocity relationship	70
4.4.2	Isometric force.....	71
4.4.3	Development of tension in a muscle.....	72
4.5	Ankle muscles mechanics and properties for gastrocnemius (GAS), soleus (SOL), tibialis anterior (TA).....	72
4.5.1	The Achilles tendon moment arm.....	74
4.5.2	Optimal pennation angle for gastrocnemius and soleus during dynamic movement.....	75
4.6	The effect of footwear features on muscle parameters	77
4.6.1	Introduction.....	77
4.6.2	Rocker sole designs, alteration to heel height and their biomechanical effect.	78
4.6.3	Alteration to heel height	79
4.6.4	Rocker sole Apex Position (AP).....	89
4.6.5	Shoe forepart flexibility	91
4.6.6	Rocker Angle (RA).....	92
4.6.7	The posterior heel curve (HC).....	93
4.6.8	Hypothesis for curved heeled shoes	95
4.7	Summary.....	95
4.8	Overarching and specific hypotheses	99
CHAPTER 5.....		109
5 METHODOLOGY.....		109
5.1	Chapter overview.....	109
5.2	The motion analysis system.....	109
5.2.1	Camera setup.....	111
5.2.2	Oqus 3+ Qualisys calibration	112
5.2.3	Calibration results.....	115
5.3	The force Platforms	116
5.3.1	Reflective marker set selection	118
5.3.2	The Calibration Anatomical System technique (CAST).....	120
5.3.3	Definition of the segment coordinate systems	121
5.4	Electromyography (EMG) data collection.....	127
5.4.1	Electromyography equipment.....	127
5.4.2	Data collection procedure	128

5.4.3	Study Design	131
5.4.4	Participants	131
5.5	Footwear selection criteria	132
5.6	Procedure used to adapt shoes with rocker sole profiles	134
5.7	Gait laboratory testing procedure	139
5.7.1	Static tests	142
5.7.2	Dynamic tests	142
5.8	Data analysis	148
5.8.1	Data processing overview.....	148
5.8.2	Kinematic data processing.....	149
5.8.3	Visual3D	150
5.8.4	Signal Processing in Visual3D	152
5.8.5	Modelling requirements for OpenSim from Visual 3D.....	156
5.8.6	Exporting data to OpenSim	156
5.8.7	OpenSim	157
5.9	Properties and models of muscles (Muscle-tendon dynamics)	161
5.10	Calculation of the outcome measures.....	165
5.10.1	Introduction.....	165
5.10.2	Joint angles	165
5.10.3	Kinetic data	166
5.10.4	Muscle-tendon properties.....	167
5.10.5	OpenSim algorithm for calculation muscles moment arm, muscle-tendon length and force	168
5.10.6	Area under the curve (impulse).....	170
5.11	Data normalisation	172
5.11.1	Normalisation techniques for the ankle joint	179
5.11.2	The first technique analysed for ankle joint normalisation	182
5.11.3	The second technique for ankle joint normalisation	183
5.11.4	Kinetic data normalisation.....	185
CHAPTER 6.....		186
6 RESULTS AND STATISTICAL ANALYSIS: KINEMATICS, KINETICS, ELECTROMYOGRAPHY AND MUSCLE FUNCTION DATA		186
6.1	Subject demographics.....	186
6.2	Trial conditions analysed	186

6.3	Gait cycle terms of reference	187
6.3.1	Ankle, knee and hip kinematics, kinetics, EMG and muscle function results ..	188
6.3.2	Ankle sagittal plane ROM	193
6.3.3	The effect of altering rocker sole apex position (AP)	197
6.3.4	The effect of altering rocker apex angle (toe angle-TA)	201
6.3.5	The effect of adding heel curves	205
6.4	The effect of altering rocker sole stiffness at the metatarsal arcade area	208
6.4.1	Alteration to sagittal plane ankle kinematics.....	208
6.4.2	Alteration to ankle ROM produced by different forefoot sole flexibilities	209
6.4.3	Summary of ankle angle results for variation in shoe forefoot flexibility.....	210
6.5	SAGITTAL PLANE KNEE KINEMATICS.....	211
6.5.1	The effect of walking with different heel heights	211
6.5.2	Alteration to kinetics of the knee during swing phase whilst walking in different heel heights	213
6.5.3	Knee sagittal plane ROM	214
6.5.4	Summary – sagittal plane knee joint angle for different heel heights.....	216
6.5.5	The effect of altering rocker sole apex position (AP)	217
6.5.6	Toe angle (apex angle).....	219
6.5.7	Heel curves	221
6.5.8	Rocker profile stiffness at the metatarsal area	223
6.6	Hip kinematics.....	226
6.6.1	The effect of walking with different heel heights	226
6.6.2	The effect of altering rocker sole apex position (AP)	229
6.6.3	Apex angle (toe angle).....	230
6.6.4	Curved heels	231
6.6.5	Rocker profile stiffness at metatarsal area	232
6.7	Ankle Moments.....	233
6.7.1	The effect of heel height alteration.....	233
6.7.2	The effect of altering rocker sole apex position (AP)	239
6.7.3	Apex angle (toe angle-TA)	242
6.7.4	Heel curves	245
6.7.5	Rocker profile stiffness at metatarsal area	248
6.8	Ankle Power	251
6.8.1	The effect of walking with different heel heights (HH).....	251

6.8.2	The effect of altering rocker sole apex position (AP)	254
6.8.3	The effect of altering apex angle (toe angle-TA).....	256
6.8.4	The effect of altering heel curve	258
6.8.5	The effect of altering rocker profile stiffness at metatarsal area	260
6.9	Electromyography data for ankle joint	261
6.9.1	The effect of walking with different heel heights	261
6.9.2	The effect of altering rocker sole apex position (AP).....	266
6.9.3	The effect of altering apex angle (toe angle-TA).....	268
6.9.4	The effect of altering heel curves.....	271
6.9.5	The effect of altering rocker profile stiffness at metatarsal area	273
6.10	Soleus electromyography results.....	274
6.10.1	The effect of walking with different heel heights	274
6.10.2	The effect of altering rocker sole apex position (AP)	279
6.10.3	The effect of altering apex angle (toe angle-TA).....	281
6.10.4	The effect of altering heel curves.....	283
6.10.5	The effect of altering rocker profile stiffness at metatarsal area	285
6.11	Tibialis anterior electromyography results.....	287
6.11.1	The effect of walking with different heel heights	287
6.11.2	The effect of altering rocker sole apex position (AP).....	290
6.11.3	The effect of altering apex angle (toe angle-TA).....	290
6.11.4	The effect of altering heel curve	291
6.11.5	The effect of altering rocker profile stiffness at metatarsal area	293
6.12	Achilles muscle moment arm	295
6.12.1	The effect of altering heel height of the sole on Achilles muscle moment arm	295
6.12.2	The effect of altering rocker sole apex position (AP) on Achilles muscle moment arm	297
6.12.3	The effect of altering apex toe angle of the sole on Achilles muscle moment arm	299
6.12.4	The effect of altering heel curve of the sole on Achilles muscle moment arm	301
6.12.5	The effect of altering rocker profile stiffness at metatarsal area on Achilles muscle moment arm	303
6.13	Gastrocnemius and Soleus fibre length alteration	304
6.13.1	Heel Height (HH).....	304
6.13.2	Apex position (AP)	306
6.13.3	Toe angle (TA).....	309

6.13.4	Heel Curve	311
6.13.5	Flexibility of the sole.....	312
6.13.6	Heel Height (HH).....	314
6.13.7	Apex position (AP)	317
6.13.8	Toe angle (TA).....	319
6.13.9	Heel Curve	321
6.13.10	Flexibility of the sole.....	323
6.14	Tendon force.....	323
6.15	Tibialis anterior fibre lengthening/shortening velocity	326
6.15.1	Heel Height (HH).....	326
6.15.2	Curved heels	330
CHAPTER 7	335
7 DISCUSSION	335
7.1	Sagittal plane ankle kinematics	335
7.1.1	The effect of walking with rocker soles incorporating different heel heights .	336
7.2	The effect of altering footwear on calf muscle functioning.....	339
7.2.1	Introduction.....	339
7.2.2	The effect of heel height alteration.....	341
7.2.3	Conclusion	345
7.3	The effect of walking with rocker soles incorporating different apex positions.....	345
7.4	The effect of different rocker apex positions (APs) on muscle function.....	346
7.4.1	Conclusion	350
7.5	The effect of different toe apex angles on muscle function	351
7.6	The effect of different curved heels on muscle function	353
7.7	Limitations to the methodology and the approach adopted	356
7.7.1	The walking trials.....	356
7.7.2	Kinetic and Kinematic data	357
7.7.3	OpenSim limitation.....	358
7.7.4	The OpenSim velocity of muscle-tendon length calculation limitations	359
7.7.5	External foot marker placement and rigid foot model	359
7.7.6	The walking speed limitation.....	360
7.7.7	Conclusion and future work	360
REFERENCES	365
APENDICES	385

LIST OF FIGURES

Figure 3.1: The determinants of gait (Cuccurullo, 2004).	23
Figure 3.2: Increase in EMG activity when walking with a negative heel rocker soled shoe [Adapted from (Li and Hong, 2007)]......	39
Figure 3.3: A negative-heel rocker soled shoe [adapted from Yamamoto et al. (2000)].	39
Figure 4.1: The anatomical position, with three reference planes and six directions.....	43
Figure 4.2: An example of a shank segment for medial/lateral aspects and proximal/distal ends of the segments.	44
Figure 4.3: Basic anatomical points for lower limb bones, segments and joints for gait analysis.....	45
Figure 4.4: Osseous structure of the foot.....	46
Figure 4.5: Motion of the lower limb joints.	46
Figure 4.6: Linear and angular movements for foot segment movement in all planes and directions...47	
Figure 4.7: The major muscles of the lower limbs.	49
Figure 4.8: The main ankle plantar/dorsiflexion muscles which were investigated to seek further understanding of their mutual relationships in performing muscle work whilst wearing different footwear features in this research, (a) - posterior view of gastrocnemius muscles, (b) posterior view of soleus muscle, (c) – anterior view of tibialis anterior muscle [picture adapted from (Palastanga and Soames, 2012)].	50
Figure 4.9: basic muscle structure.	51
Figure 4.10: Diagram representing thick and thin filaments during two stages of contraction [adapted from (Tözeren, 2000)]......	52
Figure 4.11: Typical normalised force-length relationships for a tendon.	54
Figure 4.12: Muscle fibre composition and maximum oxygen uptake rates in athletes representing different sports (Katch et al., 2011).	57
Figure 4.13: Skeletal muscle fibre recruitment during a physical workout [adapted from (Abernethy et al., 2013)]......	57
Figure 4.14: Muscle architecture of fibres: (A) fusiform, (B) sheet, (C) pennate (Palastanga and Soames, 2012).	59
Figure 4.15: The muscle-tendon actuator principle model where FM – muscle force, FT – tendon force, α – pennation angle of the muscle, IT – tendon length, IM – muscle length (Zajac, 1989, Delp, 1990, Hoy et al., 1990a, Abernethy et al., 2013).	60
Figure 4.16: Medial gastrocnemius pennation angle relationship with fibre length at rest (Narici et al., 1996).	61

Figure 4.17: The sarcomere isometric length-tension curve [adapted from (Winter, 2009, Hong and Bartlett, 2008, Rose and Gamble, 2006)].	63
Figure 4.18: Length-tension relationship for the whole muscle during isometric contraction [adapted from (Hong and Bartlett, 2008)].	65
Figure 4.19: Tendon tension resulting from various levels of muscle activation. Parallel elastic element generates tension independent of the activation of contractile element [adapted from (Winter, 2009)].	65
Figure 4.20: Comparison of normalised soleus muscle length between young adults (YA) and old adults (OA) during walking: (A) – preferred walking speed in YA and OA, (B) matched walking speed between YA and OA [adapted from (Panizzolo et al., 2013)].	68
Figure 4.21: Active plus passive soleus forces versus ankle angle with elastic and inelastic tendon. The solid black line was calculated with nominal tendon elasticity. The dotted black curve shows the effect of making the tendon inextensible.	69
Figure 4.22: Force-velocity characteristics of skeletal muscle for different levels of muscle activation: shown as 25%, 50%, 75%, and 100% levels of activation [adapted from (Winter, 2009)].	70
Figure 4.23: Force-time curve for a whole muscle contracting isometrically [adapted from (Nordin and Frankel, 2003)].	71
Figure 4.24: Mean values of optimal pennation angle with standard deviation for tiabialis anterior (TA), lateral and medial gastrocnemius, and soleus muscles (Manal et al., 2006).	76
Figure 4.25: An example during stance phase of gait of how the external dorsiflexion moment is opposed by internal plantar flexion moment generated by calf muscles.	82
Figure 4.26: A visual example of EMG activity for the calf muscle during standing on the toes [adapted from (Kirtley, 2006)].	83
Figure 4.27: GRF point of application data during initial contact (ICt) obtained in a pilot study using visual3D software (C-Motion) for 3.5 and 5.5 cm heel heights.	84
Figure 4.28: Visual example of the position of the foot and ankle at ICt for negative heeled and high heeled shoes (where d_1 and d_2 are the muscle moment arms).	84
Figure 4.29: An ankle moment calculation example. The red coloured section illustrates the extra sole thickness.	85
Figure 4.30: demonstrates a simple visual geometrical example of how different heel heights change the ankle position during terminal stance and therefore muscle biomechanics.	86
Figure 4.31: An illustration of the footwear features analysed in this thesis.	87
Figure 4.32: An example of walking in shoes with different APs.	90
Figure 4.33: An example of late stance ankle angle kinematics for flexible and solid shoes.	92

Figure 4.34: Alteration to ankle plantarflexion with a 10° rocker angle shoe versus a 20° rocker angle during late stance phase.....	93
Figure 4.35: The Masai barefoot technology shoe (MBT) during loading response [picture adapted from (Sacco et al., 2012)].	94
Figure 4.36: An example of GRF position for curved and flat-heeled shoes during loading response....	94
Figure 4.37: Internal DF/PF ankle moments during stance phase when comparing curved heels to non-curved heeled shoes.....	95
Figure 5.1: Camera set-up in the gait laboratory with an example of a typical image produced by the Qualisys software.	110
Figure 5.2: Depiction of the Qualisys cameras location, the measurement volume and walking distances available.....	112
Figure 5.3: The L-shaped frame set-up position for calibration.....	113
Figure 5.4: Qualisys calibration settings configuration.	113
Figure 5.5: Calibration procedure used in the gait laboratory.	114
Figure 5.6: Representation of the calibration volume.	114
Figure 5.7: Typical Qualisys calibration results.	115
Figure 5.8: Ground reaction vector components.....	116
Figure 5.9: The three components of the ground reaction force (GRF), with (a) the coordinate system adopted by (ISB) and (b) the coordinate system used in this research.	117
Figure 5.10: Force platform set-up positions.....	117
Figure 5.11: A 14 mm retroreflective marker attached to the skin using double-sided tape.	118
Figure 5.12: The positioning of the anatomical and technical markers.	121
Figure 5.13: Direct skin-marking technique used for the reflective marker placement.	122
Figure 5.14: Anatomical cut-outs utilised on the footwear.	122
Figure 5.15: An illustration of marker placement for the foot segment for Visual3D.....	123
Figure 5.16: Marker placement to define the shank segment for Visual3D.	124
Figure 5.17: The thigh segment marker placement used for Visual3D.....	125
Figure 5.18: the pelvic segment marker placement used for Visual3D.	126
Figure 5.19: Trunk segment marker placement.....	126
Figure 5.20: The Noraxon TeleMyo™ 2400T G2 system.	127
Figure 5.21: Noraxon TeleMyo™ 2400T G2 attachment during testing procedures.	127
Figure 5.22: Dual electrode locations on muscles recommended by SEMIAN guidelines (adopted from Noraxon guidelines).....	129
Figure 5.23: An illustration of the footwear features analysed in this thesis.....	132

Figure 5.24: The Standard high street shoe (size 8 adult UK) which was used as the base structure for adaptation.	134
Figure 5.25: Sole and heel adaptation procedure.....	136
Figure 5.26 Test footwear conditions which were used in this research.....	139
Figure 5.27: Force plates used to record GRF showing the subjects' walking direction.	140
Figure 5.28: Influence of walking speed on joint trajectories for (a) hip, (b) knee and (c) ankle joint at 10 different walking speeds (van Hedel et al., 2006).....	144
Figure 5.29: The gait speed effect on (a) EMG activity, (b) vertical ground reaction force (Chiu and Wang, 2007).	144
Figure 5.30: The Brower SpeedTrap II timing gate system.	145
Figure 5.31: The experimental set-up for gait analysis.	147
Figure 5.32: The example of mean value calculation technique.....	149
Figure 5.33: Naming standards and conventions in Visual3D.....	151
Figure 5.34: An example of the full body model in Visual3D used for this research. There were additional markers on the arms, however data acquired from these were not included in this research.	152
Figure 5.35: Filtration level example of the effect on maximum range of motion loss during 0-20% of stance phase for single trials for 12 mm rocker shoe and control shoe, which were used in the pilot study.....	153
Figure 5.36: Example of Medial Gastrocnemius EMG analysis from the pilot study using the RMS and linear envelope techniques for different shoes during stance phase.....	155
Figure 5.37: A screenshot from OpenSim, which includes a musculoskeletal model of the lower extremities.....	158
Figure 5.38: The Gait2392 musculoskeletal model in OpenSim.	158
Figure 5.39: The coordinate systems of the bone segments (Delp, 1990).	159
Figure 5.40: The ankle (ANK), subtalar (ST) and metatarsophalangeal (MTP) joints with axes and orientation (Delp, 1990).	160
Figure 5.41: Relationship between muscle fibres and tendon in a pennated muscle.	162
Figure 5.42: The muscle-tendon actuator model [adapted from (Zajac, 1989, Delp, 1990, Hoy et al., 1990a)].	163
Figure 5.43: Foot and shank segment angular relationships (ZX - sagittal plane, ZY - frontal plane and XY- transverse plane).	166
Figure 5.44: Example of an ankle joint moment calculation. Joint moments, powers and GRFs were calculated in Visual3D.....	167

Figure 5.45: Definition of terms used in moment arm calculations. Point P_1 through P_n define the muscle path. P_1 through P_{m-1} are fixed in body A. P_m through P_n are fixed in body B. \mathbf{V} is the vector from point P_{m-1} to P_m . \mathbf{r} expresses point P_m in reference frame A. In general, six generalised coordinates (three rotational angles: q_1, q_2, q_3 and three translation coordinates, not shown) are needed to characterise the orientation and position of body A relative to body B. The moment arm for each generalised coordinate is given by equation (4) (Delp, 1990).168

Figure 5.46: Example of a segment of the curve area, which is divided into areas.171

Figure 5.47: Visual3D default static ankle angle representation.173

Figure 5.48: Normalisation procedure for the ankle.174

Figure 5.49: Default Visual3D coordinate system for the lab, shank segment and anticlockwise-rotated foot segment in the Z-X axis plane.....175

Figure 5.50: Pilot study example for changing the coordinate system of the ankle segment.175

Figure 5.51: Example of how a rocker shoe can change posture for an ankle joint compared to a barefoot static trial.176

Figure 5.52: Demonstration of segmental positions.....177

Figure 5.53: Comparison of test conditions.....178

Figure 5.54: Comparison of rocker soled shoe test conditions versus barefoot statics.....179

Figure 5.55: Visual3D virtual foot example based on the C-Motion guidelines.180

Figure 5.56: This example shows how the ankle joint data were shifted by virtual foot, with virtual shank added to the static model. The raw line represents the export from visual3D and 90 degrees were subtracted to fix coordinate system rotation. The orange line shows that the virtual foot subtracted the foot segment difference between normal position and virtual foot (which lies in parallel with the ground). The blue line shows that the virtual foot and shank segments offsets were added to the ankle angle if compared with data without normalising joint angle to 0 degree.181

Figure 5.57: Resulting graph following normalisation.181

Figure 5.58: Foot-shank relationships for five footwear test conditions.182

Figure 5.59: Ankle joint kinematic data exported for 1,2,3,4,5 heel heights shoe walking trials using their own statics with virtual segments applied in Visual3D. (a) –ankle joint data with statics offsets; (b) – ankle joint data with subtracted static offsets for foot and shank.184

Figure 5.60: Raw ankle joint data from Visual3D for 1.5, 2.5, 3.5, 4.5, 5.5 heel height walking trials; (a) – all walking trials were assigned with one barefoot statics, (b) – each footwear condition was assigned with same footwear static trial.185

Figure 6.1: Sagittal plane ankle motion during the five heel height test conditions where the control shoe is 3.5 HH. (a) – without standard deviation (STD), (b) – with the lines shadowed to represent STD ranges.189

Figure 6.2: Sagittal plane ankle motion when walking with the three apex position test conditions. (a) – without standard deviation (STD), (b) – with the lines shadowed to represent STD ranges.198

Figure 6.3: sagittal plane ankle motion during the three apex angle conditions (TAs). (a) – without standard deviation (STD), (b) – with the lines shadowed to represent STD ranges.....202

Figure 6.4: Sagittal plane ankle motion for the complete gait cycle during walking with curved heels compared to a control shoe. (a) – without standard deviation (STD), (b) – with the lines shadowed to represent STD ranges.205

Figure 6.5: Sagittal plane ankle motion for shoes adapted to be more flexible at the metatarsal area compared to the control shoe. (a) – without standard deviation (STD), (b) – with the lines shadowed to represent STD ranges.208

Figure 6.6: Sagittal plane knee motion during the five heel height test conditions where the control shoe is 3.5 HH. (a) – without standard deviation (STD), (b) – with the lines shadowed to represent STD ranges.....211

Figure 6.7: Sagittal plane knee motion during the three apex position test conditions where the control shoe is 62.5AP. Legend 1 indicates where maximum knee flexion angle occurred during LR; Legend 2 indicates the point at which maximum knee extension angle occurred during terminal stance phase; legend 3 indicates the point at which maximum knee flexion angle occurred at toe-off; and legend 4 indicates the position where maximum knee flexion angle during swing occurred. (a) – without standard deviation (STD), (b) – with the lines shadowed to represent STD ranges.....217

Figure 6.8: Sagittal plane knee motion during the three apex angle test conditions where the control shoe is 15°. Legend 1 indicates where maximum knee flexion angle occurred during LR; Legend 2 indicates the point at which maximum knee extension angle occurred during terminal stance phase; legend 3 indicates the point at which maximum knee flexion angle occurred at toe-off; and legend 4 indicates the position where maximum knee flexion angle during swing occurred. (a) – without standard deviation (STD), (b) – with the lines shadowed to represent STD ranges.....220

Figure 6.9: Sagittal plane knee motion during the three different level of heel curvature of test conditions where the control shoe has no curve. (a) – without standard deviation (STD), (b) – with the lines shadowed to represent STD ranges.....221

Figure 6.10: Figure 6.6: Sagittal plane knee motion during the three different level of flexibility of the mid-part of the shoe where the control shoe is has solid sole. Legend 1 indicates where maximum knee flexion angle occurred during LR; Legend 2 indicates the point at which maximum knee extension angle occurred during terminal stance phase; legend 3 indicates the point at which maximum knee flexion angle occurred at toe-off; and legend 4 indicates the position where maximum knee flexion angle during swing occurred. (a) – without standard deviation (STD), (b) – with the lines shadowed to represent STD ranges.224

Figure 6.11: Sagittal plane hip motion during the five heel height test conditions where the control shoe is 3.5 HH. Legend 1 indicates maximum flexion and legend 2 indicates maximum hip extension.226

Figure 6.12: Sagittal plane hip motion during the three apex length footwear test conditions where the control shoe is 62.5AP. Legend 1 indicates maximum flexion and legend 2 indicates maximum hip extension. (a) – without standard deviation (STD), (b) – with the lines shadowed to represent STD ranges.229

Figure 6.13: Sagittal plane hip motion during the apex toe angle test conditions where the control shoe is 15° TA. Legend 1 indicates maximum flexion and legend 2 indicates maximum hip extension. (a) – without standard deviation (STD), (b) – with the lines shadowed to represent STD ranges.230

Figure 6.14: Sagittal plane hip motion during the three different level of heel curvature of test conditions where the control shoe has no curve. (a) – without standard deviation (STD), (b) – with the lines shadowed to represent STD ranges.231

Figure 6.15: Sagittal plane hip motion during the three different level of flexibility of the mid-part of the shoe where the control shoe has no curve (N=15). (a) – without standard deviation (STD), (b) – with the lines shadowed to represent STD ranges.232

Figure 6.16: Sagittal plane external ankle moment during the five footwear conditions highlighting the 2 area of interest (N=15). Legend 1 indicates maximum ankle plantarflexor moment; legend 2 indicates maximum ankle dorsiflexor moment. (a) – without standard deviation (STD), (b) – with the lines shadowed to represent STD ranges.234

Figure 6.17: Sagittal plane external ankle moment during the three footwear conditions highlighting the 2 area of interest (N=15). Legend 1 indicates maximum ankle plantarflexor moment; legend 2 indicates maximum ankle dorsiflexor moment. (a) – without standard deviation (STD), (b) – with the lines shadowed to represent STD ranges.239

Figure 6.18: Sagittal plane external ankle moment during the three footwear conditions highlighting the two area of interest (N=15). Legend 1 indicates maximum ankle plantarflexor moment; legend 2 indicates maximum ankle dorsiflexor moment. (a) – without standard deviation (STD), (b) – with the lines shadowed to represent STD ranges.242

Figure 6.19: Sagittal plane external ankle moment during the three footwear conditions highlighting the 2 area of interest (N=15). Legend 1 indicates maximum ankle plantarflexor moment; legend 2 indicates maximum ankle dorsiflexor moment. (a) – without standard deviation (STD), (b) – with the lines shadowed to represent STD ranges.245

Figure 6.20: Sagittal plane external ankle moment during the three footwear conditions highlighting the 2 area of interest (N=15). Legend 1 indicates maximum ankle plantarflexor moment; legend 2

indicates maximum ankle dorsiflexor moment. (a) – without standard deviation (STD), (b) – with the lines shadowed to represent STD ranges.....249

Figure 6.21: Sagittal plane external ankle joint power for HH test footwear conditions (N=15).251

Figure 6.22: Sagittal plane external ankle joint power for AP test footwear conditions (N=15).....254

Figure 6.23: Sagittal plane external ankle joint power for TA test footwear conditions (N=15).257

Figure 6.24: Sagittal plane external ankle joint power for heel-curved test footwear conditions where control shoe has no curved heel (N=15). (a) – without standard deviation (STD), (b) – with the lines shadowed to represent STD ranges.258

Figure 6.25: Sagittal plane external ankle joint power for different flexibility level of the sole where control shoe is not flexible at the metatarsal area (N=15). (a) – without standard deviation (STD), (b) – with the lines shadowed to represent STD ranges.260

Figure 6.26: The medial gastrocnemius EMG activity for test footwear conditions for % stance phase. (a) – without standard deviation (STD), (b) – with the lines shadowed to represent STD ranges.262

Figure 6.27: The gastrocnemius EMG activity for test footwear conditions (N=14).266

Figure 6.28: The gastrocnemius EMG activity for test footwear conditions. (a) – without standard deviation (STD), (b) – with the lines shadowed to represent STD ranges.269

Figure 6.29: The gastrocnemius EMG activity for test footwear conditions (N=14). (a) – without standard deviation (STD), (b) – with the lines shadowed to represent STD ranges.271

Figure 6.30: The gastrocnemius EMG activity for test footwear conditions (N=14).273

Figure 6.31: The soleus EMG activity for test footwear conditions (N=13). (a) – without standard deviation (STD), (b) – with the lines shadowed to represent STD ranges.275

Figure 6.32: The soleus EMG activity for test footwear conditions (N=13). (a) – without standard deviation (STD), (b) – with the lines shadowed to represent STD ranges.280

Figure 6.33: The soleus EMG activity for test footwear conditions (N=13). (a) – without standard deviation (STD), (b) – with the lines shadowed to represent STD ranges.282

Figure 6.34: The soleus EMG activity for test footwear conditions (N=13). (a) – without standard deviation (STD), (b) – with the lines shadowed to represent STD ranges.284

Figure 6.35: The soleus EMG activity for test footwear conditions (N=13). (a) – without standard deviation (STD), (b) – with the lines shadowed to represent STD ranges.286

Figure 6.36: The tibialis anterior EMG activity for test footwear conditions (N=14). (a) – without standard deviation (STD), (b) – with the lines shadowed to represent STD ranges.287

Figure 6.37: The tibialis anterior EMG activity for test footwear conditions (N=14). (a) – *without standard deviation (STD)*, (b) – *with the lines shadowed to represent STD ranges*.290

Figure 6.38: The tibialis anterior EMG activity for test footwear conditions (N=14). (a) – without standard deviation (STD), (b) – with the lines shadowed to represent STD ranges.291

Figure 6.39: The tibialis anterior EMG activity for test footwear conditions (N=14). (a) – without standard deviation (STD), (b) – with the lines shadowed to represent STD ranges.....292

Figure 6.40: The tibialis anterior EMG activity for test footwear conditions (N=14). (a) – without standard deviation (STD), (b) – with the lines shadowed to represent STD ranges.....293

Figure 6.41: The Achilles muscle moment arm length for different heel height test footwear conditions (N=14). Legend 1 indicates the point at which the muscle moment arm is at its maximum at 55% of stance phase, where the calf muscles are starting to generate force by eccentric contraction and gradually increasing the external DF ankle moment required for ankle movement; legend 2 indicates the mean muscle moment arm at which the peak EMG occurs.....295

Figure 6.42: The Achilles muscle moment arm length analysis for different apex length test footwear conditions (N=14). Legend 1 indicates maximum muscle moment arm at 55% of stance phase; legend 2 indicates the mean muscle moment arm at the position where the peak EMG occurs. (a) – without standard deviation (STD), (b) – with the lines shadowed to represent STD ranges.....297

Figure 6.43: The Achilles muscle moment arm length for different toe apex angle test footwear conditions (N=14). Legend 1 indicates maximum muscle moment arm at 55% of the stance; legend 2 indicates mean muscle moment arm at which the peak EMG occurs. (a) – without standard deviation (STD), (b) – with the lines shadowed to represent STD ranges.....299

Figure 6.44: The Achilles muscle moment arm length for the different curved-heel test footwear conditions where control shoe has no curve (N=14). (a) – without standard deviation (STD), (b) – with the lines shadowed to represent STD ranges.301

Figure 6.45: The Achilles muscle moment arm length analysis results from OpenSim software for different flexibility levels of the sole (N=14). Legend 1 indicates maximum muscle moment arm at 55% of the stance phase which approximates to the position where the calf muscles are starting to generate powerful force; legend 2 indicates the mean muscle moment arm at which the peak EMG occurs. (a) – without standard deviation (STD), (b) – with the lines shadowed to represent STD ranges.303

Figure 6.46: The fibre length alteration results data from OpenSim simulation software for different heel height test footwear conditions (N=14). The red line represents fibre lengths at the barefoot static position. Legend 1 indicates maximum fibre length at 55% of stance phase which approximates to where the calf muscles start to generate powerful force; legend 2 indicates the mean fibre length at which the peak EMG occurs. (a) – without standard deviation (STD), (b) – with the lines shadowed to represent STD ranges.305

Figure 6.47: The fibre length alteration results from OpenSim simulation software for different AP test footwear conditions (N=14). The red line represent fibre lengths at the barefoot static position. Legend 1 indicates maximum fibre length at 55% of stance phase which approximates to the position

where the calf muscles are starting to generate powerful force; legend 2 indicates mean fibre length at which the peak EMG occurs. (a) – without standard deviation (STD), (b) – with the lines shadowed to represent STD ranges.307

Figure 6.48: The fibre length alteration results data from OpenSim simulation software for different TA test footwear conditions (N=14). Red line represent fibre lengths at barefoot static position. Legend 1 indicates maximum fibre length at 55% of the stance phase where approximately calf muscle starting to generate powerful force; legend 2 indicates mean fibre length at which the peak EMG occurs. (a) – without standard deviation (STD), (b) – with the lines shadowed to represent STD ranges.309

Figure 6.49: The fibre length alteration results data from OpenSim simulation software for different heel curve test footwear conditions (N=14). The red line represent fibre lengths at the barefoot static position. Legend 1 indicates maximum fibre length at 55% of stance phase which approximates to the position where the calf muscles are starting to generate powerful force; legend 2 indicates mean fibre length at which the peak EMG occurs. (a) – without standard deviation (STD), (b) – with the lines shadowed to represent STD ranges.311

Figure 6.50: The fibre length alteration results data from OpenSim simulation software for different flexibility levels of the sole at the metatarsal area (N=14). The red line represents fibre lengths at the barefoot static position. Legend 1 indicates maximum fibre length at 55% of the stance phase where the calf muscle starts to generate powerful force; legend 2 indicates mean fibre length at which the peak EMG occurs.313

Figure 6.51: The fibre length velocity alteration results data from OpenSim simulation software for different HH test footwear conditions (N=14). Legend 1 indicates the area (68% stance phase) at which maximum EMG for MG muscle was recorded; legend 2 indicates the area (72% stance phase) at which maximum EMG for soleus muscle was recorded. (a) – without standard deviation (STD), (b) – with the lines shadowed to represent STD ranges.314

Figure 6.52: The fibre length velocity alteration results from OpenSim simulation software for different AP test footwear test conditions (N=14). Legend 1 indicates the area (68% stance phase) at which maximum EMG for MG muscle was recorded; legend 2 indicates the area (72% stance phase) at which maximum EMG for soleus muscle was recorded. (a) – without standard deviation (STD), (b) – with the lines shadowed to represent STD ranges.318

Figure 6.53: The fibre length velocity alteration results data from OpenSim simulation software for different toe angle test footwear conditions (N=14). Legend 1 indicates the area (68% stance phase) at which maximum EMG for MG muscle was recorded; legend 2 indicates the area (72% stance phase) at which maximum EMG for soleus muscle was recorded. (a) – without standard deviation (STD), (b) – with the lines shadowed to represent STD ranges.320

Figure 6.54: The fibre length velocity alteration results data from OpenSim simulation software for different heel curve test footwear conditions (N=14). Legend 1 indicates the area (68% stance phase) at which maximum EMG for MG muscle was recorded; legend 2 indicates the area (72% stance phase) at which maximum EMG for soleus muscle was recorded. (a) – without standard deviation (STD), (b) – with the lines shadowed to represent STD ranges.322

Figure 6.55: The fibre length velocity alteration results data from OpenSim simulation software for different level flexibly of the sole (N=14). Legend 1 indicates the area (68% stance phase) at which maximum EMG for MG muscle was recorded; legend 2 indicates the area (72% stance phase) at which maximum EMG for soleus muscle was recorded. (a) – without standard deviation (STD), (b) – with the lines shadowed to represent STD ranges.....323

Figure 6.56: The required tendon force (medial gastrocnemius) which is transmitted through the tendon for the ankle joint to oppose the external dorsiflexor moment for different footwear features. Legend 1 indicates the area at which maximum EMG activity for MG was recorded.324

Figure 6.57: The required active tendon force (medial gastrocnemius) which is transmitted through the tendon to enable the ankle joint to oppose the externally-applied moment for different footwear features. (a) – without standard deviation (STD), (b) – with the lines shadowed to represent STD ranges.....325

Figure 6.58: The tibialis anterior alterations for fibre length (mm), fibre length velocity, tibialis anterior active fibre force (N) and EMG overall area for different heel heights. Legend 1 and 2 indicate the area during LR at which maximum EMG activity occurs; legend 3 indicates the maximum active fibre force required for internal DF moment. The red line represents the barefoot static position. (a) – without standard deviation (STD), (b) – with the lines shadowed to represent STD ranges.....326

Figure 6.59: The tibialis anterior alterations in fibre length (mm), fibre length velocity, tibialis anterior active fibre force (N), EMG activity and standard deviation for different heel curves.327

Figure 6.60: The tibialis anterior alterations for fibre length (mm), fibre length velocity, tibialis anterior active fibre force (N) and EMG overall area for curved heels. Legends 1 and 2 indicate the area during LR at which maximum EMG activity occurs; legend 3 indicates the maximum active fibre force required for internal dorsiflexor moment. The red line represents the barefoot static position.....331

Figure 6.61: The tibialis anterior alteration to fibre length (mm), fibre length velocity, tibialis anterior active fibre force (N), EMG activity and standard deviation for different heel curves.332

Figure 7.1: Sagittal plane ankle motion during the five heel height test conditions with standard deviation where the control shoe is 3.5 HH.337

Figure 7.2: Summary of alteration to muscle function by different heel heights.343

Figure 7.3: Summary of alteration to muscle function caused by alteration to the rocker sole apex position.....347

Figure 7.4: Sagittal plane ankle motion when walking with the three-apex position test conditions with standard deviation where the control shoe is 62.5AP.	348
Figure 7.5: Sagittal plane knee motion during the three apex position test conditions where the control shoe is 62.5AP.....	349
Figure 7.6: Alteration to muscle function demonstrated by altering rocker apex angle.	352
Figure 7.7: The effect of different heel curves on fibre lengths.	355

LIST OF TABLES

Table 2.1: Examples of exercise training rehabilitation programmes for claudicants.	14
Table 2.2: Percentage increase in pain-free walking distance when wearing a three-curve rocker-soled shoe test condition.	21
Table 3.1: Ankle and knee kinematic data for studies which investigated the MBT shoe versus flat control shoes.	36
Table 4.1: Characteristics of muscle fibres types [adapted from (Rose and Gamble, 2006, Abernethy et al., 2013, Katch et al., 2011)].	56
Table 4.2: The characteristics of three types of muscle contraction [adapted from (Trew and Everett, 2005)].	62
Table 4.3: Muscle architecture parameters of 21 cadavers (Arnold et al., 2010).	66
Table 4.4: Pennation angle measured at rest and maximum voluntary contraction for the right (R) and left (L) legs of male and female subjects. Pennation angle is reported as degrees with standard deviations in parentheses (Manal et al., 2006).	75
Table 4.5: The effect of heel height on lower limb muscle EMG activity.	80
Table 4.6: The EMG results demonstrated by Sobhani et al (2003).	89
Table 4.7: EMG activity with varying shoe stiffness.	91
Table 4.8: Biomechanical evidence of footwear features.	96
Table 5.1: The electrode placement location over six muscles according to SENIAM guidelines (Hermens et al 1999).	130
Table 5.2: Footwear specifications.	133
Table 5.3: Filtration levels effect on maximum ankle angle range of motion.	153
Table 5.4: Muscle modelling parameters.	164
Table 6.1: Subject demographics.	186
Table 6.2: Footwear test conditions analysed and their acronyms.	187
Table 6.3: Nomenclature used for parts of stance phase.	188

Table 6.4: Mean (\pm SD) sagittal plane ankle motion for shoes with five different heel heights during stance phase.....	189
Table 6.5: Pairwise comparisons of shoe conditions for mean maximum ankle PF angle during LR phase.....	190
Table 6.6: Pairwise comparisons of shoe conditions for max ankle DF angle during second rocker of gait.....	191
Table 6.7: Pairwise comparisons of shoe conditions for max ankle PF angle during late stance.....	192
Table 6.8: Mean values for maximum ankle ROM during specific points and also the complete gait cycle for shoes with different heel heights.....	193
Table 6.9: Pairwise comparisons of shoe conditions versus ankle sagittal plane ROM during LR.....	193
Table 6.10: Pairwise significance comparisons between shoe conditions and ankle ROM angle between point 2 and 3 of the gait cycle.	194
Table 6.11: Pairwise comparisons of shoe conditions for the ankle ROM between maximum dorsiflexion and maximum PF during late stance (between points 3 and 4).	195
Table 6.12: Pairwise statistical significance comparisons between shoe conditions versus maximum ankle ROM angle during the full gait cycle.	196
Table 6.13: Alternative hypotheses accepted/not accepted for alteration to heel height test condition.	197
Table 6.14: Mean (\pm SD) sagittal plane ankle motion (deg) for three different rocker apex position test conditions.....	198
Table 6.15: Pairwise comparisons of apex positions for mean maximum ankle PF angle during LR. ..	199
Table 6.16: Pairwise comparisons of rocker APs for maximum ankle DF angle during second rocker of gait).....	199
Table 6.17: Mean values for ankle ROM during gait cycle for different AP conditions.....	200
Table 6.18: Pairwise statistical significance comparisons between shoe AP conditions and ankle ROM angle between point 2 and 3 of the gait cycle.....	200
Table 6.19: Alternative hypotheses accepted/not accepted for alteration to apex position (AP) test conditions.	201
Table 6.20: Mean (\pm SD) sagittal plane ankle motion for the three apex angles (TAs) tested.	202
Table 6.21: Pairwise comparisons of rocker toe angles (TAs) for maximum ankle DF angle during stance phase.	203
Table 6.22: Mean values for ankle ROM during the gait cycle for different apex-angled shoes.....	203
Table 6.23: Pairwise statistical significance comparisons between apex angle conditions and ankle ROM between points 2 and 3 of the gait cycle.....	204

Table 6.24: Alternative hypotheses accepted/not accepted for alteration to apex position (AP) test conditions.	204
Table 6.25: Mean (\pm SD) sagittal plane ankle rotation demonstrated by the three different curved heel test conditions.	205
Table 6.26: Mean values for sagittal plane ankle ROM during the complete gait cycle for different curved heel shoe test conditions.	206
Table 6.27: Pairwise comparisons of curved heel shoe test conditions for maximum ankle DF angle during stance phase.	206
Table 6.28: Pairwise statistical significance comparisons between curved heel conditions and ankle ROM angle between point 2 and 3 of the gait cycle.	207
Table 6.29: Alternative hypotheses accepted/not accepted for alteration to heel curve test conditions.	207
Table 6.30: Kinematic data produced when walking with shoes with different forefoot sole stiffness.	208
Table 6.31: Mean (\pm SD) sagittal plane ankle ROM (degs) for three different flexibility levels of the rocker sole at the metatarsal arcade area.	209
Table 6.32: Pairwise statistical significance comparisons for maximum ankle plantarflexion angle at toe-off phase between the forefoot shoe flexibility conditions.	209
Table 6.33: Pairwise statistical significance comparisons for maximum ankle ROM during third rocker of gait between flexible and semi-flexible sole unit conditions.	209
Table 6.34: Alternative hypotheses accepted/not accepted for alteration to heel curve test conditions.	210
Table 6.35: Mean (\pm SD) sagittal plane knee kinematics (degs) when walking with shoes with five different heel height test conditions.	212
Table 6.36: Pairwise comparisons of shoe conditions for max knee flexion at toe-off.	213
Table 6.37: Pairwise comparisons of shoe conditions for max knee flexion during swing phase.	214
Table 6.38: Mean values for maximum knee ROM between the point 2-3 and within complete stance phase for shoes with different heel heights.	214
Table 6.39: Pairwise comparisons of shoe conditions for max knee RM between point 2 and 3.	215
Table 6.40: Pairwise comparisons of shoe conditions for max ROM during stance phase.	215
Table 6.41: Alternative hypotheses accepted/not accepted for alteration to heel height test conditions.	217
Table 6.42: Mean (\pm SD) sagittal plane knee motion (degs) for three different apex position, max ROM between point 2-3 and max knee ROM during stance phase (N=15).	218
Table 6.43: Pairwise comparisons of apex positions for mean knee flexion during LR.	218

Table 6.44: Pairwise comparisons of apex positions for mean knee flexion between point 2 and 3...	219
Table 6.45: Alternative hypotheses accepted/not accepted for alteration to rocker apex positions..	219
Table 6.46: Mean (\pm SD) sagittal plane knee motion (degs) for three different toe angle test footwear conditions, max ROM between point 2-3 and max knee ROM during stance phase (N=15).....	220
Table 6.47: Mean (\pm SD) sagittal plane knee motion (degs) for three different heel curves, maximum ROM between point 2-3, and maximum knee ROM during stance phase.....	221
Table 6.48 Pairwise statistical significance comparisons between curved heel conditions and knee angle at ICt.....	222
Table 6.49: Pairwise statistical significance comparisons between shoe conditions and maximum knee ROM angle between point 2 and 3 of the gait cycle (N=15).....	222
Table 6.50: Pairwise statistical significance comparisons between shoe conditions and maximum knee ROM angle during stance phase (n=15).....	222
Table 6.51: Alternative hypotheses accepted/not accepted for different heel curves.....	223
Table 6.52: Mean (\pm SD) sagittal plane knee motion (degs) for three different flexibility of the sole, maximum ROM between point 2-3, and maximum knee ROM during stance phase.....	224
Table 6.53: Pairwise statistical significance comparisons for max knee ROM between points 2 and 3 between shoe conditions (n=15).	225
Table 6.54: Alternative hypotheses accepted/not accepted for different shoe forepart flexibility.....	226
Table 6.55: Mean (\pm SD) sagittal plane hip motion (deg) for five different heel heights, maximum hop ROM during stance and full gait cycle (N=15).....	227
Table 6.56: Pairwise comparisons of shoe conditions for max hip flexion at toe-off.....	228
Table 6.57: Alternative hypotheses accepted/not accepted for different shoe heights.....	228
Table 6.58: Mean (\pm SD) sagittal plane hip motion (deg.) for three different apex position, maximum hop ROM during stance and full gait cycle (N=15).	229
Table 6.59: Mean (\pm SD) sagittal plane hip motion (degs) for three different toe angle test footwear conditions, maximum hop ROM during stance and full gait cycle (N=15).	230
Table 6.60: Mean (\pm SD) sagittal plane hip motion (degs) for three different heel curves, maximum hop ROM during stance and full gait cycle (N=15).....	231
Table 6.61: Mean (\pm SD) sagittal plane hip motion (degs) three different level of flexibility of the mid-part of the shoe, maximum hip ROM during stance and full gait cycle (N=15).	233
Table 6.62: Mean (\pm SD) sagittal plane ankle moment (Nm/kg) for the five footwear conditions (N=15).	234
Table 6.63: Pairwise comparison of shoe conditions for mean external ankle PF moment during stance phase.	235

Table 6.64: Pairwise comparison of shoe conditions for mean external ankle DF moment during stance phase.	235
Table 6.65: The average of the area under the curves for the footwear test conditions.	236
Table 6.66: Pairwise comparison of shoe conditions for mean values of area 1.	237
Table 6.67: Pairwise comparison of shoe conditions for mean values of area 2.	238
Table 6.68: Mean (\pm SD) sagittal plane ankle moment (Nm/kg) for the three footwear conditions (N=15).	239
Table 6.69: Pairwise comparison of shoe conditions for mean external ankle PF moment during stance phase.	240
Table 6.70: Pairwise comparison of shoe conditions for mean external ankle DF moment during stance phase.	240
Table 6.71: The average of the area under the curves (external ankle moments) for the footwear test conditions (N=15).	241
Table 6.72: Pairwise comparison of the average of the area under the curves (external ankle DF moment) for test footwear conditions (N=15).	241
Table 6.73: Mean (\pm SD) sagittal plane ankle moment (Nm/kg) for the three footwear conditions (N=15).	243
Table 6.74: Pairwise comparison of shoe conditions for mean external ankle DF moment during stance phase.	243
Table 6.75: The average of the area under the curves (external ankle moments) for test footwear conditions (N=15).	244
Table 6.76: Pairwise comparison of the average of the area under the curves (external ankle DF moment) for test footwear conditions (N=15).	244
Table 6.77: Mean (\pm SD) sagittal plane ankle moment (Nm/kg) for the three footwear conditions (N=15).	246
Table 6.78: Pairwise comparison of shoe conditions for mean external ankle PF moment during stance phase.	246
Table 6.79: Pairwise comparison of shoe conditions for mean external ankle DF moment during stance phase.	246
Table 6.80: The average value of the area under the curves (external ankle moments) for test footwear conditions (N=15).	247
Table 6.81: Pairwise comparison of the average of the area under the curves (external ankle PF moment) for test footwear conditions (N=15).	247
Table 6.82: Pairwise comparison of the average of the area under the curves (external ankle DF moment) for test footwear conditions (N=15).	248

Table 6.83: Mean (\pm SD) sagittal plane ankle moment (Nm/kg) for the three footwear conditions (N=15).....	249
Table 6.84: Pairwise comparison of shoe conditions for mean external ankle PF moment during stance phase.....	249
Table 6.85: The average of the area under the curves (external ankle moments) for test footwear conditions (N=15).	250
Table 6.86: Pairwise comparison of the average of the area under the curves (external ankle PF moment) for test footwear conditions (N=15).	250
Table 6.87: Mean (\pm SD) area of ankle joint power for test footwear conditions.....	252
Table 6.88: Pairwise comparison of shoe conditions power generation area for ankle joint during whole stance phase (N=14).	252
Table 6.89: Pairwise comparison of shoe conditions for average ankle joint power absorption area for the whole stance phase (N=15).	253
Table 6.90: Mean (\pm SD) area of ankle joint power for test footwear conditions.....	255
Table 6.91: Pairwise comparison of shoe conditions power generation area for ankle joint during whole stance phase (N=15).	255
Table 6.92: Pairwise comparison of shoe conditions for average ankle joint power absorption area for the whole stance phase (N=15).	256
Table 6.93: Mean (\pm SD) area of ankle joint power for test footwear conditions.....	257
Table 6.94: Pairwise comparison of shoe conditions for average ankle joint power absorption area for the whole stance phase (N=15).	258
Table 6.95: Mean (\pm SD) area of ankle joint power for test footwear conditions.....	259
Table 6.96: Pairwise comparison of shoe conditions for average ankle joint power absorption area for the whole stance phase (N=15).	259
Table 6.97: Mean (\pm SD) area of ankle joint power for test footwear conditions.....	260
Table 6.98: Mean (\pm SD) medial gastrocnemius EMG percentage activity for test footwear conditions.	262
Table 6.99: Pairwise comparison of shoe conditions for medial gastrocnemius mean EMG activity during loading response (N=14).	263
Table 6.100: Pairwise comparison of shoe conditions for medial gastrocnemius mean EMG activity during mid-stance phase.	263
Table 6.101: Pairwise comparison of shoe conditions for medial gastrocnemius mean EMG activity during late stance phase (N=14).....	264
Table 6.102: The average (\pm SD) of the area under the curves for medial gastrocnemius EMG activity for test footwear conditions (N=14).....	265

Table 6.103: Pairwise comparison of shoe conditions for medial gastrocnemius overall area underneath the EMG activity curve during stance phase (N=14).	265
Table 6.104 Mean (\pm SD) medial gastrocnemius EMG activity for test footwear conditions.	267
Table 6.105: Pairwise comparison of shoe conditions for medial gastrocnemius mean EMG activity during mid-stance phase (N=14).	267
Table 6.106: The average (\pm SD) of the overall area under the curves for medial gastrocnemius EMG activity for test footwear conditions (N=14).	268
Table 6.107: Mean (\pm SD) medial gastrocnemius EMG activity for test footwear conditions.	269
Table 6.108: Pairwise comparison of shoe conditions for medial gastrocnemius maximum EMG activity during mid-stance phase (N=14).	269
Table 6.109: The average (\pm SD) of the overall area under the curves for medial gastrocnemius EMG activity for test footwear conditions (N=14).	270
Table 6.110: Pairwise comparison of shoe conditions for medial gastrocnemius overall area EMG activity during stance phase.	270
Table 6.111: Mean (\pm SD) maximum medial gastrocnemius EMG activity for test footwear conditions.	272
Table 6.112: The average (\pm SD) of the overall area under the curves for medial gastrocnemius EMG activity for test footwear conditions (N=14).	272
Table 6.113: Mean (\pm SD) medial gastrocnemius EMG activity for test footwear conditions.	273
Table 6.114: The average (\pm SD) of the overall area under the curves for medial gastrocnemius EMG activity for test footwear conditions (N=14).	274
Table 6.115: Mean (\pm SD) soleus EMG activity for test footwear conditions.	275
Table 6.116: Pairwise comparison of shoe conditions for soleus mean EMG activity during loading response (N=13).	275
Table 6.117: Pairwise comparison of shoe conditions for soleus mean EMG activity during mid-stance phase (N=13).	276
Table 6.118: Pairwise comparison of shoe conditions for soleus mean EMG activity during loading response (N=13).	277
Table 6.119: The average (\pm SD) of the area under the curves for medial gastrocnemius EMG activity for test footwear conditions (N=13).	278
Table 6.120: Pairwise comparison of shoe conditions for soleus overall area EMG activity during stance phase (N=13).	278
Table 6.121: Mean (\pm SD) medial gastrocnemius EMG activity for test footwear conditions.	280
Table 6.122 : Pairwise comparison of shoe conditions for soleus mean EMG activity during mid-stance phase (N=13).	280

Table 6.123: The average (\pm SD) of the overall area under the curves for soleus EMG activity for test footwear conditions (N=13).....	281
Table 6.124: Mean (\pm SD) soleus EMG activity for test footwear conditions.....	282
Table 6.125: Pairwise comparison of shoe conditions for soleus mean EMG activity during stance phase (N=13).	283
Table 6.126: The average (\pm SD) of the overall area under the curves for soleus EMG activity for test footwear conditions (N=13).....	283
Table 6.127: Mean (\pm SD) soleus EMG activity for test footwear conditions.....	284
Table 6.128: The average (\pm SD) of the overall area under the curves for medial gastrocnemius EMG activity for test footwear conditions (N=14).....	285
Table 6.129: Mean (\pm SD) soleus EMG activity for test footwear conditions.....	286
Table 6.130: The average (\pm SD) of the overall area under the curves for soleus EMG activity for test footwear conditions (N=14).....	287
Table 6.131: Mean (\pm SD) tibialis anterior EMG activity for test footwear conditions.	288
Table 6.132: Pairwise comparison of shoe conditions for tibialis mean EMG activity during loading response (N=14).	288
Table 6.133: Pairwise comparison of shoe conditions for tibialis overall area EMG activity during stance phase (N=14).	289
Table 6.134 Mean (\pm SD) tibialis anterior EMG activity for test footwear conditions.....	290
Table 6.135: Mean (\pm SD) tibialis anterior EMG activity for test footwear conditions.	291
Table 6.136: Mean (\pm SD) tibialis anterior EMG activity for test footwear conditions.	292
Table 6.137: Pairwise comparison of shoe conditions for tibialis mean EMG activity during loading response (N=14).	292
Table 6.138Table: Mean (\pm SD) tibialis anterior EMG activity for test footwear conditions.....	294
Table 6.139: Pairwise comparison of shoe conditions for tibialis mean EMG activity during loading response (N=14).	294
Table 6.140: Pairwise comparison of shoe conditions for tibialis overall area EMG activity during stance phase (N=14).	294
Table 6.141: Mean (\pm SD) Achilles muscle moment arm (mm) for heel height test footwear conditions (N=14).....	296
Table 6.142: Mean (\pm SD) Achilles muscle moment arm (mm) for apex length test footwear conditions (N=14).....	298
Table 6.143: Pairwise comparison the Achilles muscle moment arm changes at 55% stance phase for test footwear conditions (N=14).....	298

Table 6.144: Mean (\pm SD) Achilles muscle moment arm (mm) for toe angle test footwear conditions (N=14).....	300
Table 6.145: Pairwise comparison the Achilles muscle moment arm changes during peak force generation of the ankle for test footwear conditions (N=14).....	300
Table 6.146: Mean (\pm SD) Achilles muscle moment arm (mm) for curved-heel test footwear conditions (N=14).....	302
Table 6.147: Mean (\pm SD) Achilles muscle moment arm (mm) for different flexibility of the sole (N=14).	303
Table 6.148: MG and soleus fibre length (mm) mean (\pm SD) for heel height test footwear conditions (N=14).....	305
Table 6.149: MG and soleus fibre length (mm) mean (\pm SD) for the AP test footwear conditions (N=14).	307
Table 6.150: Pairwise comparison the soleus fibre length changes during peak force generation of the ankle for test footwear conditions (N=14).....	308
Table 6.151: MG and soleus fibre length (mm) mean (\pm SD) for AP test footwear conditions (N=14).	310
Table 6.152: MG and soleus fibre length (mm) mean (\pm SD) for curved heel test footwear conditions (N=14).....	312
Table 6.153: MG and soleus fibre length (mm) mean (\pm SD) for different sole flexibility level (N=14).	313
Table 6.154: MG and soleus fibre length velocity (mm/% of the stance phase) mean (\pm SD) for different heel heights (N=14).	315
Table 6.155: Pairwise comparison of medial gastrocnemius fibre velocity changes during maximum EMG activity at 68% of the stance phase for the test footwear conditions (N=14).....	315
Table 6.156: Pairwise comparison soleus fibre velocity changes during maximum EMG activity at 72% of the stance phase for test footwear conditions (N=14).....	316
Table 6.157: MG and soleus fibre length velocity (mm/% of the stance phase) mean (\pm SD) for different apex lengths of the sole (N=14).	318
Table 6.158: Pairwise comparison medial gastrocnemius fibre velocity changes during maximum EMG activity at 68% of the stance phase for test footwear conditions (N=14).....	319
Table 6.159 Table: MG and soleus fibre length velocity (mm/% of stance phase) mean (\pm SD) for different toe angles of the sole (N=14).....	320
Table 6.160: MG and soleus fibre length velocity (mm/% of the stance phase) mean (\pm SD) for different heel curves (N=14).....	322
Table 6.161: Active tendon force of MG muscle for different footwear features (N=14).	325
Table 6.162: The tibialis anterior fibre length, fibre length, active fibre force and EMG activity mean (\pm SD) for different heel heights (N=14).	328

Table 6.163: Pairwise comparison of shoe conditions for average maximum length of tibialis anterior fibres during LR (N=14).....	328
Table 6.164: Pairwise comparison of shoe conditions for average maximum length velocity of tibialis anterior fibres during LR (N=14).....	329
Table 6.165: The tibialis anterior fibre length, fibre length velocity, active fibre force and EMG activity mean (\pm SD) for different heel curves (N=14).....	332
Table 6.166: Pairwise comparison of shoe conditions for average maximum length of tibialis anterior fibres during LR (N=14).....	333
Table 6.167: Pairwise comparison of shoe conditions for maximum tibialis anterior fibre length velocity during LR (N=14).....	333
Table 7.1: Summary of comparison of factors which resulted in muscle function alteration by differing the heel heights.....	344
Table 7.2: Summary of alteration on muscle function produced by altering the rocker sole apex position.....	349
Table 7.3: Summary comparison factors which resulted in muscle functioning alteration by the rocker apex toe angle.....	353
Table 7.4: Summary and comparison of factors which resulted in muscle function alteration by altering heel curvature.....	356

ACKNOWLEDGMENTS

I am deeply thankful to my main supervisor Dr. Steven Hutchens for his help. As my supervisor, Steve has been a constant source of help and encouragement for my Ph.D. He was always very positive and supportive, had always time for me, we had lot of debates together, discussions and Steve could always cheer me up. Steve was the biggest help in my research and I am very grateful to have such supervisor and a friend.

I would like to thank my Co-supervisor Professor Richard Jones who helped me with gait analysis questions, showed me how to use SPSS for my statistical analysis and also for being very realistic with everything.

I would like to thank Professor Christopher Nester for bringing me back on track at the end of the first year of my PhD. Chris had helped me to change the topic of my study, we were discussing some new ideas and for giving me some crucial understanding in the new field.

I am thankful to Gulnaz for assisting me in the gait laboratory and being always very helpful.

I would also like to thank my aunt Dr. Valentina Volkova. She was always supportive and helped financially to finish my PhD.

I would like to thank the ORSAS and the University of Salford for funding my PhD.

I am also grateful to Dr. Glyn Heath for the support throughout my dissertation writing.

At the last, I would like to thank Daryna, as she influenced my work at the end of my research.

ABSTRACT

Introduction

Intermittent claudication (IC) is a condition which affects people with peripheral arterial disease in the lower limbs and causes calf muscle pain and limping due to the lack of blood supply to the gastrocnemius muscle in particular. This limits the distance people with IC (known as claudicants) can walk before having to stop because of the pain. The accepted best treatment currently is enrolment onto supervised exercise regimes, but these provide limited improvement and do not alter their antalgic gait. This study aims to investigate the effect of specific footwear designs on gait and lower limb muscle function with the intention of identifying which features would be recommended for inclusion in footwear designed to relieve their painful symptoms by offloading the calf muscles.

Method

Fifteen volunteer healthy subjects, age range 20-29 years (mean 25.3 ± 2.73) undertook a series of gait laboratory trials with shoes adapted with specifically-chosen outsole features. High street shoes were adapted with the test conditions which included shoes with five different heel heights (varying from a 1.5cm to 5.5cm heels), two heel profile conditions (curved and semi curved heels), three traditional (angled) rocker soles with varying apex positions (55%, 62.5% and 70% of shoe length) and three with varying apex angles (10, 15, and 20 deg.), plus three with different forepart sole stiffness (solid, semi-flexible and flexible). The baseline shoe was taken as being one with no heel curve, a heel height of 3.5mm, an apex position of 62.5% of shoe length, and apex angle of 15 deg. and a stiff forepart to the shoe. Measurement and comparisons were taken of lower limb kinetics and kinematics (Qualysis, Sweden) plus electromyographical (EMG) activity (Noraxon USA) of medial gastrocnemius, soleus, tibialis anterior, rectus femoris and biceps femoris during walking trials where the walking speed was controlled using timing gaits. Data were analysed using Visual3D and OpenSim software to enable interpretation of EMG activity to enable calculation of lower limb muscle function during gait.

Results

Changes from the baseline shoe were taken as being at a level of significance of $p < 0.05$. The most effective footwear test condition in regards to offloading of the calf muscles compared to the control shoe was that with a 4.5cm heel, a 55% of shoe length apex position, and a 20° rocker apex angle; which demonstrated significant offloading to the calf muscles. The 55% apex position had a significant offloading influence on the calf muscles whilst at the same time not significantly altering knee and hip kinematics.

Conclusion

This study demonstrates that a potentially useful shoe design was identified for treatment of claudicant calf pain which did not adversely affect more proximal joint kinetics and kinematics.

LIST OF ABBREVIATIONS

(ABPI) - measuring the ankle brachial pressure index	(MTP) - metatarsophalangeal joint
(AIM) - an automatic identification of markers	(MTU) - muscle tendon units
(AP) – apex position	(MWD) - maximum walking distance
(ASIS) - right and left anterior superior-iliac spine	(N/A) - not acceptable
(ATP) - adenosine triphosphate	(N) - newton
(bf) - barefoot	(n=) - number of subjects
(BF) - biceps femoris	(N=) - number of subjects
(CAST) - the calibration anatomical system technique	(NS) - not significant
(CI) - confidence interval	(OA) -osteoarthritis
(cm) - centimetre	(OA) - old adults
(CH) - curved heel	(PAD) - peripheral arterial disease
(COP) - centre of pressure	(PAD-IC) - peripheral vascular disease with intermittent claudication
(deg.) – degree	(PAD-ABPI) - ankle-brachial pressure index of peripheral arterial disease patients
(DM) - diabetes mellitus	(PCSA) - physiological cross-section areas
(DF) - dorsiflexion	(PCA) - physiological cross-section area
(DOF) - degrees of freedom	(PF) - plantarflexion
(6 DOF) - six degrees of freedom	(POAD) - peripheral occlusive arterial disease
(DLT) - direct linear transformation	(PRT) - progressive resistance training
(EMG) - electromyography	(PSw) - pre Swing
(ES) - erector spinae	(PSIS) - right and left posterior superior iliac spine
(FFOs) - functional foot orthoses	(PVD) - peripheral vascular disease
(Gas) - gastrocnemius	(QOL) - quality of life
(GM) - medial gastrocnemius	(QTM) - qualisys track manager
(GRF) - ground reaction force	(RA) - rocker angle
(GRV) - ground reaction vector	(RCT) - Randomized controlled trial
(HC) - heel curve	(RF) - rectus femoris
(HDP) - high density plastazote	(RFT) - right foot
(HH) - heel height	(RMS) - root mean square
(Hz) - hertz	(RPV) - pelvis
(HS) - heel strike	(RSK) - right shank
(IC) - intermittent claudication	(RTH) - right thigh
(ICt) - initial contact	(SACH) - a solid ankle and cushioned heel type of shoe
(i.e) - that is	(SET) - supervised exercise therapy
(ILIAC) - right and left iliac crests	(SOL) - soleus
(IK) - inverse kinematics	(STD) - standard deviation
(ISw) - onital Swing	(TA) - tibialis anterior
(KAFOs) - cosmetic knee ankle foot orthoses	(TA) - toe angle
(LFT) - left foot	(TO) - toes off
(LR) - loading Response	(TSt) - terminal stance
(LSK) - left shank	(TSw) - terminal Swing
(LTH) – left thigh	(YA) - young adults
(m/s) - metre/second	(1MT) - first metatarsal head
(m) - metre	(2D) - two dimensional
(mm) - millimetre	(3D) - three dimensional
(ma) - moment arm	(5MT) - the fifth metatarsal head
(MBT) - masai Barefoot Technology	
(MSt) - mid stance	
(MSw) - mid swing	

CHAPTER 1

1 INTRODUCTION

1.1 Rocker-soled shoes

Patients suffering from diseases such as diabetes mellitus (DM), spina bifida and rheumatoid arthritis are particularly susceptible to ulceration to the plantar surface of the foot resulting from excessive interface pressure between the foot and the inlay inserted in a shoe during walking. The use of rocker soles when added to footwear has historically been mainly targeted on the reduction of plantar foot pressures associated with these conditions during ambulation. Other applications for rocker soles have included the treatment of hallux rigidus by supplying a surrogate motion where lack of dorsiflexion of the first metatarsal head is experienced (Trepman and Yeo, 1995). They are also used to protect parts of the foot which have been surgically fused or become stiff and painful due to osteoarthritis (OA) in order to reduce the pain associated with walking. Such areas include the ankle, the rearfoot, the midfoot and the forefoot (Cracchiolo, 1979).

Forefoot plantar pressure in subjects with DM may be reduced using both traditional (angled) and curved rocker soles. The amount of forefoot pressure reduction achieved when analysing curved rocker soles in people with diabetes mellitus has been shown to be different for individual subjects. This is because it depends on the shape of the individual's foot, and the subsequent position of the rocker sole apex relative to the metatarsal heads, and also its orientation angle transversely across the shoe; as well as its apex angle (Chapman et al., 2013). This means that each subject should ideally have a bespoke prescription. However, it has been shown that to achieve maximal plantar pressure reduction for the great toe using angled rocker soles, the rocker angle needs to be 30° and positioned behind the metatarsal heads at a position of 55% of shoe length (Geary and Klenerman, 1987). This prevents the distal end of the foot experiencing plantar loading until as late as possible during propulsion.

This degree of rocker angle also makes the rocker sole very deep at its apex, but crucially theoretically makes the sole unit stiffest at that point so that it can rock without the shoe flexing. Rocker sole profiles which are comparatively less deep at their apex point tend to have lower apex angles, and this theoretically makes the shoe more flexible during stance phase than those with deeper profiles and larger rocker apex angles. However, the effect on

specific gait parameters of varying the thickness of the sole using rocker sole profiles in footwear and therefore also varying their stiffness is not well known and is analysed in this study.

Rocker sole designs may also affect the kinetics and kinematics of gait and also muscle function and activity in the lower limbs. However, little evidence exists with regards to these points. Although alterations to rocker sole apex angles and orientations have been extensively studied with regards to plantar pressure reductions (Hutchins et al., 2009), their effect on muscle function and activity is not well understood. Compared to barefoot walking, ambulation in a shoe incorporating a heel unit significantly alters gait parameters, but currently little is known how this affects parameters associated with muscle tendon units (MTUs) in the lower limbs. The alterations to gait kinetics and kinematics when walking with shoes adapted with the more commonly-prescribed rocker sole units such as the toe-only, the negative heel and the double rocker sole have been studied in the literature (Long et al., 2004, Van Bogart et al., 2005, Myers et al., 2006). However, these alterations have been shown to be clinically insignificant.

Currently it is unknown whether specific alterations to bespoke rocker sole design parameters can significantly affect the kinetics and kinematics of gait, and how they alter the operation of specific lower limb MTUs and the magnitude alteration which may be expected. Many studies have shown that the length and velocity of contraction of muscle fibres can have a significant effect on muscle force generation (Arnold et al., 2013). However, there is limited evidence in the literature and little understanding with regards to how much the force-length and force-velocity properties of the main muscles acting on the ankle affect force generation during walking in different footwear conditions.

Previous studies have provided limited contribution to the literature in this area, which would be potentially useful to enable footwear conditions for specific pathologies to be designed. Therefore, there is a need to expand the current knowledge in this area by analysing what effects rocker soles have on lower limb MTUs. Diseases such as intermittent claudication (IC) which adversely affect muscles acting on the ankle such as the triceps surae, may be responsive to orthotic intervention in the form of rocker soles, and evidence is needed as to which designs can, for instance, induce an offloading of this muscle group, or indeed increase loading in it for building up muscle strength. This may be achieved by

analysing a series of rocker sole profiles, which have targeted amendments to their profiles in order to identify these alterations. Therefore, muscle biomechanics and muscle parameters should be examined in relation to different footwear adaptations to understand how different designs can help in achieving the individual aims for different complications.

In addition to the conditions previously mentioned, there are numerous other conditions which affect the lower limb and foot which have been shown to be amenable to treatment using rocker soles. For instance, subjects with plantar fasciitis have been successfully treated with the toe-only rocker sole in conjunction with functional foot orthoses (FFOs) by reducing the intensity of the pain associated with the condition (Fong et al., 2012). It has been hypothesised that this improvement in symptoms may be associated with a reduction in the windlass mechanism affecting the plantar fascia due to restriction in 1st metatarsophalangeal joint (MTP) dorsiflexion during the propulsive phase of gait (Lin et al., 2013). However, analysis of the effect on the ankle plantarflexor MTUs with simultaneous analysis of kinetic and kinematics would have been useful in these studies, as it is known that subjects with plantar fasciitis may also have an ankle plantarflexor MTU contracture. Subjects with Achilles tendonitis may benefit from a reduction in the activity of the ankle plantarflexors during gait by using a rocker sole specifically designed to place the ankle in a relatively plantarflexed position during stance phase in order to reduce the work done by these muscles. This may be achieved by analysing the associated reduction in Achilles tendon lengthening and shortening during gait.

One pathology which has received a great deal of attention in the literature in recent years, and one which is known to adversely affect the ankle plantarflexor musculature is intermittent claudication (IC). This is a condition where vascular supply to the lower limbs is compromised due to peripheral vascular disease (PVD); otherwise known as peripheral occlusive arterial disease (POAD) or peripheral arterial disease (PAD). IC limits a patient's ability to walk because of pain being experienced in the calf muscles due to the muscle tissues becoming ischemic. This causes limping and eventually forces people with IC (known as claudicants) to stop walking in order to rest for a period of time after which they can continue to ambulate. This cycle of walking and resting typifies the gait of claudicants (Allaqaband et al., 2009, Wessler, 1955).

It is also important to look at muscle-tendon length changes during gait, because they actuate movement by developing force and generating internal moments (Delp, 1990). This may be an important factor when developing orthotic intervention for claudicants. Whilst the most commonly prescribed design of rocker sole profiles (such as the toe-only, double and negative heel rockers) have been shown to initiate small alterations to knee and ankle sagittal plane angles and ROMs during stance phase, little evidence exists regarding the ability of specific muscle groups to generate force when walking with rocker soles, because their effect on muscle-tendon lengths, muscle moment arms, and also their velocity of contraction is largely unknown. This is because when a muscle-tendon unit is lengthened or shortened to a certain point, the muscle fibres may be too long or too short to generate the required amount of active force in the lower limb. Skeletal muscle develops only 50% of the maximum force when its length is shortened to 85% of its resting length (Panjabi and White, 2001).

In addition, the type of muscle contraction demonstrated by specific muscles in the lower limb (i.e. concentric eccentric or isometric) may also be altered by rocker sole profiles, along with the EMG activity levels detected and the subsequent forces generated about the joint the muscle is attached to. Specific rocker sole designs may therefore affect muscle activity, and also alter gait patterns.

In order to evaluate the effects of muscle-tendon properties and skeletal geometry in determining moment-generating characteristics of selected muscles, a technique was developed by using Visual3D and OpenSim software. EMG data can indicate when a muscle is active or inactive and if larger groups of motor units are recruited to perform the task, but interpretation of EMG data does not determine what causes an increase muscle activity or which joint motion produced it.

OpenSim allows researchers to analyse exported dynamic motion data from Visual3d and examine musculoskeletal dynamic motions using a specially-developed model of the adult lower limb. This model was initially developed from data that quantified muscle architecture in cadavers (Arnold et al., 2010). It allows the user to export data, which is scaled by segments, length, mass, the average geometrical shape of bones and the height of the subject. This computer model can feasibly assist in understanding the biomechanical consequences of musculoskeletal dynamic changes when walking with different footwear

rocker sole profiles and influence the design of future footwear with the specific aim of treating patients with IC and the other conditions previously mentioned.

The focal aim of this research is to inform the development of rocker shoes for patients with IC. A significant percentage of claudicants are also diabetic. The starting age for vascular complications in the diabetic population is approximately 45 years of age. IC adversely changes claudicants' quality of life and makes them more sedentary which can cause medical complications. Such complications include muscle atrophy, stiff joints and stiff MTUs, decreased storage of muscle fuel, de-capillarisation in muscles, cardiovascular weakness, reduction in stroke volume performed by the heart to deliver oxygen, reduced oxygen extraction from the blood, reduced blood flow and distribution and increased blood pressure. Claudicants' main musculoskeletal symptom is the development of calf pain during ambulation due to vascular problems which makes them walk with a limp after walking a certain distance.

Exercise training has provided improvement for claudicants in these factors (Abernethy et al., 2013, Katch et al., 2011). Rocker soled shoes, which, if specifically-designed, may prove to reduce the work done by the ankle plantarflexors during ambulation, could be beneficial for claudicants by increasing their pain-free walking distance, reducing the intensity of their pain whilst claudicating, and by fighting against a sedentary lifestyle and naturally improving their cardiovascular system and therefore increasing oxygen delivery to the muscles without the need to attend supervised exercise programs. Moreover, alternative designs of footwear which increase work done by the muscles acting on the ankle joint could be used for short distances to build up calf musculature, increase capillary density and develop muscle fibres, which would result in improvement in oxygen delivery and muscle fuel storage.

Both these footwear features could replace supervised walking exercise programs, which are not always available or possible to attend for all patients. However, to achieve the optimal design to achieve this target would require extensive research. Before this could be achieved however, it would be necessary to more fully understand the muscular and biomechanical effects of different footwear features on muscle properties and walking patterns to inform the final designs. Therefore, in this thesis, one footwear feature was altered at a time in a series of tests to inform changes in parameters from identifiable shoe design alterations.

Walking speed was controlled within set limits during gait laboratory testing, and healthy young male subjects were recruited for the research to minimise any external influences and effects on the primary outcome measures. This approach is different from most previous studies because factors such as the control of walking speed, alteration of one distinct footwear feature at a time, and the ability to produce an analysis of muscle-tendon properties and force generation by novel use of OpenSim software during walking trials, would enable a direct comparison of shoe design alterations to be made.

In summation, the research contained in this thesis is therefore aimed at systematically understanding the precise effects of altering parameters associated with different footwear rocker sole profiles on lower limb kinematics and kinetics, linked to muscle biomechanics and alterations to muscle activity in the lower limbs (especially for the calf group of muscles and anterior leg muscles). It was thought important for the purposes of this thesis to primarily examine the effect of such interventions on healthy subjects' gait. This is because it would afford the opportunity to judge the results more precisely without other factors which may have an effect on the gait and muscle changes at the ankle and knee if subjects were to have varying amounts of disability. In addition, it would be necessary to perform gait laboratory testing on subjects who would be able to walk at similar speeds to negate the effects of walking speed on the comparative effects of altering the soles and heels of shoes. The intention was therefore to understand the precise effect of five different footwear design features (rocker sole apex position, rocker sole relative stiffness level, the type of heel shape, the rocker apex angle and alteration to heel height) on gastrocnemius medial head, soleus, tibialis anterior, rectus femoris and biceps femoris muscle activity and specific MTU parameters, plus temporal-spatial parameters during walking in adult healthy subjects. The results were intended to inform and make recommendations as to which footwear sole and heel unit design features would be suitable to alleviate symptoms associated with IC during rehabilitation protocols and also give indications for suitable intervention for various other pathologies.

By reducing the work done by the calf muscles, patients with IC may improve their free-pain walking distance and at the same time exercise their cardiovascular system by walking greater distances. Footwear which increases the work done by the calf muscles could conversely be used for exercising and strengthening their calf muscles as a parallel

treatment to also improve their fitness as well as improving their pain-free walking distances.

Therefore the overall hypothesis was, that by altering shoe features such as heel height, rocker apex position, addition of a curved heel, alteration to apex angle and relative rocker sole stiffness, this would produce significant alterations to lower limb muscle EMG activity, kinetics and kinematics, the type and velocity of muscle contractions in specific lower limb muscles and their MTUs, alteration to fibre and tendon length, joint rotations and temporal and spatial gait parameters.

A design of shoe which incorporates sole and heel unit features which maintains the calf muscle-tendon length close to its optimal length whilst simultaneously reducing the velocity of concentric contraction in the calf muscles may significantly offload the calf muscle (i.e. affect ankle power generation and absorption) more than by simply reducing the sagittal plane moments about ankle during stance phase of gait. It is as yet unknown how variation in externally-applied sagittal plane moments via the ground reaction force (GRF) affect lower limb MTUs when walking with adapted shoes. This may prove in the future to be of benefit to subjects with plantar fasciitis, Achilles tendonitis as well as IC – indeed any pathology which adversely affects the muscles acting on the foot and ankle. However, it is the intention of this thesis to base its analysis on the specific needs of patients with IC.

This study therefore presents data that permits the main muscles acting on the ankle to be studied by relating muscle fibre/tendon dynamics and force generation to the mechanical demands of walking in different footwear conditions.

1.2 Thesis content

Chapter 2 analyses how IC is diagnosed, its epidemiology, the risk factors involved and the clinical effects and known interventions for treating IC. It also presents a literature review regarding the existing evidence of the efficacy of treatment programmes and the known effects of footwear outsole features on specific gait parameters in claudicants such as heel raises and rocker soles.

Chapter 3 describes the biomechanics of normal adult gait. It also includes a section describing normal gait and the evidence to date regarding the effect of ageing on gait parameters in healthy adults and those with specific pathologies such as PAD and IC.

Chapter 4 comprises of a literature review of footwear outsole features such as rocker sole profiles which are used in clinical practise, their application in the treatment of various pathologies and describes the process which determined the features used during the gait analysis investigations.

Chapter 5 Describes the methodology used to capture the data and the software and hardware required to produce data required to accept or not accept the hypotheses stated; and also includes details on the research design and the methodology of the gait laboratory testing.

Chapter 6 presents the results for all the parameters tested and a subsequent analysis. The results from the gait laboratory data and the subsequent analysis are contained in this chapter with regards to the effect of the footwear feature test conditions on the primary outcome measures during ambulation.

Chapter 7 comprises of a discussion section which analyses and contrasts the results and makes recommendations regarding the potential relevance of performing future research using specific footwear outsole features for the potential benefit of claudicants and also those subjects with other relevant pathologies. In addition, recommendations are made for potential future research regarding other people with gait-limiting conditions such as Achilles tendonitis, diabetes and plantar fasciitis for whom the results of the gait analysis would indicate that they may benefit from interventions utilising rocker-soled shoes.

CHAPTER 2

2 INTERMITTENT CLAUDICATION (IC)

2.1 Chapter overview

Chapter 1 described how patients suffering from various pathologies could benefit from orthotic intervention in the form of footwear adapted with rocker soles by altering gait parameters. It was also explained that there may be other potential benefits of walking with rocker-soled shoes; in particular beneficial alteration to power absorption and generation by specific lower limb joints and alteration to muscle activity and muscle length during stance phase.

IC is a disease which causes specific alterations to muscle performance and also produces pain in the major ankle plantarflexor muscles. This chapter describes and contrasts the aetiology and symptoms associated with IC and the current treatments routinely available to claudicants. Treatment efficacy is discussed and an analysis is presented as to why new innovative treatments are needed to help alleviate the symptoms of IC and to potentially enable claudicants to attain higher fitness levels than can be achieved using conventional therapy.

2.2 Intermittent Claudication (IC)

IC is a disease caused by vascular insufficiency to the lower limbs; usually due to an occlusion in one of the proximal arteries of the leg (e.g. the superficial femoral artery, the iliac artery or the popliteal artery). IC is diagnosed by means of measuring the ankle brachial pressure index (ABPI), which is calculated by dividing the arterial blood pressure at the ankle by the reading obtained at the upper arm on the same side (Fowkes et al., 1991, McDermott et al., 1994, Norgren et al., 2007, Ramos et al., 2009, Feinglass et al., 1996). A positive diagnosis is recorded when the ratio of the two readings is 0.9 or less (Wang et al., 2005). Symptoms are most commonly experienced in the major calf muscles, and involve a cramp-like pain which leads to limping. A period of pain-free walking before patients experience calf pain is a symptom of the disease (Kruidenier et al., 2009). These symptoms disappear with rest; usually within a few minutes, after which it is possible to commence walking again. This produces a constant cycle of pain-free walking, followed by painful walking and

then enforced rest. Leg pain occurs unilaterally in 40% of patients and bilaterally in 60% of patients. They may also experience fatigue or pain in the thighs and buttocks (Dorland, 1994, Manzano et al., 2009).

IC is a manifestation of a more systemic disease known as peripheral arterial disease (PAD). Approximately 8 million American adults have PAD. When claudicants walk, the calf muscles receive insufficient oxygen which eventually leads to development of the muscle pain experienced by these patients. However, following a period of enforced rest, oxygen consumption in the calf muscle has been shown to return back to normal levels, which is why the pain disappears (Meru et al., 2006, NHS guidelines, 2006). Approximately 30-40% of patients diagnosed with PAD suffer from IC (Kupecz, 2000, Degischer et al., 2002). IC is caused by atheroma (fatty deposits) in the walls of the arteries leading to reduced blood flow to the muscles and tissues (NHS guidelines, 2006).

There are number of known risks factors, which cause the development of IC which include:

- Being over 45 years of age;
- Being a long-term smoker;
- Suffering from obesity;
- Having a family history of IC or vascular complications;
- The presence of cardiovascular disease and/or diabetes;
- Suffering from hypertension;
- Habitually following a poor diet;
- Having hypercholesterolemia.

IC is most commonly seen in older male subjects; especially if they are long term smokers. The Alzamora study demonstrated that the ratio between males and females with IC was approximately two to one (Alzamora et al., 2010). It has been reported that IC can affect 3% of people aged 45-64 and 18% - 27% of people over the age of 60 (Allaqaband et al., 2009).

It is important to help treat patients with IC, because in 25% of patients, their symptoms worsen and unfortunately approximately 5% of them will require an amputation within 5 years (Meru et al., 2006). IC has been associated with at least a three-fold increased risk of

coronary heart disease, stroke or cardiac failure when associated with diabetes (Stewart and Lamont, 2001).

Patients with IC can also have a significantly reduced quality of life (QOL) due to their calf pain, lack of physical mobility and their adverse emotional status, and it can be equated to that seen in cancer patients (Klevsgård et al., 1999). Another study demonstrated that the QOL of claudicants in all the respects investigated was significantly reduced compared to normal subjects (Pell, 1995, Breek et al., 2001). The severity of the disease, as measured by their ability to walk before having to stop, was a significant predictor of general health, pain, vitality and in quantifying physical and social parameters.

2.3 Treatment regimes

A number of treatments have been developed in an attempt to reduce the symptoms of the disease. This section describes an analysis of current and previous treatments and postulates why further non-invasive treatment methods are needed for this patient group.

2.3.1 Walking exercise therapy in the treatment of IC

Walking exercise therapy for claudicants has historically been prescribed by either attending structured supervised exercise sessions or by unsupervised self-regulated walking. Some studies have demonstrated that the best and safest treatment is a daily walking program; ideally 45-60 minutes per day (Stewart et al., 2002). It has been also previously stated that walking exercise programmes have clear benefits for many patients with IC (Mueller, 1998).

Exercise training has been shown to be an effective treatment by significantly increasing walking distance for patients with IC; especially in the ageing population (Remijnse-Tamerius et al., 1999). Different mechanisms were thought to be involved in producing this beneficial effect. These included adaptation or redistribution of the peripheral blood flow (otherwise referred to as the development of collateral circulation), inhibition of the progression of the atherosclerotic disease, changes in blood rheology, metabolic changes, changes in skeletal muscle morphology, economisation of walking, a change in pain perception and a positive effect on the cardiovascular system.

Endurance exercises have also been shown to be beneficial to oxygen uptake in older people (Fitzgerald, 1985, Østerås et al., 2005). Carter indicated in his study that short-term exercise programmes could be a valuable treatment for patients with IC (Carter et al., 1989). The study conducted by Andriessen et al. (1989) subsequently demonstrated the efficacy of an intensive six-months of exercise therapy performed three times per day by patients with IC.

Walking exercises are the most important treatment for IC, although drug therapy could beneficially be used in conjunction with it as well (Ernst et al., 1992, Hiatt, 2001). NHS guidelines and Ekroth et al. (1978) both stated that changes in lifestyle such as discontinuation of smoking, weight loss and daily exercise are useful to prevent and treat IC (NHS guidelines, 2006). Patterson et al. (1997) in his paper reviewed and confirmed the evidence regarding the efficacy of exercise therapy for patients with IC. Patterson noted a 337% increase in free-pain walking ability, and also illustrated the importance of supervised exercise regimes.

However, Keltikangas-Jarvinen et al. (1987), stated that personality factors such as paranoid tendencies in patients with IC should be controlled in order to optimise treatment programs. Another cautionary statement was produced by Ernst and Fialka (1993), who demonstrated that long-term continuation of exercise regimes was important, as gains in walking distance could be lost if this was not done.

A meta-analysis by Gardner and Poehlman (1995), indicated that the mean walking distance until the onset of claudication pain may be increased by an average of 179% (from 125.9 ± 57.3 m to 351.2 ± 188.7 m) following exercise programmes that include walking. The exercise level attainable by individual patients was identified as being a measure of the severity of this disorder. Subsequent publications by Gardner et al. (2000) and Gardner et al. (2001c) demonstrated an improvement in ambulatory function in patients with IC following an exercise programme. Their findings were also confirmed by Stewart et al. (2001). A long term supervised exercises (12 months) improved on average by 171% in pain free walking time and 120% in maximal walking time in a study by Crowther et al. (2008).

A previous systematic review published by Brandsma et al. (1998) investigating the effect of structured exercise programs indicated beyond doubt that walking exercises improved pain-free walking distances in patients with IC. There was, however, a large range of percentage improvements measured by the studies finally selected for review, ranging from 28% to

210%, with a mean of 105% and STD 55.8 (Larsen and Lassen, 1966, Holm et al., 1975, Ernst and Matrai, 1987, Kieseewetter et al., 1987, Lundgren et al., 1989, Creasy et al., 1990, Hiatt et al., 1990b, Mannarino et al., 1991, Hiatt et al., 1994, Regensteiner et al., 1996). It was also demonstrated that supervised exercise regimes involving only walking were more beneficial than those involving walking with other forms of exercise. Exercise therapy program for patients with IC was also recommended by Binnie et al. (1999) and Wullink et al. (2001). Hunt et al. (1999), presented a regime of supervised exercise therapy for 42 claudicants which provided successful functional outcomes. Leng et al. (2000) undertook a Cochrane systematic review, and concluded that exercise therapy should be the treatment of choice for those patients with IC who were appropriately fit enough. Stewart and Lamont recommended in their editorial that exercise therapy should be widely available to IC patients in the UK (Stewart and Lamont, 2007).

2.3.1.1 Supervised versus non-supervised walking exercise therapy

The gold standard treatment for claudicants is considered to be the use of supervised exercise therapy (SET), and this is well documented in the literature. Supervised walking exercise improves the general cardio-vascular system which leads to an increased oxygen supply to the lower limbs and improvement in the maximum pain-free walking distances by claudicants. A number of studies have suggested that a significant improvement may be achieved in the pain-free walking distance using this intervention (Table 2.1). However, there is also some evidence to suggest that long term supervised walking training exercises with a duration of up to twelve months do not demonstrate more significant improvement when compared to shorter-termed treatments.

Nevertheless, exercise programmes have been shown to be of significant benefit compared to usual care protocols in improving the walking time and distance achieved by subjects with IC (Watson et al., 2008). Fokkenrood et al. (2013) recently published a review which compared the effect of SET to that produced when following non-supervised walking therapy protocols. SET generally consisted of three exercise sessions per week, and their results suggested that SET had a statistically significant benefit with regards to treadmill walking distance (maximal and pain-free) compared with non-supervised programmes. However, the clinical relevance of this has not been demonstrated definitively. Additional

studies were therefore recommended which would focus on QOL or other disease-specific functional outcomes. They recommended that professionals in the vascular field should make SET available for all patients with IC.

Parmenter et al. (2013), also recently published a systematic review of the effect of exercise and performance-based treatment on the walking ability of claudicants as evidenced in the literature. In total 924 participants (71 % male) were studied; with a mean ankle brachial index of 0.66 ± 0.06 . Aerobic capacity was improved by $8.3 \% \pm 8.7 \%$ on average by exercise therapy. Muscle strength was measured in only five trials, improving by $42 \% \pm 74 \%$. There was a strong significant relationship between change in ankle plantarflexor muscle strength and change in pain-free walking times ($r = 0.99$; $p = 0.001$) and absolute claudication time ($r = 0.75$; $p = 0.05$) when using a treadmill to measure this parameter. The six-minute walking test distance was measured in only 14 % of trials.

Table 2.1: Examples of exercise training rehabilitation programmes for claudicants.

Source	Method	Walking test	Increase in pain-free walking distance	Increase in maximum walking distance
(Zwierska et al., 2005)	Group 1: Leg training (n=37) plus cycling. Group 2: Arm training (n=34) plus arm cranking, Group 3: Control (n=33) groups 1 and 2 were trained for 24 weeks using supervised training for 40 min/twice per week.	A shuttle test	Group 1: 93% Group 2: 122% Group 3: Not significant (NS)	Group 1: 50% Group 2: 47% Group 3: NS
(Gardner et al., 2001b)	Group 1: n=28, treadmill supervised walking exercise 3 times per week for 6 months. Group 2: n=24, the control group.	A treadmill test at a speed of 3.2 km per hour and increased by 2% every 2 minutes	Group 1: 134% Group 2: 25%	Group 1: 77% Group 2: 12%
(Patterson et al., 1997)	29 men, 26 women with IC. Group 1: 12 weeks supervised exercise using one hour of treadmill walking plus aerobic exercise three times weekly. Group 2: unsupervised walking 3 times weekly plus lectures	A treadmill test (1mph at a 5% incline); increasing at 5- minute intervals to 2.5mph and a 10% incline.	Group 1: 337% Group 2: 131% unsupervised maintained the improvement at 6 months	Group 1: 207% supervised, Group 2: 70% unsupervised; maintained for six months.

(Jones et al., 1996)	N=12 training for 12 weeks Group 1: (n=6) The Stair-master Group 2: (n=6) a treadmill	Treadmill testing at a speed of 3.2 km per hour and increased by 3.5% every 3 minutes	Group 1: Increased by 35.5s Group 2: Increased by 117.7s	Group 1: NS Group 2: increased by 171.7 s
(Hiatt et al., 1990a)	Group 1: (n=10), 3 months of supervised training, 1 hour/ 3 times per week walking on a treadmill at a speed of 2-2.5mph, with a 0-14% incline Group 2: (n=9)- a control group	Treadmill test 0-14% incline	Group 1: 165%	Group 1: 123%

2.3.2 Progressive resistance training (PRT)

The utilisation of walking allied to progressive resistance training (PRT) is a recent development which has also been shown to significantly improve claudication distances, (the point at which calf pain commences), and maximum walking distances (before having to stop) by means of undertaking a six minute walking test. The benefits of PRT in conjunction with upper body exercise appear promising (Parmenter et al., 2011), but again, more evidence is needed. A further review by Parmenter et al. (2013) also suggested that there could be a significant relationship between increased ankle plantarflexor muscle strength and treadmill walking ability following a PRT regime plus regular exercise by claudicants. Modes of aerobic exercise other than walking appeared to be equally beneficial for claudicants. However, the longer term benefit of this type of intervention has not been proven, and indeed the appetite for claudicants to undergo repeated supervised exercise programmes is doubtful; but a recent study demonstrated some improvement in claudication distance using a home-based exercise programme (McDermott et al., 2013).

Claudicants are now routinely screened and advised in the community setting as well as in hospital vascular units for lifestyle management factors like discontinuation of smoking, the need to take regular walking exercise, and control of other factors which may affect them such as diabetes, hypertension and blood cholesterol levels. In addition, various drugs have been developed to help reduce the symptoms associated with IC.

2.4 Drug therapy

Drugs such as trental, cilostazol, ramipril naftidrofuryl, pentoxifylline, inositol, nicotinate and cennarizine have been developed to potentially improve blood flow through narrowed vascular vessels and therefore increase oxygen supply to the calf muscles. Aspirin, (75mg daily) is also routinely prescribed as an anticoagulant for claudicants due to their general vascular disease. After 6 months of drug therapy using ramipril, Ahimastos et al. in their study demonstrated a 75-second (60-89 seconds) increase in mean pain-free walking time ($P < 0.001$) and a 255-second (215-295 seconds) increase in maximum walking time ($P < 0.001$) compared to a placebo (Ahimastos et al., 2013). Another study demonstrated that ramipril was also associated with a 75-second increase in mean pain-free and a 255-second increase in maximum walking time following a 6 month RCT (Kurklinsky and Levy, 2013).

The efficacy of pentoxifylline in reducing the symptoms of IC was investigated in a Cochrane review by Salhiyyah et al. (2012). There was very large variability in the reported findings between the 17 individual studies analysed even though there was no statistically significant difference in ankle brachial pressure index (ABPI) between the pentoxifylline and placebo groups. The authors therefore stated that the overall benefit of pentoxifylline for patients with IC remains uncertain. However, it was stated that drugs such as naftidrofuryl oxalate and cilostazol both appear to be effective treatments for IC patients, with the reservation that naftidrofuryl oxalate is the only treatment that is likely to be considered cost-effective, and that the long-term effectiveness of drug therapy for those analysed in the study is uncertain (Squires et al., 2011).

The evidence therefore suggests that the use of drugs in the treatment of claudicants is still uncertain when analysing their effect on increasing pain-free walking distances and absolute maximum walking distances, and further trials are warranted to identify their efficacy in improving specific gait parameters.

2.5 Discussion

There is no doubt that walking exercise, either supervised or un-supervised, is effective in improving the symptoms associated with IC. However, the results demonstrated have varied significantly, and anecdotal evidence suggests that claudicants do improve to a certain level,

at which the improvement plateaus and no further improvement is possible just by using daily exercise. New interventions have attempted to obviate this by also introducing concurrent therapy such as progressive resistance training to increase calf muscle strength and improve walking distances. However, this infers that the calf muscle will need to be constantly exercised to maintain its improved strength in order to maintain the improvement in symptoms in conjunction with regular exercise. It is as yet unknown whether a strengthened calf muscle in claudicants can be maintained at that level purely by means of walking exercise therapy, or whether special exercise regimes will be needed for much longer periods. The ramifications of this and possible alternative treatments such as the use of orthotic intervention are discussed in chapter 3. However, there is some evidence in the literature which demonstrates that orthotic intervention may provide some improvement in walking distances which could be achieved by claudicants.

2.6 Orthotic intervention

2.6.1 Rocker-soled shoes

The first investigation performed specifically to help increase pain free walking distances by claudicants was performed by Richardson, who investigated the effect of walking with angled rocker soled footwear in claudicants (n=15) and demonstrated improvement in walking distance (Richardson et al., 1989). However, the rocker was not accurately described. Richardson subsequently studied 21 claudicants and again compared the efficacy of angled rocker soled shoes to that demonstrated when walking with high street footwear (Richardson, 1991). The rocker sole used had a 15-degree angle with an apex positioned 6-7 cm proximal to metatarsal heads. For a typical adult male size 9 shoe, this would place the rocker sole apex position at approximately 50% of shoe length (authors calculation). The total walking distance, known as either the absolute or maximum walking distance, as well as the distance covered before the onset of pain (referred to as “bothered” distance or “pain free distance”), were both significantly improved for patients with IC using the traditional rocker-soled shoes [i.e. rocker sole profiles with an angled apex rather than a curved apex (Tyrrell and Carter, 2008)].

However, the study found there was a substantial variability in the patients’ responses to the rocker-soled shoes. This variability was explained by differences in walking biomechanics

amongst the patients and was also found in a study by (Honet et al., 1968). It was found that because the rocker fulcrum was positioned proximal to the metatarsal heads, the shoes were effective in facilitating heel-off rather than toe-off during gait. Therefore, the authors hypothesised that patients who pushed off more vigorously in the late-stance phase of gait during the walking trials may not have significantly decreased the work of their calf musculature. The results indicated that further work needed to be done to optimise shoe design for this patient group and indicated that the fulcrum needed to be re-positioned in future studies. However, in an un-published report, Bell and MacBain (1998) using an identical rocker design as Richardson demonstrated a significant decrease in the “bothered distance” walked by claudicants. There is therefore variance in the literature and therefore this needs further investigation.

Hutchins et al. (2012) performed a pilot study with a group of volunteer claudicants (n=8) using a shoe adapted with a rocker sole profile which comprised of three distinct circular curves in its design. This was designed to reduce the moments acting around the ankle, hip and knee joints during stance phase of gait by positioning the centres of the curves comprising the profile of the rocker sole at the sagittal plane anatomical joint centres of the ankle, hip and knee during specific parts of stance phase. This was done to encourage the ground reaction force (GRF) to pass through these joint centres and therefore to reduce moments acting on them. The study demonstrated that a significant increase in pain-free walking distance (mean 34.81m) and a significant mean percentage reduction in the intensity of calf pain once claudicating (57%) could be achieved by the claudicants in the study.

2.6.2 Raised heels

A study by Learmonth and Slessor (1952) recommended the use of raised heels for patients with PAD in the lower limbs. However, this was contradicted in a study by Chavatzas and Jamieson (1974), who added a 4cm heel raise to place the ankle in an equinus position to theoretically also reduce the amount of sagittal plane range of motion (ROM) and to unload the triceps surae muscle group. The results showed no significant improvement in pain-free walking distance in those patients tested. They also found that ankle systolic blood pressures before and after walking were not significantly affected. The onset of pain in 27 of 30

subjects tested did not alter when walking with the footwear with raised heels. This orthotic intervention was therefore not recommended by the authors. However, the reason for the lack of improvement in pain free walking distance using this type of intervention is as yet largely unknown.

2.6.3 Specifically-designed rocker profiles

The results demonstrated in the literature when utilising either rocker soled shoes or heel raises have therefore produced conflicting results. However, one study, which utilised a specifically-designed three-curve rocker sole modification has demonstrated, that in claudicants, pain-free walking distances can be significantly increased and the intensity of the calf pain experienced significantly reduced (Hutchins et al., 2012). It was thought that by reducing the power absorption and generation required to ambulate by the ankle plantarflexors in addition to reduced externally applied moments, improvements in claudication distance were achieved.

The idea of altering ankle power and absorption may be developed and expanded so that footwear could indeed be developed to not only offload the calf muscles but also alternatively make them work harder to act in the same way as PRT. Exercise programs used in parallel with footwear specifically designed to stretch and increase calf muscle activity during walking may improve not only the cardio-vascular system, but build muscle fibres which may stimulate arteries to improve blood circulation and oxygen supply, and stimulate arteries to develop new channels of blood circulation around the narrowed sites (the so-called collateral circulation). Theoretically, such a training approach could be beneficial for patients with IC. If this could be alternated with footwear developed to offload the calf muscles to enable claudicants to walk further before experiencing painful symptoms, and therefore get fitter anyway, this could prove to be a potentially novel treatment for claudicants.

The studies assessing footwear adaptations have to date still given little evidence as to why these interventions altered pain-free walking distances in claudicants because of lack of available data regarding muscle biomechanics, and in some cases, limited information about gait alterations.

A training program which focused on quadriceps femoris muscle training using a bicycle for normal subjects during an 8 week programme has demonstrated that training specific muscle groups is a powerful tool to produce an increase in capillary density by up to 20% and also increase muscle fibres by up to 20% which results in a 16% increase in oxygen supply to the muscle (Andersen and Henriksson, 1977). Capillaries serve a variety functions, such as blood supply to the muscles and tissues and an exchange between them, maintaining normal blood pressure and circulation, and serving as blood reservoir (Alter, 2004).

Footwear designs which can be shown to increase calf muscle activity and stretch such MTUs may feasibly reduce any restriction of motion at the ankle and increase capillary growth. This may be achieved by using a so-called negative rocker sole profile, (where the heel is at a lower level than the metatarsal head area) which has been demonstrated to increase the maximum range of the ankle joint during walking (Li and Hong, 2007). The negative heel may place ankle into more dorsiflexion position and therefore stretch calf muscle. A study of stretching digitorum longus muscles in rats for 2 weeks demonstrated that the capillary to fibre ratio was increased by 33% and 60%, which indicates that stretching muscle may stimulate capillary growth (Egginton et al., 1998).

This discussion therefore suggests that a new treatment approach for patients with IC may prove to be beneficial for this patient group. For instance, patients with IC may increase their pain-free and maximum walking distance (MWD) by wearing footwear which reduces calf muscle activity, and therefore their cardio-vascular system could be improved during normal walking. This may be utilised to replace supervised walking exercises and motivate claudicants to walk. Rocker soles which increase calf muscle activity could also be beneficial for more short-term walking training programs. However, before this can be proven, it will first be necessary to more succinctly understand the biomechanical and muscular consequences on human gait of walking with footwear adapted with different footwear features.

The pilot claudicant walking trial by Hutchins et al. (2007) demonstrated that subjects with IC can increased their maximum pain-free walking distance when wearing three-curved rocker shoes when compared to a standard shoe pitched with a 2.5 cm heel height. It can be

seen that the range of percentage increase in pain-free walking distance increased by average 51.8% compared to a control shoe (table 2-2).

The increase in maximum pain-free walking distance may have been due to reduced calf muscle activity and therefore a reduced oxygen demand required by the calf muscles. It may also have been due to the fact that the rocker profile placed the ankle into a relatively plantarflexed position, and this may have increased the ankle plantarflexor muscle moment arm via the Achilles tendon. However, to date this has not been investigated.

Table 2.2: Percentage increase in pain-free walking distance when wearing a three-curve rocker-soled shoe test condition.

Patient Number	Claudication Distance Increase (%)
1	40.8
2	18.9
3	75.1
4	36.32
5	116.9
6	28.8
7	92.1
8	5.8
Average increase	51.8

2.6.4 Chapter summary

The evidence therefore suggests that walking therapy using various protocols is undoubtedly effective in helping claudicants attain an increased “bothered” distance before experiencing calf pain, and also an increased maximum walking distance before having to stop due to the calf pain. However, limitations as to how much improvement may be expected have been noted and eventual outcomes still rely on the cooperation of the patient and their willingness to undergo treatment such as attendance at exercise training sessions. The use of drug therapy has shown some encouragement that it may improve their overall quality of life, but no evidence was found indicating that drugs can significantly increase their claudication distance. More evidence regarding the efficacy of drug treatment on improving the symptomatic gait associated with IC is needed and also regarding its cost effectiveness.

The use of orthotic intervention, whilst also not as yet proven, has the potential to offer an alternative adjunct therapeutic avenue for claudicants. This may take the form of specifically- adapted footwear to give the patient the choice of wearing shoes which offer a calf muscle training function to build up muscle bulk, aligned with alternative footwear to offload the ankle plantarflexors and facilitate increased pain free walking distances. However, research is needed to more fully understand which footwear outsole features increase ankle plantarflexor activity and therefore the power needed to walk and which ones reduce power generation at the ankle during propulsion.

To achieve these aims it would be necessary to more fully understand the effect of, for instance, increasing the pitch of footwear by increasing the heel height whilst still incorporating a rocker sole, or the effect of reducing heel height (to form a so-called negative heel) on specific gait parameters. The effect of various rocker sole apex positions and apex angles also needs to be investigated along with altering outsole relative stiffness of footwear in order to more fully understand which specific features demonstrate the ability to produce alterations to muscle power generation and absorption in the lower limbs, their ranges of motion, and also their effect on specific gait parameters. In this way, claudicants may have access to an alternative treatment to potentially improve their symptoms and also their QOL.

CHAPTER 3

3 ABLE-BODIED ADULT GAIT AND CLAUDICANT PATHOLOGICAL GAIT

3.1 Phases of able-bodied adult gait

The gait of able-bodied adults consist of two main phases; stance and swing. Stance phase normally comprises of 62% of the gait cycle with swing phase comprising of 38% (Winter, 1987). For the purpose of this thesis, these phases have been segmented into distinct portions as described by (Perry, 1992). These are:

- Heel strike (HS), otherwise known as initial contact (ICt);
- Loading Response (LR);
- Mid stance (MSt);
- Terminal stance (TSt);
- Pre Swing (PSw).

Swing phase may be described using the following segments:

- Initial Swing (ISw);
- Mid swing (MSw);
- Terminal Swing (TSw).

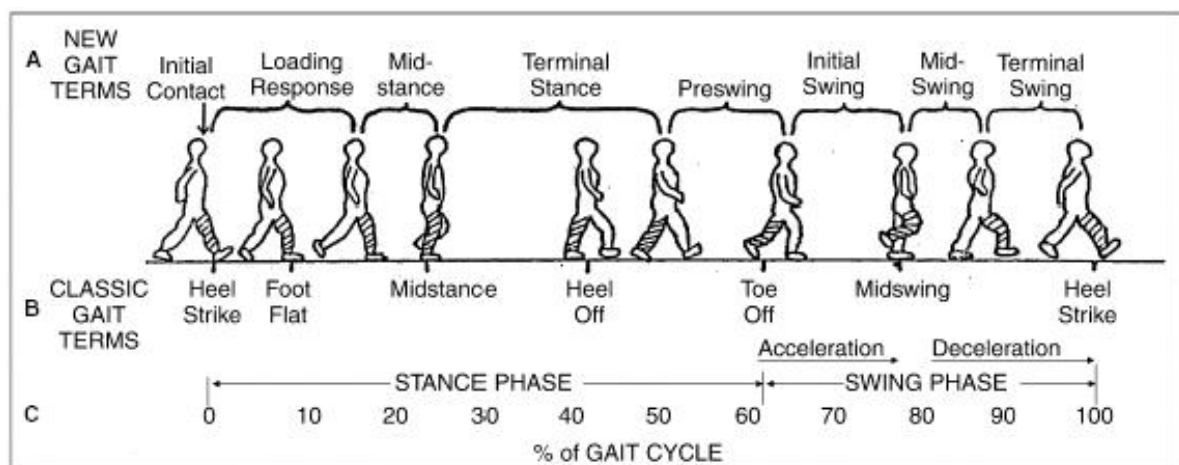


Figure 3.1: The determinants of gait (Cuccurullo, 2004).

Perry also described specific “rockers” of gait during stance phase. For the purposes of this thesis, these will be defined as the first rocker of gait, second rocker of gait and third rocker of gait, to distinguish them from rocker sole nomenclature. The first rocker of gait describes

ankle plantarflexion following heel strike and during loading response. The second rocker phase is designed to describe advancement of the shank over a stationary foot during mid-stance. The third rocker phase denotes the period during which heel rise occurs and MTP joint dorsiflexion occurs. However, a fourth rocker of gait has recently been postulated which describes a virtually locked ankle but dorsiflexion of the metatarsal heads during propulsion prior to ankle plantarflexion; which would become the third of four rocker phases during stance phase of gait (Ayyappa, 1997, Owen, 2010). However, this has not been utilised as a determinant of gait in this thesis.

3.2 Muscles of lower limb

The main muscles of interest for this thesis in the lower limb are the gastrocnemius medial head, soleus, tibialis anterior, biceps femoris and semitendinosus muscles. Gastrocnemius and soleus are the main plantarflexors of the ankle, and gastrocnemius is also influenced by knee position due to its origin being proximal to the tibial plateau. Soleus is thought to be more of a postural muscle than gastrocnemius. Symptoms of IC mainly occur in the gastrocnemius muscle due to its high oxygen demand during ambulation. Symptoms may also occur in the thigh area – if the vascular occlusion is cited proximally.

The primary reason for orthotic intervention when applied to alleviate the symptoms of IC would be to influence a reduction in the work done by the gastrocnemius and soleus muscles during stance phase, and also to reduce the intensity of their activity. However, it is unknown whether this would apply shunting of activity and power absorption or generation to the antagonist muscles (e.g. tibialis anterior). Another advantage would be the ability to reduce the power generation requirement for more proximal muscles such as the hip flexors and extensors whilst still simultaneously offloading the ankle plantarflexors as these are weak in claudicants (please refer to section 3.4).

In addition, as an alternative adjunct therapy as stated in chapter 2, regular use of a different design of rocker-soled shoes may be able to offer a training effect by increasing these parameters in place of undergoing supervised exercise therapy. In this case it could be theoretically possible to design footwear which would entice the ankle plantarflexors to work harder during the propulsive phase of gait as well as offering an alternative design of rocker sole profile which reduced their power generation requirement. This would be in

order to offer alternating therapy by building up muscle bulk on one hand and also offloading the muscle tissues during different treatment sessions to allow people with IC to become fitter by potentially reducing their painful symptoms.

3.3 The role of the ankle plantarflexor muscles

There are a number of theories pertinent to this thesis regarding the role of the ankle plantarflexors during gait. The gastrocnemius and soleus both act as the main plantarflexors of the ankle. However, the functional role of the ankle plantarflexors has been the subject of debate in the literature (Winter and Scott, 1991, Mueller et al., 1995, Nadeau et al., 1999, Winter, 2009). Three fundamental theories regarding their role during late stance have been postulated. The controlled roll-off theory (Sutherland et al., 1980, Perry, 1992) postulates that the ankle plantarflexor muscles decelerate tibial rotation and prevent knee flexion during stance by causing the body to rotate forward due to momentum and inertia. The active push-off theory (Winter, 1983) postulates that the energy generated by the ankle plantarflexors is applied to the trunk to provide active support and forward progression. Another theory supports the hypothesis that the ankle plantarflexors accelerate the legs into swing; so facilitating forward progression during late swing (Meinders et al., 1998, Hof et al., 1992).

Neptune et al. (2001) utilised SIMM software using a modelling technique in an attempt to provide definitive evidence as to which theory was most valid. The results indicated that most of the energy delivered by the soleus muscle is delivered to the trunk whilst that of the gastrocnemius is delivered to the leg for swing initiation. This would therefore suggest that a combination of the theories would most suit human locomotion. However, both soleus and gastrocnemius have been quoted as providing active push-off for support and forward progression and in initiating swing (Hof et al., 1992, Meinders et al., 1998).

The ankle plantarflexors therefore provide crucial power generation and absorption in order to not only propel the body forwards but also to control segmental rotations and enhance posture and support. People who suffer from the symptoms of IC are generally aged over 50 years of age, and the effects of ageing contribute to their reduction in walking ability. The following section analyses the evidence to date regarding the effect of ageing on gait plus

the addition burden of how gait is affected in those patients suffering from IC as a result of suffering from PAD.

3.4 The effect of IC on gait parameters and muscle strength in older people - a review of the literature regarding its effect and possible treatment regimes

For the purposes of this thesis, ABPI values linked to subjects with PAD will be denoted as PAD-ABPI values, and subjects who have IC due to PAD will be denoted as suffering from PAD-IC.

3.4.1 The effect of PAD severity and ABPI values on gait parameters and ambulatory function.

ABPI values have been quoted as being unreliable when attempting to correlate their value with alteration to walking parameters in PAD – IC subjects during ambulation (Izquierdo-Porrera et al., 2005, Chen et al., 2008). This is thought to be due to the view that ABPI values cannot reflect the effects and complexity of the effect of PAD on gait parameters (McKenna et al., 1991, Green, 2002). However, lower resting ABPI values have recently been significantly correlated with reduced bilateral hip extensor strength in claudicants [$r=0.54$ $p=0.007$, Parmenter et al. (2013)], which also potentially adversely affects claudicant walking distances. A study by Hutchins et al. (2012), when investigating the effect on the pain-free walking distances of claudicants using specifically-developed footwear, showed no correlation between subject ABPI values and increases in pain-free walking distances when walking with the footwear. The value of ABPI readings has therefore not been conclusively established when predicting severity of gait anomalies in subjects with PAD-IC. A Cochrane review has also demonstrated that enrolment by claudicants in exercise regimes does not affect PAD-ABPI readings following completion of the programme even though exercise tolerance is improved (Watson et al., 2008).

3.4.2 The effect of increasing age and PAD

Ageing also changes muscle functions and muscle properties. The most noticeable changes associated with aging are progressive muscle atrophy, a decrease in the extent of nerve tissue, a decrease in muscle length and alteration to collagen fibres (Gutmann, 1977,

Gajdosik, November 1997, Alter, 2004). Various authors have shown that older adults demonstrate altered gait patterns, particularly at the hip and ankle joints (Kerrigan et al., 1998, Graf et al., 2005). Older people have reduced hip extensor moments and reduced ankle plantarflexor moments compared to young adult subjects (Kerrigan et al., 1998, Riley et al., 2001, Kerrigan et al., 2001). However, the existence of PAD compounds these problems, as subjects with PAD use shorter swing times and longer stance times compared to age-matched controls (McCully et al., 1999).

3.4.3 The effects of a PAD-IC

3.4.3.1 The effect of PAD-IC on muscle pathology

PAD can adversely affect skeletal muscle strength. Further weakening of lower limb skeletal muscles occurs in claudicants due to the development of muscle metabolic myopathy (Brass and Hiatt, 2000), which is in turn due to oxidative damage to skeletal muscle structures and components (Pipinos et al., 2006). An axonal polyneuropathy also occurs (Weber and Ziegler, 2002). An abnormal ultra-structure of mitochondria in muscle has been demonstrated (Marbini et al., 1986), which involves abnormal mitochondrial respiration and adenosine triphosphate (ATP) production (Kemp, 2004, Pipinos et al., 2006), plus axonal nerve loss (Koopman et al., 1996, Weber and Ziegler, 2002). The overall effect can produce a reduction in muscle power and control especially during the propulsive phase of gait in the lower limbs. This means that subjects with IC may be responsive to orthotic interventions, which act as a surrogate to reduce the muscle power needed to ambulate (such as reducing the ankle plantarflexion power needed during propulsion).

3.4.3.2 The effect of PAD-IC on gait parameters

When older subjects develop PAD - IC, a further deterioration in gait parameters occurs compared to matched control groups. The onset of IC shortens step length and slows walking velocity still further in older people (McCully et al., 1999). Whilst the type of control group has varied within papers, (age-matched controls may walk with different velocities) common conclusions have been noted. These include development of slower walking speeds, shorter step lengths (Scherer et al., 1998, Gardner et al., 2001a, McDermott et al., 2001), reduced calf muscle ability (Mockford et al., 2010, Scott-Pandorf et al., 2007,

Crowther et al., 2009, Celis et al., 2009, Ayzin Rosoky et al., 2000) as well as decreased hip extension (Crowther et al., 2007). These gait adaptations are present even in the absence of pain in subjects with PAD, but worsen with the cramp-like calf pain associated with IC (Mockford et al., 2010, Scott-Pandorf et al., 2007).

Patients with PAD display gait patterns where the ankle takes longer to reach maximum dorsiflexion during TSt - PSw compared to controls. The ankle is also unable to generate the same amount of power as previously needed during push-off as the prolonged time to reach maximum ankle dorsiflexion means that the time available for the ankle to plantarflex for propulsion is limited (McDermott et al. 2001). The typical trace of GRFs (the Pedotti diagram) shows a flattened trace between the typical two peaks and also a reduction in peak values; showing that braking and propulsion phases of gait are not only so distinctly defined but also are less pronounced. Peak ankle plantarflexor moments and powers are reduced in subjects with PAD, and linked to reduced ground reaction force (GRF) values, this demonstrates an inability of PAD subjects to propel themselves effectively. Significant gait impairment results – even when the disease is unilateral (Celis et al., 2009, Koutakis et al., 2010). In comparison with controls, patients with PAD-IC, even whilst walking pain-free before claudicating, demonstrate a significant decrease in average maximum hip flexion (3.8 degrees) and a significantly mean increase in peak ankle plantar flexion (1.2 degrees) during early stance, plus a significantly increased peak ankle dorsiflexion (2.0 degrees) during late stance (Chen et al. 2008). In summary, PAD-IC subjects exhibit the following gait anomalies compared to controls:

- They walk slower;
- They have decreased cadence;
- They have increased stance phase durations as a percentage of gait cycle;
- They also have shorter step lengths and narrower step widths;
- They have reduced maximum hip flexion;
- They have increased maximum ankle plantarflexion during early stance;
- They have increased ankle dorsiflexion during late stance phase;
- They therefore have increased sagittal plane ankle ROM during stance phase;
- They have reduced peak knee power absorption during loading response;

- They have reduced peak hip power absorption during mid stance;
- They have significantly reduced peak power generation at the ankle during late stance and consequently a reduced energy output;
- They have reduced hip extension power which could also lead to weaker propulsion and reduced hip flexion by the swing leg;
- They have reduced peak power absorption at the knee during late stance. However, peak joint moments are not statistically different (Wurdeman et al. 2012);
- They take longer to dorsiflex the ankle during late stance and have a shorter time frame during which they can generate ankle plantarflexion power for propulsion (McDermott et al. 2001);
- The reduced peak knee power absorption in early stance is most likely caused by the increased ankle plantarflexion found in subjects with PAD due to a relatively reclined shank;
- The reduced hip power absorption during mid stance (which is an eccentric contraction of the hip extensors to control forward motion of the trunk) signifies weak hip musculature.

Decreased ankle power generation and decreased power absorption at the knee during push-off have been demonstrated by (Wurdeman et al., 2012, Scott-Pandorf et al., 2007). This has been linked to PAD subjects having weak hip extensors and weak ankle plantarflexors. Wurdeman et al. (2012), demonstrated that PAD patients have reduced peak hip power absorption in midstance ($p=0.017$), reduced peak knee power absorption in early and late stance ($p=0.037$ and $p=0.020$ respectively), and reduced peak ankle power generation in late stance ($p=0.021$) when compared to subjects with comparable age and self-selected walking velocity. However, peak moments were not statistically altered, and indeed may not occur at the same point in the gait cycle as peak powers (as power is calculated from moments and angular velocities). Reduced knee power absorption at loading response was thought to correlate with the increased plantarflexion at the ankle; meaning shank control did not demand as much power from the knee extensors during that period.

The decreased ankle plantarflexion power generation during late stance noted by Wurdeman et al. (2012) agreed with the findings of Scott-Pandof et al (2007) and Koutakis et al. (2010), as well as those from Chen et al. 2008 and Celis et al. (2009). However, Wurdeman et al. (2012) demonstrated this phenomenon for the first time when matching PAD subjects and controls who ambulated with similar walking velocities. This is important, since it is well known that reduced walking velocity can reduce joint powers. It was therefore confirmed that subjects with PAD- IC exhibit reduced maximal power generation at the ankle compared to accurately matched control subjects which would lead to increased metabolic cost. However, the group recommended that further research was needed to demonstrate whether peak power deficits occur as a result of reduced joint moments or angular velocities.

This led to the conclusion that there was a resultant weakness in the hip and calf muscles in subjects with PAD-IC even when not claudicating. This confirmed the hypothesis proposed by Chen et al 2008, who demonstrated that gait was altered during pain-free walking by claudicants compared to a control group, which was significantly worsened whilst claudicating. They described typical claudicant gait as being “sluggish and tired” due to the fact that the foot appeared to be in contact with the ground for a larger percentage of the gait cycle because of weak ankle plantarflexor muscles and weak propulsive muscles at the hip (the gluteal muscles). This study also confirmed previous work by Scott-Pandorf et al. (2007) and Scott-Okafor et al. (2001), who stated that the propulsion muscles of the leg were weaker than controls with reduced ankle plantarflexion strength in claudicants.

3.4.4 The effect of exercise, drug therapy on claudicant gait parameters

It is not well documented as to how exercise training can alter gait parameters in claudicants. King et al. (2012) demonstrated that there were no statistically significant alterations to any gait parameters (temporal-spatial parameters plus kinetics and kinematics) for a group of 12 claudicants following a three month supervised exercise programme, and postulated that longer exercise programmes (longer than 3 months) plus variations in intensity of training may improve gait parameters in these subjects.

With regards to drug therapy, a study by Yentes et al. (2012) found no significant improvements after 12 weeks of treatment with either cilostazol or pentoxifylline on the gait biomechanics of claudicants once the pain in the calf was felt. Huisinga et al. (2010), previously showed the same results for claudicants whilst being pain-free. This type of intervention also therefore appears to have limited potential in affecting the gait of claudicants in a positive way.

The evidence therefore suggests that although exercise regimes of various designs produce an increase in pain-free walking distance and absolute walking distance, they do not in fact alter gait parameters whilst doing so. This means that walking patterns are not altered and improvements in more severely affected individuals who, due to generalised vascular disease including PAD are unable to respond to exercise treatment with regards to altering their gait to more typical of that demonstrated by age-matched controls, are limited. Whether the extended use of PRT is useful in improving gait parameters is as yet unknown. An alternative solution is therefore required, and gives relevance to the need for methods other than drug or exercise therapy to provide alternative treatment solutions for claudicants. One such intervention could be via the use of footwear adaptations such as rocker soles which may have the ability to simultaneously alter gait parameters whilst improving claudication distances.

3.4.5 Overall analysis regarding gait parameters associated with PAD-IC

As the primary contributor to push-off, the biomechanical abnormality measured at the ankle joint should be the main target of clinical attempts at restoration of gait, and provides a clear indicator for measuring interventions directed at PAD-IC patients. Alteration to ankle plantarflexor function or offloading of the ankle plantarflexors using a rocker sole profile during stance phase could result in improved closed chain kinetics throughout the entire stance limb if it is proven to reduce the calf pain associated with IC, which may also alleviate deficits occurring at more proximal joints. The increase in ankle dorsiflexion during late stance exhibited by claudicants should be reduced by influencing a relatively plantarflexed position to be achieved during the propulsive phase of gait via implementation of a surrogate motion which may be applied via a rocker-soled shoe. This would not only provide

a potentially less dorsiflexed ankle position during TSt, but also theoretically unload the ankle plantarflexors by placing the calf muscles in an advantageous position.

An induced reduction in sagittal plane hip, knee and ankle joint power absorption and generation required for ambulation would theoretically reduce the need for the hip extensors and ankle plantarflexors to generate so much force to provide forward propulsion by claudicants. This may possibly be achieved using rocker sole profiles by positioning the joints in a more advantageous rotational position and in reducing their angular velocity of rotation in order to increase the respective muscle –joint moment arm at these joints which would therefore make propulsion and absorption more efficient.

The following sections detail the current knowledge regarding the effect of rocker soles on joint rotations and also their effects on muscle power generation and absorption.

3.5 The effect of walking with shoes adapted with rocker sole profiles

3.5.1 Reduction of plantar foot pressures

Shoes adapted with rocker sole profiles have historically primarily been utilised to reduce foot plantar pressures for people with pathologies such as diabetic peripheral neuropathy and rheumatoid arthritis; with the rocker soles being either tradition (angled) in design or shaped using a curved surface (Bauman et al., 1963, Milgram, 1964, Grundy et al., 1975, Coleman, 1985, Geary and Klenerman, 1987, Nawoczenski et al., 1988, Schaff and Cavanagh, 1990, Janisse, 1995, Stacpoole-Shea et al., 1999).

To achieve forefoot plantar pressure reduction, the apex needs to be correctly positioned to offload the forefoot, which means it must not only be positioned behind the metatarsal heads, or indeed proximal to the area on the foot which requires offloading, but also be deep enough to reduce sagittal plane motion at the metatarsal heads to provide the necessary unloading and the rocker profile must also be adequately stiff (Janisse, 1995, Schaff and Cavanagh, 1990, Nawoczenski et al., 1988).

The higher the rocker sole apex angle, the more offloading of the forefoot may be expected for a chosen apex position (Nawoczenski et al., 1988). However, practical considerations mean that maximum apex angles of 30-40 degrees for traditional (angled) rocker sole

profiles have been recommended by (Geary and Klenerman, 1987) for people with diabetic peripheral neuropathy. A 25-degree traditional metatarsal rocker was found to reduce plantar pressures more than the other designs in a study by (Stacpoole-Shea et al., 1999). To be effective, a rocker sole apex angle needs to be at least 20 degrees to be able to offer adequate forefoot unloading (Nawoczinski et al. 1988, Chapman et al. 2012).

Curved rocker soles are thought to provide a more “natural” gait by allowing a smoother transition from heel-off to toe-off with advantage of a more cosmetic appearance (Nawoczinski et al. 1988), but this means that the GRF rolls forwards without “hesitating” at the apex of a traditional rocker sole design.

Bauman et al. (1963) studied the effect on plantar pressures experienced by a range of patients using a variety of angled traditional rocker soled shoes, and demonstrated that a rigid soled shoe with a rocker placed 1.7cm proximal to the metatarsal heads was the most suitable for reducing pressure under the forefoot. Nawoczinski et al. (1988) recommended the use of a traditional rocker sole with the apex positioned at the metatarsal head level and an apex angle of 20 degrees. This was confirmed by (Coleman, 1985) and (Geary and Klenerman, 1987), but with a 30-degree apex angle for patients with diabetic neuropathy.

Brown et al. (2004) also highlighted the fact that pressure shunting can occur when offloading the forefoot using a rocker sole adaptation. They demonstrated that plantar foot pressures may be reduced when walking with the negative heel and toe traditional rocker profiles as well as a double rocker sole. However, mid-foot pressures were increased when using the negative heel and toe type traditional rocker designs.

A recent study by Chapman et al. (2012) confirmed that in diabetic subjects, a minimum rocker angle of 20 degrees with the apex positioned 60% of shoe length relative to the rear of the shoe is required to provide meaningful offloading of the forefoot.

3.5.1.1 Comment

An apex position significantly proximal to the metatarsal heads (MTHs) could be advantageous in reducing loading at the rearfoot (particularly at the ankle) by reducing the externally-applied ankle dorsiflexion moment during late stance. Indeed, (Hampton, 1979), recommended that the rocker axis should be located near the centre of the foot and the rocker sole should be thick enough to minimise contact between the end of the shoe and the floor during the toe-off phase of gait. In addition, (Cavanagh et al., 1996), demonstrated that the lowest plantar pressure measured in their study was achieved with a traditional rocker sole apex positioned 55% shoe length from the posterior heel. This may therefore indicate a potentially useful position for a rocker sole not only to offload the forefoot but also to reduce the loading on the ankle plantarflexors; but to date this has not been ascertained.

3.6 Alteration to lower limb joint kinetics and kinematics

3.6.1 Joint Rotation

The most commonly prescribed designs of rocker soles used in clinical practice do not produce significant alterations to lower limb joint kinematics. The most significant changes to kinetics has been demonstrated at the ankle in the sagittal plane followed by the hip, but have been shown to be small in magnitude (Myers et al., 2006, Van Bogart et al., 2005, Brown et al., 2004, Long et al., 2004). Myers et al. (2005), demonstrated that the most significant kinematic changes with the negative heel shoe occurred at the ankle with increases in dorsiflexion during loading response and plantarflexion at terminal stance. The toe-only rocker profile has been shown to produce increased hip extension at late stance phase. At the ankle it produced increased dorsiflexion at initial contact and loading response, and increased plantarflexion during late stance (van Bogart et al. 2005). However, this was in variance with a later study in which a toe-only rocker sole produced an increase in late stance dorsiflexion prior to the plantarflexion phase during propulsion (Hutchins et al., 2009).

There is therefore evidence in the literature which suggests that rocker soled shoes can influence ankle joint plantarflexion or dorsiflexion during stance phase of gait, although more evidence is needed to clarify the effects of some designs.

3.6.1.1 Negative heel rocker-soled shoes


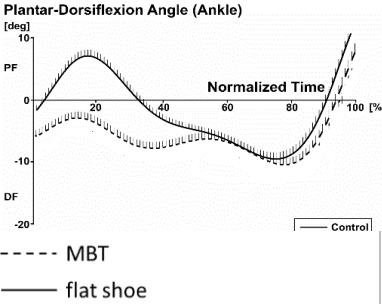

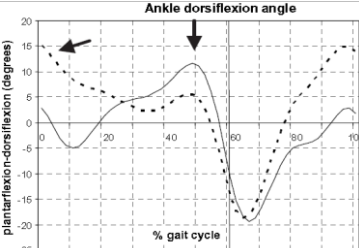
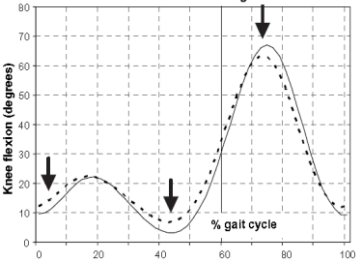
Negative heel rocker soles are deemed to be those where the heel height is lower than the depth at the tread (i.e. the point at which the sole unit contacts the ground during static standing). The same effect can be shown when walking with a cushioned heel adaptation; where soft material is added to the posterior heel area of the shoe.

Some authors have recommended the use of a rocker profile in tandem with a cushioned heel in the treatment of patients with restricted ankle motion following surgical fusion or arthritic changes to the ankle or midfoot structures (Baker, 1970, Cracchiolo, 1979, Caron et al., 1999, Marzano, 2002, Long et al., 2007). The cushioned heel is designed to simulate plantarflexion (but may not in fact do so) and cause an early transition to second rocker of gait.

Zamosky (1964), described the use of a solid ankle and cushioned heel (SACH) type adaptation with a metatarsal rocker bar combination in the treatment of patients with stiff ankle joints and limited motion. The SACH heel was described as acting as a shock absorber and by compressing, acted to bring the rocker bar into early contact with the ground. This compression of the SACH heel at heel strike afforded the patient a pseudo-plantar flexion without forcing the ankle towards plantar flexion. Since early ground contact was made at the apex of the rocker bar, the shoe was ready for roll over (i.e. second rocker of gait) and toe-off (third rocker of gait) so rapidly that motion of the tarso-metatarsal, talocrural or subtalar joints was precluded (Hutchins et al., 2009).

The MBT (Masai Barefoot Technology) shoe also has a cushioned heel, but this in fact induces a relatively dorsiflexed ankle position during loading response, and does not therefore simulate plantarflexion, (Table 3). The evidence is therefore limited regarding the effect of rocker soled shoes on lower limb kinematics and requires further investigation.

Table 3.1: Ankle and knee kinematic data for studies which investigated the MBT shoe versus flat control shoes.

Author	Subjects and footwear	Ankle and knee ROM(°)	Muscle excursion
MBT			
(Nigg et al., 2006)	<p>N=8 healthy subjects, (5 male). Walking speed was controlled at 1.38 m/s; MBT (650g) vs. Adidas supernova running shoe (358 g)</p> 	<p>Plantar-Dorsiflexion Angle (Ankle) [deg]</p>  <p>----- MBT —— flat shoe</p>	<p>Ankle: The MBT shoes induced dorsiflexion during loading response and shortening of the ankle PF muscles.</p>
(Romkes et al., 2006)	<p>N=12 healthy subjects, (6 male). 4 weeks of MBT training. Self-selected speed of walking MBT vs. regular shoe</p> 	<p>Ankle dorsiflexion angle</p>  <p>Knee flexion angle</p>  <p>----- MBT —— flat shoe</p>	<p>Ankle: MBT shoes induced dorsiflexion of the ankle for the first 30% of the gait cycle. Knee: These were relatively flexed for the first 40% of the gait cycle.</p>

3.6.1.2 Rocker soled shoes designed to reduce ankle joint rotation

It may be prudent to reduce ankle sagittal plane rotation by claudicants when using a rocker-soled shoe. This could feasibly reduce power generation by the ankle plantarflexors provided the ankle was placed in an advantageous position to increase the moment arm between the Achilles tendon and the ankle joint centre of rotation. This theoretical hypothesis is investigated in this thesis in able-bodied adults. However, there is little currently-available evidence in the literature as to which rocker sole features can reduce ankle ROM; especially during stance phase of gait.

(Wang and Hansen, 2010) published a study which demonstrated that a rocker profile with a single circular rocker profile radius equivalent to 25% of leg length, could significantly reduce ankle joint sagittal plane total ROM during stance phase to approximately 15 degrees, and that smaller radii produced more reductions in sagittal plane ankle motion than those with larger radii. Arazpour et al. (2013) when utilising a rocker profile with a central apex of 50% of shoe length, and with a 10 degree curved rocker either side of the apex and a curved heel and increased toe spring, was capable of restricting ankle joint total ROM to 17 degrees. These two studies would therefore suggest that rocker soled footwear is capable of significantly affecting ankle joint plantarflexion and dorsiflexion.

3.7 Alteration to externally-applied sagittal plane lower limb joint moments

The following effects have been demonstrated in the literature regarding alteration to lower limb joint moments by commonly-used rocker sole designs.

3.7.1 Sagittal plane knee joint moments

- Van Bogart et al. (2005) using a toe only rocker profile demonstrated increased knee extensor moments throughout stance;
- Long et al. (2007) demonstrated increased extension demand moment after LR when using the double rocker sole compared to baseline;
- Sagittal plane ankle moments;
- Myers et al. (2006) when testing the negative heel rocker profile showed that increased plantarflexion moments during LR occurred, but interestingly reduced plantarflexion demand moments at TSt, PSw and ISw;
- Van Bogart et al. (2005), demonstrated decreased plantarflexion demand moments during MSt and TSt were initiated by the toe-only rocker (which they postulated was related to the forward position of the GRF which limited the ability to generate a moment about the ankle);
- Long et al. (2007), demonstrated that the double rocker sole decreased plantarflexion demand moments between MSt. and MSw.

3.7.2 Sagittal plane ankle powers

- Myers et al. 2006 (negative heel profile) demonstrated increased ankle power generation MSt. but reduced power generation at push-off;
- Van Bogart et al. 2005 (toe-only rocker profile) demonstrated increased ankle power generation at MSt;
- Long et al. 2007 (double rocker profile) demonstrated decreased ankle power absorption between LR and MSt.

3.7.3 Alteration to EMG activity

Various authors have demonstrated that the most commonly-used rocker profiles increase the activity of the ankle plantarflexors. Harris et al. (2000) demonstrated that the toe only rocker increases gastrocnemius activity by initiating earlier firing during mid-stance and double limb support, which is related to earlier anterior tibial rotation (second rocker of gait, Perry 1992). The double rocker also produces increased muscle activity in the gastrocnemius muscle group (Wertsch et al., 2000). Harris et al. (2000), also showed that the toe-only rocker reduced tibialis anterior muscle EMG activity both during mid stance and swing phases of gait, but most noticeably during mid-stance.

A study by Romkes et al. (2006) investigated the kinematic and electromyographic changes when MBT training shoes were worn by 20 healthy volunteers. Their results indicated an increased loading to gastrocnemius medial head, soleus and tibialis anterior muscles whilst wearing the shoes. Sagittal plane ankle motion showed increased dorsiflexion at heel strike which increased gastrocnemius and soleus activity during stance phase, followed by increased plantarflexion during the remainder of stance phase with insignificant amounts of dorsiflexion prior to heel-off.

When walking with a negatively heeled shoe, an increase in total and peak gastrocnemius muscle activity (+21%) during stance phase may be expected (Li and Hong, 2007).

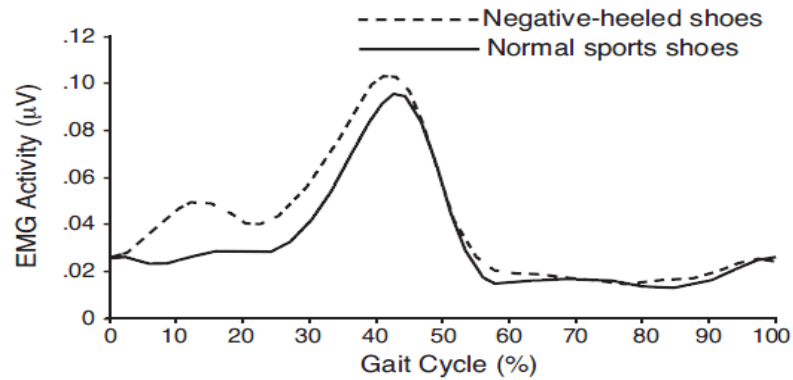


Figure 3.2: Increase in EMG activity when walking with a negative heel rocker soled shoe [Adapted from (Li and Hong, 2007)].

Yamamoto et al. (2000), demonstrated significant increases in blood flow in the calf muscles when wearing a negative heel shoe versus regular shoes in able-bodied subjects (N=6) when walking at self-selected speeds of 1.33 m/s and above. This would also indicate increased calf muscle activity.

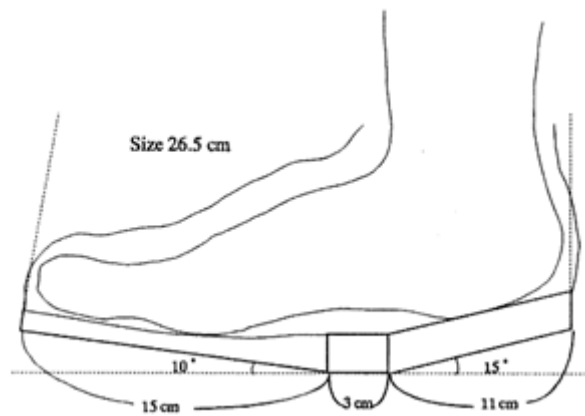


Figure 3.3: A negative-heel rocker soled shoe [adapted from Yamamoto et al. (2000)].

3.8 Comment

The evidence suggests that the majority of rocker soled shoes tested to date (which include the most commonly-used designs) induce an increase in ankle plantarflexor muscle activity during stance phase of gait. Negative heel rocker soled shoes produce a relatively dorsiflexed position during initial contact and loading response which also increases ankle plantarflexor muscle activity. Shoes with a cushioned heel (such as the MBT shoe) also induce a relatively dorsiflexed position following heel strike and therefore will have the

potential to increase ankle plantarflexor activity during early stance in order to lift the heel and advance the foot into mid stance and propulsion. However, it may be possible to identify an angled rocker sole unit following gait laboratory testing which has a prudent apex angle and position to reduce these unwanted effects for the benefit of people with PAD-IC, but as yet this is un-proven.

3.9 Alteration to oxygen consumption

Hansen and Wang (2011) compared the effect of a single curve rocker profile radius (based on % of leg length) on the oxygen consumption rate in 11 adults. They demonstrated that a rocker profile with a radius equating to 40% of leg length was the most effective by significantly reducing oxygen consumption compared to a baseline regular shoe.

3.10 Overall chapter analysis

The overall aim of this thesis is to provide enhanced and novel knowledge as to how rocker soled shoes may be designed to reduce symptoms associated with IC, but which may also be of significant benefit for people with other pathologies where offloading of the ankle plantarflexors would be of benefit. Only a few studies were found which showed some improvement in symptoms and pain-free distances by claudicants may be obtained using rocker soled shoes. These previous studies have shown little information why these changes helped to increase free-pain walking distance. There has been no information provided about muscle biomechanics and limited information about gait parameters in most of the studies examined.

It is important to look at the muscle-tendon length changes during gait, because they actuate movement by developing force and generating internal moments (Delp, 1990). For example, different footwear rocker sole profiles alter knee and ankle angles during stance phase. Therefore, when a muscle-tendon unit is lengthened or shortened to a certain point the muscle fibres may be too long or too short to generate enough active force in the lower limb. Skeletal muscle develops only 50% of the maximum force when its length is shortened to 85% of the resting length (Panjabi and White, 2001).

The type of muscle contraction may also be altered by footwear adapted with rocker soles, and they may also change EMG activity and forces generated about the joints which the muscles are attached to. This may change muscle activity, oxygen consumption and alter gait patterns.

At present, there are few tools to evaluate the effects of muscle-tendon properties and skeletal geometry in determining moment-generating characteristics of individual muscles. However, by using Visual3D and Simm/OpenSim software this gives the opportunity to analyse these effects and provide a clearer understanding as to which footwear features are capable of providing alteration to muscle performance for the potential benefit of specific patient groups.

EMG data can only indicate when a muscle is active or not, but interpretation of EMG data does not help us to determine what caused an increase muscle activity or which joint motion produced it. OpenSim allows analysts to analyse exported dynamic motion data from Visual3D and look at the musculoskeletal dynamic motions using a model of the lower limb. This computer model can assist in understanding the biomechanical consequences of musculoskeletal dynamic changes wearing different footwear rocker sole profiles and to advance the knowledge in this area as to which designs are suitable for the specific aim of reducing the activity and work done by the ankle plantarflexors. This is needed in order to help reduce the painful calf muscle symptoms which can so drastically negatively affect a claudicant's quality of life.

CHAPTER 4

4 Muscle physiology and related biomechanics

4.1 Chapter overview

This thesis seeks to investigate the relationship between walking with different footwear outsole features and the resulting alteration to gait patterns and associated kinetic and kinematic changes, plus analysis of alterations to muscle biomechanical parameters and EMG data for the lower limbs during gait. Therefore, it is appropriate to review basic principles of gait and which factors are responsible for significant alteration of lower limb muscle parameters, especially for the calf muscles. Based on logical interpretation of human biomechanics, definition of walking patterns and the alterations caused by footwear features, hypotheses may be developed to provide an enhanced understanding of the logical concepts lying behind the alterations seen during gait.

This chapter begins with basic terminology that is used when analysing the results which emanate from clinical gait analysis, plus muscle physiology, muscle mechanics and gait parameters. It finishes by presenting the information which was required to formulate the aims and hypotheses of the study to enable an investigation of the possible walking pattern alterations caused by rocker-soled shoes to be analysed.

4.2 Basic terminology used in this thesis for muscle biomechanics and gait analysis

4.2.1 Planes and axes

Movements of the body segments are described in terms of their planes and axes. The body may be considered as being composed of segments. The motion of the segments takes place around three axes and therefore three planes known as the sagittal, frontal and transverse planes (figure 4.1).

A *sagittal plane* is any plane which divides part of the body into right and left portions and describes movements such as flexion/extension of the knee and hip joints, and dorsiflexion/plantarflexion of the ankle joint. A *frontal plane* divides a body part into anterior and posterior and represents movement such as abduction/adduction. The *transverse plane*

divides body into upper and lower parts (Trew and Everett, 2005, Whittle, 2007, Kirtley, 2006).

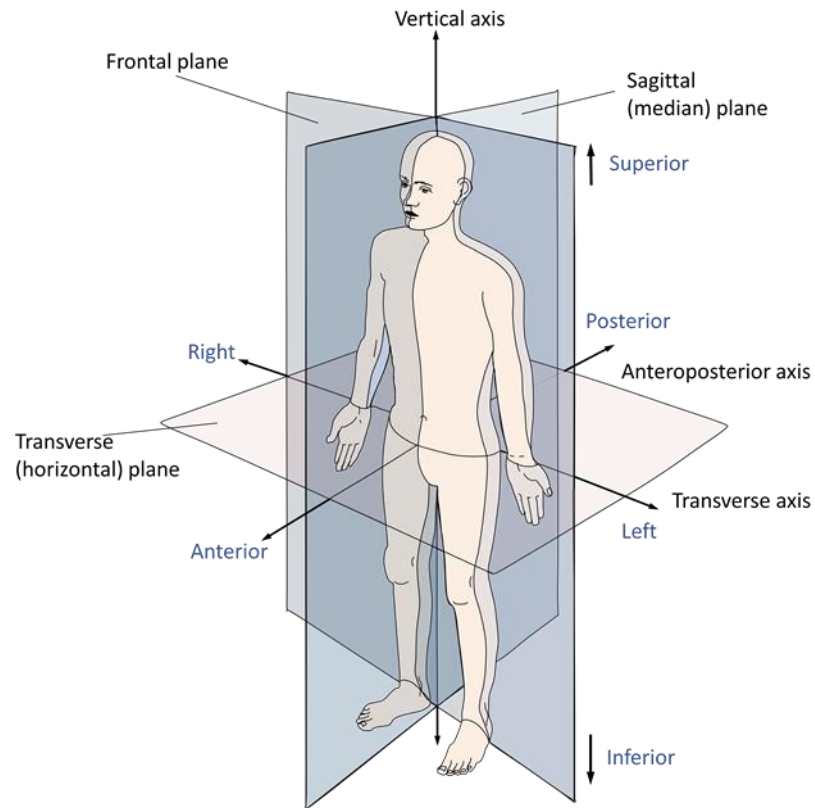


Figure 4.1: The anatomical position, with three reference planes and six directions.

There are additional terms, which are used to describe relationships between segments in gait analysis:

- *Medial* means towards the midline of the body (closest to the median);
- *Lateral* means away from the midline of the body (furthest away from the segment);
- *Distal* means away from the centre of mass;
- *Proximal* means the closer to the centre of mass (figure 4.2).

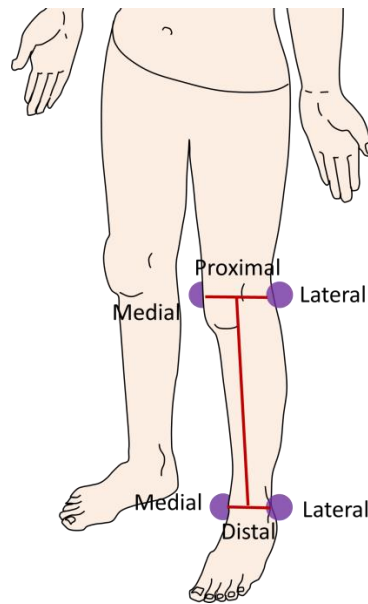


Figure 4.2: An example of a shank segment for medial/lateral aspects and proximal/distal ends of the segments.

4.2.2 Lower limb skeletal structure and joint motions

The skeletal system provides the overall shape of the body and supports its weight, whilst absorbing and dissipating stress generated by movement or external forces, facilitating movement through a network of different types of joints, and providing attachment to muscles and tendons (Trew and Everett, 2005, Palastanga and Soames, 2012). The lower body provides a locomotive function during walking whilst maintaining an upright posture. The shape and structure of individual segments are adapted to the function of supporting and resisting mechanical stresses.

The lower limb consists of the femur, tibia and fibula connected to the foot distally and the pelvis proximally via the hip joint. It is important to have knowledge of anatomical structures and anatomical points in the body to be able to define and reconstruct segments and joints for gait analysis using motion capture software. Figure 4.3 represents the basic anatomical points, segments and joints of the lower body.

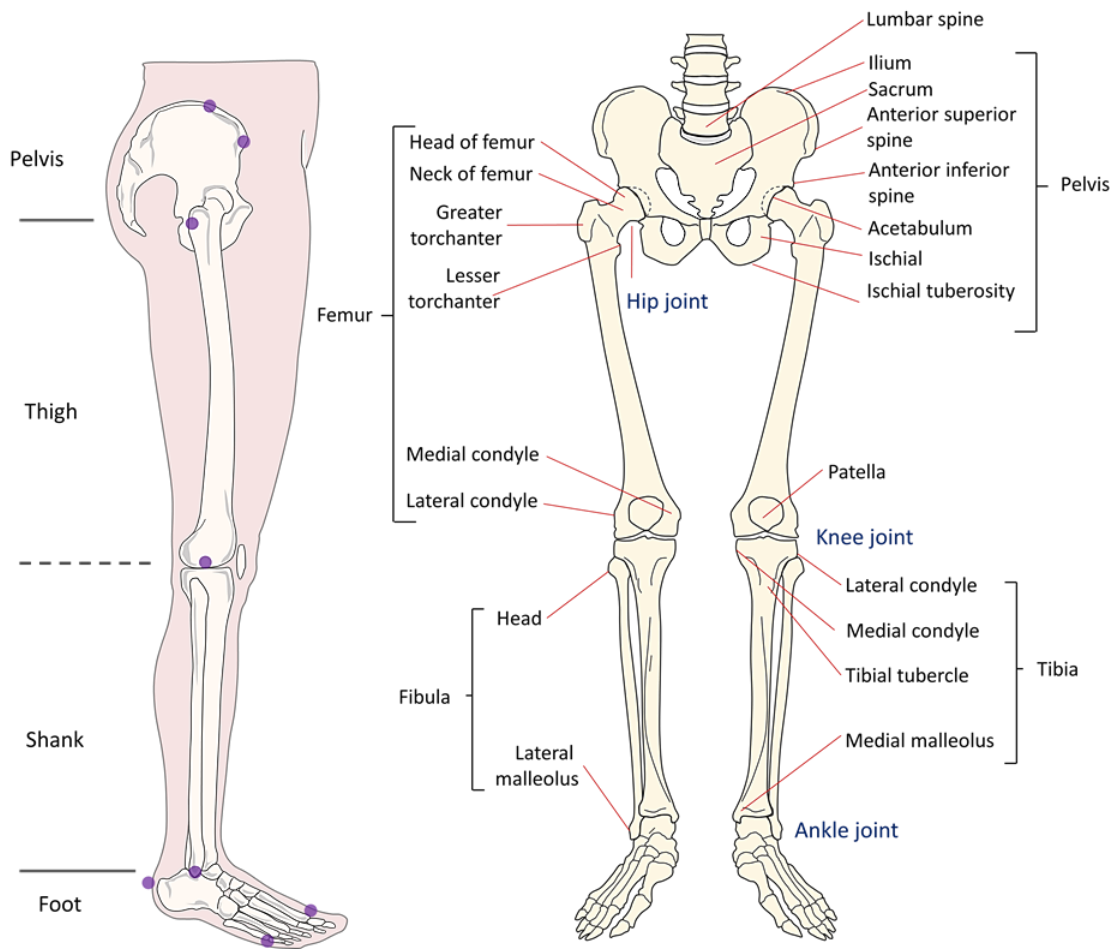


Figure 4.3: Basic anatomical points for lower limb bones, segments and joints for gait analysis.

When performing gait analysis, the foot has historically been considered as a single rigid segment. However, the foot and ankle joint complex may be better described using rearfoot, midfoot, and forefoot segments. Modelling the foot as a multiple segmental structure, rather than a rigid single one, has a significant effect on the accuracy of instantaneous power calculation between segments (Richards, 2008). Therefore, with modern motion capture systems it is possible to track the movement of the tibia, rearfoot, midfoot and forefoot as separated segments in 6 degrees of freedom (DOF) for accurate ankle joint movement, interpretation and analysis. Figure 4.4 shows the basic osseous structure of the foot as a segmental entity and relevant anatomical points.

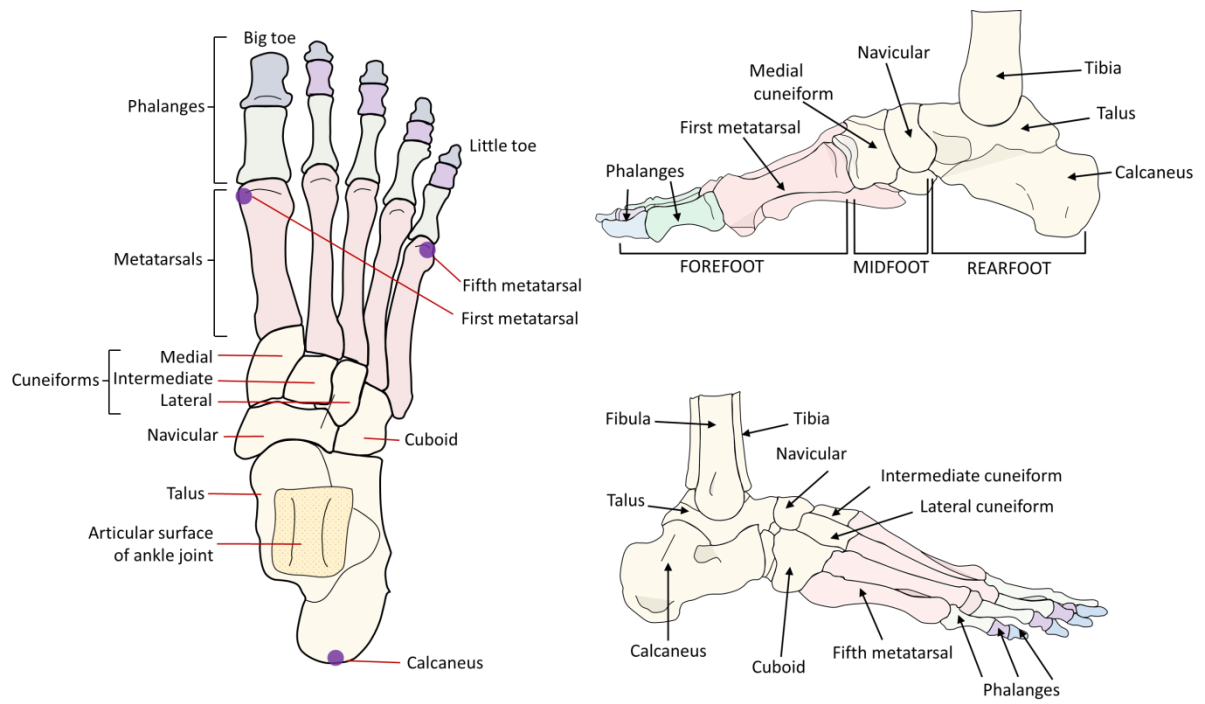


Figure 4.4: Osseous structure of the foot.

Basic joint motions of the lower limbs in the sagittal plane, which are commonly used in gait analysis research, are represented in figure 4.5.

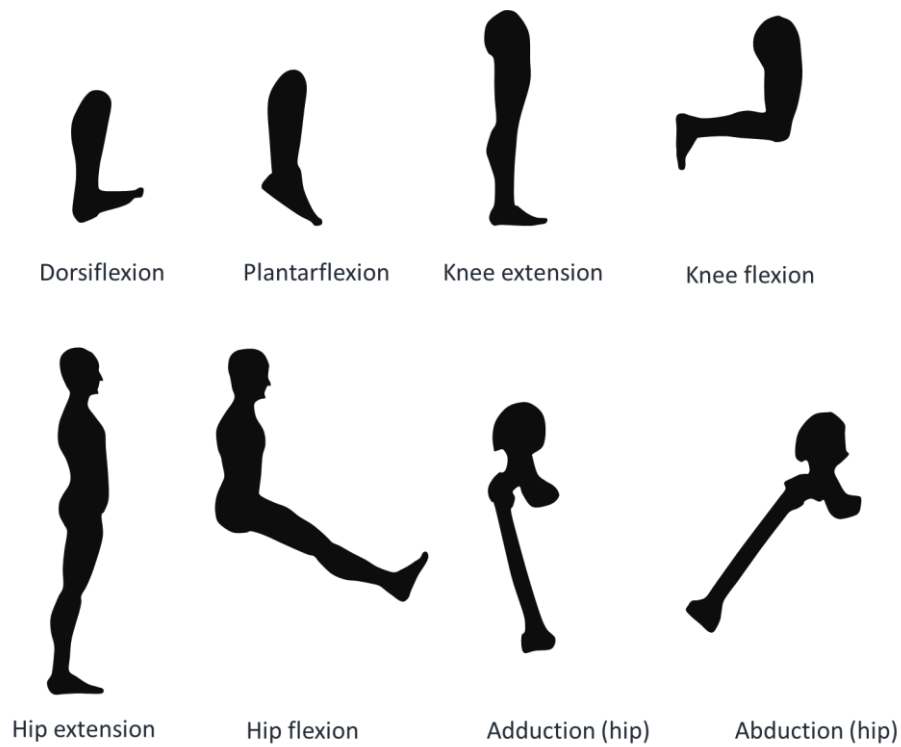


Figure 4.5: Motion of the lower limb joints.

The actual movement performed at a joint can be described in terms of the number of degrees of freedom the joint allows. Most motion analysis software for biomechanical and clinical research such as Visual3D (C-motion, USA) uses a six degrees-of-freedom (6 DOF) model for gait analysis.

Any body segment can theoretically move in six different ways independently and in human movement all these six often happen at the same time (Richards, 2008). Six degrees-of-freedom means that a body segment can utilise linear or translational movement, vertically, medio-laterally and anterior-posteriorly. It can also perform three rotational or angular movements in the sagittal, frontal and transverse planes. The possible foot segment angular and linear movements are shown on the figure 4.6.

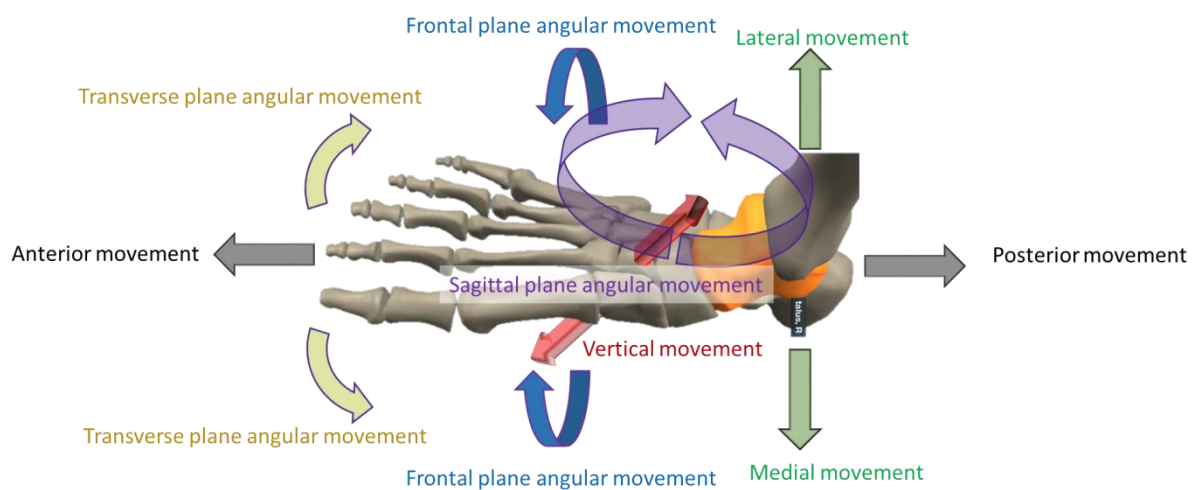


Figure 4.6: Linear and angular movements for foot segment movement in all planes and directions.

Joints can be classified into three groups based on the ROM allowed at the joint. Synarthrosis-type joints are immovable (e.g. joints found between the bones of skull and teeth). Amphiarthrosis joints allow slight movement such as the distal articulation between tibia and fibula. Diarthrosis or synovial joints allow considerable motion (Tözeren, 2000). There are different classifications for these type of joints (i.e. their DOF classification) which are also used for motion analysis, muscle simulation properties and in analysis software such as in OpenSim.

4.3 Muscle anatomy

The largest organ in the human body is the skeletal muscle system which accounts for between 40 and 45% of total body weight (Nordin and Frankel, 2003). The human body has more than 430 skeletal muscles. The role of skeletal muscles is to cause or control movements at the joints as well as performing static work (i.e. maintaining posture or position). They are attached to bones and their main function is to produce movement of one bone relative to another, to control movements produced by external forces or to hold bones to maintain posture and balance. Most of the muscles have an origin and insertion point at their attachments and also cross joints (such as the gastrocnemius muscle). Ligaments connect bones together whereas tendon connect muscles to bones (Trew and Everett, 2005, Abernethy et al., 2013). To perform a motor task, the central nervous system activates muscles that subsequently develop forces, which are transmitted by tendons to the skeleton to perform a task. An understanding of the properties of these structures, plus how to produce optimal or sub-optimal muscle performance and changes to this performance which may be demonstrated by different footwear features is potentially important to scientists who design special footwear for rehabilitation and treatment purposes.

The fundamental structure of muscles acting on the lower limb which are of relevance to this thesis are demonstrated in figure 4.7. The ankle muscles highlighted in blue text are the main group acting at the ankle or knee joints which were targeted for data analysis in this research to more fully understand the effect of different footwear features on gait than that previously demonstrated in the literature.

Rectus femoris (RF) forms part of the quadriceps muscle group which extend the knee, but it additionally flexes the hip. It originates from the anterior inferior iliac spine of the pelvis and inserts into the quadriceps tendon. Biceps femoris (BF) acts as a knee flexor and hip extensor. It has two origins – the long head comes from the ischial tuberosity and the short head from the middle of the shaft of the femur and it inserts into the lateral condyle of the tibia (Whittle, 2007).

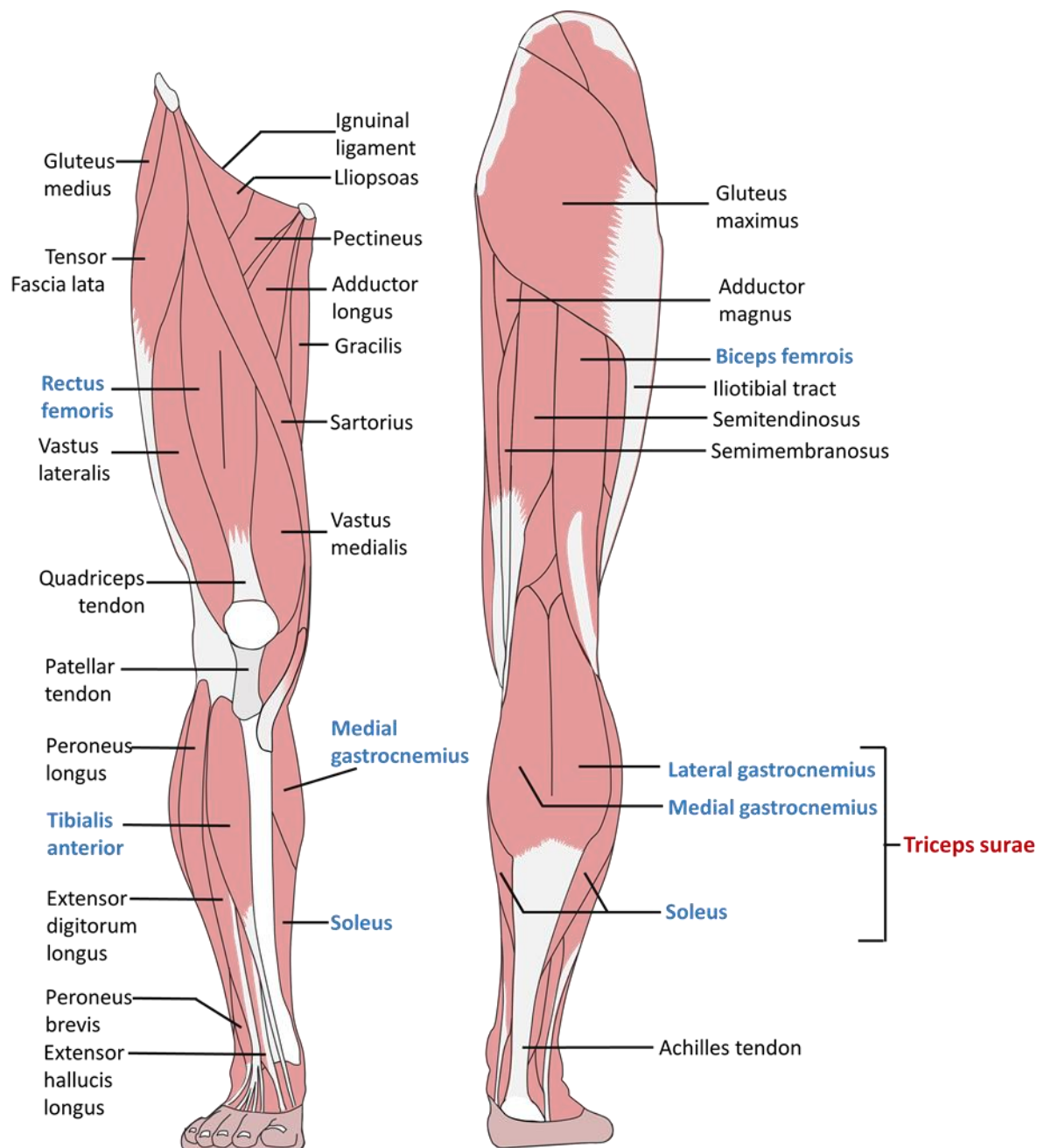


Figure 4.7: The major muscles of the lower limbs.

Muscles that plantarflex the ankle joint are the gastrocnemius, soleus, plantaris, fibularis longus, fibularis brevis, tibialis posterior, flexor digitorum longus and flexor hallucis longus muscles (Palastanga and Soames, 2012). The main plantarflexors of the ankle are known as the triceps surae muscle group. This comprises of the gastrocnemius medial and lateral heads, and soleus. The gastrocnemius muscle crosses the knee joint and originates from the posterior aspect of the medial and lateral condyles of the femur. Its tendon joins with that of the soleus to form the Achilles tendon, which inserts into the calcaneus as shown in figure

4.8. The gastrocnemius muscle also acts as a flexor of the knee whilst the soleus does not (Whittle, 2007).

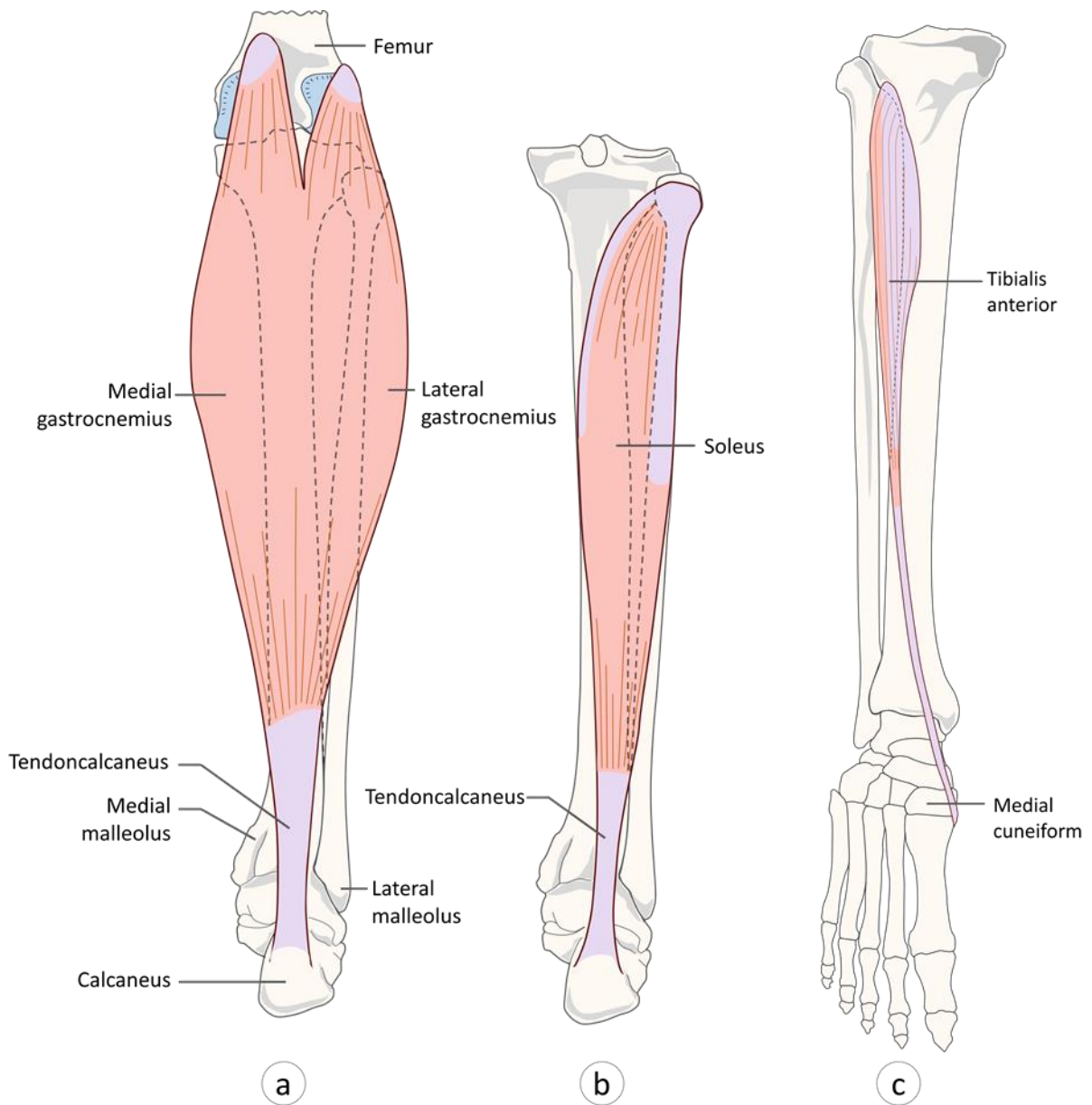


Figure 4.8: The main ankle plantar/dorsiflexion muscles which were investigated to seek further understanding of their mutual relationships in performing muscle work whilst wearing different footwear features in this research, (a) - posterior view of gastrocnemius muscles, (b) posterior view of soleus muscle, (c) – anterior view of tibialis anterior muscle [picture adapted from (Palastanga and Soames, 2012)].

The muscles which dorsiflex the ankle joint are tibialis anterior, extensor digitorum longus, extensor hallucis longus and fibularis tertius. Tibialis anterior is the main dorsiflexor of the ankle. It is a long fusiform muscle situated on the front of the leg lateral to the anterior border of the tibia as shown in figure 4.8. The muscle becomes tendinous in its lower third, passing downwards and medially over the distal end of the tibia (Palastanga and Soames, 2012, Whittle, 2007).

Intermittent claudication alters calf muscle function, and therefore the principle muscles acting on the ankle joint [medial gastrocnemius (GM), soleus (SOL) and tibialis anterior (TA)] were focused on during this research to understand their effect on gait following different footwear interventions.

4.3.1 Skeletal muscle structure

Skeletal muscle is specifically structured to meet the functional requirement for specific movement. The entire muscle is a composite of hundreds of fascicles, which in turn consist of hundreds of muscle fibres. The fibres are composed of myofibrils as shown in figure 4.9.

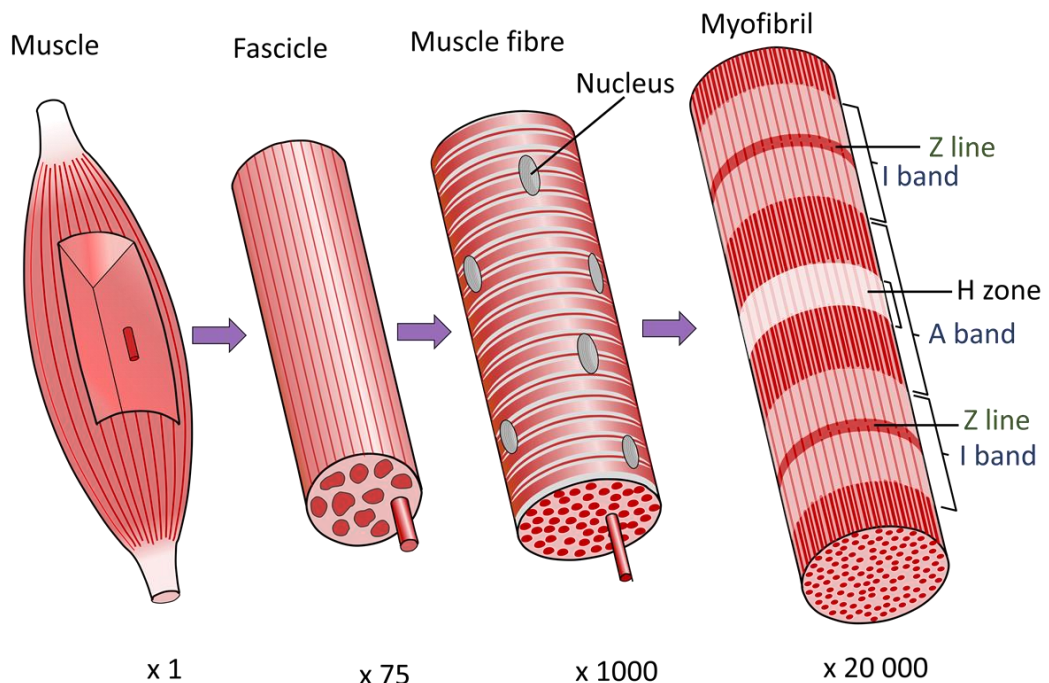


Figure 4.9: basic muscle structure.

Muscle cells convert energy from fatty acids and blood sugar glucose into movement and heat. Skeletal muscles have a regular pattern of lines or striations. These striations correspond to the basic function unit of all skeletal muscle, the sarcomere. It is the smallest contractile unit of a myofibril. It contains two contractile proteins - actin and myosin (Rose and Gamble, 2006). The actin is called the thin filament and the myosin filament is called the thick filament. When viewed through a microscope, the myofibril has dark and light bands. The various light and dark bands in the myofibril are routinely identified by letters. At each end of the sarcomere is the Z disk. The thin, dark Z line is the origin of the slender actin filaments. The distance between the Z zones is defined as the sarcomere length. These are interleaved with the thicker myosin filaments, which form the A band.

The I band and H zone change width during muscular contractions, as they represent the areas where the actin and myosin exist (Whittle, 2007). Relative translation between thick and thin filaments is responsible for much of the change in length of a muscle during contraction; figure 4.10.

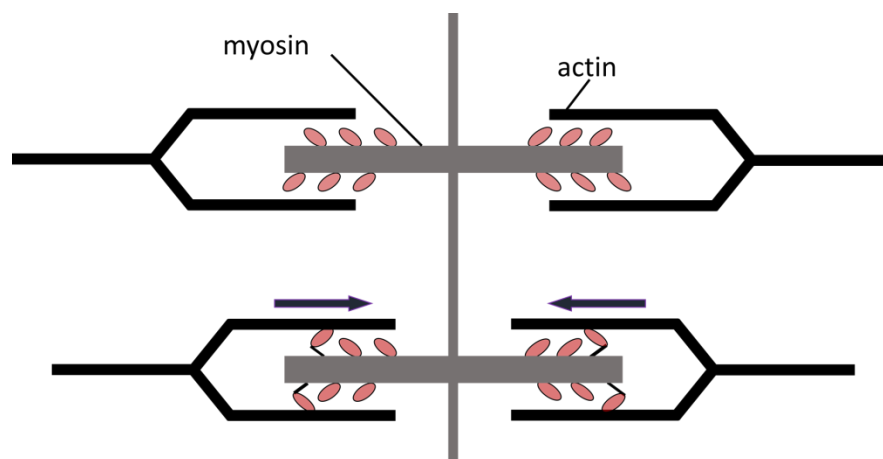


Figure 4.10: Diagram representing thick and thin filaments during two stages of contraction [adapted from (Tözeren, 2000)].

According to the “sliding filaments” theory of muscle contraction, myosin heads on the thick filaments (cross-bridges) interact with actin-binding sites on the thin filaments. These cross-bridges are believed to generate force only when they are attached to actin as shown in figure 4.10 (Tözeren, 2000). Skeletal muscles are stimulated by the central nervous system before they contract. Signals which activate muscles are transmitted from the brain to the nervous system and to individual muscle fibres. Blood capillaries encircle the muscle fibres

and the terminal branches of the motor nerve connect around 150 muscle fibres. The smallest sub-unit that can be controlled is called a motor unit, which includes a single motor neuron and all of the muscle fibres innervated by it (Nordin and Frankel, 2003). The number of muscle fibres forming a motor unit is closely related to the degree of control required of the muscle. The amount of tension produced by a skeletal muscle depends on both the frequency of stimulation and the number of motor units involved in the activation (Winter, 2009).

The energy to contract the muscles comes from the release of a substance related to the high-energy phosphate group and is known as adenosine triphosphate (ATP). Failure to provide metabolic energy to the muscles which could be due to intense performance activities and the subsequent demand can result in muscle fatigue. There are two types metabolic pathways involved in regenerating ATP. One uses up chemicals stored within the cell (phosphocreatine and glucose), without the need for oxygen and is known as *anaerobic*. The other one requires oxygen and nutrients to enter the muscle fibre from the bloodstream and is known as *aerobic* (Whittle, 2007). Anaerobic processes can provide quick powerful bursts of energy, however it can also be exhausted very quickly. For sustained muscular work, an aerobic metabolic process is used, following an oxygen debt, which will need to be repaid by aerobic respiration, to remove lactic acid which accumulates in the muscle. Muscles such as gastrocnemius and soleus have different metabolic energy pathways (and are also therefore different muscle types), and it is important to understand this for the future footwear designs for patients with IC. It is discussed in more detail in the following sections.

4.3.2 Tendons

Muscles attach either directly to bones or via a tendon. The tendons and the connective tissues in and around the muscle belly are elastic structures which help determine the mechanical characteristics of the whole muscle-tendon unit (MTU) during contraction and also during passive extension which produces muscle force to move or stabilise joints (Nordin and Frankel, 2003). The tendon actuator can be defined by specifying its geometry and force-generating properties (Delp and Loan, 1995). The length of tendon at which force begins to develop when stretched is called the tendon slack length (Delp, 1990, Zajac, 1989). Results from previous papers suggest that the tendons of soleus and gastrocnemius can

generate maximum isometric force up to maximum of 10% strain and after that they lose force generation (Zajac, 1989, Hoy et al., 1990b, Delp, 1990, Delp and Loan, 1995, Arnold et al., 2013). A typical force-length relation curve for tendinous tissue is shown in figure 4.11.

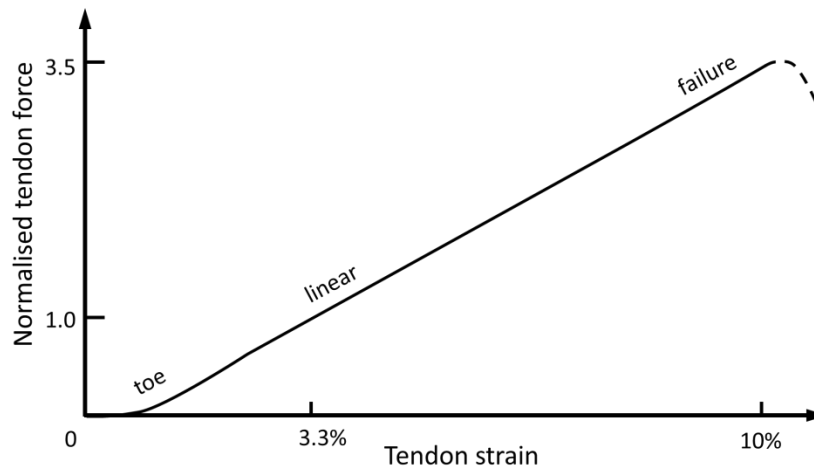


Figure 4.11: Typical normalised force-length relationships for a tendon.

Tendon is more compliant in the lower region than in the linear region as depicted in the figure above, and failure occurs at approximately 10% of strain. Tendon force is normalised by peak isometric muscle force. Tendon strain is defined by tendon stretch divided by tendon slack length, (Zajac, 1989, Delp, 1990). In a recent study it was demonstrated that tendon strain values at which maximum isometric force is generated during simulations are up to 8% in soleus and 7% in gastrocnemius medialis and lateralis (Arnold et al., 2013). The musculoskeletal model which was used in their research contained very precise muscle architecture parameters using data obtained from 21 cadavers.

4.3.3 Force generation

When a nerve is given a single, short pulse to stimulate a muscle, it produces a characteristic response called a twitch. This is a short spasm of contraction which generates a small amount of force very quickly and then declines to zero over a long period. If a second impulse is generated before the twitch has decayed to zero then it appears as a summation effect with a peak force that is higher than a single twitch. This is known as a mechanical summation. With fast and multiple stimuli, the force curve will be higher if more fibres were

activated and the motor units contract. Muscle produces electrical activity, which can be recorded with electromyography. If a muscle is contracting very weakly, only a single motor unit may be activated and if tension is increased, it means additional motor units were recruited. An EMG data acquisition system was used in this research to more fully understand the force relationship generation and muscle activity when ambulating with different footwear conditions.

4.3.4 Muscle fibre types

There are now seven recognised types of skeletal muscle fibre (Abernethy et al., 2013). However, more than 95% of human muscles may be classified into one of three categories according to their relative speed of contraction and their metabolic properties (Katch et al., 2011). The proportions of each type of muscle fibre vary from muscle to muscle and person to person. Type I fibres, also called slow twitch or slow oxidative fibres, are red, have a slow contraction velocity, are fatigue-resistant and have a high capacity to generate ATP by oxidative metabolic processes (Rose and Gamble, 2006, Katch et al., 2011).

Type IIA fibres are called fast twitch or fast oxidative fibres (fast-oxidative-glycolic fibres) which exhibit fast shortening speeds and a moderately well-developed capacity for energy transfer from both aerobic and anaerobic sources (Katch et al., 2011). They are red in colour, contain many blood capillaries, and contract and relax rapidly, but are easily fatigued. They are mainly used for brief bursts of powerful contraction.

Type IIB fibres, also called fast twitch or fast glycolytic fibres (Abernethy et al., 2013). However, they have less blood capillaries than Type I fibres and large amount of glycogen. Type IIB fibres are pale, generate ATP by anaerobic metabolic processes, and are easily fatigued.

The main characteristics of muscle fibre types are summarised in table 4.1.

Table 4.1: Characteristics of muscle fibres types [adapted from (Rose and Gamble, 2006, Abernethy et al., 2013, Katch et al., 2011)].

Fibre Type	Type I fibres	Type II A fibres	Type II B fibres
Contraction time	Slow	Fast	Very Fast
Maximum duration of use	Hours	<30 minutes	<1 minute
Fibre colour	Red	Red	White
Size of motor neuron	Small	Medium	Large
Fatigue resistance	High	Moderate	Low
Activity Used for	Aerobic	Long term anaerobic	Short term anaerobic
Force production	Low	High	Very High
Mitochondrial density	High	High	Low
Capillary density	High	Moderately high	Low
Oxidative capacity	High	Moderately high	Low
Glycolytic capacity	Low	High	High
Major storage fuel	Triglycerides	Creatine phosphate, Glycogen	Creatine phosphate, Glycogen
Metabolism	Oxidative	Oxidative glycolytic	Glycolytic

The average human's skeletal muscles comprise approximately 50% slow-twitch and 50% fast-twitch fibres; about 25% of fast-twitch muscle fibres are type IIA and 25% are type IIB. Fibre types develop depending on the muscle usage. Sprinters develop more fast twitch fibres and fewer slow twitch one (Abernethy et al., 2013). On average, sedentary children and adults possess about 50% slow-twitch fibres (Katch et al., 2011). Distance runners and cross-country skiers often have the greatest percentages of slow-twitch fibres; often as high as 90%. However, weight lifters, ice hockey players and sprinters have more fast-twitch fibres. Figure 4.12 shows typical muscle fibre compositions and maximal oxygen uptake rates in different athletes.

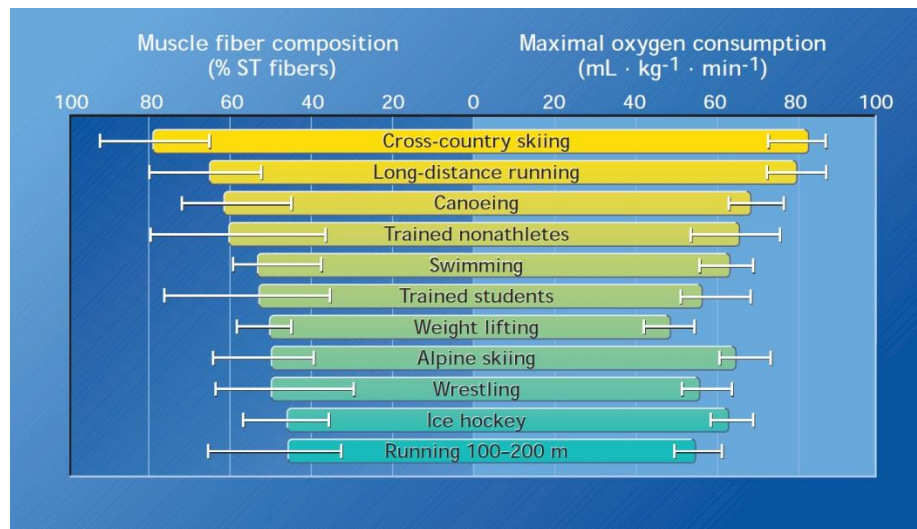


Figure 4.12: Muscle fibre composition and maximum oxygen uptake rates in athletes representing different sports (Katch et al., 2011).

When muscles contract, not all fibres are activated, or recruited, to produce force and muscle fibres are activated in proportion to the amount of force required. There is a pattern of muscle fibre recruitment which is called the size principle. Smaller slow-twitch fibres are activated first, followed by fast-twitch type IIA and then type IIB (Abernethy et al., 2013). Type IIB fibres are activated during forceful contractions requiring 70% of maximum muscular force (figure 4.13).

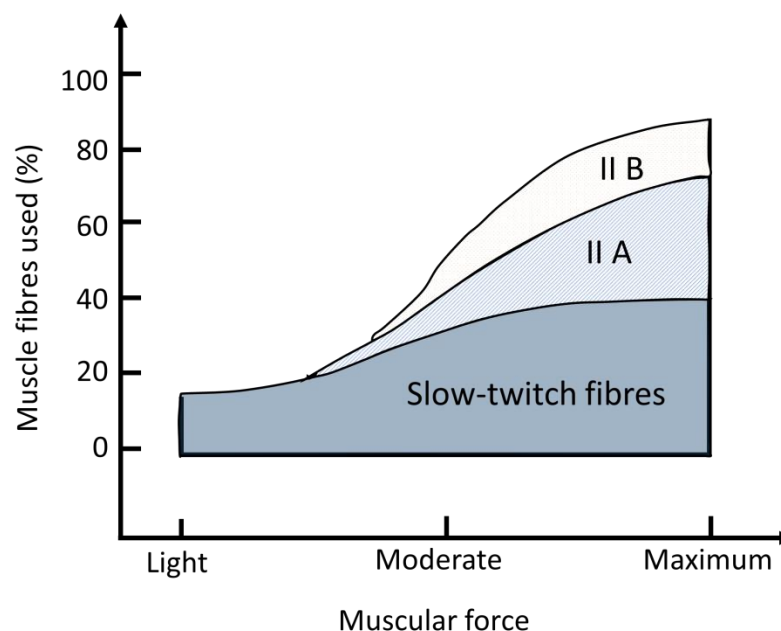


Figure 4.13: Skeletal muscle fibre recruitment during a physical workout [adapted from (Abernethy et al., 2013)].

The force of muscle activation varies from slight to maximal by means of the following mechanisms:

1. Increasing the number of motor units recruited.
2. Increasing the frequency of motor unit discharge (Katch et al., 2011).

Evidence in the literature has demonstrated that patients with IC improve their maximum pain-free walking distance after walking rehabilitation programs and this could be due to building up different types of muscle fibres during the program which therefore increases capillary density, which improves blood supply to the calves. The literature has also demonstrated that different athletes build up different type of fibres. Weightlifters have around 70% type II fibres and distance runners have around 80% type I fibres (Katch et al., 2011, Abernethy et al., 2013). Studies with humans and animals support the concept that skeletal muscle adapts to altered functional demands. Muscle fibre type transformation may occur with specific exercise training. That concept is useful to consider for patients with intermittent claudication.

4.3.5 The pennation angle of muscles

The internal structure or arrangement of muscle fibres is related to both the force of contraction and the range of movement required (Trew and Everett, 2005, Palastanga and Soames, 2012, Barlett, 2007). Co-linear muscles are those which have muscle fibres that are more or less parallel. When the line of the muscle action does not match the line of action of the fibres then the muscle is known as pennate [these muscles account for 75% of the body's muscles, mostly in the large muscle groups, including muscles of the lower extremity (Barlett, 2007)]. An example of muscles with different architectural structures is shown in figure 4.14.

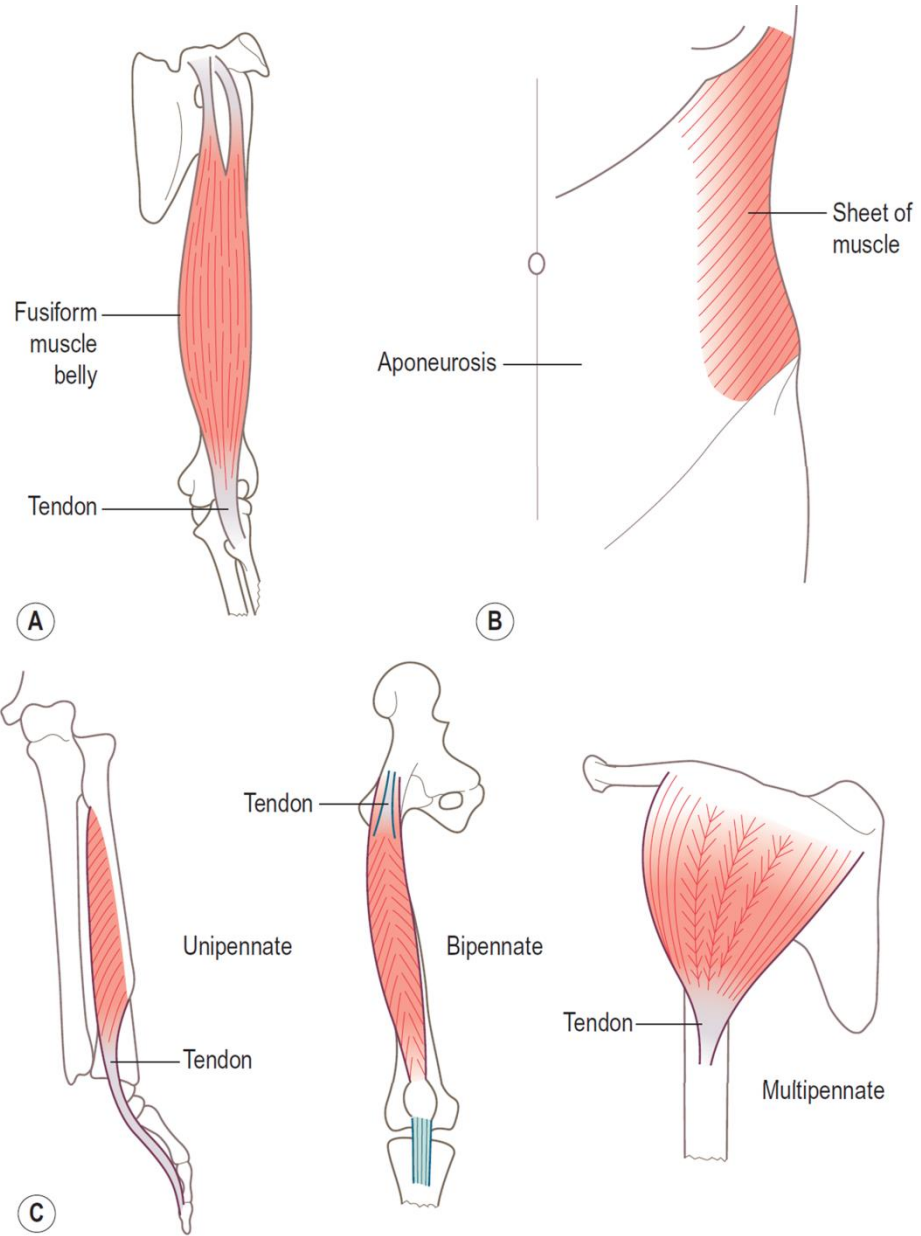


Figure 4.14: Muscle architecture of fibres: (A) fusiform, (B) sheet, (C) pennate (Palastanga and Soames, 2012).

In unipennate muscle, the fibres attach to one side of the tendon only, extending diagonally as a series of short, parallel fascicles (tibialis posterior is an example); (Barlett, 2007). Bipennate muscles have a central septum with the muscle fibres attaching to both sides and to its continuous central tendon. This group includes the rectus femoris muscle of the thigh and the flexor hallucis longus, which flexes the big toe. Mutlipennate muscles converge to several tendons.

The pennation angle of the muscle also affects the force generation properties of each muscle as it transmits force through the tendon. To understand basic muscle-tendon mechanics, the effect of pennation angle on muscle function can be ascertained from the arrangement shown in figure 4.15.

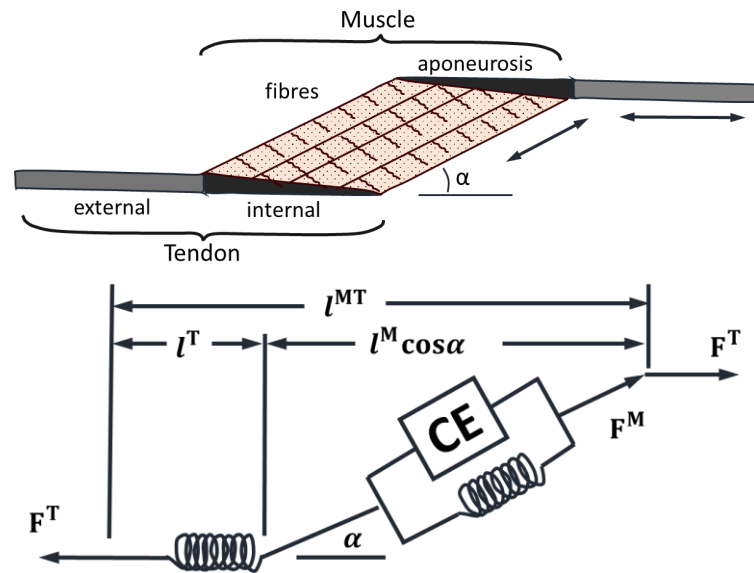


Figure 4.15: The muscle-tendon actuator principle model where F^M – muscle force, F^T – tendon force, α – pennation angle of the muscle, (l^T) – tendon length, (l^M) – muscle length (Zajac, 1989, Delp, 1990, Hoy et al., 1990a, Abernethy et al., 2013).

Force will be finally transmitted through tendon to move the joint and tendon force would be equal to fibre force multiplied by the cosine of the pennation angle:

$$F^T = F^M * (\cos \alpha)$$

The pennation angle of gastrocnemius muscle changes with fibre length change as shown in figure 4.16.

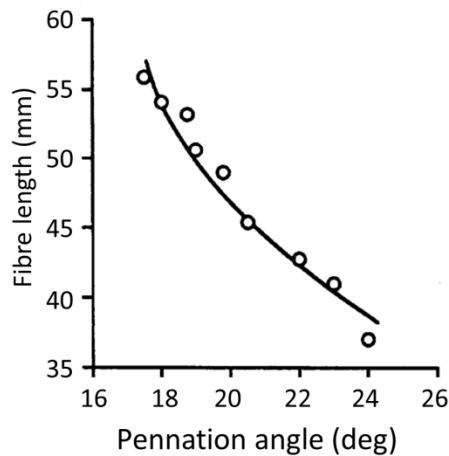


Figure 4.16: Medial gastrocnemius pennation angle relationship with fibre length at rest (Narici et al., 1996).

4.3.6 Muscle contraction

The term ‘muscle contraction’ refers to the development of tension within the muscle by changing length of the fibres (Barlett, 2007). Within the sarcomere, the force generation is performed by interaction between the thin and thick filaments. This means that both filaments slide against each other which causes a reduction of the sarcomere length. There are special terms that have been used to describe the length changes in muscle fibres when the muscle is activated.

Isometric contraction is termed when muscle force results in no movement visible of the bones. The internal tension generated by the muscle is equal to the external force and so balance is achieved (Everett, 2010).

Isotonic contraction is subdivided using the terms *concentric* and *eccentric*. *Concentric* contraction when muscle is shortening or in another words when the active muscle generates an internal force that is greater than external force (Winter, 2009, Trew and Everett, 2005).

Eccentric contraction when and active muscle generates less force than the external load and is lengthened by it.

The amount of oxygen demand during muscle activity varies according to the type of contraction. These characteristics are demonstrated in table 4.2.

Table 4.2: The characteristics of three types of muscle contraction [adapted from (Trew and Everett, 2005)].

Type of contraction	Function	External force (relative to internal)	External work by muscle	Force generated	Energy cost (oxygen demand)
Concentric	Acceleration	Less	Positive	Lowest	Highest
Isometric	Fixation	The same	None	Intermediate	Intermediate
Eccentric	Deceleration	Greater	Negative	Highest	Lowest

Eccentric muscle contraction in the literature is described as the type of contraction which consumes the least amount of oxygen compared to other contraction types. However, if this is followed by a concentric contraction this would then produce the highest oxygen demand. During both types of contraction, there would be muscle-tendon positions where the muscle is not at its most effective optimal size or position, and therefore the muscle will need to work harder to provide the same force generation and therefore consume more energy, which could result in more oxygen demand. Therefore, any footwear, which could influence muscle to act more as an isometric contraction and keep the muscle-tendon length at its optimal position (force generation efficient in relation to cost), would be ideal to reduce oxygen usage by the calf muscles. This means that the utilisation of different footwear features may have the potential to alter muscle force generation by altering the position of the muscle, its type of contraction and the velocity of contraction in order to affect muscle oxygen demand and the amount of power required to ambulate for specific muscles. Once this is more fully understood, it may be possible to also more fully understand how the type of muscle contraction can be altered to achieve a desirable effect using specifically-designed footwear.

4.3.7 Force-length relationships of muscle fibres

For a single sarcomere, the amount of tension it develops when it is stimulated to contract depends on its length. The force capacity of one sarcomere is very low. One million cross-bridges are able to produce a force of just 0.001 N, therefore the overall amount of force is

related of the ability of the muscle fibre to provide a tremendous number of cross-bridges. There is also the important factor of the length for the sarcomere unit in relation to force generation. Muscle force varies as a function of initial sarcomere length, based upon the amount of myofilament overlap (Rose and Gamble, 2006, Winter, 2009, Hong and Bartlett, 2008). At resting size, it can generate its maximum force. Sometimes muscle can be stretched or shortened and therefore it may recruit more muscle units to produce the required force. The ideal concept for footwear design to offload/load calf muscle would therefore be to manage the control of muscle-tendon length during stance phase to achieve the desirable effect. A representation of the tension produced by a sarcomere unit as it changes length about its resting length is shown on figure 4.17.

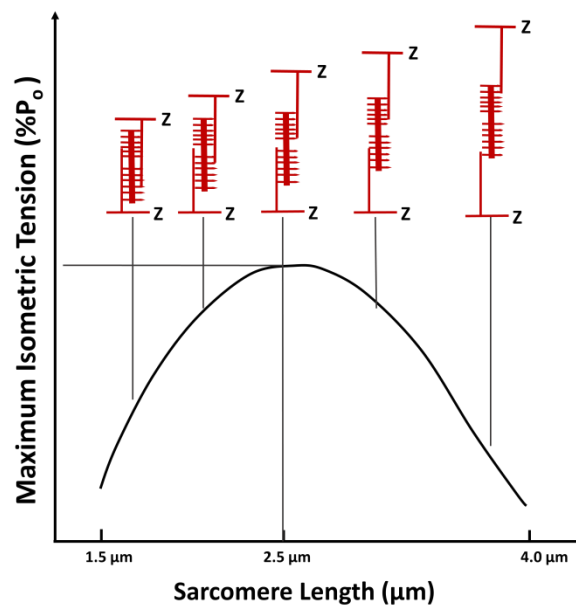


Figure 4.17: The sarcomere isometric length-tension curve [adapted from (Winter, 2009, Hong and Bartlett, 2008, Rose and Gamble, 2006)].

Figure 4.18 shows different lengths and the corresponding forces. From a sarcomere length of approximate of 3.6 μm onwards, no force can be generated because there is almost no overlap between the actin and myosin filaments. The opposite effect occurs when the length is approximately 1.7 μm (Hong and Bartlett, 2008, Rose and Gamble, 2006). At a sarcomere length of 2.0-2.2 μm a maximum overlapping of the thin and thick filaments results in a maximal force generation.

4.3.8 Force-length relationships (for the entire muscle)

For the entire muscle-tendon complex, the amount of force tension generated depends on the number of fibres recruited, their pennation angle, the velocity of contraction and on the relative length of the entire configuration with the respect of their optimal length (Hong and Bartlett, 2008).

The force developed by the muscle during isometric contraction varies with its starting length. For each muscle there is an optimal length (the length it assumes in the body at rest) at which a muscle can generate maximal active contraction (Delp, 1990, Hoy et al., 1990b, Winter, 2009, Panjabi and White, 2001). It has been shown that muscle develops only 50% of its maximum force when its length is shortened to 85% of its resting length (Panjabi and White, 2001). The connective tissues that surround the contractile elements influence the force-length curve (called the parallel elastic components) act much like an elastic band (Winter, 2009). The summation of all the connective tissues in series with the contractile component, including the tendon, are called the series elastic elements. When the muscle-tendon complex is at resting length or less, the parallel elastic component is in a slack state and is not tense. When the muscle-tendon lengthens, the elastic tension begins to build up in the muscle and tendon, slowly at first and then more rapidly. This is known as passive tension (force). The total tension is the sum of the active and passive tensions and depends on the amount of connective tissues (elastic elements) that a specific muscle-tendon complex has. For single joint muscles, the amount of stretch is less efficient with regards to passive tension when compared to two-joint muscles such as soleus and gastrocnemius. Therefore, the total force generated by two-joint muscles (i.e the sum of active and passive tension) may reach the maximum available tension in the stretched muscle.

Figure 4.18 shows the total (passive and active) tension for a muscle-tendon isometric contraction.

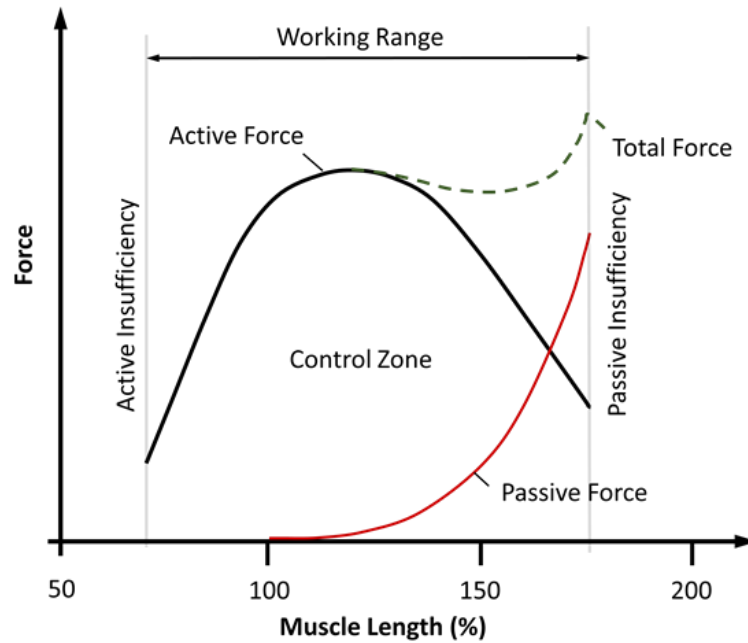


Figure 4.18: Length-tension relationship for the whole muscle during isometric contraction [adapted from (Hong and Bartlett, 2008)].

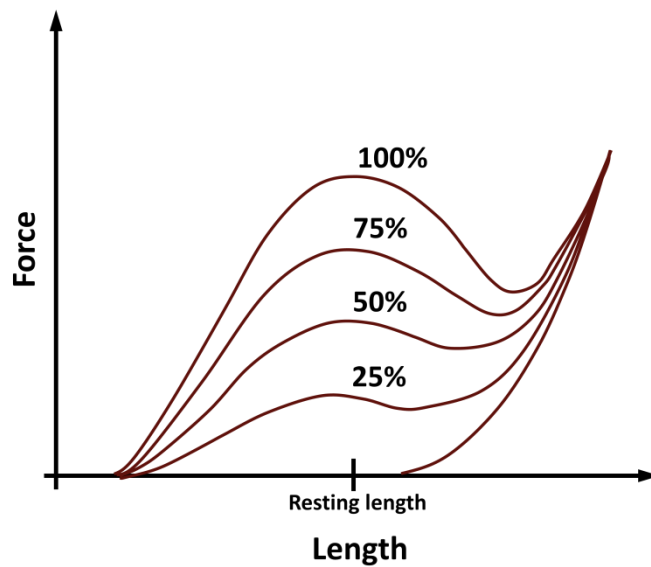


Figure 4.19: Tendon tension resulting from various levels of muscle activation. Parallel elastic element generates tension independent of the activation of contractile element [adapted from (Winter, 2009)].

The typical overall force-length characteristics of an MTU as function of the percentage of excitation is shown in figure 4.19.

Arnold et al (2010) recently published the mechanical properties and architecture of lower limb muscles obtained from 21 cadavers (table 4.3) where PCSA represents their physiological cross-section areas, and where optimal fibre length denotes the resting size of the fibre at which it can generate maximum tension.

Table 4.3: Muscle architecture parameters of 21 cadavers (Arnold et al., 2010).

Muscle	PCSA (cm)	Peak force (N)	Optimal fibre length (cm)	Tendon slack length (cm)	Pennation Angle (°)
Biceps femoris long head	11.6	705.2	9.8	32.2	11.6
Rectus femoris	13.9	848.8	7.6	34.6	13.9
Soleus	58.8	3585.9	4.4	28.2	28.3
Tibials anterior	11.0	673.7	6.8	24.1	9.6
Gastrocnemius medial head	21.4	1308.0	5.1	40.1	9.9

Tendon slack length is the length of tendon at which force begins to develop when stretched. This data can be used to calculate the maximum force of the entire muscle system and it can also be used to aid the development of gait analysis simulation software such as OpenSim to estimate the effect of gait alterations on muscle-tendon properties. It also means that this muscle-tendon unit position is the best to generate internal muscle force to perform the task with the less muscle work done.

The maximum force (F_{max}) for the whole muscle may be calculated as:

$$F_{max} = PCA * K$$

Where PCA is the physiological cross-section area and K is a constant (20 to 100 N*cm⁻²).

For pennated muscles, PCA is calculated as:

$$PCA = \frac{m * \cos\alpha}{\rho * L}$$

Where m is the mass of the muscle, ρ is its density (1.056 g*cm⁻²), L is the length of the muscle fibres and α is pennation angle of the muscle (Winter, 2009).

4.4 Comment

If a footwear test condition were designed to potentially keep the ankle plantarflexors at their optimal length during a powerful isometric contraction, this would be the most efficient tension, which would result in less muscle unit recruitment and therefore less oxygen consumption. It may not be comfortable for older people with IC to stretch their calf muscles by wearing an extremely negatively-pitched shoe in order to produce enough passive elastic force to achieve efficient tension generation in the calf muscle in order to reduce oxygen consumption. This would also alter their typical normal gait resulting in joint angle alterations in the knee, ankle and hip joints. Stretching the calf muscle would produce greater ankle dorsiflexion and would also cause different changes in knee angle. Dorsiflexion tends to be greater with a flexed knee than with it extended because of the influence of the gastrocnemius, which crosses both the ankle and knee joints. When the knee is flexed, the gastrocnemius is slacker at the knee, allowing it to stretch more at the ankle, and if the knee is extended, the gastrocnemius is more stretched proximally, allowing it to stretch less at the ankle [this is known as passive insufficiency - (Alter, 2004)].

A negative heel may therefore not be able to produce significant elastic force as the knee could adapt to the walking pattern by being flexed to facilitate more comfortable walking. Soleus is a postural muscle and stretching it may not improve posture control. The other factor is ageing. As a result of ageing, elastic fibres lose their resiliency and undergo various other alterations (Bick, 1961). When the ankle is dorsiflexed, it has a smaller gastrocnemius muscle moment arm with respect to the ankle joint centre, and it may also reduce internal moment generation about ankle joint even if elastic energy is high.

There is also evidence to suggest that older subjects tend to reduce their walking speed and it consequently reduces their soleus muscle length during the entire stance phase (Panizzolo et al., 2013). In one study, eight healthy subjects (aged 25.8 ± 3.5 years) and eight healthy older adults (66.1 ± 2.3 years) were compared by analysing their natural walking speed and matched walking speed in relation to soleus muscle lengthening using ultrasound and a motion analysis system in the gait laboratory. Natural walking speed for older subjects was reduced by 20% compared to healthy subjects. Also, because of walking speed adaptation, the kinematic data, EMG and soleus length data were very similar between elderly and young subjects (everyone walked with the comfortable their own walking speed). However,

when older subjects adjusted their walking speed to that of the younger subjects (20% faster), there were significant differences in soleus muscle lengths. For the older population, the soleus muscle was significantly stretched throughout the whole gait cycle as shown on the figure 4.20.

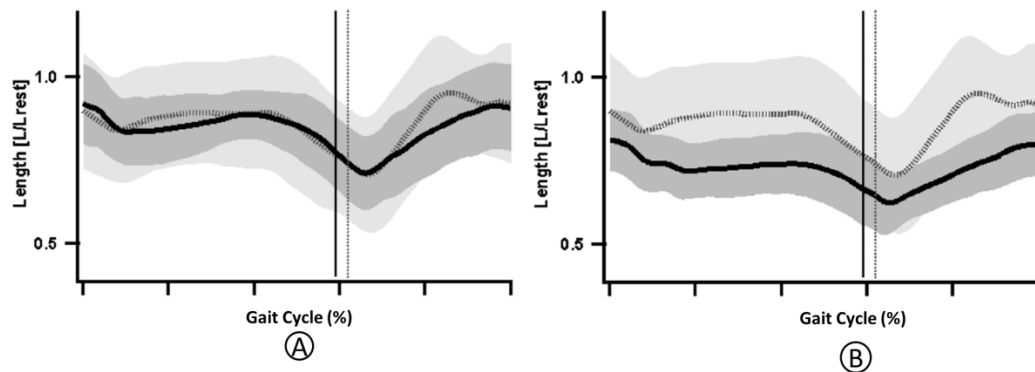


Figure 4.20: Comparison of normalised soleus muscle length between young adults (YA) and old adults (OA) during walking: (A) – preferred walking speed in YA and OA, (B) matched walking speed between YA and OA [adapted from (Panizzolo et al., 2013)].

These results suggest that older people tend to reduce stretching their soleus muscle by slowing down their walking speed to keep optimal length and sustain a more natural gait pattern similar to younger people (Panizzolo et al., 2013). This could be due to muscle architecture changes related to the muscle aging process (for example, muscles tissues become stiffer) and older people tend to reduce soleus muscle stretching to compensate this effect.

Further research which used the simulation software OpenSim and a newly developed muscle architecture data model, has demonstrated that with increasing walking speed, a reduction in soleus force generation is demonstrated (Arnold et al., 2013). Therefore, stretching muscles and walking faster would affect soleus force generation in elderly subjects and it could therefore be suggested that negative-heeled footwear may not be a good option to offload calf muscle by generating additional passive force (elastic energy) for elderly people and subjects with PAD. It is also unclear how calf muscle stretching adaptation can affect knee extension/flexion in relation to passive force generation by the ankle during walking and also muscle architecture changes for patients with IC in relation to walking pattern adaptation. Delp in his PhD demonstrated how elastic and inelastic Achilles

tendon tissue can affect the active and passive soleus force curves in relation to ankle angle as shown in figure 4.21.

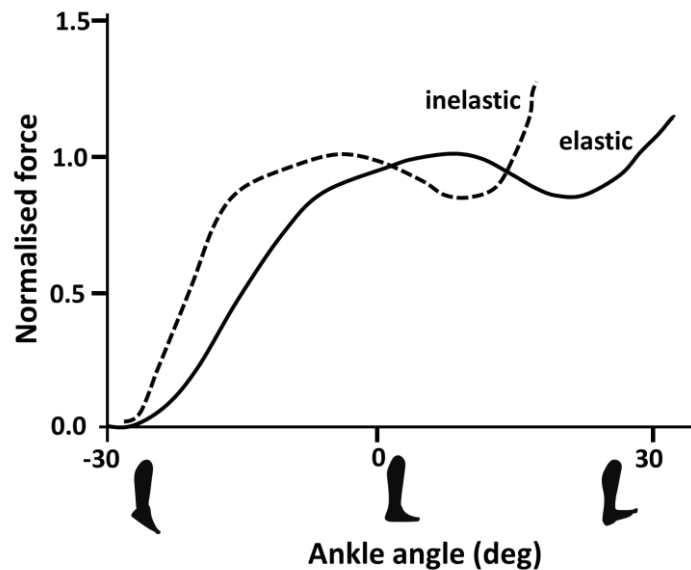


Figure 4.21: Active plus passive soleus forces versus ankle angle with elastic and inelastic tendon. The solid black line was calculated with nominal tendon elasticity. The dotted black curve shows the effect of making the tendon inextensible.

Figure 4.21 shows that if tendon and fibres are less stiff, this tends to decrease the slope of the force versus angle curve during stretching of the Achilles tendon for the soleus muscle. From the picture above it is visibly clear that for a stiffer soleus MTU, more force would be generated when it is slightly plantarflexed and for an elastic muscle-tendon complex, it would be higher when it is stretched. It is known that the aging process is related to decreased muscle and tendon elasticity and they become stiffer compared with a young healthy population (Abernethy et al., 2013). These are contributing factors to the loss of joint range of motion. Therefore, ankle force generation for older subjects in relation to the level of ankle plantar/dorsiflexion would be different versus a younger population. Another study has demonstrated that in an older age group of females, peak active and passive torque values occurred at a relatively more plantarflexed joint angle (Gajdosik et al., 1996).

This would all suggest that the muscle architecture for older subjects with specific complications or diseases should be studied in more detail to understand this relationship to ensure that an appropriate footwear rocker sole profile can be prescribed.

4.4.1 Force-velocity relationship

The force developed by a specific muscle depends upon its length and critically on its velocity of contraction (Panjabi and White, 2001, Arnold et al., 2013), figure 4.22.

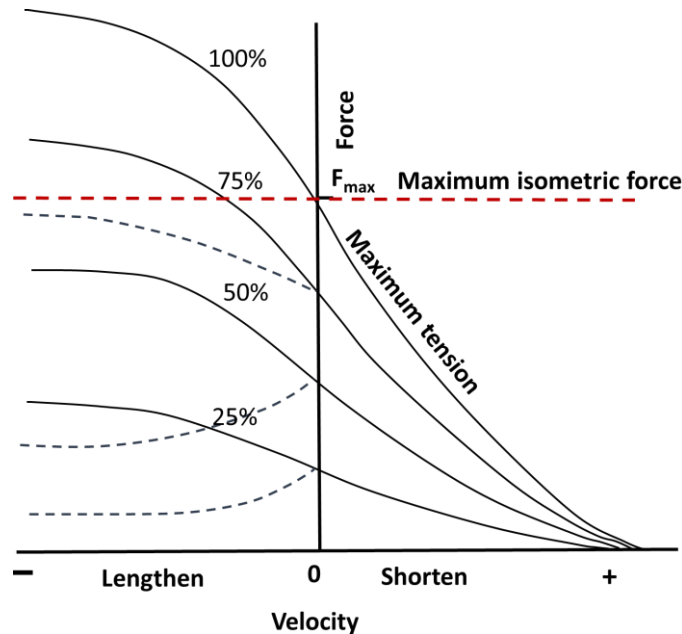


Figure 4.22: Force-velocity characteristics of skeletal muscle for different levels of muscle activation: shown as 25%, 50%, 75%, and 100% levels of activation [adapted from (Winter, 2009)].

The usual force-velocity muscle length curve is plotted for a maximum (100%) contraction. However, this condition is rarely seen in clinical practice and is reserved for athletes.

It has been demonstrated that increasing walking speed is linked to increasing fibre shortening velocity in musculoskeletal simulations of the soleus and gastrocnemius muscles (Arnold et al., 2013). A faster walking speed has also been shown to decrease peak gastrocnemius and soleus muscle force generation (Neptune and Sasaki, 2005), but interestingly generates greater EMG activity of the gastrocnemius muscle compared to when subjects walk slower (Chiu and Wang, 2007, Sousa and Tavares, 2012, Neptune and Sasaki, 2005). The results of previous studies therefore suggest that with increasing walking speed, the velocity of contraction changes along with muscle length. Force generation of the calf muscle is reduced but force which is required to perform the task is increased, thus it increases the calf muscle EMG activity. When subjects switch to a running gait, shortening velocity is decreased and gastrocnemius force generation is increased. It may therefore be

suggested that this is related to muscle length, the velocity of muscle contraction and the length of the muscle moment arm (which will be discussed later in this chapter). This indicates that it is better if all subjects are tested with the same walking speed during research protocols in order to ensure that walking speed would not affect the data results whilst walking in different footwear conditions. It would help to understand more precisely the alteration to walking patterns and MTUs caused by footwear features without additional factors, which may influence the biomechanical data.

4.4.2 Isometric force

The force generated by a muscle is proportional to the contraction time and the longer the contraction time, the greater is the force generated, up to the point of maximum tension. Slower contraction leads to developing greater force, because increased contraction time is required for the tension created by the contractile components to be transferred. However, the tension production in the contractile component can reach a maximum in as little as 10 but up to 300 milliseconds may be needed for that tension to be transferred to the elastic components (Nordin and Frankel, 2003). Figure 4.23 demonstrates the relationship for a force-time curve for the whole muscle contracting isometrically.

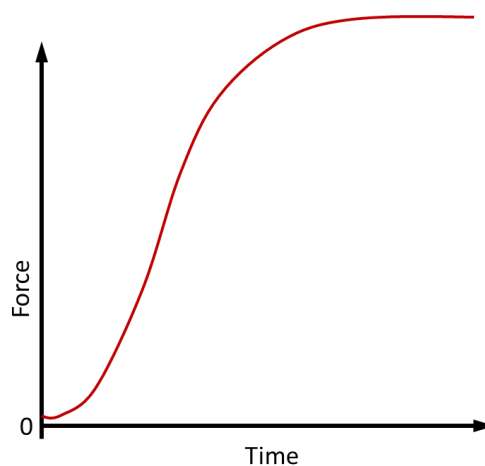


Figure 4.23: Force-time curve for a whole muscle contracting isometrically [adapted from (Nordin and Frankel, 2003)].

4.4.3 Development of tension in a muscle

The literature suggests that the main factors responsible for the force generation in a muscle depend on such parameters as:

- The number of fibres recruited and their firing rate and synchrony;
- The physiological cross-section area of the muscle;
- The optimal muscle length (with an optimal pennation angle) and for some muscles elastic energy can have a significant effect;
- The mechanical properties of the muscle such as the length-tension relationship, and velocity;
- The fibre length: short fibres produce more force and long fibres produce less force.

There are other factors such as the temperature of the muscle and muscle fatigue which can both affect muscle performance (Barlett, 2007). The force which is produced by the muscle is transmitted through tendon to the joint and therefore the muscle moment arm has a significant impact on the internal moment generation by muscles.

There are many other factors, which can influence these parameters which will be discussed in the next sections such as age related changes in muscles, moments, and how footwear features can influence muscle-tendon properties.

4.5 Ankle muscles mechanics and properties for gastrocnemius (GAS), soleus (SOL), tibialis anterior (TA)

Tibialis anterior (TA) contributes over 50% of the total dorsiflexion moment over the entire range of ankle motion (Delp, 1990). The gastrocnemius, the most superficial calf muscle, comprises of two portions, or heads, and forms the greater bulk of the calf. The soleus is a postural muscle, and is a flat muscle situated immediately deep, or anteriorly, to the gastrocnemius. Together they form a muscle group called the triceps surae, which contributes 90% of the total plantar flexion force of the posterior calf muscles (Alter, 2004). Since gastrocnemius and soleus have short fibres relative to their moment arms, the fibres change length (force) significantly as the ankle is moved (Delp, 1990). The triceps surae connects to the Achilles tendon, which is the largest and strongest tendon in the body. The

distal end is attached to the posterior surface of the calcaneus. Although it is the strongest tendon, it can be injured. The most common injury to the Achilles tendon is tendinitis, mainly caused by overuse. Footwear features could feasibly be designed to effect walking patterns and therefore to potentially aid in the recovery of an Achilles tendon injury by offloading it during rehabilitation. Gastrocnemius and soleus muscles for the average adult (i.e. not athletes) comprise of different fibre types. Slow twitch fibres (type I) which are mainly used for postural control is primarily used in soleus muscle. It also contains a high amount of oxidative fibres (Alter, 2004, Abernethy et al., 2013).

It is known that patients with IC experience pain in the calf region due to vascular complications, which results in an inadequate oxygen supply to the calf muscles. Theoretically, if footwear could be designed to offload the soleus muscle (type I muscle), it should increase pain-free walking distance, and also improve (train) the cardiovascular system. There could be benefits related to aerobic exercise and muscle performance that improve overall oxygen consumption, its delivery and muscle tissue as well as nutrition storage.

The gastrocnemius muscle provides forceful contraction and contains a high proportion of fast twitch muscle (Type II). Regular strength training of the gastrocnemius muscle could theoretically build up more muscle fibres and store more nutrition for muscle performance provided the blood vessels grow with it. Thus, footwear, which makes muscle work harder, may be a good way to strengthen gastrocnemius and could be used for short periods of walking as an adjunct therapy to strengthen the ankle plantarflexors.

Knowledge of muscle fibre types is therefore important for several reasons:

- IC patients suffer from oxygen supply deficiency to the triceps surae muscle group. It may therefore help to understand what level of oxygen usage each muscle needs and which one can be trained or offloaded with a rocker shoe and/or training programs which could be targeted for subjects with vascular complications;
- It may also help to understand what kind of footwear could be developed for IC patients.

The triceps surae's critical phase of walking cycle is the push off phase. At this time, the gastrocnemius and soleus muscles are heavily activated in order to push the centre of mass of the body forward and upward just before the heel strike of the contra-lateral leg. Recent analysis has shown that gastrocnemius and soleus both develop their peak force at the same time during the push off phase (Abernethy et al., 2013). The peak force that can be generated by GAS is around 900N, whereas the peak force in SOL is around 2000N. However, the maximum peak isometric force is around 3500N generated by SOL and around 1350N generated by GAS (Arnold et al., 2010).

4.5.1 The Achilles tendon moment arm

The range of joint angles over which a muscle can develop active force depends on its fibre length and moment arm. The change in muscle-tendon length with joint angle depends on the moment arm. For a given range of a specific joint, muscle-tendon excursion increases with the moment arm. Thus, the ratio of a muscle's fibre length to its moment arm determines the range of joint angles over which the muscle can develop active force (Delp, 1990, Hoy et al., 1990b).

The Achilles tendon moment arm length increases when the ankle moves from a dorsiflexed into a plantarflexed position (Nagano and Komura, 2003, Maganaris et al., 1998a). A study investigating alteration to the Achilles tendon moment arm with respect to the ankle joint centre using MRI scanning has shown that its length changes (i.e. increases) from 4.4 cm to 7 cm between -15° to $+30^{\circ}$ of plantarflexion (Maganaris et al., 1998a). This is one of the crucial factors for power generation and alteration to MTU moments about the ankle. Even if the triceps surae muscle force is high, if the moment arm is small, then this will cause a reduction in the internal ankle moment generated by the calf musculature. Therefore, it is crucial that MTU-joint centre moment arms be optimised and considered as one of the factors when deciding on the position the ankle joint needs to be in to reduce the work done by the calf muscles.

4.5.2 Optimal pennation angle for gastrocnemius and soleus during dynamic movement

Muscle fibre pennation angle is an important parameter with regards to musculoskeletal function (force generation). Recent developments have used ultrasound to measure muscle pennation angle and simultaneous EMG during isometric contraction of the gastrocnemius muscle. The pennation angle for the gastrocnemius muscle varies between 14° to 20° during isometric plantarflexion (Zhou et al., 2012). Maximum torque is produced at a pennation angle of around 18°. It was also noticeable from the graphs that with higher values of pennation angle, EMG was significantly higher too. With low values pennation angle was significantly lower, however tendon force is equal to fibre force multiplied by cosine of muscle pennation angle. If the pennation angle is less it consequently should increase force transferred to the tendon. However, the results suggest that the muscle produce more active force when it is shortening. Further research with MRI scanning has shown that by lengthening muscles fibres, pennation angle is reduced (Narici et al., 1996). This would help to transmit elastic force to the joint; however the muscle moment arm may be short and it may reduce the effect. It is therefore interesting to test different heel heights in footwear designs in order to understand relationships between alteration to muscle-tendon lengths, and muscle moment arms in relation to EMG and ankle moments in the lower limb.

Another study using ultrasound has calculated the pennation angle values for the gastrocnemius, soleus and tibialis anterior muscles (see table below) at rest and at maximum voluntary contraction for male and female adult subjects (Manal et al., 2006).

Table 4.4: Pennation angle measured at rest and maximum voluntary contraction for the right (R) and left (L) legs of male and female subjects. Pennation angle is reported as degrees with standard deviations in parentheses (Manal et al., 2006).

	Tibialis Anterior (TA)				Lateral Gastrocnemius (LG)				Medial Gastrocnemius (MG)				Soleus (Sol)			
	Male		Female		Male		Female		Male		Female		Male		Female	
	R	L	R	L	R	L	R	L	R	L	R	L	R	L	R	L
Rest	9.4 (2.2)	9.3 (1.4)	8.7 (1.0)	9.1 (1.0)	13.7 (4.2)	12.8 (2.4)	12.3 (3.3)	11.1 (3.4)	18.7 (2.7)	18.6 (3.3)	15.7 (2.3)	16.2 (1.6)	20.6 (7.4)	19.3 (4.6)	14.3 (4.3)	16.4 (3.8)
MVC	14.7 (2.3)	14.0 (2.2)	12.1 (1.4)	12.1 (1.5)	23.4 (8.9)	24.0 (10.6)	15.2 (3.8)	17.4 (5.5)	34.9 (6.4)	34.3 (7.3)	27.5 (5.5)	27.1 (7.4)	40.4 (7.6)	39.9 (7.8)	25.3 (8.4)	27.3 (7.5)

Optimal pennation angle angles of 8 males and 8 females for the GAS, SOL, and TA muscles were calculated. Joint angles were chosen to control muscle tendon lengths so that the muscles were near their optimal length within the length-tension relationship (figure 4.24).

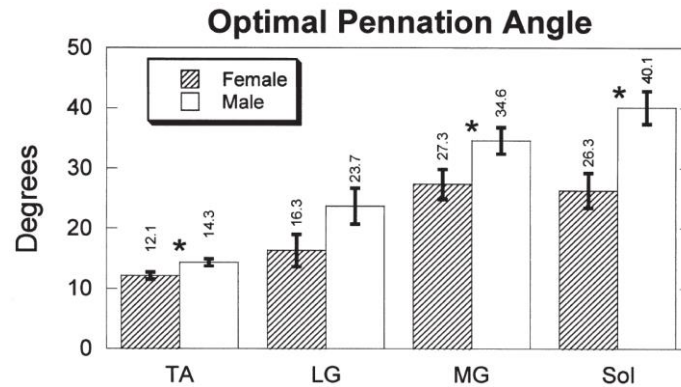


Figure 4.24: Mean values of optimal pennation angle with standard deviation for tiabialis anterior (TA), lateral and medial gastrocnemius, and soleus muscles (Manal et al., 2006).

Further ultrasound research has produced detailed measurement of the triceps surae complex architecture in six males across the muscle belly at rest and during maximum voluntary contraction trials at angles of -15° (dorsiflexion position), 0° (neutral position), $+15^{\circ}$ and $+30^{\circ}$ (plantarflexion position) (Maganaris et al., 1998b). The results demonstrated that pennation angle increases when the ankle is plantarflexing and GAS and SOL muscle fibres are shortening. Therefore, it is unclear which is the best ankle position to produce an optimal ankle moment force that would recruit less motor units to generate the internal moment by the ankle and therefore theoretically produce less oxygen consumption. This thesis was therefore designed to investigate this question using ambulatory activities with regards to footwear design by testing different footwear features, collecting kinematic, kinetic and by analysing muscle-tendon property data (lengths, velocities, Achilles moment arm) and EMG signals.

4.6 The effect of footwear features on muscle parameters

4.6.1 Introduction

Spanish cave drawings from 15,000 years ago show that people wore some kind of footwear in very ancient times (Kurup et al., 2012). The first custom-made shoes can be traced back to approximately 5500 years ago (Ravindra, 2012). Today footwear forms an integral part of our outward appearance and is also used as a functional and protective tool for walking in the modern environment. Despite this, little is known regarding the effect of footwear design on lower limb muscle function and its implications in altering gait parameters for the potential benefit of people suffering from different pathologies; especially those which affect lower limb muscle function. This chapter investigates the available evidence and discusses the biomechanical effect of different footwear features on the action of muscles such as the triceps surae group which act on the ankle, and forms subsequent hypotheses with regards to their effect on specific parameters. The chapter concludes with four over-arching hypotheses which informed the methodology and led to the subsequent results and discussion chapters.

Three specific regions of the shoe were targeted when analysing evidence available in the literature. These were:

- The rearfoot portion;
- The midfoot region, and;
- The forefoot and toe region.

The impact of the applied GRF, which can affect lower limb muscle activity, may be manipulated and altered through wearing shoes with altered heel height, varying hardness of the midsole or outsole unit and also by changing the overall shape and pitch of the shoe. The literature suggests that these parameters can alter lower limb muscle activity in conjunction with the applied external forces, as well as kinematic and kinetic data and muscle-tendon properties, and therefore can potentially change the overall work done by lower limb muscles.

Footwear can have significant effects on the musculoskeletal system and this has therefore been the subject of interest in the literature, especially with regards to lower limb muscle activity during walking (Ravindra, 2012). However, there has been little research which has investigated how footwear features change muscle-tendon properties and function in relation to force generation when walking with different rocker-soled shoes. Muscle-tendon lengths and their velocity of contraction has a significant effect on muscle force generation (Zajac, 1989, Hoy et al., 1990b, Delp, 1990) and this is therefore of interest in this thesis.

The next sections give a short analysis of the biomechanical effects of walking in shoes with various heel heights, different rocker sole apex positions relative to the length of the shoe, different apex angles, the effect of negatively-curved heels and variations in sole flexibility.

4.6.2 Rocker sole designs, alteration to heel height and their biomechanical effect

Various rocker soles designs have previously been prescribed for different pathologies and rehabilitation programs in an attempt to alter muscle working patterns, limit motion in the ankle during stance phase, or reduce pressure distribution over specific areas (Hutchins et al., 2012, Richardson, 1991, Romkes et al., 2006, Shakoor et al., 2008, Viswanathan et al., 2004, Yung-Hui and Wei-Hsien, 2005).

The actual shape of the sole unit varies in the literature according to the biomechanical effects required to be achieved, and the pathology presented. Some examples where rocker soled shoes have the potential to be used or have already been used as an orthotic intervention are:

- To improve gait performance in sport and medicine;
- To redistribute plantar foot pressures for subjects with diabetic peripheral neuropathy;
- To improve the rehabilitation of the Achilles tendon injuries;
- To improve the efficacy of rehabilitation programs in reducing pain in the ankle, knee, hip and back;
- To provide compensation for weak muscles or altered gait patterns, and to train or offload muscles to influence the work done by them;
- To alter gait parameters to make walking more efficient;

- To reduce energy expenditure, and improve comfort during walking.

Improved performance relies on efficient transformation of mechanical power output produced by the musculoskeletal system through footwear design. Understanding the biomechanical implications of different rocker-soled shoes can help ensure that the appropriate footwear selection/prescription for people with different pathologies can be made and it may also assist in the understanding of causes of lower limb injury. The following section will describe the basic biomechanical effects on specific lower limb muscles caused by different footwear features.

4.6.3 Alteration to heel height

High-heeled shoes are extensively worn by women and are influenced by fashion trends. This type of footwear has been associated with a range of foot deformities. High heel shoes can increase forefoot plantar pressures, increase loading to the toes, (especially the first metatarsal head), increase the activity of leg muscles to maintain balance and increase the activity of muscles of the lower spine. They also alter posture and gait, cause muscles to fatigue and cause pain, induce kinematic and kinetic changes, increase the risk of ankle sprains, increase anterior pelvic tilt and reduce walking speed (Ravindra, 2012, Mika et al., 2012, Stefanyshyn et al., 2000, Gefen et al., 2002, Gehlsen et al., 1986, Esenyel et al., 2003). However, high heeled shoes also have a 'benefit' in so far that they produce a positive cosmetic effect by making the legs and look slimmer and longer, and make the feet appear smaller.

Conversely, negatively-heeled shoes increase the internal PF moment, cause premature activation of the calf muscles, and place the ankle in a more dorsiflexed position during walking. They therefore stretch the triceps surae muscles and are therefore not suitable for people with Achilles tendon injuries (Li and Hong, 2007, An and Lee, 2007).

4.6.3.1 The effect of heel height on EMG activity

The effect of different heel heights on muscle activity by using EMG analysis has been investigated in several studies. The results of these studies are presented in table 4.5.

The existing evidence demonstrates variation in results with regard to EMG activity by increasing heel height, and does not clearly justify why muscle activity is increased or decreased. This is because it is unclear what causes EMG activity to be higher or lower in magnitude by altering the heel height. Gastrocnemius activity was shown by Lee et al (1990) to be reduced once the heel height exceeded 5cm, but tibialis anterior was increased once the heel height was less than 5cm. A separate study, however, showed that a 10cm heel increased EMG activity in the GM muscle compared to a 4cm heel height. Soleus increased activity with a 4cm heel compared to a 3.7cm heel. However, negatively pitched heels have been shown to increase gastrocnemius activity.

The alterations to EMG values reported in the literature may have been due to the following:

- The ankle moments and powers may have been altered or the velocity of specific muscle contractions changed due to the different footwear test conditions;
- Alteration to walking speed could have caused these consequential changes in the velocity of specific muscle contractions (Arnold et al., 2013), as velocity of contraction is related to force generation in muscles (Winter, 2009);
- Muscle-tendon lengths may not have been close to their optimal length for certain footwear test conditions or the muscle moment arms were adversely altered by the change in heel height also.

Table 4.5: The effect of heel height on lower limb muscle EMG activity.

Author/s (Date)	Subjects, Age	Footwear features	Task	Muscles (EMG) tested	Main findings
HEEL HEIGHTS					
(Lee et al., 1990)	6 Women Age range: 20-31 years	Barefoot, 2.5 cm heel, 5.0 cm heel, 7.5 cm heel	Walking	Med. Gastroc. Tib. Anterior	Med.gastroc - significantly lower mean peak EMG values with a 2.5 cm and 5 cm heel height when compared to a 7.5 cm heel. Tib. anterior - significantly greater mean peak EMG with a 2.5 cm heel compared to both 5.0 cm and 7.5 cm heel heights. Both muscles showed significantly lower mean peak EMG for all heel heights versus barefoot.

(Stefanyshyn et al., 2000)	13 female subjects Age: 40.6 (±8.3) years	Flat shoe 1.4 cm heel, Low-heeled shoe 3.7cm, 5.4cm heel and 8.5cm heel	Walking at a speed of 1.4 m/s	Gastroc. Soleus	Soleus showed a significantly greater RMS EMG amplitude with 1.4 cm heel versus a 3.7 cm heel. Soleus - significantly greater RMS EMG amplitude with an 8.5 cm heel versus all other shoes tested. EMG using a 5.4 cm heel was greater than 1.4 and 3.7 cm heel heights
(Lee et al., 2001)	5 female subjects Age: in their 20s	0 cm heel, 4.5 cm heel and 8 cm heel	Walking at a speed of 1.1 m/s	Tib. anterior	Peak tib. anterior EMG values were significantly increased with increased heel heights
(Li and Hong, 2007)	13 female subjects Age: 23.1 (±3.9)	Normal shoes plus negative-heeled shoes	Walking	Tib. anterior Lat. gastroc.	Lat. Gastroc and Tib. anterior – significantly greater EMG amplitude in negative-heeled shoes and duration of EMG activity was significantly longer for both muscles when walking in negative-heeled shoes versus normal.
(An and Lee, 2007)	15 male subjects	Flat 15° heel 20° heel	Walking at a speed of 1.33m/s	Tib. anterior Med. gastroc.	Both negative heel shoes showed significant increases in Tib. anterior EMG activity. Both negative-heel shoes showed an increase in peak EMG activity during stance phase but not significantly (p=0.08)
(Mika et al., 2012)	31 female subjects age: 20-25 15 female subjects Age: 45-55	Barefoot 4 cm heel 10 cm heel	Walking (self-selected speed)	Med. gastroc. Tib. anterior	Tib. Anterior- significantly greater EMG amplitude using a 10 cm heel compared to both barefoot and a 4 cm heel. Med. Gastrocnemius significantly greater mean peak EMG in 10 cm heel versus barefoot and 4 cm heel.
(Simonsen et al., 2012)	14 female subjects Age range: 21-38	Barefoot 9 cm heel	Walking at 4km/h	Med. gastroc. Soleus Tib. anterior	Tib. anterior - significantly greater EMG amplitude in 9 cm heel versus barefoot. Soleus – significantly greater EMG amplitude in 9 cm heel and duration of EMG activity was significantly longer. Med. Gastroc – premature activation and greater EMG amplitude during mid-stance for 9 cm heel versus barefoot

The answers to these assumptions are as yet unclear. Muscles produce movement at the joints. The forces which cause the joint to rotate produce the joint moment. External moments are produced by gravitational forces and internal moments are generated by muscles and usually oppose external forces (Kirtley, 2006, Trew and Everett, 2005, Whittle, 2003). Muscle moments or moments about the ankle are calculated as the force (muscle or GRF) multiplied by its moment arm. Therefore, both the length of the moment arm and the magnitude of the force can change the joint moment or moment produced by the muscles. The triceps surae muscle group generate internal plantarflexion (PF) moments (muscle force x internal moment arm), which is opposed by an external dorsiflexion (DF) moment (ground reaction force x external moment arm) as shown in figure 4.25 (Sobhani et al., 2013).

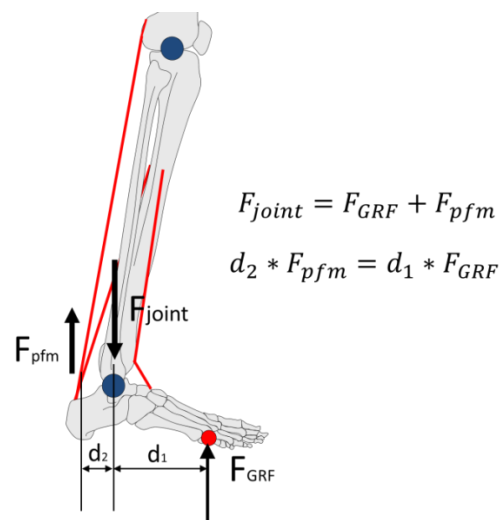


Figure 4.25: An example during stance phase of gait of how the external dorsiflexion moment is opposed by internal plantar flexion moment generated by calf muscles.

From figure 4.25 above, it is clear that changing the muscle moment arm (denoted d_2) and its projected point with the ground would also potentially change muscle force generation. High-heeled shoes place the ankle into a more plantarflexion position than flatter shoes (Simonsen et al., 2012, Esenyel et al., 2003). That would result in an increased Achilles muscle moment arm relative to the ankle joint centre (Nagano and Komura, 2003, Maganaris et al., 1998a). High-heeled shoes have also been shown to decrease the internal ankle moment (Esenyel et al., 2003). Consequently, muscle force magnitude can be increased as the Achilles tendon moment arm is increased until the muscle-tendon length reaches the length at which it loses force generation (Delp, 1990). There is therefore the potential to

influence these two parameters by footwear features so that specific muscles produce more or less muscle force generation depending on the application required.

Correlation between internal ankle moments and the related level of muscle activity at the ankle joint (i.e. the intensity of contraction and rate of motor unit recruitment) is not yet fully understood. For instance, skeletal muscles develop only 50% of its maximum available force when its length is shortened to 85% of the resting length (Panjabi and White, 2001). Figure 4.26 demonstrates that as the moment arm of the point of application of the GRF to ankle joint centre is shortened when the ankle is in plantarflexion, the calf muscles potentially work harder to generate force as their muscle-tendon length is shortened.

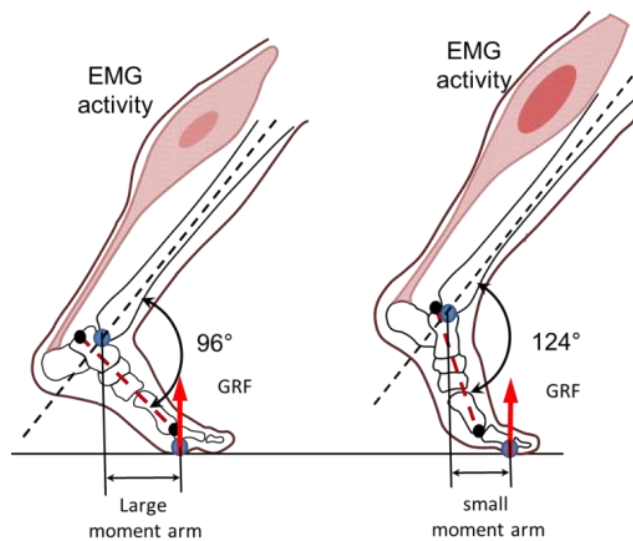


Figure 4.26: A visual example of EMG activity for the calf muscle during standing on the toes [adapted from (Kirtley, 2006)].

4.6.3.2 Heel Height (HH) hypothesis

A feasibility pilot study investigating the effect of walking with shoes with different heel heights was performed for this thesis prior to the main biomechanical testing. It showed that the point of application of the GRF during initial contact can be significantly altered (figure 4.27). These initial results resulted in the following analysis and the hypotheses being formed with regards to the effects of wearing footwear with different heel heights.

When walking with high heeled footwear, the ankle is more plantarflexed and therefore tibialis anterior (TA) muscle is stretched compare to when walking with the flat shoe. This would result in changes to TA muscle work and function.

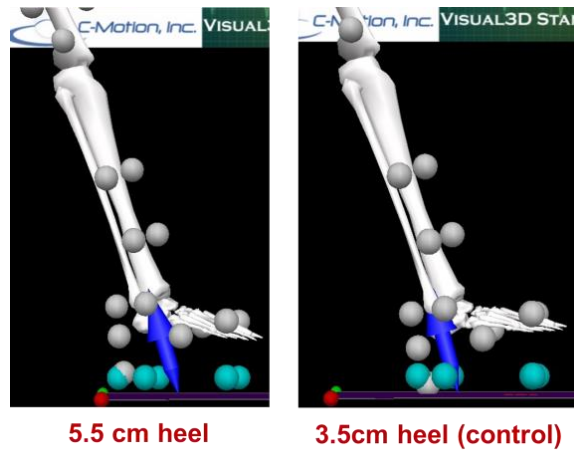


Figure 4.27: GRF point of application data during initial contact (ICt) obtained in a pilot study using visual3D software (C-Motion) for 3.5 and 5.5 cm heel heights.

High heeled shoes when compared to low or negative heels may also change the velocity of TA contraction. For instance, a negative heel would keep the ankle in a dorsiflexed position relative to the ground, but the shank would still rotate forwards. The inclination velocity of the shank relative to the foot would be different in high heel shoes compared to a negative heel. It would consequently increase the eccentric contraction velocity of TA, and EMG activity may be higher in magnitude. Figure 4.28 demonstrates visual differences for negative-heeled and high-heeled shoes during ICt.

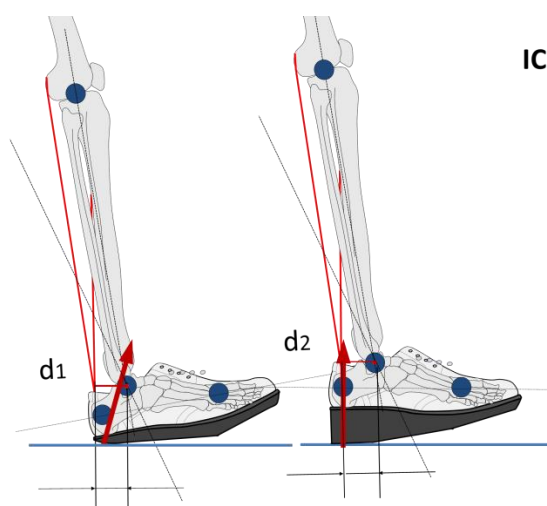


Figure 4.28: Visual example of the position of the foot and ankle at ICt for negative heeled and high heeled shoes (where d_1 and d_2 are the muscle moment arms).

Different heel heights can therefore potentially offload or load the TA muscle and may also cause premature activation of the calf muscles.

The sole thickness directly underneath ankle joint centre can also increase the ankle moment. The moment about ankle in the sagittal plane is calculated as summary of vertical GRF magnitude multiplied by the moment arm, and horizontal force multiplied by the moment arm (Richards, 2008). If the sole is thicker, it increases the vertical moment arm as shown in figure 4.29.

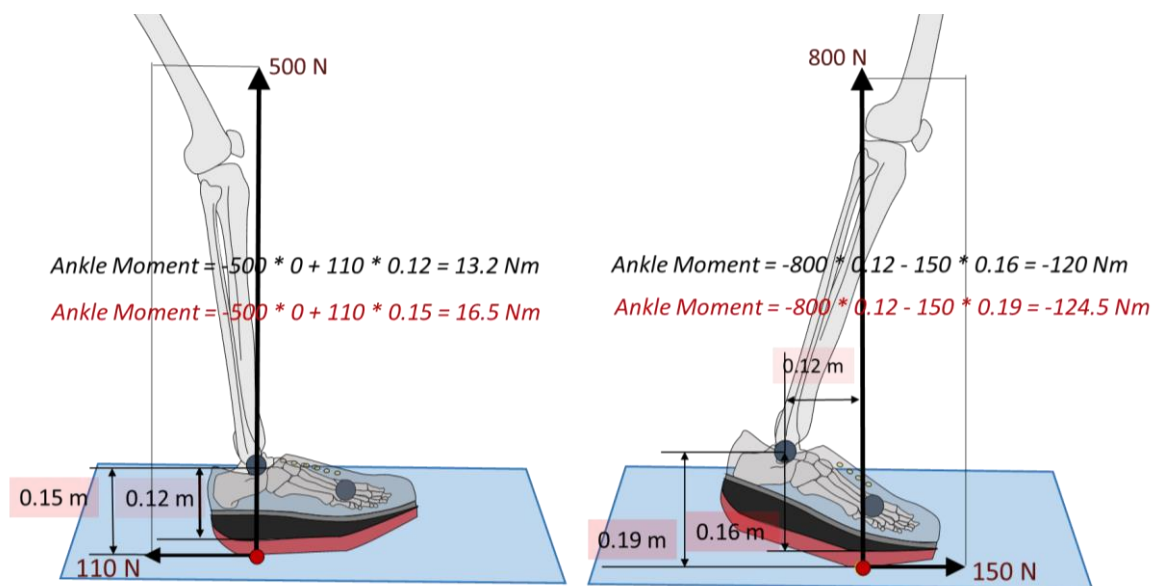


Figure 4.29: An ankle moment calculation example. The red coloured section illustrates the extra sole thickness.

However, a thicker sole may not have a significant effect on the total moment when the point of application of the GRF is moving away from the joint centre.

At mid-stance and terminal stance phases of gait, the triceps surae muscles (attached to the Achilles tendon) may produce varying force when walking with negatively-heeled, flat or high-heeled shoes if participants are walking with the same speed. There are several reasons for this:

- It can increase/decrease the external ankle moment during stance phase;
- It can change the velocity of muscle contractions along with changes to ankle angle;
- It can change passive/active muscle force generation;
- It can place the ankle into a more DF or PF position during stance phase;

- It can alter muscle-tendon lengths during stance phase;
- The calf muscle moment arm can be increased or reduced;
- It can change walking patterns and adaptation mechanisms by other part of the body.

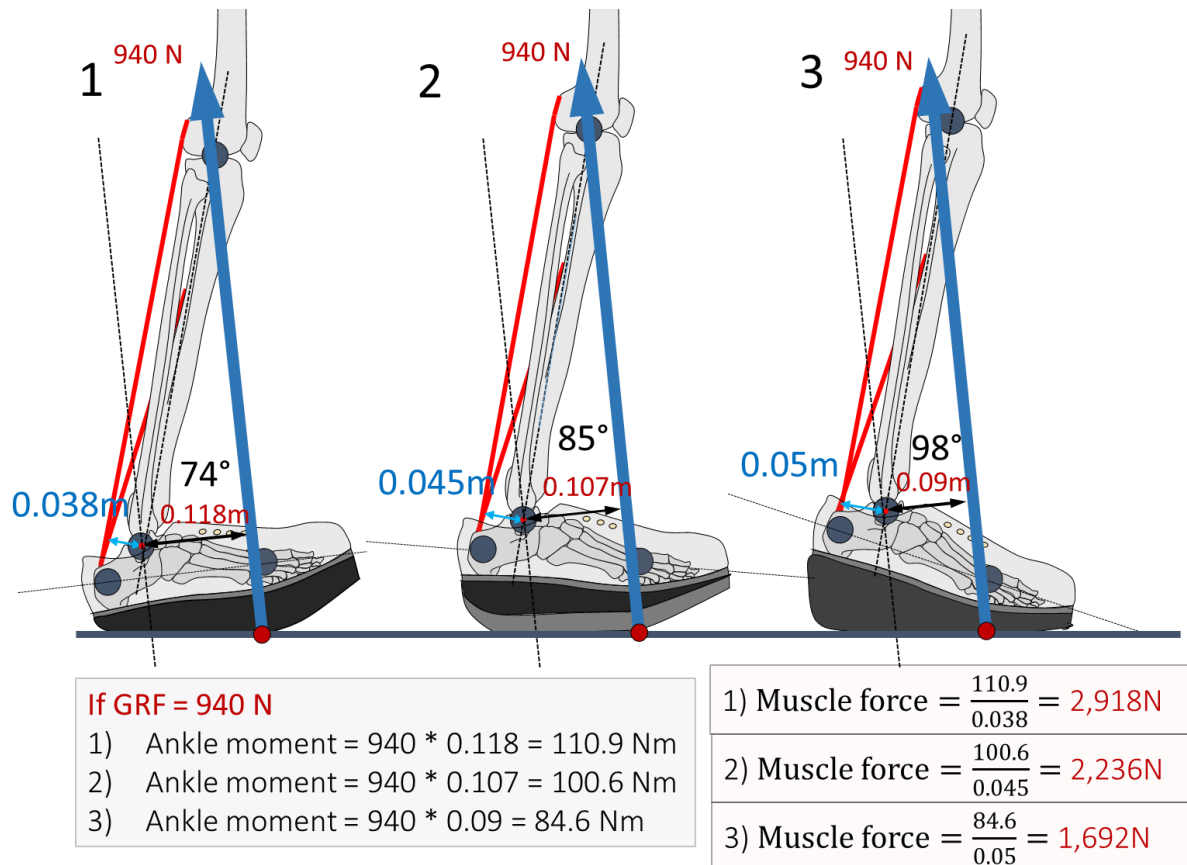


Figure 4.30: demonstrates a simple visual geometrical example of how different heel heights change the ankle position during terminal stance and therefore muscle biomechanics.

From the example above, the results of pilot/feasibility testing show that for a negative-heel shoe, the triceps surae requires around 2,918 N to perform the task, for a flat shoe 2,236 N and for a high heeled shoe 1,692 N. However, for the positively heeled shoe it requires less muscle force, but the muscles can also be shortened by 85% and consequently lose 50% of their force generation and therefore theoretically may require in excess of 3,384 N ($1,692 * 2$) of muscle force to oppose the external DF moment. This example does not include body adaptation such as knee flexion to the shoe. Gastrocnemius muscle length also depends on the knee flexion angle, and the total length can vary with force generation.

The following footwear design parameters were analysed in this study to understand their effect on muscle function:

- Rocker sole apex angle and the apex position (i.e. the position along the shoe at which the outsole begins to curve or angle upwards);
- The effect of altering the stiffness of the outsole;
- Variation in heel height (and therefore also the overall pitch of the shoe);
- Addition of a heel curve (otherwise known as a rolled, negatively-curved or chamfered heel) (figure 4.31).

Only one footwear feature was changed at a time during the gait laboratory testing to demonstrate ensure it was clear which footwear features were responsible for alterations to muscle function.

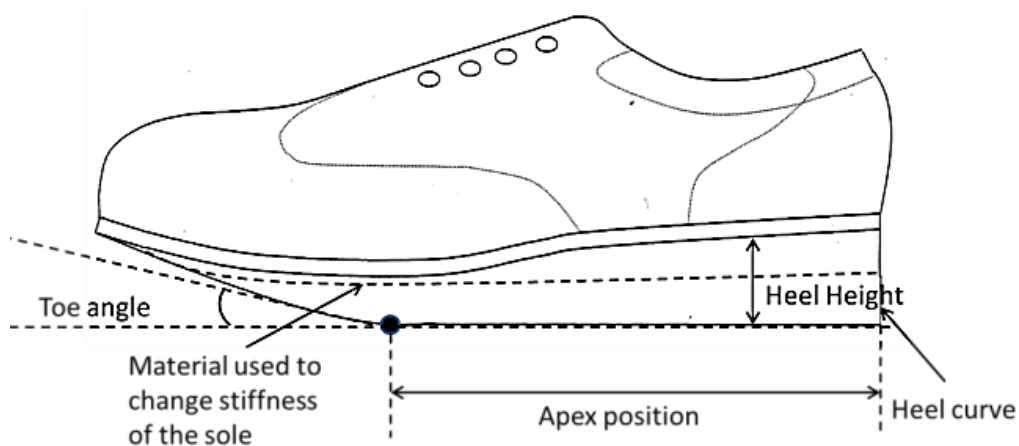


Figure 4.31: An illustration of the footwear features analysed in this thesis.

The methodology section describes in more detail the footwear rocker sole profile selection criteria for this research and illustrates the rocker sole designs, which were tested in this thesis.

4.6.3.3 Possible effects of varying heel height and resulting hypotheses

1. There is a certain heel height level at which the muscle moment arm has an optimal position in relation to the muscle-tendon length during push off phase of gait. A heel height of between 3.0 and 4.5 cm is the estimated heel height at which triceps surae can produce maximum efficient force. This heel height along with other adaptations to the sole could be beneficial in offloading the calf muscles for patients with IC.
2. High heeled shoes may increase triceps surae EMG activity even though the external ankle DF moment is reduced (this should be equal to the internal plantarflexion moment), but the muscle is too short to generate the force required compared when it is at optimal length, therefore the resulting energy cost may be increased with high-heeled shoes.
3. A negatively-heeled shoe may increase triceps surae muscle work, because it may increase the external DF ankle moment, reduce the muscle moment arm and keep the muscles stretched and therefore they may lose force generation. However, the muscles will work harder to compensate for the force required.
4. A negatively-heeled shoe may prematurely activate the calf muscles which will result in increased external ankle moment during loading response and mid stance phase and therefore an increase in EMG muscle activity will result.
5. A negatively-heeled shoe may reduce ankle ROM during loading response as the foot and shoe may not move relative to the ground, but the shank will still incline.
6. A negatively-heeled shoe may reduce the time taken during loading response and also activate mid stance phase earlier due to a more dorsiflexed foot position.
7. A high-heeled shoe may increase ankle plantarflexion during loading response because it may change the point of application of the GRF (more ankle movement could also result, for example a more inclined shank may result in order to achieve a more comfortable ankle position when compared to a low heeled shoe) and this will increase the external plantarflexion moment.
8. A negatively-heeled shoe will stretch the calf muscles and therefore change their velocity of contraction, EMG activity, and keep the ankle more dorsiflexed through the entire gait cycle and also affect the knee and hip.
9. A positive (high) heel will shift the ankle into a more plantarflexion position during the entire gait cycle and therefore change kinematic, kinetic, EMG and muscle function.

4.6.4 Rocker sole Apex Position (AP)

Some studies have been conducted to more fully understand the effect of rocker sole apex positions (APs) on plantar pressures as well as kinematics, kinetics and EMG data (van Schie et al., 2000, Chapman et al., 2012, Sobhani et al., 2013). Two studies have analysed plantar pressures in relation to AP and they have reported results indicating which area was maximally offloaded for a given AP (van Schie et al., 2000, Chapman et al., 2012). Alteration to muscle activity has also been studied by comparing a standard shoe with rocker-soled shoes with APs positioned at 53% and 65% of length from the heel (table 4.6). The results demonstrated no significant difference in gastrocnemius EMG values but significantly greater EMG values for tibialis anterior with the apex positioned at 65% of shoe length.

Table 4.6: The EMG results demonstrated by Sobhani et al (2003).

Author/s (Date)	Subjects, Age	Footwear features	Task	Muscles (EMG)	Main findings
ROCKER SOLE APEX POSITION (AP)					
(Sobhani et al., 2013)	8 females 8 males Age: 29±9	53% shoe length from the heel 65% shoe length from the heel (thicker sole)	Walking at a controlled speed	Med. Gastroc. Lat. Gastroc. Tib. anterior	Med.gastroc – not significant Lat. Gastroc – not significant Tib. anterior significantly greater mean peak EMG with 65% apex position

There were therefore no significant change in triceps surae muscle activity for different apex positions; however, the external DF moment was significantly different for both shoes and a 53% AP demonstrated reduction in mean values for this parameter. These results suggest that calf muscles work less hard according to the ankle moment in a 53% AP shoe, but there were no significant differences in data for their EMG activity. There was not enough evidence to arrive at a definitive conclusion to explain the reason for this. It could have been due to the velocity of contractions, muscle moment arm and/or muscle-tendon length changes. There were also other factors such as different shoe weights ($467 \pm 87g$ versus $805 \pm 157g$), different thicknesses of the sole units (65% AP shoe was thicker by 2.2 cm versus 53% AP) and different shoe sizes (36 to 46). Thicker-soled shoes demonstrated significant increases in mean EMG activity for the tibialis anterior muscle. It may therefore be suggested that it would be better to test shoes with different AP length but with the same thickness of the sole, as similar a weight as possible and similar sizes. Lighter-weight shoes have

demonstrated an improvement in oxygen consumption by 1% for every 100g lost in weight (Williams and Cavanagh, 1987, Morgan et al., 1989). This may also result in less work done by lower limb muscles.

4.6.4.1 Rocker sole apex position hypotheses

Different rocker sole APs may therefore have following biomechanical implications:

1. Shoes with more proximal APs can theoretically cause premature plantarflexion during late stance as shown in figure 4.32.

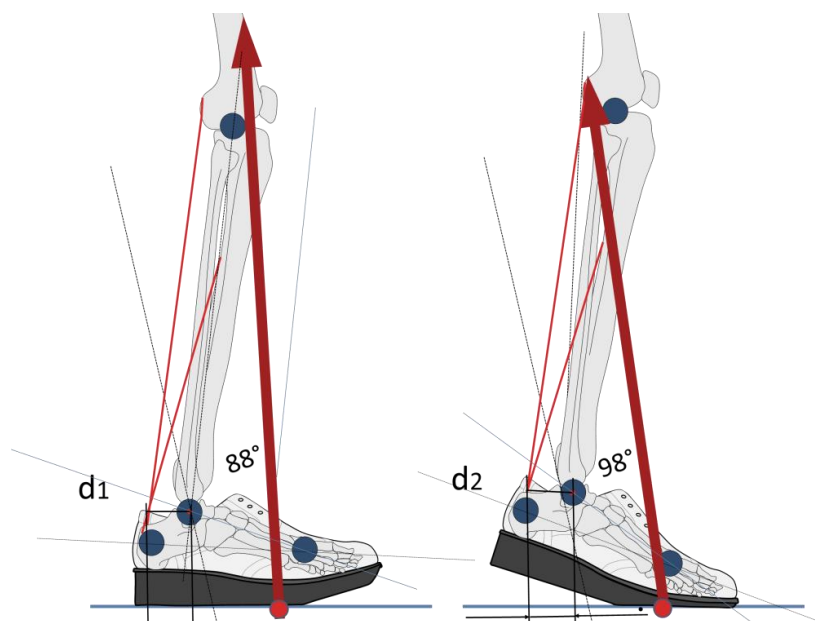


Figure 4.32: An example of walking in shoes with different APs.

This would also change ankle kinematics, moments, velocity of muscle contractions, GRF force direction, muscle-tendon lengths, and muscle moment arms.

2. A short AP length may offload the triceps surae muscles because it may cause premature plantar flexion and therefore keep the ankle at a neural position near to where the muscle-tendon length is optimal, and consequently muscle fibres can generate force without less effort;
3. By increasing AP length of the shoe it may load up the calf muscles as it may resist plantarflexion, and also increase the external ankle DF moment;
4. A short AP may result in reduction of maximum DF and therefore stretch the triceps surae less than were it to be placed more distally.

4.6.5 Shoe forepart flexibility

The foot is naturally a very flexible structure when walking barefoot. The kinematic and kinetic responses associated with barefoot walking, differ from those associated with rocker-soled shoes. There have been many benefits reported related to extremely flexible running shoe designs (Ravindra, 2012). It has been reported that changes can occur in muscle cross-section areas and increased strength after using such footwear for more than 5 months (Bruggemann et al., 2005). It has also been reported that well cushioned shoes reduced oxygen cost by up to 2.8% over stiffer shoes of the same weight whilst running, and may also have some effect during walking (Saunders et al., 2004). With increased shoe flexibility at the metatarsal joint area, a reduction in the load on the Achilles tendon and triceps surae muscle group may be expected as well as reduction in lever arm about the ankle in the sagittal plane (Ravindra, 2012).

Table 4.7: EMG activity with varying shoe stiffness.

Author (Date)	Subjects, Age range	Footwear features	Task	Muscles (EMG)	Main findings
ROCKER SOLE STIFFNESS					
(Kersting et al., 2005)	8 males Age: 27.9±2.3 8 females Age: 23.9 ± 2	Standard shoe with a stiff midsole; Neutral shoe with a flexible midsole; Shoe with soft midsole	Walking	Med. gastroc. Tib. anterior	Med. gastrcnemius – significantly greater EMG with a stiff midsole compared to a soft midsole. Tib. anterior – not significantly altered
(Bohm and Hosl, 2010)	15 healthy males Age: 29±5	Stiff shafted boot; Soft shafted boot.	Walking	Med. Gastroc. Tib. anterior	Med.gastroc – not significant Tib. anterior – not significant

Kersting et al. (2005) investigated three shoes with different midsole stiffness during walking. He showed that increased stiffness of the outsole resulted in significantly greater muscle effort by the gastrocnemius muscle. Bohm et al. (2010) tested two boots; one with a stiff shaft and one with a soft shaft. The results did not show any significant changes in gastrocnemius EMG activity. However, this study mentioned that the stiff-shafted boot decreased the ankle range of motion as well as the eccentric energy absorbed at the ankle

(Bohm and Hosl, 2010). Therefore, the efficiency of the stiff boots might be decreased as they may have influenced oxygen consumption. There has been significant research done on investigating the effect of running with a stiff-soled shoe but there is little information regarding their effect on walking in different stiffness level of shoes with regards to muscle function.

4.6.5.1 Shoe forefoot stiffness hypotheses

The above analysis means that the following may occur during adult gait:

1. A very stiff mid-sole area of the shoe may load the calf muscles, because the sole will resist metatarsal joint motion (figure 4.23), and therefore may also alter knee flexion, ankle angle, ankle moments, muscle tendon-lengths, the velocity of muscle contraction, produce a reduced stride length, and change walking speed.

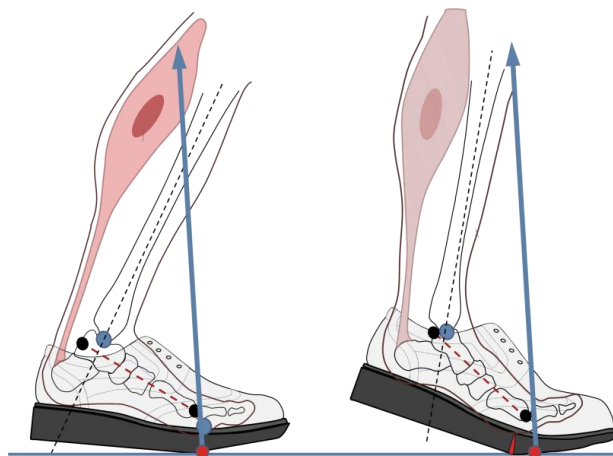


Figure 4.33: An example of late stance ankle angle kinematics for flexible and solid shoes.

2. A soft-soled shoe can achieve a more natural walking (barefoot) pattern, and therefore walking can be adapted to most comfortable way and muscle function will vary according to adaptation and walking speed.

4.6.6 Rocker Angle (RA)

The effect of different rocker angles (RAs) on plantar pressure, kinetics and kinematics have been investigated in several studies (van Schie et al., 2000, Van Bogart et al., 2005, Chapman et al., 2012). Van Bogart's study found that angled rocker soles increased the plantarflexion

angle during late stance phase and decreased the internal rotation moment during mid-stance and terminal stance. The results suggested that the ankle was more plantarflexed and therefore could be at more natural position at which fibres and tendons are closer in length to the optimal size. Internal PF moments were also reduced (figure 4.34).

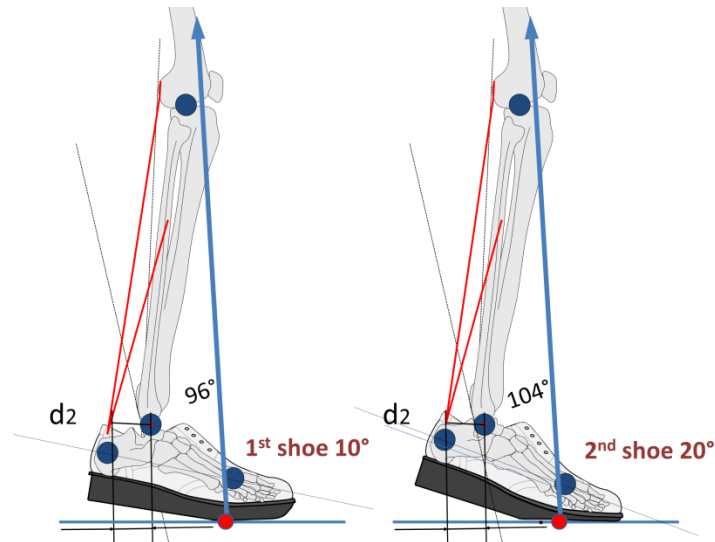


Figure 4.34: Alteration to ankle plantarflexion with a 10° rocker angle shoe versus a 20° rocker angle during late stance phase.

Therefore, specifically angled (between 10°- 25°) rocker soles may offload the calf muscles.

4.6.6.1 Hypothesis for alteration to rocker angle (RA)

The hypothesis would be that for a given AP, the RA would alter the kinematics of the ankle during late stance phase. The foot could be more dorsiflexed or plantarflexed, and therefore muscle length, velocity of contraction, muscle force generation, and moments would be affected. A flat and stiff shoe (i.e. with zero RA) may increase the load applied to the calf muscle as the shoe will resist ankle plantarflexion.

4.6.7 The posterior heel curve (HC)

The heel curve modification is routinely applied to the design of training shoes as well as contemporary footwear such as so-called “unstable shoes”; an example of which is the MBT shoe. However, most unstable shoes have reinforcement placed in the shoe upper around

the heel to provide shock absorption during initial contact and loading response (Ravindra, 2012). It has been demonstrated that MBT shoes reduce peak EMG activity for tibialis anterior muscle (Sacco et al., 2012, Romkes et al., 2006, Nigg et al., 2006). However, the MBT shoe has a cushioned heel and during loading response it partly acts as negative heel, and therefore it offloads the TA muscle (figure 4.35).



Figure 4.35: The Masai barefoot technology shoe (MBT) during loading response [picture adapted from (Sacco et al., 2012)].

The reasons why unstable shoes such as the MBT shoe reduce tibialis anterior muscle activity are as follows:

1. A curved heel changes point of application of the GRF with the ground by moving it anteriorly nearer to the ankle joint, and therefore the internal DF moment is reduced (figure 4.34).

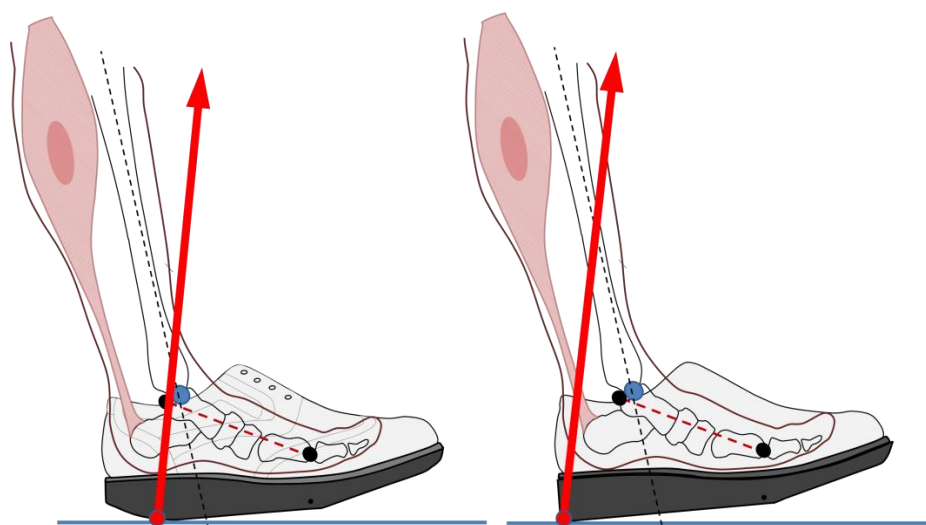


Figure 4.36: An example of GRF position for curved and flat-heeled shoes during loading response.

- The heel curvature could theoretically reduce the velocity of the tibialis anterior eccentric contraction during IC and LR, and therefore tension generation by the muscle is reduced.

4.6.8 Hypothesis for curved heeled shoes

A curved-heel shoe may offload tibialis anterior muscle. Due to the geometrical construction of the curved heel it may shift the point of application with the ground to the ankle joint as well as the GRF direction to be closer to the centre of the ankle joint, and consequently it might lead to offloading of the TA muscle but premature activation of triceps surae. Figure 4.37 demonstrates that a curved heel may shift the point of application of the GRF, and therefore remove the internal DF moment, and thus overall muscle work by the triceps surae may be increased.

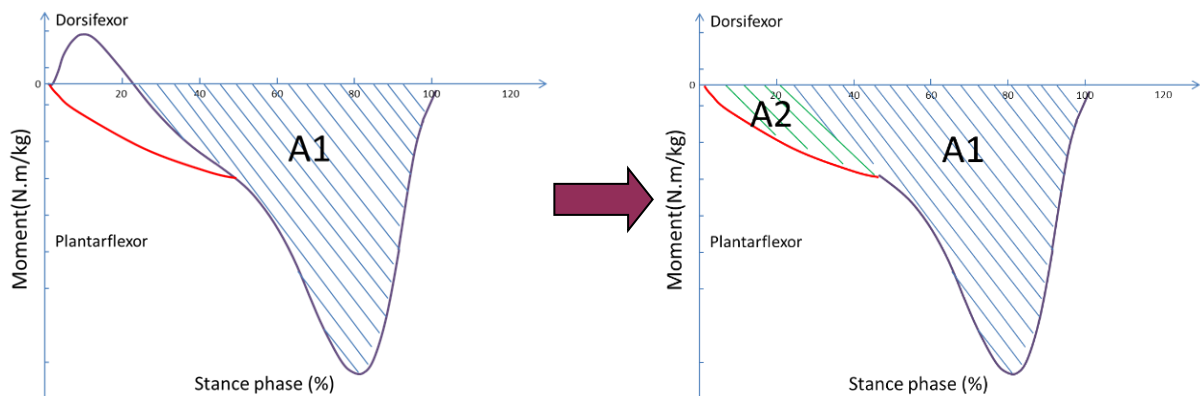


Figure 4.37: Internal DF/PF ankle moments during stance phase when comparing curved heels to non-curved heeled shoes.

If the internal DF moment was removed/reduced by a curved heel it may prematurely activate the calf muscles. A1 – represents the total area of the internal PF moment and A2 the area which can be transposed by alteration to the heel. The sum of areas A1+A2 may increase the total work done by the triceps surae by transposing the initial internal DF moment into a PF one.

4.7 Summary

Footwear profiles were designed in this research so that only one footwear feature was altered. For example, previous studies have investigated the effect of altering the apex position, but at the same time they also changed the thickness of the sole and the resulting

weight. This may have resulted in an additional parameter alteration (i.e. large differences in weight) which could have affected the results. Therefore this research has a systematic approach to more fully understand the precise effect of footwear features by reducing factors that can influence the results (such as walking speed, previous injuries and current pathologies, and differences in age groups).

This research used same standard shoe profile without changing thickness of the sole or significant weight of the shoe, to facilitate a better understanding than previously as to how rocker shoes alter gait and muscle function. Additional software was used to analyse muscle properties and it is discussed in the methodology chapter. The summary biomechanical result of footwear features, which can result in alteration of triceps surae muscle work, is presented in table 4.8 below.

Table 4.8: Biomechanical evidence of footwear features.

Footwear features (FF)	Definition (Biomechanical explanation in text)	Hypotheses	Measures
Back of heel			
Heel Height (HH)	<p>The heel height of shoes can be varied by increasing the heel height or reducing it. Different heel heights will have an effect on the anatomical shape of the shoe and raised heels can also affect apex position in relationship to the toe angle.</p> <p>A high heel places the ankle in a plantarflexion position during the whole stance phase as it alters the pitch of footwear as well.</p> <p>A low heel shoe may be called negative shoe as the sole apex position is lower than heel height level with the shoe on a level surface (the heel is lower than the front of the foot).</p>	<p>A Heel height profile would theoretically alter direction of ground reaction force (GRF), moment arm of external moment and therefore reduce/increase moment generation about the ankle and knee. Heel height can shift the ankle kinematics to be into more dorsiflexion or plantarflexion position during stance phase. It may change muscle-tendon properties, velocity and type of muscle contraction during stance phase. Consequently, it may change the magnitude of the EMG for lower leg muscles. Gastrocnemius is responsible for knee flexion as well and increased HH of the shoe will place the knee into a more flexed position during stance phase, therefore it may also affect the gastrocnemius muscle activity. Heel height can change the triceps surae muscle moment arm. When moving from a DF position into PF, the muscle moment arm is increasing. There should be an optimal heel height at which the MTU can be at its optimal length during</p>	<p>Different heel heights in relationship to different measurements detailed below:</p> <ol style="list-style-type: none"> 1. GRF point of application. 2. GRF direction. 3. Kinematic and kinetic data. 4. EMG activity during stance phase. 5. Muscle-tendon length and velocity of contraction. 6. The type of muscle contraction. 7. The muscle moment arm. 8. Shank angle (reclined or inclined). 9. Walking speed.

		mid-stance and terminal-stance to make the calf muscles work efficient and offload them.	
Curved heel (CH) or SACH heel	<p>A curved heel could be designed purely by shape or changing the material property of the heel. For example, a SACH heel will also allow the heel to deform into a curved heel shape during IC phase.</p> <p>A curved heel places the ankle into a more dorsiflexion position after IC phase (in MBT) compared with normal shoes.</p>	<p>CH changes the point of application during IC and shifts it closer to the ankle, and therefore it reduces the dorsiflexion moment (as ankle moment arm is reduced) which can result in tibialis anterior (TA) muscle activity being reduced during 0-10% of the gait cycle. If the point of application of the GRF is closer to or forwards of the ankle it may activate triceps surae group prematurely. Therefore, CH may alter kinematics, kinetics, muscle-tendon length and contraction velocity of the muscles acting on the ankle, which may result in EMG changes for the lower limb during IC, LR and partly mid-stance phases.</p>	<p>Different material properties of the heel in relationship to different measurements below:</p> <ol style="list-style-type: none"> 1. Point of application. 2. GRF direction. 3. Kinematic and kinetic data. 4. Level of EMG during stance phase. 5. Muscle-tendon length, velocity. 6. Type of muscle contraction 7. Muscle moment arm. 8. Shank angle (reclined or inclined). 9. Walking speed.
Midsole area			
Bending flexibility or stiffness (BF)	<p>Stiffness of the sole is defined by how much force is required to bend the mid sole of the shoe. Baseline stiffness occurs during barefoot walking, and an extremely stiff sole is produced when reinforced by steel plating or by a deep rocker sole. A low level of stiffness (i.e. a more easily bent sole) approximates more to barefoot walking.</p>	<p>Shoe flexibility of the mid-shoe area may alter plantar flexor moment during end of mid stance, terminal stance and pre-swing phases, and therefore alter lower limb (particularly calf muscle) activity. If the sole is more flexible, it may require less plantarflexor moment and power to plantarflex the ankle during the end of mid stance, terminal stance and pre-swing phases. If the sole has increased the level of bending stiffness in the middle of the sole it means bending resistance is increased and it can alter walking strategy, for example, it may affect the knee and increase flexion during second half of the stance phase. Stiffness of the sole may alter calf muscle firing patterns during the end of mid stance, terminal stance and pre-swing phases, and it may also alter type of contraction, velocity of muscle contraction, reduce ankle range of motion, muscle-tendon properties and consequently EMG activity.</p>	<p>Different flexibility levels of the mid area of the sole in a relationship to different measurements below:</p> <ol style="list-style-type: none"> 1. Point of application. 2. GRF direction. 3. Kinematic and kinetic data. 4. Level of EMG during stance phase. 5. Muscle-tendon length, velocity. 6. Type of muscle contraction 7. Muscle moment arm. 8. Shank angle (reclined or inclined). 9. Walking speed.

Apex position (AP)	Shoes with angled rocker soles have a single apex position on the sole where the shoe contacts a level surface. In a baseline shoe this defined by the last the shoe is made from and decided by heel height and toe spring. In the MBT shoe, the apex position is positioned at approx 50% shoe length as a result of the curve shape of the sole. The apex position of a shoe may be varied by adding a rocker sole, and the apex position will still be the point at which the sole contacts the ground on a level surface. If there is a flat surface from heel to apex position, it is the position after which the toe shape raises above the flat surface. The apex position can be anywhere between the heel and the sole.	Moving the apex position alters direction of ground reaction force (GRF) during different percentages of the stance phase, and changes kinematics and kinetic data of lower limbs as well. It can also affect the flexibility by changing the thickness of the sole at the apex position. If the apex is further forwards towards the toe, there is more material behind the apex position and therefore the shoe may be stiffer. An apex position at 50% of shoe length may alter stability, because the metatarsal head area during plantar flexion phase, positioned at the area of 60% of the shoe would be shaped upward. This may force an increased acceleration of the ankle and increase muscle activity of the ankle and knee to control balance. Muscle tendon properties and the type of contraction can be rapidly changed. AP can be varied and tuned to be optimal at the stance phase by keeping muscle fibres and tendons close to their optimal length, and therefore muscle force can be more efficiently applied. Also, less oxygen can be used.	<ol style="list-style-type: none"> 1. Point of application. 2. GRF direction. 3. Kinematic and kinetic data. 4. Level of EMG during stance phase. 5. Muscle-tendon length, velocity. 6. Type of muscle contraction. 7. Muscle moment arm. 8. Shank angle (reclined or inclined). 9. Walking speed.
Toe (forefoot) area			
Angle of the toe area (toe spring angle)	The toe spring angle is determined by the position and orientation of the sole at the apex. The higher the angle the deeper the sole unit and stiffer the sole for a given material.	This will have an effect on the GRF position and direction. Therefore ankle external ankle dorsiflexion and/or plantarflexion moments may be altered.	<ol style="list-style-type: none"> 1. Point of application. 2. GRF direction. 3. Kinematic and kinetic data of ankle, knee and pelvis. 4. Level of EMG during stance phase. 5. Muscle-tendon length, velocity and acceleration. 6. Type of muscle contraction 7. Muscle moment arm. 8. Shank angle (reclined or inclined). 9. Walking speed.
Curve level of the toes area (toe spring).	Same as above	Same as above	Same as above

4.8 Overarching and specific hypotheses

The first overarching null hypothesis (Ho1) therefore states the following:

There is no statistically significant difference between specific lower limb kinetic and/or kinematic measures caused by walking whilst wearing shoes adapted with specific rocker profiles or different heel heights or forepart outsole stiffness compared to a baseline control shoe.

The alternative overarching hypothesis (Ha1) states that:

There is a statistically significant difference between specific lower limb kinetic and/or kinematic measures caused by walking whilst wearing shoes adapted with specific rocker profiles or different heel heights, heel curves or different forepart outsole stiffness compared to a baseline control shoe.

The second overarching null hypothesis (Ho2) states the following:

There is no statistically significant difference between lower limb EMG RMS values of targeted muscles caused by walking whilst wearing shoes adapted with specific rocker profiles or different heel heights, heel curves or different forepart outsole stiffness compared to a baseline control shoe.

The alternative hypothesis (Ha2) states that:

There is a statistically significant difference between lower limb EMG RMS values of targeted muscles caused by walking whilst wearing shoes adapted with specific rocker profiles or different heel heights, heel curves or different forepart outsole stiffness compared to a baseline control shoe.

The third overarching null hypothesis (Ho3) states the following:

There is no statistically significant difference between lower limb temporal and spatial parameter values caused by walking whilst wearing shoes adapted with specific rocker profiles or different heel heights, heel curves or different outsole stiffness compared to a baseline control shoe.

The alternative hypothesis (Ha3) states that:

There is a statistically significant difference between lower limb temporal and spatial parameter values caused by walking whilst wearing shoes adapted with specific rocker profiles or different heel heights, heel curves or different outsole stiffness compared to a baseline control shoe.

The fourth overarching null hypothesis (Ho4) states the following:

There is no statistically significant difference between specific lower limb muscle/tendon lengths, muscle moment arms, velocity of contractions, fibre lengths caused by walking whilst wearing shoes adapted with specific rocker profiles or different heel heights, heel curves or different outsole forepart stiffness compared to a baseline control shoe.

The alternative hypothesis (Ha4) states that:

There is a statistically significant difference between specific lower limb muscle/tendon lengths, muscle moment arms, velocity of contractions, fibre lengths caused by walking whilst wearing shoes adapted with specific rocker profiles or different heel heights, heel curves or different outsole forepart stiffness compared to a baseline control shoe

Definitive hypotheses

The first definitive null hypothesis (Ho1a) states the following:

There is no statistically significant difference between lower limb kinematic measures for maximum ankle plantarflexion during LR, caused by walking whilst wearing shoes adapted with specific rocker profiles or different heel heights, heel curves or forepart outsole stiffness compared to a baseline control shoe.

The alternative definitive hypothesis (Ha1a) states that:

There is a statistically significant difference between lower limb kinematic measures for maximum ankle plantarflexion during LR, caused by walking whilst wearing shoes adapted with specific rocker profiles or different heel heights, heel curves or different forepart outsole stiffness compared to a baseline control shoe.

The second definitive null hypothesis (Ho1b) states the following:

There is no statistically significant difference between lower limb kinematic measures for maximum ankle ROM during LR, caused by walking whilst wearing shoes adapted with specific rocker profiles or different heel heights, heel curves or forepart outsole stiffness compared to a baseline control shoe.

The alternative definitive hypothesis (Halb) states that:

There is a statistically significant difference between lower limb kinematic measures for maximum ankle ROM during LR, caused by walking whilst wearing shoes adapted with specific rocker profiles or different heel heights, heel curves or different forepart outsole stiffness compared to a baseline control shoe.

The third definitive null hypothesis (Ho1c) states the following:

There is no statistically significant difference between lower limb kinematic measures for maximum ankle dorsiflexion during second rocker of gait, caused by walking whilst wearing shoes adapted with specific rocker profiles or different heel heights, heel curves or forepart outsole stiffness compared to a baseline control shoe.

The alternative third definitive hypothesis (Halc) states that:

There is a statistically significant difference between lower limb kinematic measures for maximum ankle dorsiflexion during second rocker of gait, caused by walking whilst wearing shoes adapted with specific rocker profiles or different heel heights, heel curves or different forepart outsole stiffness compared to a baseline control shoe.

The fourth definitive null hypothesis (Ho1d) states the following:

There is no statistically significant difference between lower limb kinematic measures for maximum ankle ROM during second rocker of gait, caused by walking whilst wearing shoes adapted with specific rocker profiles or different heel heights, heel curves or forepart outsole stiffness compared to a baseline control shoe.

The alternative definitive hypothesis (H_{ald}) states that:

There is a statistically significant difference between lower limb kinematic measures for maximum ankle ROM during second rocker of gait, caused by walking whilst wearing shoes adapted with specific rocker profiles or different heel heights, heel curves or different forepart outsole stiffness compared to a baseline control shoe.

The fifth definitive null hypothesis (H_{o1e}) states the following:

There is no statistically significant difference between lower limb kinematic measures for maximum ankle plantarflexion during third rocker of gait, caused by walking whilst wearing shoes adapted with specific rocker profiles or different heel heights, heel curves, or forepart outsole stiffness compared to a baseline control shoe.

The alternative definitive hypothesis (H_{ale}) states that:

There is a statistically significant difference between lower limb kinematic measures for maximum ankle plantarflexion during the third rocker of gait, caused by walking whilst wearing shoes adapted with specific rocker profiles or different heel heights, heel curves or different forepart outsole stiffness compared to a baseline control shoe.

The sixth definitive null hypothesis (H_{o1f}) states the following:

There is no statistically significant difference between lower limb kinematic measures for maximum overall ankle ROM during stance phase of gait, caused by walking whilst wearing shoes adapted with specific rocker profiles or different heel heights, heel curves or forepart outsole stiffness compared to a baseline control shoe.

The alternative definitive hypothesis (H_{alf}) states that:

There is a statistically significant difference between lower limb kinematic measures for maximum overall ankle ROM during stance phase of gait, caused by walking whilst wearing shoes adapted with specific rocker profiles or different heel heights, heel curves or different forepart outsole stiffness compared to a baseline control shoe.

The seventh definitive null hypothesis (H_{01g}) states the following:

There is no statistically significant difference between lower limb kinematic measures for maximum ankle ROM during third rocker of gait, caused by walking whilst wearing shoes adapted with specific rocker profiles or different heel heights, heel curves or forepart outsole stiffness compared to a baseline control shoe.

The alternative definitive hypothesis (H_{1g}) states that:

There is a statistically significant difference between lower limb kinematic measures for maximum ankle ROM during third rocker of gait, caused by walking whilst wearing shoes adapted with specific rocker profiles or different heel heights, heel curves or different forepart outsole stiffness compared to a baseline control shoe.

The eighth definitive null hypothesis (H_{01h}) states the following:

There is no statistically significant difference between lower limb kinematic measures for maximum knee flexion during LR, caused by walking whilst wearing shoes adapted with specific rocker profiles or different heel heights, heel curves or forepart outsole stiffness compared to a baseline control shoe.

The alternative definitive hypothesis (H_{1h}) states that:

There is a statistically significant difference between lower limb kinematic measures for maximum knee flexion during LR, caused by walking whilst wearing shoes adapted with specific rocker profiles or different heel heights, heel curves or different forepart outsole stiffness compared to a baseline control shoe.

The ninth definitive null hypothesis (H_{01i}) states the following:

There is no statistically significant difference between lower limb kinematic measures for maximum knee extension during stance, caused by walking whilst wearing shoes adapted with specific rocker profiles or different heel heights, heel curves or forepart outsole stiffness compared to a baseline control shoe.

The alternative definitive hypothesis (H_{al}i) states that:

There is a statistically significant difference between lower limb kinematic measures for maximum knee extension during stance, caused by walking whilst wearing shoes adapted with specific rocker profiles or different heel heights, heel curves or different forepart outsole stiffness compared to a baseline control shoe.

The tenth definitive null hypothesis (H_o1j) states the following:

There is no statistically significant difference between lower limb kinematic measures for maximum knee flexion at TO, caused by walking whilst wearing shoes adapted with specific rocker profiles or different heel heights, heel curves or forepart outsole stiffness compared to a baseline control shoe.

The alternative definitive hypothesis (H_{al}j) states that:

There is a statistically significant difference between lower limb kinematic measures for maximum knee flexion at TO, caused by walking whilst wearing shoes adapted with specific rocker profiles or different heel heights, heel curves or different forepart outsole stiffness compared to a baseline control shoe.

The eleventh definitive null hypothesis (H_o1k) states the following:

There is no statistically significant difference between lower limb kinematic measures for maximum knee flexion during swing, caused by walking whilst wearing shoes adapted with specific rocker profiles or different heel heights, heel curves or forepart outsole stiffness compared to a baseline control shoe.

The alternative definitive hypothesis (H_{al}k) states that:

There is a statistically significant difference between lower limb kinematic measures for maximum knee flexion during swing, caused by walking whilst wearing shoes adapted with specific rocker profiles or different heel heights, heel curves or different forepart outsole stiffness compared to a baseline control shoe.

The twelve definitive null hypothesis (Ho1l) states the following:

There is no statistically significant difference between lower limb kinematic measures for maximum knee ROM late stance, caused by walking whilst wearing shoes adapted with specific rocker profiles or different heel heights, heel curves or forepart outsole stiffness compared to a baseline control shoe.

The alternative definitive hypothesis (Hal) states tha:

There is a statistically significant difference between lower limb kinematic measures for maximum knee ROM late stance, caused by walking whilst wearing shoes adapted with specific rocker profiles or different heel heights, heel curves or different forepart outsole stiffness compared to a baseline control shoe.

The thirteenth definitive null hypothesis (Ho1m) states the following:

There is no statistically significant difference between lower limb kinematic measures for maximum knee ROM during stance, caused by walking whilst wearing shoes adapted with specific rocker profiles or different heel heights, heel curves or forepart outsole stiffness compared to a baseline control shoe.

The alternative definitive hypothesis (Halm) states that:

There is a statistically significant difference between lower limb kinematic measures for maximum knee ROM during stance, caused by walking whilst wearing shoes adapted with specific rocker profiles or different heel heights, heel curves or different forepart outsole stiffness compared to a baseline control shoe.

The fourteenth definitive null hypothesis (Ho1n) states the following:

There is no statistically significant difference between lower limb kinematic measures for sagittal knee angle position at ICt, caused by walking whilst wearing shoes adapted with specific rocker profiles or different heel heights, heel curves or forepart outsole stiffness compared to a baseline control shoe.

The alternative definitive hypothesis (H_{aln}) states that:

There is a statistically significant difference between lower limb kinematic measures for sagittal knee angle position at ICt, caused by walking whilst wearing shoes adapted with specific rocker profiles or different heel heights, heel curves or different forepart outsole stiffness compared to a baseline control shoe.

The fifteenth definitive null hypothesis (H_{o1o}) states the following:

There is no statistically significant difference between lower limb kinematic measures for sagittal hip angle position at ICt, caused by walking whilst wearing shoes adapted with specific rocker profiles or different heel heights, heel curves or forepart outsole stiffness compared to a baseline control shoe.

The alternative definitive hypothesis (H_{alo}) states that:

There is a statistically significant difference between lower limb kinematic measures for sagittal hip angle position at ICt, caused by walking whilst wearing shoes adapted with specific rocker profiles or different heel heights, heel curves or different forepart outsole stiffness compared to a baseline control shoe.

The sixteenth definitive null hypothesis (H_{o1p}) states the following:

There is no statistically significant difference between lower limb kinematic measures for maximum sagittal hip angle during LR, caused by walking whilst wearing shoes adapted with specific rocker profiles or different heel heights, heel curves or forepart outsole stiffness compared to a baseline control shoe.

The alternative definitive hypothesis (H_{alp}) states that:

There is a statistically significant difference between lower limb kinematic measures for maximum hip flexion angle during LR, caused by walking whilst wearing shoes adapted with specific rocker profiles or different heel heights, heel curves or different forepart outsole stiffness compared to a baseline control shoe.

The seventeenth definitive null hypothesis (Ho1q) states the following:

There is no statistically significant difference between lower limb kinematic measures for maximum hip extension, caused by walking whilst wearing shoes adapted with specific rocker profiles or different heel heights, heel curves or forepart outsole stiffness compared to a baseline control shoe.

The alternative definitive hypothesis (Ha1q) states that:

There is a statistically significant difference between lower limb kinematic measures for maximum hip extension, caused by walking whilst wearing shoes adapted with specific rocker profiles or different heel heights, heel curves or different forepart outsole stiffness compared to a baseline control shoe.

The eighteenth definitive null hypothesis (Ho1r) states the following:

There is no statistically significant difference between lower limb kinematic measures for maximum hip ROM during stance, caused by walking whilst wearing shoes adapted with specific rocker profiles or different heel heights, heel curves or forepart outsole stiffness compared to a baseline control shoe.

The alternative definitive hypothesis (Ha1r) states that:

There is a statistically significant difference between lower limb kinematic measures for maximum hip ROM during stance, caused by walking whilst wearing shoes adapted with specific rocker profiles or different heel heights, heel curves or different forepart outsole stiffness compared to a baseline control shoe.

The nineteenth definitive null hypothesis (Ho1s) states the following:

There is no statistically significant difference between lower limb kinematic measures for maximum hip ROM during the gait cycle, caused by walking whilst wearing shoes adapted with specific rocker profiles or different heel heights, heel curves or forepart outsole stiffness compared to a baseline control shoe.

The alternative definitive hypothesis (H_{alt}) states that:

There is a statistically significant difference between lower limb kinematic measures maximum hip ROM during the gait cycle, caused by walking whilst wearing shoes adapted with specific rocker profiles or different heel heights, heel curves or different forepart outsole stiffness compared to a baseline control shoe.

The twentieth definitive null hypothesis (H_{01t}) states the following:

There is no statistically significant difference between lower limb kinematic measures for maximum hip ROM during the gait cycle, caused by walking whilst wearing shoes adapted with specific rocker profiles or different heel heights, heel curves or forepart outsole stiffness compared to a baseline control shoe.

The alternative definitive hypothesis (H_{alt}) states that:

There is a statistically significant difference between lower limb kinematic measures maximum hip ROM during the gait cycle, caused by walking whilst wearing shoes adapted with specific rocker profiles or different heel heights, heel curves or different forepart outsole stiffness compared to a baseline control shoe.

CHAPTER 5

5 METHODOLOGY

5.1 Chapter overview

The purpose of this thesis is to investigate the differences in gait caused by altering footwear outsole features during ambulation in healthy male volunteer subjects. The specific objective of this thesis was to especially target analysis on the alterations demonstrated to soleus (SOL), tibialis anterior (TA) and medial gastrocnemius (MGAS) muscle activity and the performance of their MTUs. This information should lead to new clinical treatments and further research; for example to recommend techniques to offload the ankle plantarflexors for patients with IC or other complications by using this innovative database to inform the design of new footwear features.

The aim of this chapter is to introduce the methods which were utilised in order to collect and investigate the primary outcome measures which were changes in the movement (kinematics), forces (kinetics) and muscle activation (EMG) and muscle properties of the lower limbs whilst walking in different specifically-chosen footwear test conditions. Ethical approval was granted by the University of Salford ethics committee to perform the walking trials and the experimental protocol (ethics application HSCR12/04).

Various footwear features were examined by changing one outsole or heel feature at a time, and were compared to a baseline shoe test condition.

Walking speed was controlled within defined limits for all subjects during the testing procedure to ensure that it was not a factor in influencing alteration to ankle kinematic data, nor muscle-tendon properties or the work done by the muscles. This would then not add additional factors which could influence the gait pattern detected; apart from when ambulating with different footwear conditions (Kirtley et al., 1985, Kirtley, 2006). Participants were trained to walk with speeds within specific limits during the initial test walks using timing gates.

5.2 The motion analysis system

Motion analysis involves specific methods and techniques to systematically analyse movement. Modern gait laboratories use motion analysis systems to acquire dynamic

changes in the three-dimensional coordinates of specific body landmarks from the images recorded by each camera. Three-dimensional kinematic data were obtained during this study with ten high-speed SXGA OQUS™ 3+, five OQUS3 and one OQUS1 Qualisys infrared cameras with 1.3 megapixel (1280x1024) resolution and passive retro-reflective markers using Qualisys Track Manager™ software (Qualisys AB, Gothenburg, Sweden).

The Qualisys cameras used are based on video technology. The lens is surrounded by diodes which emit strobed infra-red light which cannot be seen by the human eye. This is reflected back from the markers, and the sensors of the camera record that information. The gait laboratory set up used is illustrated in figure 5.1.



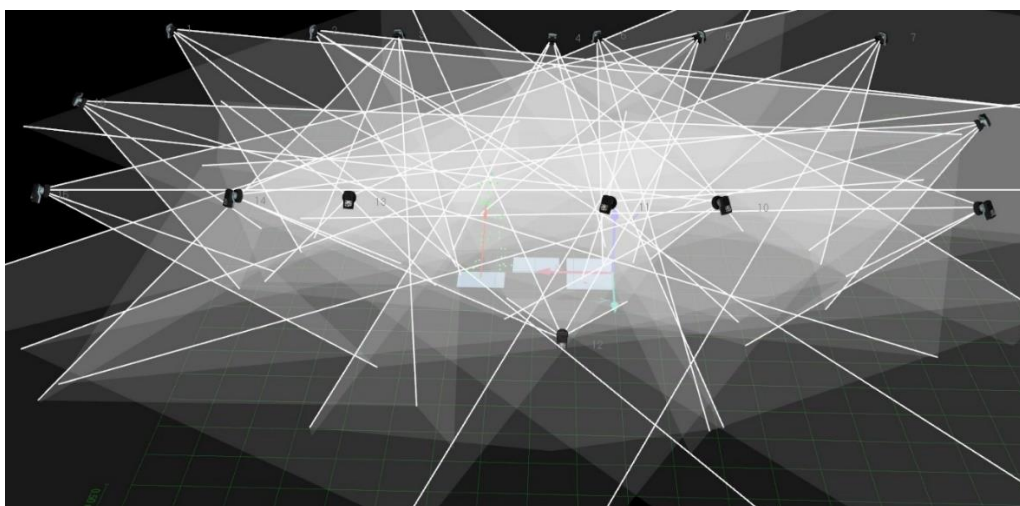
Figure 5.1: Camera set-up in the gait laboratory with an example of a typical image produced by the Qualisys software.

The measurement frequency of the cameras was set at 100Hz with a 1.3 megapixel resolution. A high resolution for the sensors was utilised to achieve precise marker position recognition in the coordinate system in order to enable the ability of the system to measure small changes in marker position (Whittle, 2007).

5.2.1 Camera setup

Each marker must be seen by at least two cameras during data recording (Payton and Bartlett, 2008). All cameras are permanently mounted in specific positions, which allow all anatomically-placed body markers to be clearly visible and accurately processed by the Qualisys software. The measurement volume was fully visible for body marker placement within two gait cycles within a volume of 8 m (x) by 3.5 m (y) by 2 m (z) (figure 5.2).

Camera focal lengths, apertures and the sensitivities of each camera were adjusted to ensure that calibration and tracking of the retro-reflective markers could achieve the optimal results for each testing session. Each camera lens direction was positioned to prevent any opposing cameras from detecting each other's infrared light. If this was not possible, then a mask area was placed in Qualisys software to ensure that camera views were adjusted to avoid stray reflection from being picked up, as if a reflection were to be picked up by more than one camera, it would be reconstructed as a marker and static calibration would fail.



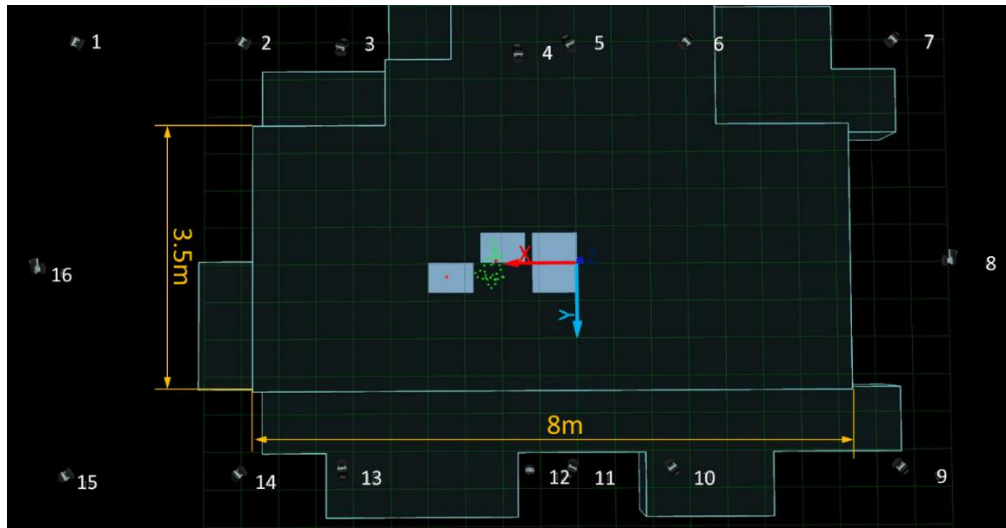


Figure 5.2: Depiction of the Qualisys cameras location, the measurement volume and walking distances available.

5.2.2 Oqus 3+ Qualisys calibration

As with any motion analysis system, the volume space to be used for data collection must be calibrated before use. The purpose of the calibration is to define the precise position of markers in a three dimensional (3D) coordinate system during static and dynamic movement by using one of the direct linear transformation (DLT) techniques as recommended in the literature (Abdel-Aziz and Karara, 1971, Miller et al., 1980). Each camera was synchronised and recorded x-y coordinates which were then reconstructed into a single set of X, Y, Z real-life coordinates. This technique was achieved using DLT. This method does not require careful camera positioning and therefore allows more flexibility in the choice of camera location. The DLT algorithm establishes the linear relationship between the 2D image coordinates and 3D real world coordinates of markers; thus an object space or data collection volume must be defined by using calibration technique (Grimshaw et al., 2006).

To perform that task, two calibration frames were used. The first static reference frame was 'L' shaped with four reflective markers mounted on it in known locations and with a known distance between them (figure5.3).

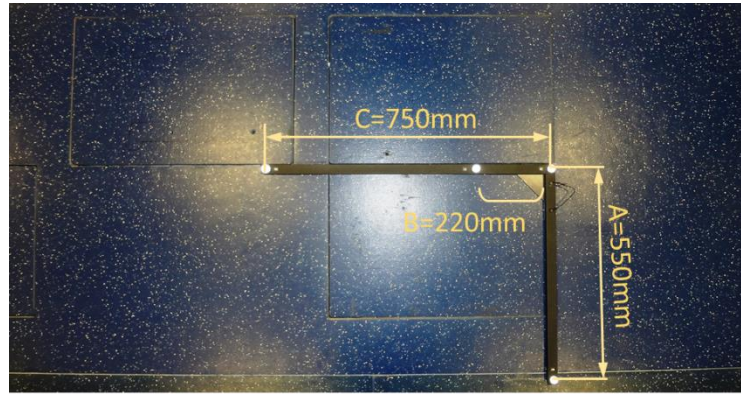


Figure 5.3: The L-shaped frame set-up position for calibration.

The static L-shaped frame defined the location of the origin and the orientation of the laboratory reference frame (Payton and Bartlett, 2008). The L-shaped frame was placed on top of the first force platform in the direction of travel to match the corners and sides of the frame according to the calibration rules recommended during use of the Qualisys software (figures 5.3 and 5.4).

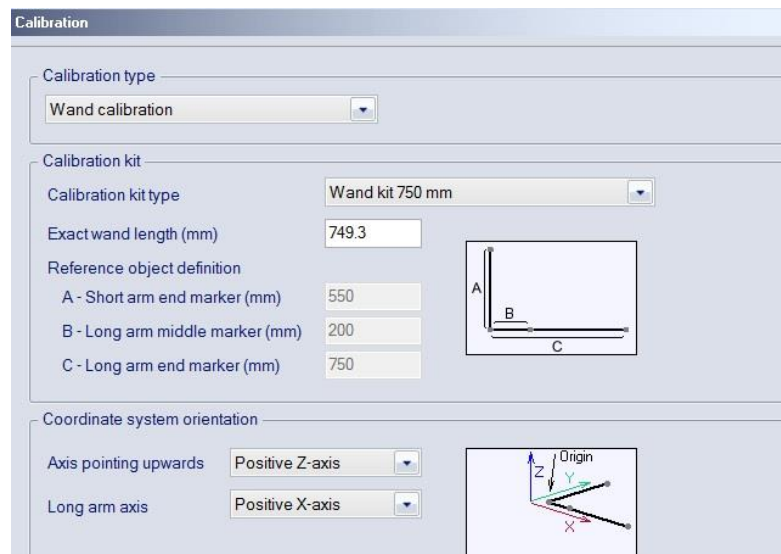


Figure 5.4: Qualisys calibration settings configuration.

For dynamic calibration, a hand-held T-shaped wand with reflective markers positioned with an exact wand length of 749.3 mm was used to calibrate the walking volume to be used during the subject walking trials (figure 5.5).

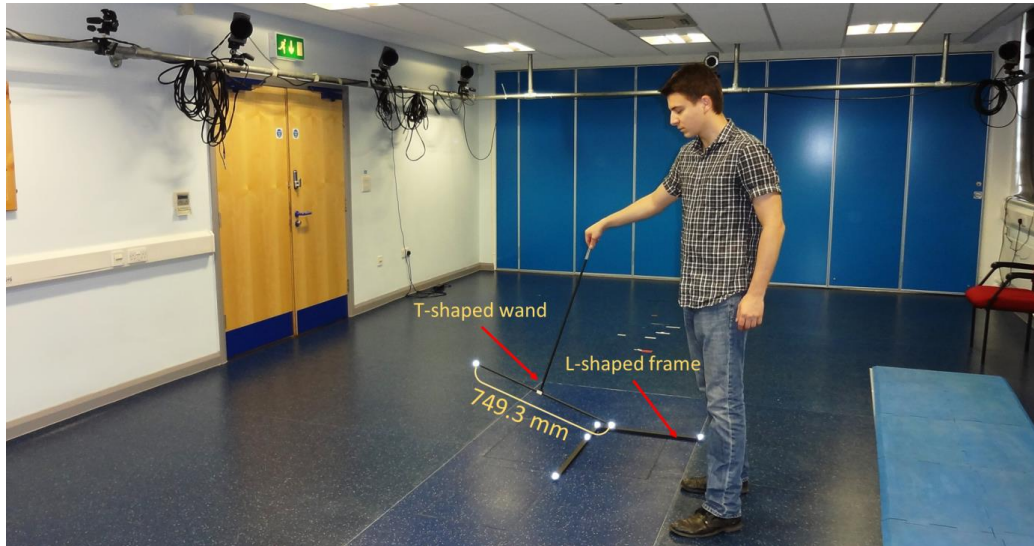


Figure 5.5: Calibration procedure used in the gait laboratory.

It was important to manually move the wand throughout the 3D space volume where data were recorded by using as many orientations as possible in all three orthogonal directions. A capture time was set for 60 seconds to calibrate the measurement volume to ensure that both the lower limbs and torso were covered completely during kinematic data recording for the walking trials. The T-shape wand was dynamically moved by hand in the area where data were captured.

This then created a calibration volume to enable marker position tracking of the body and lower limbs (Figure 5.6).

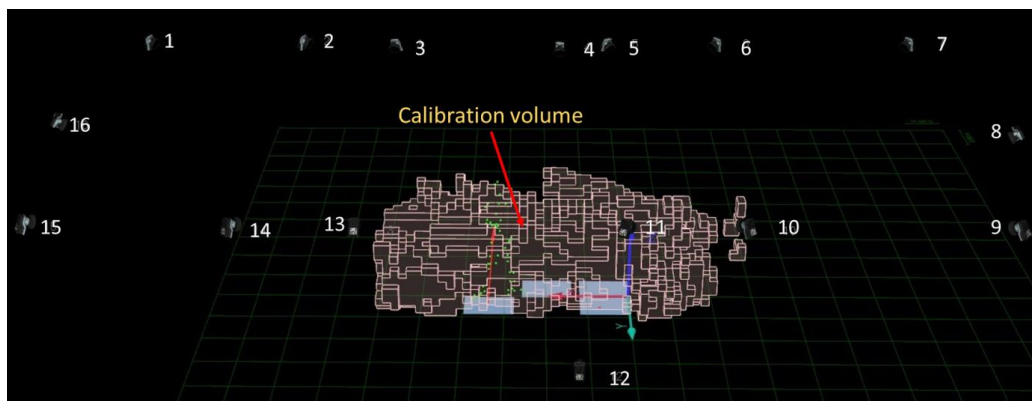


Figure 5.6: Representation of the calibration volume.

5.2.3 Calibration results

The most important parameter for successful calibration is low error accuracy, which describes the relationship between where the reflective markers are and where the system shows they are. The calibration procedure showed the magnitude of the errors present during calibration, and if the process was successful. Result figures were given for each camera, such as the average residual of each camera, which demonstrated the error between static marker positions and also in dynamic movement and it also showed the standard deviation of the wand length (figure 5.7). The aim was to obtain calibration results numerically as low as possible and to cover the full volume where kinematic data were recorded. A good calibration is fundamental to the collection of high quality of data. Therefore, the higher the residual number; the less accurately the calibration was performed.

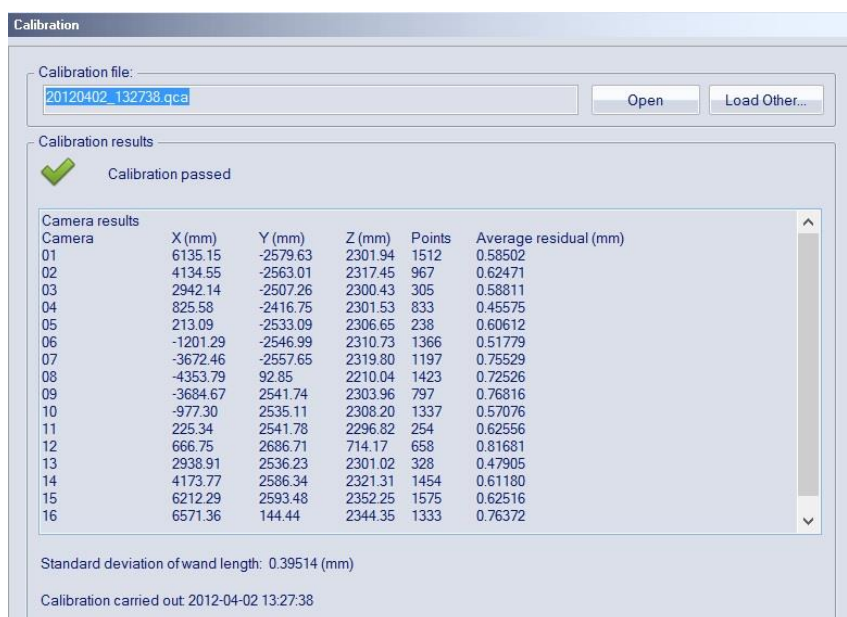


Figure 5.7: Typical Qualisys calibration results.

If a dynamic calibration is performed according to the manufacture rules, the accuracy of residual values should be no more than 1 mm (Grimshaw et al., 2006). In this study, the average residuals of the calibration trials were accepted if all the camera average residual values were ≤ 0.8 mm as this indicated that a marker's position in space was located within 0.8 mm of its true position. Earlier systems had typical measurement errors of 2-3 mm in all three dimensions (Whittle, 1982).

5.3 The force Platforms

During quiet standing on the force platform, a ground reaction component acts in opposition to body weight. During dynamic walking the ground reaction vector magnitude and direction is further influenced by three vector forces as shown on figure 5.8 (Richards, 2008).

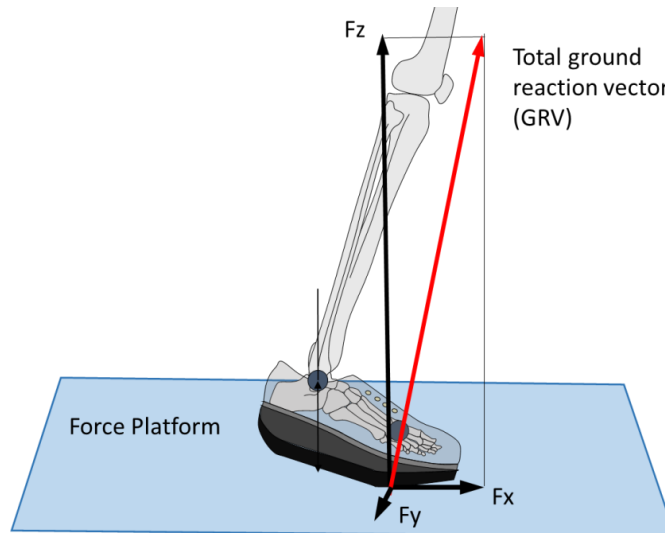


Figure 5.8: Ground reaction vector components.

Forces acting on the human body can be divided into external and internal forces. The internal forces are those transmitted by body tissues, which include muscular forces, ligaments forces and forces transmitted through joint contact. The external forces represent all physical interactions between the body and the environment such as gravitational, ground reaction and inertial forces (Bronstein et al., 2004).

The largest of the forces acting during normal walking speed is the support force and the second largest is the friction force. The force platform was used to measure the ground reaction force (GRF) or body's response to gravitational forces as subjects walked across it.

The ground reaction vector magnitude in the horizontal plane is calculated as:

$$GRV = \sqrt{F_x^2 + F_y^2 + F_z^2}$$

In this research, the gait laboratory coordinate system used was different from that used by The International Society of Biomechanics (ISB) system, (figure 5.9). For the purposes of this thesis, the gait laboratory was set up with the vertical direction denoted as the "z" direction and the transverse, the "y" direction.

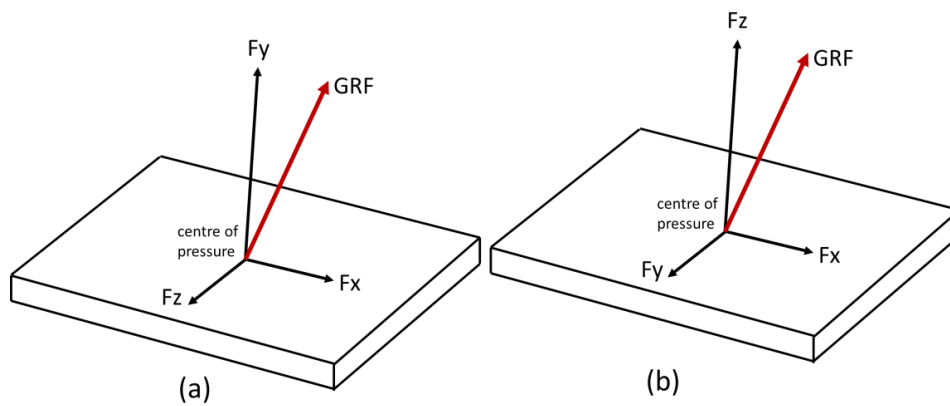


Figure 5.9: The three components of the ground reaction force (GRF), with (a) the coordinate system adopted by (ISB) and (b) the coordinate system used in this research.

GRF data were collected using four AMTI force plates (AMTI, Watertown, MA, USA, model BP600400). They were mounted to be flush with the gait laboratory floor and at the same level as the floor to minimise them being noticeable by subjects during the walking trials. To obtain good quality data, the whole of the subject's foot must land on the platform (Kirtley, 2006). Therefore, the walking patterns of all the subjects were observed, and slight adjustment in the starting position using markers on the floor was used to ensure that a clean foot-strike occurred on the force platforms without alteration to their walking pattern at that time. The location of force platforms used in the gait laboratory for kinetic data collection is demonstrated in figure 5.10.

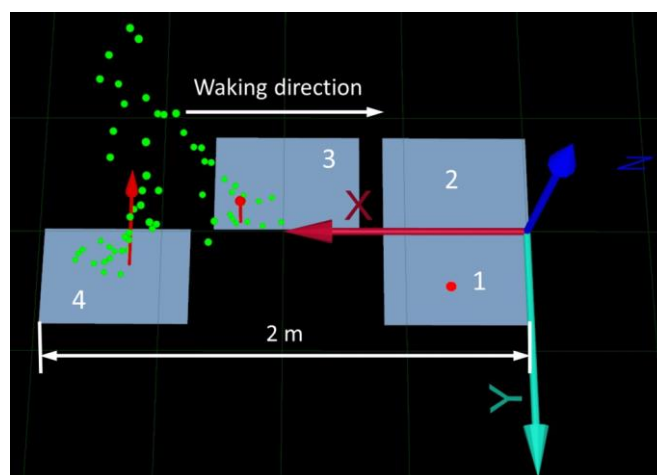


Figure 5.10: Force platform set-up positions.

Force platforms were used to define gait events from heel strike (HS) [otherwise known as initial contact (ICt)] to toe off (TO) to enable calculation of kinematics, external ankle/knee moments, EMG plus muscle-tendon property data during stance phase of gait. The force

platform system used was factory-calibrated, but manual calibration was also performed during each testing session by pressing the calibration button or null ground when there was no load acting on of the force plates to ensure that the reading was equal to zero weight. Caltestster was routinely applied in the gait laboratory with errors of less than 1 degree in orientation angle and <1 mm in centre of pressure (COP).

5.3.1 Reflective marker set selection

Lightweight reflective markers of 14 mm diameter were used in all of walking trials in the gait laboratory. The markers were attached to the skin at specifically chosen anatomical landmarks using hypo-allergenic double-sided tape (figure 5.11).



Figure 5.11: A 14 mm retroreflective marker attached to the skin using double-sided tape.

The marker set used was configured as recommended by Cappozzo et al. (2005). Two markers can only define a line and cannot fully provide information about movement in 3D nor indicate whether rotation about that line is occurring. A minimum of three non-collinear markers is required per rigid segment for three-dimensional analysis with 6 degrees-of-freedom (Cappozzo et al., 1995).

For the purpose of the thesis, OpenSim 3.0 software was used to analyse the properties of the muscle movements. Visual3D 4.0 allows the export of OpenSim-compatible motion files designed for use in OpenSim gait models. Therefore, Visual3D was used to export a scaled model using body segment and motion data for further analysis in OpenSim, hence providing the software requirements used to build up static models in the C-Motion software. The Visual3d model used for OpenSim output must include the right foot (RFT), right shank (RSK), right thigh (RTH), left foot (LFT), left shank (LSK), left thigh (LTH), pelvis

(RPV) and a Thorax/Ab. Full body marker landmark positioning was required in this research to be able to do so, according to exportation standards by Visual3D (C-Motion, Rockville, MD, USA). To build up a static model, Visual3d does not require the adoption of a special marker configuration. The skeletal model defined in it has a precise definition that can be followed to create any number of segments within a model. Two rules should be followed to allow Visual3D to calculate the six degree of freedom motion of every segment using optimal techniques. The two basics rules are:

- At least 3 tracking markers must be attached to each segment and recorded during the movement trial;
- A standing trial must identify four static markers that represent medial and lateral locations at the proximal end of the segment, and the medial and lateral locations at the distal end of the segment.

A number of studies have demonstrated that if markers are placed directly onto the skin, soft tissue motion artefacts can be produced during dynamic motion data collection (Fuller et al., 1997, Reinschmidt et al., 1997, Holden et al., 1997b). These studies showed that that data contained less noise if markers were mounted on pins which were inserted directly to the bones. Additional artefacts are also produced by the weight of the marker (Karlsson and Tranberg, 1999). Therefore, very light-weight markers were used in this research. Although direct attachment of the markers to the bones has been shown to be the most accurate technique to measure of motion of that segment, it was not practical for this research due to ethical and safety considerations. In previous gait analysis techniques, researches have placed non-collinear markers on a rigid structure and attached that rigid marker cluster to the body segment (Hutchins, 2007, Jones, 2010). The markers were therefore fixed to rigid anatomically-shaped polypropylene plates on the anterior thigh and lower leg to prevent the markers moving independently from each other (as they would have done had they been individually attached to the skin). This meant that the system had the advantage that the markers in each individual cluster would not move relative to each other. Manal et al. (2000) compared marker clusters for tibia rotation versus surface mounted markers and discovered that the rigid structure of marker placement produced less skin artefacts and produced more accurate data.

5.3.2 The Calibration Anatomical System technique (CAST)

The CAST technique enables a local coordinate system defined by external markers to be given anatomical relevance (Cappozzo et al., 1995). The CAST protocol also offers the ability to model each body segment in six degrees of freedom as long as the segments have an anatomical frame by using the static markers and a cluster of dynamic tracking markers (Richards, 2008).

This technique requires two sets of markers. One group of markers needed to be worn in all the trials (these included the marker clusters) whilst anatomical markers were used to define the coordinate system and body segments. The first group of markers were not related to any anatomical points, but defined segments and also 3D motion while performing the walking activities. Therefore, there were not less than three non-collinear markers placed on a segment and normally positioned on the rigid cluster approximating to the mid-point of the segment. The anatomical markers were positioned and related to define anatomical characteristics at the proximal and distal end, lateral and medial sides of lower leg segments; for example at the tibial tuberosity, fibular head, medial and lateral malleoli; and therefore rigid segments could be defined. A modified version of the CAST method was used to reconstruct segments of lower limbs during walking trials, using clusters of markers mounted on polypropylene plates on the anterior thigh and shin bilaterally and the pelvis. The anatomical markers were used to build body segments while marker clusters were placed on segments also.

Static trials were initially recorded and then reflective markers could be removed, leaving only the marker clusters used to define motion, which also allowed reconstruction of the global coordinates of each anatomical marker in each frame of all dynamic trials from the coordinates of the marker cluster by the C-Motion software (Cappello et al., 1997). This method is now being integrated into movement analysis software Visual3D (motion analysis software by C-Motion), which allows this method of anatomical referencing to be applied simply and quickly.

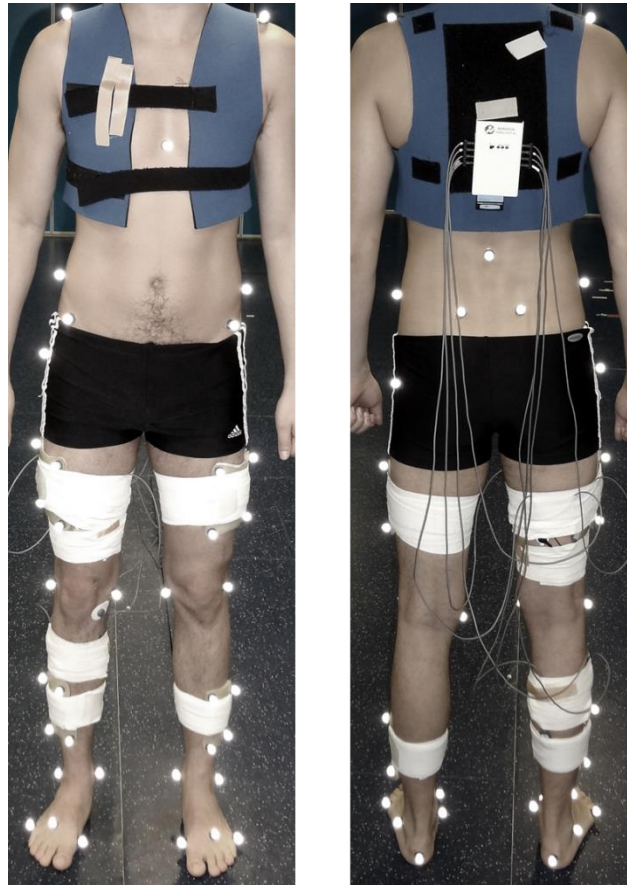


Figure 5.12: The positioning of the anatomical and technical markers.

The marker clusters were placed on the right/left thigh and the right/left shank. Direct skin mounted markers were used for dynamic motion tracking for the foot, pelvis and thorax segments.

5.3.3 Definition of the segment coordinate systems

5.3.3.1 The Foot segment model

Direct marker placement on the skin of the foot was used in this study. The barefoot position of the foot segment should be parallel to the ground for all shoes, to ensure that static offsets caused by sole design would be removed. It was very important to do so, because small angular changes in the position of the shank and foot segment would cause a significant change in muscle property data and these data would not have any meaning for the further analysis and comparison. Therefore, it was important to ensure that all markers were placed on the same position on the foot during walking trials for all footwear

conditions. Hence, anatomical markers were kept on the same landmark positions during entire testing procedure. There was only one potential complication that markers of the foot segment were constantly replaced after changing footwear conditions. To ensure that all markers were placed on the same location on the foot, the circumference outline of the marker base was drawn on the skin of the foot where it was to be attached (figure 5.13). That technique ensured that foot markers were placed and re-placed on the exact same position with an estimated standard deviation of ± 0.5 mm. Therefore, only one static model was used for all footwear conditions to be able to export motion data without static shifts caused by the shape of the soles and shank position.



Figure 5.13: Direct skin-marking technique used for the reflective marker placement.

The foot model for the foot segment was defined as a single rigid body. Three non-collinear markers were attached directly to the skin of the foot to define motion of the foot segment. Three holes were cut (figure 5.14) for each of the fifteen same-sized pair of shoes used during the testing to enable reflective markers to be placed at the following points:

- The dorsal aspect of the great toe (first metatarsal denoted as 1MT);
- The fifth metatarsal head (5MT);
- The posterior aspect of the heel counter of the shoe (proximal calcaneus).



Figure 5.14: Anatomical cut-outs utilised on the footwear.

The second reason of using the method of directly attaching skin markers on the foot was to be sure that a precise foot segment tracking motion technique was used for different footwear conditions, rather than if markers were placed on the leather uppers of the shoe. This is because it would not be possible to place markers on exactly the same position on all footwear conditions, and therefore muscle property data would be less precisely captured than when compared to the method used in this thesis.

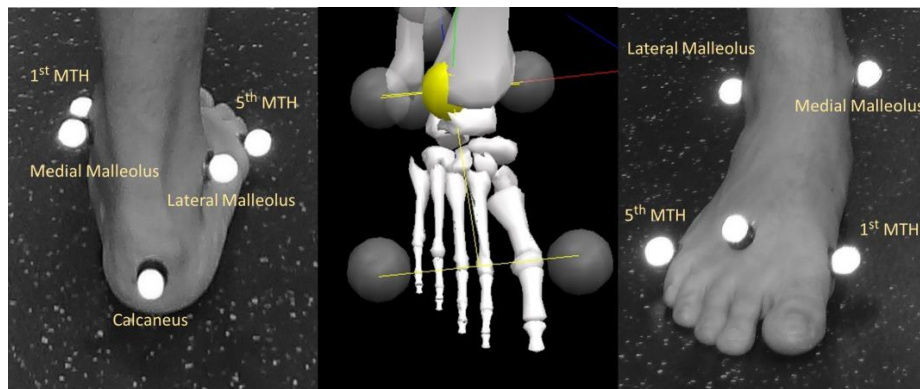


Figure 5.15: An illustration of marker placement for the foot segment for Visual3D.

Figure 5.15 shows the retroreflective marker positions on the foot and ankle. The centre of the ankle joint was taken to be the midpoint between the apices of the lateral and medial malleolus. The calcaneus, the first metatarsal head (1st MTH) and the fifth metatarsal head (5th MTH) were used as anatomical points to represent the skin cluster for dynamic motion tracking for foot the segment. Three markers were also placed on the shoes to compare the kinematic data of the ankle when markers were attached on the skin of the foot inside the shoe and also with markers attached to the shoe uppers. However, the results derived from this data are not presented in the thesis.

5.3.3.2 The shank segment

The shank segment model was adopted from that described by (Cappozzo et al., 1995). The centre of the knee joint was taken to be the midpoint between the femoral epicondyles. The shank segment was defined as a rigid structure. The proximal knee joint position was defined by lateral and medial epicondyle markers. The distal end of the shank was defined by the lateral and medial malleolus positions. Marker clusters were placed on the shank to reconstruct the segment during movement trials recording (figure 5.16).

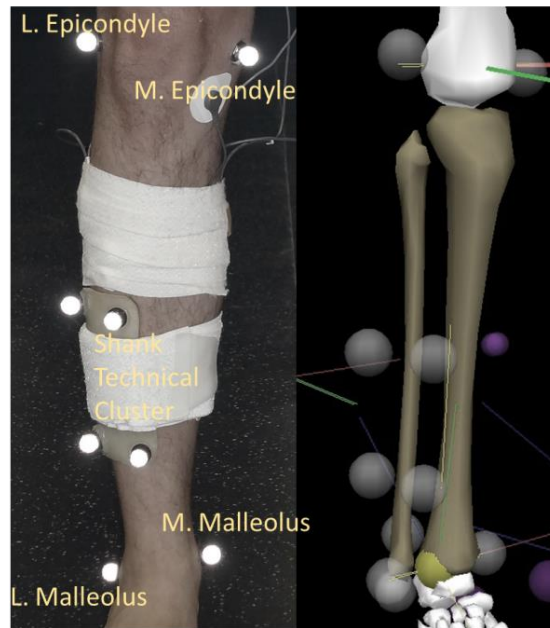


Figure 5.16: Marker placement to define the shank segment for Visual3D.

This technique was utilized to reconstruct the segment and reduce marker motion artefacts. If dynamic motion had been calculated by using a skin knee marker placement technique, skin displacement of the individual markers relative to the knee could have been as much as 40 mm (Reinschmidt et al., 1997).

5.3.3.3 The thigh segment

The thigh segment was defined by the position of the thigh anatomical markers relative to the knee joint centre. The proximal anatomical landmarks were the greater trochanter and hip joint centre. To locate the greater trochanter it was required to detect movement of one segment relative to another segment - in this case the thigh relative to the pelvis. The distal end of the thigh was defined as centre of the knee joint (based on the position of the lateral and medial epicondyles); figure 5.17.



Figure 5.17: The thigh segment marker placement used for Visual3D.

Marker clusters were used for the thigh and shank with the markers mounted on polypropylene plates moulded to provide a close fit to the thigh and leg. The plates on which the reflective markers were mounted were initially attached to the skin with double sided tape, and then elastic rubber bandage was also applied over the top of the plates and around the leg to ensure that they were prevented from moving during the walking trials. The bandage was applied so that it did not cover any of the reflective markers.

5.3.3.4 The pelvic segment

The pelvic geometry was estimated by using the most accurate procedure described by (Seidel et al., 1995) who conducted an anthropometric study of the adult pelvis using 65 cadaveric specimens (thirty males and thirty five females) to investigate the relationship between the hip joint centre and selected aspects of pelvic geometry. For this study, the hip joint centre was calculated using markers which were placed on the anterior superior-iliac spine (ASIS), the iliac crests and the sacrum (mid-PSIS); figure 5.18.

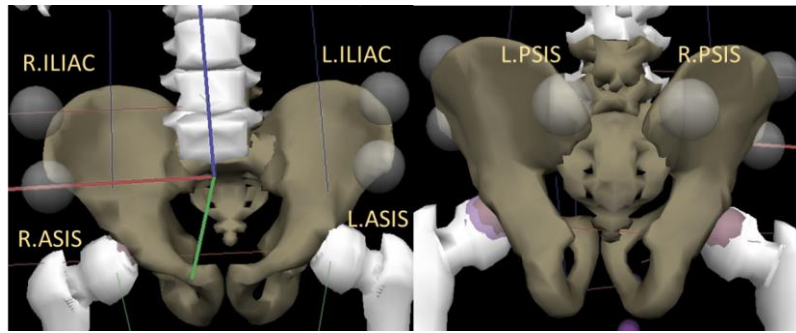


Figure 5.18: the pelvic segment marker placement used for Visual3D.

For dynamic motion tracking of the pelvic segment, four markers were therefore used: R.ASIS, L.ASIS, R.PSIS, L.PSIS.

5.3.3.5 The Trunk segment

The Thorax/Ab segment was built up according to Visual3D instructions. The proximal end of the thorax was created at the same location as the proximal end of pelvis. The distal end of the thorax was built up with right and left acromium (figure 5.19).

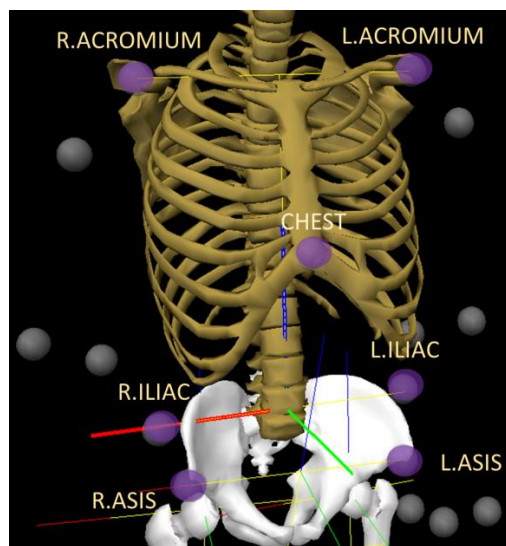


Figure 5.19: Trunk segment marker placement.

To track trunk motion, three markers were used: R.ACROMIUM, L.ACROMIUM and CHEST as shown on the figure 5.19. Markers were also placed on the arms, however results were not included in this research.

5.4 Electromyography (EMG) data collection

5.4.1 Electromyography equipment

Electromyography is a technique used for recording changes in the electrical potential of muscle fibres that are associated with their contraction at a given electrode location (Payton and Bartlett, 2008). Electromyographic data for lower leg muscles were recorded in this study by the 8-channel Noraxon wireless EMG system (Noraxon TeleMyo™ 2400T G2) (figure 5.20)



Figure 5.20: The Noraxon TeleMyo™ 2400T G2 system.

EMG data were collected at sample rate of 3000 Hz to ensure optimal quality of the data. The TeleMyo™ 2400T G2 is a real-time EMG system that sends analogue signals across a distance of up to 100 meters by wireless transmission to a desktop computer. Every subject was asked to wear a neoprene vest to which the Noraxon TeleMyo™ 2400T G2 system could be conveniently attached (figure 5.21), which also offered a convenient position for the electrode leads to be attached in a central point of the torso.

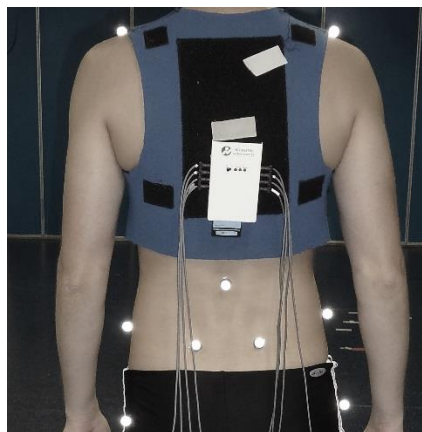


Figure 5.21: Noraxon TeleMyo™ 2400T G2 attachment during testing procedures.

5.4.2 Data collection procedure

With regards to the targeted muscles in the lower limbs, the aim of the thesis was to investigate the changes in EMG activity in conjunction with an analysis as to what type of contraction was occurring concurrently with alteration to muscle length when walking with different footwear conditions. Since it was deemed important to target the main muscles acting on the ankle and knee, as well as the lower back, surface EMG data were therefore obtained from the following six muscles on the right side of the body only:

- Medial Gastrocnemius (GAS);
- Soleus (SOL);
- Tibialis anterior (TA);
- Rectus femoris (RF);
- Biceps femoris (BF);
- Erector spinae (ES).

The EMG signal was collected via six Noraxon dual hypo-allergenic surface gel adhesive Ag/AgCl electrodes; with the EMG signal being recorded as the voltage difference between the two electrodes. Motion capture data, GRF and EMG data were synchronised during walking trials. Before placing electrodes on the muscles, the skin was shaved, rubbed with abrasive skin preparation gel (Nuprep tm ECG & EEG) and then cleaned with alcohol (Isopropyl Alcohol 70%) to reduce skin impedance. Skin preparation and surface electrode placement was performed according to the guidelines issued by SENIAM (surface EMG for a non-invasive assessment of muscles), (Hermens et al., 2000). The electrodes were attached along the line of muscle action and over the area of the greatest muscle bulk during muscle contraction and overlaid with elastic bands to minimise movement artefacts as per the SENIAM guidelines. These guidelines were followed, which recommended the placement of dual electrodes in a distal to proximal orientation over the muscle bulk as shown in figure 5.22 and table 5.1 with a separation distance of 2cm.

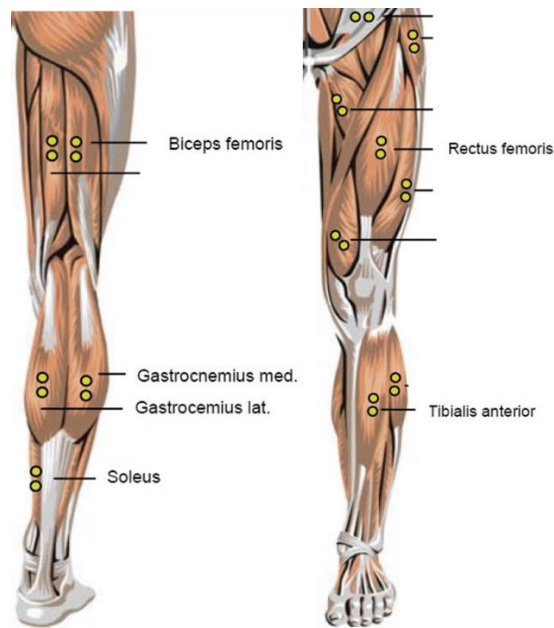


Figure 5.22: Dual electrode locations on muscles recommended by SENIAM guidelines (adopted from Noraxon guidelines).

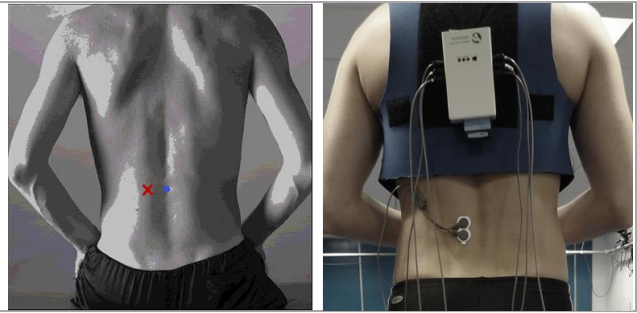
The gastrocnemius medial head muscle is attached to the proximal and posterior part of medial condyle and the adjacent part of the femur, and the capsule of the knee joint. The electrodes were attached over the greatest muscle bulk on the medial gastrocnemius muscle belly by asking the subjects to plantarflex the ankle during standing (i.e. standing on their toes). If this task was not successful subjects were asked to lie on the table with flexed knee and with a plantarflexed ankle. The perceived optimal location was then marked with a pen for the subsequent electrode attachment procedure. The location of the soleus muscle was taken as two-thirds along the line between the medial condyle of the femur to the medial malleolus. The electrodes were placed at the most prominent muscle bulk using the method of plantarflexing and inverting the ankle whilst seated and with the knee flexed (as per SENIAM recommendations). Tibialis anterior (TA) muscle bulk position was taken as being one-third along the line joining the tip of the fibula and the tip of the medial malleolus. The electrodes were again attached over the area of greatest muscle bulk. Rectus femoris arises by two tendons: one is a straight head from the anterior inferior iliac spine and another one from a groove above the rim of the acetabulum (SENIAM). To locate the rectus femoris electrode position, subjects were asked to sit on the table with knees in slight flexion and the upper body tilted slightly backwards (table 5.1).

Table 5.1: The electrode placement location over six muscles according to SENIAM guidelines (Hermens et al 1999).

Muscle	Placement position	Electrode orientation
<p>Medial Gastrocnemius</p> <p>The electrodes need to be placed on the most prominent bulge of the muscle.</p>		
<p>Soleus</p> <p>The electrodes need to be placed at 2/3 of the line between the medial condyles of the femur and the medial malleolus.</p>		
<p>Tibialis Anterior</p> <p>The electrodes need to be placed at 1/3 on the line between the tip of the fibula and the tip of the medial malleolus.</p>		
<p>Rectus Femoris</p> <p>The electrodes need to be placed at a position 50% along a line from the anterior superior iliac spine to the superior part of the patella.</p>		
<p>Biceps Femoris</p> <p>The electrodes need to be placed at 50% along the line between the ischial tuberosity and the lateral epicondyle of the tibia.</p>		

Erector Spinae

The electrodes need to be placed at 2 finger width lateral from the upper lumbar spine



Biceps femoris long head originates from the distal part of sacrotuberous ligament and the posterior part of the tuberosity; the short head originates from the lateral lip of linea aspera, the proximal two-thirds of the supracondylar line and the lateral intramuscular septum. To attach electrodes to biceps femoris subjects were asked to lie in a prone position face down with the thigh down on the table and knees flexed (to less than 90 degrees). This meant they could flex their knee with the hand holding the ankle and to resist flexion, which allowed the muscle location to be marked with a pen.

5.4.3 Study Design

This was a randomised, one visit study design. Test conditions were randomised to minimise any carry-over effects, although these have been shown to be minimal in previous rocker shoe studies.

5.4.4 Participants

Healthy young male subjects were recruited via a poster and information sheet, and after giving informed consent, were tested in the gait laboratory. This subject group was chosen to minimise data variability in walking patterns which could be caused by previous injury or age differences in the test subjects. The exclusion criteria included subjects with a history of any orthopaedic or other pathology which could adversely affect ambulation, evidence of previous back pain, injury to the lower limbs, leg length discrepancy, or loss in sensation in the lower limbs. Subject demographics are demonstrated in the results section. All subjects gave informed consent and signed a consent form and were also given a subject information sheet. They also understood that they were free to remove themselves from the study at any time.

5.5 Footwear selection criteria

It was decided to select footwear test conditions which could feasibly be used in clinical practise and reflected the designs commonly seen in rocker sole and other outsole designs. The literature suggests that footwear features regarding their outsole design may be divided into three regions (van Schie et al., 2000); namely:

1. The back of the heel (or the so-called rearfoot portion);
2. The midfoot region, and;
3. The forefoot region and toes.

The results of the literature review suggested that alteration to lower limb muscle activity can be achieved by varying footwear features, which alter the internal and external forces acting on the body segments, and therefore alter muscle-tendon properties and muscle activity.

The following outsole features were therefore investigated:

- The rocker apex angle at the distal (toe) end and the apex position (the position along the shoe at which the outsole begins to curve or angle upwards);
- The relative stiffness of the outsole (the relative amount of force required to bend the shoe or deform it);
- The heel height (and also the overall pitch of the shoe);
- The heel curve (otherwise known as a rolled or chamfered heel) (figure 5.23).

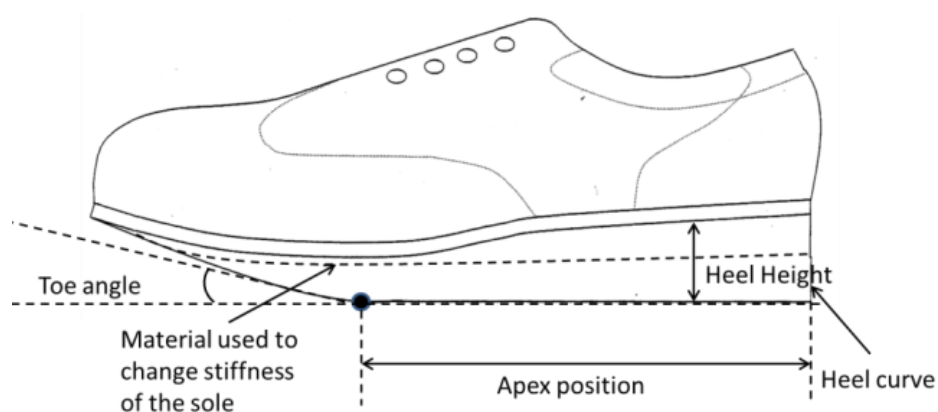


Figure 5.23: An illustration of the footwear features analysed in this thesis.

Most of the research found in the literature has investigated ambulation using single designs of footwear rocker profiles and most papers using this approach have not demonstrated any evidence of systematic changes to the human musculoskeletal gait pattern. It was thought that by varying one parameter at a time for each design in this study, the interpretation of the resulting gait changes would be more efficiently analysed and obvious than previously. Therefore, in this research, each rocker sole was modified with the intention to enable identification of the causes and effects of altering specific design parameters on the primary outcome measures. There were fifteen footwear profiles tested which are described in table 5.2. Illustrations for each rocker sole profile test conditions are shown in figure 5.26.

Table 5.2: Footwear specifications.

Shoe	Heel Height (HH)	Sole Stiffness (SS)	Rocker Apex Position (AP)	Rocker Toe Angle (TA)	Heel Curve (HC)
Rearfoot heel height					
1 Heel Height	1.5 cm	stiff sole	62.5%	15°	No curve
2 Heel Height	2.5 cm	stiff sole	62.5%	15°	No curve
3 (HH3) (control)	3.5 cm	stiff sole	62.5%	15°	No curve
4 Heel Height	4.5 cm	stiff sole	62.5%	15°	No curve
5 Heel Height	5.5 cm	stiff sole	62.5%	15°	No curve
Rocker profile stiffness					
8 Sole stiffness	3.5 cm	medium flexibility	62.5%	15°	No curve
10 (SS) (control)	3.5 cm	stiff sole	62.5%	15°	No curve
11 Sole stiffness	3.5 cm	flexible sole	62.5%	15°	No curve
Apex position					
9 Apex position	3.5 cm	stiff sole	55%	15°	No curve
10 (AP) (control)	3.5 cm	stiff sole	62.5%	15°	No curve
12 Apex position	3.5 cm	stiff sole	70%	15°	No curve
Apex angle					
14 Toe Angle	3.5 cm	stiff sole	62.5%	10°	No curve
15 (TA2) (control)	3.5 cm	stiff sole	62.5%	15°	No curve
15 Toe Angle	3.5 cm	stiff sole	62.5%	20°	No curve
Heel curve					
16 Heel Curve	3.5 cm	stiff sole	62.5%	15°	Small curve
17 (HC)(control)	3.5 cm	stiff sole	62.5%	15°	No curve
18 Heel Curve	3.5 cm	stiff sole	62.5%	15°	Big curve
Baseline condition					
19 Standard	2.5 cm	Medium flex	62.5%	15°	No curve
20 Barefoot	-	-	-	-	-

5.6 Procedure used to adapt shoes with rocker sole profiles

High street footwear was obtained for use in the study. The shoe selected was a four-hole tie Gibson-styled shoe with semi-brogue punching, padded collars, synthetic lining and a moulded polyurethane sole and heel unit. All were size eight adult UK fitting. The shoes had an initial heel height of 2.5cm, a toe box depth of 30mm and a forefoot width suitable for use by people with an average forefoot width (figure 5.24).



Figure 5.24: The Standard high street shoe (size 8 adult UK) which was used as the base structure for adaptation.

To manufacture the shoe test conditions, the waist area of the shoe (the area between the breast of the heel and the tread point of the sole where the sole contacted the ground with the heel also in full contact) was initially roughened slightly to provide an adherent surface, and filled in with sheets of 10 mm thick high density plastazote (HDP), (Algeo UK Ltd, Liverpool UK). This material is a high density expanded polyethylene which is ideally suited to footwear adaptation. It is mouldable at a temperature of 120°C and is easily ground to provide a flat or curved surface. In addition, it does not compress easily under load which makes it ideal for the addition to the base of shoes for such adaptations such as external raises and rocker profiles. The HDP material and the shoe surface were both brushed with contact adhesive and then placed under ultraviolet light heaters to activate the adhesive and to heat up the HDP to make it flexible. Once the HDP was flexible enough it was applied underneath the waist area of the shoe and left to cool.

Once cool and adhered to the waist area, it was ground down on a flat grinder to make a flush surface with the base of the heel and the sole. This then facilitated the addition of extra layers of 25 mm HDP to be adhered to this base shape and which could be ground to the desired shape required according to the design of rocker sole selected.

The rocker profile designs utilized are shown on the footwear specification table (table 5.3). The rocker profile and its orientation to the pitch and plantar shape of the un-adapted shoe was drawn on the HDP using a template derived from a scale drawing generated from a computer programme which accounted for apex position, heel height, toe angle and heel shape. Following this, they were all ground according to the line structure drawn on the HDP. The final thickness of the added material made the rocker sole rigid enough to allow the rocker profile to act as a rigid shape.

Once the shoe was appropriately adapted with the rocker sole profile a final layer of 1 mm vibram material was adhered to the base of the rocker sole to ensure that the surface in contact with the ground was non-slip and also to ensure the plantar surface did not wear down.

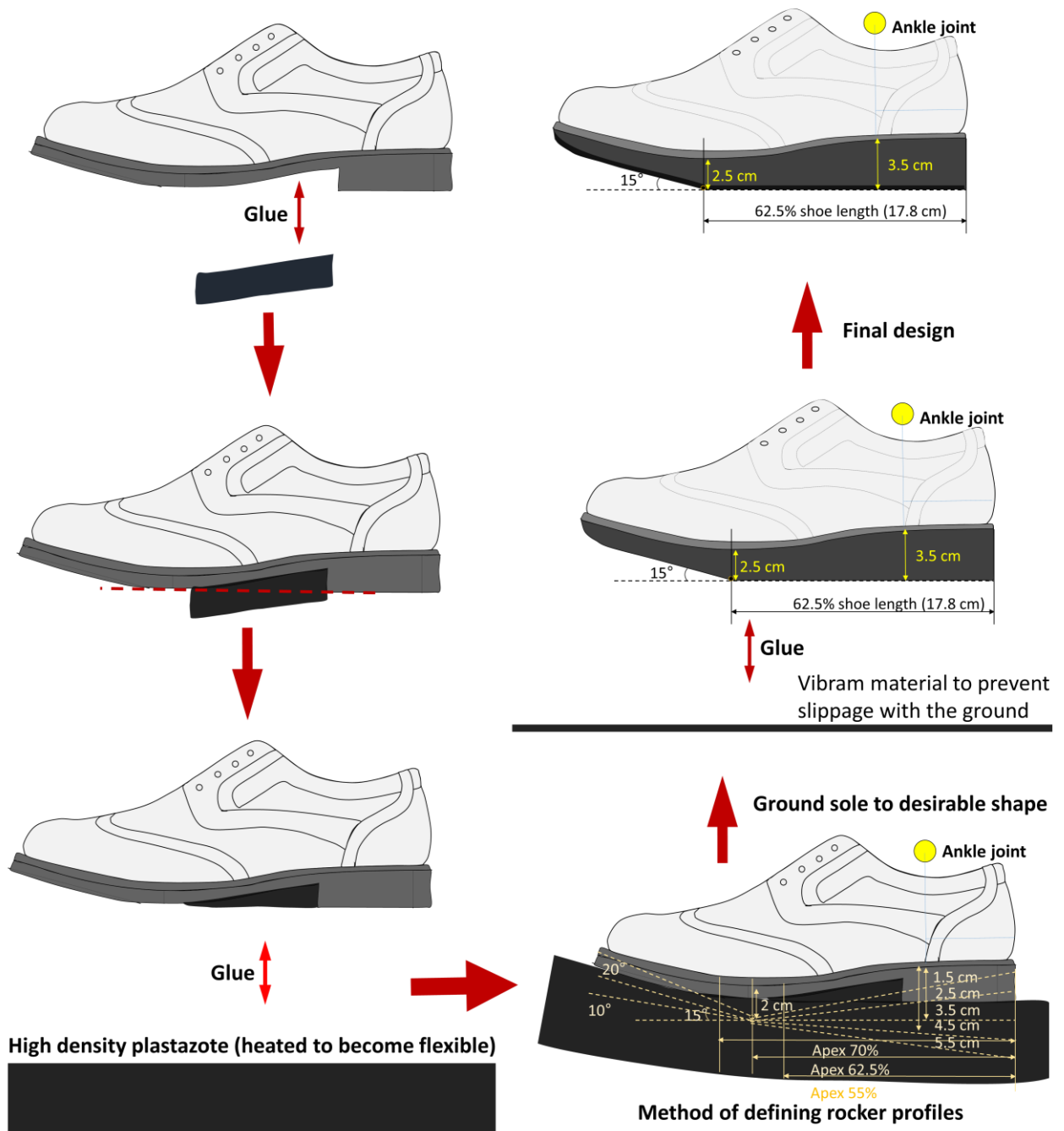

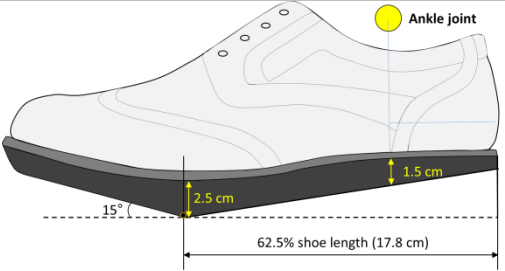

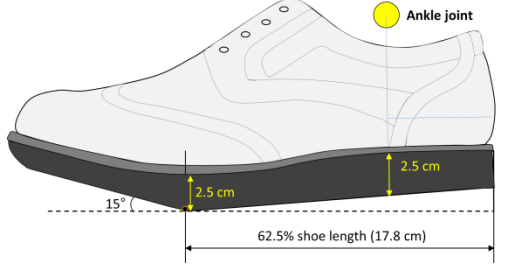

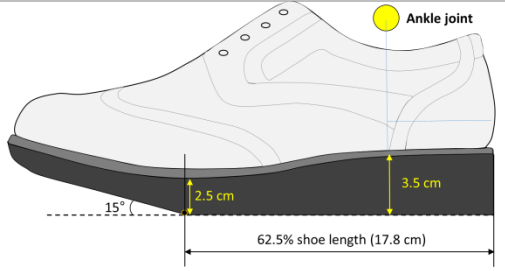

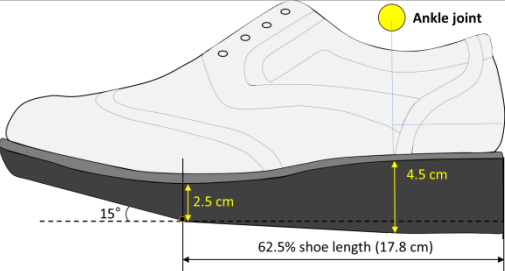



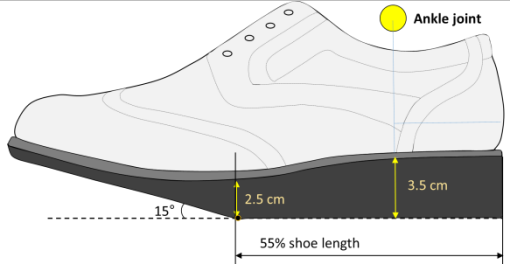



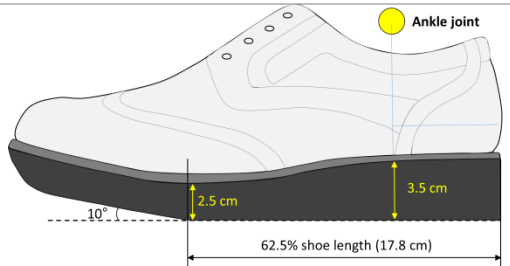
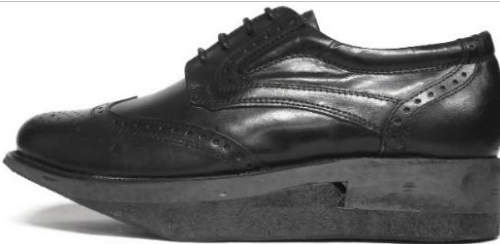
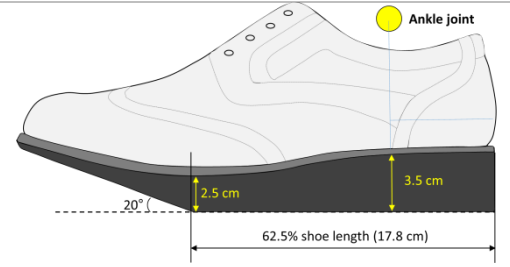

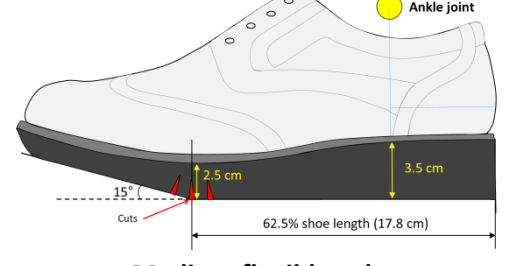

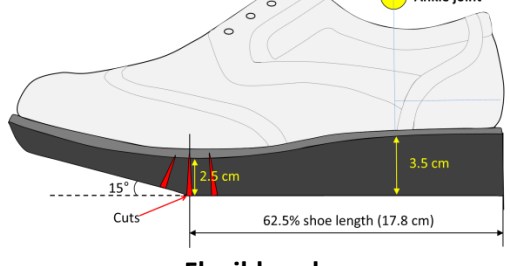


Figure 5.25: Sole and heel adaptation procedure.

The footwear test conditions which were used in this research are illustrated in figure 5.26.

 <p>1.5 cm heel</p>	 <p>1.5 cm heel</p>
 <p>2.5 cm heel</p>	 <p>2.5 cm heel</p>
 <p>Control shoe, 62.5% Apex position, solid, 15° Toe angle</p>	 <p>Control shoe, 62.5% Apex position, solid, 15° Toe angle</p>
 <p>4.5 cm heel</p>	 <p>4.5 cm heel</p>
 <p>5.5 cm heel</p>	 <p>5.5 cm heel</p>

 <p>55% Apex position</p>	 <p>55% Apex position</p>
 <p>70% Apex position</p>	 <p>70% Apex position</p>
 <p>10° Toe angle</p>	 <p>10° Toe angle</p>
 <p>20° Toe angle</p>	 <p>20° Toe angle</p>
 <p>Medium flexible sole</p>	 <p>Medium flexible sole</p>
 <p>Flexible sole</p>	 <p>Flexible sole</p>

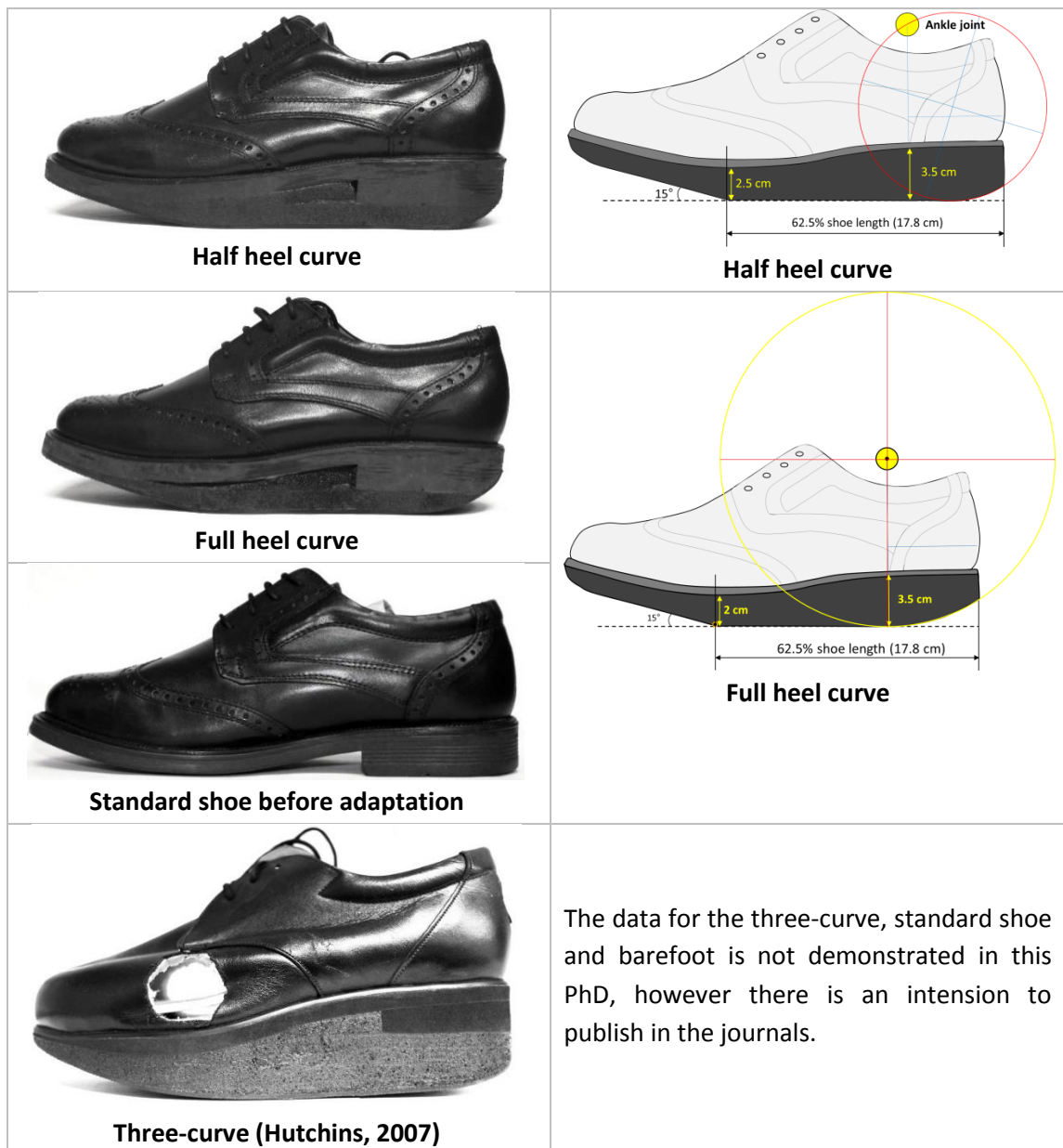


Figure 5.26 Test footwear conditions which were used in this research.

The comparison results for three-curve and standard shoe without adaptation, which are not presented in result section are planned to be published in journals.

5.7 Gait laboratory testing procedure

The gait laboratory was prepared before each testing session to ensure that all of the equipment was working correctly. An acceptable calibration of the Qualysis was performed, and the timing gates were tested. It was ensured that all the batteries required for the walking test equipment were fully charged that the EMG system was synchronised with the

gait laboratory software, and that the trigger was able to start simultaneous kinematic, kinetic and EMG data collection.

Retro-reflective markers were prepared with double-sided tape, and elastic bandages to bind on top of the marker clusters were made available. EMG electrodes, shaving razors, EMG gel and alcoholic wipes, cleaning wipes, scissors, a pen, and towels were all made ready in preparation for testing.

On attendance at the gait laboratory, each participant was familiarised with the testing procedure and agreed to undertake the gait laboratory test protocol by signing a consent form. Once everything was prepared, each participant was then instructed to change into tight fitting shorts (or swimming underwear). The ambient temperature in the laboratory was adjusted to be comfortable for each participant. The testing procedure and walking direction was explained to each participant, who was then asked to repeatedly walk over force plates where recording was to be performed to assess their walking speed and to ensure it was within the envelope set of 5 kilometres per hour \pm 5%. The walking speed was checked using the timing gate system. Once the participants' speed was proven to be constant, the starting point of gait initiation was adjusted to make sure that they stepped in centre area of the first right hand platform in the direction of travel with the right foot first without looking down. Subjects were asked to look straight ahead whilst walking. It was possible to record two gait cycles for most of the walking trials. The walk was adjusted so that the right foot struck the first force platform, followed by a left heel strike on the next platform; meaning a second right heel strike could then occur on the subsequent right hand platform (denoted number 1) as show in figure 5.27.

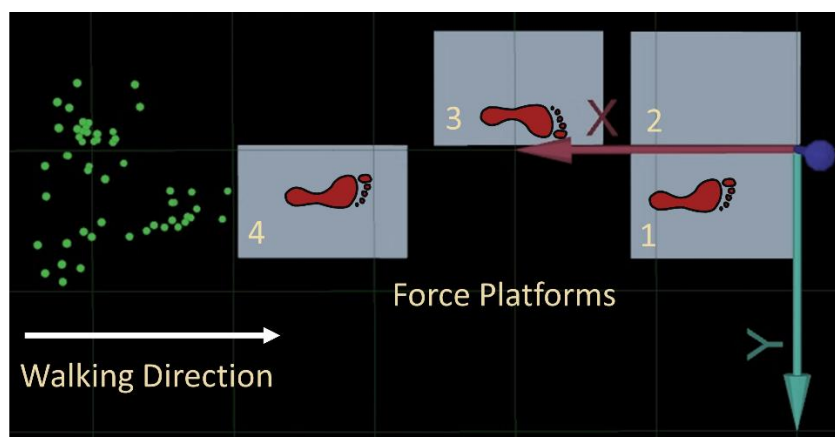


Figure 5.27: Force plates used to record GRF showing the subjects' walking direction.

The walking trials confirmed symmetry between the left and right lower limb data for all the subjects as the individuals were healthy. Therefore, only the right side was eventually chosen for analysis. In addition, there were only eight EMG channels available, and six of them were already used for the right side lower limb and the back muscles.

After familiarisation, SENIAM recommendations were used to locate and mark the targeted muscles for surface EMG recording for the right leg and the lower back. The subject's skin surface was prepared to reduce electrical resistance by shaving the skin surface of the muscle belly area, and removal of dead skin cells was performed using gel (Nuprep tm ECG & EEG) and alcohol (Isopropyl Alcohol 70%) (Sousa and Tavares, 2012).

Once this was done, participants were asked to don the neoprene vest to which the Noraxon TeleMyo™ 2400T G2 EMG system was attached posteriorly with six numbered electrode leads connected. The EMG for each muscle was collected by an eight-channel unit at a frequency of 3000 Hz. The measurement electrodes were placed over the muscle belly of the medial gastrocnemius, soleus, tibialis anterior, rectus femoris, biceps femoris and erector spinae muscles according to the quoted anatomical references, and positioned with adhesive tape (as per SENIAM recommendations).

Each electrode was marked with a number to ensure to which muscle it belonged for the further data processing. Each subject wore cushioned socks manufactured by Nike to make sure blisters did not form during the testing procedure, as this had occurred during the pilot study. Holes were made in the socks to enable the reflective markers to be placed directly onto the skin covering the first and fifth metatarsal heads and the superior aspect of the calcaneus. Participants were then asked to wear the control shoe to which the holes had been made to ensure that these holes matched the position of circular rings depicting the position of the plastic base onto which the reflective markers were placed which had been drawn on the foot with a pen. The next step was to place anatomical markers. The total amount of markers was 46; however additional markers were placed on the arms and shoe uppers. The shoe uppers were altered by making holes in the uppers at strategic places and markers were placed on the skin of the foot which protruded through these holes cut in the uppers, as detailed in section 5.3.3.1. All the markers and electrodes were positioned by the author. An assistant helped to press the trigger and to name the trial data acquired by Qualysis during the walking trials.

With the markers and electrodes in situ, the EMG system was then tested to ensure full functionality. Participants were asked to stand up on their toes to ensure that the electrodes were accurately positioned over the muscle bellies of medial GAS and SOL, and that an adequate signal was being recorded by the data acquisition system. They were then asked to dorsiflex the foot to check the electrodes were correctly positioned over the tibialis anterior muscle (TA), and also asked to bend their knees to check that the muscle firing for the more proximal leg muscles were being detected adequately. All the connecting leads were arranged to be appropriately positioned without interfering with gait and were taped to the leg and torso to reduce motion artefacts.

5.7.1 Static tests

Static tests were performed for each subject and for each footwear condition prior to undertaking the walking trials in the gait laboratory. Participants stood on force platform number 3 with their feet parallel to each other and then stepped onto force platform number 2 to ensure that the static test was of good quality and that all the markers were visible for data analysis. Each subject was asked to stand up straight with their knees fully extended, their feet pointing forward towards the walking direction and with both legs symmetrically positioned.

5.7.2 Dynamic tests

Barefoot recording was undertaken after the static capture and at the beginning of the testing. Ten walking trials of acceptable quality were recorded and saved for further analysis for each subject. Once data collection for barefoot was finished, one of the shoes used was randomly selected as a test condition and donned, and the retro-reflective markers were repositioned again on the area where the circles had previously been drawn on the foot and through the holes cut in the uppers of the shoes. The testing order for each shoe test was randomised for all subjects throughout their walking trials. After donning each pair of shoes, a static test was recorded and then a small number of walking trials were performed to monitor the walking speed for repeatability and to identify the optimal gait initiation point before walking data were recorded. It typically took five minutes to record the walking trials and five minutes to replace the shoes for each footwear test condition and to ensure that

the leg muscles being tested were not getting fatigued. A five minute period of habituation was given for each test condition, and also a number test runs were performed for each shoe test condition to ensure each subject could walk confidently for each run by striking the force plates in the correct area and also maintaining gait speed within the set time parameters using the timing gates.

At the end of the testing session the subject's weight and height was measured with the clinical equipment available in the gait laboratory.

5.7.2.1 Walking speed

Various sources from the literature and scientific articles for the effect of walking speed on kinematic, kinetic and EMG data for lower limb suggest that it has a significant impact on these changes (Kirtley et al., 1985, Chen et al., 1997, Holden et al., 1997a, Waters and Mulroy, 1999, Hof et al., 2002, den Otter et al., 2004, van Hedel et al., 2006, Byrne et al., 2007, Chiu and Wang, 2007, Stoquart et al., 2008, Chung and Wang, 2010, Sousa and Tavares, 2012).

It was therefore decided that the best method for kinematic, kinetic and EMG data collection for this study was to closely control walking speed during the gait laboratory trials. Previous studies have demonstrated that speed of walking effects gait patterns and EMG data, and would therefore have an effect on the results obtained with regards to muscle properties, which were based on Qualisys kinematic motion capture data. Chung and Wang (2010) conducted research to investigate the gait performance of subjects aged between 20-60 years of age utilising walking speeds of 80%, 100%, 120%, 140% of their preferred walking speed. The most significant alterations to gait parameters were noted once subjects attained walking speeds greater than 20% of their preferred walking speed. Holden et al (1997a) demonstrated that if subjects walk at lower natural speed by a factor of 25%, it results in reduced knee flexion and lower knee moments. Additional research, which investigated the effect of varying walking speed and the effects of additional weight on lower limb muscles and gait, has demonstrated that significant changes in joint kinematics for healthy subjects at walking speeds slower than 3 km/h (kilometres per hour) versus the 5 km/h figure (van Hedel et al., 2006) can occur.

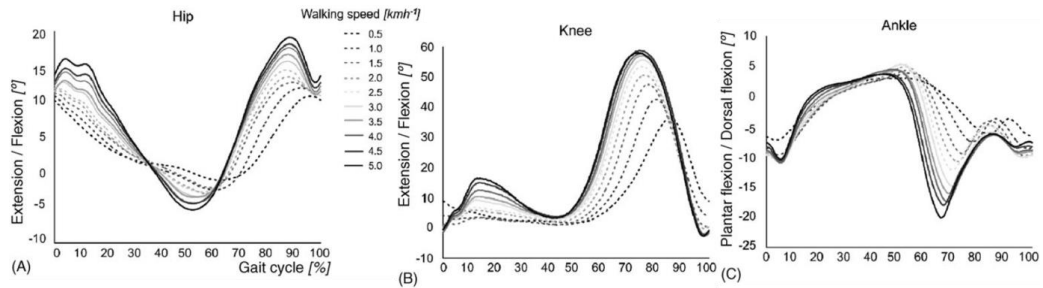


Figure 5.28: Influence of walking speed on joint trajectories for (a) hip, (b) knee and (c) ankle joint at 10 different walking speeds (van Hedel et al., 2006).

Chiu and Wang investigated the effect of speed and gender on muscle activity, joint motion in lower extremity plus GRF values and demonstrated that walking speed had a significant influence on the perceived extension of the whole body, as well as the buttock, rear thigh, front thigh and rear shank areas. An increased walking speed caused significant increases in the muscle activity of erector spinae, biceps femoris, and medial gastrocnemius, as well as GRF values as shown in figure 5.29.

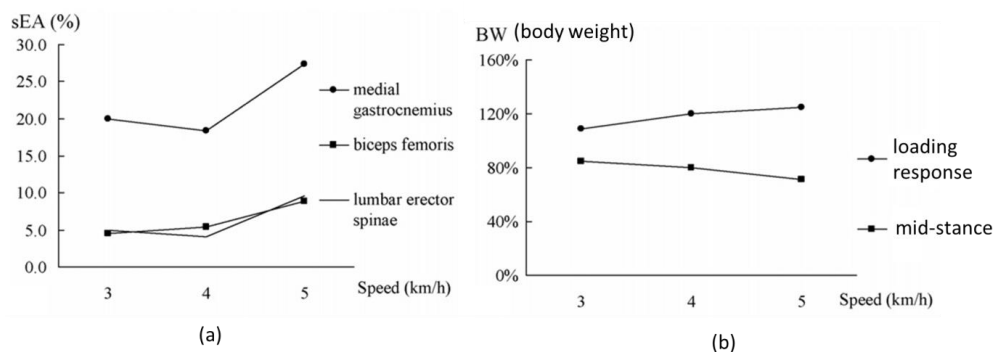


Figure 5.29: The gait speed effect on (a) EMG activity, (b) vertical ground reaction force (Chiu and Wang, 2007).

One recent study of the effect of gait speed on muscle patterns and magnitude during stance phase on thirty-five healthy individuals for gastrocnemius medialis, biceps femoris and rectus femoris muscles showed significant changes due to walking speed. In general, muscle activity was significantly higher at + 25% of self-selected walking speed and significant lower at -25% of self-selected walking speed (Sousa and Tavares, 2012).

Most adults prefer to walk at a speed of between 3600 and 6012 metres/hour. The average walking speed observed by Walters and Mulroy (1999) for adult pedestrians aged between 20-60 years old (who were unaware they were observed) was 4932 meters per hour. The

participants who volunteered for this thesis were young, aged 25.3 ± 2.73 years with an average height of 1.74 ± 0.06 m, and were healthy. Therefore, the ideal selected walking speed for all subjects to attain during the walking trials in this study was chosen as 5 kilometres per hour. The evidence demonstrates that walking speeds within a range of $\pm 5\%$ have no significant comparative effects on knee and ankle kinematics or EMG readings for lower extremities during stance phase. Therefore, the acceptable speed range within the trials was set at $5\text{km/h} \pm 5\%$ for this research.

5.7.2.2 The timing gates

Timing gates were utilised to ensure each walk taken with each footwear test condition was performed within set time parameters. A short period of habituation was allowed for each subject prior to walking in each test condition. No evidence was found in the literature of the existence of carry-over effects when walking with rocker-soled footwear. The timing gates utilised were manufactured by Brower SpeedTrap II (figure 5.30) and gave an audible sound when passed through by the subject both on commencement and completion of the walk in question.



Figure 5.30: The Brower SpeedTrap II timing gate system.

The speed of walking was shown using the remote controller of the system. If a walk was seen to not be within the prescribed limits of time, then further walks were undertaken to ensure an adequate number of walks for subsequent analysis were performed.

5.7.2.3 Gait laboratory synchronisation equipment setup

Qualisys Track Manager (QTM) software and hardware had complete integration with the Noraxon's wireless EMG system. All the basic settings below were selected:

- The muscle channel name;
- The sampling rate;
- The channel output;
- Trigger synchronisation;
- Device setup and synchronisation check.

The EMG settings for EMG devices were set using the QTM software and all data were captured directly to the Qualisys software. Only one single desktop computer was used for integration. The EMG integration was added to the existing integration with four force plates. It was possible to start Qualisys recording EMG, force and motion capture data from the QTM software. An external trigger was used to control the start of recording. The basic experimental setup for the gait analysis and synchronisation is shown on figure 5.31. The EMG capture frequency was set at 3000 Hz. Motion data capture frequency was set at 100 Hz and the force plate frequency for all plates was set at 100 Hz.

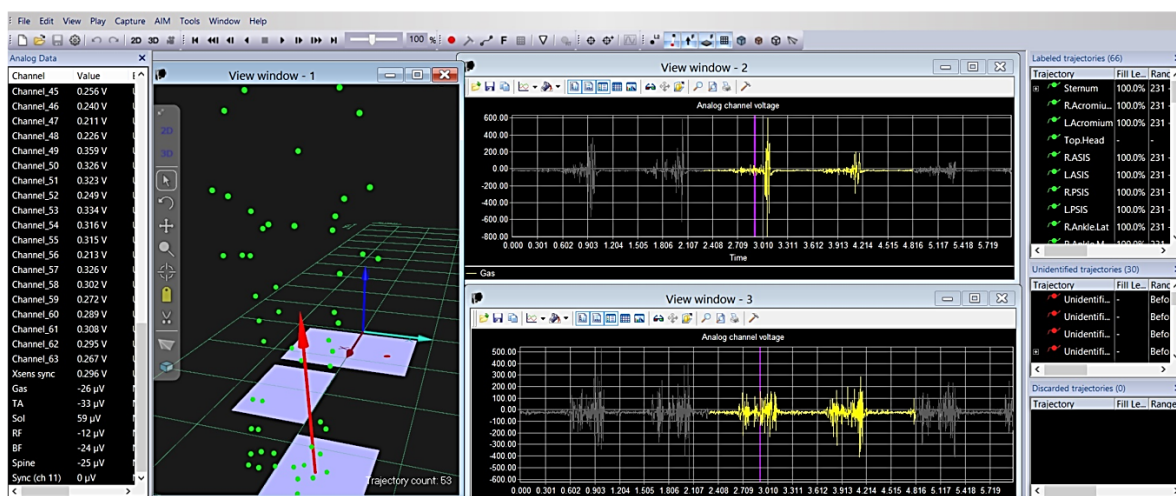
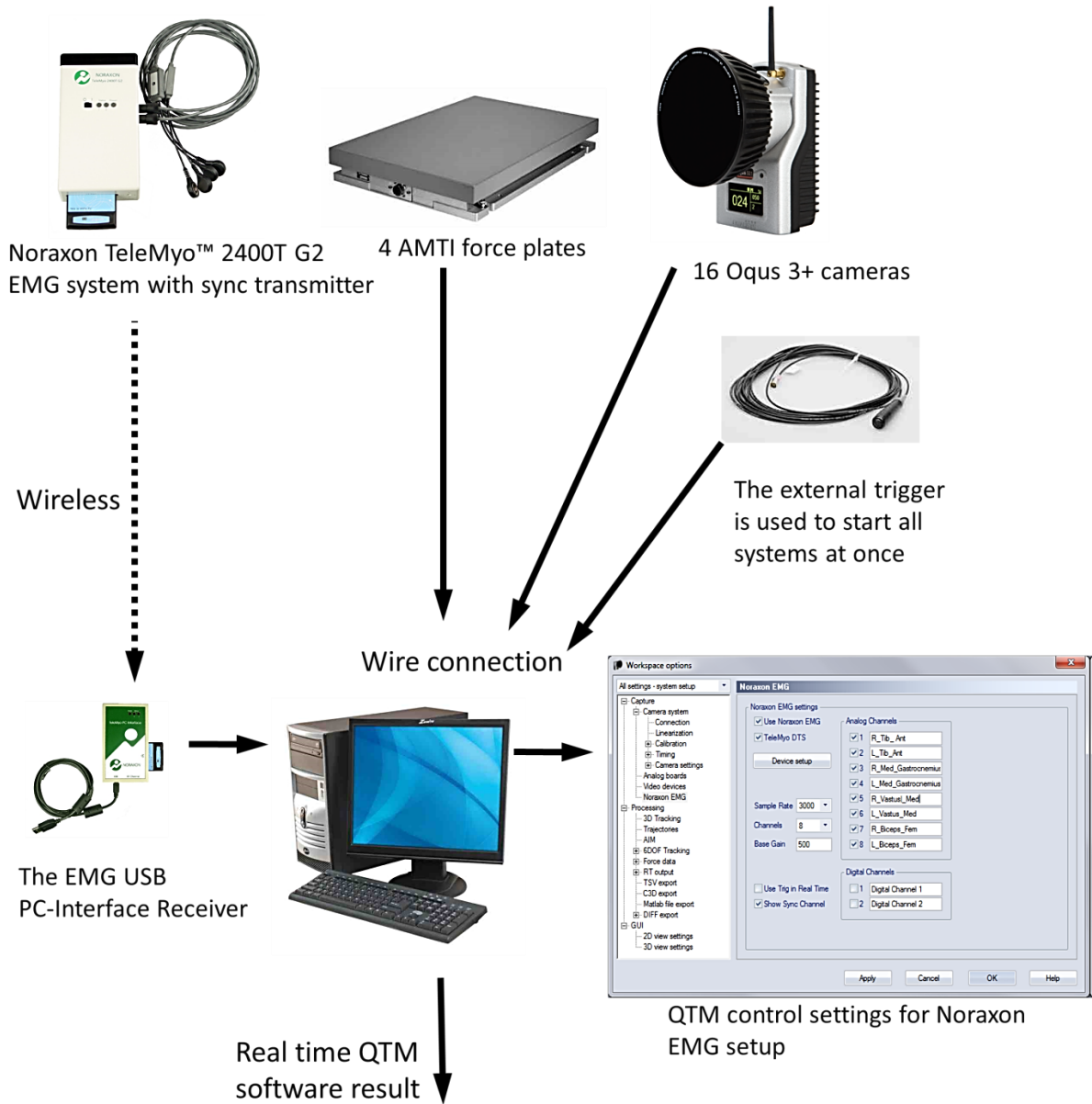


Figure 5.31: The experimental set-up for gait analysis.

5.8 Data analysis

5.8.1 Data processing overview

Kinematic, kinetic and EMG data were collected and stored by Qualisys Track Manager (QTM) software. All markers were labelled and checked for any errors in QTM. Thus use of numerous cameras meant that all markers were visible for each frame during motion capturing for the most part. Typically, there were no any gaps at all and if there were missing gaps in the tracking data, they were reconstructed within 10 frames by system default. Static trials were prepared for each footwear condition and they were exported within 1-2 frame range. Motion data were exported with at least 10 frames before heel-strike on the force platform. The exportation format was C3D for the further processing in Visual3D software. All data were then imported to Visual3D. Static models were built for each footwear condition and assigned with motion files. Each static model for each subject was scaled with mass and height. Kinematic data were smoothed using a 4th order Butterworth low-pass filter with a cut off frequency of 6 Hz and kinematic data were filtered with the same filter of frequency 25 Hz. Once it was finished, automatic gait events were generated in pipeline and then checked to be correct for each trial. Following this, EMG data were processed using a linear envelope technique and a moving root mean square technique (RMS). Kinematic, kinetic and EMG data were then analysed and presented in the reports. To export data to OpenSim, one barefoot static model was used for all motion files. Five trials per shoe condition were exported with a low-pass filter of 12 Hz being applied. Once it was finished all data were imported to OpenSim and the following parameters were analysed for GAS, SOL, TA, RF, BF and ES muscles:

- Fibre length, tendon length, muscle-tendon length;
- Fibre and tendon lengthening velocities and acceleration;
- Fibre force, tendon force;
- Muscle moment arm.

Once all analysis was finished for each subject, it was then exported to an ASCII file and imported back to Visual3D for further definition of gait event and normalisation process. Once all data analysis was completed in Visual3D, it was exported to ASCII format for the further processing in Excel and statistical analysis in SPSS. The mean values were calculated

in Excel. Each mean value was obtained for each trial separately and the average of the means were calculated for each footwear condition and subject. This was done because the mean value for each line can be different in time/frame scale, therefore the mean value for the same point in time might be different for each trial as shown in the figure 5.32.

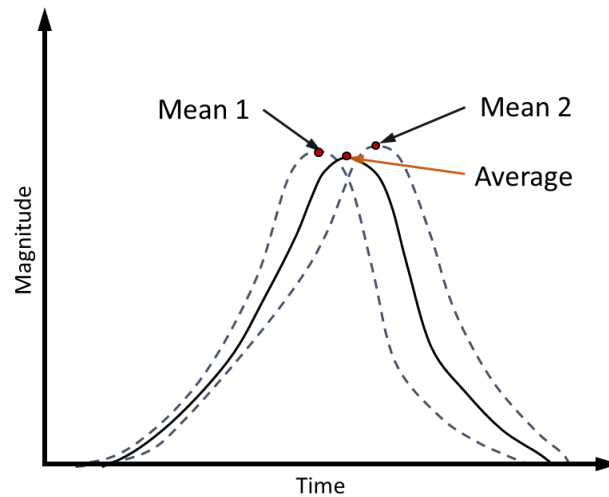


Figure 5.32: The example of mean value calculation technique.

5.8.2 Kinematic data processing

The Oqus 3+ system incorporates Qualisys Track Manager (QTM) software, which handled the motion capturing process. The QTM software allowed the use of the following features for this research:

- 2D / 3D / 6DOF data tracking;
- Marker / high-speed video data;
- Real-time streaming;
- Automatic marker identification;
- Marker masking;
- Passive markers;
- Supported all Oqus 3+ cameras, Noraxon EMG system and AMTI force plates to be synchronised.

The kinematic, kinetic and EMG data were collected simultaneously and captured by QTM software and kept in the single trial which could be exported for further analysis by

Visual3D. An automatic identification of markers (AIM) function was utilised to expedite data processing. In order for this method to be valid, the first walking trial was labelled to allow the rest of the trials be automatically labelled afterwards. The data were subsequently inspected for any marker labelling errors and corrected. Numerous cameras were used for this research, and therefore most of time, all the dynamic markers were visible throughout the measurement volume during data recording. However, QTM allows the user to pre-define gap-missing markers and fill with acceptable level of ten frames. These data were then exported via C3D files at least 10 frames before the heel strike on the force platform to be analysed by Visual3D software.

5.8.3 Visual3D

Visual3D is designed and developed by C-Motion. Inc (Maryland, USA), and is one of Qualisys' global, strategic partners for research application. This software can process complex motion capture data and analogue signals (e.g. force platforms and EMG signals) and provides informative reports. For this study, Visual3D was used for:

- 6 degrees of freedom modelling;
- Defining gait event from heel strike (HS) to toe off (TO) for every trial for data analysis during stance phase;
- Filtering/smoothing data and normalising data for standard biomechanical analysis;
- EMG analysis;
- Kinematic and kinetic data analysis;
- Exporting kinematic data to OpenSim software;
- Muscle property data synchronisation with OpenSim;
- Report design;
- Exporting kinematic, kinetic, EMG data and muscle property data to Excel.

5.8.3.1 Modelling

The Visual3D biomechanical model defines each joint as having six degrees of freedom. The kinematics of the model were calculated by determining the transformation from the recorded tracking targets to the pose of the model using an optimal approach (Cappello et

al., 1997). The trunk, pelvis, thigh, shank and foot were modelled in Visual3D as rigid segments, which were linked with joints. Each segment is specified by a proximal endpoint, which is defined as being the closest point to the centre of mass and the distal endpoint, which is further away. The following picture illustrates a segment definition, and shows the terminology used for defining segments in anatomy and Visual3D (figure 5.33).

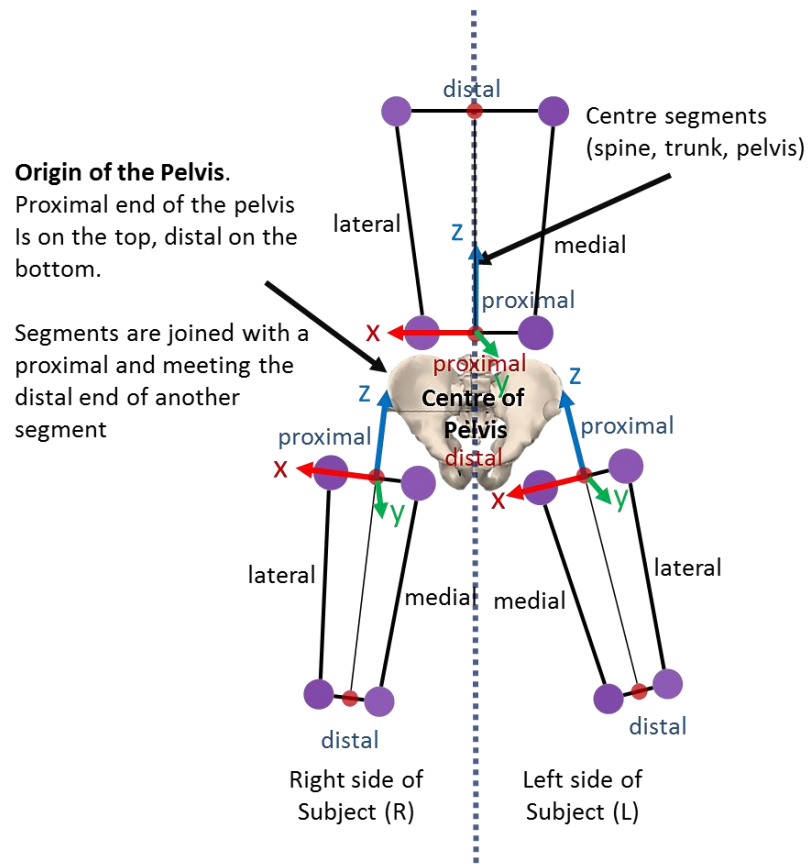


Figure 5.33: Naming standards and conventions in Visual3D.

The segmental coordinate system in visual3D is defined by the location of the proximal and/or distal ends of the segment and lateral/medial aspects. The coordinate system of the segment in Visual3D shows at the proximal end of the joint centre as shown in figure 5.33.

In section 5.3, the anatomical marker placements method utilised was explained in detail, and also marker placement for building up the segments in Visual3D. The picture below illustrates the full body model which was built in Visual3D using this method (figure 5.34).

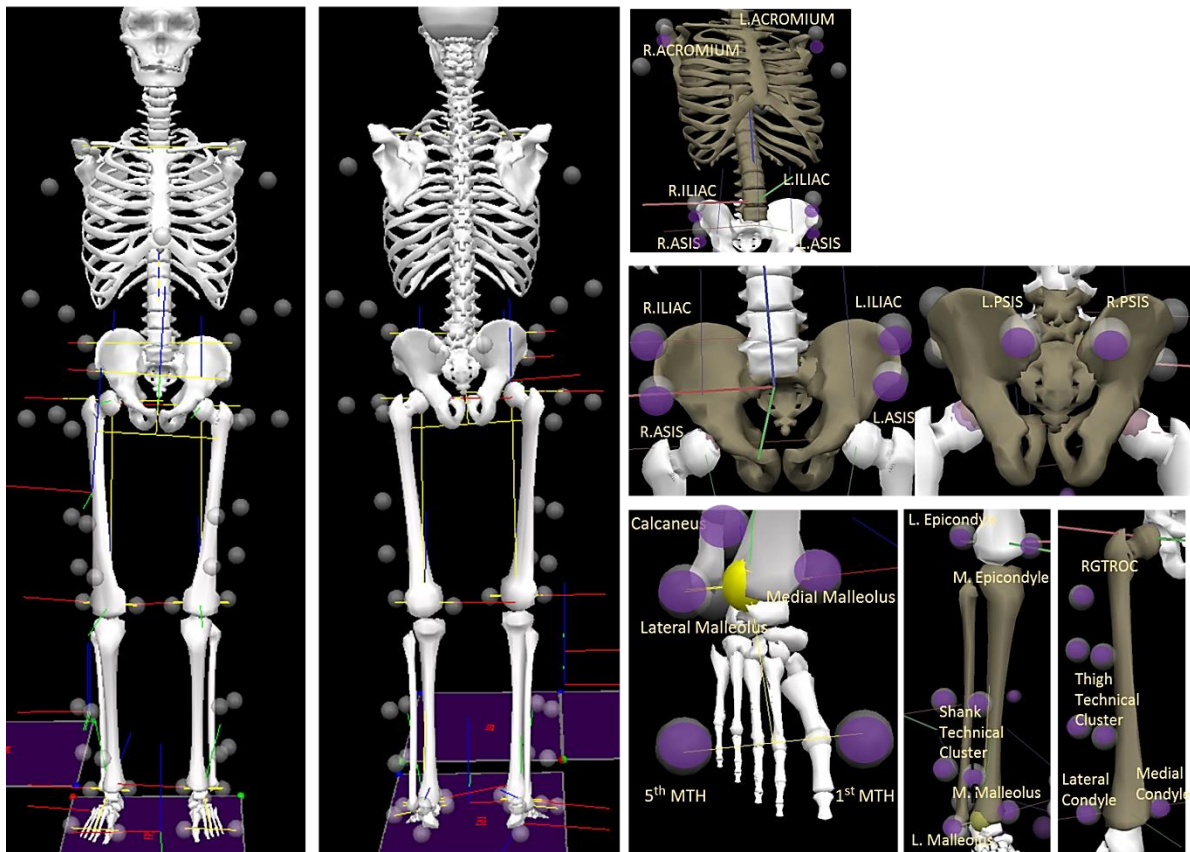


Figure 5.34: An example of the full body model in Visual3D used for this research. There were additional markers on the arms, however data acquired from these were not included in this research.

One limitation to the model used was that the foot was modelled as one rigid segment and therefore, did not distinguish between the ankle and subtalar joints.

5.8.4 Signal Processing in Visual3D

5.8.4.1 Kinematic and kinetic data

Filtering is an important consideration with human movement data. The cut-off frequency of the filter can have a significant effect on the shape of the marker trajectory line in three-dimensional movement. If the frequency were to be set too low, the curve may become over-smoothed and peaks could be flattened. For example, if the ankle angle curve were to change shape and duration during loading response, too low a filter value could cut out too much data and useful information (such as muscle-tendon length, velocity, muscle moment arm etc.) and could therefore be partially lost. If the cut-off frequency used is too high, the

curve will contain noise. Walking data are typically filtered at 6 Hz, and running at 8 to 12 Hz (Payton and Bartlett, 2008).

Three pilot studies were conducted for this thesis with at least 10 trials being collected for each footwear condition. The results showed that a filter with a 6 Hz cut-off frequency, cut the maximum ankle range of motion (ROM) during 0-20% of stance phase by 17% for different shoes and a 12 Hz filter reduced it on average by a figure of 2%. Therefore, a 12 Hz filter was chosen to be used on all raw kinematic data.

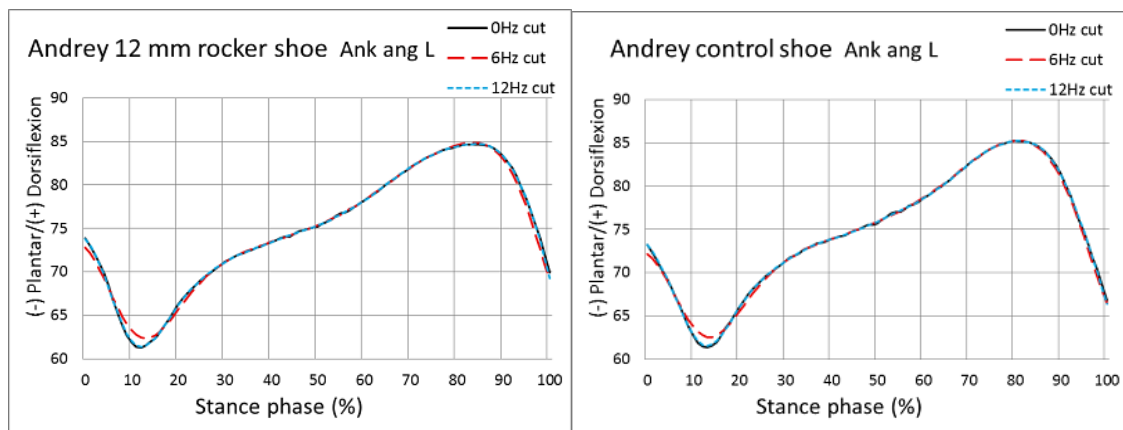


Figure 5.35: Filtration level example of the effect on maximum range of motion loss during 0-20% of stance phase for single trials for 12 mm rocker shoe and control shoe, which were used in the pilot study.

Table 5.3 below demonstrates a pilot study example for kinematic data of maximum ankle angle range of motion smoothing levels with different cut-off frequencies for three different shoes during 0-20% of the stance phase.

Table 5.3: Filtration levels effect on maximum ankle angle range of motion.

Shoe type	Cut-off frequency 0-20% stance phase	Cut-off frequency 0-20% stance phase	Cut-off frequency 0-20% stance phase
12 mm rocker shoe	0 Hz	6 Hz	12 Hz
Max ankle ROM (deg.)	12.6	10.5	12.4
Reduction in ROM	0%	17%	1%
Control shoe	0 Hz	6 Hz	12 Hz
Max ankle ROM (deg.)	11.9	9.6	11.7
Reduction in ROM	0%	19%	2%
Scholl shoe	0 Hz	6 Hz	12 Hz
Max ankle ROM (deg.)	12.3	10.3	12.3
Reduction in ROM	0%	16%	0%

Kinetic data for the force platforms is usually filtered with a 15 or 25 Hz low pass filter. A cut-off frequency of 25 Hz was used for this research.

5.8.4.2 EMG analysis in Visual3D

Visual3D software processes electromyography signals, which were stored as analogue data in Qualisys motion capture trials and within the exported *.c3d file.

Raw EMG signals can be processed in numerous ways and the most common technique is use of the average rectified EMG, Root Mean Square (RMS) or Linear Envelope (Payton and Bartlett, 2008, Winter, 2009, Konrad, 2005). All these techniques are recognised as appropriate processing methods by researchers. Some authors have claimed that they prefer the RMS evaluation technique over other EMG analysis techniques for the reason that the RMS is a measure of the power of the signal and has a clear physical meaning; so that a low level isometric contraction shows less variability than the average rectified value (ARV) when calculated over successive time windows. The RMS method has the potential to detect signal changes that could be masked by the greater variability of the ARV (Payton and Bartlett, 2008, De Luca, 1997). The RMS and linear envelope techniques were therefore tested to analyse EMG data. The typical settings for the RMS technique in Visual3d were:

- A high pass filter with 50 Hz cut-off was applied (surface EMG signals typically have a frequency content between 50 and 500 Hz. These signals may have a DC bias. It is common to apply a high pass filter with a cut-off frequency of 50 Hz to EMG signals prior to any other processing.);
- A low pass filter of 500 Hz (this can only can be used if the EMG signal frequency is greater 1500 Hz) was used to remove electrode and equipment noise;
- Moving RMS with 100ms window was used (to detect rapid changes in muscle activity in a short distance within a time frame of 100ms);
- A 4th order Butterworth low-pass filter with a cut off frequency of 8 Hz was applied to smooth the resulting signal.

For the linear envelope technique:

- A full wave rectified EMG signal;
 - The 4th order Butterworth low-pass filter with a cut off frequency of 8 Hz was applied to smooth the resulting signal.

Both methods showed no significant change in the shape of the signal during the pilot study. However, the RMS technique demonstrated more power in the signal and therefore the moving RMS analysis technique was used in this research to process EMG data, (figure 5.36).

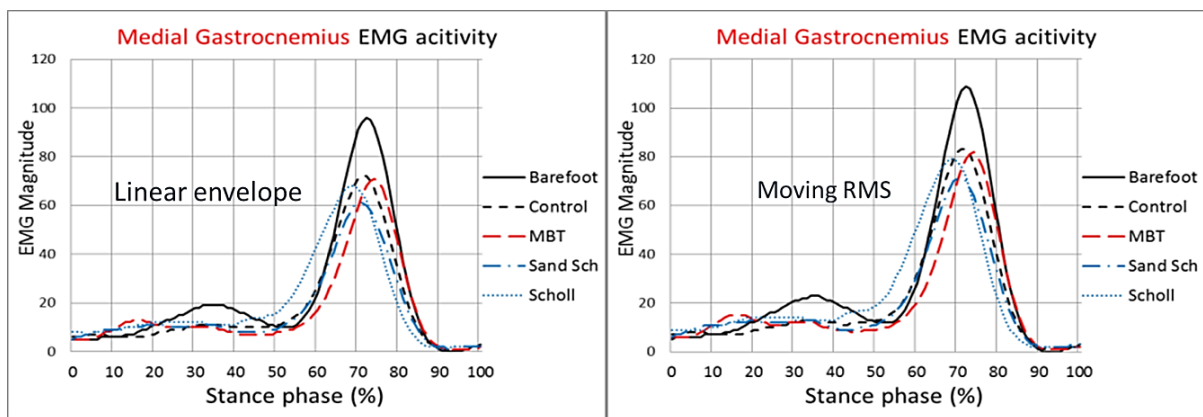


Figure 5.36: Example of Medial Gastrocnemius EMG analysis from the pilot study using the RMS and linear envelope techniques for different shoes during stance phase.

5.8.4.3 EMG normalisation

Comparison of the EMG signals between footwear trials and participants can be difficult. The EMG normalisation technique, which has been used extensively, is the maximum voluntary contraction. This involves recording a maximal isometric contraction and relating the EMG data subsequently obtained to this value. However, this technique has the drawback that it is unknown if the subject did indeed give their maximal possible contraction. In addition, it is also difficult to compare and relate concentric and eccentric contractions to isometric contractions which produce different EMG signals (Richards, 2008). Therefore, another technique was used to normalise the EMG data obtained.

All participants' EMG data were collected within a 2-hour period. Within this time, each five-minute duration of walking was followed by five minutes of rest to minimise muscle fatigue. The baseline shoe was the control shoe. All data were compared to the baseline shoe to

enable the effect of small changes in footwear features to be detected. The averaged values of all control EMG signal values were calculated and scaled to 0-100% signal (from minimum to maximum).

5.8.5 Modelling requirements for OpenSim from Visual 3D

The following model requirements were completed before exporting data to OpenSim:

- The Visual3d model used for OpenSim output must include the right foot (RFT), right shank (RSK), right thigh (RTH), left foot (LFT), left shank (LSK), left thigh (LTH), pelvis (RPV) and a Thorax/Ab;
- The positions denoting the proximal end the thorax segments were created at the exact same location as the proximal end of pelvis and if the coordinate system of trunk was different from the rest of the segments it was altered to be exactly the same to avoid trunk segment being 180 degrees out of phase (i.e upside down);
- The coordinate system of pelvic motion in Visual3D is different from OpenSim, and therefore a virtual lab (named as the v3d_lab) was created with +Y direction of walking, +Z axis in vertical direction and +X axis pointing to the right to be able to use the correct motion data and model in OpenSim.

5.8.6 Exporting data to OpenSim

Visual3D exports an OpenSim motion *.mot file which is compatible with gait23*.osim models in OpenSim software. Motion file bypasses the scaling and Inverse Kinematics (IK) in OpenSim. Visual3D's writes OpenSim comparable .mot files, which are based on Visual3D's own inverse kinematics algorithm solutions which are based on the implementation by Lu and O'Connor (1999). A three-stage process was necessary to achieve that:

- During exportation, Visual3D created the scale factors, which scaled the OpenSim gait model (mass and height) to the Visual3D static calibration model. These scale factors were written to a special OpenSim scale set file named Visial3d_Scale_ScaleSet.xml;
- Visual3D used IK to fit the scaled OpenSim gait model to the Visual3D static calibration model;
- Visual3D then used IK to fit the gait data to the newly calibrated model.

Inverse kinematics is the process of determining the parameters of a jointed flexible object (a kinematic chain) in order to achieve a desired pose (Visual3D guidelines).

The IK steps through each time frame of experimental data and positions the model in a pose that 'best matches' experimental marker and coordinate data for that time step. This 'best match' is the pose that minimizes a sum of weighted squared errors of markers and/or coordinates. Obtaining accurate results from the IK is essential for using OpenSim (OpenSim help guidelines).

5.8.7 OpenSim

In the 1990s Delp and Loan introduced a musculoskeletal modelling software that allows the user to create, alter and evaluate models of many different musculoskeletal structures (Delp, 1990). This software is used extensively to create computer models of musculoskeletal structures and to simulate movements (Delp et al., 2007). Models of the lower and upper extremities have been developed to examine the following biomechanical parameters in gait laboratory testing:

- Studying how surgical changes in musculoskeletal geometry (e.g. origin-to-insertion path) and muscle-tendon parameters (e.g. optimal muscle-fibre length and tendon slack length) can affect the moment-generating capacity of the different muscles on the human body(Hoy et al., 1990b);
- Examining the biomechanical consequences of surgical procedures including tendon surgeries, osteotomies and joint replacements (Delp and Maloney, 1993, Delp and Zajac, 1992, Delp et al., 1995, Erdemir and Piazza, 2004);
- The lower-extremity models have been used to estimate muscle-tendon lengths, velocities, moments arms during normal and pathological gait (Arnold et al., 2000, Arnold et al., 2006, Jonkers et al., 2006, Kimmel and Schwartz, 2006);
- To investigate the causes of abnormal gait (Piazza and Delp, 1996, Kerrigan et al., 1998, Higginson et al., 2006).

OpenSim is an open-source platform for modelling, simulating and analysing the neuromusculoskeletal system. It includes low-level computational tools that are invoked by an application (figure 5.37).

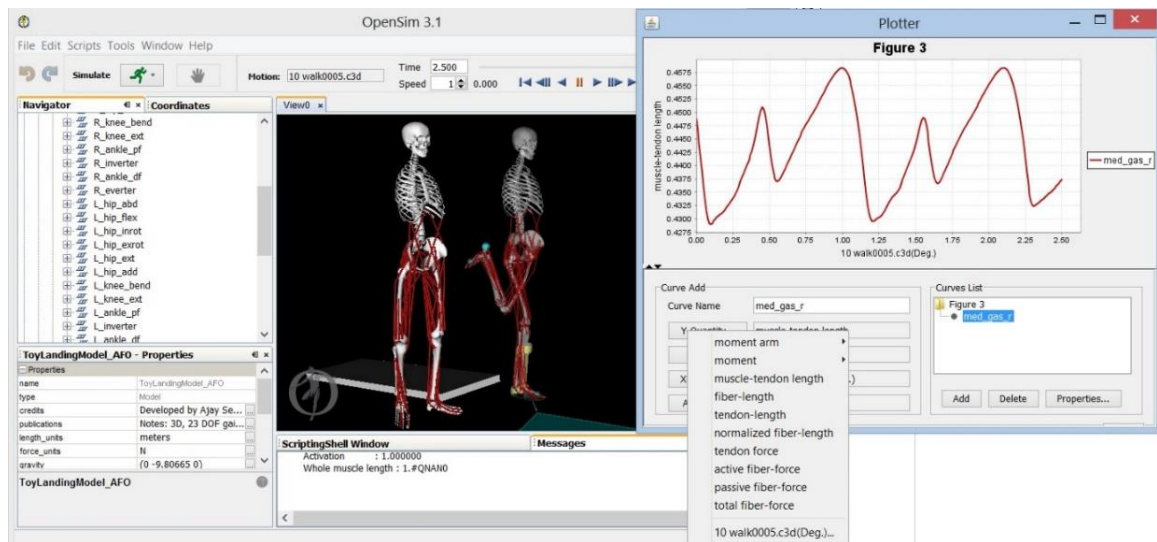


Figure 5.37: A screenshot from OpenSim, which includes a musculoskeletal model of the lower extremities.

5.8.7.1 The OpenSim model

The Gait2392 model is a three-dimensional, 23 degree of freedom computer model of the human musculoskeletal system was used for muscle property data analysis. It is also compatible with Visual3D *.mot exported files and scaling procedure. The model was created by Darryl Thelen (University of Wisconsin-Madison) and Ajay Seth, Frank C. Anderson, and Scott L. Delp (Stanford University). It features 92 musculo-tendon actuators to represent 76 muscles in the lower extremities and torso (figure 5.38).



Figure 5.38: The Gait2392 musculoskeletal model in OpenSim.

The musculoskeletal model describes not only the geometric relationships of the muscles and bones (the musculoskeletal geometry), but also the muscle-tendon parameters and it consists of coordinates for muscle attachments and a model for each muscle tendon compartment.

The model's bone geometry of the shank and foot were adopted from (Stredney, 1982).

The model of the lower extremity consists of seven rigid-body segments: pelvis, femur, patella, tibia/fibula, talus, foot (which includes the calcaneus, navicular, cuboid, cuneiforms, metatarsals), and toes. Reference frames are fixed in each segment (Delp, 1990). Figure 5.39 shows location of the body-segmental reference frame.

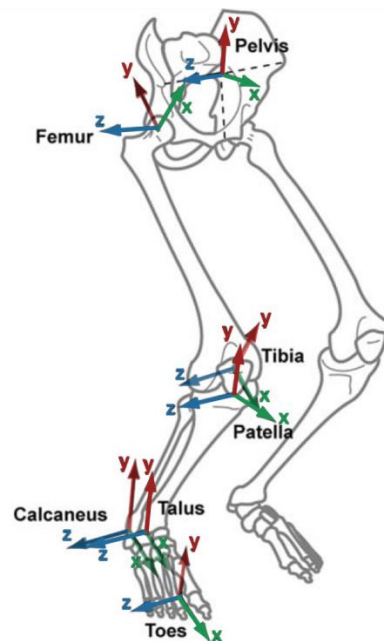


Figure 5.39: The coordinate systems of the bone segments (Delp, 1990).

- **Pelvis:** The pelvic reference frame is fixed at the midpoint of the line connecting the two anterior superior iliac spines;
- **Femur:** The femoral frame is fixed at the centre of the femoral head;
- **Tibia:** The tibial frame is located at the midpoint of the line between the medial and lateral femoral epicondyles;
- **Patella:** The patellar frame is located at the most distal point of the patella;
- **Talus:** The talar frame is located at the midpoint of the line between the apices of the medial and lateral malleoli;

- **Calcaneus:** The calcaneal frame is located at the most interior, lateral point on the posterior surface of the calcaneus;
- **Toe:** The toe frame is located at the base of the second metatarsal.

5.8.7.2 Ankle, subtalar, and metatarsophalangeal joints

The ankle, subtalar and metatarsophalangeal joints are represented as a frictionless revolute as shown in figure 5.40.

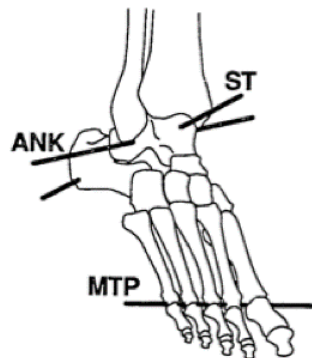


Figure 5.40: The ankle (ANK), subtalar (ST) and metatarsophalangeal (MTP) joints with axes and orientation (Delp, 1990).

Each foot is modelled using two segments: a hindfoot and the toes. The hindfoot joins with the shank via a two degrees of freedom (dof) joint and the toes joins with the hindfoot via a one degree of freedom hinge joint. The metatarsophalangeal axis is rotated by -8 degrees on a right-handed vertical axis to minimize disarticulation of the joint. In this research, the entire foot segment was rigid due to the need to place marker positions through holes drilled in shoe uppers. The foot segment was used as a single rigid body in this research.

5.8.7.3 Muscle geometry

The paths of the muscles were based on geometric data (i.e., musculo-tendon origin and insertion sites) as reported by (Delp, 1990). In all case, tendons were assumed to attach at a point to the bone. The muscle-tendon actuators in the lower extremity portion of the model were defined on the anatomical landmarks on the bone surface models. In some cases, for example the soleus, origin and insertion landmarks are sufficient for describing the muscle path. In other cases, where muscle wraps over bone or is constrained by retinacula,

intermediate points or “via” points are introduced to represent the muscle path more accurately. The number of points activated for the muscle can depend on body position. Straight-line segments were used whenever an actuator can run freely from one point to another (for example SOL muscle), with intermediate or via points introduced to model contact of the muscle with bony prominences. Cylinders were used to model the path of muscle when the muscle wraps completely around the underlying bone and/or other muscles (for example a medial and lateral GAS cylinder was utilised to simulate the tissues swapping around the medial and lateral condyles of the femur). This was designed because by using a via-cylinder rather than a series of via-points, muscle moment arms at some of the joints can be represented more accurately (Anderson and Pandy, 1999). The parameters for the cylinders at the knee were estimated by inspecting MR images of the hamstrings and gastrocnemius muscles as reported by (Reicher, 1993).

5.8.7.4 Model Anthropometry

The model mass and inertial properties for all segments, except for foot segment, were based on average anthropometric data of the five male subjects who participated in that study (age 26 ± 3 years, height 177 ± 3 cm and weight 70.1 ± 7.8 kg). All data were recorded according to the methods described by (McConville et al., 1980). The mass, position of the centre of mass and principal moments of inertia for each segment in the model except for foot segment were calculated by averaging the anthropometric data for the subjects (Anderson and Pandy, 1999).

The mass of the rearfoot and toes in the models were similar to the mass of the whole foot reported by (McConville et al., 1980) plus the mass of a size 10 tennis shoe.

5.9 Properties and models of muscles (Muscle-tendon dynamics)

A muscle-tendon unit is defined by specifying its geometry and force generating properties. Muscle force is transmitted to the skeleton via tendon. The properties of muscle and tendon were integrated in OpenSim into a model of the muscle-tendon complex (muscle-tendon actuator). In the model, muscles were considered as a set of equally-long fibres that were in

series with the tendon. The fibres are in the line with the tendon, as in a parallel-fibred muscle, or at an angle (the pennation angle, α to the tendon) - figure 5.41

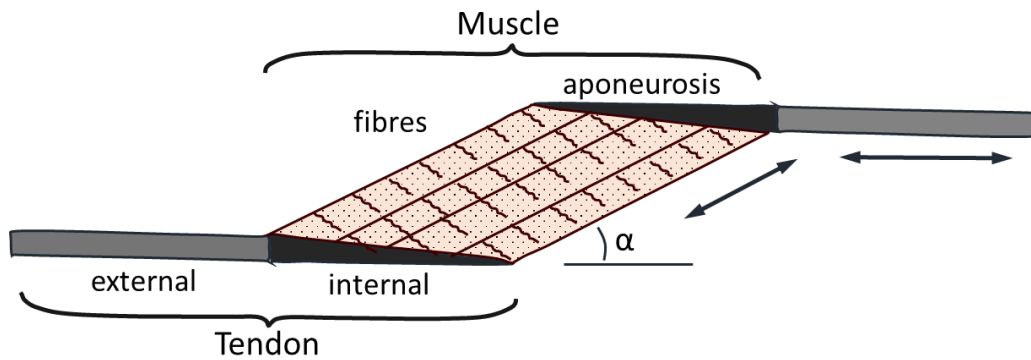


Figure 5.41: Relationship between muscle fibres and tendon in a pennated muscle.

Muscle fibres (shaded region) lie in parallel, have the same length and are oriented at an angle α to the tendon axis of pull. Tendon consists of a component internal (i.e., the aponeurosis) and external to the muscle belly (Zajac, 1989, Hoy et al., 1990a).

The static properties of tendon were included in the muscle-tendon model. The force-length property of the tendon were determined by specifying peak active force F_o^M and its tendon slack length l_s^T (Zajac, 1989). Tendon length was considered to consist of both internal and external portions and it included the length of internal and external tendon. The length of tendon at which force begins to develop when stretched is called the tendon slack length l_s^T . The model's muscle and tendon force-length properties were summarised. These properties were scaled to represent individual muscle-tendon complex by specifying four parameters:

- Peak isometric force F_o^M and optimal fibre length l_o^M scale the muscle force-length property;
- Peak isometric force F_o^M and tendon slack length l_s^T scale the tendon force-length property;
- Pennation angle (α) specified the angle between the muscle fibres and the tendon.

The Muscle-tendon actuator principle model, which is used in the 2392gait model is shown in figure5.42.

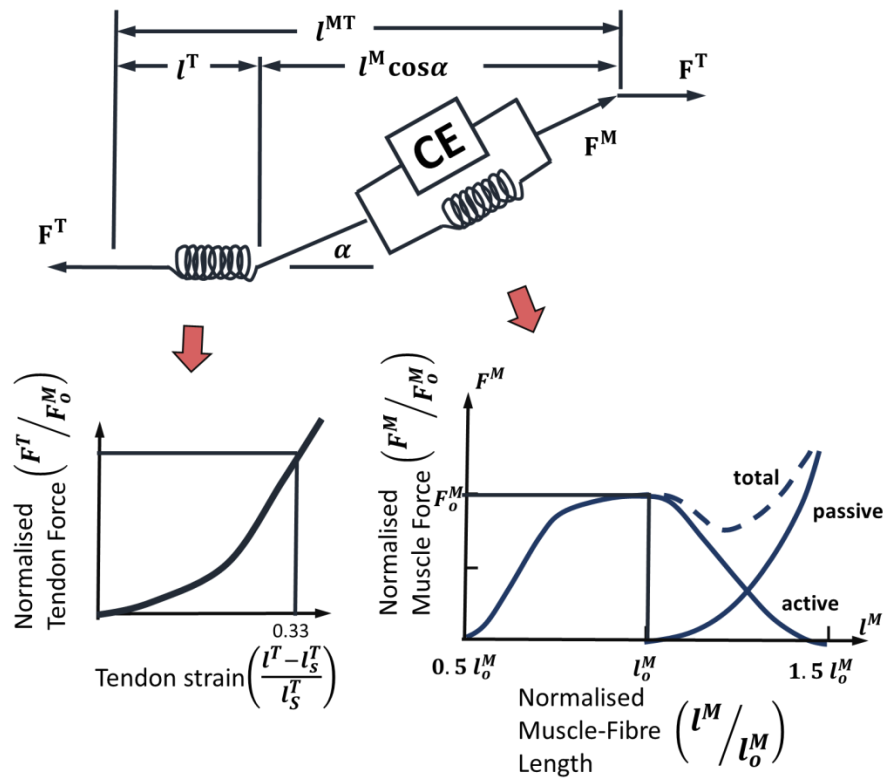


Figure 5.42: The muscle-tendon actuator model [adapted from (Zajac, 1989, Delp, 1990, Hoy et al., 1990a)].

The isometric properties of muscle are represented by an active contractile element (CE) in parallel with a passive elastic element. Isometric muscle force is assumed to be the sum of muscle force when it is inactive (passive) and when it is active. The muscle is in series with tendon, which is represented by a non-linear elastic element. The forces in muscle F^M and tendon F^T are normalised by peak isometric muscle force (F_o^M). Tendon length (l^T) and muscle-fibre length (l^M) are normalised by optimal muscle-fibre length (l_o^M). Note that: $l^{MT} = l^T + l^M * (\cos \alpha)$ and $F^T = F^M * (\cos \alpha)$ where l^{MT} is the muscle-tendon length and α is the pennation angle. l_s^T is the tendon slack length. For a given muscle-tendon length and activation level the model determines muscle and tendon forces (Zajac, 1989, Delp, 1990, Hoy et al., 1990a).

Muscle-tendon parameters for 43 lower-limb muscles used in the model based on data reported by Delp is demonstrated in table 5.4.

Table 5.4: Muscle modelling parameters.

Muscle	Peak force (N)	Optimal fibre Length (cm)	Pennation Angle (°)	Tendon slack length (cm)	Tendon length, fibre length(cm)
Gluteus medius1 ^a	550	5.4	8	7.8	1.4
Gluteus medius2 ^a	380	8.4	0	5.3	0.6
Gluteus medius3 ^a	435	6.5	19	5.3	0.8
Gluteus minimus1 ^a	180	6.8	10	1.6	0.2
Gluteus minimus2 ^a	190	5.6	0	2.6	0.5
Gluteus minimus3 ^a	215	3.8	1	5.1	1.3
Gluteus maximus1 ^a	380	14.2	5	12.5	0.9
Gluteus maximus2 ^a	550	14.7	0	12.7	0.9
Gluteus maximus3 ^a	370	14.4	5	14.5	1
Adductor magnus1 ^a	345	8.7	5	6	0.7
Adductor magnus2 ^a	310	12.1	3	13	1
Adductor magnus3 ^a	445	13.1	5	26	2
Adductor longus ^a	420	13.8	6	11	0.8
Adductor brevis ^a	285	13.3	0	2	0.2
Pectineus ^a	175	13.3	0	0.1	0.1
Iliacus ^a	430	10	7	9	0.9
Psoas ^a	370	10.4	8	13	1.3
Quadratus femoris ^a	255	5.4	0	2.4	0.4
Gemelli ^a	110	2.4	0	3.9	1.6
Piriformis ^a	295	2.6	10	11.5	4.4
Rectus femoris ^b	780	8.4	5	34.6	4
Semimembranosus ^b	1030	8	15	35.9	4.5
Semitendinosus ^b	330	20.1	5	26.2	1.3
Biceps femoris ^b	720	10.9	0	34.1	3.1
Gracilis ^b	110	35.2	3	14	0.4
Sartorius ^b	105	57.9	0	4	0.1
Tensor fasciae latae ^b	155	9.5	3	42.5	4.5
Vastus medialis ^b	1295	8.9	5	12.6	1.4
Vastus intermedius ^b	1235	8.7	3	13.6	1.6
Vastus lateralis ^b	1870	8.4	5	15.7	1.9
Biceps femoris ^b	400	17.3	23	10	0.6
Medial gastrocnemius ^c	1115	4.5	17	40.8	9
Lateral gastrocnemius ^c	490	6.4	8	38.5	6
Soleus ^d	2830	3	25	26.8	8.9
Tibialis posterior ^e	1270	3.1	12	31	10
Flexor digitorum longus ^e	310	3.4	7	40	11.8
Flexor hallucis longus ^e	320	4.3	10	38	8.8
Peroneus brevis ^e	350	5	5	16.1	3.2
Peroneus longus ^e	755	4.9	10	34.5	7
Tibialis anterior ^e	600	9.8	5	22.3	2.2
Peroneus tertius ^e	90	7.9	13	10	1.3
Extensor digitorum longus ^e	340	10.2	8	34.5	3.4
Extensor hallucis longus ^e	110	5.4	6	30.5	2.6

^a Peak force derived from (Brand et al., 1986); fibre length and pennation from (Friederich and Brand, 1990). ^b Peak force, fibre length and penation angle derived from (Wickiewicz et al., 1983). ^c Peak force derived from (Brand et al., 1986); fibre length and pennation derived

from (Wickiewicz et al., 1983).^e Peak force derived from (Wickiewicz et al., 1983) multiplied by 0.8; fibre length from (Friederich and Brand, 1990).

5.10 Calculation of the outcome measures

5.10.1 Introduction

Using data analysis software Visual3D, OpenSim and Excel, the following desired gait outcome variables were analysed for all test conditions and compared to baseline data with regards to kinematics, kinetics, EMG activity and muscle-tendon properties data acquired from gait laboratory tests. The outcome results for the stance phase were:

- **Kinematic data in the sagittal plane:** ankle angle, knee angle, hip angle, foot plantar/dorsiflexion, shank incline/decline, flexion velocities;
- **Kinetic data:** GRF, ankle moment, knee moment, ankle power, knee power, area under the curve (impulse) for ankle moment;
- **EMG activity:** EMG signals (for medial GAS, SOL, TA), area under the curve (impulse) for medial GAS, SOL and TA muscles;
- **Muscle-tendon properties:** Fibre/tendon lengths and velocities, fibre/tendon forces, medial GAS and SOL muscle moment arms.

5.10.2 Joint angles

Visual3D software was used for kinematic data analysis. Segments of the body were defined as a rigid body with a local coordinate system defined to coincide with the set of anatomical axes by knowing the coordinates of the proximal and distal end of a body segment in particular plane. The segments angles were then found by using simple trigonometry. The foot was aligned in the sagittal plane by Visual3D software. The ankle motion in the sagittal plane was then calculated as an angular relationship of foot and shank segment by subtracting the two angles (figure 5.43).

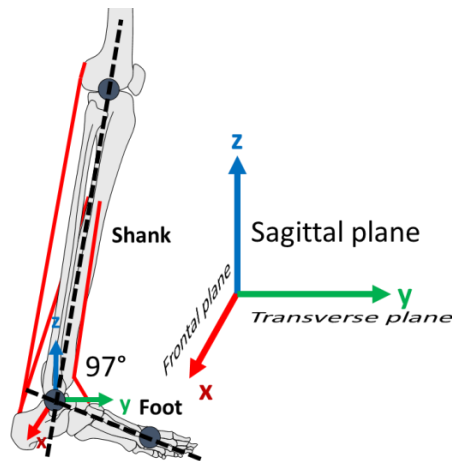


Figure 5.43: Foot and shank segment angular relationships (ZX - sagittal plane, ZY - frontal plane and XY- transverse plane).

Knee motion in the sagittal plane was calculated as the angular relationship between the shank and thigh segments. Hip motion data were calculated as pelvis versus the thigh segment. Shank incline/decline and foot flexion were obtained as relationship those rigid segment with the ground surface (for example force platforms) and it was 0 degrees.

5.10.3 Kinetic data

All the joint moments, powers and GRFs were calculated in Visual3D. The anthropometric data such as segment lengths were calculated by the transformation from the tracking of markers to the position and orientation of each segment. The mass of the segments were scaled by weight of the individual subject. To calculate joint moment data such as point of application, and GRF moment arms to joint centres were obtained from the data processed in Visual3D (figure 5.44).

Joint moments are commonly used in gait analysis by researches. Factors like height and body mass, gender can influence these moments (Moisio et al., 2003). Joint moments may be normalised to the participants' body weight and height or just body weight. Normalisation by mass decreasing variability by about 50% (Winter, 2009). As there is only one gender the ankle and knee moments were normalised by body mass (Nm/kg) (Moisio et al., 2003). The ground reaction force and powers by default were normalised by bodyweight in Visual3D.

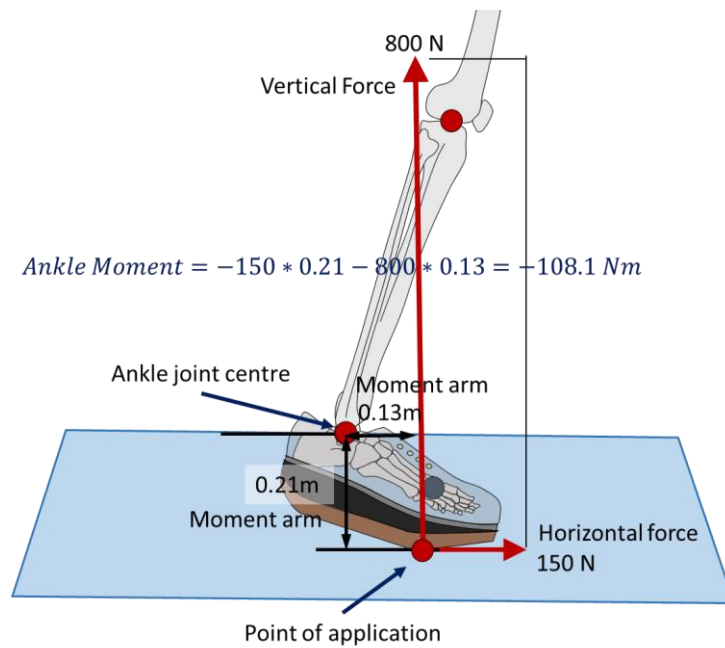


Figure 5.44: Example of an ankle joint moment calculation. Joint moments, powers and GRFs were calculated in Visual3D.

5.10.4 Muscle-tendon properties

Muscle tendon properties were calculated in OpenSim software. Each muscle has a unique set of muscle tendon parameters (peak force, optimal fibre length, pennation angle and tendon length) which determine its isometric force-generating characteristics. Muscle architecture parameters and bone geometry were obtained in the literature and applied in the model, which was included in OpenSim software. Muscle insertion points and muscle geometry were used in the model in OpenSim based on the research from Delp. Each gait model used in this research was scaled by body weight and height for each participant in OpenSim.

5.10.5 OpenSim algorithm for calculation muscles moment arm, muscle-tendon length and force

For every joint that a muscle is connected to via tendon, the muscle has a moment arm. For example, medial gastrocnemius connects to both the rearfoot and the knee and it has a moment arm for both the ankle and knee angle. OpenSim calculates these moment arms using the “partial velocity” method, which is defined by equations (1) – (4) below.

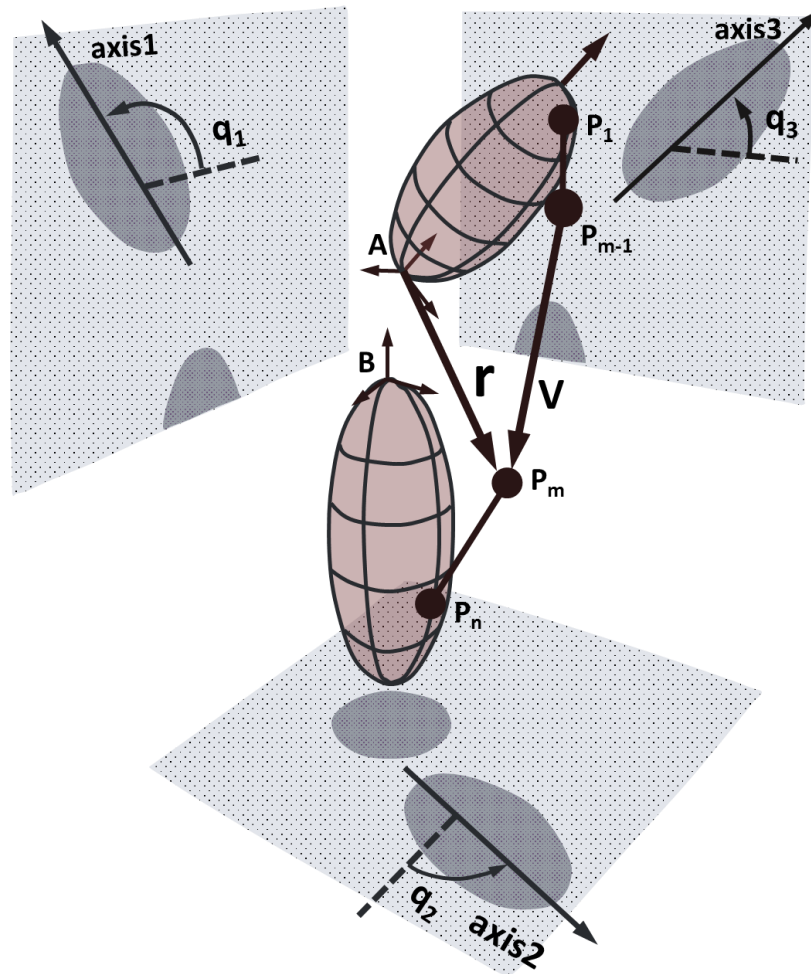


Figure 5.45: Definition of terms used in moment arm calculations. Point P_1 through P_n define the muscle path. P_1 through P_{m-1} are fixed in body A . P_m through P_n are fixed in body B . \mathbf{V} is the vector from point P_{m-1} to P_m . \mathbf{r} expresses point P_m in reference frame A . In general, six generalised coordinates (three rotational angles: q_1 , q_2 , q_3 and three translation coordinates, not shown) are needed to characterise the orientation and position of body A relative to body B . The moment arm for each generalised coordinate is given by equation (4) (Delp, 1990).

u is the translational component of the partial velocity and defined as:

$$u = (\partial tx / \partial q_i)x + (\partial ty / \partial q_i)y + (\partial tz / \partial q_i)z \quad (1)$$

where tx , ty and tz are the constants of kinematic functions that define the translation between the two reference frames. ω is the angular component of the partial velocity and defines as:

$$\omega = (\partial r1 / \partial q_i)\lambda_1 + (\partial r2 / \partial q_i)\lambda_2 + (\partial r3 / \partial q_i)\lambda_3 \quad (2)$$

where $r1$, $r2$ and $r3$ are the constants or kinematic functions that define the rotations about λ_1 (*axis1*), λ_2 (*axis2*) and λ_3 (*axis3*) respectively. Then ${}^A P V^{P_m}$ the partial velocity of the muscle point P_m in reference frame A is:

$${}^A P V^{P_m} = \omega * r + u \quad (3)$$

where r is P_m in reference frame A (figure ...). And the moment arm (ma) of the muscle for generalised coordinate q_i was calculated as:

$$ma = {}^A P V^{P_m} * V \quad (4)$$

where V is the vector along the muscle line of action (figure....). If the muscle line of action connects more than one joint (i.e., biarticular muscles) the moment arm was computed by summing the partial velocity terms for each joint connected (Delp, 1990). Equation (3) was used to determine the component of partial velocity at each joint. These components were then summarised to determine ${}^A P V^{P_m}$ which was used in equation (4).

This method is equivalent to computing moment arms with a vector cross-product for ball and socket and revolute joints (Hoy et al., 1990a). This method calculates the moment arm of a muscle about the instant centre of rotation as determined from the joint kinematics. The partial velocity method calculates a muscle moment arm (ma) equal to the change in muscle-tendon length (∂l^{MT}) with respect to a change in the generalised coordinate (∂q_i). That is, (4) is equivalent to

$$ma = (\partial l^{MT} / \partial q_i) \quad (5)$$

This method provides a consistent technique to calculate moment arms for all types of joints (Delp, 1990, Hoy et al., 1990a).

Muscle-tendon length was calculated as the sum of the length of the line segments that connect the point defining the muscle path. If a muscle path was defined by points P_1 through P_n , then muscle-tendon length (l^{MT}) was determined by first transforming the muscle points to a common reference frame and the computing

$$l^{MT} = \sum_{0 < i < n} |P_{i+1} - P_i| \quad (6)$$

Muscle-tendon actuator force for the gait2392 model was used following an interactive algorithm. Once the muscle-tendon length was computed, an initial estimation of the muscle and tendon length was made. The force in the muscle was found by summing active and passive forces, each of which was calculated by using the length estimation to interpolate the appropriate force-length curve. Similarly, the force in the tendon was found by using its length to interpolate the force-length curve of the tendon. In static equilibrium, the force in the tendon (F^T) and muscle (F^M) were related by:

$$F^T = F^M (\cos \alpha) \quad (7)$$

where α is the pennation angle. If the computed muscle and tendon force satisfy the equation, then the muscle and tendon force have been found. Otherwise, the muscle and tendon lengths are adjusted based on the slopes of their force-length curves at their respective lengths and the process is repeated. A more detailed algorithm of this muscle-tendon properties calculation which was adopted in the model has been explained in the literature (Zajac, 1989, Hoy et al., 1990b, Delp, 1990).

There some important problems for using models to study individual patients as:

Models represent anatomy and function of average healthy adult subjects (no deformities, altered joint kinematics, age difference).

5.10.6 Area under the curve (impulse)

The area under the curves were calculated for ankle moment and EMG data to understand and compare changes in the summary of EMG activity and moment data during stance phase. It can demonstrate clearly if a muscle has worked harder overall and if more muscle force used to generate an internal ankle moment for ankle movement. This information is

valuable to understand effect on muscle overall work whilst walking with different rocker shoes.

The simplest method to calculate the area under the curve is the *trapezoid rule* (Liengme, 2009). If the area under the curve is divided into a sufficient large number or parts (figure 5.46), then the area under the curve (the approximate integral) is given by:

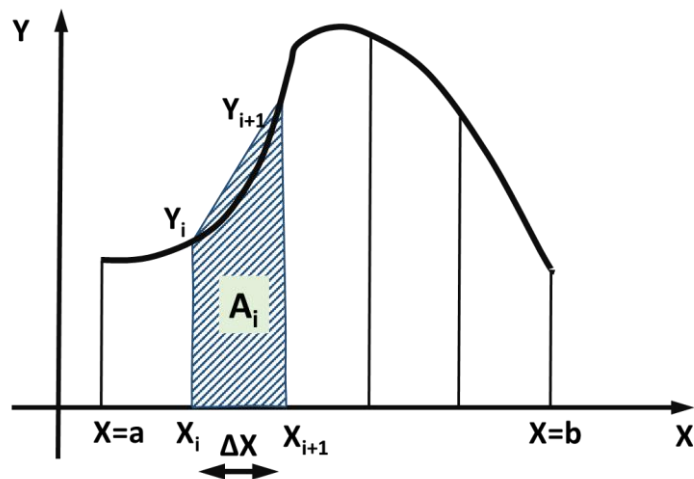


Figure 5.46: Example of a segment of the curve area, which is divided into areas.

$$I = \int_a^b f(x)dx \approx \sum_{i=1}^n A_i$$

It effectively approximates the representative strip to a trapezoid. For a clearer explanation only a few strips were used in this example. More, and smaller strips are needed for a good approximation. The area of a typical strip is equivalent to:

$$A_i = \Delta x \frac{y_i + y_{i+1}}{2}$$

Combining the two equations, the area under the curve will be equivalent to:

$$I \approx \Delta x \frac{y_1 + y_2}{2} + \Delta x \frac{y_2 + y_3}{2} + \dots + \Delta x \frac{y_n + y_{n+1}}{2}$$

or

$$I \approx \frac{\Delta x}{2} (y_1 + 2y_2 + 2y_3 + 2y_4 + \dots + 2y_n + y_{n+1})$$

or

$$I \approx \frac{\Delta x}{2} \left(y_1 + 2 \sum_{i=2}^n y_i + y_{n+1} \right)$$

The last equation is called the *trapezoid rule* and it was used to calculate the area under the curves. To calculate I EMG and moment data were not normalised to 100% time scale. The data contained enough “strips” to be accurate, as EMG was recorded at a 3000 Hz frequency and therefore there were around 3000 strips in the graph. Walking speed was controlled by time and therefore walking pattern was consistent. The I for ankle moment was calculated with approximately 65 strips per stance phase. Data were consistent and followed the same pattern for each trial to be more accurate.

Every single raw trial was analysed without normalising it to the 0-100% time scale. It was important to do so, because time scale normalisation was interpolating the curves areas and therefore data would not be valid, it could contain more area or less. Data were tested and showed that if normalised curve could contain up to 25% more area under the curve versus raw data. For that reason, each trial was analysed separately.

5.11 Data normalisation

Stance phase is the most important phase of gait in this study. During stance phase, it was possible to evaluate rocker sole shapes, which would have influenced forward propulsion generation and absorption by the muscles. Stance phase was subdivided into the following phases according to (Perry, 1992):

- Initial contact (weight acceptance 0-2% of gait cycle);
- Loading response (weight acceptance 0-10% of gait cycle);
- Mid-stance (single limb support 10-30% of gait cycle);
- Terminal stance (single limb support 30-50% of gait cycle);
- Pre-swing phase (50-60% of gait cycle).

The five stance phase gait events [initial contact (ICt), loading response (LR), mid-stance (MSt), terminal stance (TSt) and pre-swing (PS)], were expressed as a percentage of gait cycle. The gait cycle was defined as a gait event from heel strike to heel strike and stance phase was event from heel strike to toe-off. All data were normalised on a 0-100% time

scale. Force platforms were used to define gait events from heel strike to toe-off. The mean values were analysed within five gait events for all trials.

To normalise data to one standard for all participants in Visual3D is a challenging task. If the ankle angle during static barefoot standing is at neutral position (i.e. not plantarflexed or dorsiflexed), it will be equal to 0° or 90° with one expectation; that the shank segment is not inclined/declined and foot has full contact with the ground for a healthy person. If the person were to be standing barefoot on the force platform to record a static trial in visual3D, ankle angle would be around 73.1° . In Visual3D barefoot static posture (which has full contact with the force platform or in parallel to the ground) of the foot segment relative to the ground is not equal to 0° but equal to around 25.5° (data derived from one of the participants). The reason for this, is that the foot segment is built up in Visual3D, with the proximal end starting at the ankle joint centre and the lateral end along a line joining the metatarsal heads. Therefore, the segment line direction does not lie parallel to the ground (force plates), but has 25.5° inclination. In other words, the segments' line direction is coming from the ankle joint centre to metatarsals heads. The shank also had an inclination of 8.6° for this participant during static standing recording. Figure 5.47 shows why the static ankle joint angle is equal to 73.1° in Visual3D in more detail.

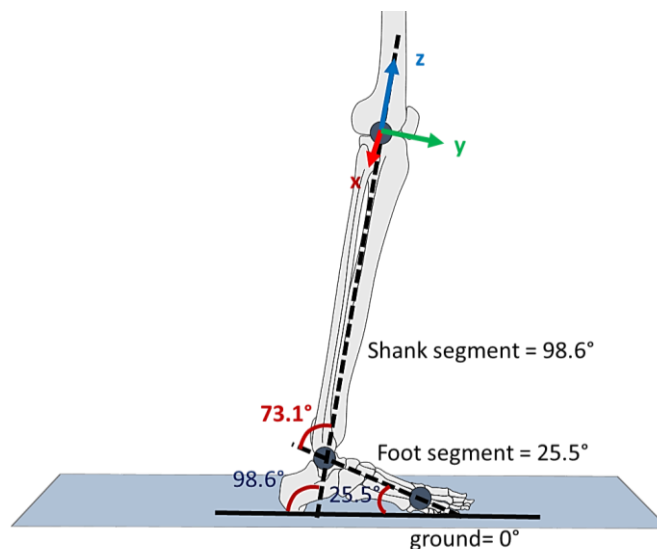


Figure 5.47: Visual3D default static ankle angle representation.

This is the default reference posture of the coordinate system for a barefoot static trial when standing on a force platform. The example for barefoot ankle kinematics derived from it is shown in figure 5.48, and it was not close to 90° or 0° . One of the manual ways available

to normalise ankle angle to the neutral position (0 degrees) to be able to define plantarflexion/dorsiflexion, is by subtracting 90° from raw kinematic data, then subtract the shank incline of 8.6 degrees and adding a 25.5° foot offset caused by defining the foot segment in visual3D. The overall equation for this example is $-90^\circ - 8.6^\circ + 25.5^\circ$. This would set a 0 degrees position of the ankle joint angle in the sagittal plane (Z-X plane).

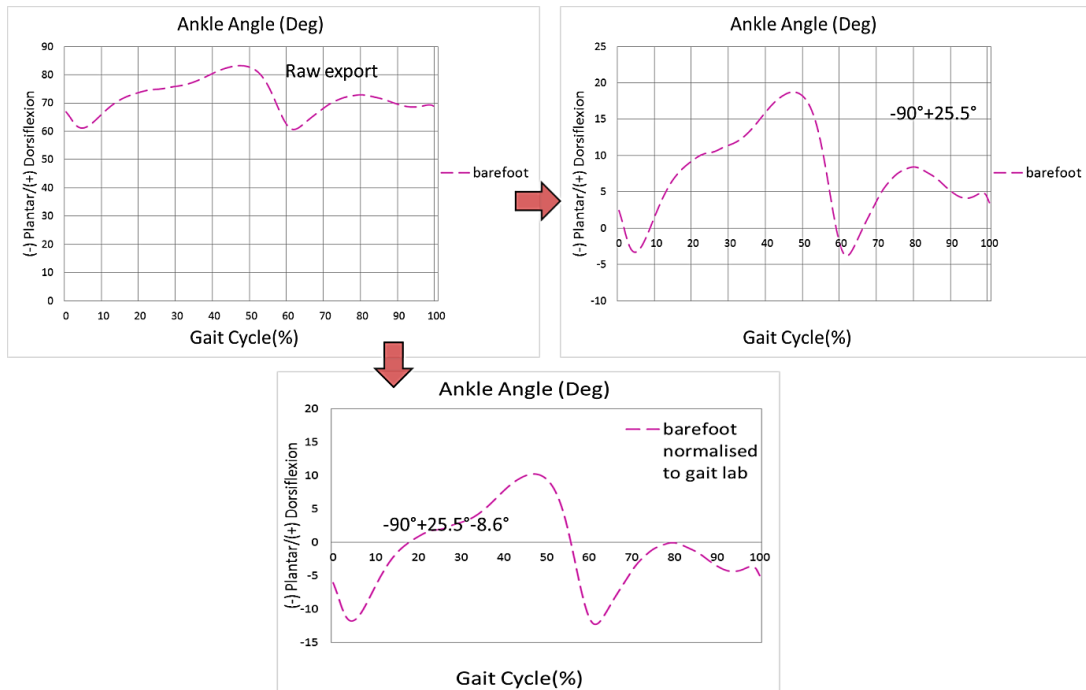


Figure 5.48: Normalisation procedure for the ankle.

Ninety degrees was subtracted because the foot segment default coordinate system in Visual3D is rotated anticlockwise by 90 degrees in the Z-X plane versus the laboratory. Other segments in the coordinate system are shown in figure 5.49.

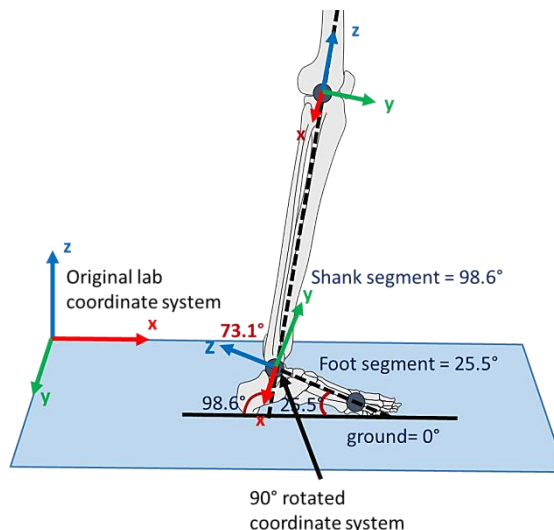


Figure 5.49: Default Visual3D coordinate system for the lab, shank segment and anticlockwise-rotated foot segment in the Z-X axis plane.

Results from the pilot study and the literature suggested that it would not be prudent to change between global and segment coordinate systems as this can lead to errors (Richards, 2008), figure 5.50.

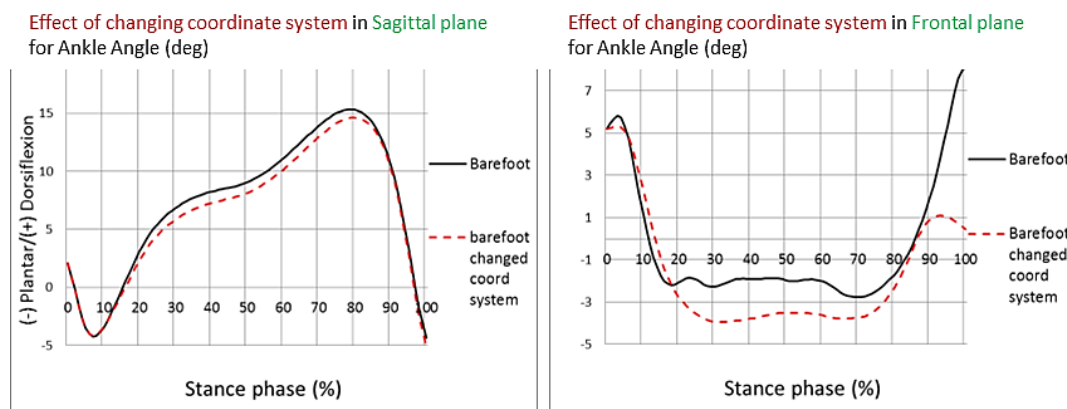


Figure 5.50: Pilot study example for changing the coordinate system of the ankle segment.

Therefore, the coordinate system for calculating segments were kept to the Visual3D default without changing them.

Depending on how the ankle angle is desired to be presented, researchers choose their own techniques for ankle kinematic data interpretation. In this thesis, ankle joint neutral position was considered to be at 0 degrees. Ankle angle was calculated as an angular relationship of the shank and foot segments.

Different static postures caused by different footwear conditions, would set 3 offsets from a reference posture (0 degrees joint angles). All statics trials recorded in this research have different static positions for all the segments. One subject stood with shank incline of 2° in the high heeled shoe with the foot plantarflexed at 35 degrees relative to the ground and with the barefoot shank at 10 degrees and foot segment at 25.5° (figure 5.51).

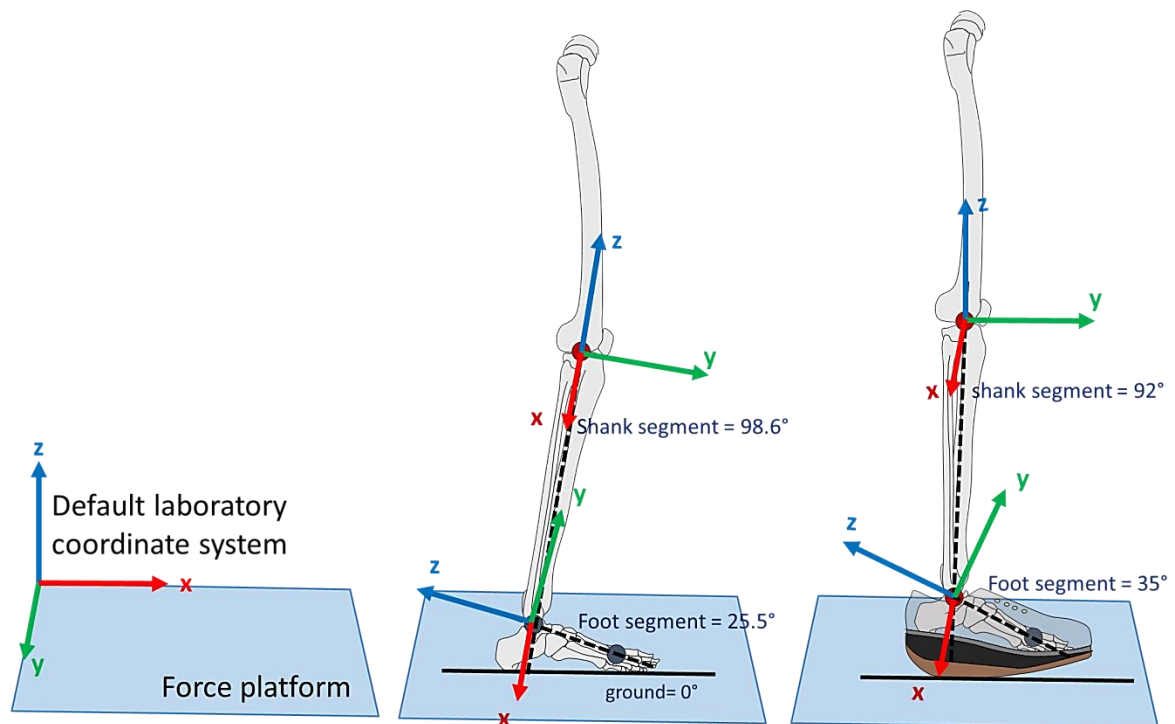


Figure 5.51: Example of how a rocker shoe can change posture for an ankle joint compared to a barefoot static trial.

A total of 160 trials were collected per subject and 16 different footwear conditions were used, and therefore 16 different static positions were recorded. All static body positions were altered in all 3 axes during standing postures. This could have been due to the shoes or just the participant being comfortable in that standing position at that time. Each static position was linked to 10 walking trials. Therefore, to analyse the precise relationship if the ankle was more in a plantar or dorsiflexed position when comparing different rocker shoes would not make any sense without a default segmental reference system for all footwear conditions and participants. The ideal case scenario would be if all statics were the same (all joints were set as 0 degree). In this case, joint kinematic data contained offsets in the coordinate system for each segment when compared to each other.

New updated software Visual3D versions 4.9xx and 5xx have included improved automatic features to remove static offsets between different static positions in data. Therefore, if all dynamic trials (with different shoes) are assigned to one barefoot static it would not theoretically be different if all trials were assigned to their own statics, unless marker positions were not the same. To investigate that, the test was conducted using one walking trial with the 70 % apex position shoe compared to two different statics; the first static was

a 1.5 cm heel (negative shoe) and the second was a 5.5 cm heel (high heel shoe). These both shoes made a big difference to the standing position for the foot segment, with the negative heel foot segment being dorsiflexed and in the high heel shoe it was plantarflexed relative to the ground. If all markers were placed at the same location for each static then after exporting data from Visual3D, it should not show any differences in kinematic data and no offsets caused by reference statics. Figure 5.52 demonstrates a visual example of static posture alteration caused by different rocker soles in Visual3D.

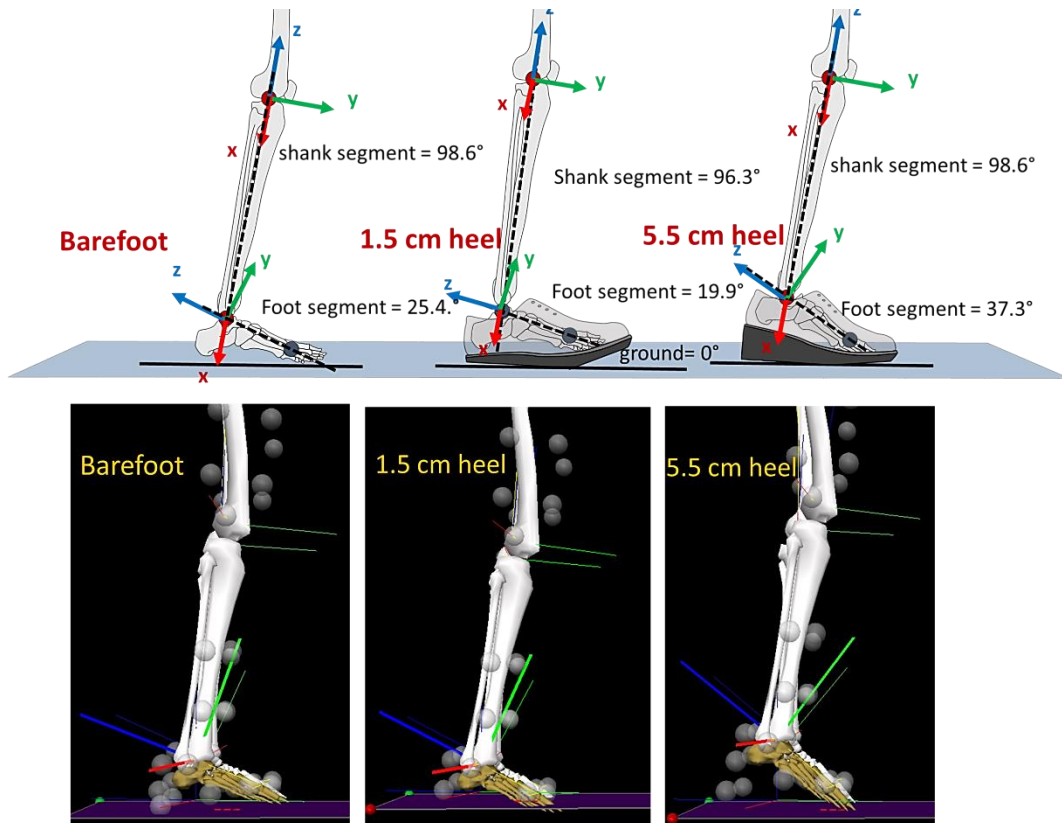


Figure 5.52: Demonstration of segmental positions.

Ankle angle kinematic data for the 70 % apex position shoe walking trial was assigned with 1.5 cm heel and 5.5 cm heel static trials and then data were exported to be compared. The data looked the same (average angle difference mean STD $\pm 0.095^\circ$ for the full gait cycle) as shown in figure 5.53, even though for both shoes, static positions were different, the 5.5 cm heel was more plantarflexed by 17.4 degrees compared to the 1.5 cm heel shoe, and shank incline differences were 2.3 degrees, Visual3D removed static offset by default.

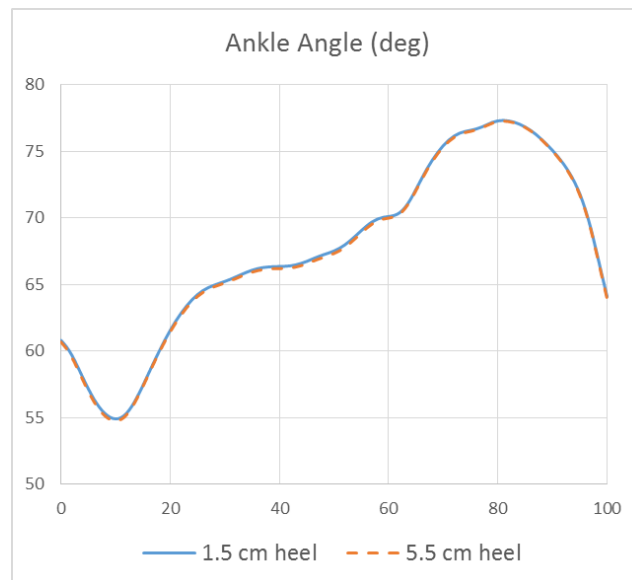


Figure 5.53: Comparison of test conditions.

However, there were some factors which were unclear:

- This method does not show the joint angles in relation to the real coordinate system as we see;
- If the data have to be normalised between different participants and therefore statics, there is no information about what the foot or shank positioning relative to the lab coordinate system was, or which reference segment was used for normalising statics offsets and therefore how different it is between the subjects.

For this reason, a new method of normalisation joint kinematics was tested and used to solve both uncertainties. Before that, the question was raised: if different statics were assigned for the walking trial wearing completely different shoes, how it can be guaranteed that all markers were placed at the same location?

Previously the method of marker placement was described that all footwear conditions had holes and markers location were drawn on to the skin, where markers were to be re-attached (only for the foot segments) after changing footwear conditions. If marker locations were wrong, it would change the shape of the joint kinematics. Figure 5.54 demonstrates the ankle joint angle result data on effect of marker relocation for several different rocker shoes. In this example, it shows that the walking trial wearing a 1.5 cm negative heel and 5.5 cm heel was compared versus a barefoot static trial, (1.5 cm heel static and 5.5 cm heel static trial). The shape of kinematic data were almost identical with

differences in average mean for the 1.5 cm heel STD of ± 0.0106 degrees and for 5.5 cm heel raise mean STD of ± 0.0185 degrees. It means that markers were positioned very precisely.

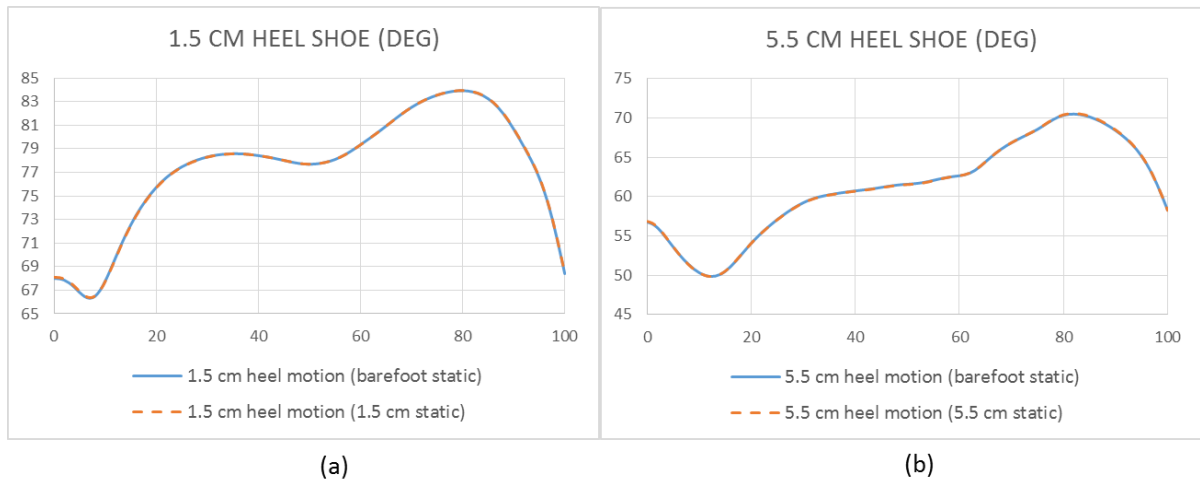


Figure 5.54: Comparison of rocker soled shoe test conditions versus barefoot statics.

Figure 5.54 demonstrates that there is no difference in the shape of the ankle joint kinematics if markers were reattached for different static trials and it means that markers were attached very close to the previous one. (a) - 1.5 cm walking trial compared versus barefoot and 1.5 cm heel static trials (STD $\pm 0.0106^\circ$), (b) – 5.5 cm walking trial compared versus barefoot and 5.5 cm heel static trials (STD $\pm 0.0185^\circ$).

That proves that marker placement for each footwear conditions was almost identical for this example or very close to the true and there is no significant change in kinematic data caused by relocating markers.

5.11.1 Normalisation techniques for the ankle joint

Ankle joint angle normalisation explained by Visual3D guidelines involve making virtual foot segments, which remove offsets in all three components (X-Y-Z). This means that the procedure sets joint angles at 0 degrees. By using virtual segments, it switches static offsets normalisation between footwear conditions and it adds to each static trial and consequently in kinematic data. When a virtual foot is applied, foot segment coordinate systems become similar as for all segments and therefore there is no 90 degrees coordinate system change in the sagittal plane. The difference between foot segment and virtual foot is that virtual foot markers are all at the same level as force platform and therefore it sets foot segment angle

as 0° relative to the ground as shown in the figure 5.53, the virtual segments were also built up for shank, thigh and hip.

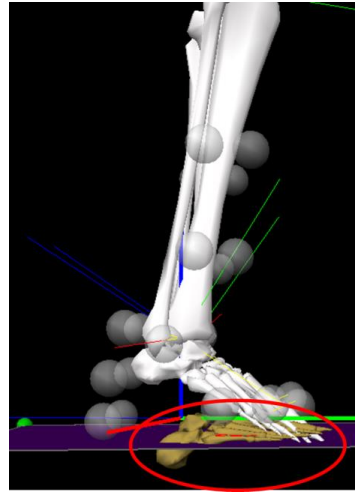


Figure 5.55: Visual3D virtual foot example based on the C-Motion guidelines.

The next step for normalisation was to make virtual segments whose segment coordinate systems were consistent. Visual3d guidelines explains how to make virtual foot segments in detail. Figure 5.56 demonstrates that creating virtual segments applies static offsets for shank and foot segments in the ankle joint kinematic data. In this example a 1.5 cm heel height static trial was built with virtual shank and virtual foot to test normalisation effect on ankle joint data. The static foot segment for the 1.5 cm heel had a 20° angle (barefoot 25.4° and in negative it was slightly dorsiflexed) and the shank had a 6.3° angle compared to the gait laboratory coordinate system. When the virtual foot was applied, it can be seen that the ankle angle default data were shifted by 20° upwards relative to the raw data and when the virtual shank and virtual foot were applied together, then the shank incline was also subtracted from the data in Visual3D. This technique is designed to remove automatic shift correction between static trials in kinematic data in Visual3D, and angles are compared versus one reference pose with postural offsets added to the data. These static offsets should be subtracted manually for each static condition depending on the amount of offset. Each static angular pose was calculated versus virtual segments to know the offset of the shoes for each static.

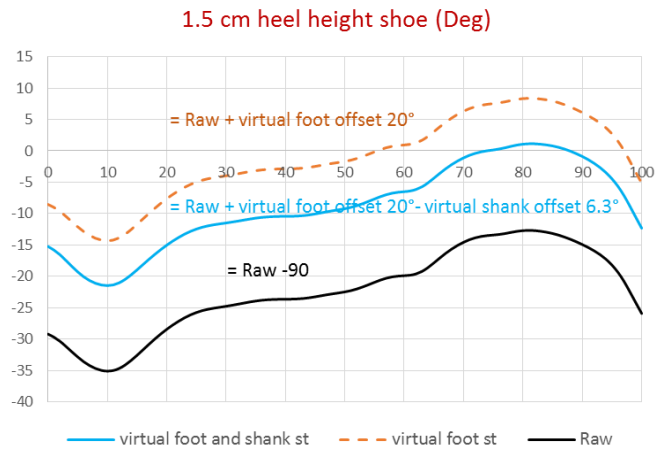


Figure 5.56: This example shows how the ankle joint data were shifted by virtual foot, with virtual shank added to the static model. The raw line represents the export from visual3D and 90 degrees were subtracted to fix coordinate system rotation. The orange line shows that the virtual foot subtracted the foot segment difference between normal position and virtual foot (which lies in parallel with the ground). The blue line shows that the virtual foot and shank segments offsets were added to the ankle angle if compared with data without normalising joint angle to 0 degree.

Virtual segments represent default reference system for all static trials and participants, however all segments offsets were applied to the joint kinematic data and therefore each static offset cause by footwear conditions should be subtracted. The final graph obtained for that example is shown in figure 5.57. It shows the ankle joint data versus default coordinate system (as we see) in the gait laboratory.

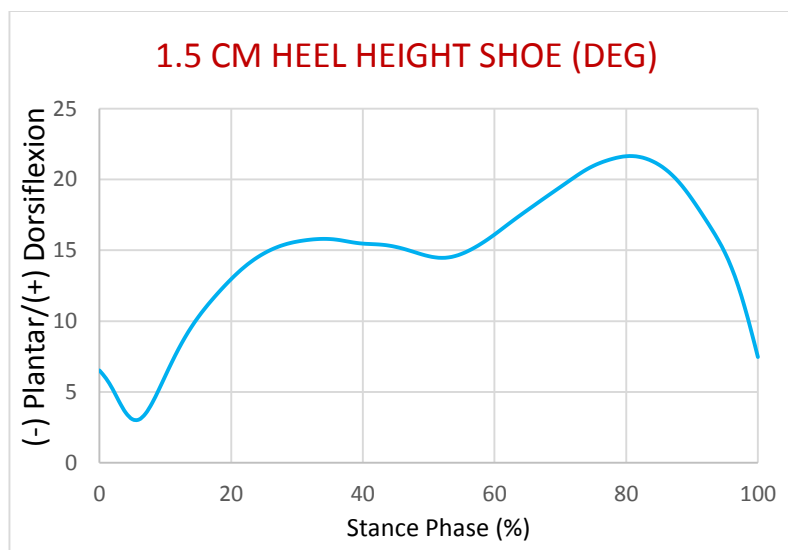


Figure 5.57: Resulting graph following normalisation.

Normalisation demonstrates that the 1.5 cm negative heel shoe placed the ankle into 6.5 degrees of dorsiflexion during IC and kept the ankle in a dorsiflexion position during stance phase; this would also lengthen the calf muscles.

The next pictorial example demonstrates five different heel heights for ankle kinematic data and a comparison versus Visual3D automatic offset normalisation. One barefoot static was applied to different footwear dynamic trials, five own statics and the new technique of normalisation ankle joint, which was used in this thesis. Figure 5.58 shows statics trial offset angles for different shoes in Visual3D during static trials recording for 5 different footwear test conditions.

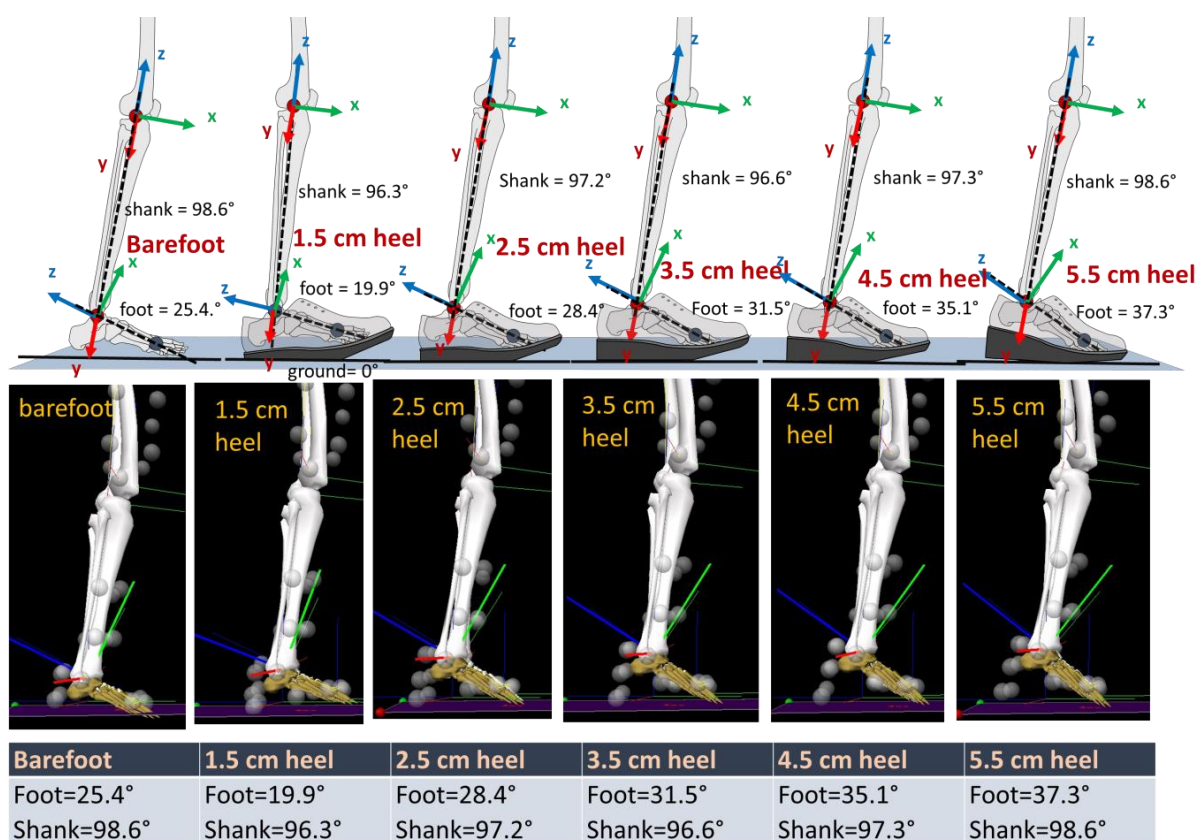


Figure 5.58: Foot-shank relationships for five footwear test conditions.

5.11.2 The first technique analysed for ankle joint normalisation

The next example shows the first normalisation technique investigated. Raw kinematic data were exported for the 1.5, 2.5, 3.5, 4.5, 5.5 cm heel height (HH) shoes. Each footwear condition was assigned with the static shoe trial, which was used for walking trials. Then 90 degrees was subtracted from the data and then a barefoot foot segment angle of 25.4° was

added. In this example, no static footwear segment offsets were applied as Visual3D does it automatically.

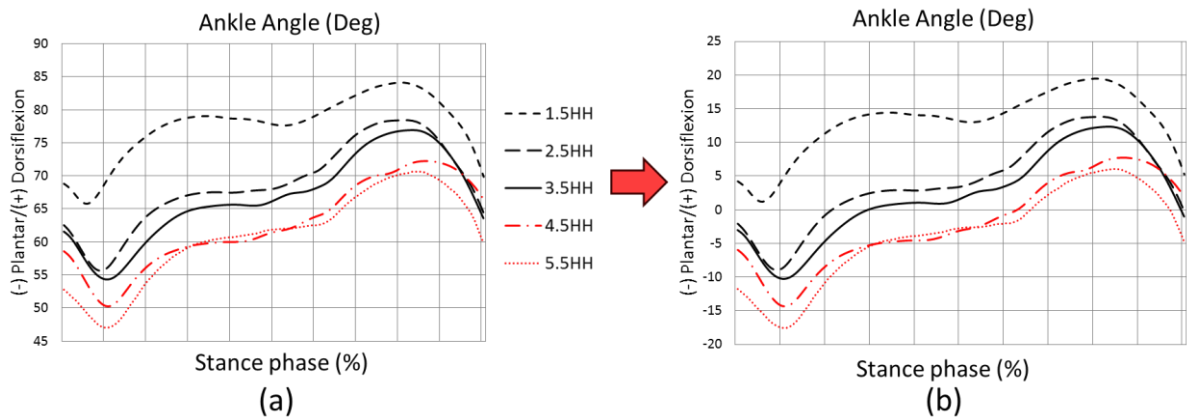


Figure 5.57: Ankle joint kinematic data exported for 1,2,3,4,5 heel heights shoe walking trials using their own statics in Visual3D. (a) – raw ankle joint data; (b) – raw ankle data - $90^\circ +$ barefoot foot segment position 25.4° relative to the ground.

Figure 5.57 shows that static positions for different shoes had shank inclines and it is unclear which angle should be used to normalise it to 0 degrees, therefore this method was not used in this thesis.

5.11.3 The second technique for ankle joint normalisation

Virtual segments were used in static models to have one reference system for all statics and participants (to keep segments at 0 or 90 degrees relative to the force platforms). Static offsets were calculated for each shoe static trial relative to the barefoot. Then offsets were subtracted from kinematic data to be normalised to barefoot static position (when foot segment is in parallel to the ground). After that, barefoot shank incline was subtracted from the data and it made ankle joints to be at neutral position. Figure 5.59 demonstrates this procedure for normalising ankle joint data.

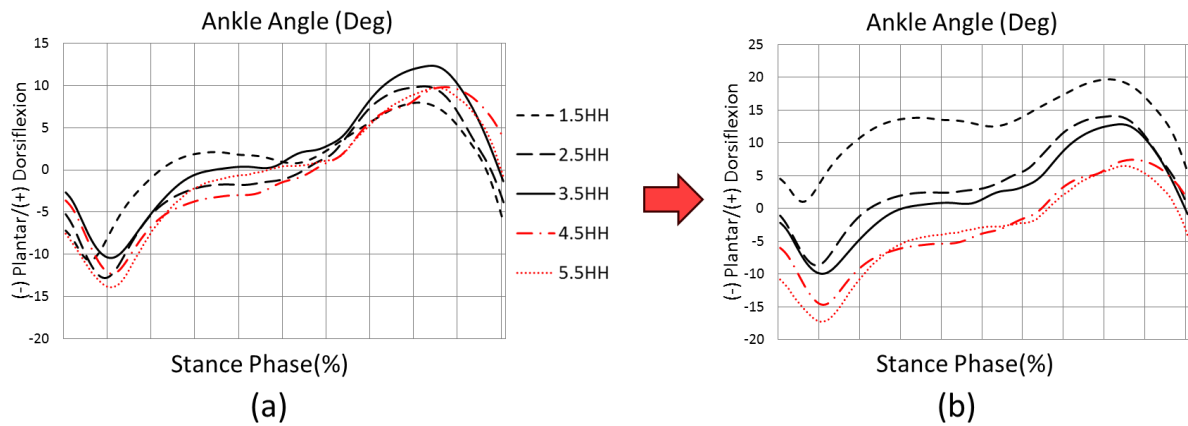


Figure 5.59: Ankle joint kinematic data exported for 1,2,3,4,5 heel heights shoe walking trials using their own statics with virtual segments applied in Visual3D. (a) –ankle joint data with statics offsets; (b) – ankle joint data with subtracted static offsets for foot and shank.

Figure 5.59 (b) shows a neutralised ankle joint angle and this represents real ankle angles as we see them or as a coordinate system of the gait laboratory. The results show that a 1.5 cm negative heel keeps the ankle more dorsiflexed and during initial contact the angle is about 5 degrees of dorsiflexion. With increasing the heel height the ankle becomes more plantarflexed and with the 5.5 cm heel ankle angle at around 10° (100°) degrees of plantarflexion at initial contact and keeps the ankle more plantarflexed throughout stance phase.

All statics offsets were calculated and were removed to normalise it to barefoot static with no shank incline. *All kinematic data such as ankle angle, knee angle and hip angle used the second technique for data normalisation which used the laboratory coordinate system as reference for all trials and participants.*

The next example is a comparison of shoes with 1.5, 2.5, 3.5, 4.5, 5.5 cm heel heights walking trials which were assigned to 1 barefoot static and to their own statics without normalisation.

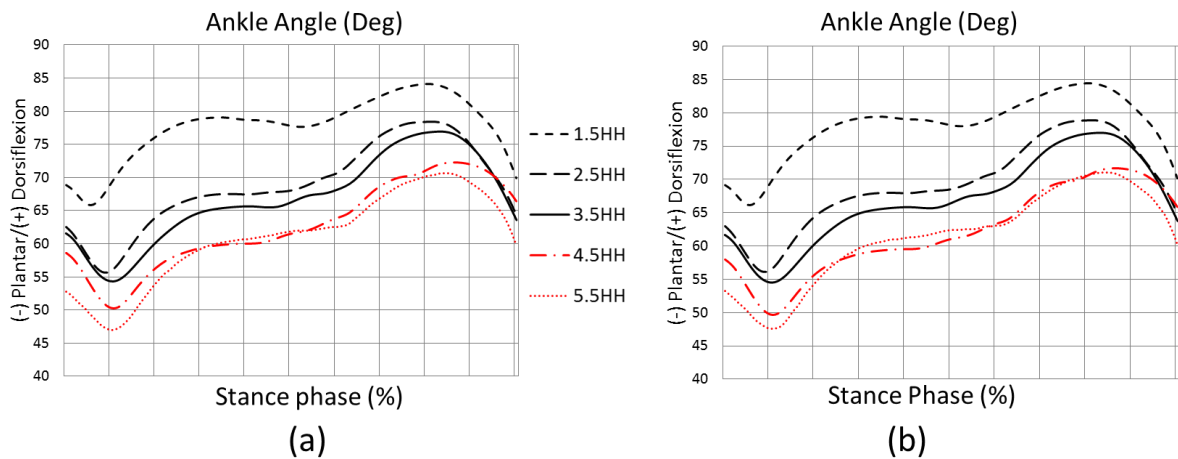


Figure 5.60: Raw ankle joint data from Visual3D for 1.5, 2.5, 3.5, 4.5, 5.5 heel height walking trials; (a) – all walking trials were assigned with one barefoot static, (b) – each footwear condition was assigned with same footwear static trial.

One barefoot static was used for all trials in Visual3D to export kinematic data to OpenSim. There are no other techniques available that allow manual removal of static offsets in the OpenSim software, and therefore barefoot static was the best option for the following reasons:

- An OpenSim requirement for Visual3D statics is that the foot should be parallel to the ground;
- Visual3D use an IK process which makes the foot segment to be parallel with the ground; and if statics were used for different rocker shoes, it would add offsets in the data and therefore muscle-tendon property data would not be valid.

5.11.4 Kinetic data normalisation

Joint moments are commonly used in gait analysis by researchers. Factors like height and body mass, plus gender can influence these moments (Moisio et al., 2003). Joint moments may be normalised to the participants' body weight and height or just body weight. Normalisation by mass decreases variability by about 50% (Winter, 2009). As there was only one gender tested in this study, the ankle and knee moments were normalised by body weight (Nm/kg) (Moisio et al., 2003). The ground reaction force and powers by default were normalised by bodyweight in Visual3D.

CHAPTER 6

6 RESULTS AND STATISTICAL ANALYSIS: KINEMATICS, KINETICS, ELECTROMYOGRAPHY AND MUSCLE FUNCTION DATA

6.1 Subject demographics

Fifteen healthy male subjects, with an age range between 20 and 29 years of age volunteered for this research. It was decided to analyse healthy participant data to minimise the effects of additional factors, which could influence the effect of different footwear features on gait patterns and musculoskeletal biomechanics of the lower limbs during gait. All the subjects tested stated they were healthy with no previous history injuries or pathology that would result in an abnormal walking patterns. Table 6.1 demonstrates the subject demographics.

Table 6.1: Subject demographics.

Male Subject No.	Age on testing date (years)	Body Mass (kg)	Height (m)
1	22	65	1.78
2	24	81	1.77
3	29	71	1.83
4	23	65	1.70
5	29	67	1.72
6	26	64	1.68
7	25	81	1.77
8	24	77	1.83
9	29	84	1.72
10	27	88	1.71
11	24	63	1.68
12	25	66	1.75
13	27	63.5	1.62
14	20	68	1.76
15	27	66	1.74
Mean value	25.3 ± 2.73	71.3 ± 8.50	1.74 ± 0.06

6.2 Trial conditions analysed

Lower limb kinematic, kinetic and muscle function data were analysed to ascertain alterations produced by walking with footwear adapted with features using the method described in section 5.5. Footwear features were divided and analysed in groups. The short

abbreviations chosen for the footwear testing conditions and testing grouping are described in table 6.2.

Table 6.2: Footwear test conditions analysed and their acronyms.

Footwear condition	Short name
1. Rearfoot heel height	
1.5 cm heel height (Negative heel)	1.5HH
2.5 cm heel height (almost flat)	2.5HH
3.5 cm heel height (control shoes)	3.5HH (control)
4.5 cm heel height (heel raised by 1cm)	4.5HH
5.5 cm heel height (heel raised by 2cm)	5.5HH
2. Rocker Apex position (AP)	
Apex position 55% of shoe length (from rear of shoe)	55AP
Apex position 62.5% of shoe length	62.5AP (control)
Apex position 70% of shoe length	70 AP
3. Rocker Apex Angle (RA)	
10°	10° toe
15°	15° toe (control)
20°	20° toe
4. Heel Curve Type (HC)	
A half-curved heel (the curve ended half way between the posterior heel line and the ankle joint centre position)	Half curve
A full curve (the curve ended directly beneath ankle joint centre)	Full curve
The control shoe (no heel curve)	Control (no curve)
5. Rocker profile stiffness at metatarsal area	
A stiff sole (inherent in the control shoe)	Solid (control)
Medium flexibility (half the sole thickness was removed at the metatarsal arcade area)	Med flex
A flexible shoe (transverse incisions were cut into the sole across the metatarsal arcade area to a depth of almost the entire thickness leaving a small base layer; making it very flexible in that area only)	Flex sole

6.3 Gait cycle terms of reference

The results were collated and analysed with reference to specific points during the gait cycle in order to systematically interpret and clarify the effect of different rocker sole test conditions on gait patterns and muscle function. Stance phase was sub-divided into the following phases according to (Perry, 1992):

- Initial contact (weight acceptance 0-2% of gait cycle);
- Loading response (weight acceptance 0-10% of gait cycle);

- Mid-stance (single limb support 10-30% of gait cycle);
- Terminal stance (single limb support 30-50% of gait cycle);
- Pre-swing (50-60% of gait cycle).

The abbreviations used for these distinct phases are illustrated in table 6.3.

Table 6.3: Nomenclature used for parts of stance phase.

Initial contact	IC
Loading response	LR
Mid-stance	MSt.
Terminal stance	TSt.
Pre-swing phase	PSw.

6.3.1 Ankle, knee and hip kinematics, kinetics, EMG and muscle function results

6.3.1.1 The effect of heel height alteration

The following figures show plots with and without standard deviation (STD) demonstrated in colour shading. This was done to show the range of STD for each plot to confirm that the plot can be represented by single line.

Following the analysis of STD values for the figures illustrated in this thesis. It was confirmed that a single line would represent the data obtained. The result shows that the STD were consistent and single line was valid.

Figure 6.1 represents the average ankle angle for all the walking trials utilised for assessing the different heel heights (HHs). It can be seen that through the first and second rockers of gait, shoes with lower heel heights kept the ankle joint relatively dorsiflexed and in those with raised heels the ankle joint shifted into a more plantarflexed position compared to the control shoe test condition (denoted as 3.5HH). However, at maximum plantarflexion (point 4) this effect was not so significant except for the 1.5HH test condition.

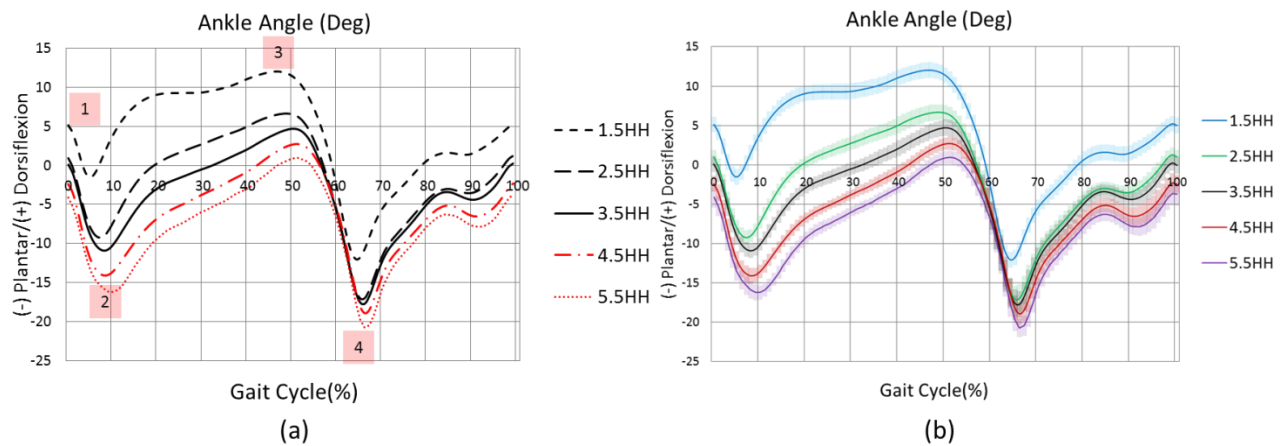


Figure 6.1: Sagittal plane ankle motion during the five heel height test conditions where the control shoe is 3.5 HH. (a) – without standard deviation (STD), (b) – with the lines shadowed to represent STD ranges.

The 0° degree horizontal line represents the barefoot static stance position with the foot parallel to the ground and with the shank positioned with a 0° incline/recline angle. Legend 1 indicates ankle angle at initial contact; legend 2 indicates the area where maximum ankle plantarflexion occurred during LR; legend 3 indicates the point at which maximum ankle dorsiflexion angle occurred during the second rocker of gait during MSt and legend 4 indicates the position where maximum ankle plantarflexion at toe-off (TO), during the third rocker of gait, occurred. The mean sagittal plane ankle angles at ICt and other specific points during stance phase are shown in table 6.4.

Table 6.4: Mean (\pm SD) sagittal plane ankle motion for shoes with five different heel heights during stance phase.

	1.5 HH	2.5 HH	3.5 HH	4.5 HH	5.5 HH
Ankle angle (degrees) at ICt (deg): (+) DF/(-) PF	5.1 (0.9)	1.0 (0.9)	0.1 (1.0)	-2.4 (1.0)	-4.2 (1.3)
Max ankle PF angle during LR (deg)	-1.9 (3.5)	-9.4 (2.4)	-11.2 (3.0)	-14.4 (2.7)	-16.7 (2.5)
Max ankle DF angle during stance phase (deg)	12.3 (1.0)	7.0 (1.0)	5.1 (1.0)	3.0 (0.8)	1.2 (0.8)
Max ankle PF angle at TO (deg)	-12.9 (1.5)	-18.0 (1.4)	-18.6 (1.4)	-19.6 (1.2)	-21.6 (1.0)

6.3.1.2 Ankle position at initial contact (ICt) and during loading response (LR)

At IC, the 1.5 cm negative heel test condition increased the ankle dorsiflexion angle by 5.1° (SD: 0.9) compared to the control shoe (0.1°, SD:1.0). However, when walking with shoes incorporating heels of more than 3.5 cm in height, a plantarflexion shift appeared at the ankle joint for this point in the gait cycle. A distinct pattern emerged during the first two rockers of gait whereby lower-heeled shoes produced a dorsiflexion shift whilst higher heeled shoes produced a plantarflexion shift compared to the control test condition.

During loading response (LR), all shoe test conditions demonstrated significant changes in maximum mean plantarflexion relative to each other (table 6.5) and a gradual plantarflexion shift from the negative heel shoe (1.5 cm) to the positive heel (5.5 cm) occurred (table 6.4) during stance phase overall.

Table 6.5 demonstrates relevant data and the significance value of comparison between the five heel height test conditions for maximum PF angle of the ankle during LR. These display the mean and standard deviations for the test conditions parameters concerned, and the significance level of the mean difference between footwear conditions. A 95% confidence interval (CI) was utilised. The results for one-way ANOVA pairwise comparisons with Bonferroni correction in this chapter will be presented in a similar format as below for clarity. All data followed a normal distribution.

Table 6.5: Pairwise comparisons of shoe conditions for mean maximum ankle PF angle during LR phase.

Cond.	Cond.	Mean Difference	Std. Error	Sig.	95% Confidence Interval for Difference	
					Lower Bound	Upper Bound
1.5HH	2.5HH	7.441*	0.655	0.000	5.261	9.621
	3.5HH	9.259*	0.503	0.000	7.585	10.934
	4.5HH	12.486*	0.581	0.000	10.552	14.420
	5.5HH	14.647*	0.602	0.000	12.644	16.651
2.5HH	1.5HH	-7.441*	0.655	0.000	-9.621	-5.261
	3.5HH	1.818*	0.316	0.000	0.768	2.869
	4.5HH	5.045*	0.311	0.000	4.012	6.078
	5.5HH	7.206*	0.353	0.000	6.031	8.382
3.5HH	1.5HH	-9.259*	0.503	0.000	-10.934	-7.585
	2.5HH	-1.818*	0.316	0.000	-2.869	-0.768
	4.5HH	3.227*	0.289	0.000	2.266	4.187
	5.5HH	5.388*	0.370	0.000	4.156	6.620

4.5HH	1.5HH	-12.486*	0.581	0.000	-14.420	-10.552
	2.5HH	-5.045*	0.311	0.000	-6.078	-4.012
	3.5HH	-3.227*	0.289	0.000	-4.187	-2.266
	5.5HH	2.161*	0.360	0.000	0.965	3.357

Table 6.5 confirms significance (one-way ANOVA with Bonferroni correction) for any value of 0.05 or less in bold font. The greatest difference in maximum ankle plantarflexion value was between the 1.5 cm heel test condition and all the other test conditions (7.5 – 14.8 deg.) during LR.

6.3.1.3 Ankle angle at the point of maximum dorsiflexion during stance phase

Maximum ankle dorsiflexion angle during second rocker of gait also demonstrated significant differences between all heel heights when compared to each other (table 6.6). Negatively-heeled shoes placed the ankle into more dorsiflexion compared to the control shoe; but with increases in heel height, the ankle was gradually shifted into being less dorsiflexed.

Table 6.6 demonstrates the significance of the differences demonstrated between the heel height test conditions at the point of maximum ankle dorsiflexion during stance phase. A plantarflexion shift again occurred for this parameter with increasing heel height, and significance was noted between all the test conditions.

Table 6.6: Pairwise comparisons of shoe conditions for max ankle DF angle during second rocker of gait.

Cond.	Cond.	Mean Difference	Std. Error	Sig.	95% Confidence Interval for Difference	
					Lower Bound	Upper Bound
1.5HH	2.5HH	5.242*	0.923	0.001	2.173	8.311
	3.5HH	7.186*	1.047	0.000	3.705	10.667
	4.5HH	9.242*	1.047	0.000	5.760	12.725
	5.5HH	11.077*	1.014	0.000	7.707	14.448
2.5HH	1.5HH	-5.242*	0.923	0.001	-8.311	-2.173
	3.5HH	1.944*	0.477	0.011	0.359	3.529
	4.5HH	4.000*	0.388	0.000	2.710	5.291
	5.5HH	5.835*	0.311	0.000	4.802	6.868
3.5HH	1.5HH	-7.186*	1.047	0.000	-10.667	-3.705
	2.5HH	-1.944*	0.477	0.011	-3.529	-0.359
	4.5HH	2.056*	0.317	0.000	1.003	3.110

	5.5HH	3.891*	0.457	0.000	2.373	5.410
4.5HH	1.5HH	-9.242*	1.047	0.000	-12.725	-5.760
	2.5HH	-4.000*	0.388	0.000	-5.291	-2.710
	3.5HH	-2.056*	0.317	0.000	-3.110	-1.003
	5.5HH	1.835*	0.381	0.003	0.569	3.100

6.3.1.4 Maximum plantarflexion angle at TO

At toe-off, the 1.5 cm heel shoe was significantly less plantarflexed when compared to the 3.5 cm heel control shoe ($p=0.002$) and indeed all the other test conditions. There were significant differences between 2.5HH and 4.5HH and 5.5HH, but no significant differences between the 2.5 HH and 3.5HH, and 3.5HH and 4.5 HH and 4.5HH and 5.5HH shoes. The 5.5HH shoe was significantly more plantarflexed versus all footwear conditions except for the 4.5 cm heel test condition (table 6.7).

Table 6.7: Pairwise comparisons of shoe conditions for max ankle PF angle during late stance.

Cond.	Cond.	Mean Difference	Std. Error	Sig.	95% Confidence Interval for Difference	
					Lower Bound	Upper Bound
1.5HH	2.5HH	5.065*	1.192	0.008	1.101	9.028
	3.5HH	5.629*	1.130	0.002	1.873	9.386
	4.5HH	6.699*	1.153	0.000	2.865	10.533
	5.5HH	8.673*	1.126	0.000	4.929	12.418
2.5HH	1.5HH	-5.065*	1.192	0.008	-9.028	-1.101
	3.5HH	0.565	0.483	1.000	-1.043	2.172
	4.5HH	1.634*	0.483	0.045	0.027	3.242
	5.5HH	3.609*	0.575	0.000	1.697	5.520
3.5HH	1.5HH	-5.629*	1.130	0.002	-9.386	-1.873
	2.5HH	-0.565	0.483	1.000	-2.172	1.043
	4.5HH	1.070	0.414	0.216	-0.307	2.446
	5.5HH	3.044*	0.392	0.000	1.742	4.346
4.5HH	1.5HH	-6.699*	1.153	0.000	-10.533	-2.865
	2.5HH	-1.634*	0.483	0.045	-3.242	-0.027
	3.5HH	-1.070	0.414	0.216	-2.446	0.307
	5.5HH	1.974	0.634	0.076	-0.134	4.082

6.3.2 Ankle sagittal plane ROM

Table 6.8 demonstrates the ankle ROMs produced when walking with shoes adapted with different heel heights.

Table 6.8: Mean values for maximum ankle ROM during specific points and also the complete gait cycle for shoes with different heel heights.

	1.5 HH	2.5 HH	3.5 HH	4.5 HH	5.5 HH
Ankle ROM during LR (points 1-2) degrees	7.2 (0.8)	10.4 (0.9)	11.4 (0.9)	12.1 (0.9)	12.5 (1.1)
Ankle ROM between points 2 and 3 (end of LR to max DF during stance phase) degrees	14.3 (1.2)	16.5 (1.3)	16.3 (1.2)	17.5 (1.2)	17.9 (1.2)
Ankle ROM between max DF and maximum PF during late stance (between points 3 and 4)	25.2 (1.5)	25.0 (1.5)	23.7 (1.6)	22.7 (1.2)	22.8 (1.1)
Maximum ROM during gait cycle (deg)	26.5 (1.6)	25.2 (1.4)	23.8 (1.5)	23.4 (1.1)	23.0 (1.1)

6.3.2.1 Ankle ROM during LR

The 1.5 cm and 2.5cm heel test conditions both significantly reduced ankle ROM during LR compared to all the other heel height test conditions (table 6.9). The 3.5cm, 4.5 cm and 5.5 cm heeled shoes did not show any significant increase in ROM between themselves.

Table 6.9: Pairwise comparisons of shoe conditions versus ankle sagittal plane ROM during LR.

Cond.	Cond.	Mean Difference	Std. Error	Sig.	95% Confidence Interval for Difference	
					Lower Bound	Upper Bound
1.5HH	2.5HH	-3.278*	0.405	0.000	-4.624	-1.931
	3.5HH	-4.220*	0.421	0.000	-5.621	-2.819
	4.5HH	-4.924*	0.600	0.000	-6.918	-2.930
	5.5HH	-5.382*	0.630	0.000	-7.478	-3.286
2.5HH	1.5HH	3.278*	0.405	0.000	1.931	4.624
	3.5HH	-0.942*	0.226	0.009	-1.694	-0.190
	4.5HH	-1.647*	0.424	0.017	-3.057	-0.236
	5.5HH	-2.105*	0.542	0.016	-3.906	-0.303
3.5HH	1.5HH	4.220*	0.421	0.000	2.819	5.621

	2.5HH	0.942*	0.226	0.009	0.190	1.694
	4.5HH	-0.704	0.388	0.909	-1.994	0.586
	5.5HH	-1.162	0.506	0.376	-2.845	0.521
4.5HH	1.5HH	4.924*	0.600	0.000	2.930	6.918
	2.5HH	1.647*	0.424	0.017	0.236	3.057
	3.5HH	0.704	0.388	0.909	-0.586	1.994
	5.5HH	-0.458	0.356	1.000	-1.643	0.727

It was hypothesised in chapter 5, that with low heel heights, the sagittal plane ankle ROM during LR would be reduced. Table 6.9 confirms that this did indeed occur.

6.3.2.2 Ankle ROM during second rocker of gait (i.e. between points 2 and 3)

The ankle ROM between points 2 and 3 was significantly increased for the 5.5 cm heel versus 3.5 cm control shoe.

Table 6.10: Pairwise significance comparisons between shoe conditions and ankle ROM angle between point 2 and 3 of the gait cycle.

Cond.	Cond.	Mean Difference	Std. Error	Sig.	95% Confidence Interval for Difference	
					Lower Bound	Upper Bound
1.5HH	2.5HH	-2.158	1.033	0.554	-5.593	1.277
	3.5HH	-2.033	1.079	0.804	-5.620	1.554
	4.5HH	-3.203	1.136	0.137	-6.982	0.576
	5.5HH	-3.528*	1.052	0.047	-7.025	-0.030
2.5HH	1.5HH	2.158	1.033	0.554	-1.277	5.593
	3.5HH	0.125	0.429	1.000	-1.301	1.552
	4.5HH	-1.045	0.339	0.081	-2.171	0.081
	5.5HH	-1.370*	0.334	0.011	-2.479	-0.260
3.5HH	1.5HH	2.033	1.079	0.804	-1.554	5.620
	2.5HH	-0.125	0.429	1.000	-1.552	1.301
	4.5HH	-1.170	0.473	0.268	-2.743	0.403
	5.5HH	-1.495*	0.387	0.017	-2.781	-0.209
4.5HH	1.5HH	3.203	1.136	0.137	-0.576	6.982
	2.5HH	1.045	0.339	0.081	-0.081	2.171
	3.5HH	1.170	0.473	0.268	-0.403	2.743
	5.5HH	-0.325	0.396	1.000	-1.642	0.993

6.3.2.3 Ankle ROM during third rocker of gait (i.e. between points 3 and 4)

The ankle ROM between maximum dorsiflexion and maximum plantarflexion during late stance (between points 3 and 4) showed a significant increase for the 2.5 cm heel height versus the 4.5 and 5.5 cm heeled shoes. No other significance was found.

Table 6.11: Pairwise comparisons of shoe conditions for the ankle ROM between maximum dorsiflexion and maximum PF during late stance (between points 3 and 4).

Cond.	Cond.	Mean Difference	Std. Error	Sig.	95% Confidence Interval for Difference	
					Lower Bound	Upper Bound
1.5HH	2.5HH	0.178	0.706	1.000	-2.169	2.524
	3.5HH	1.557	0.832	0.825	-1.211	4.325
	4.5HH	2.543	0.903	0.138	-0.461	5.548
	5.5HH	2.404	0.778	0.080	-0.183	4.992
2.5HH	1.5HH	-0.178	0.706	1.000	-2.524	2.169
	3.5HH	1.379	0.505	0.162	-0.299	3.058
	4.5HH	2.366*	0.479	0.002	0.773	3.959
	5.5HH	2.227*	0.502	0.006	0.557	3.896
3.5HH	1.5HH	-1.557	0.832	0.825	-4.325	1.211
	2.5HH	-1.379	0.505	0.162	-3.058	0.299
	4.5HH	0.987	0.503	0.701	-0.687	2.660
	5.5HH	0.847	0.467	0.912	-0.706	2.401
4.5HH	1.5HH	-2.543	0.903	0.138	-5.548	0.461
	2.5HH	-2.366*	0.479	0.002	-3.959	-0.773
	3.5HH	-0.987	0.503	0.701	-2.660	0.687
	5.5HH	-0.139	0.490	1.000	-1.768	1.490

6.3.2.4 The overall ankle ROM during the complete gait cycle

The total ankle sagittal plane mean ROM differences during the full gait cycle are shown in table 6.12. Overall ankle ROM angle during the full gait cycle was significantly increased for the 1.5 cm heel versus the control shoe, the 4.5 cm and the 5.5 cm heel height test conditions. The shoe with the 5.5 cm heel height produced a significant reduction in overall ankle ROM compared to the 1.5cm and 2.5cm heel heights. The shoes with heels higher than the control shoe (3.5mm) did not demonstrate any significant difference in ankle joint ROM when compared to the control shoe or between themselves.

Table 6.12: Pairwise statistical significance comparisons between shoe conditions versus maximum ankle ROM angle during the full gait cycle.

Cond.	Cond.	Mean Difference	Std. Error	Sig.	95% Confidence Interval for Difference	
					Lower Bound	Upper Bound
1.5HH	2.5HH	1.268	0.811	1.000	-1.429	3.965
	3.5HH	2.680*	0.726	0.024	0.266	5.093
	4.5HH	3.123*	0.820	0.019	0.398	5.849
	5.5HH	3.473*	0.809	0.007	0.783	6.164
2.5HH	1.5HH	-1.268	0.811	1.000	-3.965	1.429
	3.5HH	1.412	0.512	0.154	-0.290	3.114
	4.5HH	1.855*	0.548	0.045	0.031	3.680
	5.5HH	2.205*	0.570	0.017	0.311	4.100
3.5HH	1.5HH	-2.680*	0.726	0.024	-5.093	-0.266
	2.5HH	-1.412	0.512	0.154	-3.114	0.290
	4.5HH	0.444	0.473	1.000	-1.130	2.017
	5.5HH	0.794	0.465	1.000	-0.753	2.340
4.5HH	1.5HH	-3.123*	0.820	0.019	-5.849	-0.398
	2.5HH	-1.855*	0.548	0.045	-3.680	-0.031
	3.5HH	-.444	.473	1.000	-2.017	1.130
	5.5HH	.350	.371	1.000	-.884	1.584

6.3.2.5 Summary of sagittal plane ankle joint angles for shoes with different heel heights

One of the aims of the thesis was to determine whether different rocker sole profiles may be specifically designed to place the ankle joint at an optimal position at which the plantarflexor muscles keep the loading to the calf muscles to a minimum for a given gait speed; especially during the propulsive phase. Therefore, the following results for heel height conditions are pertinent to this thesis:

- Despite a reduction in sagittal plane ankle ROM for lower-heeled shoes demonstrated when compared to higher-heeled shoes during the LR phase, walking in lower-heeled shoes produced significant increases in overall ROM during the full gait cycle;
- Lower heel heights significantly increased ankle ROM between maximum dorsiflexion and maximum plantarflexion during stance phase of gait. Low-heeled shoes caused

the ankle to be more dorsiflexed during the whole gait cycle compared to high-heeled ones;

- High heeled shoes placed the ankle into a relatively more PF position during the gait cycle compared to low-heeled shoes;
- The 1.5 cm heel placed the ankle at an angle so that the calf muscle MTU would be theoretically stretched where maximum DF occurred during the end of second rocker of gait. However, the 1.5 cm heel, the 2.5 cm, 3.5 cm and 4.5 cm heel kept the ankle closer to its natural resting position, and indeed, the 5.5 cm heel only produced less than 2° of dorsiflexion at this point in the gait cycle.

Therefore, with regards to hypotheses *Ha1a* to *Ha1g*, these hypotheses are accepted with regards to the effect of alteration to shoe heel height as demonstrated in table 6.13.

Table 6.13: Alternative hypotheses accepted/not accepted for alteration to heel height test condition.

	1.5 HH	2.5 HH	3.5 HH	4.5 HH	5.5 HH
Maximum PF during LR (<i>Ha1a</i>)	Accepted	Accepted	control	Accepted	Accepted
Ankle ROM during LR (points 1-2) degrees (<i>Ha1b</i>)	Accepted	Accepted	control	Not accepted	Not accepted
Max DF during 2 nd rocker (<i>Ha1c</i>)	Accepted	Accepted	control	Accepted	Accepted
Ankle ROM 2 nd rocker of gait (<i>Ha1d</i>)	Not accepted	Not accepted	control	Not accepted	Accepted
Max. PF 3 rd rocker of gait (<i>Ha1e</i>)	Accepted	Not accepted	control	Not accepted	Accepted
Ankle ROM 3 rd rocker of gait (<i>Ha1g</i>)	Not accepted	Not accepted	control	Not accepted	Not accepted
Maximum ROM during gait cycle (<i>Ha1f</i>)	Accepted	Not accepted	control	Not accepted	Not accepted

6.3.3 The effect of altering rocker sole apex position (AP)

Sagittal plane ankle angle plots are shown in figure 6.2, which compares the effect on ankle kinematics with shoes adapted with different rocker apex positions but the same heel height. These demonstrate that the shoe with a 55% apex rocker position (55AP), shifted the ankle into a more plantarflexed position during LR compared to the control shoe (where the

control shoe is 62.5AP) and also produced less maximum dorsiflexion during second rocker of gait. Additionally, it placed the ankle into more plantarflexion during third rocker of gait compared to both the other test conditions. This meant that a plantarflexion shift occurred during the whole of stance as well as during swing phase.

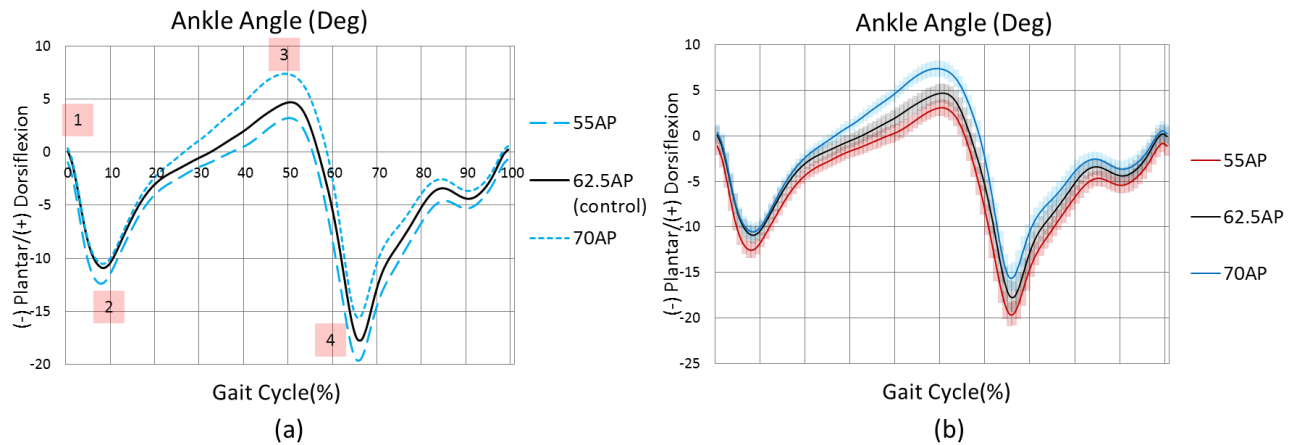


Figure 6.2: Sagittal plane ankle motion when walking with the three apex position test conditions. (a) – without standard deviation (STD), (b) – with the lines shadowed to represent STD ranges.

Table 6.14: Mean (\pm SD) sagittal plane ankle motion (deg) for three different rocker apex position test conditions.

	55AP	62.5AP	70AP
Ankle angle at initial contact (-)plantar/(+)dorsiflexion	-0.9 (1.0)	0.1 (1.0)	0.1 (1.0)
Max ankle PF angle during LR (deg)	-12.6 (0.9)	-11.3 (0.9)	-11.0 (0.9)
Max ankle DF angle during double support (deg)	3.5 (0.8)	5.1 (1.0)	7.7 (0.9)
Max ankle PF angle at toe-off (deg)	-20.5 (1.1)	-18.6 (1.4)	-16.4 (1.4)

Pairwise comparison between AP conditions (table 6.15) shows that mean maximum ankle PF angle for the 55% apex rocker was significantly more plantarflexed than the other two test conditions during LR. The 70 AP rocker shoe did not show any significant difference compared to the control shoe (62.5% AP).

Table 6.15: Pairwise comparisons of apex positions for mean maximum ankle PF angle during LR.

Cond.	Cond.	Mean Difference	Std. Error	Sig.	95% Confidence Interval for Difference	
					Lower Bound	Upper Bound
55AP	62.5AP	-1.320*	0.268	0.001	-2.050	-0.591
	70 AP	-1.607*	0.164	0.000	-2.052	-1.161
62.5AP	55AP	1.320*	0.268	0.001	0.591	2.050
	70 AP	-0.286	0.222	0.656	-0.890	0.318

6.3.3.1 Alteration to ankle angle at maximum dorsiflexion during stance for different rocker APs

Table 6.16 demonstrates that compared to the control shoe, the 55AP rocker test condition produced significantly less maximum dorsiflexion during the second rocker of gait when compared to the control shoe, whilst the 70AP shoe produced significantly more dorsiflexion. This means that all test conditions using different apex positions demonstrated statistically significant differences in maximum dorsiflexion during stance compared to each other.

Table 6.16: Pairwise comparisons of rocker APs for maximum ankle DF angle during second rocker of gait).

Cond.	Cond.	Mean Difference	Std. Error	Sig.	95% Confidence Interval for Difference	
					Lower Bound	Upper Bound
55AP	62.5AP	-1.571*	0.441	0.009	-2.769	-0.372
	70 AP	-4.234*	0.306	0.000	-5.067	-3.402
62.5AP	55AP	1.571*	0.441	0.009	0.372	2.769
	70 AP	-2.663*	0.425	0.000	-3.820	-1.507

6.3.3.2 Alteration to maximum plantarflexion during stance for different rocker APs

At the end of the third rocker of gait (toe-off phase) the 55% AP shoe produced significantly more PF compared to the control shoe, but in comparison, the shoe with the 70% AP induced significantly less PF .

6.3.3.3 Ankle ROM for different rocker APs

The sagittal plane ankle ROM data did not show any significant differences ($p>0.05$) between any rocker APs during LR. Table 6.17 shows the mean and standard deviation values for ankle ROM for the AP conditions at specific points in the gait cycle.

Table 6.17: Mean values for ankle ROM during gait cycle for different AP conditions.

	55AP	62.5AP	70AP
Ankle ROM during loading response (1-2) degrees	11.7 (1.2)	11.4 (0.9)	11.4 (1.0)
Ankle ROM between point 2 and 3 (including LR to maximum angle DF phase) degrees	16.1 (1.1)	16.4 (1.2)	18.7 (1.1)
Ankle ROM between max DF and max PF during late stance (between points 3 and 4) degrees	24.0 (1.1)	23.7 (1.6)	24.1 (1.4)
Max ROM during gait cycle (deg)	24.1 (1.1)	23.8 (1.5)	24.5 (1.3)

Ankle ROM during second rocker of gait (i.e. between points 2 and 3) did not show any statistical significance between the 55% and 62.5% rocker AP test conditions. However, the 70% AP shoe increased ankle ROM significantly compared to the other two test conditions (table 6.18).

Table 6.18: Pairwise statistical significance comparisons between shoe AP conditions and ankle ROM angle between point 2 and 3 of the gait cycle.

Cond.	Cond.	Mean Difference	Std. Error	Sig.	95% Confidence Interval for Difference	
					Lower Bound	Upper Bound
55AP	62.5AP	-0.251	0.502	1.000	-1.614	1.113
	70 AP	-2.628*	0.321	0.000	-3.499	-1.756
62.5AP	55AP	0.251	0.502	1.000	-1.113	1.614
	70 AP	-2.377*	0.398	0.000	-3.458	-1.296

With regards to maximum ROM within points 3 and 4 and maximum ROM during full gait cycle results did not show any significant differences between any apex length conditions.

6.3.3.4 Summary: ankle kinematics for different rocker AP conditions

- The 70% AP condition increased ankle ROM during stance phase up to pre-swing. However overall ROM during the full gait cycle was not significantly changed;

- The 55% AP shoe kept ankle significantly more plantarflexed during the gait cycle compared to the other AP but this did not significantly reduce ankle ROM;
- Compared to the control shoe, a more distal apex position produced a more dorsiflexed ankle joint except during LR;
- The 55% apex position cause earlier plantarflexion motion during late stance phase (as was hypothesised in chapter 5).

Table 6.19: Alternative hypotheses accepted/not accepted for alteration to apex position (AP) test conditions.

	55%	62.5 %	70%
Maximum PF during LR (Ha1a)	Accepted	control	Not accepted
Ankle ROM during LR (points 1-2) degrees (Ha1b)	Not accepted	control	Not accepted
Max DF during 2 nd rocker (Ha1c)	Accepted	control	Accepted
Ankle ROM 2 nd rocker of gait (Ha1d)	Not accepted	control	Accepted
Max. PF 3 rd rocker of gait (Ha1e)	Accepted	control	Accepted
Ankle ROM 3 rd rocker of gait (Ha1g)	Not accepted	control	Accepted
Maximum ROM during gait cycle (Ha1f)	Accepted	control	Not accepted

6.3.4 The effect of altering rocker apex angle (toe angle-TA)

6.3.4.1 Alteration to sagittal plane ankle kinematics

In chapter 5 it was discussed and hypothesised that for rocker apex angles, higher angles would cause the ankle to be more plantarflexed during third rocker of gait (and also produce premature PF during late stance phase) and lower apex angles would cause the opposite effect.

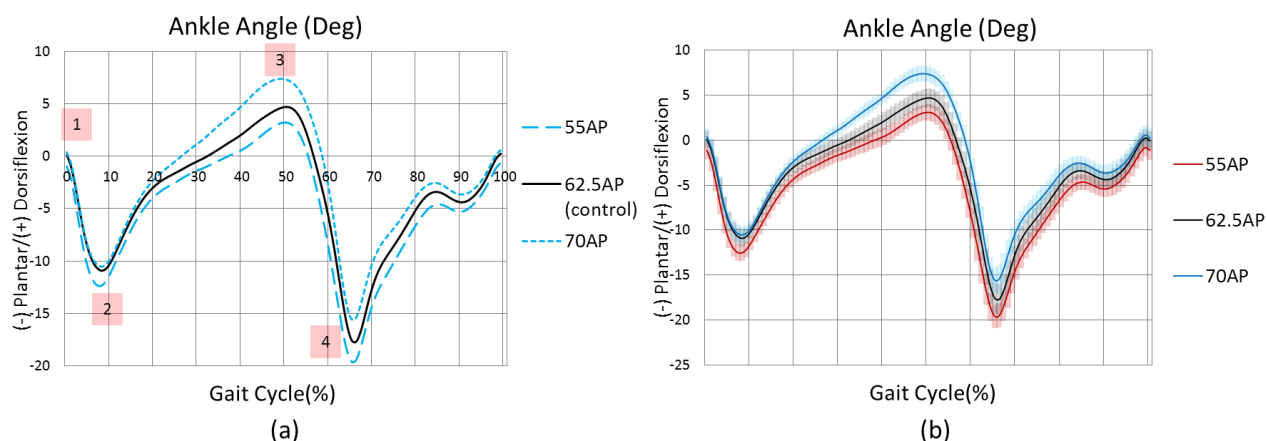


Figure 6.3: sagittal plane ankle motion during the three apex angle conditions (TAs). (a) – without standard deviation (STD), (b) – with the lines shadowed to represent STD ranges.

6.3.4.2 Alteration to maximum plantarflexion and dorsiflexion during stance phase caused by different TA conditions.

The mean values of ankle angle for the rocker sole TA conditions during stance phase are shown in table 6.20.

Table 6.20: Mean (\pm SD) sagittal plane ankle motion for the three apex angles (TAs) tested.

	10° TA	15° TA	20° TA
Ankle angle at initial contact (+)PF/(-)DF (deg.)	0.0 (1.0)	0.1 (1.0)	-0.2 (1.1)
Max ankle plantarflexion angle during LR (deg)	-11.5 (0.9)	-11.3 (0.9)	-11.7 (0.7)
Max ankle dorsiflexion angle during stance (deg)	6.7 (0.9)	5.1 (1.0)	4.3 (1.0)
Max ankle PF angle at toe-off phase (deg)	-17.9 (1.4)	-18.6 (1.4)	-20.3 (1.6)

There were no significant differences between test conditions for maximum plantarflexion during LR. Table 6.21 demonstrates the relevant data and the significance value of comparison between test conditions utilising different toe angles for maximum dorsiflexion of the ankle during second rocker of gait during stance phase. It shows significance for the 10°TA rocker shoe for maximal DF compared to the control condition (15°) and the 20° test condition. The 20° rocker sole TA test condition heel did not show any significance that it was less dorsiflexed compared to the control shoe.

Table 6.21: Pairwise comparisons of rocker toe angles (TAs) for maximum ankle DF angle during stance phase.

Cond.	Cond.	Mean Difference	Std. Error	Sig.	95% Confidence Interval for Difference	
					Lower Bound	Upper Bound
10° TA	15° TA	1.643*	0.377	0.002	0.620	2.667
	20° TA	2.412*	0.416	0.000	1.282	3.542
15° TA	10° TA	-1.643*	0.377	0.002	-2.667	-0.620
	20° TA	0.769	0.497	0.432	-.581	2.118

During toe-off phase (third rocker of gait) the 20° test condition produced significantly more maximum PF compared to the other two rocker apex test conditions. These results confirm the toe angle hypothesis alteration.

6.3.4.3 Ankle ROM when walking with shoes adapted with different rocker TAs

Table 6.22 shows the effect of different rocker apex angles on ankle ROM during the complete gait cycle. Ankle ROM between point 2 and 3 (LR to late stance phase at which maximum DF occurs) did not show any statistical significance between the 15° apex angle test condition (control) and the 20° test condition. However, the 10° apex angled-shoe increased ROM significantly compared to the other two test conditions during second rocker of gait, as shown in table 6.22.

Table 6.22: Mean values for ankle ROM during the gait cycle for different apex-angled shoes.

	10° TA	15° TA	20° TA
Ankle ROM during loading response (1-2) (deg.)	11.5 (0.9)	11.4 (0.9)	11.5 (1.0)
Ankle ROM between point 2 and 3 (including LR to max angle DF phase degrees)	18.2 (1.3)	16.4 (1.2)	16.0 (1.3)
Ankle ROM between max DF and max PF during late stance (between points 3 and 4 degrees)	24.6 (1.3)	23.7 (1.6)	24.6 (1.6)
Max ROM during gait cycle (deg)	25.3 (1.2)	23.8 (1.5)	24.7 (1.6)

Table 6.23: Pairwise statistical significance comparisons between apex angle conditions and ankle ROM between points 2 and 3 of the gait cycle.

Cond.	Cond.	Mean Difference	Std. Error	Sig.	95% Confidence Interval for Difference	
					Lower Bound	Upper Bound
10° TA	15° TA	1.881*	0.334	0.000	0.974	2.788
	20° TA	2.191*	0.422	0.000	1.045	3.337
15° TA	10° TA	-1.881*	0.334	0.000	-2.788	-0.974
	20° TA	0.310	0.513	1.000	-1.083	1.704

There were no statistically significant differences in ankle ROM between maximum dorsiflexion and maximum plantarflexion during stance phase. However, the 10° test condition increased maximum ROM during the whole gait cycle to a significant level compared to the control shoe (p=0.013).

6.3.4.4 Summary of sagittal ankle angle for the different rocker TA conditions

- The 10° TA shoe increased the maximum ankle DF angle during stance and also significantly increased the maximum ankle ROM during the full gait cycle compared to the control test condition;
- The 20° TA caused premature plantarflexion during late stance phase, and produced a plantarflexion shift throughout the remainder of stance phase and most of swing phase compared to both the other test conditions up to the point of TSw., at which point the ankle angle at IC was not significantly different from the other two test conditions.

Table 6.24 demonstrates the significance of the TA conditions relative to the control condition (15° TA).

Table 6.24: Alternative hypotheses accepted/not accepted for alteration to apex position (AP) test conditions.

	10° TA	15° TA	20° TA
Maximum PF during LR (Ha1a)	Not accepted	control	Not accepted
Ankle ROM during LR (points 1-2) degrees (Ha1b)	Not accepted	control	Not accepted
Max DF during 2 nd rocker (Ha1c)	Accepted	control	Not accepted
Ankle ROM 2 nd rocker of gait (Ha1d)	Accepted	control	Accepted
Max. PF 3 rd rocker of gait (Ha1e)	Not Accepted	control	Accepted
Ankle ROM 3 rd rocker of gait (Ha1g)	Not accepted	control	Not accepted
Maximum ROM during gait cycle (Ha1f)	Accepted	control	Not accepted

6.3.5 The effect of adding heel curves

The sagittal plane ankle joint kinematics (Figure 6.4, Table 6.25, Table 6.26) demonstrate that a dorsiflexion shift occurred for both curved heel test conditions during LR, MS and TS. It also can be seen that a significant ($p < 0.001$) reduction in ROM occurred for the half curved heel shoe and greater reduction for full curve profile and mean PF values during LR between all conditions.

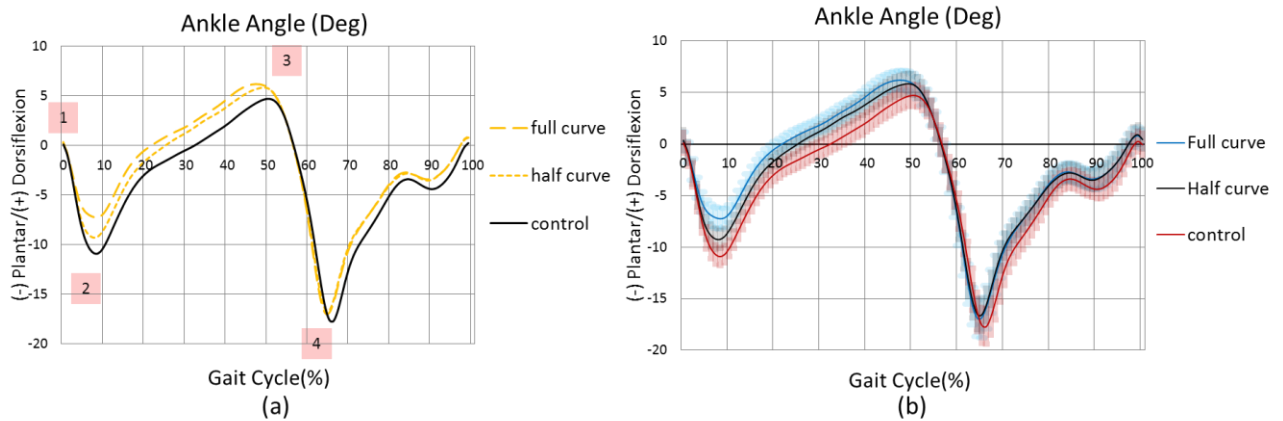


Figure 6.4: Sagittal plane ankle motion for the complete gait cycle during walking with curved heels compared to a control shoe. (a) – without standard deviation (STD), (b) – with the lines shadowed to represent STD ranges.

The 0° degree line represents the barefoot static position with the foot in parallel to the ground and the shank has a 0° incline/recline. Legend 1 indicates the point at which the ankle is at ICt; legend 2 indicates the area where maximum ankle plantarflexion occurred during LR; legend 3 indicates the area at which maximum ankle dorsiflexion angle occurred during MSt; and legend 4 indicates the position where maximum ankle plantarflexion at toe-off occurred.

Table 6.25: Mean (\pm SD) sagittal plane ankle rotation demonstrated by the three different curved heel test conditions.

	Full curve	Half curve	control
Ankle angle at initial contact (deg) (-)plantar/(+)dorsiflexion	0.3 (1.0)	0.4 (1.0)	0.1 (1.0)
Max ankle PF angle during LR (deg)	-7.8 (0.9)	-9.5 (0.9)	-11.3 (0.9)
Max ankle DF angle during stance phase (deg)	6.4 (0.9)	6.2 (1.0)	5.1 (1.0)
Max ankle PF angle at toe-off phase (deg)	-18.0 (1.7)	-17.5 (1.4)	-18.6 (1.4)

Table 6.26: Mean values for sagittal plane ankle ROM during the complete gait cycle for different curved heel shoe test conditions.

	Full curve	Half curve	control
Ankle ROM during loading response (1-2) degrees	8.0 (1.0)	9.9 (0.8)	11.4 (0.9)
Ankle ROM between point 2 and 3 (including LR to maximum angle DF phase) degrees	14.2 (1.3)	15.7 (1.3)	16.4 (1.2)
Ankle ROM between maximum dorsiflexion and maximum plantarflexion during late stance (between points 3 and 4) degrees	24.4 (1.5)	23.7 (1.5)	23.7 (1.5)
Maximum ROM during gait cycle (deg)	24.6 (1.6)	23.9 (1.4)	23.8 (1.5)

The full curve and half curve-heeled shoes produced a statistically significant increase in maximum ankle DF angle during stance phase compared to the shoes with no heel curve as shown in the table 6.25. However, there was no significant difference between the curved heels for this parameter. Whilst ankle angle at IC was not significantly altered between any of the test conditions, a dorsiflexion shift appeared during loading response commensurate with a reduction in ankle plantarflexion ROM during LR, and continued through second rocker of gait for both the curved heel test conditions to produce the dorsiflexion shift noted at the maximum DF position (table 6.27).

Table 6.27: Pairwise comparisons of curved heel shoe test conditions for maximum ankle DF angle during stance phase.

Cond.	Cond.	Mean Difference	Std. Error	Sig.	95% Confidence Interval for Difference	
					Lower Bound	Upper Bound
Full curve	Half curve	0.237	0.200	0.764	-0.305	0.779
	No curve	1.364*	0.436	0.022	0.179	2.548
Half curve	Full curve	-0.237	0.200	0.764	-0.779	0.305
	No curve	1.127*	0.392	0.037	0.060	2.193

During toe-off phase the half curved heel showed significance in reduction of max PF (P=0.043).

Ankle ROM between point 2 and 3 (second rocker of gait) for the full- curved heel showed a statistically significant increase in ankle ROM when compared to both the half- curved heel and baseline control shoes as shown in table 6.25.

Table 6.28: Pairwise statistical significance comparisons between curved heel conditions and ankle ROM angle between point 2 and 3 of the gait cycle.

Cond.	Cond.	Mean Difference	Std. Error	Sig.	95% Confidence Interval for Difference	
					Lower Bound	Upper Bound
Full curve	Half curve	-1.494*	0.266	0.000	-2.217	-0.771
	No curve	-2.137*	0.456	0.001	-3.375	-0.898
Half curve	Full curve	1.494*	0.266	0.000	0.771	2.217
	No curve	-0.643	0.380	0.339	-1.676	0.391

There were no statistical significant differences between any footwear conditions for maximum ROM between point 3 and 4 and during full gait cycle.

6.3.5.1 Summary of sagittal plane ankle angle alterations produced by curved heel test conditions

- Both curved heel test conditions shifted the ankle joint into a more DF position during LR, second rocker of gait and the majority of swing phase and therefore calf muscle lengths would have been lengthened compared to the control condition;
- The curved heels reduced the maximal ankle plantarflexion angle during third rocker of gait and also reduced ankle ROM during LR.
- The curved heels not only altered the beginning of the stance phase but also full gait cycle kinematics.

Table 6.29: Alternative hypotheses accepted/not accepted for alteration to heel curve test conditions.

	Full curve	Half curve	control
Maximum PF during LR (<i>Ha1a</i>)	accepted	accepted	control
Ankle ROM during LR (points 1-2) degrees (<i>Ha1b</i>)	accepted	accepted	control
Max DF during 2 nd rocker (<i>Ha1c</i>)	Accepted	accepted	control
Ankle ROM 2 nd rocker of gait (<i>Ha1d</i>)	Accepted	Not accepted	control
Max. PF 3 rd rocker of gait (<i>Ha1e</i>)	Not Accepted	Accepted	control
Ankle ROM 3 rd rocker of gait (<i>Ha1g</i>)	Not accepted	Not accept	control

6.4 The effect of altering rocker sole stiffness at the metatarsal arcade area

6.4.1 Alteration to sagittal plane ankle kinematics

Sagittal plane ankle kinematics did not show any statistical significant differences during the gait cycle except during the third rocker of gait. A plantarflexion shift occurred during third rocker of gait, which continued into swing phase for the two more flexible test conditions, but even this was limited to less than 2 degrees at the point of maximal ankle plantarflexion during third rocker of gait.

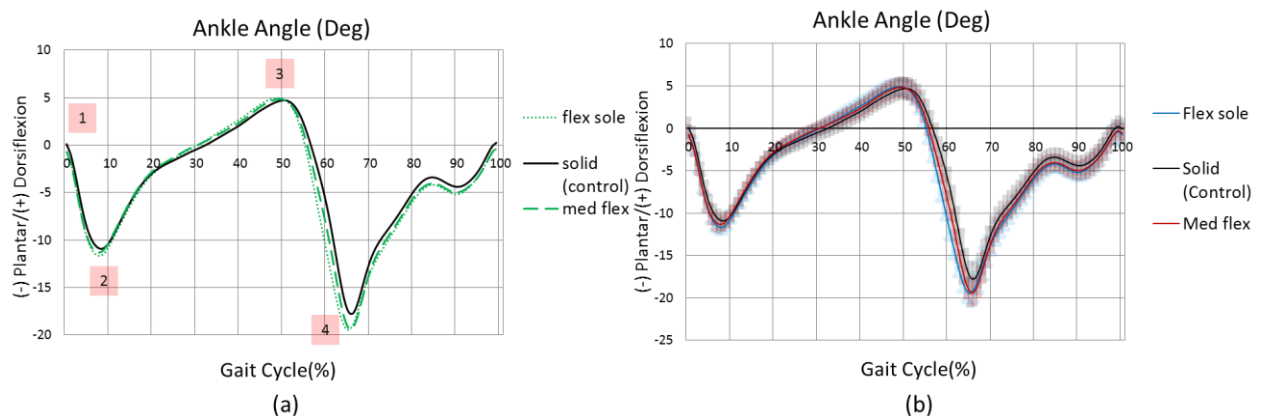


Figure 6.5: Sagittal plane ankle motion for shoes adapted to be more flexible at the metatarsal area compared to the control shoe. (a) – without standard deviation (STD), (b) – with the lines shadowed to represent STD ranges.

Table 6.30: Kinematic data produced when walking with shoes with different forefoot sole stiffness.

	Flexible sole	Medium flexibility	Solid
Ankle angle at initial contact (deg) (+)plantar/(-)dorsiflexion	0.0 (1.0)	-0.7 (1.0)	0.1 (1.0)
Max ankle PF angle during LR (deg)	-11.9 (0.8)	-11.6 (0.8)	-11.3 (0.9)
Max ankle DF angle during stance phase (deg)	5.2 (0.9)	5.1 (0.9)	5.1 (1.0)
Max ankle PF angle at toe-off phase (deg)	-20.1 (1.4)	-20.0 (1.5)	-18.6 (1.4)

Table 6.31: Mean (\pm SD) sagittal plane ankle ROM (degs) for three different flexibility levels of the rocker sole at the metatarsal arcade area.

	Flex sole	Med. flex	Solid
Ankle ROM during LR (1-2)	11.1 (0.9)	10.9 (0.8)	11.4 (0.9)
Ankle ROM between point 2 and 3 (including LR to max angle DF phase)	17.1 (1.1)	16.7 (1.1)	16.4 (1.2)
Ankle ROM between max DF and max PF during late stance (between points 3 and 4)	25.3 (1.5)	25.1 (1.6)	23.7 (1.6)
Max ROM during gait cycle.	25.7 (1.4)	25.2 (1.5)	23.8 (1.5)

During toe-off phase the most solid rocker sole kept the ankle significantly less plantarflexed compared to the flexible and semiflexible footwear conditions ($P < 0.04$) as shown in the table 6.32.

Table 6.32: Pairwise statistical significance comparisons for maximum ankle plantarflexion angle at toe-off phase between the forefoot shoe flexibility conditions.

Cond.	Cond.	Mean Difference	Std. Error	Sig.	95% Confidence Interval for Difference	
					Lower Bound	Upper Bound
Flex sole	Med. flex	-0.117	0.615	1.000	-1.789	1.556
	Solid	-1.515*	0.461	0.016	-2.767	-0.263
Med. flex	Flex sole	0.117	0.615	1.000	-1.556	1.789
	Solid	-1.398*	0.494	0.040	-2.741	-0.056

6.4.2 Alteration to ankle ROM produced by different forefoot sole flexibilities

The more flexible and semi-flexible sole units demonstrated significant increase in maximum ROM between point 3 and 4 compared to the control solid shoe condition as shown in table 6.33.

Table 6.33: Pairwise statistical significance comparisons for maximum ankle ROM during third rocker of gait between flexible and semi-flexible sole unit conditions.

Cond.	Cond.	Mean Difference	Std. Error	Sig.	95% Confidence Interval for Difference	
					Lower Bound	Upper Bound
Flex sole	Med. flex	0.217	0.527	1.000	-1.216	1.650
	Solid	1.675*	0.509	0.016	.291	3.058
Med. flex	Flex sole	-0.217	0.527	1.000	-1.650	1.216
	Solid	1.458*	0.474	0.025	.170	2.745

Maximum ankle ROM angle was increased to significant level for flexible shoe ($p < 0.001$) and increased for medium flexible shoe ($p = 0.037$) versus solid shoe.

6.4.3 Summary of ankle angle results for variation in shoe forefoot flexibility

- The shoes with semi-flexible and flexible areas at the metatarsal head area produced an increase in the maximum PF angle during toe-off phase to a statistically-significant level compared to the less flexible control shoe condition;
- The footwear conditions (flexible and that with medium flexibility) increased maximum ROM during push off phase (between max DF at terminal stance and max PF at toe-off phase). That would also alter the concentric contraction velocity and of the calf muscle and alter the MTU length of travel of the calf muscles;
- The flexible profile shoe increased the maximum range of motion detected during the whole gait cycle.

Table 6.34: Alternative hypotheses accepted/not accepted for alteration to heel curve test conditions.

	Flex sole	Med. flex	Solid
Maximum PF during LR (<i>Ha1a</i>)	Not accepted	Not accepted	control
Ankle ROM during LR (points 1-2) degrees (<i>Ha1b</i>)	Not accepted	Not accepted	control
Max DF during 2 nd rocker (<i>Ha1c</i>)	Not accepted	Not accepted	control
Ankle ROM 2 nd rocker of gait (<i>Ha1d</i>)	Not accepted	Not accepted	control
Max. PF 3 rd rocker of gait (<i>Ha1e</i>)	Accepted	Accepted	control
Ankle ROM 3 rd rocker of gait (<i>Ha1g</i>)	Accepted	Accepted	control

6.5 SAGITTAL PLANE KNEE KINEMATICS

6.5.1 The effect of walking with different heel heights

In figure 6.6, legend 1 indicates where maximum knee flexion occurs during LR; Legend 2 indicates the point at which maximum knee extension angle occurred during stance phase; legend 3 indicates the point at which maximum knee flexion angle occurred during toe-off and legend 4 indicates the position where maximum knee flexion occurs during swing phase of normal adult gait.

Figure 6.6 shows the average of the data (n=15) analysed for knee kinematics in the sagittal plane for footwear with different heel heights acquired during the walking trials. It can be seen that the 1.5 cm heel increased knee flexion during IC and the LR phase and also caused premature maximal knee flexion during LR; and consequently caused a reduction in the time taken for LR. This could have been due to alteration to the ankle ROM resulting in the shorter time taken during LR phase. The 1.5 cm heel also induced maximum knee extension prematurely (at point 2 in figure 6.6) compared to the other heel height test conditions and also increased knee flexion during 40%-62% of the gait cycle including toe-off phase, which is the main interest for the calf muscle work. The opposite effect was produced by wearing shoes with the higher heel test conditions during late stance.

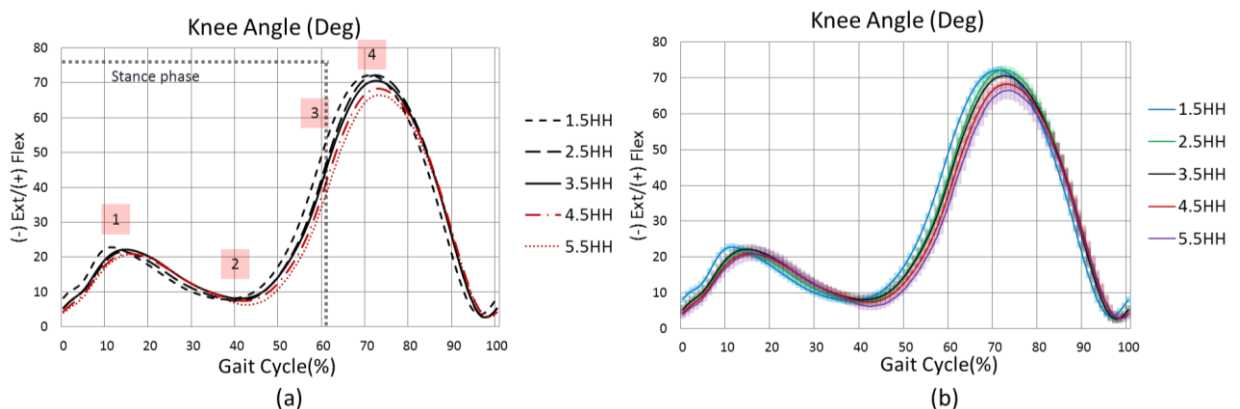


Figure 6.6: Sagittal plane knee motion during the five heel height test conditions where the control shoe is 3.5 HH. (a) – without standard deviation (STD), (b) – with the lines shadowed to represent STD ranges.

6.5.1.1 Sagittal plane knee kinematics during IC

At ICt, the 1.5 cm negative heel test condition increased knee flexion by 2.9° (SD:1.4°) when compared with the control shoe (table 6.29). The 5.5 cm heel test condition kept the knee more extended when compared to the negative heels tested and the control shoe.

6.5.1.2 The effect of heel height test conditions during loading response (LR)

During LR, there were no statistically significant differences in maximum knee flexion values. Premature knee flexion occurred when walking with the 1.5 cm heel and slightly increased knee extension for the high-heeled shoes.

Table 6.35: Mean (\pm SD) sagittal plane knee kinematics (degs) when walking with shoes with five different heel height test conditions.

	1.5 HH	2.5 HH	3.5 HH	4.5 HH	5.5 HH
Knee angle at ICt (deg)	8.2 (1.4)	5.4 (1.2)	5.3 (1.4)	4.5 (1.2)	4.0 (1.4)
Maximum knee flexion angle during LR (deg)	23.0 (1.5)	21.8 (1.1)	22.4 (1.4)	21.3 (1.1)	21.1 (2.0)
Max knee extension during stance (deg)	7.2 (1.3)	6.8 (1.2)	7.4 (1.3)	6.8 (1.2)	5.7 (1.2)
Max knee flexion angle at toe-off (deg)	58.1 (2.8)	52.3 (2.4)	50.7 (2.6)	46.7 (3.0)	43.6 (3.2)
Max knee flexion angle during swing (deg)	72.5 (1.6)	72.5 (1.0)	70.9 (0.9)	68.6 (1.1)	66.8 (2.5)
Max Knee ROM between point 2-3 (deg)	50.9 (2.7)	45.6 (2.5)	43.3 (2.9)	39.9 (3.1)	37.9 (3.3)
Max knee ROM during support (deg)	55.6 (2.8)	50.8 (2.7)	48.9 (2.7)	45.1 (3.2)	42.2 (3.4)

6.5.1.3 The effect of heel height test conditions on knee angle during late stance

During late stance, the 5.5 cm heel height produced significantly increased knee extension compared to the control shoe ($p=0.025$) and the maximum extension phase was delayed versus control and negative-heel test footwear conditions.

6.5.1.4 The effect of heel height test conditions on knee angle at TO (maximum knee flexion)

At toe-off, the 1.5 cm heel was significantly more flexed when compared to the 3.5 cm heel and even more flexed compared to the heels, which were more raised (table 6.30). With raising the heel height, the knee was gradually more extended at toe-off.

Table 6.36: Pairwise comparisons of shoe conditions for max knee flexion at toe-off.

Cond.	Cond.	Mean Difference	Std. Error	Sig.	95% Confidence Interval for Difference	
					Lower Bound	Upper Bound
1.5HH	2.5HH	5.732*	0.755	0.000	3.222	8.241
	3.5HH	7.393*	1.034	0.000	3.955	10.832
	4.5HH	11.336*	1.083	0.000	7.736	14.937
	5.5HH	14.474*	1.125	0.000	10.732	18.216
2.5HH	1.5HH	-5.732*	0.755	0.000	-8.241	-3.222
	3.5HH	1.661	0.879	0.796	-1.262	4.584
	4.5HH	5.604*	0.819	0.000	2.882	8.327
	5.5HH	8.742*	0.858	0.000	5.890	11.594
3.5HH	1.5HH	-7.393*	1.034	0.000	-10.832	-3.955
	2.5HH	-1.661	0.879	0.796	-4.584	1.262
	4.5HH	3.943*	0.609	0.000	1.918	5.968
	5.5HH	7.081*	0.927	0.000	3.997	10.164
4.5HH	1.5HH	-11.336*	1.083	0.000	-14.937	-7.736
	2.5HH	-5.604*	0.819	0.000	-8.327	-2.882
	3.5HH	-3.943*	0.609	0.000	-5.968	-1.918
	5.5HH	3.137*	0.904	0.038	0.129	6.146

6.5.2 Alteration to kinetics of the knee during swing phase whilst walking in different heel heights

During swing phase, a similar effect on knee kinematics was noted as seen during toe-off phase between footwear test conditions; where the 1.5 cm heel was significantly more flexed compared to the 4.5 cm and 5.5 cm heel-height shoes. The 4.5 cm and 5.5 cm heeled shoes were significantly more extended compared to the control shoe as shown in the table 6.31.

Table 6.37: Pairwise comparisons of shoe conditions for max knee flexion during swing phase.

Cond.	Cond.	Mean Difference	Std. Error	Sig.	95% Confidence Interval for Difference	
					Lower Bound	Upper Bound
1.5HH	2.5HH	-0.025	0.731	1.000	-2.456	2.406
	3.5HH	1.600	0.895	0.955	-1.377	4.577
	4.5HH	3.861*	0.801	0.003	1.199	6.523
	5.5HH	5.697*	1.069	0.001	2.144	9.251
2.5HH	1.5HH	0.025	0.731	1.000	-2.406	2.456
	3.5HH	1.625	0.511	0.067	-0.075	3.326
	4.5HH	3.886*	0.353	0.000	2.711	5.061
	5.5HH	5.722*	0.806	0.000	3.042	8.403
3.5HH	1.5HH	-1.600	0.895	0.955	-4.577	1.377
	2.5HH	-1.625	0.511	0.067	-3.326	0.075
	4.5HH	2.261*	0.496	0.004	0.610	3.911
	5.5HH	4.097*	0.792	0.001	1.464	6.730
4.5HH	1.5HH	-3.861*	0.801	0.003	-6.523	-1.199
	2.5HH	-3.886*	0.353	0.000	-5.061	-2.711
	3.5HH	-2.261*	0.496	0.004	-3.911	-0.610
	5.5HH	1.836	0.764	0.306	-0.703	4.376

6.5.3 Knee sagittal plane ROM

Table 6.38 demonstrates the knee ROMs produced when walking with shoes adapted with different heel heights.

Table 6.38: Mean values for maximum knee ROM between the point 2-3 and within complete stance phase for shoes with different heel heights.

	1.5 HH	2.5 HH	3.5 HH	4.5 HH	5.5 HH
Max Knee ROM between point 2-3 (deg)	50.9 (2.7)	45.6 (2.5)	43.3 (2.9)	39.9 (3.1)	37.9 (3.3)
Max knee ROM during support (deg)	55.6 (2.8)	50.8 (2.7)	48.9 (2.7)	45.1 (3.2)	42.2 (3.4)

The 1.5 cm HH significantly increased knee ROM versus all test footwear conditions and it can be seen that with raising the heel height the knee ROM was gradually reduced between maximum extension at TSt and maximum flexion at toe-off phase. The 5.5 cm heel reduced

maximum knee ROM between points 2-3 when compared to all the other footwear conditions except for the 4.5 cm heel as shown in table below.

Table 6.39: Pairwise comparisons of shoe conditions for max knee RM between point 2 and 3.

Cond.	Cond.	Mean Difference	Std. Error	Sig.	95% Confidence Interval for Difference	
					Lower Bound	Upper Bound
1.5HH	2.5HH	5.302*	0.962	0.001	2.104	8.500
	3.5HH	7.579*	0.771	0.000	5.014	10.144
	4.5HH	11.002*	1.136	0.000	7.223	14.781
	5.5HH	12.954*	1.052	0.000	9.455	16.454
2.5HH	1.5HH	-5.302*	0.962	0.001	-8.500	-2.104
	3.5HH	2.277	0.902	0.242	-0.722	5.276
	4.5HH	5.700*	0.898	0.000	2.713	8.687
	5.5HH	7.652*	0.613	0.000	5.615	9.690
3.5HH	1.5HH	-7.579*	0.771	0.000	-10.144	-5.014
	2.5HH	-2.277	0.902	0.242	-5.276	0.722
	4.5HH	3.423*	0.644	0.001	1.280	5.566
	5.5HH	5.375*	0.849	0.000	2.553	8.198
4.5HH	1.5HH	-11.002*	1.136	0.000	-14.781	-7.223
	2.5HH	-5.700*	0.898	0.000	-8.687	-2.713
	3.5HH	-3.423*	0.644	0.001	-5.566	-1.280
	5.5HH	1.952	0.810	0.303	-0.742	4.646

The 1.5 cm HH significantly increased maximum knee ROM during stance phase versus all test footwear conditions. It also can be seen that with raising heel height it resulted in significant gradual reduction of ROM during stance phase versus lower heels (table 6.40).

Table 6.40: Pairwise comparisons of shoe conditions for max ROM during stance phase.

Cond.	Cond.	Mean Difference	Std. Error	Sig.	95% Confidence Interval for Difference	
					Lower Bound	Upper Bound
1.5HH	2.5HH	4.785*	0.848	0.001	1.963	7.607
	3.5HH	6.780*	0.934	0.000	3.674	9.886
	4.5HH	10.521*	1.133	0.000	6.752	14.290
	5.5HH	13.393*	0.967	0.000	10.177	16.610
2.5HH	1.5HH	-4.785*	0.848	0.001	-7.607	-1.963
	3.5HH	1.995	0.856	0.353	-0.852	4.842
	4.5HH	5.736*	0.922	0.000	2.670	8.802
	5.5HH	8.608*	0.705	0.000	6.263	10.954
3.5HH	1.5HH	-6.780*	0.934	0.000	-9.886	-3.674
	2.5HH	-1.995	0.856	0.353	-4.842	0.852

	4.5HH	3.741*	0.657	0.001	1.557	5.925
	5.5HH	6.614*	0.911	0.000	3.584	9.644
4.5HH	1.5HH	-10.521*	1.133	0.000	-14.290	-6.752
	2.5HH	-5.736*	0.922	0.000	-8.802	-2.670
	3.5HH	-3.741*	0.657	0.001	-5.925	-1.557
	5.5HH	2.873*	0.841	0.042	.074	5.671

The 1.5 cm HH significantly increased maximum knee ROM during stance phase versus all test footwear condition. It also can be seen that with raising heel height it resulted in gradual increase of knee extension during LR, an increase knee flexion during TS phase if compared versus negative-heeled shoes and increase extension of the knee ROM between maximum extension at TS and maximum flexion at toe-off phase. The 5.5 cm heel reduced max knee ROM between points 2-3 if compared versus all footwear conditions except for 4.5 cm heel.

6.5.4 Summary – sagittal plane knee joint angle for different heel heights

- The 1.5 cm heel increased knee flexion during ICt and raised heels slightly increased knee extension. The results suggest that the knee was more flexed, thus shank incline was increased, and therefore negative profile and shank incline caused huge alterations to ankle joint kinematics.
- There were no statistically significant differences demonstrated between conditions for maximum knee flexion during loading response. However, 1.5 cm heel caused premature knee flexion during LR and raised heel test conditions showed slight knee extension.
- During mid-stance phase the 1.5 cm heel resulted in knee extension and considerable less knee extension occurred for the 2.5 cm heel test condition when compared to all test conditions.
- During 40%-50% of terminal stance phase the positive heel shoes stayed longer in knee extension position when compared to control and the 1.5 cm heel was significantly more flexed.
- The 1.5 cm heel significantly increased knee flexion ROM within 40% - 62% stance phase, and the opposite effect was noted for raised heels.

Table 6.41: Alternative hypotheses accepted/not accepted for alteration to heel height test conditions.

	1.5 HH	2.5 HH	3.5 HH	4.5 HH	5.5 HH
Knee angle at ICT	accepted	Not accepted	control	Not accepted	Not accepted
Maximum knee flexion angle during LR (Ha1h)	Not accepted	Not accepted	control	Not accepted	Not accepted
Max knee extension during stance (Ha1i)	Not accepted	Not accepted	control	Not accepted	accepted
Max knee flexion angle at toe-off (Ha1j)	accepted	Not accepted	control	accepted	accepted
Max knee flexion angle during swing (Ha1k)	Not accepted	Not accepted	control	accepted	accepted
Max Knee ROM between point 2-3 (Ha1l)	accepted	Not accepted	control	accepted	accepted
Max knee ROM during support (Ha1m)	accepted	Not accepted	control	accepted	accepted

6.5.5 The effect of altering rocker sole apex position (AP)

Figure 6.7 shows the average of the knee kinematics in the sagittal plane for different apex length shoes.

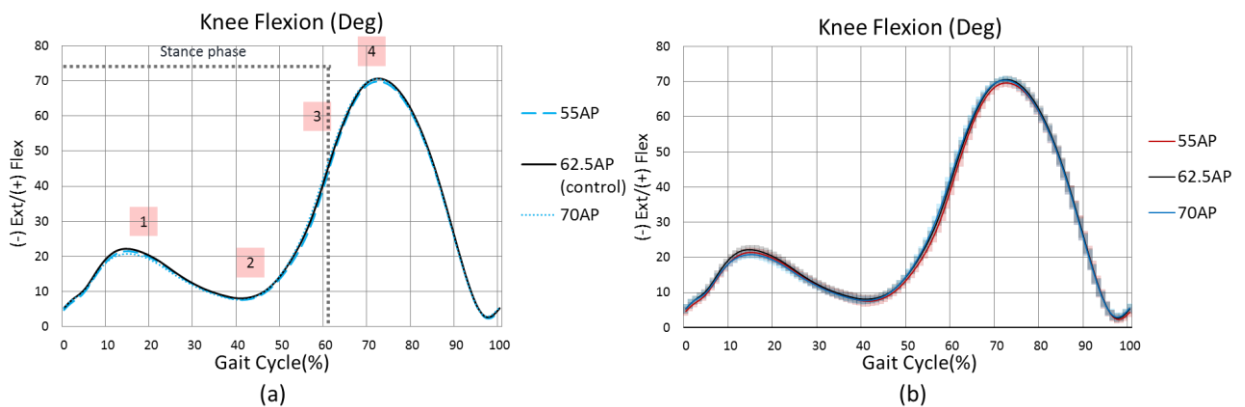


Figure 6.7: Sagittal plane knee motion during the three apex position test conditions where the control shoe is 62.5AP. Legend 1 indicates where maximum knee flexion angle occurred during LR; Legend 2 indicates the point at which maximum knee extension angle occurred during terminal stance phase; legend 3 indicates the point at which maximum knee flexion angle occurred at toe-off; and legend 4 indicates the position where maximum knee flexion angle during swing occurred. (a) – without standard deviation (STD), (b) – with the lines shadowed to represent STD ranges.

Table 6.42 shows mean values and ROM for knee motion in sagittal conditions for different apex length test conditions.

Table 6.42: Mean (\pm SD) sagittal plane knee motion (degs) for three different apex position, max ROM between point 2-3 and max knee ROM during stance phase (N=15).

	55AP	62.5AP	70AP
Knee angle at ICt (deg)	4.7 (1.4)	5.3 (1.4)	5.4 (1.3)
Maximum knee flexion angle during LR (deg)	21.7 (1.3)	22.4 (1.4)	21.0 (1.2)
Max knee extension during TSt (deg)	6.8 (1.4)	7.4 (1.3)	7.1 (1.0)
Max knee flexion angle at toe-off (deg)	49.3 (3.1)	50.7 (2.6)	51.8 (2.5)
Max knee flexion angle during swing (deg)	70.2 (1.0)	70.9 (0.9)	70.6 (1.2)
Max Knee ROM between point 2-3 (deg)	42.4 (3.3)	43.3 (2.9)	44.7 (2.4)
Max knee ROM during support (deg)	48.0 (3.3)	48.9 (2.7)	49.9 (2.7)

6.5.5.1 Loading response

Pairwise comparison between different AP conditions (table 6.36) demonstrates that the 70 AP test condition had significantly less knee flexion ($p=0.044$) when compared to control shoe.

Table 6.43: Pairwise comparisons of apex positions for mean knee flexion during LR.

Cond.	Cond.	Mean Difference	Std. Error	Sig.	95% Confidence Interval for Difference	
					Lower Bound	Upper Bound
55AP	62.5AP	-0.664	0.574	0.800	-2.225	0.896
	70 AP	0.657	0.630	0.944	-1.055	2.368
62.5AP	55AP	0.664	0.574	0.800	-0.896	2.225
	70 AP	1.321*	0.475	0.044	0.029	2.613

6.5.5.2 Knee range of motion

The sagittal plane knee ROM showed that the 70AP footwear condition significantly increased ROM between point 2 and 3 (maximum extension during terminal stance and maximum flexion during toe-off phase) when compared to the 55AP footwear condition ($p=0.024$) as shown in the table 6.44.

Table 6.44: Pairwise comparisons of apex positions for mean knee flexion between point 2 and 3.

Cond.	Cond.	Mean Difference	Std. Error	Sig.	95% Confidence Interval for Difference	
					Lower Bound	Upper Bound
55AP	62.5AP	-0.874	0.604	.510	-2.516	0.768
	70 AP	-2.233*	0.723	.024	-4.197	-0.268
62.5AP	55AP	0.874	0.604	.510	-0.768	2.516
	70 AP	-1.359	0.683	.200	-3.215	0.497

6.5.5.3 Summary of knee joint flexion results for different apex position conditions:

- The 70AP footwear test condition significantly reduced knee flexion when compared to control ($p=0.044$).
- The 70AP footwear test condition significantly increased ROM between point 2 and 3 (maximum extension during terminal stance and maximum flexion during toe-off phase) when compared to 55AP footwear condition ($p=0.024$).

Table 6.45: Alternative hypotheses accepted/not accepted for alteration to rocker apex positions.

	55AP	62.5AP	70AP
Max knee flexion angle during LR (Ha1h)	Not accepted	control	accepted
Max knee extension during stance (Ha1i)	Not accepted	control	Not accepted
Max knee flexion angle at toe-off (Ha1j)	Not accepted	control	Not accepted
Max knee flexion angle during swing (Ha1k)	Not accepted	control	Not accepted
Max Knee ROM between point 2-3 (Ha1l)	Not accepted	control	accepted
Max knee ROM during support (Ha1m)	Not accepted	control	Not accepted

6.5.6 Toe angle (apex angle)

Figure 6.8 shows the average data for knee kinematics in sagittal plane for different apex angle footwear conditions acquired during the walking trials for N=15. Figure 6.8 demonstrates that there was a slight change in maximum knee flexion during LR phase where the 10° toe angle test condition produced more knee extension versus the control

shoe. During swing phase maximum knee flexion was reduced for the 20° toe angle test condition.

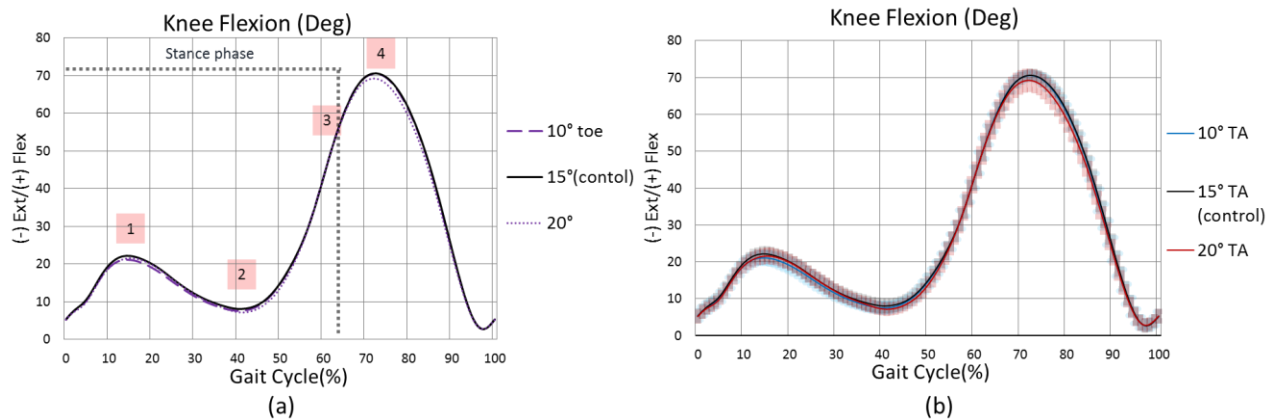


Figure 6.8: Sagittal plane knee motion during the three apex angle test conditions where the control shoe is 15°. Legend 1 indicates where maximum knee flexion angle occurred during LR; Legend 2 indicates the point at which maximum knee extension angle occurred during terminal stance phase; legend 3 indicates the point at which maximum knee flexion angle occurred at toe-off; and legend 4 indicates the position where maximum knee flexion angle during swing occurred. (a) – without standard deviation (STD), (b) – with the lines shadowed to represent STD ranges.

Mean values for knee kinematics in sagittal plane are shown in the table below.

Table 6.46: Mean (\pm SD) sagittal plane knee motion (degs) for three different toe angle test footwear conditions, max ROM between point 2-3 and max knee ROM during stance phase (N=15).

	10° TA	15° TA	20° TA
Knee angle at ICt (deg)	5.3 (1.2)	5.3 (1.4)	5.2 (1.2)
Maximum knee flexion angle during LR (deg)	21.4 (1.5)	22.4 (1.4)	21.8 (1.5)
Max knee extension during TSt (deg)	6.9 (1.1)	7.4 (1.3)	6.6 (1.0)
Max knee flexion angle at toe-off (deg)	50.8 (2.8)	50.7 (2.6)	50.7 (3.7)
Max knee flexion angle during swing (deg)	70.8 (0.9)	70.9 (0.9)	69.5 (2.5)
Max Knee ROM between point 2-3 (deg)	43.9 (2.8)	43.3 (2.9)	44.5 (2.7)
Max knee ROM during support (deg)	49.0 (3.0)	48.9 (2.7)	49.5 (2.8)

However, one-way Anova did not show any statistical significance changes for all parameters. All alternative hypotheses appertaining to parameters listed in table 6.46 were therefore not accepted.

6.5.7 Heel curves

Figure 6.9 shows the average knee kinematic data in the sagittal plane for different heel-curved shoes. The alteration caused by the full heel curve test condition resulted in a slight reduction in the time taken for LR. It also increased knee extension within 10-40% of the gait cycle and also subsequently increased knee flexion during push-off and toe-off phases.

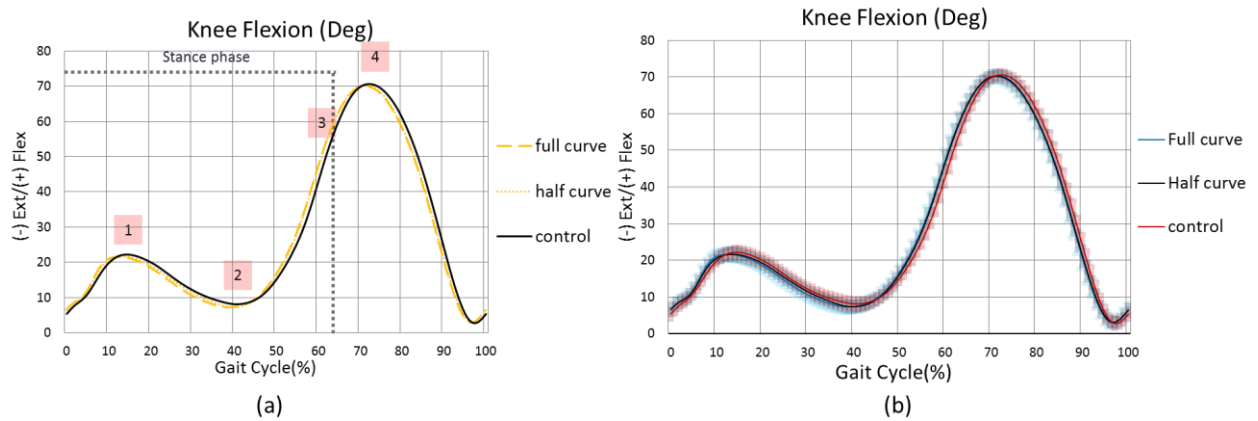


Figure 6.9: Sagittal plane knee motion during the three different level of heel curvature of test conditions where the control shoe has no curve. (a) – without standard deviation (STD), (b) – with the lines shadowed to represent STD ranges.

Table 6.47: Mean (\pm SD) sagittal plane knee motion (degs) for three different heel curves, maximum ROM between point 2-3, and maximum knee ROM during stance phase.

	Full curve	Half curve	control
Knee angle at ICt (deg)	6.6 (1.3)	6.5 (1.5)	5.3 (1.4)
Maximum knee flexion angle during LR (deg)	22.0 (1.6)	21.9 (1.4)	22.4 (1.4)
Max knee extension during TSt (deg)	6.6 (1.3)	6.7 (1.2)	7.4 (1.3)
Max knee flexion angle at toe-off (deg)	54.5 (2.6)	54.1 (2.5)	50.7 (2.6)
Max knee flexion angle during swing (deg)	70.4 (1.3)	70.6 (1.2)	70.9 (0.9)
Max Knee ROM between point 2-3 (deg)	47.9 (3.0)	47.3 (2.6)	43.3 (2.9)
Max knee ROM during support (deg)	52.7 (3.1)	52.1(2.4)	48.9 (2.7)

6.5.7.1 The knee kinematics during IC

The full heel curve footwear placed the knee into a more flexion position by 1.3 degrees when compared to the control shoe ($p=0.049$) at initial contact phase.

Table 6.48 Pairwise statistical significance comparisons between curved heel conditions and knee angle at ICt.

Cond.	Cond.	Mean Difference	Std. Error	Sig.	95% Confidence Interval for Difference	
					Lower Bound	Upper Bound
Full curve	Half curve	0.023	0.463	1.000	-1.235	1.282
	No curve	1.221*	0.448	0.049	0.003	2.439
Half curve	Full curve	-0.023	0.463	1.000	-1.282	1.235
	No curve	1.198	0.564	0.156	-0.334	2.729

6.5.7.2 Knee range of motion

Heel curves demonstrated a significant increase in knee ROM between points 2 -3 when compared to the control shoe ($p < 0.001$) as shown in the table 6.49.

Table 6.49: Pairwise statistical significance comparisons between shoe conditions and maximum knee ROM angle between point 2 and 3 of the gait cycle (N=15).

Cond.	Cond.	Mean Difference	Std. Error	Sig.	95% Confidence Interval for Difference	
					Lower Bound	Upper Bound
Full curve	Half curve	0.577	0.732	1.000	-1.412	2.565
	No curve	4.570*	0.646	0.000	2.814	6.326
Half curve	Full curve	-0.577	0.732	1.000	-2.565	1.412
	No curve	3.993*	0.878	0.001	1.608	6.379

Similar results for maximum knee ROM angle during stance phase were demonstrated where curved heel profiles significantly increased maximum knee ROM ($p < 0.05$) as show in the table below.

Table 6.50: Pairwise statistical significance comparisons between shoe conditions and maximum knee ROM angle during stance phase (n=15).

Cond.	Cond.	Mean Difference	Std. Error	Sig.	95% Confidence Interval for Difference	
					Lower Bound	Upper Bound
Full curve	Half curve	0.553	0.554	1.000	-0.952	2.059
	No curve	3.834*	0.606	0.000	2.187	5.481
Half curve	Full curve	-0.553	0.554	1.000	-2.059	0.952
	No curve	3.281*	0.813	0.004	1.072	5.489

6.5.7.3 Summary knee kinematics for different heel curves:

- The curvature of the heel (both shoes) resulted in an increase in maximum ROM during point 2-3 and stance phase to significant level when compared to the shoe without curve;
- The alteration of the heel curve caused in slight reduction in the time taken for LR;
- The curvature of the heel increased knee extension within 10-40% of the gait cycle and then it increased knee flexion during push-off and toe-off phases.

Table 6.51: Alternative hypotheses accepted/not accepted for different heel curves.

	Full curve	Half curve	control
Maximum knee flexion angle during LR (Ha1h)	Not accepted	Not accepted	control
Max knee extension during stance (Ha1i)	Not accepted	Not accepted	control
Max knee flexion angle at toe-off (Ha1j)	Not accepted	Not accepted	control
Max knee flexion angle during swing (Ha1k)	Not accepted	Not accepted	control
Max Knee ROM between point 2-3 (Ha1l)	accepted	accepted	control
Max knee ROM during support (Ha1m)	accepted	accepted	control
Knee flexion angle at ICt (Ha1n)	accepted	Not accepted	control

6.5.8 Rocker profile stiffness at the metatarsal area

Figure 6.10 shows the average of the knee kinematics in the sagittal plane for different rocker profiles stiffness at metatarsal area. It shows that flexible and mid-flexible shoes reduced maximum knee flexion during LR and increased maximum extension during terminal stance versus solid (control shoe). It is also noticeable that the flexible sole increased maximum flexion during swing phase versus all the other footwear conditions.

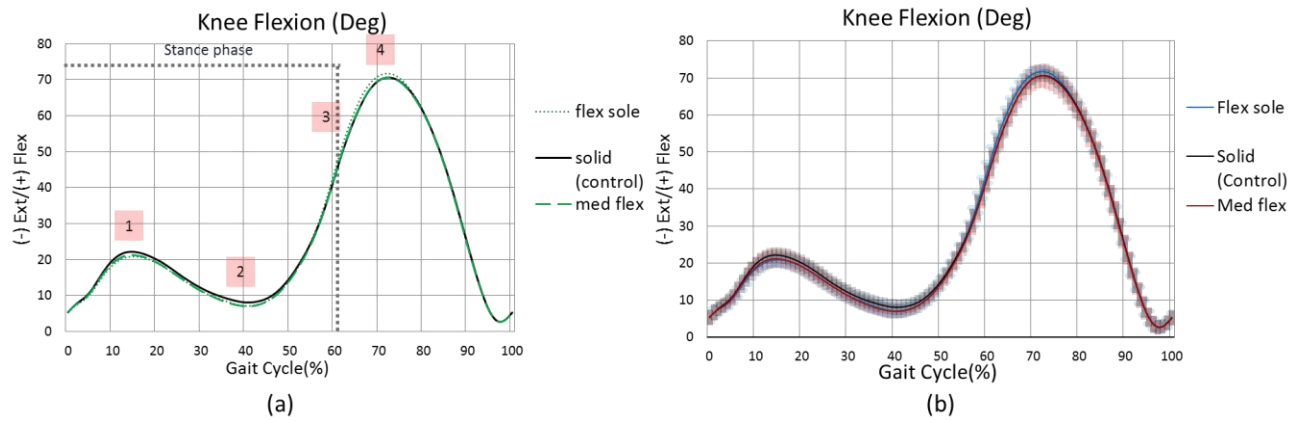


Figure 6.10: Figure 6.6: Sagittal plane knee motion during the three different level of flexibility of the mid-part of the shoe where the control shoe is has solid sole. Legend 1 indicates where maximum knee flexion angle occurred during LR; Legend 2 indicates the point at which maximum knee extension angle occurred during terminal stance phase; legend 3 indicates the point at which maximum knee flexion angle occurred at toe-off; and legend 4 indicates the position where maximum knee flexion angle during swing occurred. (a) – without standard deviation (STD), (b) – with the lines shadowed to represent STD ranges.

Table 6.52: Mean (\pm SD) sagittal plane knee motion (degs) for three different flexibility of the sole, maximum ROM between point 2-3, and maximum knee ROM during stance phase.

	Flex sole	Med. flex	Solid
Knee angle at ICt (deg)	5.4 (1.2)	5.4 (1.3)	5.3 (1.4)
Maximum knee flexion angle during LR (deg)	21.1 (1.3)	21.4 (1.8)	22.4 (1.4)
Max knee extension during TSt (deg)	6.4 (1.4)	6.2 (1.1)	7.4 (1.3)
Max knee flexion angle at toe-off (deg)	52.7 (2.6)	50.9 (3.5)	50.7 (2.6)
Max knee flexion angle during swing (deg)	72.0 (1.0)	70.8 (2.7)	70.9 (0.9)
Max Knee ROM between point 2-3 (deg)	46.3 (3.1)	44.7 (3.7)	43.3 (2.9)
Max knee ROM during support (deg)	51.0 (2.8)	49.3 (3.6)	48.9 (2.7)

6.5.8.1 Maximum knee flexion at toe-off

Max knee flexion angle at toe off did not show any statistical significance between the test conditions, however without Bonferroni adjustment, the flexible sole was significantly more flexed when compared to the stiff sole ($p=0.024$).

6.5.8.2 6.5.8.2 Knee range of motion

The flexible sole significantly increased maximum knee ROM between points 2-3 (table below) when compared to the control shoe.

Table 6.53: Pairwise statistical significance comparisons for max knee ROM between points 2 and 3 between shoe conditions (n=15).

Cond.	Cond.	Mean Difference	Std. Error	Sig.	95% Confidence Interval for Difference	
					Lower Bound	Upper Bound
Flex sole	Med. flex	1.591	0.699	0.117	-0.307	3.490
	Solid	2.948*	1.070	0.047	0.039	5.857
Med. flex	Flex sole	-1.591	0.699	0.117	-3.490	0.307
	Solid	1.356	0.843	0.390	-0.936	3.649

Maximum ROM during stance phase did not show any statistical significance with Bonferroni adjustment. However, with simple pairwise test Anova it showed that the flexible shoe increased maximum knee ROM during stance phase versus solid shoe (p=0.028).

Figure 6.10 shows the average of the knee kinematics in the sagittal plane for different rocker profiles stiffness at the metatarsal area. It shows that the flexible and mid-flexible shoes reduced maximum flexion during LR and increased maximum extension during terminal stance versus the solid (control) shoe. It is also noticeable that the flexible sole increased maximum flexion during swing phase versus all footwear conditions.

6.5.8.3 Summary for knee kinematics:

- The flexible and mid-flexible soled shoes slightly reduced maximum flexion during LR when compared to control and slightly increased maximum extension during terminal stance when compared to the solid soled shoe (control shoe).
- The flexible sole produced significantly increased maximum knee ROM between points 2-3 when compared to control shoe (table 6.54).

Table 6.54: Alternative hypotheses accepted/not accepted for different shoe forepart flexibility.

	Flex sole	Med. flex	Solid
Maximum knee flexion angle during LR (Ha1h)	Not accepted	Not accepted	control
Max knee extension during stance (Ha1i)	Not accepted	Not accepted	control
Max knee flexion angle at toe-off (Ha1j)	Not accepted	Not accepted	control
Max knee flexion angle during swing (Ha1k)	Not accepted	Not accepted	control
Max Knee ROM between point 2-3 (Ha1l)	accepted	Not accepted	control
Max knee ROM during support (Ha1m)	Not accepted	Not accepted	control
Knee flexion angle at ICt (Ha1n)	Not accepted	Not accepted	control

6.6 Hip kinematics

6.6.1 The effect of walking with different heel heights

Figure 6.11 shows the average hip kinematics in the sagittal plane for different heel height footwear conditions acquired during the walking trials. It can be seen that at ICt raised heels reduced hip flexion. During 10-40% of the gait cycle the 1.5 cm heel increased knee extension versus all footwear condition. Maximum extension was increased for raised heels and during toe-off phase raised heel shoes increased hip extension and negative heels increased hip flexion.

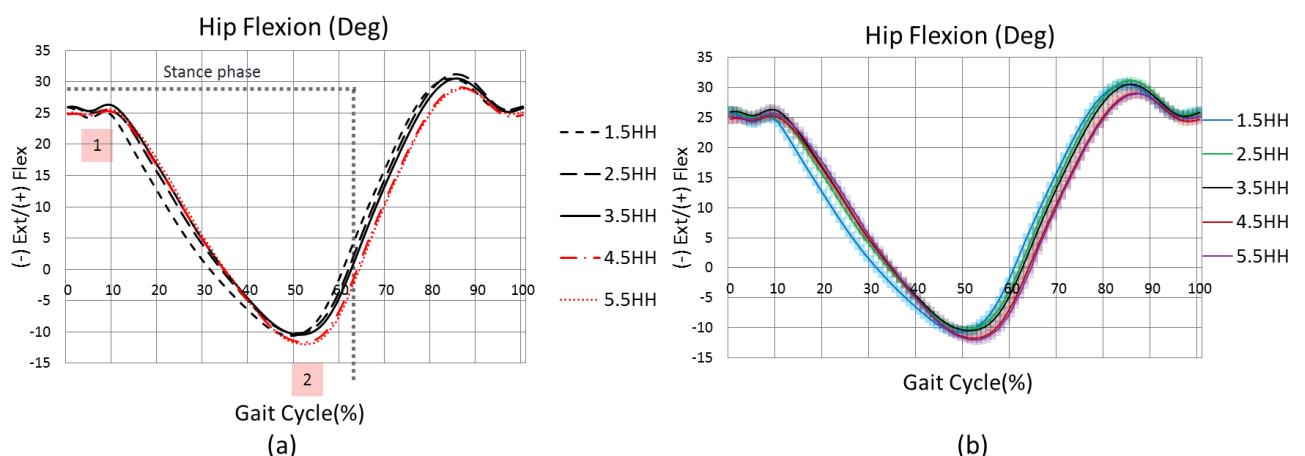


Figure 6.11: Sagittal plane hip motion during the five heel height test conditions where the control shoe is 3.5 HH. Legend 1 indicates maximum flexion and legend 2 indicates maximum hip extension.

6.6.1.1 The hip kinematics during IC

At ICt, the 4.5HH footwear condition reduced hip flexion by 1.1 degree when compared to control. The 4.5HH did not show any significant difference using the Anova test with Bonferroni adjustments, however with the Anova only, the significance was $p=0.011$.

Table 6.55: Mean (\pm SD) sagittal plane hip motion (deg) for five different heel heights, maximum hop ROM during stance and full gait cycle (N=15).

	1.5 HH	2.5 HH	3.5 HH	4.5 HH	5.5 HH
Hip angle at ICt (deg)	25.9 (0.8)	25.9 (0.9)	25.9 (0.9)	24.8 (1.0)	25.0 (1.1)
Max Hip flexion angle during LR (deg)	26.7 (0.8)	26.8 (0.8)	27.2 (0.8)	26.2 (1.1)	26.6 (1.1)
Max Hip extension (deg)	-10.9 (0.9)	-10.5 (0.6)	-10.6 (0.8)	-11.9 (0.8)	-12.2 (0.8)
Max Hip ROM during stance (deg)	37.6 (1.1)	37.2 (0.9)	37.8 (1.0)	38.1 (1.1)	38.7 (1.2)
Max Hip ROM during gait cycle (deg)	42.0 (1.2)	42.0 (0.9)	41.6 (1.0)	41.5 (1.1)	42.0 (1.2)

6.6.1.2 Loading response (LR)

During LR, there were no statistically significant differences in maximum hip flexion values. However, with one-way Anova without Bonferroni correction the 4.5HH shoe showed significant reduction in knee flexion versus the control shoe ($p=0.08$).

6.6.1.3 Max Hip extension

The 5.5HH showed significant increase maximum hip extension when compared to control shoe ($p=0.42$).

6.6.1.4 Max Hip ROM during stance

The 2.5 cm heel height significantly reduced maximum ROM when compared to the 4.5 and 5.5 cm heel raised shoes ($p<0.035$). The 5.5HH shoe increased maximum ROM when compared to control shoe ($p=0.017$) as shown in the table below.

Table 6.56: Pairwise comparisons of shoe conditions for max hip flexion at toe-off.

Cond.	Cond.	Mean Difference	Std. Error	Sig.	95% Confidence Interval for Difference	
					Lower Bound	Upper Bound
1.5HH	2.5HH	.341	.363	1.000	-.868	1.550
	3.5HH	-.257	.345	1.000	-1.403	.889
	4.5HH	-.536	.425	1.000	-1.949	.877
	5.5HH	-1.173	.415	.135	-2.555	.208
2.5HH	1.5HH	-.341	.363	1.000	-1.550	.868
	3.5HH	-.598	.340	1.000	-1.729	.533
	4.5HH	-.878*	.250	.034	-1.708	-.047
	5.5HH	-1.514*	.347	.007	-2.670	-.359
3.5HH	1.5HH	.257	.345	1.000	-.889	1.403
	2.5HH	.598	.340	1.000	-.533	1.729
	4.5HH	-.279	.226	1.000	-1.030	.471
	5.5HH	-.916*	.236	.017	-1.701	-.132
4.5HH	1.5HH	.536	.425	1.000	-.877	1.949
	2.5HH	.878*	.250	.034	.047	1.708
	3.5HH	.279	.226	1.000	-.471	1.030
	5.5HH	-.637	.274	.358	-1.549	.275

6.6.1.5 Max Hip ROM during gait cycle

There were no significant changes in maximum hip ROM during the full gait cycle.

6.6.1.6 Summary – sagittal plane hip joint angle for different heel heights.

- The 5.5HH shoe increase max ROM during stance phase when compared to control shoe ($p=0.017$).

Table 6.57: Alternative hypotheses accepted/not accepted for different shoe heights.

	1.5 HH	2.5 HH	3.5 HH	4.5 HH	5.5 HH
Hip angle at ICt (<i>Halo</i>)	Not accepted	Not accepted	control	Not accepted	Not accepted
Maximum Hip flexion angle during LR (<i>Halp</i>)	Not accepted	Not accepted	control	Not accepted	Not accepted
Max Hip extension (<i>Halq</i>)	Not accepted	Not accepted	control	Not accepted	accepted
Max Hip ROM during stance (<i>Halr</i>)	Not accepted	Not accepted	control	Not accepted	accepted
Max Hip ROM during gait cycle (<i>Hals</i>)	Not accepted	Not accepted	control	Not accepted	Not accepted
Maximum hip flexion at TO (<i>Halt</i>)	Not accepted	Not accepted	control	Not accepted	Not accepted

6.6.2 The effect of altering rocker sole apex position (AP)

Figure 6.12 shows the average of the hip kinematics in the sagittal plane for different apex length shoes. There was slight increase in knee flexion for the 55AP shoe during maximum extension when compared to the 70AP test condition. However, there were no statistically significant differences noted.

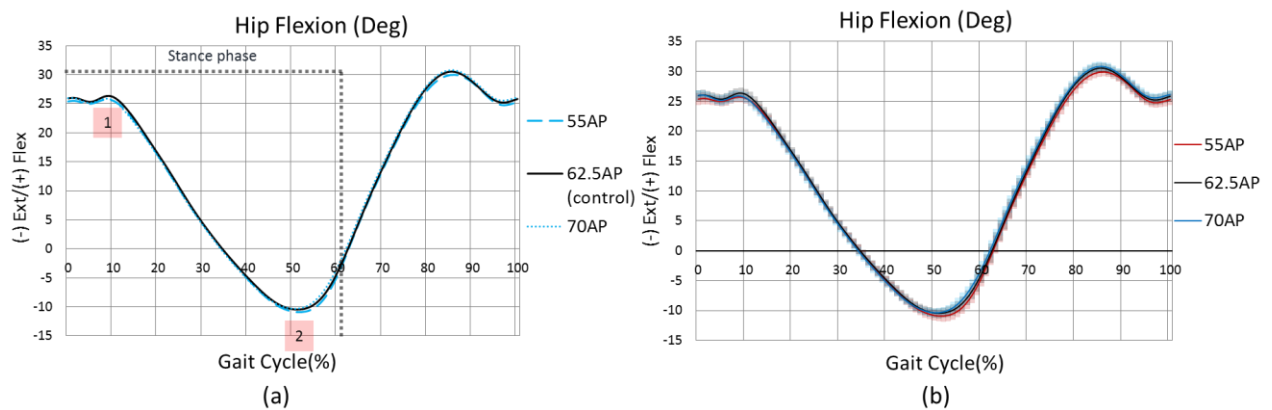


Figure 6.12: Sagittal plane hip motion during the three apex length footwear test conditions where the control shoe is 62.5AP. Legend 1 indicates maximum flexion and legend 2 indicates maximum hip extension. (a) – without standard deviation (STD), (b) – with the lines shadowed to represent STD ranges.

Table 6.58: Mean (\pm SD) sagittal plane hip motion (deg.) for three different apex position, maximum hop ROM during stance and full gait cycle (N=15).

	55AP	62.5AP	70AP
Hip angle at ICt (deg)	25.4 (1.0)	25.9 (0.9)	26.0 (0.8)
Maximum Hip flexion angle during LR (deg)	26.8 (0.9)	27.2 (0.8)	27.0 (0.9)
Max Hip extension (deg)	-11.1 (1.0)	-10.6 (0.8)	-10.6 (0.7)
Max Hip ROM during stance (deg)	37.9 (1.2)	37.8 (1.0)	37.6 (1.1)
Max Hip ROM during gait cycle (deg)	41.8 (1.1)	41.6 (1.0)	41.8 (1.1)

6.6.2.1 Summary hip joint flexion results for different apex position conditions:

- There was a slight increase in knee flexion for the 55AP shoe test condition during maximum extension when compared to the 70AP test condition.

6.6.3 Apex angle (toe angle)

Figure 6.13 shows the average data for hip kinematics in sagittal plane for different apex angle footwear conditions acquired during the walking trials for N=15. Figure 6.15 demonstrates that the 10° toe angle test condition produced a noticeable increase in hip extension during 0-55% of the gait cycle during when compared to the control shoe. During push-off and toe-off phases, the 10°TA increased knee flexion.

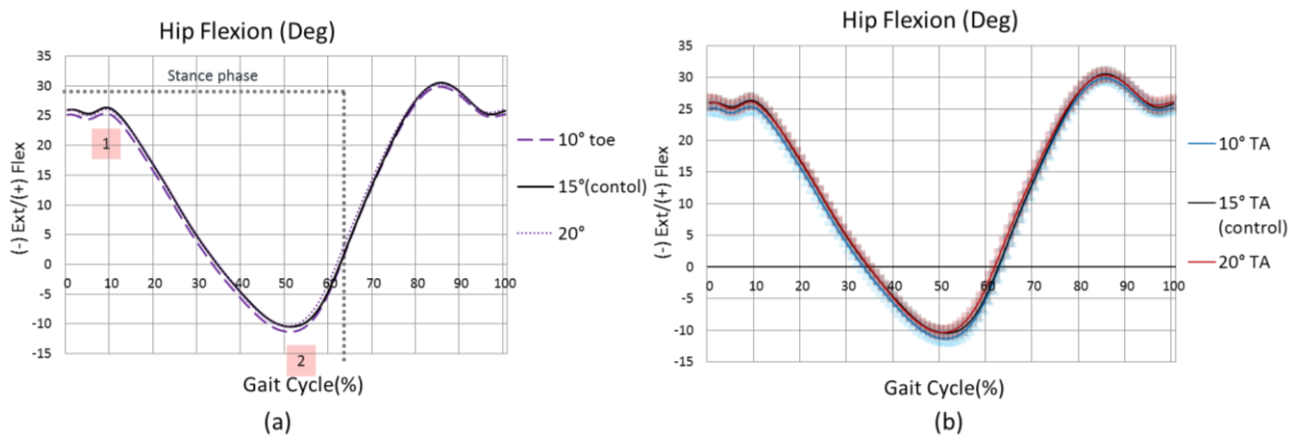


Figure 6.13: Sagittal plane hip motion during the apex toe angle test conditions where the control shoe is 15° TA. Legend 1 indicates maximum flexion and legend 2 indicates maximum hip extension. (a) – without standard deviation (STD), (b) – with the lines shadowed to represent STD ranges.

Table 6.59: Mean (\pm SD) sagittal plane hip motion (deg) for three different toe angle test footwear conditions, maximum hop ROM during stance and full gait cycle (N=15).

	10° TA	15° TA	20° TA
Hip angle at ICt (deg)	25.1 (1.0)	25.9 (0.9)	26.0 (1.0)
Maximum Hip flexion angle during LR (deg)	26.4 (0.9)	27.2 (0.8)	27.2 (0.9)
Max Hip extension (deg)	-11.5 (0.9)	-10.6 (0.8)	-10.5 (1.0)
Max Hip ROM during stance (deg)	37.9 (1.2)	37.8 (1.0)	37.7 (1.3)
Max Hip ROM during gait cycle (deg)	41.9 (1.0)	41.6 (1.0)	41.7 (1.0)

There were no significant differences noted between any of the TA test conditions for the parameters listed in the above table.

6.6.4 Curved heels

Figure 6.14 shows the average hip kinematic data in the sagittal plane for different heel-curved shoe test conditions. The alteration in the test condition with the full heel curve resulted in increased hip flexion during 0-50% of the gait cycle and then slight hip extension during the rest of the gait cycle when compared to the control shoe.

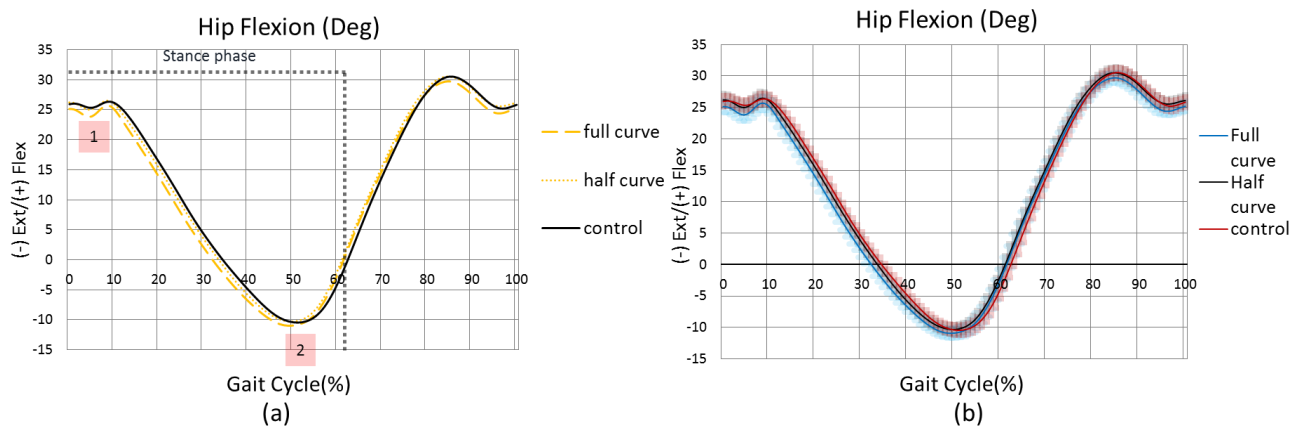


Figure 6.14: Sagittal plane hip motion during the three different level of heel curvature of test conditions where the control shoe has no curve. (a) – without standard deviation (STD), (b) – with the lines shadowed to represent STD ranges.

Table 6.60: Mean (\pm SD) sagittal plane hip motion (degs) for three different heel curves, maximum hop ROM during stance and full gait cycle (N=15).

	Full curve	Half curve	control
Hip angle at ICt (deg)	25.1 (0.9)	26.2 (1.0)	25.9 (0.9)
Maximum Hip flexion angle during LR (deg)	26.5 (1.0)	27.4 (1.0)	27.2 (0.8)
Max Hip extension (deg)	-11.1 (0.7)	-10.5 (0.7)	-10.6 (0.8)
Max Hip ROM during stance (deg)	37.6 (1.4)	38.0 (1.1)	37.8 (1.0)
Max Hip ROM during gait cycle (deg)	41.3 (1.0)	41.7 (1.0)	41.6 (1.0)

Statistical tests did not show any significance for mean values and knee ROM shown in table 6.60.

6.6.4.1 Summary of heel kinematics for different heel curves:

- The alteration in the heel by adding a full curve resulted in increased hip flexion during 0-50% gait cycle and then slight hip extension during the rest gait cycle when compared to control shoe.

6.6.5 Rocker profile stiffness at metatarsal area

Figure 6.15 shows the average of the hip kinematics in the sagittal plane for different rocker profiles stiffnesses at the metatarsal area of the shoes. It shows that flexible shoes and those with medium-flexibility increased hip extension during 0-53% of the gait cycle when compared to the solid (control) shoe. It is also noticeable that the flexible sole increased maximum flexion during swing phase versus all the other footwear conditions. Similar results were demonstrated for the knee flexion data.

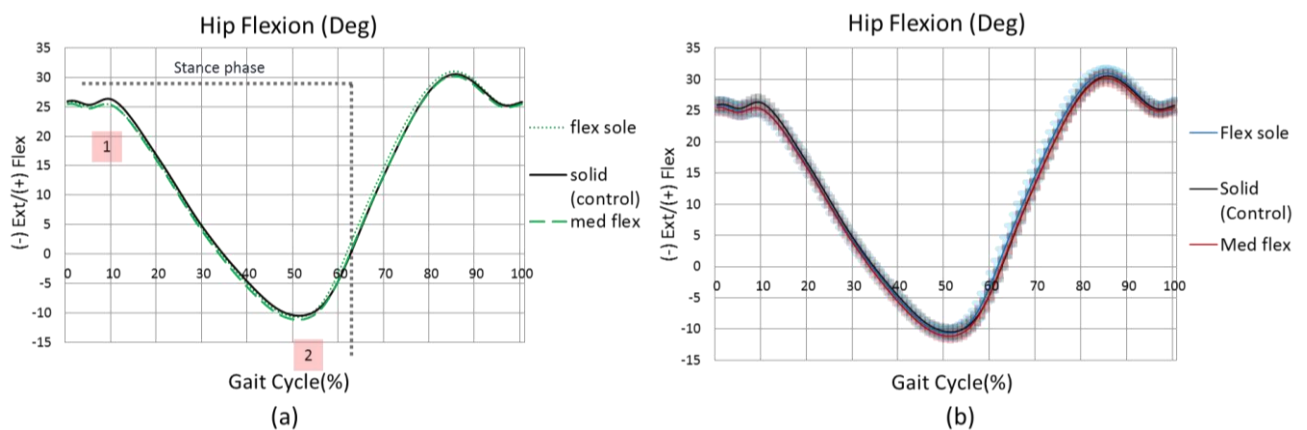


Figure 6.15: Sagittal plane hip motion during the three different level of flexibility of the mid-part of the shoe where the control shoe has no curve (N=15). (a) – without standard deviation (STD), (b) – with the lines shadowed to represent STD ranges.

The results in table 6.61 show that no statistically significant alterations in hip flexion were produced in different footwear forepart flexibility test conditions.

Table 6.61: Mean (\pm SD) sagittal plane hip motion (degs) three different level of flexibility of the mid-part of the shoe, maximum hip ROM during stance and full gait cycle (N=15).

	Flex sole	Med. flex	Solid
Hip angle at ICt (deg)	25.8 (1.0)	25.4 (0.9)	25.9 (0.9)
Maximum Hip flexion angle during LR (deg)	26.7 (1.0)	26.5 (0.9)	27.2 (0.8)
Max Hip extension (deg)	-10.9 (0.9)	-11.3 (0.7)	-10.6 (0.8)
Max Hip ROM during stance (deg)	37.6 (1.3)	37.9 (1.0)	37.8 (1.0)
Max Hip ROM during gait cycle (deg)	42.2 (1.2)	42.1 (1.0)	41.6 (1.0)

6.6.5.1 Summary hip kinematics for different sole flexibilities:

The flexible and medium-flexibility shoes increased hip extension during 0-53% of the gait cycle when compared to the solid (control) shoe. It is also noticeable that the flexible sole increased maximum flexion during swing phase versus all the other footwear conditions.

6.7 Ankle Moments

6.7.1 The effect of heel height alteration

Figure 6.16, illustrates the alteration to external ankle moments induced by the heel height test conditions. It can be seen that the 1.5 cm heel significantly reduced external PF moment and increased the external DF moment between 12-80% of stance phase when compared to all the other footwear test conditions. It resulted in an increase in the overall external DF moment at the ankle joint experienced by the calf muscles. The negative heel profile produced a shorter PF external moment period and premature DF external moment initiation. The opposite effect was seen for raised heels. The 5.5HH increased the overall external PF moment and resulted in a delay of the external DF moment initiation. It also reduced the moment during 25-70% of stance phase as shown in figure 6.16.

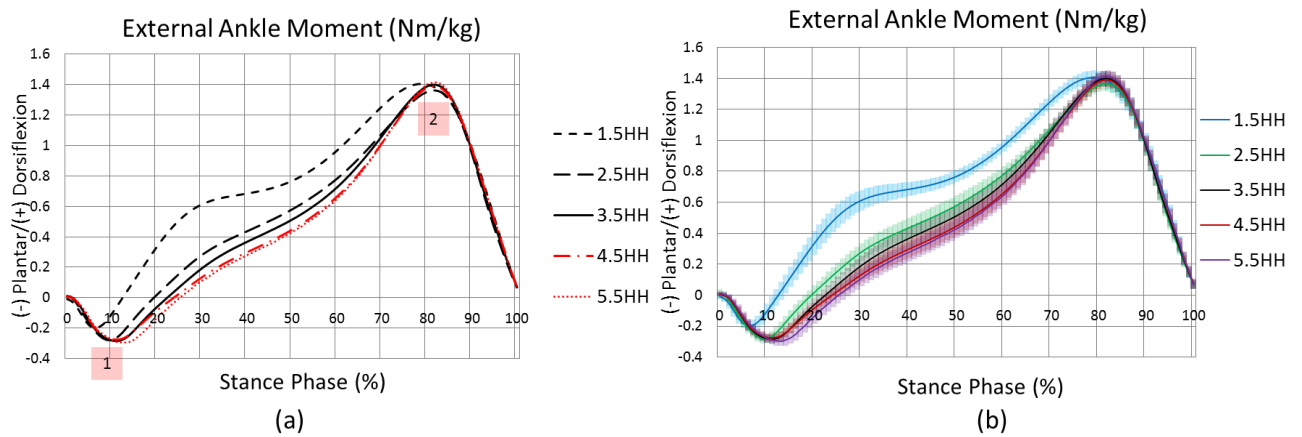


Figure 6.16: Sagittal plane external ankle moment during the five footwear conditions highlighting the 2 area of interest (N=15). Legend 1 indicates maximum ankle plantarflexor moment; legend 2 indicates maximum ankle dorsiflexor moment. (a) – without standard deviation (STD), (b) – with the lines shadowed to represent STD ranges.

The mean results from the figure 6.16 are demonstrated in the table 6.62.

Table 6.62: Mean (\pm SD) sagittal plane ankle moment (Nm/kg) for the five footwear conditions (N=15).

	1.5 HH	2.5 HH	3.5 HH	4.5 HH	5.5 HH
Maximum external ankle plantarflexor moment (Nm/kg)	-0.22 (0.02)	-0.29 (0.03)	-0.30 (0.03)	-0.29 (0.03)	-0.31 (0.03)
Maximum external ankle dorsiflexor moment (Nm/kg)	1.41 (0.05)	1.37 (0.04)	1.41 (0.05)	1.40 (0.05)	1.42 (0.04)

6.7.1.1 Maximum external ankle plantarflexor moment

The 1.5 cm heel demonstrated significant reduction in maximum external ankle moment versus all the other footwear conditions (table 6.63). The 2.5HH did not show any significance versus the 3.5HH and the 4.5HH; however it was significantly reduced when compared to the 5.5 cm heel. The 3.5 cm heel produced a significant increase in the maximum external ankle PF moment when compared to the 1.5 cm heel test condition. The 4.5 and 5.5 cm heels showed significant increase versus 1.5 cm heel raise test condition.

Table 6.63: Pairwise comparison of shoe conditions for mean external ankle PF moment during stance phase.

Cond.	Cond.	Mean Difference	Std. Error	Sig.	95% Confidence Interval for Difference	
					Lower Bound	Upper Bound
1.5HH	2.5HH	.070*	.008	.000	.042	.097
	3.5HH	.074*	.008	.000	.045	.102
	4.5HH	.064*	.009	.000	.034	.094
	5.5HH	.085*	.011	.000	.050	.120
2.5HH	1.5HH	-.070*	.008	.000	-.097	-.042
	3.5HH	.004	.007	1.000	-.020	.028
	4.5HH	-.006	.008	1.000	-.034	.021
	5.5HH	.016	.007	.478	-.008	.039
3.5HH	1.5HH	-.074*	.008	.000	-.102	-.045
	2.5HH	-.004	.007	1.000	-.028	.020
	4.5HH	-.010	.007	1.000	-.033	.013
	5.5HH	.012	.008	1.000	-.015	.039
4.5HH	1.5HH	-.064*	.009	.000	-.094	-.034
	2.5HH	.006	.008	1.000	-.021	.034
	3.5HH	.010	.007	1.000	-.013	.033
	5.5HH	.022	.007	.101	-.003	.046

6.7.1.2 Maximum external ankle dorsiflexor moment

There were no significant results demonstrated for maximum external ankle DF moment except for the 2.5HH test condition which showed a significant reduction when compared to the 5.5 cm heel raised footwear condition ($p=0.027$) as shown in table 6.64.

Table 6.64: Pairwise comparison of shoe conditions for mean external ankle DF moment during stance phase.

Cond.	Cond.	Mean Difference	Std. Error	Sig.	95% Confidence Interval for Difference	
					Lower Bound	Upper Bound
1.5HH	2.5HH	.048	.023	.551	-.029	.124
	3.5HH	.008	.023	1.000	-.070	.086
	4.5HH	.015	.027	1.000	-.077	.107
	5.5HH	-.015	.026	1.000	-.102	.072
2.5HH	1.5HH	-.048	.023	.551	-.124	.029
	3.5HH	-.040	.015	.233	-.092	.012

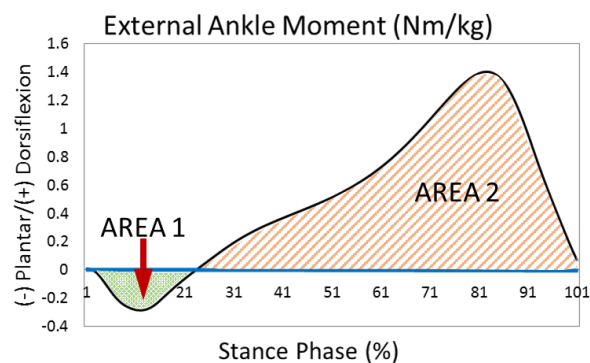
	4.5HH	-0.033	.011	.077	-0.069	.002
	5.5HH	-0.063*	.017	.027	-0.120	-.006
3.5HH	1.5HH	-0.008	.023	1.000	-0.086	.070
	2.5HH	.040	.015	.233	-0.012	.092
	4.5HH	.006	.012	1.000	-0.034	.047
	5.5HH	-.023	.016	1.000	-.077	.031
4.5HH	1.5HH	-.015	.027	1.000	-.107	.077
	2.5HH	.033	.011	.077	-.002	.069
	3.5HH	-.006	.012	1.000	-.047	.034
	5.5HH	-.029	.012	.255	-.069	.010

6.7.1.3 External ankle moment impulse values

The results were converted to be presented as percentage difference and the control shoe was therefore considered to be a baseline shoe; meaning its value was 100%. The results were divided into area 1 – the area under the curve for external ankle PF moment, and area 2 – the area under the curve for external ankle DF moment as shown in table 6.65.

Table 6.65: The average of the area under the curves for the footwear test conditions.

	1.5 HH	2.5 HH	3.5 HH	4.5 HH	5.5 HH
Area 1 (%)	42.2 (8.0)	82.3 (13.7)	100.0 (14.3)	103.3 (16.3)	119.4 (20.8)
Differences between control shoe (%)	-57.8	-17.7	0.0	3.3	19.4
Area 2 (%)	128.0 (3.8)	104.7 (5.5)	100.0 (5.9)	95.1 (5.4)	95.4 (5.1)
Differences between control shoe (%)	28.0	4.7	0.0	-4.9	-4.6



6.7.1.4 Area 1 (External PF ankle moment)

For the heel height test conditions (1.5HH to the 5.5HH), a significant gradual significant increase of external ankle PF moment area under the curve was demonstrated as shown in table 6.66 and table 6.67. These results clearly demonstrate that the overall work done by the internal DF muscles to rotate the ankle joint was significantly increased with raising heel heights. For example, the 1.5HH reduced the overall area 1 by 57.8%, the 2.5HH shoe by -17.7% when compared to control shoe. The 5.5HH increased this parameter by 19.4% versus the control shoe.

Table 6.66: Pairwise comparison of shoe conditions for mean values of area 1.

Cond.	Cond.	Mean Difference	Std. Error	Sig.	95% Confidence Interval for Difference	
					Lower Bound	Upper Bound
1.5HH	2.5HH	-40.089*	3.439	.000	-51.527	-28.650
	3.5HH	-57.771*	3.719	.000	-70.141	-45.401
	4.5HH	-61.038*	4.906	.000	-77.353	-44.723
	5.5HH	-77.213*	7.556	.000	-102.343	-52.083
2.5HH	1.5HH	40.089*	3.439	.000	28.650	51.527
	3.5HH	-17.682*	2.999	.000	-27.658	-7.707
	4.5HH	-20.949*	3.280	.000	-31.858	-10.041
	5.5HH	-37.125*	6.360	.000	-58.276	-15.973
3.5HH	1.5HH	57.771*	3.719	.000	45.401	70.141
	2.5HH	17.682*	2.999	.000	7.707	27.658
	4.5HH	-3.267	4.302	1.000	-17.574	11.041
	5.5HH	-19.442	6.589	.105	-41.357	2.472
4.5HH	1.5HH	61.038*	4.906	.000	44.723	77.353
	2.5HH	20.949*	3.280	.000	10.041	31.858
	3.5HH	3.267	4.302	1.000	-11.041	17.574
	5.5HH	-16.175	6.031	.179	-36.233	3.883

6.7.1.5 Area 2 (External DF ankle moment)

A significant reduction in area 1 for the 1.5HH was demonstrated, but at the same time a significant increase in area 2 was noted (+28%) when compared to the control shoe and was significantly increased compared to all the other footwear test conditions. The 2.5HH value for area 2 was significantly increased when compared to the 1.5HH test condition, but significantly reduced when compared to the 4.5 and 5.5 cm heel height shoes. The 3.5 cm

heel (control shoe) demonstrated a significant increase in area 2 versus the 1.5 cm heel height shoe.

Table 6.67: Pairwise comparison of shoe conditions for mean values of area 2.

Cond.	Cond.	Mean Difference	Std. Error	Sig.	95% Confidence Interval for Difference	
					Lower Bound	Upper Bound
1.5HH	2.5HH	23.316*	3.034	.000	13.224	33.408
	3.5HH	28.030*	3.669	.000	15.828	40.233
	4.5HH	32.883*	3.620	.000	20.842	44.924
	5.5HH	32.628*	4.128	.000	18.901	46.355
2.5HH	1.5HH	-23.316*	3.034	.000	-33.408	-13.224
	3.5HH	4.714	1.900	.264	-1.606	11.034
	4.5HH	9.567*	1.361	.000	5.040	14.094
	5.5HH	9.311*	2.254	.010	1.815	16.808
3.5HH	1.5HH	-28.030*	3.669	.000	-40.233	-15.828
	2.5HH	-4.714	1.900	.264	-11.034	1.606
	4.5HH	4.853	1.594	.088	-.450	10.155
	5.5HH	4.597	2.228	.581	-2.811	12.006
4.5HH	1.5HH	-32.883*	3.620	.000	-44.924	-20.842
	2.5HH	-9.567*	1.361	.000	-14.094	-5.040
	3.5HH	-4.853	1.594	.088	-10.155	.450
	5.5HH	-.255	1.443	1.000	-5.054	4.543

6.7.1.6 Summary for heel height:

- The low heel profiles demonstrated reductions in maximum external PF ankle moment when compared with higher heel profiles and the opposite effect was seen for high heeled shoes;
- The 2.5 cm heel produced a significant a reduction in the maximum external DF ankle moment when compared with the 5.5 cm heel test condition;
- From 1.5HH to the 5.5HH test conditions, a significant gradual increase of external ankle PF moment area under the curve was demonstrated which indicated that the internal DF muscles (tibialis anterior and others) worked less hard to generate the moment. The (H₀) hypothesis is therefore accepted;

- Negative heel profiles significantly increased the overall area under the curve for the external DF ankle moment (area 2) when compared to all higher heeled test conditions. The (Hal) hypothesis is accepted;
- The 4.5HH and 5.5HH did not produce any significant changes when compared to control shoe but a significant reduction in area 2 versus the 1.5 and 2.5 cm heel height footwear conditions was demonstrated. The (Hal) hypothesis is rejected.

6.7.2 The effect of altering rocker sole apex position (AP)

Figure 6.17, illustrates the alteration to external ankle moments induced by the shoe apex length (position) footwear test conditions. A noticeable change was noted in increased maximum external DF ankle moment for the 70% apex length shoe test condition and a reduction of 55% was seen when compared to the control shoe for the 55AP test condition. .

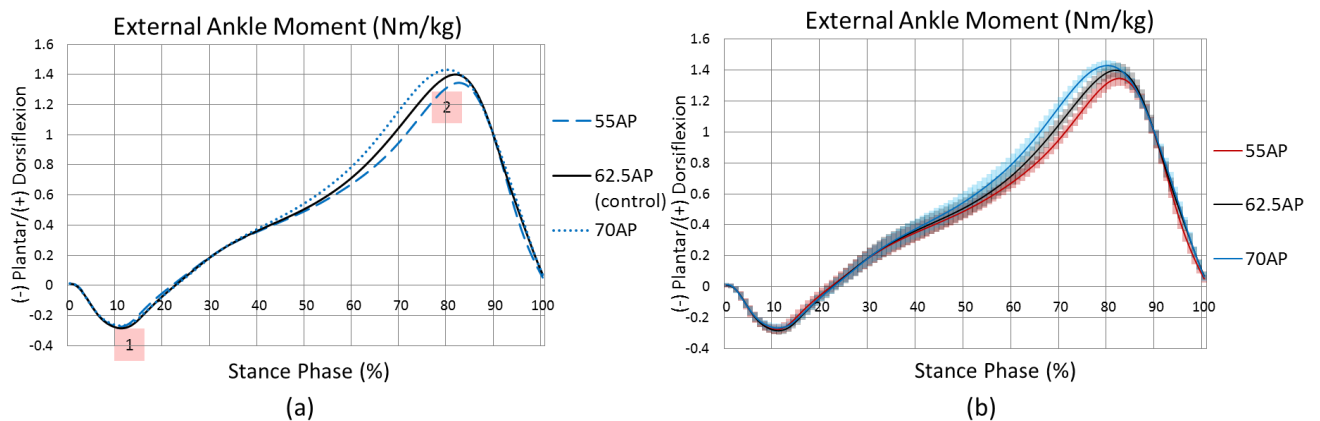


Figure 6.17: Sagittal plane external ankle moment during the three footwear conditions highlighting the 2 area of interest (N=15). Legend 1 indicates maximum ankle plantarflexor moment; legend 2 indicates maximum ankle dorsiflexor moment. (a) – without standard deviation (STD), (b) – with the lines shadowed to represent STD ranges.

Table 6.68: Mean (\pm SD) sagittal plane ankle moment (Nm/kg) for the three footwear conditions (N=15).

	55AP	62.5AP	70AP
Maximum ankle external plantarflexor moment (Nm/kg)	-0.29 (0.03)	-0.30 (0.03)	-0.28 (0.03)
Maximum ankle external dorsiflexor moment (Nm/kg)	1.35 (0.05)	1.41 (0.05)	1.44 (0.03)

6.7.2.1 Maximum external ankle plantarflexor moment

The 70% apex length showed a significant maximum external ankle PF moment reduction when compared to the control shoe (p=0.048) as shown in the table below.

Table 6.69: Pairwise comparison of shoe conditions for mean external ankle PF moment during stance phase.

Cond.	Cond.	Mean Difference	Std. Error	Sig. ^b	95% Confidence Interval for Difference ^b	
					Lower Bound	Upper Bound
55AP	62.5AP	.011	.006	.192	-.004	.026
	70 AP	-.005	.006	1.000	-.023	.012
62.5AP	55AP	-.011	.006	.192	-.026	.004
	70 AP	-.016*	.006	.048	-.032	.000
70 AP	55AP	.005	.006	1.000	-.012	.023
	62.5AP	.016*	.006	.048	.000	.032

Based on estimated marginal means

*. The mean difference is significant at the .05 level.

b. Adjustment for multiple comparisons: Bonferroni.

6.7.2.2 Maximum external ankle dorsiflexor moment

The 55% apex length shoe (55AP) demonstrated a significant mean ankle DF moment reduction when compared to the control (p=0.04) and 70AP test conditions (p=0.008) as shown in table 6.70. There was no significant maximum external ankle dorsiflexor moment increase produced by the 70AP test condition when compared to control, however it was significantly higher versus the 55AP shoe test condition.

Table 6.70: Pairwise comparison of shoe conditions for mean external ankle DF moment during stance phase.

Cond.	Cond.	Mean Difference	Std. Error	Sig.	95% Confidence Interval for Difference	
					Lower Bound	Upper Bound
55AP	62.5AP	-.058*	.014	.004	-.097	-.018
	70 AP	-.091*	.025	.008	-.159	-.023
62.5AP	55AP	.058*	.014	.004	.018	.097
	70 AP	-.033	.019	.303	-.084	.018

6.7.2.3 External ankle moment impulse (overall area of the moment curve)

Table 6.71 shows the results of the overall area of the moment curves for different apex position footwear conditions. The results for area 1 which are shown in table 6.71, represents the area under the curve representing the external ankle PF moment, and area 2 is the area under the curve for the external ankle DF moment.

Table 6.71: The average of the area under the curves (external ankle moments) for the footwear test conditions (N=15).

	55AP	62.5AP	70AP
Area 1 (%)	94.1 (16.3)	100.0 (14.3)	96.5 (12.3)
Differences between control shoe (%)	-5.9	0.0	-3.5
Area 2 (%)	94.3 (5.4)	100.0 (5.9)	106.4 (5.1)
Differences between control shoe (%)	-5.7	0.0	6.4

6.7.2.4 Area 1 (External ankle PF moment)

The apex length (position) alteration for the test conditions did not show any significant difference for external ankle PF moment impulse value (area 1).

6.7.2.5 Area 2 (External ankle DF moment)

There were significant changes in the overall external ankle DF moment curve for all the footwear test conditions. It shows that the 55AP test condition significantly reduced the area of the moment curve when compared to the control shoe (p=0.016). The 70AP footwear test condition significantly increased the value calculated for area 2 versus the control shoe (p=0.007) and the 55AP test condition significantly reduced it when compared to the control shoe (p<0.001) as shown in the table below.

Table 6.72: Pairwise comparison of the average of the area under the curves (external ankle DF moment) for test footwear conditions (N=15).

Cond.	Cond.	Mean Difference	Std. Error	Sig.	95% Confidence Interval for Difference	
					Lower Bound	Upper Bound
55AP	62.5AP	-5.655*	1.713	.016	-10.312	-.998
	70 AP	-12.069*	1.618	.000	-16.465	-7.672
62.5AP	55AP	5.655*	1.713	.016	.998	10.312
	70 AP	-6.414*	1.725	.007	-11.103	-1.724

6.7.2.6 Summary for apex length position:

- The 70% apex length position produced significant maximum external ankle PF moment reduction when compared to the control shoe ($p=0.048$). The (H₀) hypothesis is accepted;
- The 55% apex length shoe demonstrated a significant mean ankle DF moment reduction when compared to the control shoe ($p=0.04$), and reduction when compared with 70AP ($p=0.008$). The (H₀) hypothesis is accepted;
- The 55% apex length shoe demonstrated a significant reduction for the area under curve 2 when compared to the control test condition. This meant that the triceps surae group of muscles would have had to work less to produce the ankle moment. The (H₀) hypothesis is accepted;
- The 70% apex length shoe significantly increased the external ankle DF moment impulse (area 2) compared to the control and 55AP shoes, which means that there would have been more total muscle force required for the triceps surae to produce the internal PF moment. The (H₀) hypothesis is accepted.

6.7.3 Apex angle (toe angle-TA)

Figure 6.18, illustrates the alteration to external ankle moments induced by the shoe apex toe angle. The 20° toe angle demonstrated a visible reduction of maximum external ankle DF moment when compared to the control and 10° toe angle test conditions.

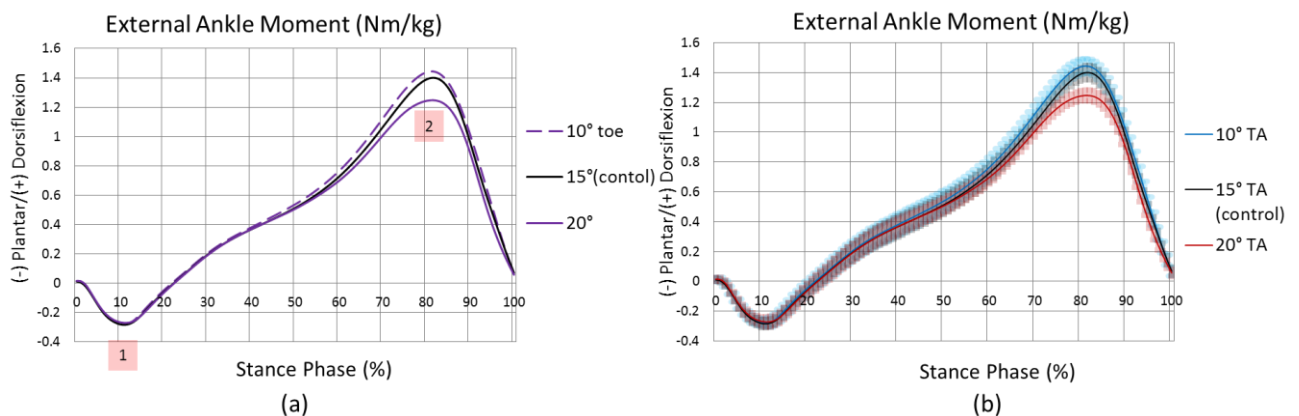


Figure 6.18: Sagittal plane external ankle moment during the three footwear conditions highlighting the two area of interest (N=15). Legend 1 indicates maximum ankle

plantarflexor moment; legend 2 indicates maximum ankle dorsiflexor moment. (a) – without standard deviation (STD), (b) – with the lines shadowed to represent STD ranges.

The results for mean external moments values are demonstrated in the table below.

Table 6.73: Mean (\pm SD) sagittal plane ankle moment (Nm/kg) for the three footwear conditions (N=15).

	10° TA	15° TA	20° TA
Maximum ankle external plantarflexor moment (Nm/kg)	-0.29 (0.03)	-0.30 (0.03)	-0.28 (0.03)
Maximum ankle external dorsiflexor moment (Nm/kg)	1.45 (0.05)	1.41 (0.05)	1.26 (0.04)

6.7.3.1 Maximum external ankle plantarflexor moment

There were no significant alterations for maximum external ankle PF moment demonstrated for different toe angle footwear test conditions. The (H_0) hypothesis is rejected.

6.7.3.2 Maximum external ankle dorsiflexor moment

The 15° toe angle (control shoe) demonstrated significant decrease in mean external ankle DF moment when compared to the 10 ° toe angle ($p=0.009$) and a significant increase when compared to the 20° toe angle test condition ($p<0.001$), as shown in table 6.74.

Table 6.74: Pairwise comparison of shoe conditions for mean external ankle DF moment during stance phase.

Cond.	Cond.	Mean Difference	Std. Error	Sig.	95% Confidence Interval for Difference	
					Lower Bound	Upper Bound
10° TA	15° TA	.044*	.012	.009	.011	.077
	20° TA	.194*	.021	.000	.138	.250
15° TA	10° TA	-.044*	.012	.009	-.077	-.011
	20° TA	.150*	.021	.000	.092	.208

6.7.3.3 External ankle moment impulse (overall area of the moment curve)

Table 6.75 demonstrates the mean results of the overall area of the moment curves for different toe angle footwear test conditions. Area 1 represents the area under the curve for the external ankle PF moment. Area 2 is the area under the curve for the external ankle DF

moment. Table 6.75 below indicates that the 10° TA test condition increased area 2 value (DF moment) by 5.4% and the 20° TA decreased this parameter by 7.5% when compared to the control shoe.

Table 6.75: The average of the area under the curves (external ankle moments) for test footwear conditions (N=15).

	10° TA	15° TA	20° TA
Area 1 (%)	97.1 (16.1)	100.0 (14.3)	101.3 (17.7)
Differences between control shoe (%)	-2.9	0.0	1.3
Area 2 (%)	105.4 (5.4)	100.0 (5.9)	92.5 (4.1)
Differences between control shoe (%)	5.4	0.0	-7.5

6.7.3.4 Area 1 (External ankle PF moment)

Alteration to the sole apex toe angle did not produce any significant differences for external ankle PF moment impulse values (area 1).

6.7.3.5 Area 2 (External ankle DF moment)

There were significant changes in the overall external ankle DF moment curve for all footwear conditions. The 10° toe angle footwear test condition significantly increased area 2 versus the control shoe ($p=0.002$), but the 20° toe angle significantly reduced this parameter when compared to control ($p=0.026$) as shown in table 6.76.

Table 6.76: Pairwise comparison of the average of the area under the curves (external ankle DF moment) for test footwear conditions (N=15).

Cond.	Cond.	Mean Difference	Std. Error	Sig.	95% Confidence Interval for Difference	
					Lower Bound	Upper Bound
10° TA	15° TA	5.359*	1.219	.002	2.047	8.671
	20° TA	12.880*	2.545	.001	5.964	19.795
15° TA	10° TA	-5.359*	1.219	.002	-8.671	-2.047
	20° TA	7.521*	2.467	.026	.816	14.226

6.7.3.6 Summary for toe apex length (position):

- The 15° toe angle (control shoe) demonstrated a significant decrease in mean external ankle DF moment value when compared to the 10° toe angle test condition ($p=0.009$), and a significant increase when compared to the 20° toe angle ($p<0.001$). The (H_{a1}) hypothesis is accepted;
- The 10° toe angle footwear test condition significantly increased the value of area 2 versus the control shoe ($p=0.002$) and the 20° toe angle significantly reduced it when compared to control ($p=0.026$). The (H_{a1}) hypothesis is accepted.

6.7.4 Heel curves

Figure 6.19, shows the alteration to external ankle moments induced by the shoe heel curve test conditions. It is noticeable that curved heels reduced the external ankle PF moments and increased DF moments between 0-75% of stance phase. There was also a visible reduction in the maximum mean external DF moment for curved heel test conditions.

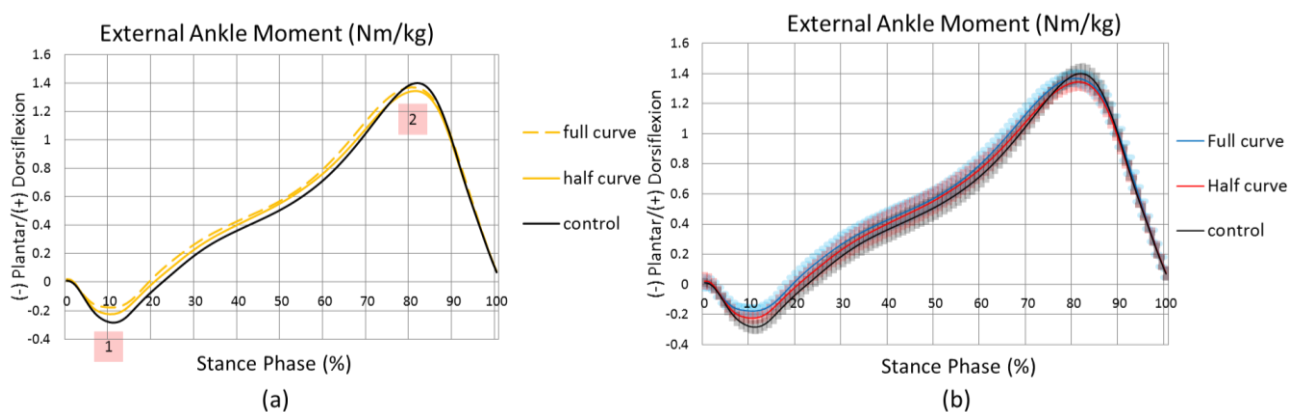


Figure 6.19: Sagittal plane external ankle moment during the three footwear conditions highlighting the 2 area of interest ($N=15$). Legend 1 indicates maximum ankle plantarflexor moment; legend 2 indicates maximum ankle dorsiflexor moment. (a) – without standard deviation (STD), (b) – with the lines shadowed to represent STD ranges.

The results for mean external moment values are demonstrated in table 6.77.

Table 6.77: Mean (\pm SD) sagittal plane ankle moment (Nm/kg) for the three footwear conditions (N=15).

	Full curve	Half curve	control
Maximum ankle external plantarflexor moment (Nm/kg)	-0.19 (0.02)	-0.23 (0.02)	-0.30 (0.03)
Maximum ankle external dorsiflexor moment (Nm/kg)	1.37 (0.04)	1.35 (0.04)	1.41 (0.05)

6.7.4.1 Maximum external ankle plantarflexor moment

There were significant PF moment reductions for curved heels when compared to the control test condition ($p < 0.001$). The full curve shoe showed a significant PF moment reduction when compared to the half curve test condition as shown in table 6.78.

Table 6.78: Pairwise comparison of shoe conditions for mean external ankle PF moment during stance phase.

Cond.	Cond.	Mean Difference	Std. Error	Sig.	95% Confidence Interval for Difference	
					Lower Bound	Upper Bound
Full curve	Half curve	.041*	.004	.000	.029	.052
	No curve	.104*	.005	.000	.089	.118
Half curve	Full curve	-.041*	.004	.000	-.052	-.029
	No curve	.063*	.005	.000	.049	.077

6.7.4.2 Maximum external ankle dorsiflexor moment

The half curve shoe demonstrated a significant mean DF moment reduction when compared to the control shoe ($p = 0.04$) as shown in table 6.79.

Table 6.79: Pairwise comparison of shoe conditions for mean external ankle DF moment during stance phase.

Cond.	Cond.	Mean Difference	Std. Error	Sig.	95% Confidence Interval for Difference	
					Lower Bound	Upper Bound
Full curve	Half curve	.024	.012	.190	-.008	.056
	No curve	-.032	.017	.261	-.078	.015
Half curve	Full curve	-.024	.012	.190	-.056	.008
	No curve	-.055*	.014	.004	-.093	-.018

6.7.4.3 External ankle moment impulse (overall area of the moment curve)

The full curved heel shoe test condition reduced the PF moment curve area by 40.2% when compared to control shoe. The half curve reduced the PF moment curve area 1 by 25.6% versus the control shoe as shown in table 6.80.

The full curve increased the DF moment area 2 by 6% when compared to the control shoe.

Table 6.80: The average value of the area under the curves (external ankle moments) for test footwear conditions (N=15).

	Full curve	Half curve	control
Area 1 (%)	59.8 (11.0)	74.4 (13.1)	100.0 (14.3)
Differences between control shoe (%)	-40.2	-25.6	0.0
Area 2 (%)	106.0 (5.3)	100.6 (5.8)	100.0 (5.9)
Differences between control shoe (%)	6.0	0.6	0.0

6.7.4.4 Area 1 (External ankle PF moment)

The full and half curved heel shoes demonstrated a significant reduction in area 1 when compared to the control shoe and half curve as shown in the table below.

Table 6.81: Pairwise comparison of the average of the area under the curves (external ankle PF moment) for test footwear conditions (N=15).

Cond.	Cond.	Mean Difference	Std. Error	Sig.	95% Confidence Interval for Difference	
					Lower Bound	Upper Bound
Full curve	Half curve	-14.697*	2.692	.000	-22.013	-7.382
	No curve	-40.249*	1.806	.000	-45.158	-35.340
Half curve	Full curve	14.697*	2.692	.000	7.382	22.013
	No curve	-25.552*	2.319	.000	-31.853	-19.250

6.7.4.5 Area 2 (External ankle DF moment)

There was a significant change in overall external ankle DF moment area curve for the full curve shoe versus control and the half curve shoe ($p < 0.013$) as shown in the table below.

Table 6.82: Pairwise comparison of the average of the area under the curves (external ankle DF moment) for test footwear conditions (N=15).

Cond.	Cond.	Mean Difference	Std. Error	Sig.	95% Confidence Interval for Difference	
					Lower Bound	Upper Bound
Full curve	Half curve	5.353*	1.553	.012	1.133	9.573
	No curve	5.979*	1.302	.001	2.441	9.518
Half curve	Full curve	-5.353*	1.553	.012	-9.573	-1.133
	No curve	.626	1.465	1.000	-3.356	4.609

6.7.4.6 Summary of ankle moment alterations produced by curved heel test conditions

- Both curved heel test conditions reduced the mean external ankle PF moment when compared to control. This also resulted in a reduction of the overall area of PF moment when compared to control and therefore the muscle work by DF muscles were theoretically reduced to produce the ankle joint moment. The (Hal) hypothesis is accepted;
- The heel curvature reduced the maximum external ankle DF moment. However, the curved heel reduced LR time and would have induced premature activation of PF muscles. It resulted in an increased overall external ankle DF moment area for the full curve shoe and therefore also the overall calf muscle force applied to produce the moment and a possible increase in oxygen consumption.

6.7.5 Rocker profile stiffness at metatarsal area

Figure 6.20 shows the alteration to external ankle moment induced by the shoe flexibility level. From the figure below, there was a slight noticeable change during PF moment where the overall area and mean values are visually reduced. There was however, no significant change during late stance except for during late push off phase where the flexible sole reduced the DF moment.

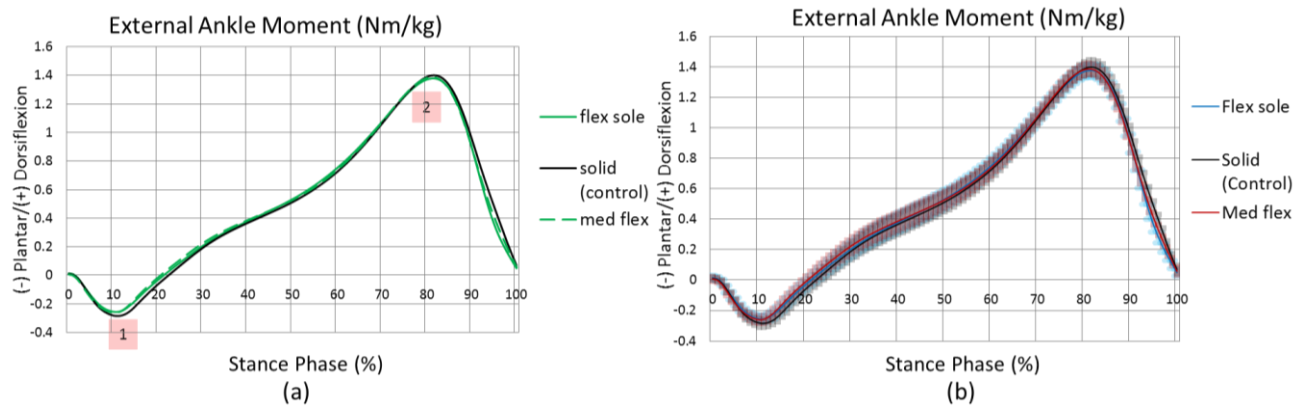


Figure 6.20: Sagittal plane external ankle moment during the three footwear conditions highlighting the 2 area of interest (N=15). Legend 1 indicates maximum ankle plantarflexor moment; legend 2 indicates maximum ankle dorsiflexor moment. (a) – without standard deviation (STD), (b) – with the lines shadowed to represent STD ranges.

The results for mean external moments values are demonstrated in the table below.

Table 6.83: Mean (\pm SD) sagittal plane ankle moment (Nm/kg) for the three footwear conditions (N=15).

	Flex sole	Med. flex	Solid
Max ankle external PF moment (Nm/kg)	-0.26 (0.03)	-0.27 (0.03)	-0.30 (0.03)
Max ankle external DF moment (Nm/kg)	1.39 (0.04)	1.39 (0.04)	1.41 (0.05)

6.7.5.1 Maximum external ankle plantarflexor moment

There was a significant PF moment reduction demonstrated for the flexible soles when compared to the solid control shoe ($p < 0.02$) as shown in the table below.

Table 6.84: Pairwise comparison of shoe conditions for mean external ankle PF moment during stance phase.

Cond.	Cond.	Mean Difference	Std. Error	Sig.	95% Confidence Interval for Difference	
					Lower Bound	Upper Bound
Flex sole	Med. flex	.004	.007	1.000	-.016	.023
	Solid	.032*	.009	.010	.007	.056
Med. flex	Flex sole	-.004	.007	1.000	-.023	.016
	Solid	.028*	.006	.001	.012	.044

6.7.5.2 Maximum external ankle dorsiflexor moment

There were no significant changes. The (H_0) hypothesis is rejected.

6.7.5.3 External ankle moment impulse (overall area of the moment curve)

The flexible sole reduced the impulse value of the PF moment curve by 14.9% and the medium flexibility sole by 15.7% when compared to the control shoe as shown in table 6.85. There were no significant changes for area 2 which is the main interest of this research.

Table 6.85: The average of the area under the curves (external ankle moments) for test footwear conditions (N=15).

	Flexible sole	Medium flexible sole	Solid
Area 1 (%)	85.1 (12.1)	84.3.4 (13.0)	100.0 (14.3)
Differences between control shoe (%)	-14.9	-15.7	0.0
Area 2 (%)	98.0 (5.3)	100.0 (5.6)	100.0 (5.9)
Differences between control shoe (%)	-2.0	0.0	0.0

6.7.5.4 Area 1 (External ankle PF moment)

The both flexible shoes significantly reduced area 1 when compared to the control shoe ($p < 0.024$).

Table 6.86: Pairwise comparison of the average of the area under the curves (external ankle PF moment) for test footwear conditions (N=15).

Cond.	Cond.	Mean Difference	Std. Error	Sig.	95% Confidence Interval for Difference	
					Lower Bound	Upper Bound
Flex sole	Med. flex	.751	3.614	1.000	-9.071	10.573
	Solid	-14.915*	4.798	.023	-27.956	-1.875
Med. flex	Flex sole	-.751	3.614	1.000	-10.573	9.071
	Solid	-15.667*	3.887	.004	-26.229	-5.104

6.7.5.5 Area 2 (External ankle DF moment)

There were no significant differences noted. The (H_0) hypothesis is rejected.

6.7.5.6 Summary of ankle moment alterations produced by curved heel test conditions.

- Both flexible sole profiles significantly reduced maximum PF moment values when compared to control. The (H₀₁) hypothesis is accepted;
- The flexible sole reduced PF moment curve area impulse by 14.9% and the medium flexible sole by 15.7% when compared to the control shoe;
- There were no significant results seen between any footwear test conditions for external ankle DF moment. The (H₀₁) hypothesis is rejected.

6.8 Ankle Power

6.8.1 The effect of walking with different heel heights (HH)

Figure 6.21 illustrates the alteration to sagittal plane external ankle joint power for the heel height test conditions.

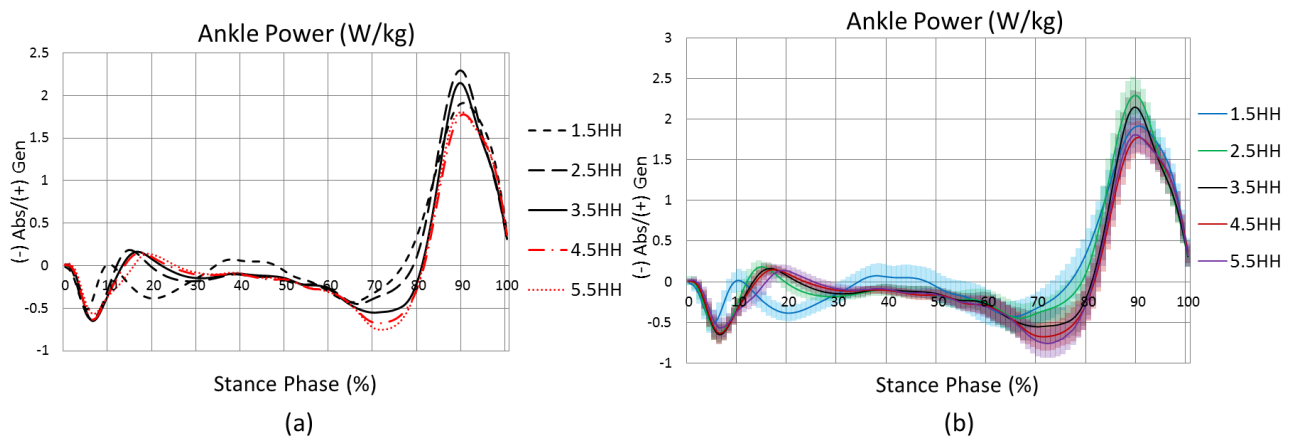


Figure 6.21: Sagittal plane external ankle joint power for HH test footwear conditions (N=15).

The mean results for maximum area of sagittal plane external ankle joint power for different footwear conditions are demonstrated in table 6.87.

Table 6.87: Mean (\pm SD) area of ankle joint power for test footwear conditions.

	1.5 HH	2.5 HH	3.5 HH	4.5 HH	5.5 HH
Generation area % (overall area of power generation)	118.9 (11.7)	111.6 (9.8)	100.0 (9.2)	90.6 (12.3)	93.5 (11.1)
Differences between control shoe (%)	18.9	11.6	0	-9.4	-6.5
Absorption area % (overall area of power absorption)	90.7 (14.0)	88.2 (11.5)	100.0 (13.4)	105.6 (10.9)	108.9 (14.0)
Differences between control shoe (%)	-9.3	-11.8	0	5.6	8.9

6.8.1.1 The ankle power generation area

The 1.5HH increased the power generation area for the ankle joint by 18.9% versus the control shoe, but it did not show any significant difference versus any of the other footwear conditions. The 2.5HH test condition produced a significant increase in the power generation area when compared to the 4.5HH (21% $p < 0.000$) and the 5.5HH (18.1% $p = 0.001$). The 4.5HH significantly reduced power generation area by 9.4% when compared to the control shoe ($p = 0.017$) as shown in table 6.88 below.

Table 6.88: Pairwise comparison of shoe conditions power generation area for ankle joint during whole stance phase (N=14).

Cond.	Cond.	Mean Difference	Std. Error	Sig.	95% Confidence Interval for Difference	
					Lower Bound	Upper Bound
1.5HH	2.5HH	7.260	10.038	1.000	-26.123	40.643
	3.5HH	18.854	8.246	.383	-8.569	46.277
	4.5HH	28.251	9.313	.089	-2.720	59.222
	5.5HH	25.317	9.994	.239	-7.921	58.554
2.5HH	1.5HH	-7.260	10.038	1.000	-40.643	26.123
	3.5HH	11.594	4.137	.141	-2.164	25.352
	4.5HH	20.991*	3.460	.000	9.483	32.498

	5.5HH	18.056*	3.470	.001	6.515	29.598
3.5HH	1.5HH	-18.854	8.246	.383	-46.277	8.569
	2.5HH	-11.594	4.137	.141	-25.352	2.164
	4.5HH	9.397*	2.424	.017	1.336	17.458
	5.5HH	6.462	3.611	.952	-5.547	18.472
4.5HH	1.5HH	-28.251	9.313	.089	-59.222	2.720
	2.5HH	-20.991*	3.460	.000	-32.498	-9.483
	3.5HH	-9.397*	2.424	.017	-17.458	-1.336
	5.5HH	-2.935	3.166	1.000	-13.464	7.595

6.8.1.2 The ankle power absorption area

The results show that the 1.5HH significantly reduced the ankle power absorption area by 18.2% when compared to the 5.5HH footwear test condition ($p=0.017$). The 3.5HH test condition significantly increased the ankle power absorption area by 11.8% when compared to the 2.5HH ($p=0.008$) (table 6.89). The 2.5HH significantly reduced the ankle power absorption area when compared to the 3.5HH (11.8%, $p=0.08$), the 4.5HH (17.7%, $p<0.000$) and the 5.5HH (20.7%, $p<0.000$).

Table 6.89: Pairwise comparison of shoe conditions for average ankle joint power absorption area for the whole stance phase (N=15).

Cond.	Cond.	Mean Difference	Std. Error	Sig.	95% Confidence Interval for Difference	
					Lower Bound	Upper Bound
1.5HH	2.5HH	2.510	4.179	1.000	-11.386	16.407
	3.5HH	-9.281	4.521	.593	-24.316	5.754
	4.5HH	-14.906	4.983	.097	-31.477	1.666
	5.5HH	-18.153*	4.709	.017	-33.813	-2.494
2.5HH	1.5HH	-2.510	4.179	1.000	-16.407	11.386
	3.5HH	-11.792*	2.783	.008	-21.048	-2.536
	4.5HH	-17.416*	2.789	.000	-26.692	-8.140
	5.5HH	-20.664*	3.488	.000	-32.263	-9.065
3.5HH	1.5HH	9.281	4.521	.593	-5.754	24.316
	2.5HH	11.792*	2.783	.008	2.536	21.048
	4.5HH	-5.624	2.622	.500	-14.343	3.095
	5.5HH	-8.872	3.172	.143	-19.421	1.677
4.5HH	1.5HH	14.906	4.983	.097	-1.666	31.477
	2.5HH	17.416*	2.789	.000	8.140	26.692
	3.5HH	5.624	2.622	.500	-3.095	14.343
	5.5HH	-3.248	2.389	1.000	-11.191	4.696

6.8.1.3 Summary of sagittal plane ankle joint power area alteration produced by different heel heights:

- The 2.5HH test condition produced a significant increase in power generation area (for the whole of stance phase) when compared to the 4.5HH (21% $p < 0.000$) and the 5.5HH (18.1% $p = 0.001$) test conditions. The 4.5HH significantly reduced the power generation area by 9.4% when compared to the control shoe ($p = 0.017$). The (H₀) hypothesis is accepted.
- The results show that the 1.5HH test condition significantly reduced the ankle power absorption area by 18.2% when compared to the 5.5HH footwear ($p = 0.017$).
- The 3.5HH significantly increased the ankle power absorption area by 11.8% when compared to the 2.5HH ($p = 0.008$). The (H₀) hypothesis is accepted.
- The 2.5HH test condition significantly reduced the ankle power absorption area when compared to the 3.5HH (11.8%, $p = 0.08$), the 4.5HH (17.7%, $p < 0.000$) test conditions and the 5.5HH (20.7%, $p < 0.000$).

6.8.2 The effect of altering rocker sole apex position (AP)

Figure 6.37 illustrates the alteration to sagittal plane external ankle joint power by the apex length sole changes.

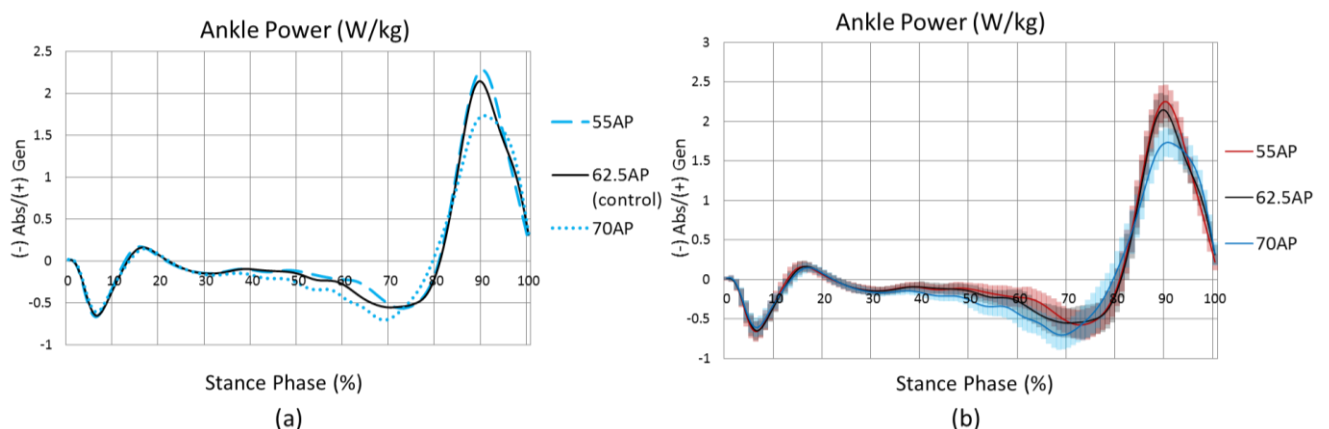


Figure 6.22: Sagittal plane external ankle joint power for AP test footwear conditions (N=15).

The mean results for average area of sagittal plane external ankle joint power for different footwear conditions are demonstrated in table 6.90. (a) – without standard deviation (STD), (b) – with the lines shadowed to represent STD ranges.

Table 6.90: Mean (\pm SD) area of ankle joint power for test footwear conditions.

	55AP	62.5AP	70AP
Generation area % (overall area of power generation)	104.9 (9.5)	100.0 (9.2)	94.6 (10.2)
Differences between control shoe (%)	4.9	0	-5.4
Absorption area % (overall area of power absorption)	91.4 (11.4)	100.0 (13.4)	113.8 (11.5)
Differences between control shoe (%)	-8.6	0	13.8

6.8.2.1 The ankle power generation area

The 55AP footwear condition increased average ankle power generation area by 10.3% when compared to the 70AP ($p=0.23$).

Table 6.91: Pairwise comparison of shoe conditions power generation area for ankle joint during whole stance phase (N=15).

Cond.	Cond.	Mean Difference	Std. Error	Sig.	95% Confidence Interval for Difference	
					Lower Bound	Upper Bound
55AP	62.5AP	4.850	4.070	.760	-6.212	15.913
	70 AP	10.212*	3.277	.023	1.307	19.117
62.5AP	55AP	-4.850	4.070	.760	-15.913	6.212
	70 AP	5.362	2.792	.226	-2.226	12.949

6.8.2.2 The ankle power absorption area

The 55AP footwear significantly reduced the average ankle joint power absorption area by 8.6% when compared to control 62.5AP shoe ($p=0.01$) and significantly reduced it by 22.4% when compared to the 70AP ($p=0.001$) as shown in the table below.

Table 6.92: Pairwise comparison of shoe conditions for average ankle joint power absorption area for the whole stance phase (N=15).

Cond.	Cond.	Mean Difference	Std. Error	Sig.	95% Confidence Interval for Difference	
					Lower Bound	Upper Bound
55AP	62.5AP	-8.602*	2.422	.010	-15.185	-2.019
	70 AP	-22.355*	4.502	.001	-34.591	-10.119
62.5AP	55AP	8.602*	2.422	.010	2.019	15.185
	70 AP	-13.753*	4.737	.035	-26.627	-.880

6.8.2.3 Summary of sagittal plane ankle joint power area alteration produced by AP of the sole:

- The 55AP footwear condition increased the average ankle power generation area by 10.3% when compared to the 70AP (p=0.23) footwear for the whole stance phase. The (H₀) hypothesis is rejected;
- The 55AP footwear significantly reduced the average ankle joint power absorption area by 8.6% when compared to control 62.5AP shoe (p=0.01) and significantly reduced by 22.4% when compared to the 70AP (p=0.001) as shown in the table below. The (H₀) hypothesis is accepted.

6.8.3 The effect of altering apex angle (toe angle-TA)

Figure 6.23 illustrates the alteration to sagittal plane external ankle joint power induced by the apex toe angle changes.

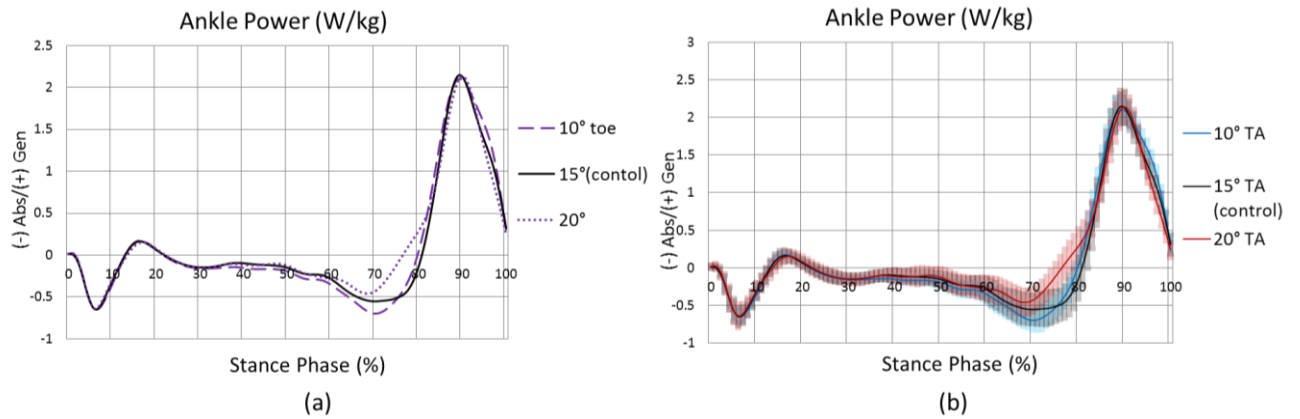


Figure 6.23: Sagittal plane external ankle joint power for TA test footwear conditions (N=15). The mean results for average area of sagittal plane external ankle joint power for different footwear conditions are demonstrated in table 6.93 below.

Table 6.93: Mean (\pm SD) area of ankle joint power for test footwear conditions.

	10° TA	15° TA	20° TA
Generation area % (overall area of power generation)	107.7 (9.1)	100.0 (9.2)	102.0 (10.6)
Differences between control shoe (%)	7.7	0	2.0
Absorption area % (overall area of power absorption)	111.1 (11.8)	100.0 (13.4)	79.8 (11.0)
Differences between control shoe (%)	11.1	0	-20.2

6.8.3.1 The ankle power generation area

The results did not show any significance. The (H_0) hypothesis is rejected.

6.8.3.2 The ankle power absorption area

The 20°TA footwear significantly reduced ankle joint power absorption area by 20.2% when compared to control 15°TA shoe ($p=0.007$) and significantly reduced by 31.3% when compared to 10°TA ($p<0.000$).

Table 6.94: Pairwise comparison of shoe conditions for average ankle joint power absorption area for the whole stance phase (N=15).

Cond.	Cond.	Mean Difference	Std. Error	Sig.	95% Confidence Interval for Difference	
					Lower Bound	Upper Bound
10° TA	15° TA	11.144*	2.999	.007	2.994	19.295
	20° TA	31.362*	2.492	.000	24.590	38.133
15° TA	10° TA	-11.144*	2.999	.007	-19.295	-2.994
	20° TA	20.217*	3.102	.000	11.788	28.646

6.8.3.3 Summary for sagittal plane ankle joint power area alteration produced by alteration to toe angle of the sole:

- The 20°TA footwear significantly reduced ankle joint power absorption area by 20.2% when compared to control 15°TA shoe ($p=0.007$) and significantly reduced by 31.3% when compared to 10°TA ($p<0.000$). The (H_0) hypothesis is accepted.

6.8.4 The effect of altering heel curve

Figure 6.24 illustrates the alteration to sagittal plane external ankle joint power induced by the curvature of the heel.

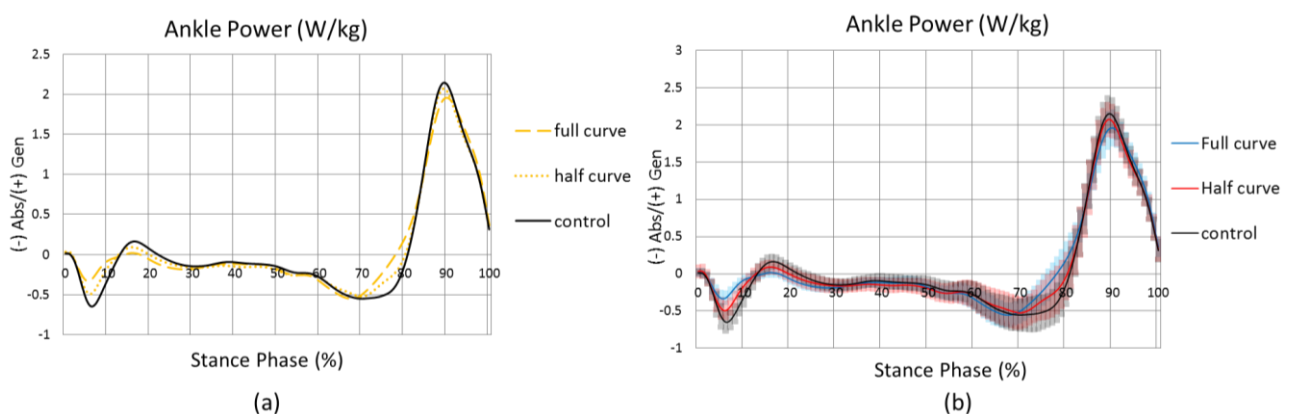


Figure 6.24: Sagittal plane external ankle joint power for heel-curved test footwear conditions where control shoe has no curved heel (N=15). (a) – without standard deviation (STD), (b) – with the lines shadowed to represent STD ranges.

The mean results for average area of sagittal plane external ankle joint power for different footwear conditions are demonstrated in the table below.

Table 6.95: Mean (\pm SD) area of ankle joint power for test footwear conditions.

	Full curve	Half curve	control
Generation area % (overall area of power generation)	95.8 (12.1)	93.5 (9.8)	100.0 (9.2)
Differences between control shoe (%)	-4.2	-6.5	0
Absorption area % (overall area of power absorption)	83.3 (13.1)	90.8 (11.5)	100.0 (13.4)
Differences between control shoe (%)	-16.7	-9.2	0

6.8.4.1 The ankle power generation area

There were no statistically significant differences noted in ankle power generation. The (H₀) hypothesis is accepted.

6.8.4.2 The ankle power absorption area

The control shoe without a curved heel significantly increased the ankle joint power absorption area by 9.2%% when compared to half curved heel shoe ($p=0.006$) and significantly increased it by 16.7% when compared to full curved heel shoe ($p<0.001$) as shown in table 6.96.

Table 6.96: Pairwise comparison of shoe conditions for average ankle joint power absorption area for the whole stance phase (N=15).

Cond.	Cond.	Mean Difference	Std. Error	Sig.	95% Confidence Interval for Difference	
					Lower Bound	Upper Bound
Full curve	Half curve	-7.493*	2.713	.046	-14.866	-.121
	No curve	-16.729*	3.408	.001	-25.993	-7.466
Half curve	Full curve	7.493*	2.713	.046	.121	14.866
	No curve	-9.236*	2.415	.006	-15.799	-2.673

6.8.4.3 Summary for sagittal plane ankle joint power area alteration produced by curved heel test conditions:

- The control shoe without a curved heel significantly increased the average ankle joint power absorption area by 9.2% when compared to half curve shoe ($p=0.006$) and significantly increased by 16.7% when compared to full curve heel ($p<0.001$). The (Hal) hypothesis is accepted.

6.8.5 The effect of altering rocker profile stiffness at metatarsal area

Figure 6.25 illustrates the alteration to sagittal plane external ankle joint power induced by the flexibility of the sole.

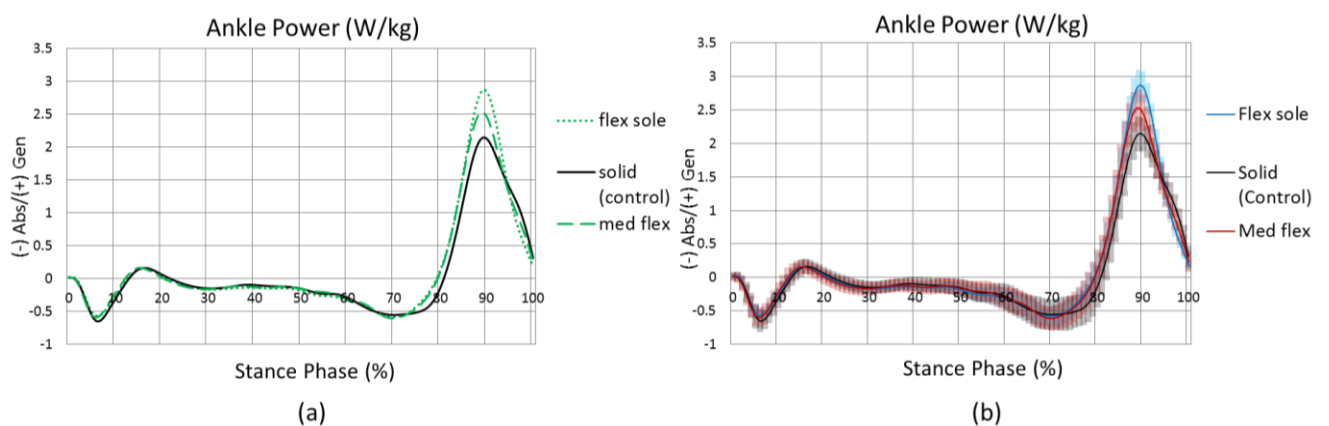


Figure 6.25: Sagittal plane external ankle joint power for different flexibility level of the sole where control shoe is not flexible at the metatarsal area (N=15). (a) – without standard deviation (STD), (b) – with the lines shadowed to represent STD ranges.

The mean results for average area of sagittal plane external ankle joint power for different footwear conditions are demonstrated in the table below.

Table 6.97: Mean (\pm SD) area of ankle joint power for test footwear conditions.

	Flex sole	Med. flex	Solid
Generation area % (overall area of power generation)	116.2 (8.3)	111.6 (9.3)	100.0 (9.2)
Differences between control shoe (%)	16.2	11.6	0
Absorption area % (overall area of power absorption)	95.5 (9.2)	94.8 (10.2)	100.0 (13.4)
Differences between control shoe (%)	-4.5	-5.2	0

6.8.5.1 The ankle power generation area

The flexible sole produced a significant increase in the average ankle joint power generation area by 16.2% when compared to the solid soled shoe ($p=0.25$).

6.8.5.2 The ankle power absorption area

There were no statistically significant alterations to this parameter. The (Hal) hypothesis is accepted.

6.8.5.3 Summary for sagittal plane ankle joint power area alteration produced by footwear stiffness level at the metatarsal area:

- The flexible sole showed significant increases in the average ankle joint power generation area by 16.2% when compared to solid soled shoe ($p=0.25$). The (Hal) hypothesis is accepted.

6.9 Electromyography data for ankle joint

It is important to collect EMG activity data for medial gastrocnemius and soleus muscles to understand the level of their activation altered by different footwear features. There were only 16 subjects used for EMG data, two subjects were excluded from the study, as the data were not good for some footwear features due to electrode movement or other artefacts. Therefore, $N=14$ in total were used for analysis of medial gastrocnemius activity.

6.9.1 The effect of walking with different heel heights

Figure 6.26 illustrates the alteration to the medial gastrocnemius EMG RMS values for the heel height test conditions. The results were converted to present as a percentage of the maximum in the control shoe. It can be seen that the 1.5HH increased EMG activity within 10-40% of the stance phase versus all footwear profiles because of premature activation. The 2.5HH increased maximum EMG activity when compared to the rest and the 4.5 cm heel showed visible less activity when compared to all the other footwear conditions.

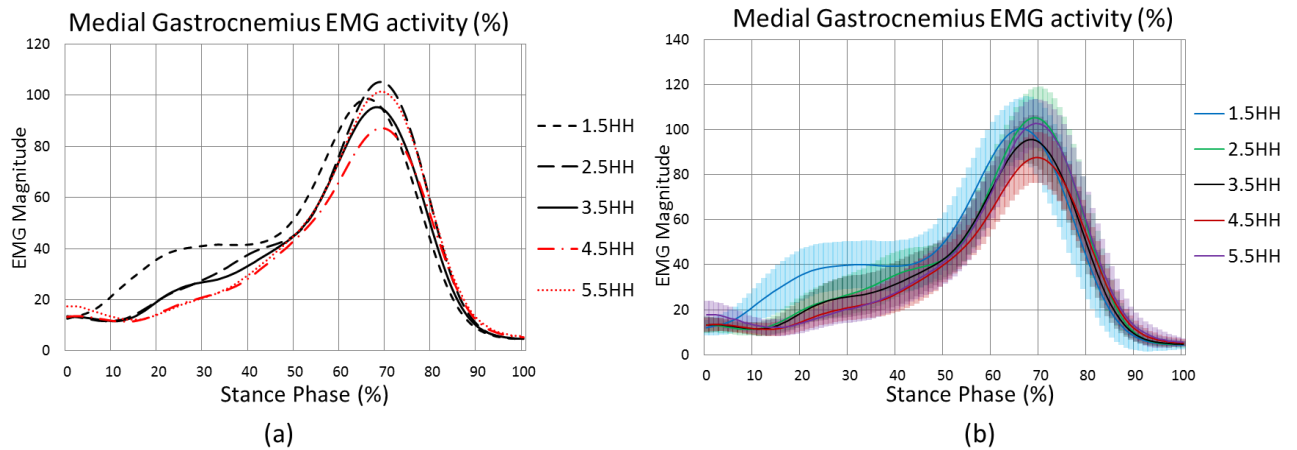


Figure 6.26: The medial gastrocnemius EMG activity for test footwear conditions for % stance phase. (a) – without standard deviation (STD), (b) – with the lines shadowed to represent STD ranges.

The mean results for maximum EMG RMS activity for different footwear conditions during different part of the stance phase are demonstrated in the table below.

Table 6.98: Mean (\pm SD) medial gastrocnemius EMG percentage activity for test footwear conditions.

	1.5 HH	2.5 HH	3.5 HH	4.5 HH	5.5 HH
Maximum EMG activity during LR (%)	34.2	20.7	19.7	17.2	20.5
	11.2	(6.4)	(6.6)	(4.0)	(7.0)
Maximum EMG activity during mid-stance (%)	58.1	50.2	48.5	45.6	46.7
	(11.6)	(9.1)	(9.7)	(9.7)	(10.7)
Maximum EMG activity during stance phase (%)	104.2	110.1	100.0	93.5	108.1
	(13.7)	(11.8)	(8.8)	(9.1)	(9.6)

6.9.1.1 Loading response

The 1.5HH significantly increased medial gastrocnemius (MG) EMG activity when compared to all the other footwear conditions except for the 5.5HH footwear condition as shown in table 6.99. The 4.5HH significantly reduced muscle activity versus the 1.5HH but it was not significant versus the control shoe.

Table 6.99: Pairwise comparison of shoe conditions for medial gastrocnemius mean EMG activity during loading response (N=14).

Cond.	Cond.	Mean Difference	Std. Error	Sig.	95% Confidence Interval for Difference	
					Lower Bound	Upper Bound
1.5HH	2.5HH	13.543*	3.367	.015	2.188	24.899
	3.5HH	14.474*	2.945	.003	4.541	24.406
	4.5HH	16.970*	3.167	.001	6.288	27.651
	5.5HH	13.749	4.174	.058	-.327	27.826
2.5HH	1.5HH	-13.543*	3.367	.015	-24.899	-2.188
	3.5HH	.930	2.280	1.000	-6.758	8.619
	4.5HH	3.427	1.309	.213	-.989	7.842
	5.5HH	.206	2.083	1.000	-6.818	7.230
3.5HH	1.5HH	-14.474*	2.945	.003	-24.406	-4.541
	2.5HH	-.930	2.280	1.000	-8.619	6.758
	4.5HH	2.496	1.729	1.000	-3.334	8.326
	5.5HH	-.724	2.508	1.000	-9.182	7.733
4.5HH	1.5HH	-16.970*	3.167	.001	-27.651	-6.288
	2.5HH	-3.427	1.309	.213	-7.842	.989
	3.5HH	-2.496	1.729	1.000	-8.326	3.334
	5.5HH	-3.221	1.556	.589	-8.467	2.026

6.9.1.2 Mid-stance phase

The 4.5 cm heel height shoe significantly reduced mean EMG activity during mid-stance phase when compared to the 1.5HH footwear test condition ($p=0.20$) as shown in table 6.100.

Table 6.100: Pairwise comparison of shoe conditions for medial gastrocnemius mean EMG activity during mid-stance phase.

Cond.	Cond.	Mean Difference	Std. Error	Sig.	95% Confidence Interval for Difference	
					Lower Bound	Upper Bound
1.5HH	2.5HH	7.891	3.024	.216	-2.307	18.089
	3.5HH	9.569	3.332	.131	-1.668	20.807
	4.5HH	12.511*	3.243	.020	1.574	23.448
	5.5HH	11.387	4.488	.248	-3.747	26.521
2.5HH	1.5HH	-7.891	3.024	.216	-18.089	2.307
	3.5HH	1.679	2.018	1.000	-5.129	8.486
	4.5HH	4.620	1.707	.180	-1.138	10.378

	5.5HH	3.496	3.527	1.000	-8.397	15.389
3.5HH	1.5HH	-9.569	3.332	.131	-20.807	1.668
	2.5HH	-1.679	2.018	1.000	-8.486	5.129
	4.5HH	2.941	2.161	1.000	-4.346	10.229
	5.5HH	1.818	2.950	1.000	-8.130	11.766
4.5HH	1.5HH	-12.511*	3.243	.020	-23.448	-1.574
	2.5HH	-4.620	1.707	.180	-10.378	1.138
	3.5HH	-2.941	2.161	1.000	-10.229	4.346
	5.5HH	-1.124	2.754	1.000	-10.413	8.165

6.9.1.3 Late stance phase

The 4.5HH reduced MG mean EMG activity during stance phase when compared to the 2.5 cm heel height ($p=0.003$). The 5.5HH footwear condition significantly increase mean EMG when compared to control (3.5HH) shoe.

Table 6.101: Pairwise comparison of shoe conditions for medial gastrocnemius mean EMG activity during late stance phase (N=14).

Cond.	Cond.	Mean Difference	Std. Error	Sig.	95% Confidence Interval for Difference	
					Lower Bound	Upper Bound
1.5HH	2.5HH	-5.900	7.386	1.000	-30.808	19.008
	3.5HH	4.223	6.302	1.000	-17.031	25.478
	4.5HH	10.732	8.332	1.000	-17.367	38.830
	5.5HH	-3.891	6.364	1.000	-25.352	17.570
2.5HH	1.5HH	5.900	7.386	1.000	-19.008	30.808
	3.5HH	10.123	3.904	.223	-3.042	23.288
	4.5HH	16.632*	3.412	.003	5.126	28.137
	5.5HH	2.009	5.031	1.000	-14.959	18.977
3.5HH	1.5HH	-4.223	6.302	1.000	-25.478	17.031
	2.5HH	-10.123	3.904	.223	-23.288	3.042
	4.5HH	6.508	3.465	.830	-5.178	18.195
	5.5HH	-8.114*	2.264	.033	-15.751	-.478
4.5HH	1.5HH	-10.732	8.332	1.000	-38.830	17.367
	2.5HH	-16.632*	3.412	.003	-28.137	-5.126
	3.5HH	-6.508	3.465	.830	-18.195	5.178
	5.5HH	-14.623	4.783	.092	-30.754	1.509

6.9.1.4 EMG Impulse

The results show that the 1.5HH increased overall EMG activity by MG muscle by 14.4% when compared to control and the 4.5HH reduced overall EMG activity by 21.9% when compared to the 1.5HH. The 4.5HH reduced overall EMG area by 7.4% when compared to control shoe as demonstrated in the table below.

Table 6.102: The average (\pm SD) of the area under the curves for medial gastrocnemius EMG activity for test footwear conditions (N=14).

	1.5 HH	2.5 HH	3.5 HH	4.5 HH	5.5 HH
EMG impulse (overall area of EMG activity (%))	114.4 (13.0)	107.4 (9.1)	100.0 (10.1)	92.6 (10.5)	103.6 (10.5)
Differences between control shoe (%)	14.4	7.4	0	-7.4	3.6

The pairwise Anova test with Bonferroni adjustment demonstrate that the 1.5HH and 2.5HH significantly increased EMG area under the curve for MG muscle when compared to the 4.5HH footwear condition ($p < 0.014$).

Table 6.103: Pairwise comparison of shoe conditions for medial gastrocnemius overall area underneath the EMG activity curve during stance phase (N=14).

Cond.	Cond.	Mean Difference	Std. Error	Sig.	95% Confidence Interval for Difference	
					Lower Bound	Upper Bound
1.5HH	2.5HH	10.275	5.472	.849	-8.484	29.034
	3.5HH	18.130	5.589	.070	-1.034	37.293
	4.5HH	25.795*	6.212	.013	4.497	47.092
	5.5HH	15.147	5.177	.127	-2.601	32.894
2.5HH	1.5HH	-10.275	5.472	.849	-29.034	8.484
	3.5HH	7.854	4.242	.889	-6.691	22.399
	4.5HH	15.519*	2.045	.000	8.507	22.532
	5.5HH	4.871	4.130	1.000	-9.288	19.031
3.5HH	1.5HH	-18.130	5.589	.070	-37.293	1.034
	2.5HH	-7.854	4.242	.889	-22.399	6.691
	4.5HH	7.665	3.859	.703	-5.565	20.895
	5.5HH	-2.983	2.655	1.000	-12.086	6.120
4.5HH	1.5HH	-25.795*	6.212	.013	-47.092	-4.497
	2.5HH	-15.519*	2.045	.000	-22.532	-8.507
	3.5HH	-7.665	3.859	.703	-20.895	5.565
	5.5HH	-10.648	3.950	.195	-24.189	2.893

6.9.1.5 Summary of gastrocnemius EMG activity alteration produced by different heel heights:

- The 1.5HH footwear significantly increased EMG activity within 10-40% of stance phase when compared to all the other heel height test conditions and the maximum activation was seen at 20% stance phase with an 80% level of increase when compared to the control shoe. It positively accepted the (H_{a2}) hypothesis;
- The 2.5HH increased maximum EMG activity when compared to the other footwear test conditions;
- Negative heel profiles increase overall EMG activity. The 1.5HH increased the overall area of MG EMG activity by 14.4% when compared to control and the 4.5HH reduced overall EMG activity by 21.9% when compared to the 1.5HH. The (H_{a2}) hypothesis is therefore positively accepted;
- The slight raise if the heel height resulted in overall reduction of the area MG EMG activity. The 4.5HH reduced overall EMG area by 7.4% when compared to control.

6.9.2 The effect of altering rocker sole apex position (AP)

Figure 6.27 illustrates the alteration to medial gastrocnemius EMG activity induced by the apex position changes. The 55AP caused a reduction in maximum MG EMG activity when compared to control and more reduction when compared to the 70AP.

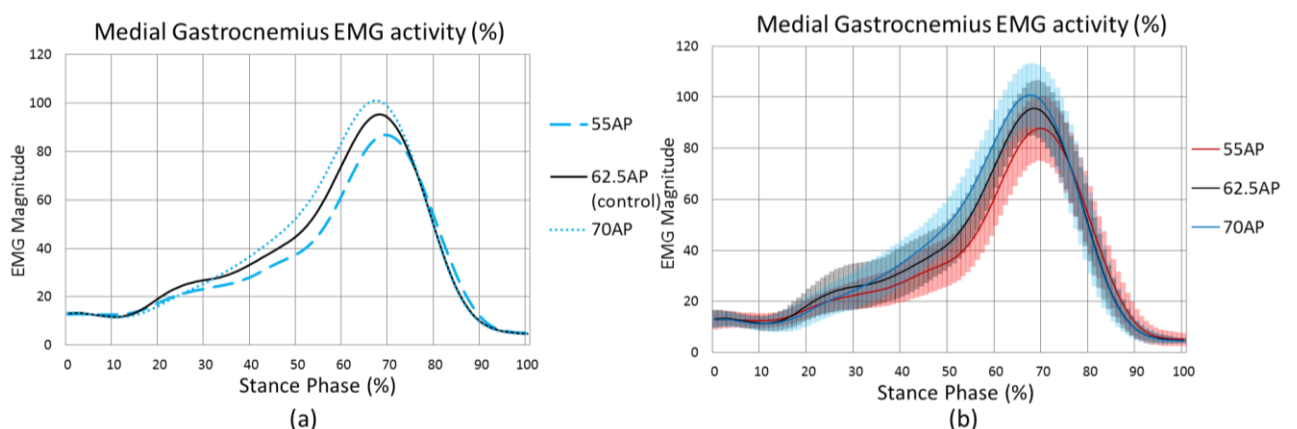


Figure 6.27: The gastrocnemius EMG activity for test footwear conditions (N=14).

The mean results for maximum EMG RMS activity for different footwear conditions during different parts of stance phase are demonstrated in the table below. (a) – without standard deviation (STD), (b) – with the lines shadowed to represent STD ranges.

Table 6.104 Mean (\pm SD) medial gastrocnemius EMG activity for test footwear conditions.

	55AP	62.5AP	70AP
Maximum EMG activity during LR (%)	18.7 (4.4)	19.7 (6.6)	17.7 (5.5)
Maximum EMG activity during mid-stance (%)	40.9 (9.5)	48.5 (9.7)	55.0 (10)
Maximum EMG activity during stance phase (%)	91.3 (11.3)	100.0 (8.8)	107.1 (9.3)

6.9.2.1 Mid-stance phase.

The 55AP demonstrated significant mean EMG reduction when compared to the 70AP footwear test condition ($p=0.02$). The 62.5AP control shoe reduced EMG activity during mid-stance phase when compared to the 70AP footwear ($p=0.011$) as shown in table6.105.

Table 6.105: Pairwise comparison of shoe conditions for medial gastrocnemius mean EMG activity during mid-stance phase (N=14).

Cond.	Cond.	Mean Difference	Std. Error	Sig.	95% Confidence Interval for Difference	
					Lower Bound	Upper Bound
55AP	62.5AP	-7.613	3.017	.076	-15.897	.672
	70 AP	-14.071*	3.112	.002	-22.616	-5.525
62.5AP	55AP	7.613	3.017	.076	-.672	15.897
	70 AP	-6.458*	1.823	.011	-11.464	-1.452

6.9.2.2 Stance phase

The 55AP produced a significant reduction in the MG muscle maximum EMG activity during stance phase when compared to the control shoe ($p=0.018$) and also a reduction when compared to the 70AP test condition ($p=0.005$).

6.9.2.3 EMG Impulse for MG muscle

The table below shows that the 55AP reduced overall EMG area by 8.9% when compared to control and reduced it by 15.6% when compared to the 70AP footwear.

Table 6.106: The average (\pm SD) of the overall area under the curves for medial gastrocnemius EMG activity for test footwear conditions (N=14).

	55AP	62.5AP	70AP
EMG impulse (overall area of EMG activity %)	91.1 (12.6)	100.0 (10.1)	106.7 (9.0)
Differences between control shoe (%)	-8.9	0	6.7

The 55AP significantly reduced GM muscle overall EMG activity area when compared to the 70AP footwear ($p=0.01$).

6.9.2.4 Summary of gastrocnemius EMG activity alteration produced apex length of testing footwear conditions:

- The 55AP produced a significant reduction in the MG muscle maximum EMG activity during stance phase when compared to the control shoe ($p=0.018$) and reduced it when compared to the 70AP test condition ($p=0.005$). It positively answered the (H_{a2}) hypothesis;
- The 55AP reduced overall MG muscle EMG activity area by 8.9%, when compared to control, and reduced it by 15.6% when compared to the 70AP footwear test condition.

6.9.3 The effect of altering apex angle (toe angle-TA)

Figure 6.28 illustrates the alteration to the medial gastrocnemius EMG activity induced by the apex toe angle changes. From the figure below it can be seen that the maximum EMG activity reduced for the 20° angled-toe shoe versus control, with the 10° toe angle shoe increasing the maximum EMG activity when compared to control.

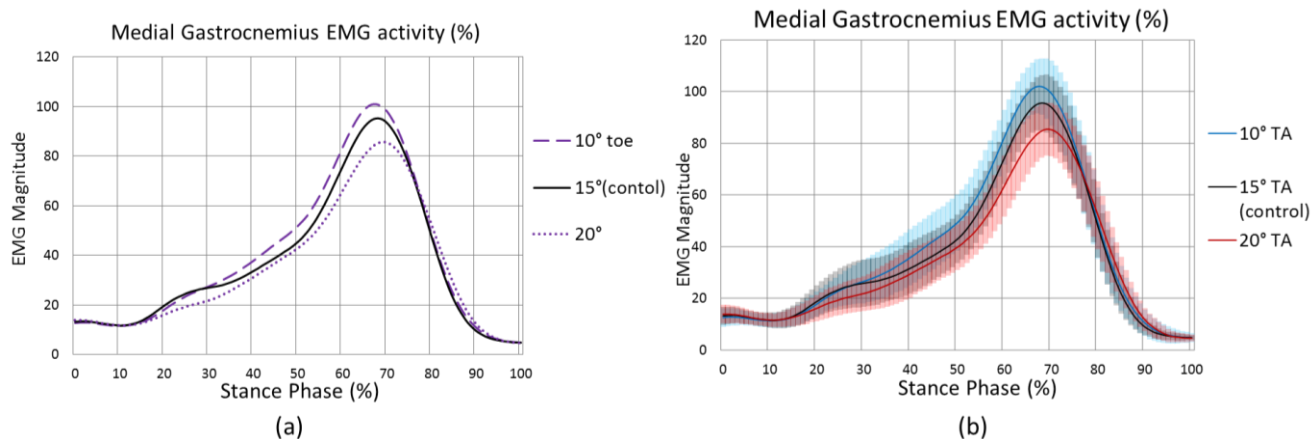


Figure 6.28: The gastrocnemius EMG activity for test footwear conditions. (a) – without standard deviation (STD), (b) – with the lines shadowed to represent STD ranges.

The mean results for maximum EMG RMS activity for different footwear conditions during different part of the stance phase are presented in the table below.

Table 6.107: Mean (\pm SD) medial gastrocnemius EMG activity for test footwear conditions.

	10° TA	15° TA	20° TA
Max EMG activity during LR (%)	17.9 (4.9)	19.7 (6.6)	18.3 (5.3)
Max EMG activity during mid-stance (%)	54.4 (11.5)	48.5 (9.7)	45.2 (8.9)
Max EMG activity during stance phase (%)	107.2 (15.3)	100.0 (8.8)	89.4 (9.3)

6.9.3.1 Mid-stance phase

The 10° TA test condition showed a significant increase in maximum EMG activity during mid-stance phase when compared to control ($p=0.018$) and 20° TA ($p=0.004$).

Table 6.108: Pairwise comparison of shoe conditions for medial gastrocnemius maximum EMG activity during mid-stance phase (N=14).

Cond.	Cond.	Mean Difference	Std. Error	Sig.	95% Confidence Interval for Difference	
					Lower Bound	Upper Bound
10° TA	15° TA	5.871*	1.788	.018	.961	10.781
	20° TA	9.172*	2.256	.004	2.976	15.368
15° TA	10° TA	-5.871*	1.788	.018	-10.781	-.961
	20° TA	3.301	1.576	.169	-1.026	7.628

6.9.3.2 Late stance phase

The 20° TA shoe significantly reduced maximum EMG activity by 10.6% when compared to control shoe ($p=0.006$), and significantly reduced maximum EMG activity by 17.8% when compared to the 10° TA ($p=0.007$).

6.9.3.3 EMG Impulse

The 10° toe angle footwear increased the overall area of MG EMG activity by 7.2% when compared to the control and increased by 13.5% when compared to 20° toe angle footwear. The 20° toe angle footwear test condition significantly reduced area 1 for the MG EMG activity when compared to the 10° toe angle footwear profile.

Table 6.109: The average (\pm SD) of the overall area under the curves for medial gastrocnemius EMG activity for test footwear conditions (N=14).

	10° TA	15° TA	20° TA
EMG impulse (overall area of EMG activity %)	107.2 (11.2)	100.0 (10.1)	93.7 (10.1)
Differences between control shoe (%)	7.2	0	-6.3

Table 6.110: Pairwise comparison of shoe conditions for medial gastrocnemius overall area EMG activity during stance phase.

Cond.	Cond.	Mean Difference	Std. Error	Sig.	95% Confidence Interval for Difference	
					Lower Bound	Upper Bound
10° TA	15° TA	7.217	3.675	.214	-2.874	17.307
	20° TA	13.548*	3.918	.013	2.788	24.308
15° TA	10° TA	-7.217	3.675	.214	-17.307	2.874
	20° TA	6.331	3.957	.401	-4.534	17.197

6.9.3.4 Summary of medial gastrocnemius EMG activity alteration produced by apex toe angle footwear conditions:

- The 10° TA produced a significant increase in mean EMG activity during mid-stance phase when compared to control ($p=0.018$) and 20° TA ($p=0.004$) which is also accepted (H_{a2}) hypothesis;
- The 20° TA shoe significantly reduced maximum EMG activity by 10.6% when compared to control shoe ($p=0.006$), and significantly reduced maximum EMG activity by 17.8% when compared to the 10° TA ($p=0.007$). This is also answered the hypothesis that the 20° TA place ankle more PF during terminal stance and therefore theoretically offloaded medial gastrocnemius muscle by reducing its EMG activity [and positively confirmed the general hypothesis (H_{a2})];
- The 10° toe angle footwear increased overall area of MG EMG activity by 7.2% compared to control and increased it by 13.5% when compared to the 20° toe angle footwear.

6.9.4 The effect of altering heel curves

Figure 6.29 illustrates the alteration to the medial gastrocnemius EMG activity induced by the curvature of the heel. The picture visually shows that the full curve shoe increased MG EMG activity within 5-70% of the stance phase when compared to the other heel curve footwear test conditions.

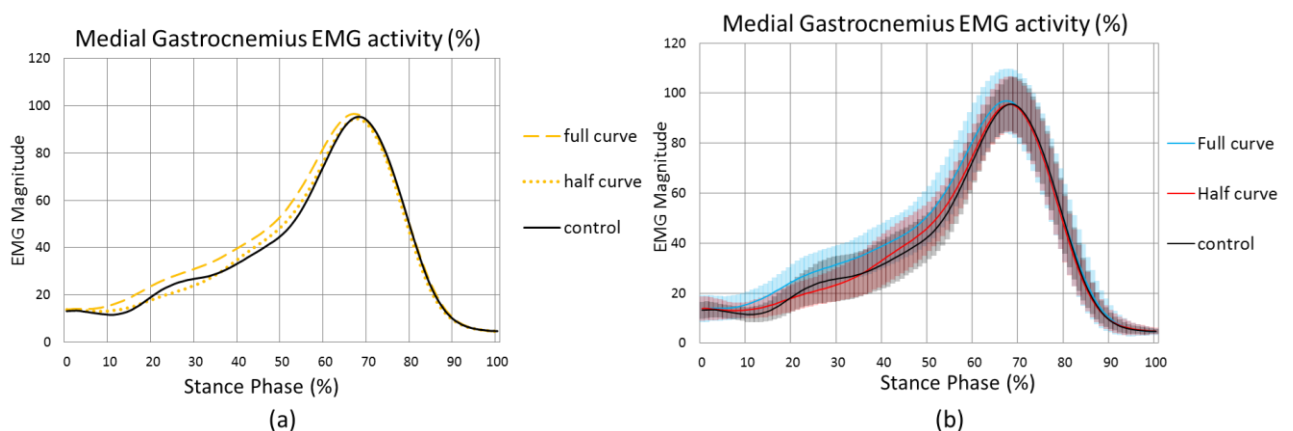


Figure 6.29: The gastrocnemius EMG activity for test footwear conditions (N=14). (a) – without standard deviation (STD), (b) – with the lines shadowed to represent STD ranges.

The results for maximum EMG RMS activity for different footwear conditions during different part of the stance phase are demonstrated in the table below.

Table 6.111: Mean (\pm SD) maximum medial gastrocnemius EMG activity for test footwear conditions.

	Full curve	Half curve	control
Max EMG activity during LR (%)	24.3 (7.0)	20.7 (6.2)	19.7 (6.6)
Max EMG activity during mid-stance (%)	57.2 (11.3)	50.7 (10.6)	48.5 (9.7)
Max EMG activity during stance phase (%)	102.6 (11.6)	99.9 (9.8)	100.0 (8.8)

6.9.4.1 Mid-stance phase

The control shoe (without a curved heel) showed a significant reduction in MG muscle maximum EMG activity during mid-stance phase when compared to the full curve shoe test condition ($p=0.008$).

6.9.4.2 The overall summary area for EMG activity

The full curve increased overall EMG area by 7.7% when compared to the control shoe with no curve added.

Table 6.112: The average (\pm SD) of the overall area under the curves for medial gastrocnemius EMG activity for test footwear conditions (N=14).

	Full curve	Half curve	control
EMG impulse (overall area of EMG activity %)	107.7 (10.5)	99.1 (10.4)	100.0 (10.1)
Differences between control shoe (%)	7.7	-0.9	0

The full curve showed a significant increase in area 1 of EMG activity when compared to the half curve footwear ($p=0.034$).

6.9.4.3 Summary of gastrocnemius EMG activity alteration produced by curved heel test conditions.

- The control shoe without a curved heel showed significant reductions in MG muscle maximum EMG activity during mid-stance phase when compared to the full curve shoe ($p=0.008$). It is positively confirmed H_0 hypothesis;
- The full curve showed a significant increase in EMG impulse when compared to half curve footwear ($p=0.034$) as shown in the table below.

6.9.5 The effect of altering rocker profile stiffness at metatarsal area

Figure 6.30 illustrates the alteration to the medial gastrocnemius EMG activity induced by the flexibility of the sole. The picture below shows that the medium flexibility footwear increased maximum MG muscle EMG activity when compared to all footwear conditions.

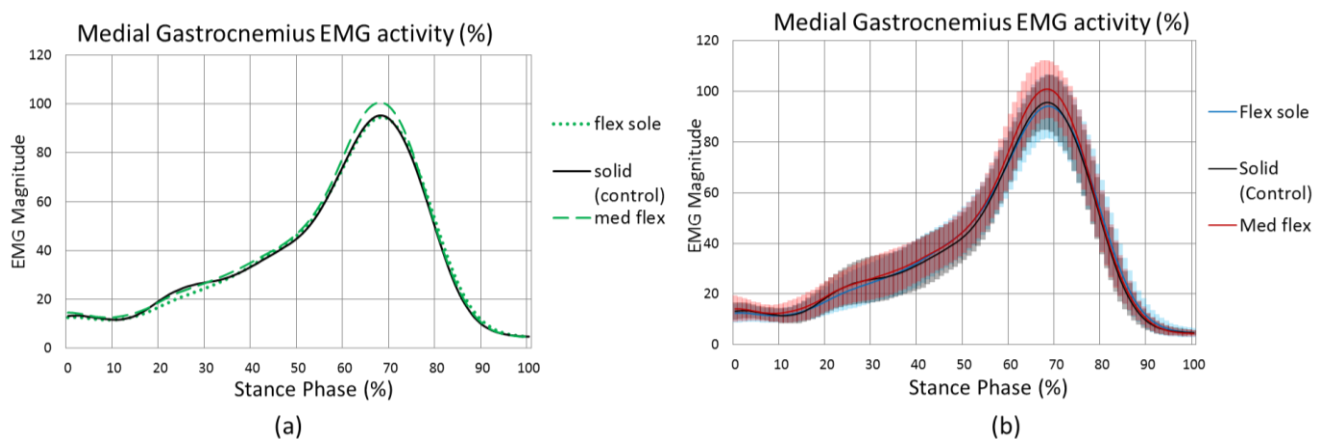


Figure 6.30: The gastrocnemius EMG activity for test footwear conditions (N=14).

The mean results for maximum EMG RMS activity for different footwear conditions during different part of the stance phase are presented in the table below.

Table 6.113: Mean (\pm SD) medial gastrocnemius EMG activity for test footwear conditions.

	Flexible sole	Medium flexible	Solid
Max EMG activity during LR (%)	18.3 (5.2)	20.2 (6.9)	19.7 (6.6)
Max EMG activity during mid-stance (%)	48.2 (9.2)	48.9 (9.3)	48.5 (9.7)
Max EMG activity during stance phase (%)	100.0 (10.4)	105.3 (10.3)	100.0 (8.8)

The statistical analysis did not show any statistical significance.

6.9.5.1 The overall summary area for EMG activity

The table below shows that medium flexibility footwear increased overall EMG area by 4.3% when compared to control and reduced by 4.7 % when compared to the flexible sole footwear, however it was not significant.

Table 6.114: The average (\pm SD) of the overall area under the curves for medial gastrocnemius EMG activity for test footwear conditions (N=14).

	Flexible sole	Medium flexibility	Solid
EMG impulse (overall area of EMG activity %)	99.6 (9.7)	104.3 (8.7)	100.0 (10.1)
Differences between control shoe (%)	-0.4	4.3	0

6.9.5.2 Summary of gastrocnemius EMG activity alteration produced by sole flexibility

The results did not show any statistical significant alteration for medial gastrocnemius EMG activity caused by flexible footwear. It positively confirmed the second overarching null hypothesis (H_02) and rejected (H_a2).

6.10 Soleus electromyography results

6.10.1 The effect of walking with different heel heights

Figure 6.31 illustrates the alteration to the soleus EMG RMS values for the heel height test conditions. The results were converted to present as percentage of the results demonstrated for the control shoe as a baseline shoe, which was deemed to be 100%. It can be seen that the 1.5HH increased (by premature activation) EMG activity within 10-65% of the stance phase versus all footwear profiles. The 5.5HH increased maximum EMG activity when compared to the rest and the 4.5 cm heel showed visible less activity when compared to all footwear conditions. Similar results were demonstrated for the medial gastrocnemius muscle.

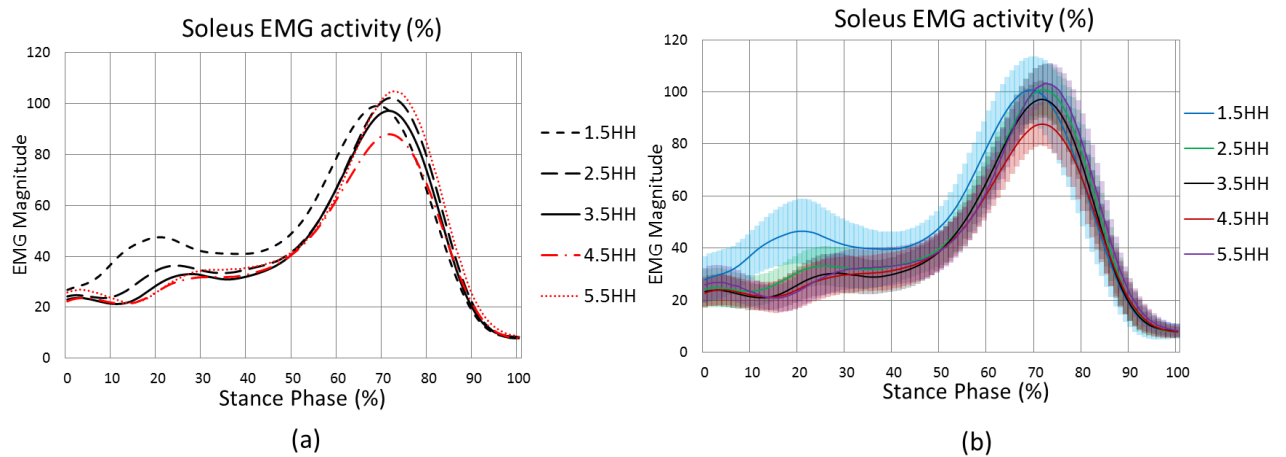


Figure 6.31: The soleus EMG activity for test footwear conditions (N=13). (a) – without standard deviation (STD), (b) – with the lines shadowed to represent STD ranges.

The mean results for maximum EMG RMS activity for different footwear conditions during different parts of stance phase are demonstrated in the table below.

Table 6.115: Mean (\pm SD) soleus EMG activity for test footwear conditions.

	1.5 HH	2.5 HH	3.5 HH	4.5 HH	5.5 HH
Maximum EMG activity during LR (%)	49.8 (11.8)	37.0 (9.0)	31.2 (7.2)	30.3 (7.8)	32.5 (7.7)
Maximum EMG activity during mid-stance (%)	59.0 (9.9)	47.6 (7.5)	44.1 (7.1)	44.0 (8.0)	45.0 (7.6)
Maximum EMG activity during stance phase (%)	104.7 (11.0)	105.8 (9.0)	100.0 (6.5)	91.2 (7.3)	107.5 (7.4)

6.10.1.1 Loading response

The 1.5HH significantly increased soleus EMG activity when compared to all footwear conditions as shown in the table below.

Table 6.116: Pairwise comparison of shoe conditions for soleus mean EMG activity during loading response (N=13).

Cond.	Cond.	Mean Difference	Std. Error	Sig.	95% Confidence Interval for Difference	
					Lower Bound	Upper Bound
1.5HH	2.5HH	12.846*	3.555	.036	.657	25.035
	3.5HH	18.633*	3.783	.004	5.665	31.601
	4.5HH	19.537*	3.405	.001	7.864	31.211
	5.5HH	17.361*	4.403	.020	2.267	32.456
2.5HH	1.5HH	-12.846*	3.555	.036	-25.035	-.657

	3.5HH	5.787	2.086	.168	-1.364	12.937
	4.5HH	6.691	2.637	.261	-2.350	15.733
	5.5HH	4.515	3.276	1.000	-6.716	15.746
3.5HH	1.5HH	-18.633*	3.783	.004	-31.601	-5.665
	2.5HH	-5.787	2.086	.168	-12.937	1.364
	4.5HH	.905	1.562	1.000	-4.449	6.258
	5.5HH	-1.272	2.327	1.000	-9.249	6.706
4.5HH	1.5HH	-19.537*	3.405	.001	-31.211	-7.864
	2.5HH	-6.691	2.637	.261	-15.733	2.350
	3.5HH	-.905	1.562	1.000	-6.258	4.449
	5.5HH	-2.176	2.062	1.000	-9.245	4.892

6.10.1.2 Mid-stance phase

The 1.5HH significantly increased maximum soleus EMG activity when compared to all footwear conditions ($p < 0.015$).

Table 6.117: Pairwise comparison of shoe conditions for soleus mean EMG activity during mid-stance phase (N=13).

Cond.	Cond.	Mean Difference	Std. Error	Sig.	95% Confidence Interval for Difference	
					Lower Bound	Upper Bound
1.5HH	2.5HH	11.401*	2.742	.013	1.999	20.804
	3.5HH	14.872*	3.048	.004	4.421	25.324
	4.5HH	14.963*	2.889	.002	5.058	24.869
	5.5HH	14.038*	3.391	.014	2.414	25.662
2.5HH	1.5HH	-11.401*	2.742	.013	-20.804	-1.999
	3.5HH	3.471	1.337	.234	-1.112	8.054
	4.5HH	3.562	1.957	.937	-3.146	10.270
	5.5HH	2.637	2.043	1.000	-4.368	9.641
3.5HH	1.5HH	-14.872*	3.048	.004	-25.324	-4.421
	2.5HH	-3.471	1.337	.234	-8.054	1.112
	4.5HH	.091	1.500	1.000	-5.050	5.232
	5.5HH	-.834	1.798	1.000	-6.997	5.329
4.5HH	1.5HH	-14.963*	2.889	.002	-24.869	-5.058
	2.5HH	-3.562	1.957	.937	-10.270	3.146
	3.5HH	-.091	1.500	1.000	-5.232	5.050
	5.5HH	-.925	1.306	1.000	-5.402	3.552

6.10.1.3 Late stance phase

The 4.5HH significantly reduced soleus mean EMG activity during stance phase when compared to the 2.5, 3.5 and 5.5 cm heel heights ($p < 0.025$).

Table 6.118: Pairwise comparison of shoe conditions for soleus mean EMG activity during loading response (N=13).

Cond.	Cond.	Mean Difference	Std. Error	Sig.	95% Confidence Interval for Difference	
					Lower Bound	Upper Bound
1.5HH	2.5HH	-1.146	6.238	1.000	-22.534	20.243
	3.5HH	4.693	4.670	1.000	-11.317	20.703
	4.5HH	13.460	6.013	.449	-7.156	34.076
	5.5HH	-2.826	5.406	1.000	-21.359	15.707
2.5HH	1.5HH	1.146	6.238	1.000	-20.243	22.534
	3.5HH	5.838	4.012	1.000	-7.917	19.594
	4.5HH	14.606*	3.817	.024	1.520	27.692
	5.5HH	-1.681	4.941	1.000	-18.622	15.260
3.5HH	1.5HH	-4.693	4.670	1.000	-20.703	11.317
	2.5HH	-5.838	4.012	1.000	-19.594	7.917
	4.5HH	8.767*	2.167	.016	1.336	16.198
	5.5HH	-7.519	2.575	.128	-16.347	1.309
4.5HH	1.5HH	-13.460	6.013	.449	-34.076	7.156
	2.5HH	-14.606*	3.817	.024	-27.692	-1.520
	3.5HH	-8.767*	2.167	.016	-16.198	-1.336
	5.5HH	-16.286*	3.806	.011	-29.335	-3.238

6.10.1.4 The overall summary area for EMG activity

The results show that the 1.5HH increased overall soleus EMG activity by 9.6% when compared to control and the 4.5HH reduced overall EMG activity by 15.4% when compared to the 1.5HH test condition. The 4.5HH adaptation reduced overall EMG area by 5.8% when compared to control shoe as demonstrated in the table below.

Table 6.119: The average (\pm SD) of the area under the curves for medial gastrocnemius EMG activity for test footwear conditions (N=13).

	1.5 HH	2.5 HH	3.5 HH	4.5 HH	5.5 HH
EMG impulse (overall area of EMG activity)	109.6 (8.6)	105.5 (7.7)	100.0 (7.3)	94.2 (7.0)	105.8 (7.7)
Differences between control shoe (%)	9.6	5.5	0	-5.8	5.8

The graph shows the EMG activity of the soleus muscle during the stance phase. The y-axis represents EMG Magnitude from 0 to 120, and the x-axis represents Stance Phase (%) from 0 to 100. A solid line represents the control condition, and the area beneath it is shaded orange and labeled 'Area'. The activity starts at approximately 20 at 0% stance phase, rises to a peak of about 100 at 70% stance phase, and then declines to near 0 by 100% stance phase.

A pairwise Anova test with Bonferroni adjustment demonstrated that the 2.5HH significantly increased EMG area for soleus muscle when compared to the 4.5HH footwear test condition. The 4.5HH showed significant reduction in the soleus EMG area when compared to the control shoe ($p=0.008$).

Table 6.120: Pairwise comparison of shoe conditions for soleus overall area EMG activity during stance phase (N=13).

Cond.	Cond.	Mean Difference	Std. Error	Sig.	95% Confidence Interval for Difference	
					Lower Bound	Upper Bound
1.5HH	2.5HH	4.060	3.262	1.000	-7.123	15.243
	3.5HH	9.588	4.541	.564	-5.982	25.158
	4.5HH	15.374	4.662	.064	-.610	31.357
	5.5HH	3.814	5.936	1.000	-16.538	24.166
2.5HH	1.5HH	-4.060	3.262	1.000	-15.243	7.123
	3.5HH	5.528	3.054	.953	-4.941	15.998
	4.5HH	11.313*	3.176	.039	.423	22.204
	5.5HH	-.246	4.076	1.000	-14.219	13.727
3.5HH	1.5HH	-9.588	4.541	.564	-25.158	5.982
	2.5HH	-5.528	3.054	.953	-15.998	4.941
	4.5HH	5.785*	1.311	.008	1.292	10.279
	5.5HH	-5.774	2.299	.273	-13.655	2.107
4.5HH	1.5HH	-15.374	4.662	.064	-31.357	.610
	2.5HH	-11.313*	3.176	.039	-22.204	-.423
	3.5HH	-5.785*	1.311	.008	-10.279	-1.292
	5.5HH	-11.559*	2.160	.002	-18.966	-4.153

6.10.1.5 Summary of soleus EMG activity alteration produced heel heights of the sole:

- The 1.5HH increased EMG activity within 10-65% of the stance phase versus all footwear profiles by initiating premature activation. The hypothesis (H_{a2}) is positively accepted;
- During LR the 1.5HH test condition significantly increased soleus EMG activity when compared to all footwear conditions;
- During mid-stance phase the 1.5HH significantly increased maximum soleus EMG activity when compared to all footwear conditions ($p < 0.015$);
- During stance phase the 4.5HH significantly reduced soleus mean EMG activity during stance phase when compared to the 2.5, 3.5 and 5.5 cm heel heights ($p < 0.025$). The hypothesis (H_{a2}) is positively accepted;
- The results show that the 1.5HH increased overall soleus EMG activity by 9.6% when compared to control and the 4.5HH reduced overall EMG activity by 15.4% when compared to the 1.5HH. The 4.5HH reduced overall EMG area by 5.8% when compared to control shoe;
- The 4.5HH showed a significant reduction of the soleus EMG area when compared to the control shoe ($p = 0.008$) which positively confirmed (H_{a2}) hypothesis;
- The 2.5HH significantly increased EMG area for soleus muscle when compared to the 4.5HH footwear condition.

6.10.2 The effect of altering rocker sole apex position (AP)

Figure 6.27 illustrates the alteration to the soleus EMG activity induced by the apex length sole changes. The 55AP test condition caused reduction in maximum soleus EMG activity and slightly altered the point during stance phase where maximum EMG activity occurred when compared to control.

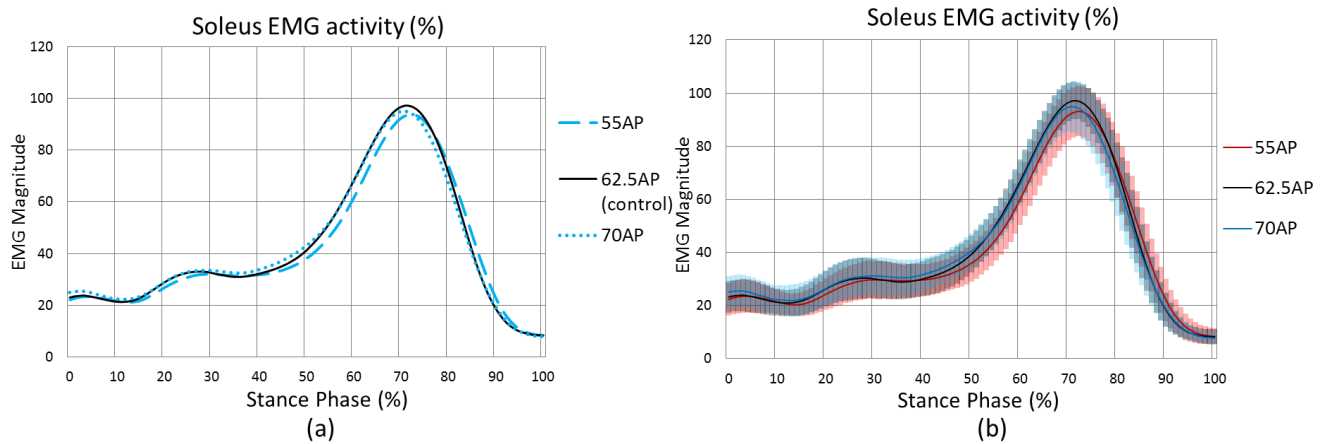


Figure 6.32: The soleus EMG activity for test footwear conditions (N=13). (a) – without standard deviation (STD), (b) – with the lines shadowed to represent STD ranges.

The mean results for maximum EMG RMS activity for different footwear conditions during different part of the stance phase are demonstrated in the table below.

Table 6.121: Mean (\pm SD) medial gastrocnemius EMG activity for test footwear conditions.

	55AP	62.5AP	70AP
Maximum EMG activity during LR (%)	29.6 (6.5)	31.2 (7.1)	32.8 (8.4)
Maximum EMG activity during mid-stance (%)	41.5 (6.8)	44.1 (7.1)	46.4 (7.4)
Maximum EMG activity during stance phase (%)	96.2 (9.2)	100.0 (6.5)	98.5 (8.2)

Loading response

The results did not show any statistical significant difference between the test conditions.

Mid-stance phase

The 55AP demonstrated significant mean EMG reduction when compared to the 70AP footwear during mid-stance phase ($p=0.042$).

Table 6.122 : Pairwise comparison of shoe conditions for soleus mean EMG activity during mid-stance phase (N=13).

Cond.	Cond.	Mean Difference	Std. Error	Sig.	95% Confidence Interval for Difference	
					Lower Bound	Upper Bound
55AP	62.5AP	-2.586	1.589	.389	-7.002	1.831
	70 AP	-4.824*	1.676	.042	-9.483	-.165
62.5AP	55AP	2.586	1.589	.389	-1.831	7.002
	70 AP	-2.239	1.000	.135	-5.019	.542

Late stance phase

The results did not show any statistical significant difference between the test conditions.

6.10.2.1 Overall summary area of EMG activity

There were no significant changes in the area of EMG activity.

Table 6.123: The average (\pm SD) of the overall area under the curves for soleus EMG activity for test footwear conditions (N=13).

	55AP	62.5AP	70AP
EMG impulse (overall area of EMG activity %)	98.7 (6.8)	100.0 (7.3)	99.7 (8.3)
Differences between control shoe (%)	-1.3	0	-0.3

6.10.2.2 Summary of soleus EMG activity alteration produced apex length of testing footwear conditions:

- During mid-stance phase the 55AP demonstrated significant mean EMG reduction when compared to the 70AP footwear during mid-stance phase ($p=0.042$). The (H_0) hypothesis is rejected;
- The maximum peak EMG activity was not significantly altered and so the (H_0) hypothesis is rejected.

6.10.3 The effect of altering apex angle (toe angle-TA)

Figure 6.33 illustrates the alteration to the soleus EMG activity induced by the apex toe angle changes. From the figure below, it can be seen maximum EMG activity reduction for the 20° angled-toe shoe versus control.

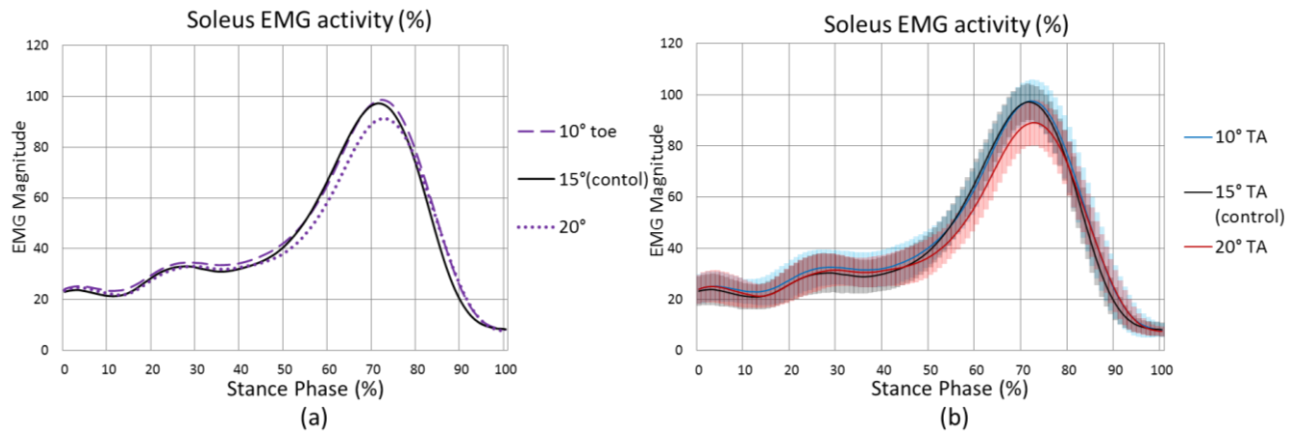


Figure 6.33: The soleus EMG activity for test footwear conditions (N=13). (a) – without standard deviation (STD), (b) – with the lines shadowed to represent STD ranges.

The mean results for maximum EMG RMS activity for different footwear conditions during different part of the stance phase are presented in the table below.

Table 6.124: Mean (\pm SD) soleus EMG activity for test footwear conditions.

	10° TA	15° TA	20° TA
Max EMG activity during LR (%)	33.3 (7.4)	31.2 (7.1)	30.9 (7.2)
Max EMG activity during mid-stance (%)	46.4 (7.9)	44.1 (7.1)	42.5 (7.7)
Max EMG activity during stance phase (%)	102.3 (7.6)	100.0 (6.5)	94.2 (8.0)

Loading response

The results did not show any statistically significance alterations.

Mid-stance phase

The results did not show any statistically significance alterations.

Stance phase

The 20° TA shoe significantly reduced maximum EMG activity when compared to the 10° TA ($p=0.023$).

Table 6.125: Pairwise comparison of shoe conditions for soleus mean EMG activity during stance phase (N=13).

Cond.	Cond.	Mean Difference	Std. Error	Sig.	95% Confidence Interval for Difference	
					Lower Bound	Upper Bound
10° TA	15° TA	2.309	1.923	.759	-3.036	7.653
	20° TA	8.142*	2.542	.023	1.075	15.208
15° TA	10° TA	-2.309	1.923	.759	-7.653	3.036
	20° TA	5.833	2.885	.198	-2.185	13.851
20° TA	10° TA	-8.142*	2.542	.023	-15.208	-1.075
	15° TA	-5.833	2.885	.198	-13.851	2.185

The overall summary area for EMG activity

The 10° toe angle footwear increased the overall area of soleus EMG activity by 5.7% when compared to the 20° toe angle footwear as demonstrated in table 6.126.

Table 6.126: The average (\pm SD) of the overall area under the curves for soleus EMG activity for test footwear conditions (N=13).

	10° TA	15° TA	20° TA
EMG impulse (overall area of EMG activity %)	102.5 (7.4)	100.0 (7.3)	96.8 (8.8)
Differences between control shoe (%)	2.5	0	-3.2

Statistical results are not significant.

6.10.3.1 Summary of soleus EMG activity alteration produced by apex toe angle footwear conditions:

- The 20° TA shoe significantly reduced soleus maximum EMG activity when compared to the 10° TA ($p=0.023$) and positively confirmed the (H_{a2}) hypothesis;
- The 10° toe angle footwear increased the overall area of soleus EMG activity by 5.7% when compared to the 20° toe angle footwear test condition.

6.10.4 The effect of altering heel curves

Figure 6.34 illustrates the alteration to the soleus EMG activity induced by the curvature of the heel. The figure below visually shows that the full heel curve footwear test condition

resulted in increase of soleus EMG activity within 0-40% of the stance phase when compared to the other footwear test conditions. The half curve heeled shoe reduced maximum soleus EMG activity when compared to control shoe and a slightly less effect was seen for the full curved heel.

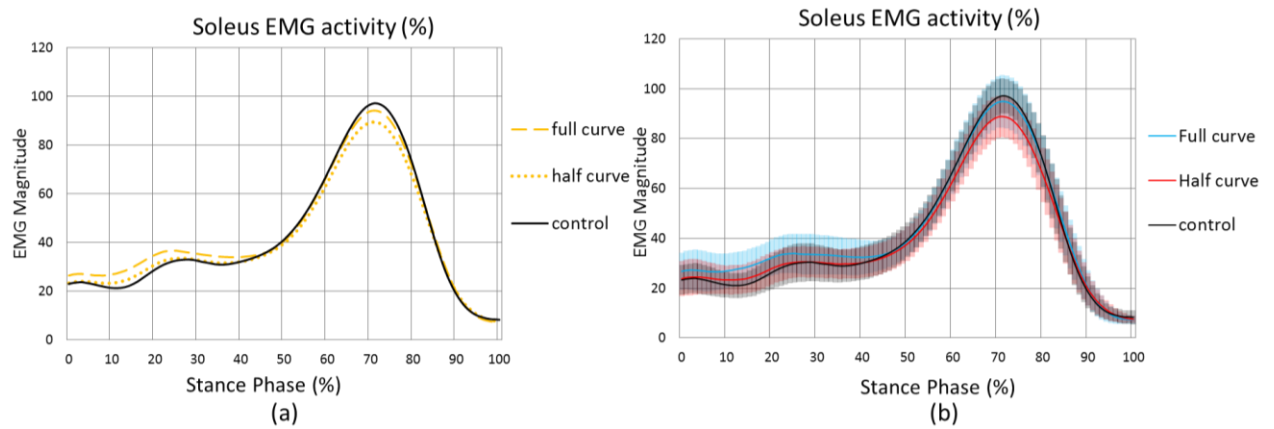


Figure 6.34: The soleus EMG activity for test footwear conditions (N=13). (a) – without standard deviation (STD), (b) – with the lines shadowed to represent STD ranges.

The mean results for maximum EMG RMS activity for different footwear conditions during different part of the stance phase are demonstrated in the table below.

Table 6.127: Mean (\pm SD) soleus EMG activity for test footwear conditions.

	Full curve	Half curve	control
Max EMG activity during LR (%)	39.9 (8.1)	33.9 (8.4)	31.2 (7.1)
Max EMG activity during mid-stance (%)	47.9 (9.1)	43.3 (7.1)	44.1 (7.1)
Max EMG activity during stance phase (%)	97.5 (9.8)	92.9 (7.2)	100.0 (6.5)

Loading response

The results did not show any statistically significance alterations.

Mid-stance phase

The results did not show any statistically significance alterations.

Stance phase

The results did not show any statistically significance alterations.

The overall summary area for EMG activity

The half curved heel footwear test condition reduced the overall EMG area by 5.1% when compared to the control shoe with no heel curve added.

Table 6.128: The average (\pm SD) of the overall area under the curves for medial gastrocnemius EMG activity for test footwear conditions (N=14).

	Full curve	Half curve	control
EMG impulse (overall area of EMG activity %)	100.9 (7.7)	94.9 (8.1)	100.0 (7.3)
Differences between control shoe (%)	0.9	-5.1	0

The results did not show any statistically significance alterations.

6.10.4.1 Summary of soleus EMG activity alteration produced by curved heel test conditions.

- The half curve footwear reduced the overall EMG area by 5.1% when compared to the control shoe with no heel curve.
- The full curved heel footwear test condition resulted in an overall increase of soleus EMG activity within 0-40% of the stance phase when compared to the other footwear test conditions. The (H_{a2}) hypothesis is accepted.

6.10.5 The effect of altering rocker profile stiffness at metatarsal area

Figure 6.35 illustrates the alteration to the soleus muscle EMG activity induced by the flexibility of the sole. The picture below shows that the medium flexible footwear slightly increased maximum soleus muscle EMG activity when compared to all footwear conditions. However, statistical analysis did not show any significant results for the whole stance phase.

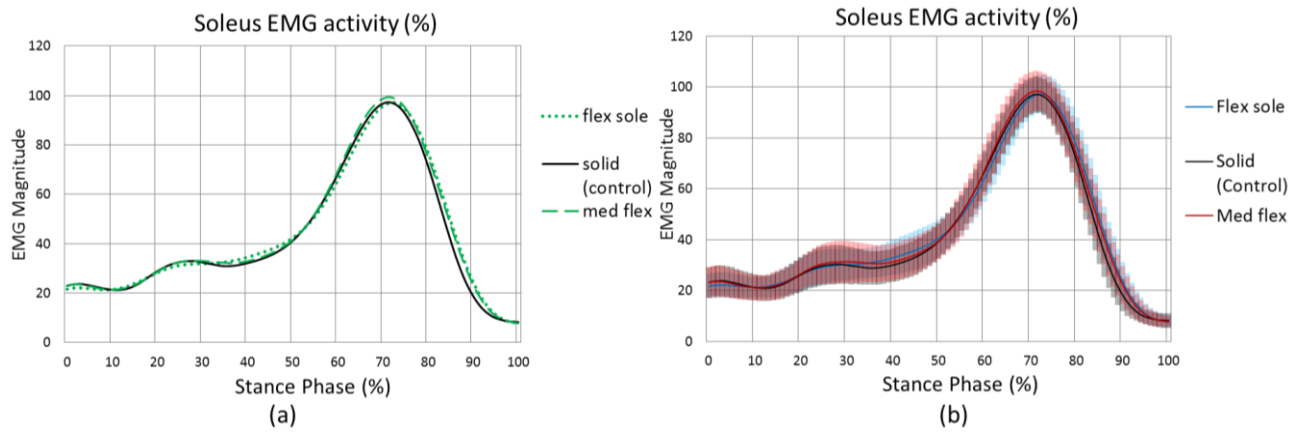


Figure 6.35: The soleus EMG activity for test footwear conditions (N=13). (a) – without standard deviation (STD), (b) – with the lines shadowed to represent STD ranges.

The mean results for maximum EMG RMS activity for different footwear conditions during different part of the stance phase are presented in the table below.

Table 6.129: Mean (\pm SD) soleus EMG activity for test footwear conditions.

	Flex sole	Med. flex	Solid
Max EMG activity during LR (%)	31.0 (6.1)	31.0 (7.9)	31.2 (7.1)
Max EMG activity during mid-stance (%)	45.1 (7.2)	45.3 (8.4)	44.1 (7.1)
Max EMG activity during stance phase (%)	100.4 (6.9)	103.1 (6.6)	100.0 (6.5)

Loading response

The results did not show any statistically significance alterations.

Mid-stance phase

The results did not show any statistically significance alterations.

Stance phase

The results did not show any statistically significance alterations.

The overall summary area for EMG activity

Table 6.130: The average (\pm SD) of the overall area under the curves for soleus EMG activity for test footwear conditions (N=14).

	Flex sole	Med. flex	Solid
EMG impulse (overall area of EMG activity %)	99.9 (7.3)	101.7 (7.2)	100.0 (7.3)
Differences between control shoe (%)	-0.1	1.7	0

The results did not show any statistical significant differences between each other and rejected the generated hypothesis in chapter 4 (H_0 2).

6.11 Tibialis anterior electromyography results

6.11.1 The effect of walking with different heel heights

Figure 6.36 illustrates the alteration to the tibialis anterior EMG RMS values for the heel height test conditions. It can be seen that negative heel profiles reduced tibialis anterior EMG activity when compared to higher heels.

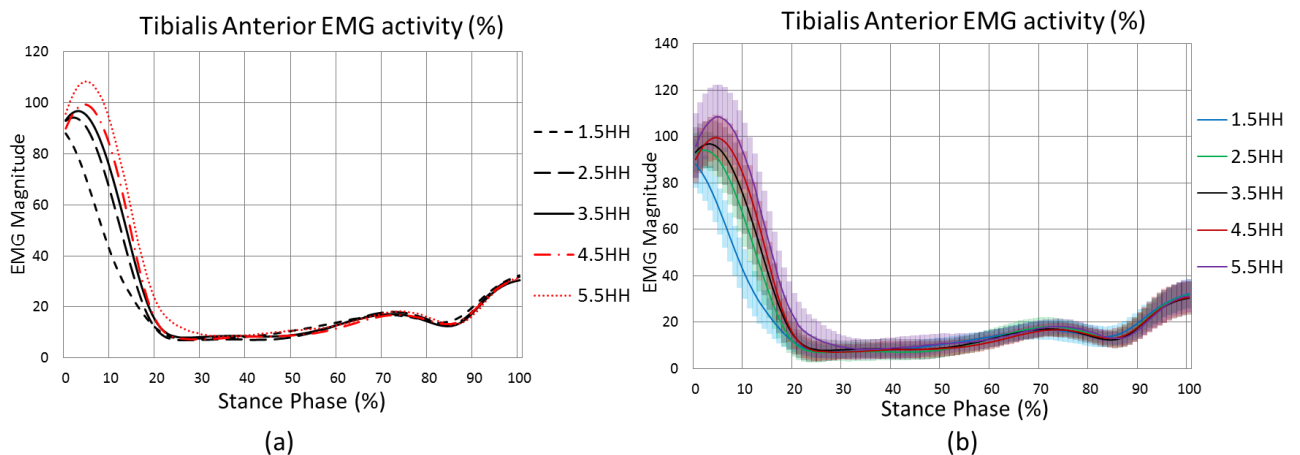


Figure 6.36: The tibialis anterior EMG activity for test footwear conditions (N=14). (a) – without standard deviation (STD), (b) – with the lines shadowed to represent STD ranges. The mean results for maximum EMG RMS activity for different footwear conditions during different parts of stance phase are demonstrated in table 6.131.

Table 6.131: Mean (\pm SD) tibialis anterior EMG activity for test footwear conditions.

	1.5 HH	2.5 HH	3.5 HH	4.5 HH	5.5 HH
Maximum EMG activity during stance phase (%)	88.6 (10.2)	96.7 (8.0)	100.0 (10.3)	101.7 (9.9)	112.1 (13.5)
EMG impulse (overall area of EMG activity)	80.1 (10.8)	94.3 (12.8)	100.0 (12.1)	104.3 (11.6)	114.2 (12.7)
Differences between control shoe (%)	-19.9	-5.7	0	4.3	14.2

Loading response

The 1.5HH significantly reduced mean soleus EMG activity when compared to 4.5HH ($p=0.036$) and 5.5HH ($p=0.003$) as shown in table 6.132.

Table 6.132: Pairwise comparison of shoe conditions for tibialis mean EMG activity during loading response (N=14).

Cond.	Cond.	Mean Difference	Std. Error	Sig.	95% Confidence Interval for Difference	
					Lower Bound	Upper Bound
1.5HH	2.5HH	-8.104	5.751	1.000	-27.500	11.292
	3.5HH	-11.406	4.506	.251	-26.601	3.789
	4.5HH	-13.133*	3.704	.036	-25.625	-.641
	5.5HH	-23.484*	4.721	.003	-39.406	-7.563
2.5HH	1.5HH	8.104	5.751	1.000	-11.292	27.500
	3.5HH	-3.302	2.631	1.000	-12.176	5.573
	4.5HH	-5.029	5.503	1.000	-23.589	13.531
	5.5HH	-15.380	4.982	.087	-32.183	1.422
3.5HH	1.5HH	11.406	4.506	.251	-3.789	26.601
	2.5HH	3.302	2.631	1.000	-5.573	12.176
	4.5HH	-1.727	3.565	1.000	-13.751	10.296
	5.5HH	-12.079	4.035	.104	-25.687	1.530
4.5HH	1.5HH	13.133*	3.704	.036	.641	25.625
	2.5HH	5.029	5.503	1.000	-13.531	23.589
	3.5HH	1.727	3.565	1.000	-10.296	13.751
	5.5HH	-10.351	3.200	.065	-21.142	.439

The overall summary area for EMG activity

The results show that the 1.5HH reduced tibialis anterior area EMG activity by 19.9% when compared to the control shoe ($p=0.001$) and produced a significant reduction against the

other test conditions; especially by 34.1% when compared with the 5.5HH test condition ($p < 0.000$). The 3.5HH significantly reduced tibialis anterior area EMG activity by 14.2% when compared with the 5.5HH ($p = 0.016$) as shown in the table below.

Table 6.133: Pairwise comparison of shoe conditions for tibialis overall area EMG activity during stance phase (N=14).

Cond.	Cond.	Mean Difference	Std. Error	Sig.	95% Confidence Interval for Difference	
					Lower Bound	Upper Bound
1.5HH	2.5HH	-14.250*	3.137	.006	-24.828	-3.671
	3.5HH	-19.902*	3.731	.001	-32.485	-7.320
	4.5HH	-24.215*	4.660	.002	-39.931	-8.500
	5.5HH	-34.091*	4.092	.000	-47.893	-20.290
2.5HH	1.5HH	14.250*	3.137	.006	3.671	24.828
	3.5HH	-5.653	2.714	.575	-14.804	3.499
	4.5HH	-9.966	4.233	.350	-24.243	4.312
	5.5HH	-19.842*	4.165	.004	-33.887	-5.797
3.5HH	1.5HH	19.902*	3.731	.001	7.320	32.485
	2.5HH	5.653	2.714	.575	-3.499	14.804
	4.5HH	-4.313	2.885	1.000	-14.042	5.417
	5.5HH	-14.189*	3.585	.016	-26.281	-2.097
4.5HH	1.5HH	24.215*	4.660	.002	8.500	39.931
	2.5HH	9.966	4.233	.350	-4.312	24.243
	3.5HH	4.313	2.885	1.000	-5.417	14.042
	5.5HH	-9.876	3.800	.221	-22.692	2.940

6.11.1.1 Summary of tibialis anterior EMG activity alteration produced heel heights of the sole:

- The 1.5HH significantly reduced mean soleus EMG activity when compared to the 4.5 and 5.5 cm heel height shoe test conditions ($p < 0.037$) as shown in the table below. The (H_0) hypothesis is rejected;
- The results show that the low heel profile gradually reduced tibialis anterior EMG activity impulse value (the positive area under the curve) to a significant level by altering the heel to 1.5 cm in depth. Higher heel profiles demonstrated an increase in EMG impulse for the tibialis anterior muscle. The (H_0) hypothesis is accepted.

6.11.2 The effect of altering rocker sole apex position (AP)

Figure 6.32 illustrates the alteration to the tibialis anterior EMG activity induced by the sole apex length (position) changes.

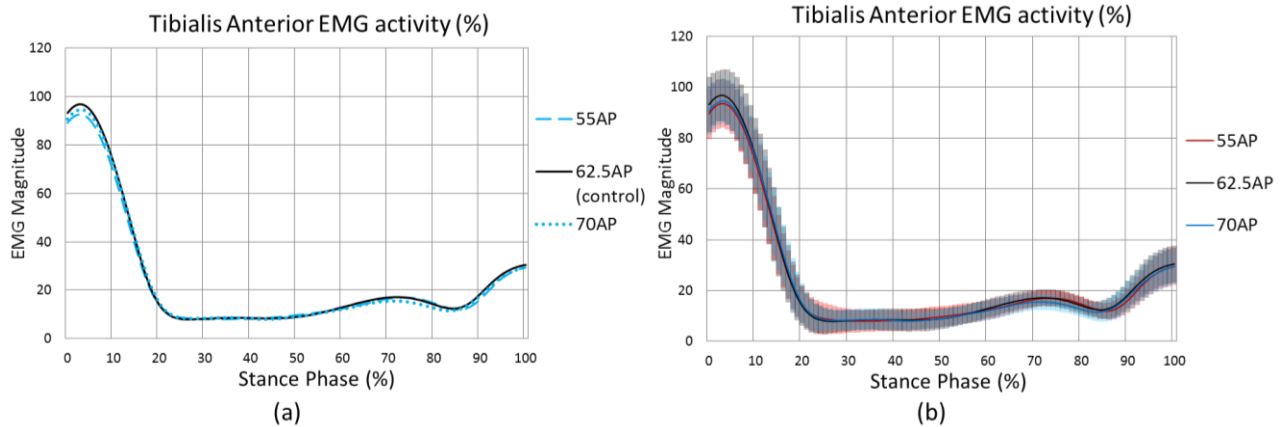


Figure 6.37: The tibialis anterior EMG activity for test footwear conditions (N=14). (a) – without standard deviation (STD), (b) – with the lines shadowed to represent STD ranges. The mean results for maximum EMG RMS activity for different footwear conditions are demonstrated in the table below.

Table 6.134 Mean (\pm SD) tibialis anterior EMG activity for test footwear conditions.

	55AP	62.5AP	70AP
Max EMG activity during stance phase	95.1 (9.2)	100.0 (10.3)	97.7 (8.7)
EMG impulse (overall area of EMG activity)	96.5 (12.2)	100.0 (12.1)	98.5 (12.0)
Differences between control shoe (%)	-3.5	0	-1.5

The results did not show any statistically significant differences between the test conditions and the (H_{a2}) hypothesis is rejected.

6.11.3 The effect of altering apex angle (toe angle-TA)

Figure 6.38 illustrates the alteration to the tibialis anterior EMG activity induced by the apex toe angle changes.

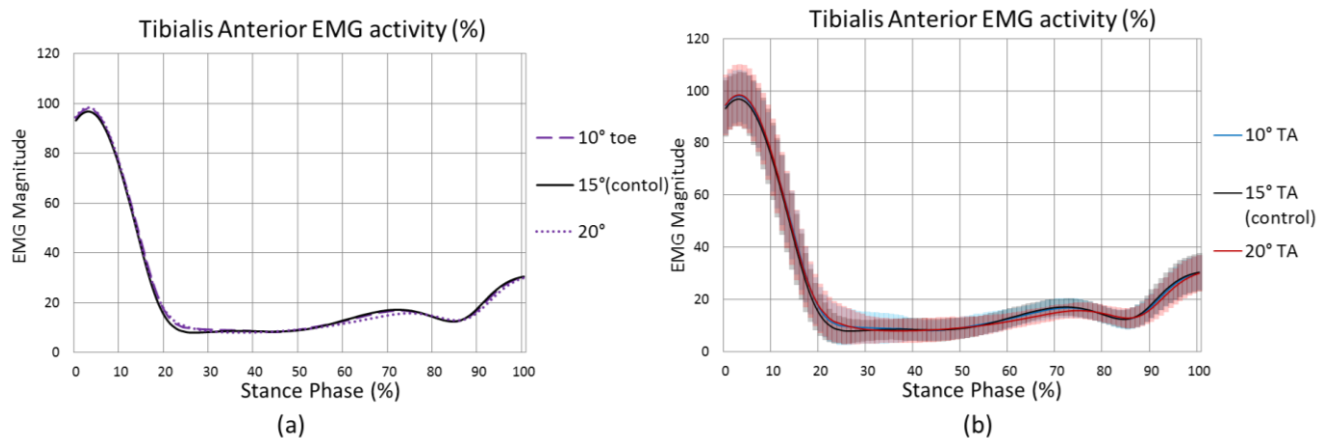


Figure 6.38: The tibialis anterior EMG activity for test footwear conditions (N=14). (a) – without standard deviation (STD), (b) – with the lines shadowed to represent STD ranges.

The mean results for maximum EMG RMS activity for different footwear conditions are presented in the table below.

Table 6.135: Mean (\pm SD) tibialis anterior EMG activity for test footwear conditions.

	10° TA	15° TA	20° TA
Max EMG activity during stance phase	101.6 (9.4)	100.0 (10.3)	101.0 (11.5)
EMG impulse (overall area of EMG activity)	101.4 (11.6)	100.0 (12.1)	100.7 (12.8)
Differences between control shoe (%)	1.4	0	0.7

The results did not show any statistically significant differences between the test conditions and the (H_{a2}) hypothesis is rejected.

6.11.4 The effect of altering heel curve

Figure 6.39 illustrates the alteration to the tibialis anterior EMG activity induced by the curvature of the heel. The figure below visually shows that the curved-heel footwear conditions resulted in reduction of mean tibialis anterior EMG activity when compared to the control shoe without a heel curve.

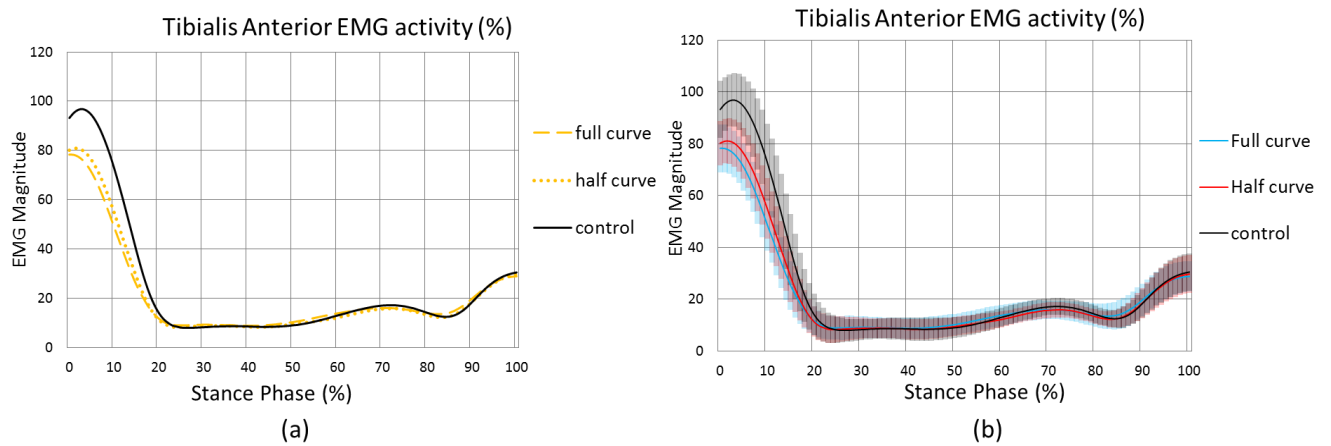


Figure 6.39: The tibialis anterior EMG activity for test footwear conditions (N=14). (a) – without standard deviation (STD), (b) – with the lines shadowed to represent STD ranges. The mean results for maximum EMG RMS activity for different footwear conditions are shown in the table below.

Table 6.136: Mean (\pm SD) tibialis anterior EMG activity for test footwear conditions.

	Full curve	Half curve	control
Maxi EMG activity during stance phase	79.9 (9.1)	83.0 (8.7)	100.0 (10.3)
EMG impulse (overall area of EMG activity)	84.1 (12.9)	86.3 (11.8)	100.0 (12.1)
Differences between control shoe (%)	-15.9	-13.7	0

6.11.4.1 Loading response

The control shoe without a curve significantly increased mean tibialis anterior EMG activity during loading response when compared to the other footwear conditions with curved heels ($p < 0.000$).

Table 6.137: Pairwise comparison of shoe conditions for tibialis mean EMG activity during loading response (N=14).

Cond.	Cond.	Mean Difference	Std. Error	Sig.	95% Confidence Interval for Difference	
					Lower Bound	Upper Bound
Full curve	Half curve	-3.038	2.766	.876	-10.635	4.559
	No curve	-20.067*	2.824	.000	-27.820	-12.313
Half curve	Full curve	3.038	2.766	.876	-4.559	10.635
	No curve	-17.029*	2.841	.000	-24.829	-9.228

The overall summary area for EMG activity

The full heel curve footwear reduced the overall EMG area for the tibialis anterior muscle by 15.9% ($p < 0.000$) and the half curved-heel shoe reduced it by 13.7% ($p = 0.001$) when compared to the control shoe.

6.11.4.2 Summary of tibialis anterior EMG activity alteration produced by curved heel test conditions

- The control shoe significantly increased mean tibialis anterior EMG activity during loading response when compared to footwear conditions with curved-heels ($p < 0.000$);
- The full curve footwear reduced overall EMG area by 15.9% ($p < 0.000$) and the half curved-heel shoe reduced it by 13.7% ($p = 0.001$) when compared to the control shoe without a curve;
- It confirmed the hypothesis that curvature of the heel may reduce tibialis anterior maximum EMG activity.

6.11.5 The effect of altering rocker profile stiffness at metatarsal area

Figure 6.40 illustrates the alteration to the tibialis anterior muscle EMG activity induced by the flexibility of the sole. It shows that flexible footwear profiles reduced mean tibialis anterior EMG activity when compared to a solid sole (control shoe).

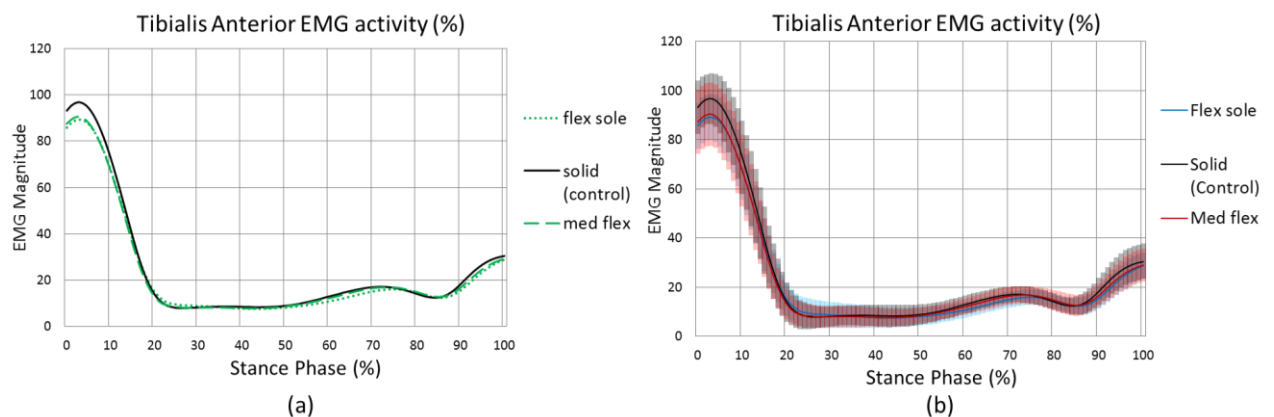


Figure 6.40: The tibialis anterior EMG activity for test footwear conditions (N=14). (a) – without standard deviation (STD), (b) – with the lines shadowed to represent STD ranges.

The mean results for maximum EMG RMS activity for different footwear conditions are presented in the table below.

Table 6.138 Table: Mean (\pm SD) tibialis anterior EMG activity for test footwear conditions.

	Flex sole	Med. flex	Solid
Max EMG activity during stance phase	91.6 (9.6)	93.6 (12.2)	100.0 (10.3)
EMG impulse (overall area of EMG activity)	92.0 (12.8)	93.9 (12.5)	100.0 (7.3)
Differences between control shoe (%)	-8.0	-6.1	0

The solid sole showed significant increase tibialis anterior EMG activity when compared to the flexible shoe ($p=0.003$) and medium flexibility shoe ($p=0.04$) as shown in the table below.

Table 6.139: Pairwise comparison of shoe conditions for tibialis mean EMG activity during loading response (N=14).

Cond.	Cond.	Mean Difference	Std. Error	Sig.	95% Confidence Interval for Difference	
					Lower Bound	Upper Bound
Flex sole	Med. flex	-1.959	2.112	1.000	-7.760	3.841
	Solid	-8.382*	1.946	.003	-13.725	-3.039
Med. flex	Flex sole	1.959	2.112	1.000	-3.841	7.760
	Solid	-6.423*	2.247	.040	-12.593	-.253

The overall summary area for EMG activity

The solid shoe significantly increased overall tibialis anterior EMG activity by 8% when compared to a flexible sole profile.

Table 6.140: Pairwise comparison of shoe conditions for tibialis overall area EMG activity during stance phase (N=14).

Cond.	Cond.	Mean Difference	Std. Error	Sig.	95% Confidence Interval for Difference	
					Lower Bound	Upper Bound
Flex sole	Med. flex	-1.893	2.869	1.000	-9.772	5.985
	Solid	-8.015*	2.112	.007	-13.815	-2.214
Med. flex	Flex sole	1.893	2.869	1.000	-5.985	9.772
	Solid	-6.121	2.335	.063	-12.533	.290

6.11.5.1 Summary results for tibialis anterior EMG results altered by footwear stiffness level at metatarsal area:

- The solid-soled showed significantly increased tibialis anterior EMG activity when compared to a flexible shoe ($p=0.003$) and a medium flexibility shoe ($p=0.040$). The (H_{a2}) hypothesis is accepted;
- The solid shoe significantly increased overall tibialis anterior EMG activity by 8% when compared to the flexible sole profile.

6.12 Achilles muscle moment arm

6.12.1 The effect of altering heel height of the sole on Achilles muscle moment arm

Figure 6.41, illustrates the alteration produced to the Achilles muscle moment arm by the heel height test conditions. The results shows that low heel kept the muscle moment arm shorter when compared to raised heels. The red line represents the Achilles muscle moment arm length at barefoot standing (the natural position where the foot is parallel to the ground). The closest position to the barefoot standing at which muscle is not shortened or lengthened during powerful ankle contraction at the late stance phase is the 4.5HH footwear condition.

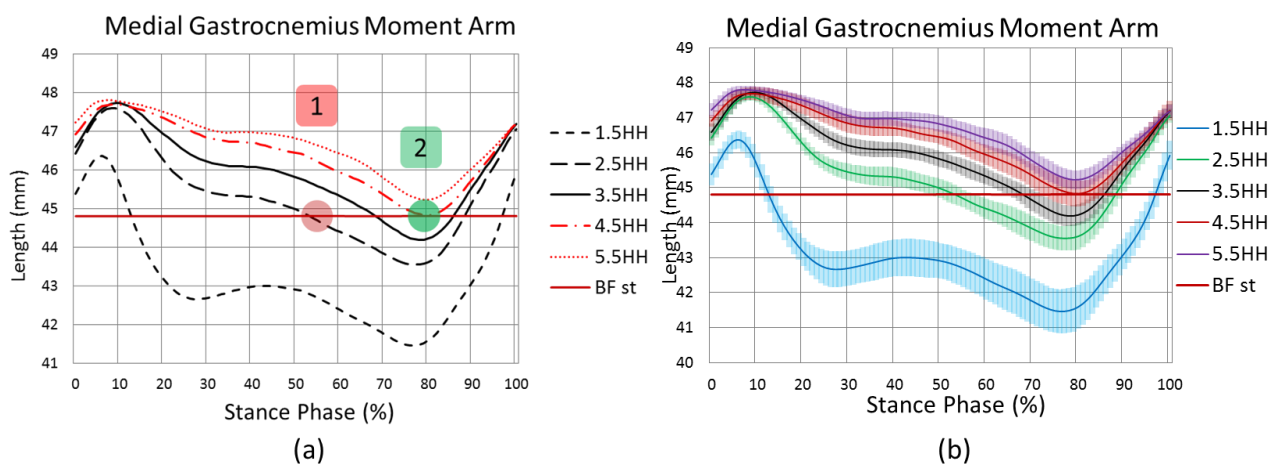


Figure 6.41: The Achilles muscle moment arm length for different heel height test footwear conditions (N=14). Legend 1 indicates the point at which the muscle moment arm is at its maximum at 55% of stance phase, where the calf muscles are starting to generate force by eccentric contraction and gradually increasing the external DF ankle moment required for

ankle movement; legend 2 indicates the mean muscle moment arm at which the peak EMG occurs.

The results for the Achilles muscle moment arm change within highlighted points of interest are demonstrated in the table below.

Table 6.141: Mean (\pm SD) Achilles muscle moment arm (mm) for heel height test footwear conditions (N=14).

Maximum ROM Achilles moment arm for all footwear conditions used for this study (mm)					7.04
	1.5 HH	2.5 HH	3.5 HH	4.5 HH	5.5 HH
Maximum moment arm length during 55% of stance phase (mm)	42.70 (0.54)	44.69 (0.25)	45.58 (0.24)	46.21 (0.26)	46.64 (0.23)
Differences between control 3.5HH shoe (mm)	-4.15 (0.54)	-0.89 (0.25)	0.00 (0.24)	0.63 (0.26)	1.06 (0.23)
Maximum moment arm length during peak force generation (mm)	40.95 (0.56)	43.39 (0.34)	44.11 (0.30)	44.67 (0.28)	44.99 (0.29)
Differences between control 3.5HH shoe (mm)	-3.16 (0.56)	-0.72 (0.34)	0.00 (0.30)	0.55 (0.28)	0.88 (0.29)

6.12.1.1 Maximum moment arm length during 55% of stance phase.

All heel heights showed significant changes in the Achilles muscle moment arm when compared to the other conditions ($p < 0.001$). A significant gradual increase in muscle moment arm from low heel to high was demonstrated. The maximum length change with all the footwear conditions in this study was 7.04 mm for the Achilles muscle moment arm.

6.12.1.2 Maximum moment arm length during peak force generation.

With raising the heel the muscle moment arm was significantly increased ($p < 0.004$) for all test conditions, except for the 4.5HH and the 5.5HH which did not show any significant difference between each other. However, it is difficult to choose level of significance for the muscle moment arm value because a small change can increase the internal muscle moment more significantly, if more muscle force was applied.

6.12.1.3 Summary results for Achilles muscle moment arm changes affected by heel heights:

- The Achilles muscle moment arm was significantly increased with raising heel heights at 55% of stance phase and peak force generation by the calf muscle and the (Ha4) hypothesis is accepted;
- The 4.5 heel height kept the muscle moment arm closer to its natural position at which there is no calf lengthening or shortening at peak calf muscle force generation. The (Ha4) hypothesis is accepted.

6.12.2 The effect of altering rocker sole apex position (AP) on Achilles muscle moment arm

Figure 6.42, illustrates the alteration to the Achilles muscle moment arm by the apex length of the shoe. The 55AP kept the muscle moment arm longer between 20-100% of stance phase versus the other apex position footwear conditions. It can be seen that the 55AP increased length of the Achilles muscle moment arm at propulsion performed by the calf muscle.

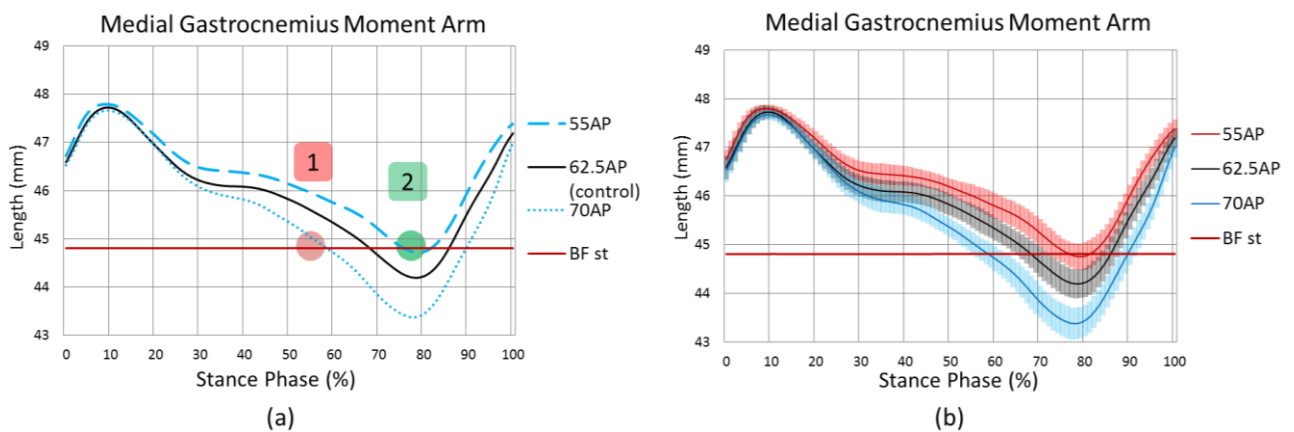


Figure 6.42: The Achilles muscle moment arm length analysis for different apex length test footwear conditions (N=14). Legend 1 indicates maximum muscle moment arm at 55% of stance phase; legend 2 indicates the mean muscle moment arm at the position where the peak EMG occurs. (a) – without standard deviation (STD), (b) – with the lines shadowed to represent STD ranges.

Table 6.142: Mean (\pm SD) Achilles muscle moment arm (mm) for apex length test footwear conditions (N=14).

Maximum ROM Achilles moment arm for all footwear conditions used for this study (mm)	7.04		
	55AP	62.5AP	70AP
Maximum moment arm length during 55% of stance phase (mm)	45.95 (0.23)	45.58 (0.24)	45.03 (0.22)
Differences between control 3.5HH shoe (mm)	0.37 (0.23)	0.00 (0.24)	-0.55 (0.22)
Maximum moment arm length during peak force generation (mm)	44.59 (0.26)	44.11 (0.30)	43.26 (0.33)
Differences between control 3.5HH shoe (mm)	0.48 (0.26)	0.00 (0.30)	-0.86 (0.33)

6.12.2.1 Maximum moment arm length during 55% of stance phase

The short apex length (55AP) test condition resulted in a significant increase in the Achilles muscle moment arm at 55% stance phase versus 62.5% and 70% ($P < 0.023$) as shown in the table below.

Table 6.143: Pairwise comparison the Achilles muscle moment arm changes at 55% stance phase for test footwear conditions (N=14).

Cond.	Cond.	Mean Difference	Std. Error	Sig.	95% Confidence Interval for Difference	
					Lower Bound	Upper Bound
55AP	62.5AP	.374*	.118	.023	.048	.699
	70 AP	.929*	.096	.000	.666	1.191
62.5AP	55AP	-.374*	.118	.023	-.699	-.048
	70 AP	.555*	.109	.001	.256	.854

6.12.2.2 Maximum moment arm length during peak force generation

The 55AP footwear significantly increased the length of the moment arm at peak muscle force generation when compared to the 62.5AP and 70AP ($p < 0.021$).

6.12.2.3 Summary results for AP changes in the Achilles muscle moment arm:

- The 55AP test condition kept the muscle moment arm longer between 20-100% of stance phase versus all footwear conditions;
- The 55AP footwear significantly increased the length of the moment arm at peak muscle force generation when compared to the 62.5AP and 70AP test conditions ($p < 0.021$). It accepted the hypothesis that the 55AP placed ankle angle at earlier plantarflexion during terminal stance which resulted in increase the length of Achilles tendon moment arm when compared to longer apex position of the sole. The (Ha4) hypothesis is accepted.

6.12.3 The effect of altering apex toe angle of the sole on Achilles muscle moment arm

Figure 6.43, illustrates the alteration to the Achilles muscle moment arm by the toe angle footwear test conditions. The figure below shows that the 10 degrees toe angle reduced the Achilles moment arm from 20-100% of stance phase versus the 15 and 20 degrees toe-angled footwear conditions. The 20 degrees toe angle shoe slightly increased the moment arm between 80-95% of stance phase when compared to the control shoe.

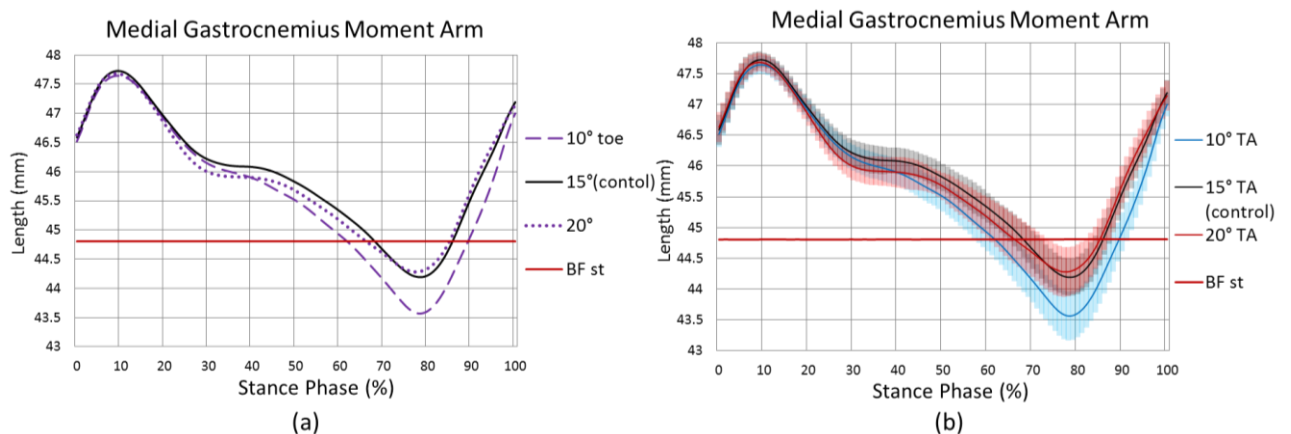


Figure 6.43: The Achilles muscle moment arm length for different toe apex angle test footwear conditions (N=14). Legend 1 indicates maximum muscle moment arm at 55% of the stance; legend 2 indicates mean muscle moment arm at which the peak EMG occurs. (a) – without standard deviation (STD), (b) – with the lines shadowed to represent STD ranges.

The results for the Achilles muscle moment arm change within highlighted points of interest are demonstrated in the table below.

Table 6.144: Mean (\pm SD) Achilles muscle moment arm (mm) for toe angle test footwear conditions (N=14).

Maximum ROM Achilles moment arm for all footwear conditions used for this study (mm)	7.04		
	10° TA	15° TA	20° TA
Maximum moment arm length during 55% of stance phase (mm)	45.21 (0.26)	45.58 (0.24)	45.42 (0.28)
Differences between control 3.5HH shoe (mm)	-0.37 (0.26)	0.00 (0.24)	-0.16 (0.28)
Maximum moment arm length during peak force generation (mm)	43.48 (0.37)	44.11 (0.30)	44.12 (0.37)
Differences between control 3.5HH shoe (mm)	-0.64 (0.37)	0.00 (0.30)	0.01 (0.37)

6.12.3.1 Maximum moment arm length during 55% of stance phase

The 10° TA reduced the length of the Achilles moment arm to a significant level when compared to the control shoe at 55% of stance phase ($p=0.028$).

6.12.3.2 Maximum moment arm length during peak force generation

The 10° TA reduced length of the Achilles moment arm to significant level when compared to control ($p=0.01$) and reduced it when compared to the 20° TA test condition ($p=0.03$) as shown in table 6.145.

Table 6.145: Pairwise comparison the Achilles muscle moment arm changes during peak force generation of the ankle for test footwear conditions (N=14).

Cond.	Cond.	Mean Difference	Std. Error	Sig.	95% Confidence Interval for Difference	
					Lower Bound	Upper Bound
10° TA	15° TA	-.635*	.128	.001	-.986	-.285
	20° TA	-.673*	.159	.003	-1.110	-.235
15° TA	10° TA	.635*	.128	.001	.285	.986
	20° TA	-.037	.130	1.000	-.395	.320

6.12.3.3 Summary for toe angle alteration to rocker shoes:

- The 10 degree toe angle reduced the Achilles moment arm from 20-100% of the stance phase versus the 15 and 20 degrees toe-angled footwear conditions;
- The 20 degree toe angle shoe slightly increased the moment within 80-95% stance phase when compared to control shoe. The (H_{a4}) hypothesis is rejected.

6.12.4 The effect of altering heel curve of the sole on Achilles muscle moment arm

Figure 6.44, illustrates the alteration to the Achilles muscle moment arm by the heel curvature footwear test conditions. The curvature of the heel resulted in shortening the Achilles moment arm within the whole of stance phase when compared to the control shoe.

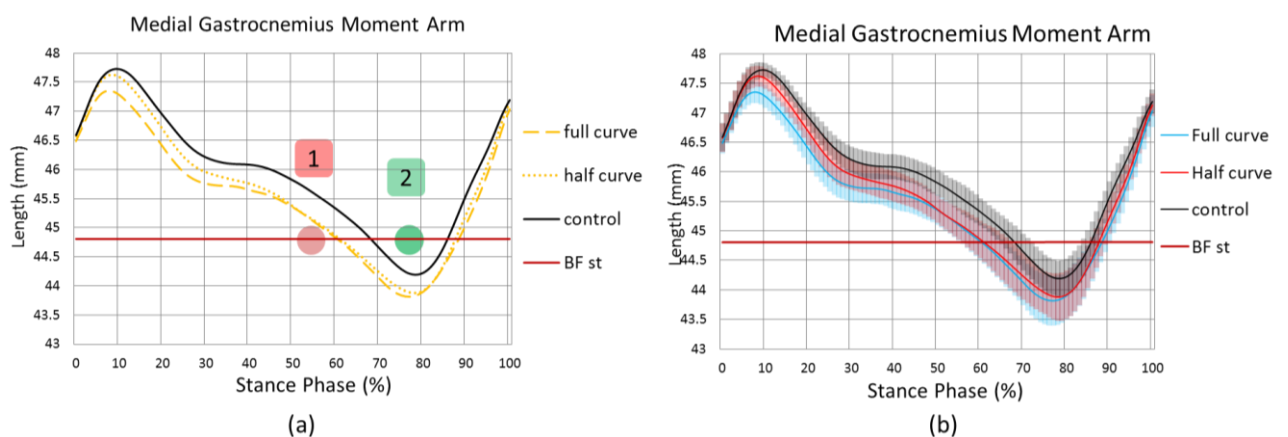


Figure 6.44: The Achilles muscle moment arm length for the different curved-heel test footwear conditions where control shoe has no curve (N=14). (a) – without standard deviation (STD), (b) – with the lines shadowed to represent STD ranges.

The results for the Achilles muscle moment arm change within highlighted points of interest are demonstrated in the table below.

Table 6.146: Mean (\pm SD) Achilles muscle moment arm (mm) for curved-heel test footwear conditions (N=14).

Maximum ROM Achilles moment arm for all footwear conditions used for this study (mm)			7.04
	Full curve	Half curve	control
Maximum moment arm length during 55% of stance phase (mm)	45.09 (0.26)	45.12 (0.27)	45.58 (0.24)
Differences between control 3.5HH shoe (mm)	-0.49 (0.26)	-0.46 (0.27)	0.00 (0.24)
Maximum moment arm length during peak force generation (mm)	43.68 (0.36)	45.12 (0.27)	44.11 (0.30)
Differences between control 3.5HH shoe (mm)	-0.43 (0.36)	-0.34 (0.27)	0.00 (0.30)

6.12.4.1 Maximum moment arm length during 55% of stance phase

The control shoe (without curve on the heel) significantly increased the Achilles moment arm at 55% stance phase when compared to full and half curved heel footwear conditions ($p < 0.004$).

6.12.4.2 Maximum moment arm length during peak force generation

The control shoe without any heel curve increased the moment arm to a significant level when compared to both the curved heel test conditions during the phase of peak ankle force generation performed by the calf muscles ($p < 0.048$).

6.12.4.3 Summary of results for curved heel footwear test conditions:

- A curvature of the heel resulted in shortening of the Achilles moment arm within the whole of stance phase when compared to the control shoe;
- The control shoe without a curved heel increased the moment arm to a significant level when compared to both the curved heel test conditions at 55% stance phase ($p < 0.004$). The (H_{a4}) hypothesis is accepted;
- The control shoe increased the moment arm to a significant level when compared to both the curved heeled shoes during the peak ankle force generation phase performed by the calf muscle ($p < 0.048$). The (H_{a4}) hypothesis is accepted;

6.12.5 The effect of altering rocker profile stiffness at metatarsal area on Achilles muscle moment arm

Figure 6.45, illustrates the alteration to the Achilles muscle moment arm by the flexibility of the sole where control shoe has solid sole.

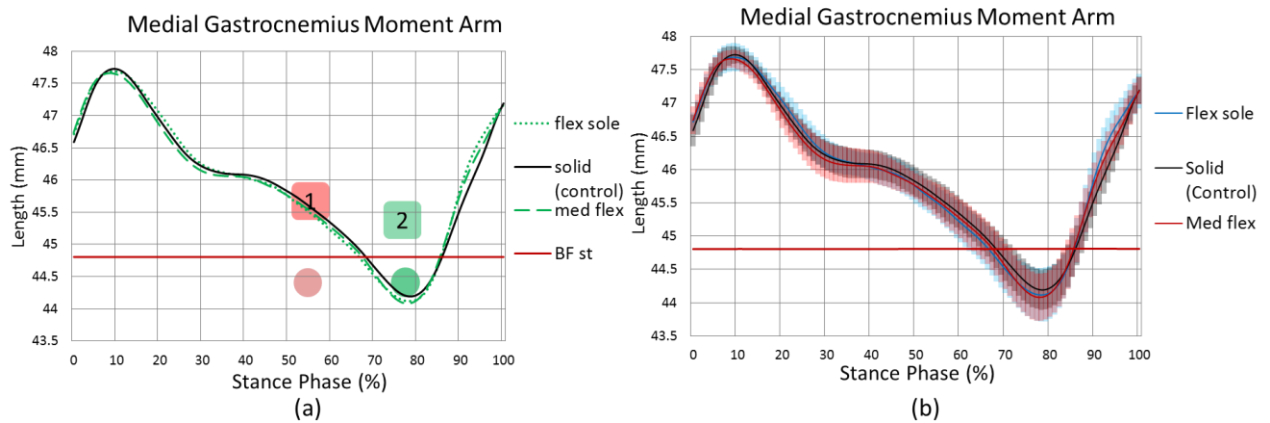


Figure 6.45: The Achilles muscle moment arm length analysis results from OpenSim software for different flexibility levels of the sole (N=14). Legend 1 indicates maximum muscle moment arm at 55% of the stance phase which approximates to the position where the calf muscles are starting to generate powerful force; legend 2 indicates the mean muscle moment arm at which the peak EMG occurs. (a) – without standard deviation (STD), (b) – with the lines shadowed to represent STD ranges.

The results for the Achilles muscle moment arm change within the highlighted points of interest are demonstrated in table 6.147.

Table 6.147: Mean (\pm SD) Achilles muscle moment arm (mm) for different flexibility of the sole (N=14).

Maximum ROM Achilles moment arm for all footwear conditions used for this study (mm)			7.04
	Flex sole	Med. flex	Solid
Maximum moment arm length during 55% of stance phase (mm)	45.49 (0.24)	45.52 (0.26)	45.58 (0.24)
Differences between control 3.5HH shoe (mm)	-0.19 (0.24)	-0.06 (0.26)	0.00 (0.24)
Maximum moment arm length during peak force generation (mm)	43.92 (0.34)	43.92 (0.35)	44.11 (0.30)
Differences between control 3.5HH shoe (mm)	-0.19 (0.34)	-0.19 (0.35)	0.00 (0.30)

6.12.5.1 Maximum moment arm length during 55% of stance phase

No significant differences in the data were calculated. The (H_{a4}) hypothesis is rejected.

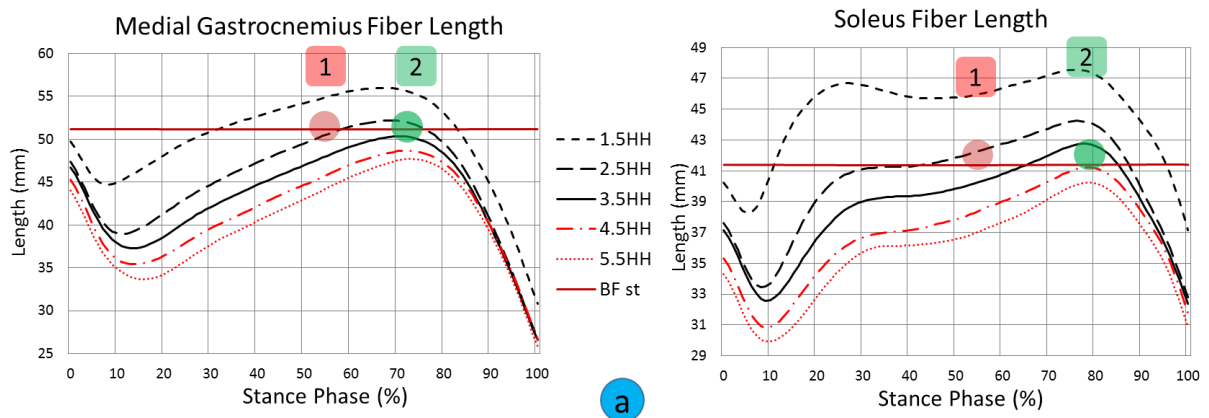
6.12.5.2 Maximum moment arm length during peak force generation

No significant differences in the data were noted. The (H_{a4}) hypothesis is rejected.

6.13 Gastrocnemius and Soleus fibre length alteration

6.13.1 Heel Height (HH)

Figure 6.46, illustrates the alteration to the MG and Soleus fibre lengths by the heel height test conditions. The soleus fibre length is only related to ankle joint movement but gastrocnemius muscle is also related to the knee flexion. The barefoot static position (red line) for the soleus muscle shows the neutral position (optimal position when it is not shortened or lengthened) of the ankle at which maximum force can be generated. The 4.5HH placed ankle at the position where fibre length for soleus is at optimal length position during peak force generation (point 2). The 1.5 HH is too stretched during stance phase and raised heel reduce length of MG and soleus fibres during whole stance phase.



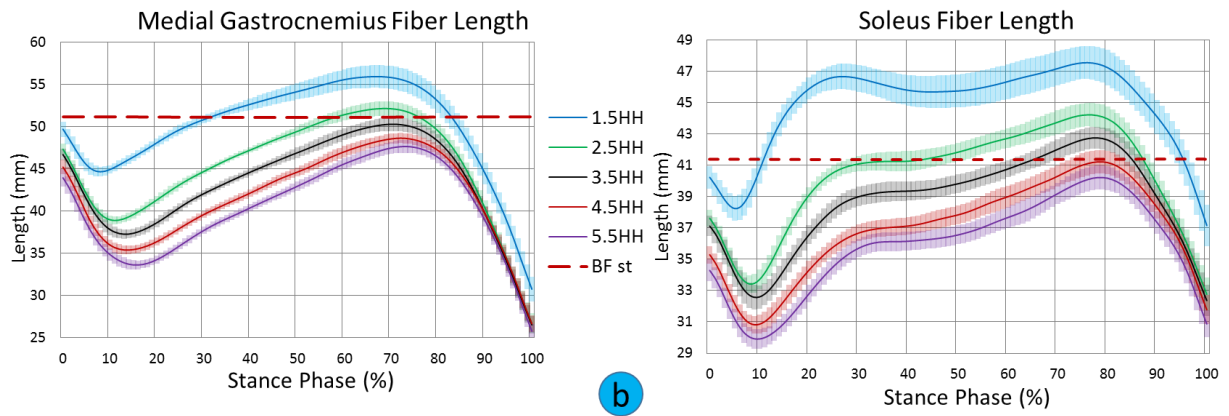


Figure 6.46: The fibre length alteration results data from OpenSim simulation software for different heel height test footwear conditions (N=14). The red line represents fibre lengths at the barefoot static position. Legend 1 indicates maximum fibre length at 55% of stance phase which approximates to where the calf muscles start to generate powerful force; legend 2 indicates the mean fibre length at which the peak EMG occurs. (a) – without standard deviation (STD), (b) – with the lines shadowed to represent STD ranges.

The average results for the changes in fibre lengths of GM and soleus muscles within the highlighted points of interest are demonstrated in table 6.148.

Table 6.148: MG and soleus fibre length (mm) mean (\pm SD) for heel height test footwear conditions (N=14).

	1.5 HH	2.5 HH	3.5 HH	4.5 HH	5.5 HH
Medial Gastrocnemius					
Maximum fibre length at 55% of stance phase (mm)	54.93 (1.11)	50.57 (0.63)	48.07 (0.72)	45.88 (0.61)	44.31 (0.56)
Differences between control 3.5HH shoe (mm)	6.85 (1.11)	2.49 (0.63)	0.00 (0.72)	-2.20 (0.61)	-3.76 (0.56)
Maximum fibre length during peak force generation (mm)	56.31 (1.29)	52.45 (0.88)	50.47 (0.83)	48.80 (0.63)	47.77 (0.77)
Differences between control 3.5HH shoe (mm)	5.85 (1.29)	1.99 (0.88)	0.00 (0.83)	-1.66 (0.63)	-2.70 (0.77)
Soleus					
Maximum fibre length at 55% of stance phase (mm)	45.98 (1.16)	42.31 (0.64)	40.26 (0.63)	38.42 (0.69)	37.05 (0.65)
Differences between control 3.5HH shoe (mm)	5.72 (1.16)	2.05 (0.64)	0.00 (0.63)	-1.84 (0.69)	-3.21 (0.65)
Maximum fibre length during peak force generation (mm)	47.89 (1.07)	44.48 (0.77)	42.89 (0.69)	41.44 (0.75)	40.40 (0.81)
Differences between control 3.5HH shoe (mm)	5.00 (1.07)	2.05 (0.77)	0.00 (0.69)	-1.84 (0.75)	-3.21 (0.81)

6.13.1.1 Maximum fibre length during peak calf muscle force generation

All footwear altered by using different heel heights produced significant changes in GM and soleus fibre lengths when compared to each other ($p < 0.003$). A significant gradual lengthening (stretching) of MG and soleus fibre lengths was noted when walking from high heeled to low heeled shoes.

6.13.1.2 Summary of the results for MG and soleus fibre length changes affected by heel heights:

- All footwear features altered by heel height showed significant changes in GM and soleus fibre lengths when compared to each other ($p < 0.003$). A significant gradual lengthening (stretching) of MG and soleus fibre lengths from high heels to low heels was demonstrated. The (H_04) hypothesis is accepted;
- The 4.5HH placed the ankle at the position where the fibre length for soleus is at its optimal length/position during peak force generation (point 2);
- The 1.5HH shoe test condition altered soleus muscle fibres length to increase at 35% of the stance phase, then shortening until 50% of stance phase and then lengthening again. There were no similar alterations for other footwear conditions.

6.13.2 Apex position (AP)

Figure 6.47, illustrates the alteration to the MG and soleus fibre lengths by rocker apex position shoe test conditions. The medial gastrocnemius fibre length is stretching with a fairly constant and similar velocity; probably due to concurrent knee flexion. The soleus fibre length changes to isometric contraction at 20% of stance phase and then rapid lengthens at terminal stance phase. The 55% AP footwear shows that fibre length at peak muscle generation at point 2 is more stretched when compared to the control and 70AP footwear.

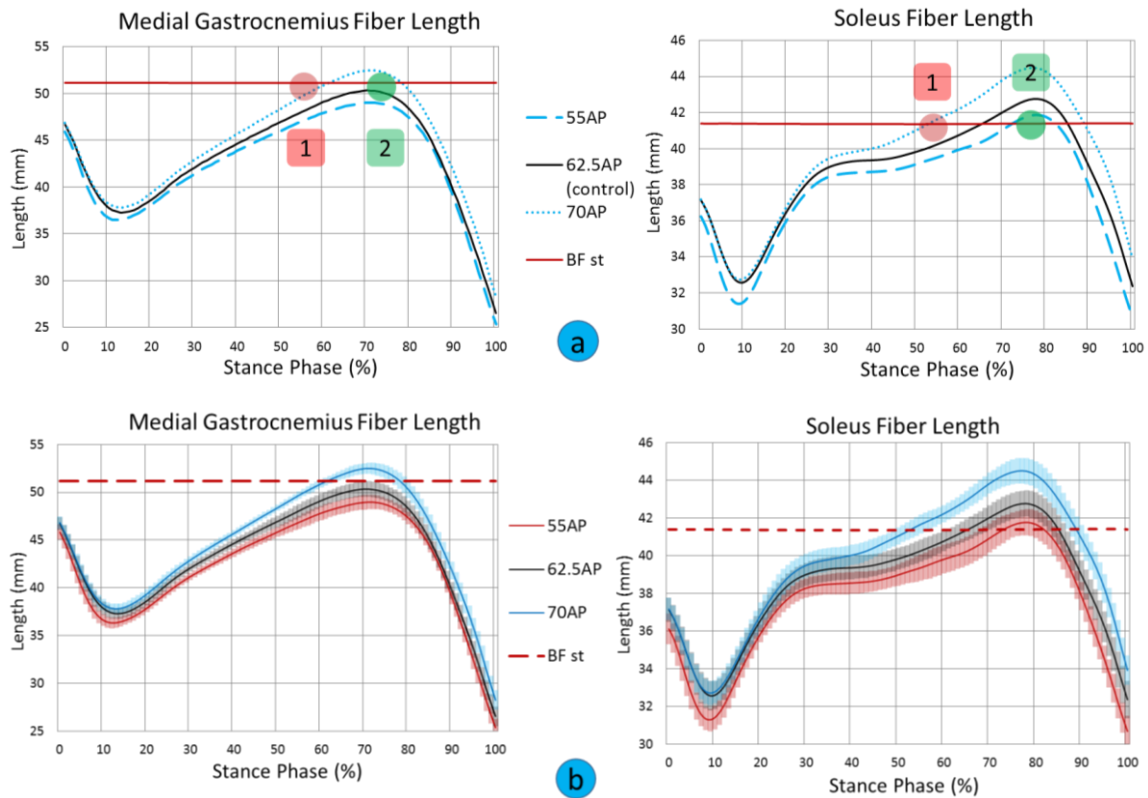


Figure 6.47: The fibre length alteration results from OpenSim simulation software for different AP test footwear conditions (N=14). The red line represent fibre lengths at the barefoot static position. Legend 1 indicates maximum fibre length at 55% of stance phase which approximates to the position where the calf muscles are starting to generate powerful force; legend 2 indicates mean fibre length at which the peak EMG occurs. (a) – without standard deviation (STD), (b) – with the lines shadowed to represent STD ranges. The average results for the fibre lengths of GM and soleus muscles change within highlighted points of interest are demonstrated in table 6.149.

Table 6.149: MG and soleus fibre length (mm) mean (\pm SD) for the AP test footwear conditions (N=14).

	55AP	62.5AP	70AP
Medial Gastrocnemius			
Max fibre length at 55% of stance phase (mm)	47.04 (0.70)	48.07 (0.72)	49.71 (0.37)
Differences between control 3.5HH shoe (mm)	-1.03 (0.70)	0.00 (0.72)	1.64 (0.37)
Max fibre length during peak force generation (mm)	49.15 (0.74)	50.47 (0.83)	52.68 (0.60)
Differences between control 3.5HH shoe (mm)	-1.32 (0.74)	0.00 (0.83)	2.21 (0.60)
Soleus			
Max fibre length at 55% of stance phase (mm)	39.53 (0.76)	40.26 (0.63)	41.67 (0.54)
Differences between control 3.5HH shoe (mm)	-0.73 (0.76)	0.00 (0.63)	1.41 (0.54)
Max fibre length during peak force generation (mm)	42.03 (0.73)	42.89 (0.69)	44.73 (0.74)
Differences between control 3.5HH shoe (mm)	-0.86 (0.73)	0.00 (0.69)	1.41 (0.74)

6.13.2.1 Maximum fibre length during peak calf muscle force generation

The 62.5AP footwear significantly increased MG fibre length at peak calf muscle force generation when compared to the 55AP ($p < 0.001$) and significantly reduced GM fibre length when compared to the 70AP footwear ($p < 0.001$).

The 55AP footwear did not reach significant shortening of soleus fibre length when compared to the control shoe ($p = 0.07$). However, the significance level should be low for the fibres length because 10% of shortening can reduce force generation of skeletal muscles by 50%. The 70AP footwear significantly stretched soleus fibres when compared to both footwear conditions ($p < 0.000$) as shown in table 6.150.

Table 6.150: Pairwise comparison the soleus fibre length changes during peak force generation of the ankle for test footwear conditions (N=14).

Cond.	Cond.	Mean Difference	Std. Error	Sig.	95% Confidence Interval for Difference	
					Lower Bound	Upper Bound
10° TA	15° TA	-.857	.337	.070	-1.783	.069
	20° TA	-2.700*	.219	.000	-3.302	-2.098
15° TA	10° TA	.857	.337	.070	-.069	1.783
	20° TA	-1.843*	.261	.000	-2.560	-1.127

6.13.2.2 Summary results for MG and soleus fibre lengths changes affected by apex length of the sole:

- The 55% apex position shoe shows that the soleus fibre lengths are close to their natural position at which peak force is generated during push off phase;
- The 62.5AP footwear significantly increased MG fibre length at peak calf muscle force generation when compared to the 55AP ($p < 0.001$) and significantly reduced GM fibre length when compared to the 70AP footwear ($p < 0.001$). This answered the hypothesis that shorter apex length resulted in less calf muscle stretching when compared to longer AP. The hypothesis (H_{a4}) is accepted.

6.13.3 Toe angle (TA)

Figure 6.48 shows the alteration to the MG and soleus fibre lengths by toe angle of the shoe. Figure shows that the 10 degree toe angle footwear increased MG and soleus fibre length (stretched) during terminal stance and push-off phase when compared to the 15 and 20 degree toe angle shoe test conditions.

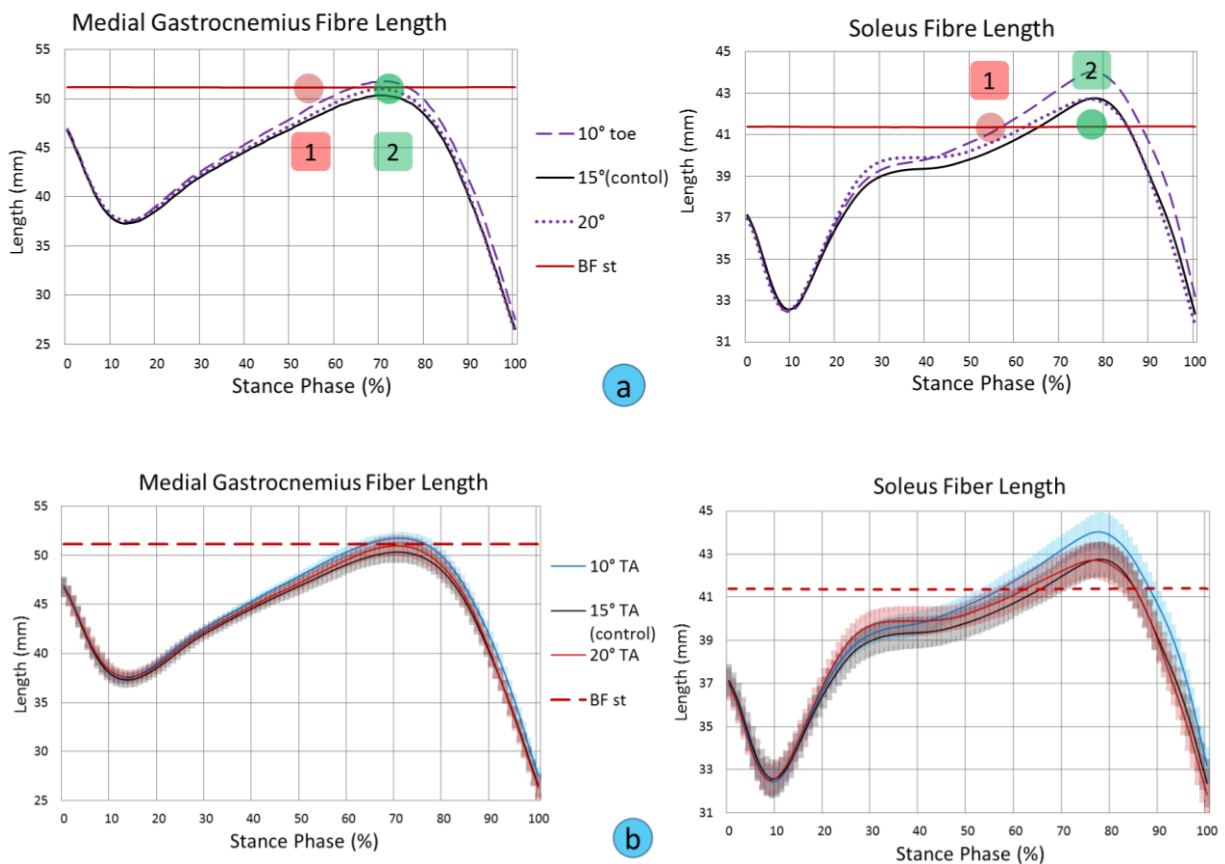


Figure 6.48: The fibre length alteration results data from OpenSim simulation software for different TA test footwear conditions (N=14). Red line represent fibre lengths at barefoot static position. Legend 1 indicates maximum fibre length at 55% of the stance phase where approximately calf muscle starting to generate powerful force; legend 2 indicates mean fibre length at which the peak EMG occurs. (a) – without standard deviation (STD), (b) – with the lines shadowed to represent STD ranges.

The average results for the fibre lengths of GM and soleus muscles change within highlighted points of interest are demonstrated in table 6.151.

Table 6.151: MG and soleus fibre length (mm) mean (\pm SD) for AP test footwear conditions (N=14).

	10° TA	15° TA	20° TA
Medial Gastrocnemius			
Max fibre length at 55% of stance phase (mm)	49.28 (0.51)	48.07 (0.72)	48.47 (0.46)
Differences between control 3.5HH shoe (mm)	1.21(0.51)	0.00 (0.72)	0.40 (0.46)
Max fibre length during peak force generation (mm)	51.95 (0.65)	50.47 (0.83)	51.23 (0.81)
Differences between control 3.5HH shoe (mm)	1.48 (0.65)	50.47 (0.83)	0.76 (0.81)
Soleus			
Max fibre length at 55% of stance phase (mm)	41.15 (0.58)	40.26 (0.63)	40.66 (0.61)
Differences between control 3.5HH shoe (mm)	0.89 (0.58)	0.00 (0.63)	0.40 (0.61)
Max fibre length during peak force generation (mm)	44.23 (0.80)	42.89 (0.69)	43.01 (0.63)
Differences between control 3.5HH shoe (mm)	1.34 (0.80)	0.00 (0.69)	0.12 (0.63)

6.13.3.1 Maximum fibre length during peak calf muscle force generation

The 10°TA significantly increased GM fibre length at peak force generation by calf muscle during late stance phase when compared to control shoe ($p < 0.000$).

The 10°TA significantly increased soleus fibre length at peak force generation by calf muscle during late stance phase when compared to the 20°TA ($p < 0.000$).

6.13.3.2 Summary for toe angle alteration rocker shoes:

- The 10 degrees toe angle footwear increased MG and soleus fibre length (stretched) during terminal stance and push-off phases when compared to 15 and 20 degrees toe angle. The hypothesis (H_{a4}) is accepted.
- The 10°TA significantly increased GM fibre length at peak force generation by calf muscle during late stance phase when compared to control shoe ($p < 0.000$). The hypothesis (H_{a4}) is accepted.
- The 10°TA significantly increased soleus fibre length at peak force generation by calf muscle during late stance phase when compared to the 20°TA ($p < 0.000$). The hypothesis (H_{a4}) is not accepted.

6.13.4 Heel Curve

Figure 6.49 shows the alteration to the MG and soleus fibre lengths by heel curve of the shoe where control shoe has no curve. The curved profiles resulted in lengthening MG and soleus fibres during whole stance phase.

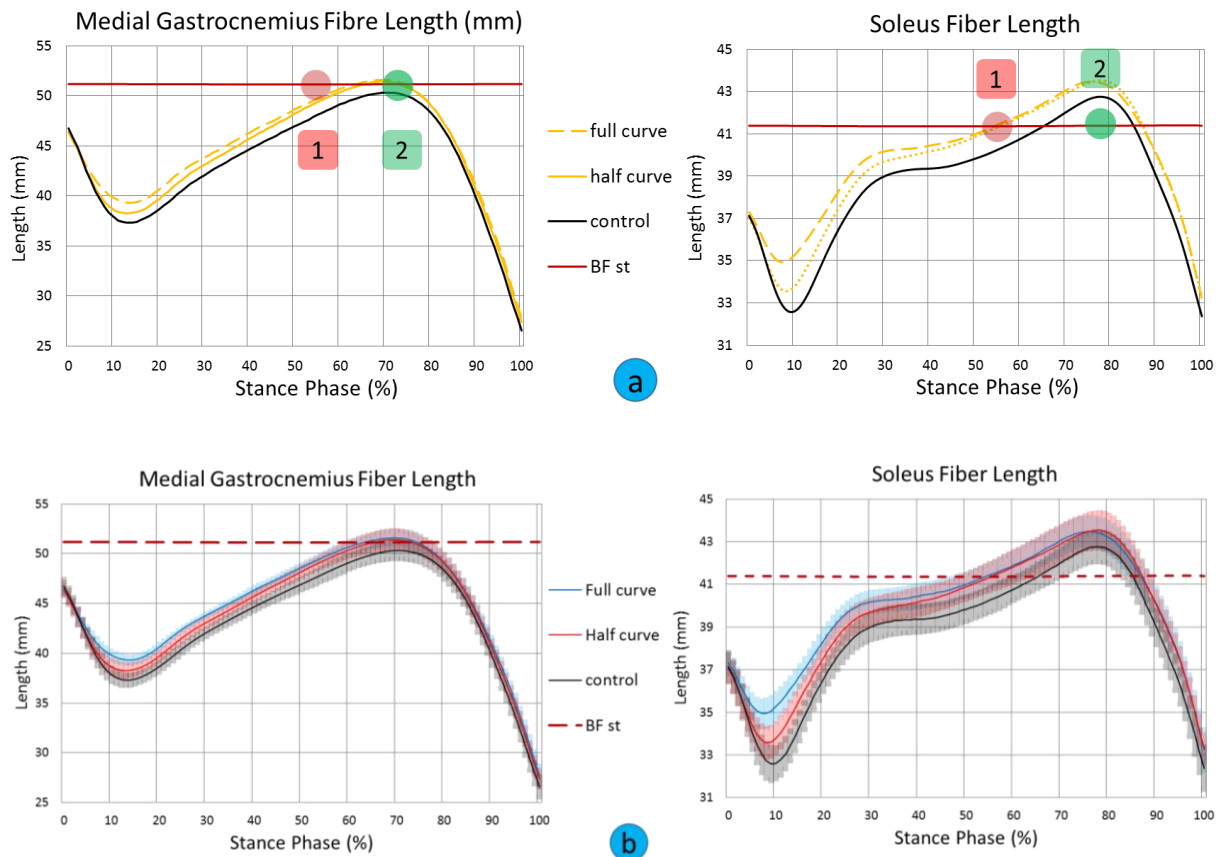


Figure 6.49: The fibre length alteration results data from OpenSim simulation software for different heel curve test footwear conditions (N=14). The red line represent fibre lengths at the barefoot static position. Legend 1 indicates maximum fibre length at 55% of stance phase which approximates to the position where the calf muscles are starting to generate powerful force; legend 2 indicates mean fibre length at which the peak EMG occurs. (a) – without standard deviation (STD), (b) – with the lines shadowed to represent STD ranges.

The average results for the fibre lengths of GM and soleus muscles change within highlighted points of interest are demonstrated in table 6.152.

Table 6.152: MG and soleus fibre length (mm) mean (\pm SD) for curved heel test footwear conditions (N=14).

	Full curve	Half curve	control
Medial Gastrocnemius			
Max fibre length at 55% of stance phase (mm)	49.73 (0.64)	49.37 (0.56)	48.07 (0.72)
Differences between control 3.5HH shoe (mm)	1.66 (0.64)	1.30 (0.56)	0.00 (0.72)
Max fibre length during peak force generation (mm)	51.90 (0.85)	51.62 (0.84)	50.47 (0.83)
Differences between control 3.5HH shoe (mm)	1.44 (0.85)	1.15 (0.84)	0.00 (0.83)
Soleus			
Max fibre length at 55% of stance phase (mm)	41.45(0.69)	41.34 (0.66)	40.26 (0.63)
Differences between control 3.5HH shoe (mm)	1.19 (0.69)	1.07(0.66)	0.00 (0.63)
Max fibre length during peak force generation (mm)	43.72 (0.73)	43.72 (0.81)	42.89 (0.69)
Differences between control 3.5HH shoe (mm)	0.83 (0.73)	0.83 (0.81)	42.89 (0.69)

6.13.4.1 Maximum fibre length during peak calf muscle force generation

The full heel curve and half heel curve shoe test conditions significantly increased GM and soleus fibre length at peak calf muscle force generation during late stance phase when compared to control shoe ($p < 0.000$).

6.13.4.2 Summary results for curved heel footwear test conditions:

- The curved heel shoes resulted in lengthening of both MG and soleus fibres during the whole of stance phase.
- The full curve and half curve rockers significantly increased GM and soleus fibre length at peak calf muscle force generation during late stance phase when compared to the control shoe ($p < 0.000$). The hypothesis (H_{a4}) is accepted.

6.13.5 Flexibility of the sole

Figure 6.50 shows the alteration to the MG and soleus fibre lengths caused by altering the flexibility of the sole.

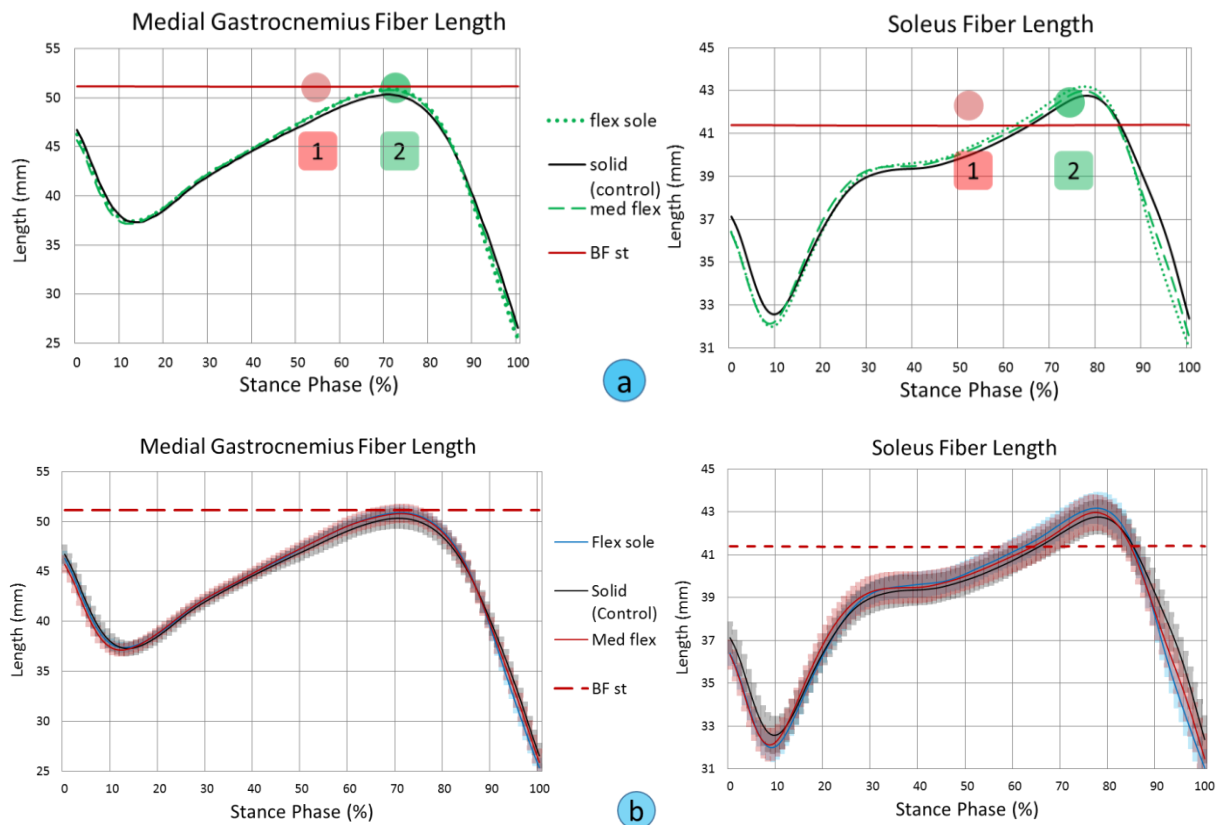


Figure 6.50: The fibre length alteration results data from OpenSim simulation software for different flexibility levels of the sole at the metatarsal area (N=14). The red line represents fibre lengths at the barefoot static position. Legend 1 indicates maximum fibre length at 55% of the stance phase where the calf muscle starts to generate powerful force; legend 2 indicates mean fibre length at which the peak EMG occurs.

The average results for the fibre lengths of GM and soleus muscles change within highlighted points of interest are demonstrated in table 6.153 below.

Table 6.153: MG and soleus fibre length (mm) mean (\pm SD) for different sole flexibility level (N=14).

	Flex sole	Med. flex	Solid
Medial Gastrocnemius			
Max fibre length at 55% of stance phase (mm)	48.52 (0.56)	48.54 (0.60)	48.07 (0.72)
Differences between control 3.5HH shoe (mm)	0.44 (0.56)	0.46 (0.60)	0.00 (0.72)
Max fibre length during peak force generation (mm)	51.06 (0.76)	50.94 (0.75)	50.47 (0.83)
Differences between control 3.5HH shoe (mm)	0.59 (0.76)	0.47 (0.75)	0.00 (0.83)
Soleus			
Max fibre length at 55% of stance phase (mm)	40.64 (0.62)	40.48 (0.68)	40.26 (0.63)
Differences between control 3.5HH shoe (mm)	0.38 (0.62)	0.22 (0.68)	0.00 (0.63)
Max fibre length during peak force generation (mm)	43.37 (0.81)	43.12 (0.78)	42.89 (0.69)
Differences between control 3.5HH shoe (mm)	0.48 (0.81)	0.23 (0.78)	0.00 (0.69)

Flexible and medium flexibility profiles did not show any significant differences for MG and soleus fibre lengths. The hypothesis (Ha4) is rejected.

6.13.5.1 MG and soleus fibre length velocity alteration by footwear features

6.13.6 Heel Height (HH)

Figure 6.51 shows the alteration to the MG and soleus fibre length velocity caused by differing heel heights.

The 1.5HH shoe test condition altered MG and soleus fibre velocity during 0-70% stance phase when compared to the other heel height test conditions. It resulted in higher EMG activity at the beginning of stance phase until terminal stance.

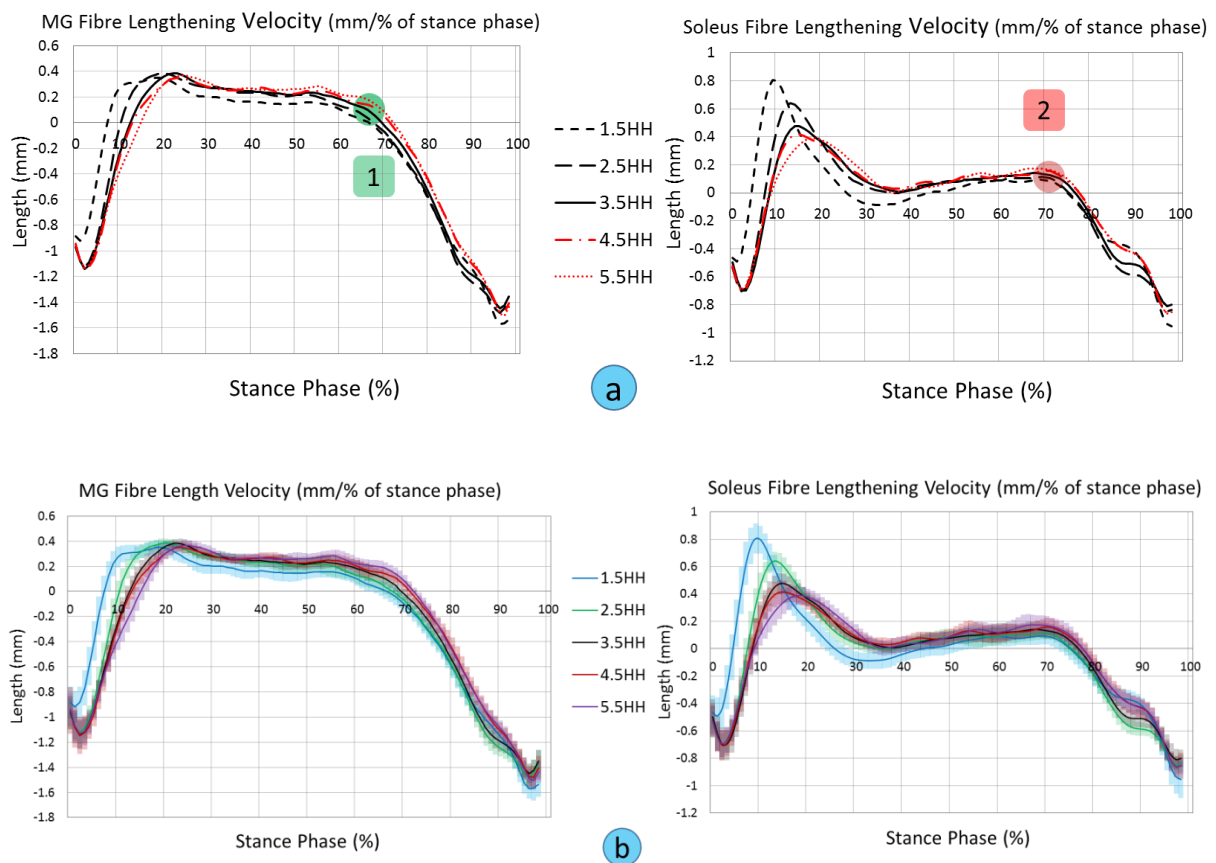


Figure 6.51: The fibre length velocity alteration results data from OpenSim simulation software for different HH test footwear conditions (N=14). Legend 1 indicates the area (68% stance phase) at which maximum EMG for MG muscle was recorded; legend 2 indicates the

area (72% stance phase) at which maximum EMG for soleus muscle was recorded. (a) – without standard deviation (STD), (b) – with the lines shadowed to represent STD ranges.

The average results for the alteration to fibre length velocity of the GM and soleus muscles cwithin the highlighted points of interest are demonstrated in table 6.154.

Table 6.154: MG and soleus fibre length velocity (mm/% of the stance phase) mean (\pm SD) for different heel heights (N=14).

	1.5 HH	2.5 HH	3.5 HH	4.5 HH	5.5 HH
Medial Gastrocnemius					
Fibre velocity at 68% stance phase where maximum MG EMG activity.	0.001 (0.080)	0.043 (0.060)	0.094 (0.054)	0.137 (0.040)	0.185 (0.054)
Soleus					
Fibre velocity at 72% stance phase where maximum Sol EMG activity.	0.07 (0.08)	0.09 (0.05)	0.12 (0.05)	0.14 (0.06)	0.15 (0.07)

6.13.6.1 Fibre velocity at 68% of stance phase where maximum MG EMG activity occurs.

The 1.5HH test condition reduced MG lengthening velocity (as calf muscle is contracting eccentrically from LR until late stance phase) at 68% of stance phase to a significant level when compared to the 3.5HH test condition ($p=0.03$). The 4.5HH test condition significantly increased MG lengthening velocity at 68% of stance phase when compared to the 3.5HH test condition ($p=0.007$). The 5.5HH test condition significantly increased MG lengthening velocity at 68% of stance phase when compared to the 3.5HH test condition ($p=0.000$). There was a gradual increase in lengthening velocity of the MG muscle at 68% of the stance phase where ankle is in dorsiflexion. It was also noted that a lower heel reduced the fibre lengthening velocity.

Table 6.155: Pairwise comparison of medial gastrocnemius fibre velocity changes during maximum EMG activity at 68% of the stance phase for the test footwear conditions (N=14).

Cond.	Cond.	Mean Difference	Std. Error	Sig.	95% Confidence Interval for Difference	
					Lower Bound	Upper Bound
1.5HH	2.5HH	-.042	.017	.297	-.101	.016
	3.5HH	-.094*	.019	.003	-.158	-.030
	4.5HH	-.137*	.018	.000	-.199	-.075
	5.5HH	-.184*	.022	.000	-.257	-.112

2.5HH	1.5HH	.042	.017	.297	-.016	.101
	3.5HH	-.052*	.010	.002	-.086	-.017
	4.5HH	-.095*	.011	.000	-.133	-.057
	5.5HH	-.142*	.016	.000	-.195	-.090
3.5HH	1.5HH	.094*	.019	.003	.030	.158
	2.5HH	.052*	.010	.002	.017	.086
	4.5HH	-.043*	.010	.007	-.077	-.010
	5.5HH	-.091*	.010	.000	-.123	-.058
4.5HH	1.5HH	.137*	.018	.000	.075	.199
	2.5HH	.095*	.011	.000	.057	.133
	3.5HH	.043*	.010	.007	.010	.077
	5.5HH	-.047*	.013	.033	-.092	-.003

6.13.6.2 Fibre velocity at 72% stance phase where maximum soleus EMG activity occurs

The 3.5HH test condition significantly increased soleus fibre lengthening velocity at 72% of stance phase when compared to the 1.5HH shoe ($p=0.016$). The 1.5HH test condition significantly reduced soleus lengthening velocity of fibres at 72% of stance phase when compared to the 4.5HH shoe ($p=0.004$) and the 5.5HH shoe ($p=0.001$) as shown in table 6.155.

Table 6.156: Pairwise comparison soleus fibre velocity changes during maximum EMG activity at 72% of the stance phase for test footwear conditions (N=14).

Cond.	Cond.	Mean Difference	Std. Error	Sig.	95% Confidence Interval for Difference	
					Lower Bound	Upper Bound
1.5HH	2.5HH	-.018	.015	1.000	-.067	.032
	3.5HH	-.047*	.012	.016	-.087	-.007
	4.5HH	-.072*	.015	.004	-.124	-.021
	5.5HH	-.083*	.015	.001	-.132	-.034
2.5HH	1.5HH	.018	.015	1.000	-.032	.067
	3.5HH	-.030	.019	1.000	-.094	.034
	4.5HH	-.055	.020	.181	-.123	.014
	5.5HH	-.065	.021	.089	-.137	.006
3.5HH	1.5HH	.047*	.012	.016	.007	.087
	2.5HH	.030	.019	1.000	-.034	.094
	4.5HH	-.025	.017	1.000	-.083	.033

	5.5HH	-.035	.016	.456	-.089	.019
4.5HH	1.5HH	.072*	.015	.004	.021	.124
	2.5HH	.055	.020	.181	-.014	.123
	3.5HH	.025	.017	1.000	-.033	.083
	5.5HH	-.010	.012	1.000	-.050	.029

6.13.6.3 Summary of results for MG and soleus fibre velocity changes affected by heel heights:

- The 1.5HH test condition reduced MG lengthening velocity at 68% stance phase to significant level when compared to the 3.5HH shoe(p=0.03);
- The 4.5HH test condition significantly increased MG lengthening velocity at 68% of stance phase when compared to the 3.5HH shoe (p=0.007);
- The 5.5HH test condition significantly increased MG lengthening velocity at 68% of stance phase when compared to the 3.5HH shoe (p=0.000). There was a gradual increase in lengthening velocity of the MG muscle at 68% of the stance phase where ankle is dorsiflexion, and it was noted that walking with lower heeled shoes resulted in reduced fibre lengthening velocity;
- The 3.5HH test condition significantly increased the soleus fibre lengthening velocity at 72% of stance phase when compared to the 1.5HH test condition (p=0.016);
- The 1.5HH test condition significantly reduced soleus lengthening velocity of fibres at 72% of stance phase when compared to the 4.5HH and 5.5HH test conditions (p<0.005).

6.13.7 Apex position (AP)

Figure 6.52 shows the alteration to the MG and soleus fibre length velocity by AP. The 70AP test condition increased soleus fibre lengthening velocity between 35% and 68% of stance phase; however there was no significant alteration demonstrated for soleus muscle length changes.

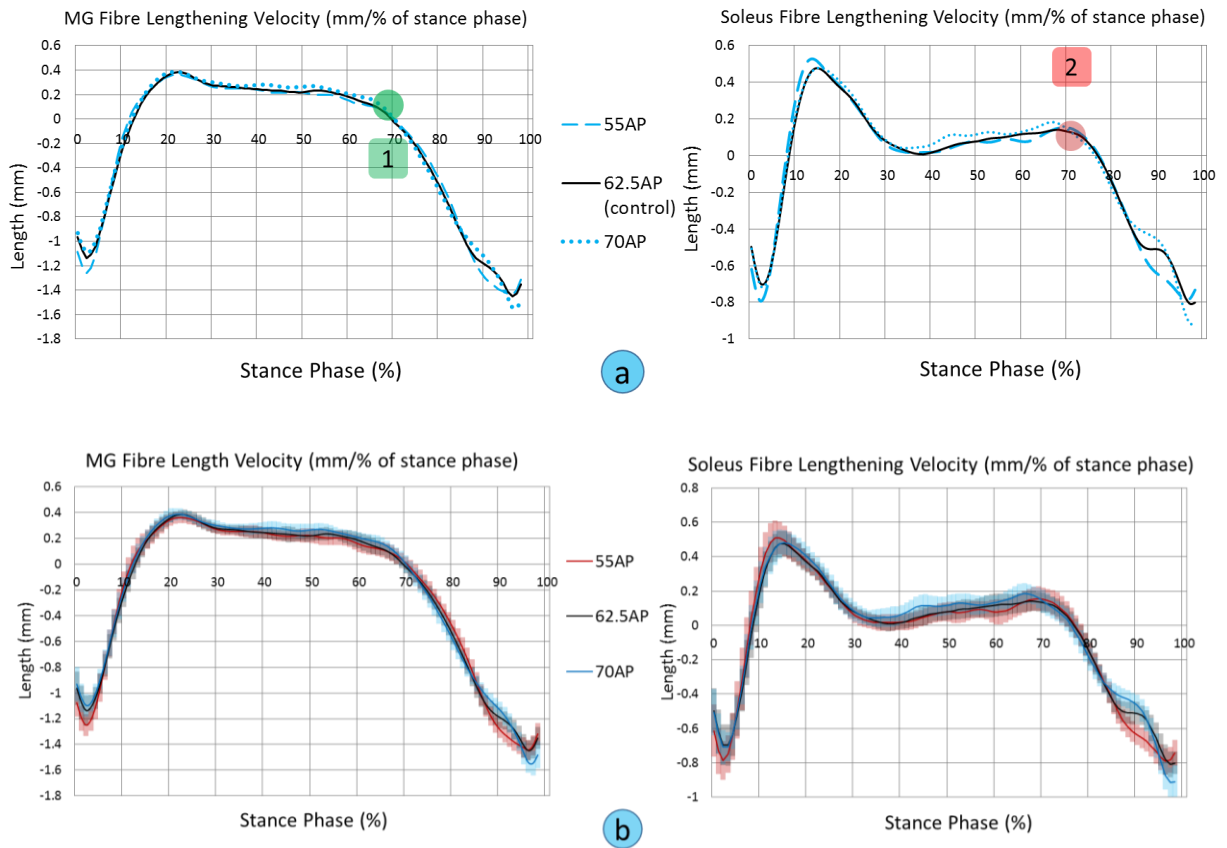


Figure 6.52: The fibre length velocity alteration results from OpenSim simulation software for different AP test footwear test conditions (N=14). Legend 1 indicates the area (68% stance phase) at which maximum EMG for MG muscle was recorded; legend 2 indicates the area (72% stance phase) at which maximum EMG for soleus muscle was recorded. (a) – without standard deviation (STD), (b) – with the lines shadowed to represent STD ranges.

The average results for the changes to fibre length velocity of GM and soleus muscles within the highlighted points of interest are demonstrated in table 1.157.

Table 6.157: MG and soleus fibre length velocity (mm/% of the stance phase) mean (\pm SD) for different apex lengths of the sole (N=14).

	55AP	62.5AP	70AP
Medial Gastrocnemius			
Fibre velocity at 68% stance phase where max MG EMG activity.	0.094 (0.059)	0.094 (0.054)	0.135 (0.053)
Soleus			
Fibre velocity at 72% stance phase where max Sol EMG activity.	0.13 (0.08)	0.12 (0.05)	0.10 (0.07)

6.13.7.1 Fibre velocity at 68% stance phase where maximum MG EMG activity occurs

The 62.5AP footwear showed significant reduction of MG fibre lengthening velocity at 68% stance phase when compared to the 70AP test condition (p=0.045).

Table 6.158: Pairwise comparison medial gastrocnemius fibre velocity changes during maximum EMG activity at 68% of the stance phase for test footwear conditions (N=14).

Cond.	Cond.	Mean Difference	Std. Error	Sig.	95% Confidence Interval for Difference	
					Lower Bound	Upper Bound
55AP	62.5AP	.000	.018	1.000	-.050	.049
	70 AP	-.041	.027	.442	-.114	.032
62.5AP	55AP	.000	.018	1.000	-.049	.050
	70 AP	-.041*	.015	.045	-.081	-.001

6.13.7.2 Fibre velocity at 72% stance phase where maximum soleus EMG activity occurs

There were no significant alterations demonstrated. The hypothesis (H_{a4}) is rejected.

6.13.7.3 Summary results for MG and soleus fibre velocity changes affected by AP:

- The 62.5AP footwear test condition produced a significant reduction in MG fibre lengthening velocity at 68% stance phase when compared to the 70AP test condition (p=0.045). This may have resulted in increased EMG activity for the MG muscle. The hypothesis (H_{a4}) is accepted.

6.13.8 Toe angle (TA)

Figure 6.53 shows the alteration to the MG and soleus fibre length velocity by toe angle. The 10° TA test condition increased MG fibre lengthening velocity within 30-55% stance phase, therefore it may have resulted in an EMG activity increase within 35-70% of stance phase.

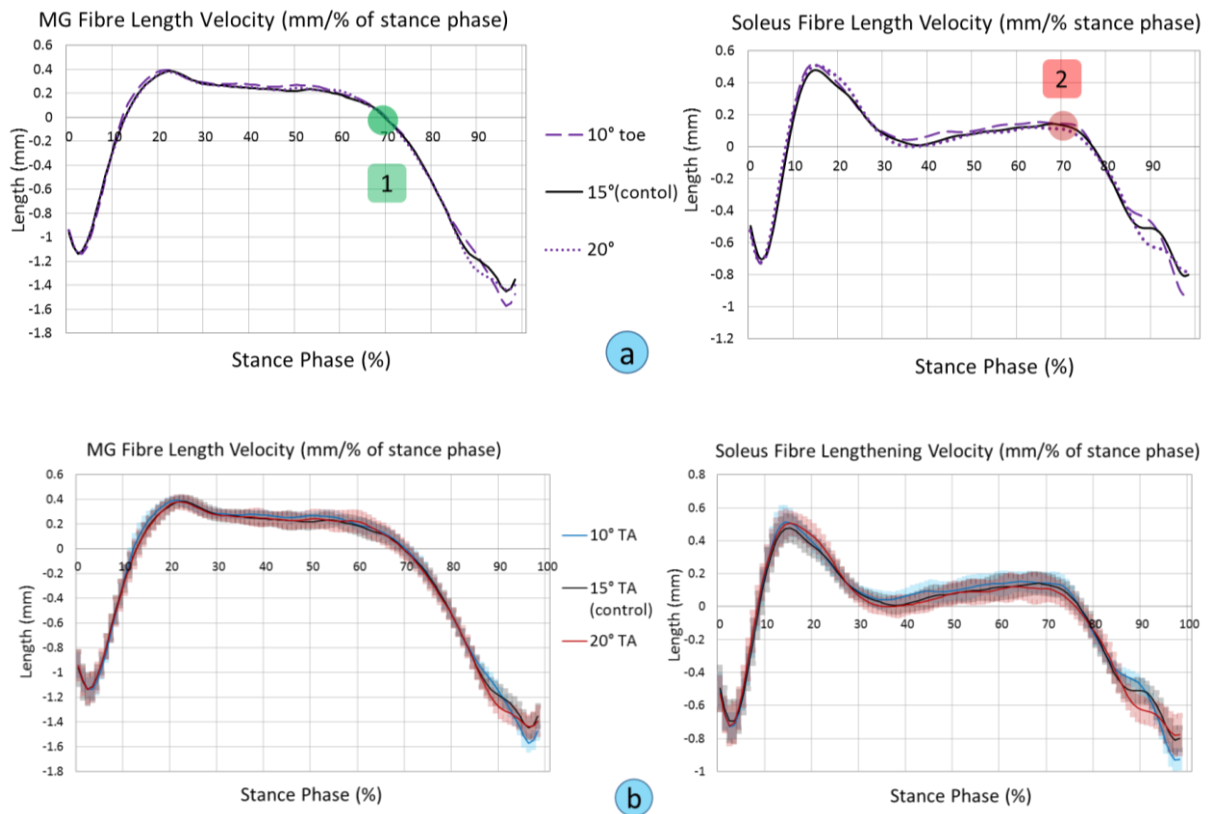


Figure 6.53: The fibre length velocity alteration results data from OpenSim simulation software for different toe angle test footwear conditions (N=14). Legend 1 indicates the area (68% stance phase) at which maximum EMG for MG muscle was recorded; legend 2 indicates the area (72% stance phase) at which maximum EMG for soleus muscle was recorded. (a) – without standard deviation (STD), (b) – with the lines shadowed to represent STD ranges.

The average results for the alterations demonstrated for fibre length velocity of GM and soleus muscles within the highlighted points of interest are demonstrated in table 6.159 below.

Table 6.159 Table: MG and soleus fibre length velocity (mm/% of stance phase) mean (\pm SD) for different toe angles of the sole (N=14).

	10° TA	15° TA	20° TA
Medial Gastrocnemius			
Fibre velocity at 68% stance phase where maximum MG EMG activity.	0.120 (0.051)	0.094 (0.054)	0.097 (0.067)
Soleus			
Fibre velocity at 72% stance phase where maximum Sol EMG activity.	0.14 (0.08)	0.12 (0.05)	0.09 (0.07)

6.13.8.1 Fibre velocity at 68% stance phase where maximum MG EMG activity occurs.

The 10° TA footwear produced an increase in MG fibre lengthening velocity at 68% of stance phase when compared to the control footwear; however it did not reach a level of significance ($p=0.053$).

6.13.8.2 Fibre velocity at 72% stance phase where maximum soleus EMG activity occurs

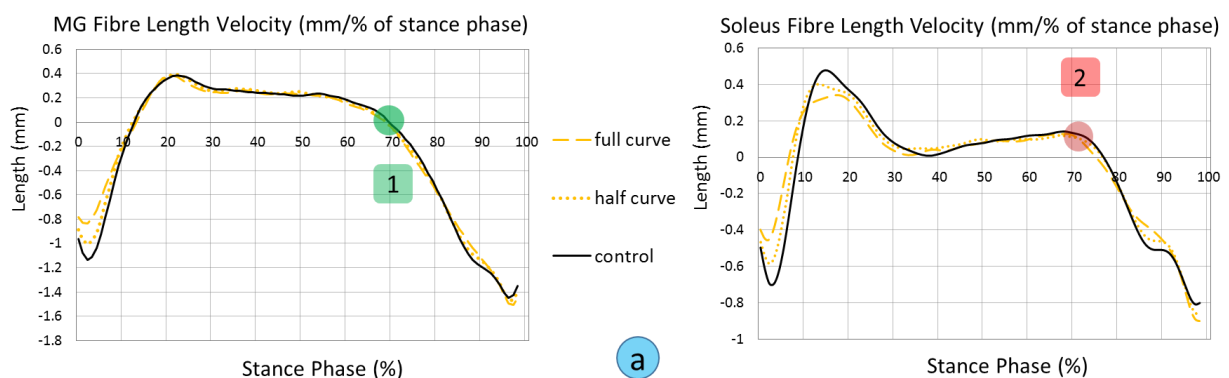
The alterations to this parameter were not significant. The hypothesis (H_{a4}) is not accepted.

6.13.8.3 Summary of results for MG and soleus fibre velocity changes affected by alteration to rocker sole toe angle:

- The 10° TA test condition increased MG fibre lengthening velocity during 30-55% of stance phase; therefore, it may result in an EMG activity increase within 35-70% of stance phase. This will be discussed in the discussion chapter.

6.13.9 Heel Curve

Figure 6.54 shows the alteration to the MG and soleus fibre length velocity by heel curve.



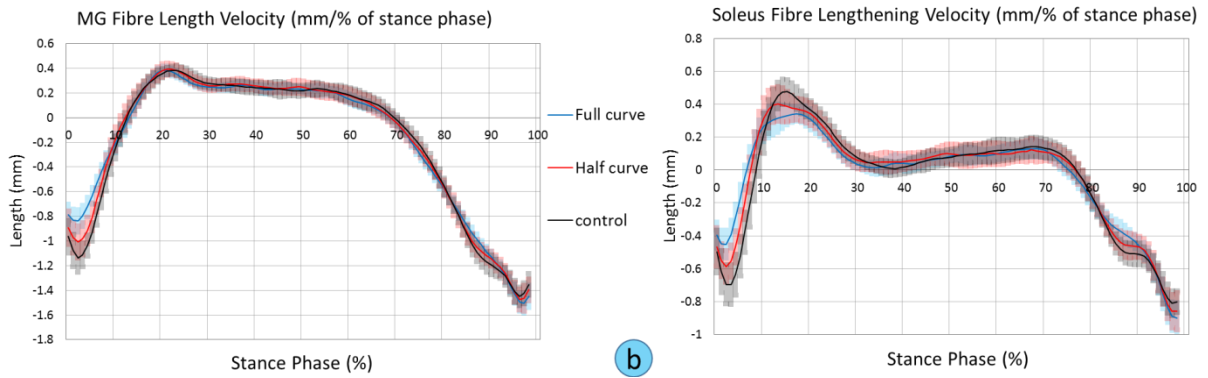


Figure 6.54: The fibre length velocity alteration results data from OpenSim simulation software for different heel curve test footwear conditions (N=14). Legend 1 indicates the area (68% stance phase) at which maximum EMG for MG muscle was recorded; legend 2 indicates the area (72% stance phase) at which maximum EMG for soleus muscle was recorded. (a) – without standard deviation (STD), (b) – with the lines shadowed to represent STD ranges.

The average results for alteration to the fibre length velocity of GM and soleus muscles within highlighted points of interest are demonstrated in the table below.

Table 6.160: MG and soleus fibre length velocity (mm/% of the stance phase) mean (\pm SD) for different heel curves (N=14).

	Full curve	Half curve	control
Medial Gastrocnemius			
Fibre velocity at 68% stance phase where maximum MG EMG activity.	0.060 (0.050)	0.070 (0.052)	0.048 (0.050)
Soleus			
Fibre velocity at 72% stance phase where maximum Sol EMG activity.	0.08 (0.07)	0.09 (0.06)	0.12 (0.05)

6.13.9.1 Summary results for MG and soleus fibre velocity changes affected by heel curves:

There were no significant changes and therefore the hypothesis (H_{a4}) is rejected.

6.13.10 Flexibility of the sole

Figure 6.55 shows the alteration to the MG and soleus fibre length velocity by the flexibility of the sole. The flexible profiles increased MG and soleus fibre lengthening velocity within 5-18% stance phase. However, the calf muscle was not active at LR.

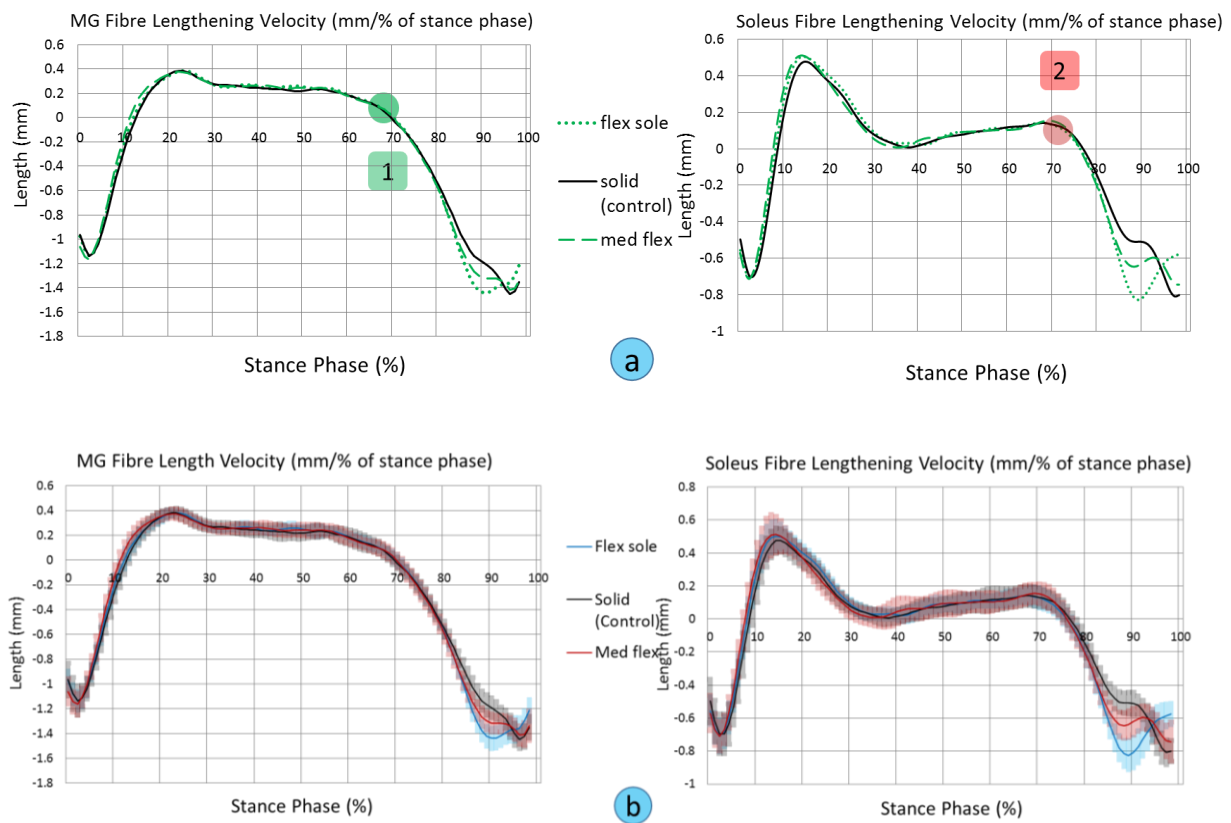


Figure 6.55: The fibre length velocity alteration results data from OpenSim simulation software for different level flexibly of the sole (N=14). Legend 1 indicates the area (68% stance phase) at which maximum EMG for MG muscle was recorded; legend 2 indicates the area (72% stance phase) at which maximum EMG for soleus muscle was recorded. (a) – without standard deviation (STD), (b) – with the lines shadowed to represent STD ranges.

There were nosignificant changes demonstrated at points 1 and 2 for MG and soleus fibre length and therefore, the hypothesis (H_{a4}) is rejected.

6.14 Tendon force

The active fibre force data shows what is the internal active fibre force required to produce the ankle moment. Different footwear features require different force because the muscle moment arm changes. However, it does not give the information how hard the muscle has

to work as it is also related to fibre length and velocity of contraction. However, the data demonstrates what maximum MG active fibre force is required when subjects walk in different footwear conditions. Figure 6.56 shows the example for active fibre force produced through the tendon for medial gastrocnemius muscle. Similar results were demonstrated for the soleus muscle. However, the force, which is generated by soleus muscle is higher in magnitude at approximately 4000N.

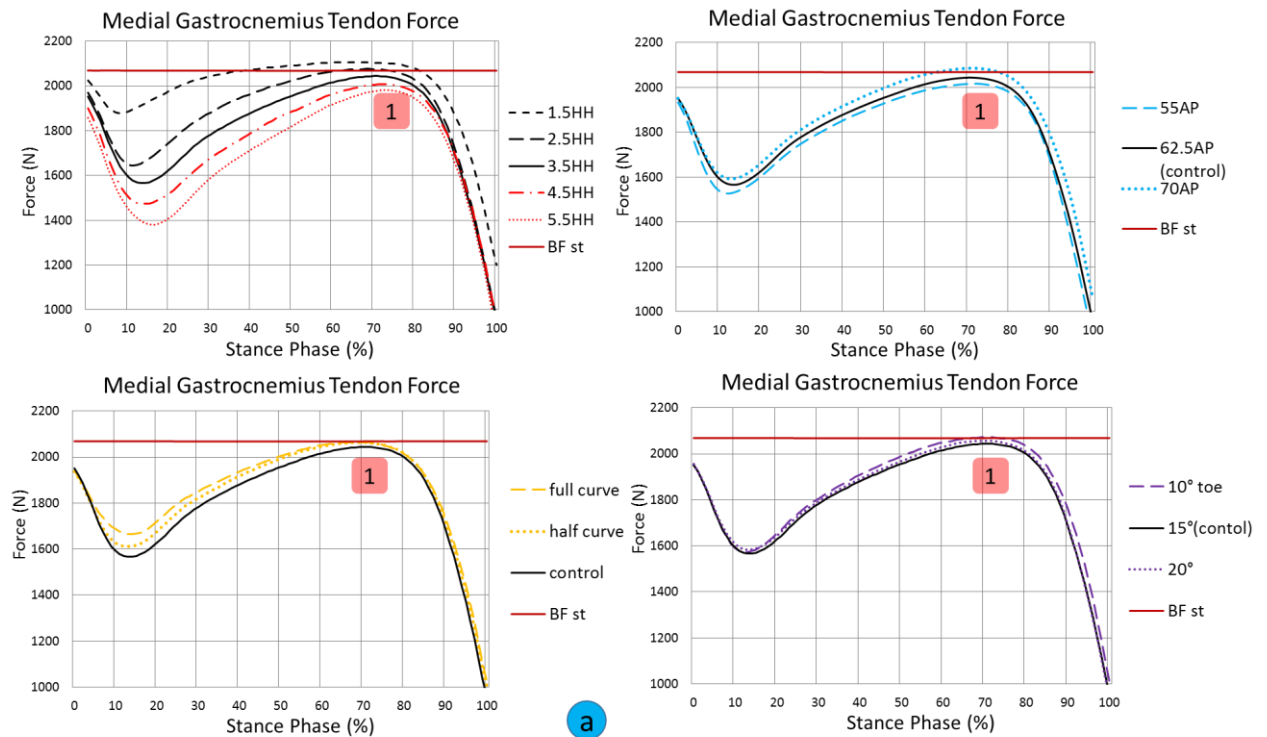


Figure 6.56: The required tendon force (medial gastrocnemius) which is transmitted through the tendon for the ankle joint to oppose the external dorsiflexor moment for different footwear features. Legend 1 indicates the area at which maximum EMG activity for MG was recorded.

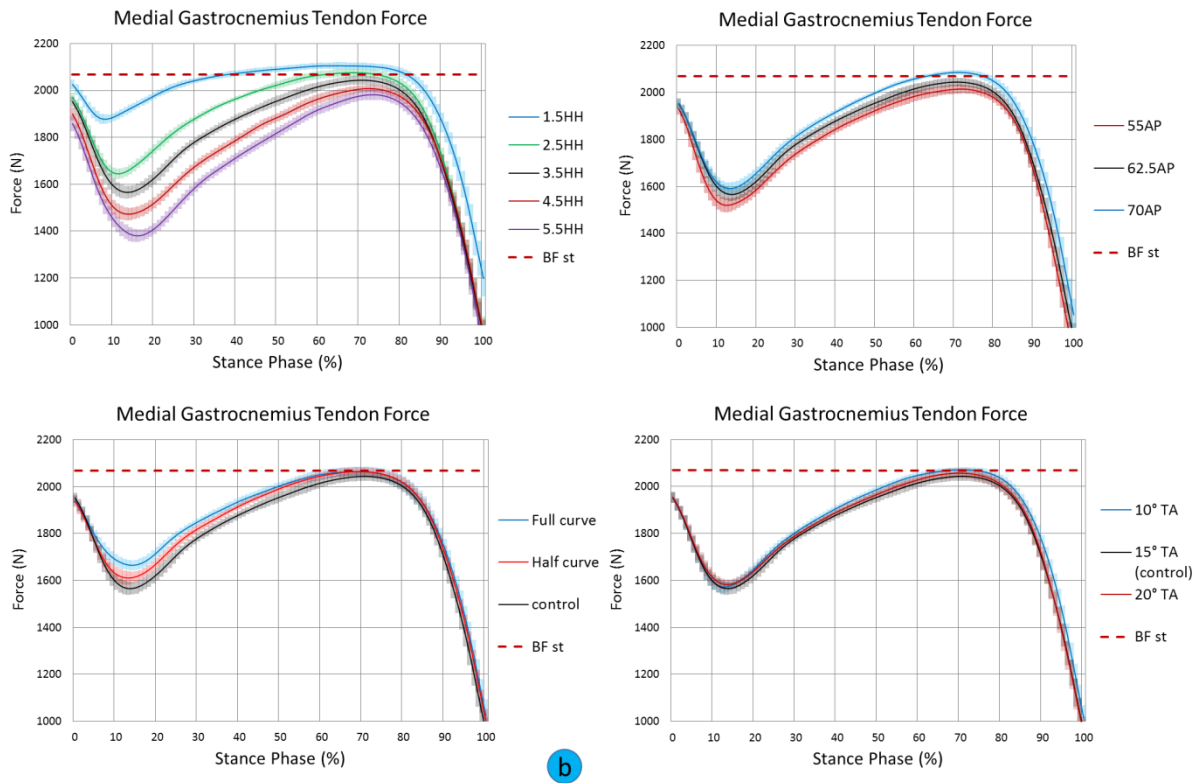


Figure 6.57: The required active tendon force (medial gastrocnemius) which is transmitted through the tendon to enable the ankle joint to oppose the externally-applied moment for different footwear features. (a) – without standard deviation (STD), (b) – with the lines shadowed to represent STD ranges.

Table 6.161 demonstrates the maximum active tendon force produced by medial gastrocnemius for different footwear features.

Table 6.161: Active tendon force of MG muscle for different footwear features (N=14).

	1.5HH	2.5HH	3.5HH control	4.5HH	5.5HH	55AP	70AP	10° TA	20° TA	Full curve	Half curve
Medial Gastrocnemius											
Force required (N) at peak EMG	2107.9 (13.7)	2078.6 (18.2)	2046.6 (19.0)	2010.9 (15.0)	1983.9 (21.7)	2019.0 (18.2)	2088.0 (9.2)	2074.8 (10.5)	2060.5 (21.7)	2068.2 (19.8)	2067.1 (17.5)
Differences between control 3.5HH shoe (N)	61.3 (13.7)	32.0 (18.2)	0.0 (19.0)	-35.7 (15.0)	-62.7 (21.7)	-27.5 (18.2)	41.4 (9.2)	28.2 (10.5)	14.0 (21.7)	21.6 (19.8)	19.8 (17.5)

The results demonstrated that the 1.5HH required 61.3 (13.7)N more MG muscle force when compared to the control shoe. The 4.5HH required less [35.7 (15.0)N] to perform the task versus control. The 5.5HH test condition reduced the force generated by 62.7N. The 55AP required less fibre force [27.8 (18.2)N]. A longer apex position (i.e. more distal) resulted in an increased force requirement by MG which was 41.4 (9.2)N for the 70AP footwear.

6.15 Tibialis anterior fibre lengthening/shortening velocity

6.15.1 Heel Height (HH)

Figure 6.58 shows the alteration to the tibialis anterior fibre length, active fibre force and EMG activity caused by varying heel heights. It can be seen that by raising the heel, fibres were also lengthened, and that resulted in increases in active fibre force requirement to dorsiflex the ankle as well as an increase in EMG activity.

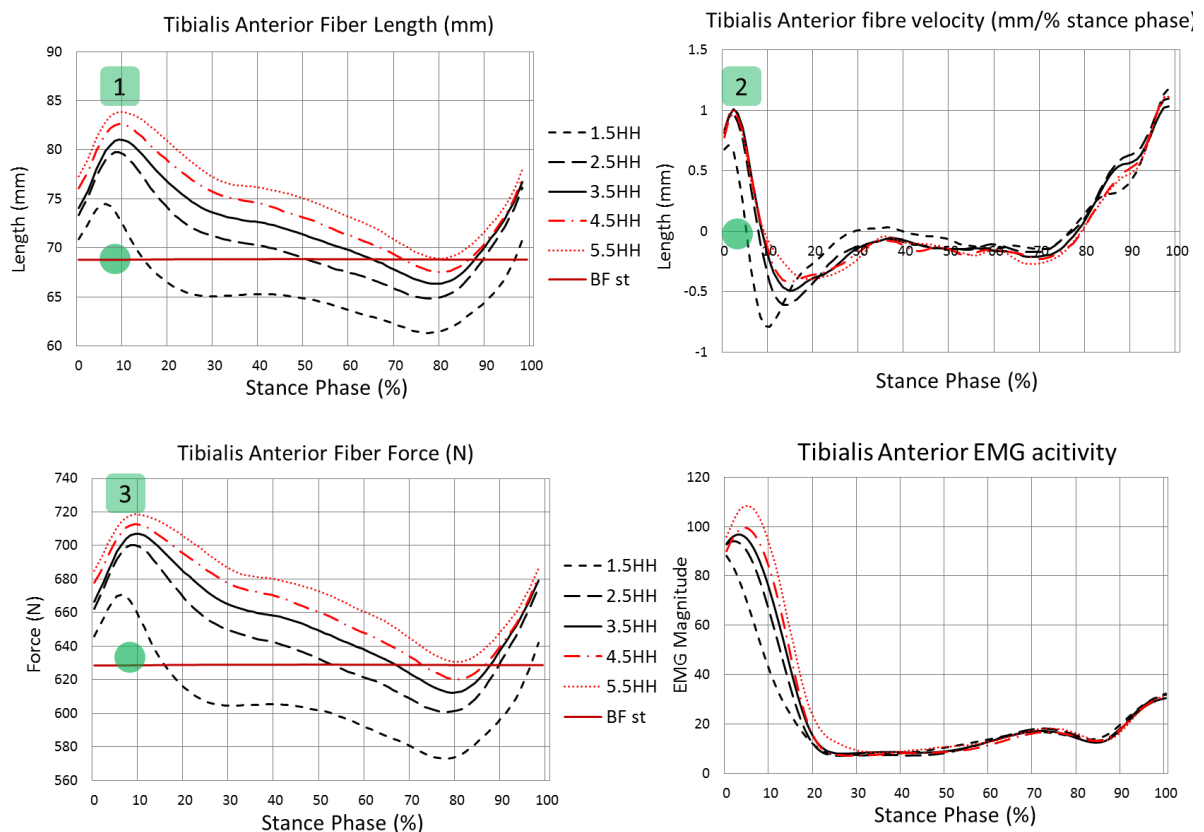


Figure 6.58: The tibialis anterior alterations for fibre length (mm), fibre length velocity, tibialis anterior active fibre force (N) and EMG overall area for different heel heights. Legend 1 and 2 indicate the area during LR at which maximum EMG activity occurs; legend 3

indicates the maximum active fibre force required for internal DF moment. The red line represents the barefoot static position. (a) – without standard deviation (STD), (b) – with the lines shadowed to represent STD ranges.

Exactly the same graphs from figure 6.58, but with standard deviations added are demonstrated below.

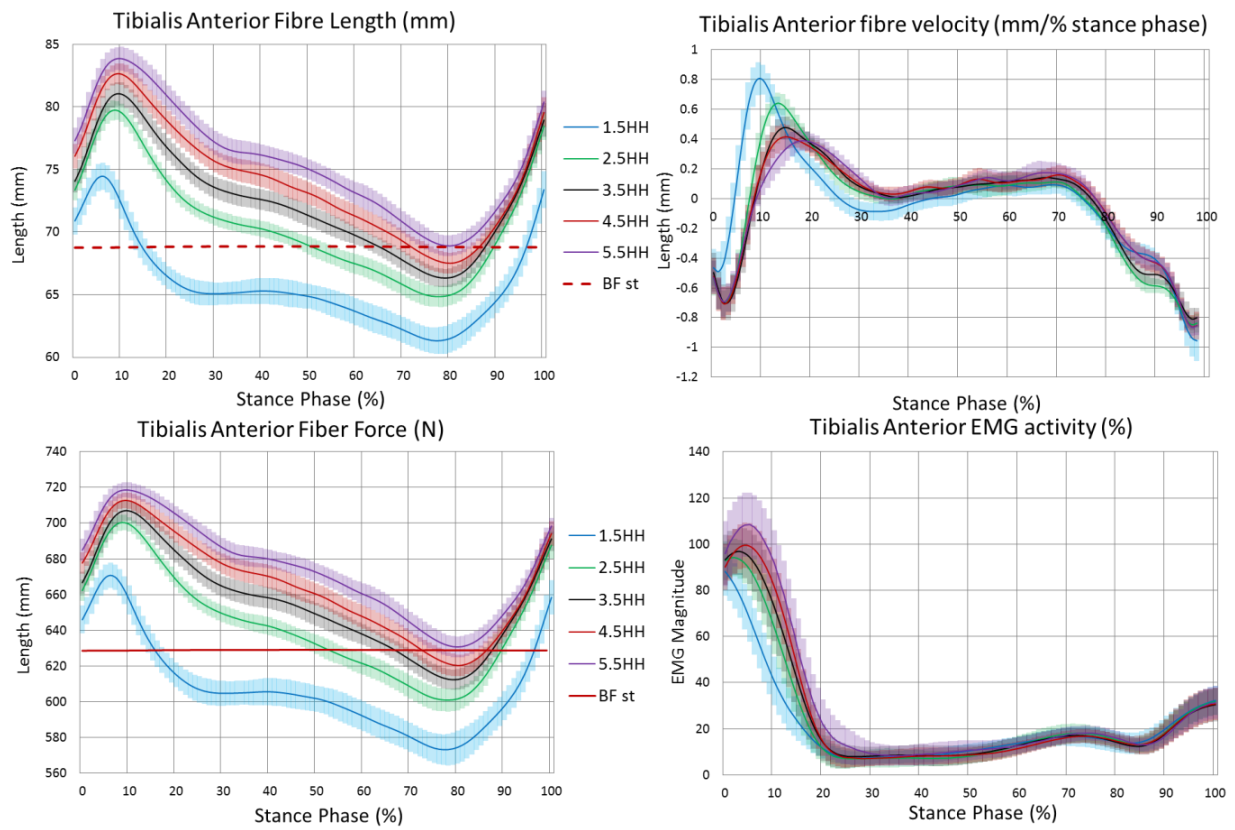


Figure 6.59: The tibialis anterior alterations in fibre length (mm), fibre length velocity, tibialis anterior active fibre force (N), EMG activity and standard deviation for different heel curves.

The average results for the tibialis anterior fibre length velocity change within highlighted points of interest, are presented in table 6.162.

Table 6.162: The tibialis anterior fibre length, fibre length, active fibre force and EMG activity mean (\pm SD) for different heel heights (N=14).

	1.5 HH	2.5 HH	3.5 HH	4.5 HH	5.5 HH
Tibialis anterior					
Max fibre length during LR (mm)	74.86 (1.16)	79.98 (0.78)	81.33 (0.97)	83.02 (0.86)	84.28 (1.13)
Fibre length difference versus control (mm)	-6.47 (1.16)	-1.35 (0.78)	0.00 (0.97)	1.69 (0.86)	2.95 (1.13)
Max fibre length velocity (mm/% stance phase)	0.78 (0.15)	1.03 (0.11)	1.07 (0.14)	1.16 (0.11)	1.08 (1.12)
Active fibre force (N)	673.73 (7.28)	701.91 (4.35)	708.81 (5.1)	714.56 (4.28)	721.15 (4.34)
Active fibre force difference versus control (N)	-35.08 (7.28)	-6.90 (4.35)	0.00 (5.1)	5.10 (4.28)	12.35 (4.34)
Overall EMG area (%)	80.1 (10.8)	94.3 (12.8)	100.0 (12.1)	104.3 (11.6)	114.2 (12.7)
Differences EMG area versus control shoe (%)	-19.9	-5.7	0.0	4.3	14.2

6.15.1.1 Max fibre length during LR (mm)

Raising the heel height gradually but also significantly increased the maximum length of tibialis anterior fibres during LR when compared to lower heels ($p < 0.000$).

Table 6.163: Pairwise comparison of shoe conditions for average maximum length of tibialis anterior fibres during LR (N=14).

Cond.	Cond.	Mean Difference	Std. Error	Sig.	95% Confidence Interval for Difference	
					Lower Bound	Upper Bound
1.5HH	2.5HH	-5.114*	.536	.000	-6.922	-3.307
	3.5HH	-6.466*	.444	.000	-7.964	-4.967
	4.5HH	-8.160*	.486	.000	-9.800	-6.519
	5.5HH	-9.412*	.653	.000	-11.615	-7.210
2.5HH	1.5HH	5.114*	.536	.000	3.307	6.922
	3.5HH	-1.352*	.256	.001	-2.214	-.489
	4.5HH	-3.045*	.327	.000	-4.147	-1.944
	5.5HH	-4.298*	.302	.000	-5.315	-3.281
3.5HH	1.5HH	6.466*	.444	.000	4.967	7.964
	2.5HH	1.352*	.256	.001	.489	2.214
	4.5HH	-1.694*	.272	.000	-2.613	-.775
	5.5HH	-2.947*	.350	.000	-4.125	-1.768

4.5HH	1.5HH	8.160*	.486	.000	6.519	9.800
	2.5HH	3.045*	.327	.000	1.944	4.147
	3.5HH	1.694*	.272	.000	.775	2.613
	5.5HH	-1.253*	.298	.010	-2.257	-.249

6.15.1.2 Max fibre length velocity (mm/% stance phase)

The 1.5HH footwear test condition significantly reduced tibialis anterior fibre length velocity when compared to the other footwear heel height conditions ($p < 0.021$) as shown in table 6.164.

Table 6.164: Pairwise comparison of shoe conditions for average maximum length velocity of tibialis anterior fibres during LR (N=14).

Cond.	Cond.	Mean Difference	Std. Error	Sig.	95% Confidence Interval for Difference	
					Lower Bound	Upper Bound
1.5HH	2.5HH	-.270*	.049	.001	-.439	-.101
	3.5HH	-.316*	.058	.001	-.514	-.117
	4.5HH	-.307*	.078	.020	-.575	-.040
	5.5HH	-.324*	.075	.009	-.580	-.069
2.5HH	1.5HH	.270*	.049	.001	.101	.439
	3.5HH	-.046	.038	1.000	-.176	.085
	4.5HH	-.037	.062	1.000	-.249	.174
	5.5HH	-.055	.059	1.000	-.256	.147
3.5HH	1.5HH	.316*	.058	.001	.117	.514
	2.5HH	.046	.038	1.000	-.085	.176
	4.5HH	.008	.054	1.000	-.177	.194
	5.5HH	-.009	.062	1.000	-.221	.203
4.5HH	1.5HH	.307*	.078	.020	.040	.575
	2.5HH	.037	.062	1.000	-.174	.249
	3.5HH	-.008	.054	1.000	-.194	.177
	5.5HH	-.017	.040	1.000	-.155	.121

6.15.1.3 Summary for tibialis anterior muscle properties:

- Raised heels significantly increased the maximum length of tibialis anterior fibres during LR when compared to lower heels ($p < 0.000$). The hypothesis (H_{a4}) is accepted;
- Stretching tibialis anterior resulted in increased muscle work. When fibre length were close it neutral position, the EMG activity and overall EMG were significantly reduced;
- The 1.5HH footwear test condition significantly reduced tibialis anterior fibre length velocity when compared to the other footwear conditions ($p < 0.021$). The hypothesis (H_{a4}) is accepted.

6.15.2 Curved heels

Figure 6.59 shows the alteration to the tibialis anterior fibre length, active fibre force and EMG activity by adding heel curves. The curved heels reduced maximum tibialis anterior fibre length during LR, which resulted in a reduction in the eccentric velocity contraction of the tibialis anterior muscle. Therefore, less force would be required to dorsiflex the ankle, and tibialis anterior EMG activity was therefore reduced for curved heels when compared to the control shoe without a heel curve.

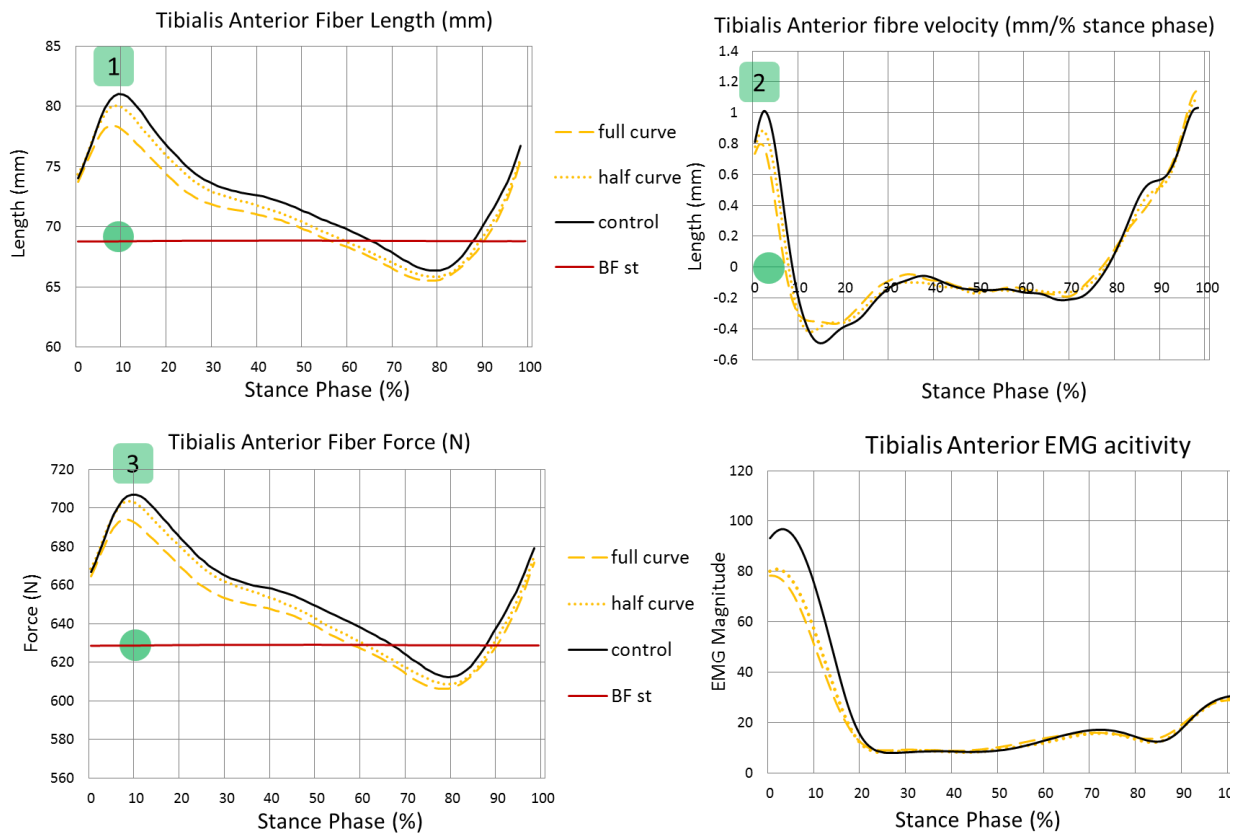


Figure 6.60: The tibialis anterior alterations for fibre length (mm), fibre length velocity, tibialis anterior active fibre force (N) and EMG overall area for curved heels. Legends 1 and 2 indicate the area during LR at which maximum EMG activity occurs; legend 3 indicates the maximum active fibre force required for internal dorsiflexor moment. The red line represents the barefoot static position.

The graphs with standard deviation added are demonstrated in figure 6.61.

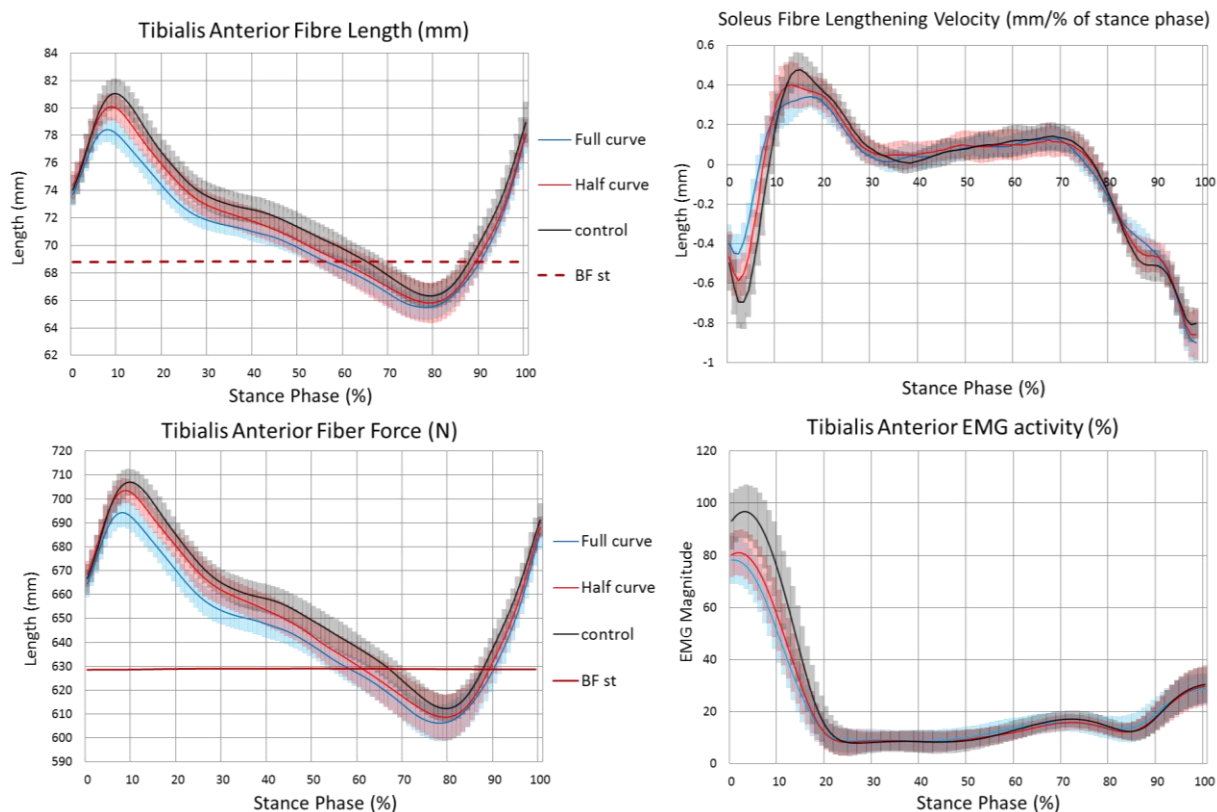


Figure 6.61: The tibialis anterior alteration to fibre length (mm), fibre length velocity, tibialis anterior active fibre force (N), EMG activity and standard deviation for different heel curves.

The average results for the tibialis anterior fibre length velocity change within highlighted points of interest which are presented in table 6.165.

Table 6.165: The tibialis anterior fibre length, fibre length velocity, active fibre force and EMG activity mean (\pm SD) for different heel curves (N=14).

	Full curve	Half curve	control
Tibialis anterior			
Max fibre length during LR (mm)	78.77 (0.94)	80.47 (0.88)	81.33 (0.97)
Fibre length difference versus control (mm)	-2.56 (0.94)	-0.86 (0.88)	0.00 (0.97)
Max fibre length velocity (mm/% stance phase)	0.91 (0.14)	1.04 (0.17)	1.07 (0.14)
Active fibre force (N)	696.64 (6.28)	705.94 (5.18)	708.81 (5.1)
Active fibre force difference versus control (N)	-12.16 (6.28)	-2.87 (5.18)	0.00 (5.1)
Overall EMG area (%)	84.1 (12.9)	86.3 (11.8)	100.0 (12.1)
Differences EMG area versus control shoe (%)	-15.9	-13.7	0.0

6.15.2.1 Maximum tibialis anterior fibre length during LR

The full curve significantly reduced maximum tibialis anterior fibre length during LR when compared to the other footwear conditions ($p < 0.000$).

Table 6.166: Pairwise comparison of shoe conditions for average maximum length of tibialis anterior fibres during LR (N=14).

Cond.	Cond.	Mean Difference	Std. Error	Sig.	95% Confidence Interval for Difference	
					Lower Bound	Upper Bound
Full curve	Half curve	-1.702*	.321	.000	-2.583	-.821
	No curve	-2.558*	.397	.000	-3.648	-1.468
Half curve	Full curve	1.702*	.321	.000	.821	2.583
	No curve	-.856	.368	.110	-1.865	.154

6.15.2.2 Maximum tibialis anterior fibre length velocity (mm/% stance phase)

The full curve and half curve footwear conditions significantly reduced the velocity of tibialis anterior fibre eccentric contraction ($p < 0.030$) as shown in table 6.167.

Table 6.167: Pairwise comparison of shoe conditions for maximum tibialis anterior fibre length velocity during LR (N=14).

Cond.	Cond.	Mean Difference	Std. Error	Sig.	95% Confidence Interval for Difference	
					Lower Bound	Upper Bound
Full curve	Half curve	-.155*	.051	.030	-.296	-.014
	No curve	-.315*	.042	.000	-.431	-.199
Half curve	Full curve	.155*	.051	.030	.014	.296
	No curve	-.160*	.052	.029	-.306	-.015

6.15.2.3 Summary of results for tibialis anterior muscle.

- The full curved heel test condition significantly reduced maximum tibialis anterior fibre length during LR when compared to the other footwear conditions ($p < 0.000$). The hypothesis (H_{a4}) is accepted;
- The full curve and half curve footwear conditions significantly reduced the velocity of tibialis anterior fibre eccentric contraction when compared to control ($p < 0.030$). The hypothesis (H_{a4}) is accepted;

- A curvature of the heel resulted in less active fibre force required to dorsiflex the ankle at LR when compared to a sole without a heel curve;
- The total tibialis anterior EMG activity area was significantly reduced for shoes with curved heels.

CHAPTER 7

7 DISCUSSION

7.1 Sagittal plane ankle kinematics

The results from this study demonstrated that statistically significant alterations to ankle kinematics can be induced by introducing variations to rocker sole designs in footwear. Previous studies analysing the effects of kinematics and kinetics on the more commonly seen rocker sole interventions (Long et al 2004, Myers et al 2005, van Bogart 2005) did not demonstrate any significant alteration to ankle kinematics during stance phase of gait.

Myers et al (2005), confirmed the findings of this study in that a negatively- heeled rocker sole profile produced an increase in dorsiflexion both at the ankle during LR and plantarflexion at terminal stance, but in their study, these outcome measures were not significant. However, the pitch of the shoe (i.e. the heel-sole differential) was not accurately defined in that study, which makes it difficult to provide a direct comparison with the results of this study.

Chapter 4 described newly published designs of rocker-soled shoes, which were developed in an attempt to reduce ankle joint rotation or accommodate limited ankle joint rotation during the whole of the gait cycle, but particularly during stance phase of gait (Arazpour et al 2013, Wang and Hansen 2010). This was done to improve gait for patients suffering from conditions such as paraplegia; necessitating the need to wear cosmetic knee ankle foot orthoses (KAFOs) with AFO sections, which are designed to support the foot and ankle but restrict motion in all planes by providing an ankle blocking function. They were also used to provide restriction to ankle joint sagittal plane rotation in the presence of pain associated with joint degeneration and arthritic changes. In both these cases, there was a need to facilitate forward rotation of the shank during stance phase. The designs illustrated that a rocker sole can indeed be designed to significantly reduce sagittal plane motion whilst being suitable for ambulation by specific patient groups. Both the studies not involving an AFO reduced total ankle ROM to below 18 degrees. Rocker soles have also been recently studied as an adjunct treatment in the reduction of pain experienced with plantar fasciitis in association with FFOs, by using a toe-only rocker sole to utilise its proven effect of pressure shunting extra loading to the midfoot and helping the effect of the FFO (Fong et al 2012).

The rocker sole test conditions utilised in this study were chosen following an analysis of the literature. Traditional (angled) rocker soles were originally tested for use by claudicants, but the three studies which did so produced conflicting results. The efficacy of traditional rocker soles in reducing forefoot plantar pressures by utilising an anterior-placed apex position indicated that they may be useful in offloading the ankle plantarflexors. A small pilot feasibility study was performed prior to the main testing phase to ensure that data could be reliably obtained for the chosen primary outcome measures using the gait analysis equipment available, and to also confirm that alteration to shoe outsole features could provide meaningful differences in the data. The shoe conditions tested in the pilot study were an ortho-wedge negatively-heeled shoe with an apex angle of 35 degrees, a control shoe with no rocker sole but a heel height of 3cm, and a three curve rocker shoe which had previously been shown to induce plantarflexion compared to the control shoe (Hutchins et al 2008). The results of this trial gave the author confidence to proceed using the test conditions chosen for this study.

7.1.1 The effect of walking with rocker soles incorporating different heel heights

7.1.1.1 The effect of different heel heights on ankle joint kinematics

The concept of this thesis was to inform the indications for using rocker-soled shoes by claudicants and those subjects suffering from other pathologies who would benefit from walking with a reduced power requirement by the ankle plantarflexors; especially during the propulsive phase of gait.

One hypothesis of this thesis was, that by placing the ankle in an advantageous position, both in regards to maximising the Achilles tendon ankle joint moment arm, but also by reducing the ankle sagittal plane ROM around an optimal position, then this could prove potentially beneficial for claudicants when tested during future walking trials, if a traditional rocker sole could be developed to achieve this. Traditional rocker soles also have the advantage that they cause the GRF to “hesitate” at the angled rocker fulcrum position, and

therefore the GRF does not move forwards as quickly as when walking with known curved rocker designs.

The experimental design protocol developed for this thesis was therefore intended to demonstrate which design features would be recommended to achieve calf muscle unloading during stance phase. To achieve this, the features of the rearfoot (posterior) section of a rocker profile design needed to be determined.

The testing of five different heel heights (varying from 1.5 to 5.5 cm in depth) induced significant alterations to ankle joint kinematics in this study as shown in the figure 7.1.

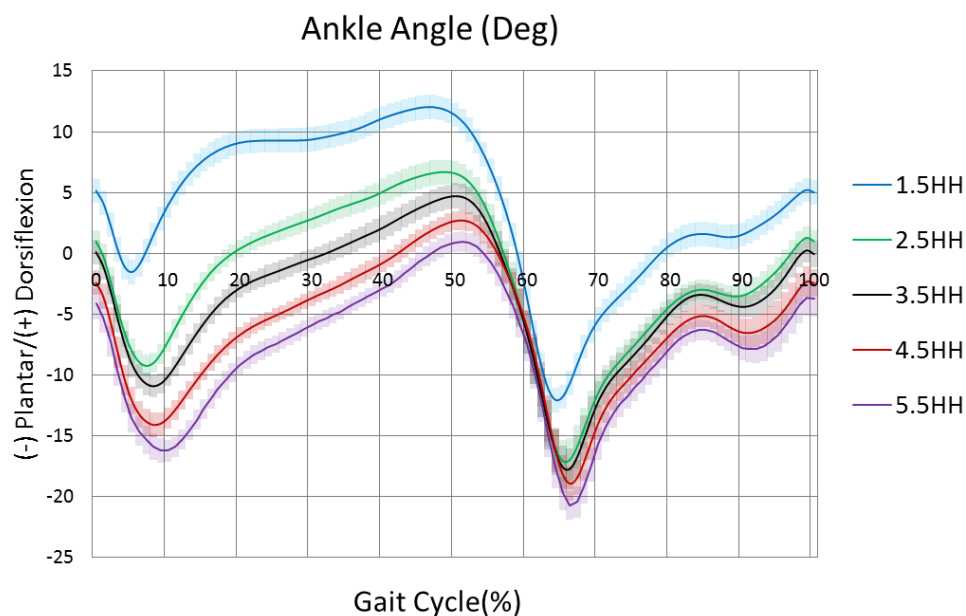


Figure 7.1: Sagittal plane ankle motion during the five heel height test conditions with standard deviation where the control shoe is 3.5 HH.

Shoes with lower heel heights kept the ankle joint relatively dorsiflexed and in those with raised heels the ankle joint shifted into a more plantarflexed position compared to the control shoe test condition (denoted as 3.5HH) during the whole of stance phase. The 3.5cm heel height test condition was the transition height between producing a relatively plantarflexed or dorsiflexed ankle during LR which continued during stance phase of gait. All test conditions were significantly different from each other for the maximum ankle plantarflexion angle during LR ($p=0.00$). The maximal ankle dorsiflexion during stance was

also significantly altered between all the test conditions with an 11.1⁰ degree difference in the range of values. The maximal plantarflexion position was not significantly different between the 2.5, 3.5 and 4.5 cm heel heights. The 1.5 cm (negative heel) induced a relatively dorsiflexed position throughout swing phase also, whilst the other test conditions did not.

With respect to the total sagittal plane ankle ROM, the 1.5 cm and 2.5cm heel test conditions both significantly reduced ankle ROM during LR compared to all the other heel height test conditions (table 6.9). The 3.5cm, 4.5 cm and 5.5 cm heeled shoes did not show any significant increase in ROM between themselves, with only a 10 degree maximal difference in range.

7.1.1.2 The effect of varying heel height on knee joint kinematics

The 1.5cm negative heel test condition significantly increased knee flexion at toe-off ($p=0.00$) by 2.9° (SD:1.4°) when compared with the control shoe (table 6.30). The 5.5 cm heel test condition kept the knee more extended when compared to the negative heels tested and the control shoe ($p=0.00$). During LR, there were no statistically significant differences in maximum knee flexion values. Premature knee flexion occurred when walking with the 1.5 cm heel and slightly increased knee extension for the high-heeled shoes. During late stance, the 5.5 cm heel height produced significantly increased knee extension compared to the control shoe ($p=0.025$) and the maximum extension phase was delayed versus the control and the negative-heel test footwear conditions. At toe-off, the 1.5 cm heel test condition produced a significantly more flexed knee when compared to the 3.5 cm heel ($p=0.00$). The evidence therefore demonstrated that lower heeled shoes produce statistically significantly more knee flexion during mid to late stance and swing than higher heeled ones.

To offload the calf muscles it would be advantageous to have a more flexed knee to reduce the extension loading on the proximal insertion of the gastrocnemius muscle during propulsion. However, the negative heel which produced this effect also placed the ankle into a significantly more dorsiflexed position during mid stance. There were no statistically significant differences between the 2.5 and 3.5 cm heel in knee flexion angle during propulsive phase, but these were still significantly more flexed than wearing the lower heeled shoe ($p=0.00$).

7.1.1.3 The effect of varying heel height on hip joint kinematics

With regards to the hip, the 5.5cm increased maximum hip extension significantly by 1.6 deg.($p=0.042$) compared to the control shoe and also increased the total hip ROM. Lower heeled shoes produced increased hip extension during stance and increased hip flexion during swing, but did not produce the maximal hip extension. Total hip ROM was not significantly altered between the heel height test conditions.

7.2 The effect of altering footwear on calf muscle functioning

7.2.1 Introduction

The shape of the sole changes the way in which the foot moves relative to the ground. A negative heel keeps foot more dorsiflexed through the whole gait cycle and a raised heel keeps ankle more plantarflexed. Therefore, the point of application and direction of GRF changes as well, which results in compensation by the other parts of the body to keep balance during walking in the joints. This causes an alteration to shank, thigh and hip movement. If the ankle angle is too plantarflexed, the fibres in the calf muscle lose force generation capabilities and it then requires the use of more motor units to provide propulsion. However, the moment arm is also lengthening with ankle plantarflexion to compensate for it. There is a specific range at which the calf muscle starts to lose efficient force generation capabilities and this makes the muscle work harder with a lower ankle moment. The 5.5HH demonstrated that effect. The 1.5 cm differences in heel height significantly reduced MG and soleus mean EMG values when compared to lower heeled profiles. However, with raising the heel height beyond the point of 4.5 cm, the calf muscles work harder to compensate for the disadvantageous fibre length-force relationship. Therefore, just a 1cm raise of the heel height from 4.5cm increased the calf mean EMG activity (the 5.5HH increased by 14.6% for MG muscle and increase by 17.3% for soleus muscle when compared to the 4.5HH) and resulted in increase the area underneath the EMG curve (5.5HH increased by 11.0% (MG muscle) and increase by 11.6% for soleus muscle when compared to the 4.5HH). Therefore, if a footwear profile were to be carefully designed according to proven muscle-tendon force capabilities, it could be possible to produce the

ideal footwear, which would not alter knee, hip kinematics and kinetics, but offload calf muscle, as their fibres would be at their optimal position during the walking. This may also result in efficient lower limb body movement without firing up muscles and therefore potentially reduce overall oxygen consumption. The 55% apex length shoe test position proved to be the most effective footwear to offload the calf muscle. It did not significantly change hip and knee kinematics but reduced EMG and ankle moments when compared to the control or 70% apex shoe.

Chapter 6 demonstrated the individual alterations in gait parameters produced by the footwear test conditions. The following sections summarise all the effects of the medial gastrocnemius and soleus force generation changes caused by different footwear features. The results for the flexible forepart shoe were not included as there were no significant alterations compared to the other test conditions. Footwear with flexible foreparts did not demonstrate any significant alterations to the primary outcome measures; probably due to walking speed being kept within strict limits during the walking trials. However, if the participants had chosen their own self-selected walking speed, their gait pattern might have adapted to the most comfortable walking speed and footwear with flexible sole might not limit their walking pattern as a more solid shoe would, as the sole may resist the ankle movement.

Theoretically it could be postulated that a shoe which gave the least resistance to plantarflexion during stance would be the most effective in offloading the calf muscles even if was designed into a solid rocker sole profile – and this may be why the 55% apex shoe position was the most effective in doing this during the walking trials. Indeed this apex position, as stated above, has been shown to be very effective in reducing forefoot plantar pressures; which may be explained by the fact that it did this by reducing the activity of the ankle plantarflexors, which if excessive, could increase forefoot loading. However, a definitive link between forefoot plantar pressures and ankle plantarflexor muscle parameters is as yet unproven, and requires further investigation.

7.2.2 The effect of heel height alteration

Whilst it is important to understand the external measurable effects caused by walking in different shoes, (such as plantar pressures, externally applied moments, kinetics and kinematics), it is becoming increasingly important to also analyse and determine what effect this has on the internal structures of the lower limb; especially when developing footwear for specific applications such as reduction in the calf pain symptoms experienced by claudicants.

Figure 7.2 summarises the alterations to the MG and SOL muscles for different external parameters when walking in shoes with different heel heights. The maximum externally applied ankle dorsiflexion moment at which point the calf muscle works the most is denoted by legend 1. It did not show any significance differences except for the 1.5HH test condition when compared to the other footwear conditions. This demonstrates that the mean externally applied ankle DF moment was similar for all footwear conditions in this study. The extent to which this result applies to other rocker profiles needs to be determined in future studies.

The internal ankle moment is correlated to muscle force generation and the internal MTU moment arm. Therefore, it is not clear without further clarification, if the muscle is applying higher or lower magnitudes of force for a given moment value. Legend 2 in figure 7.1, shows that there was a significant change in the Achilles tendon moment arm between all footwear conditions caused by the heel height change as shown in table 7.1. It can be seen that with the 1.5HH test condition, the muscle moment arm was significantly reduced and it required an additional 61.3N of force generation to produce ankle motion when compared to the control shoe. However, there were no significant changes seen to the EMG data when comparing all the footwear test conditions even though the MG and soleus muscles were significantly stretched which would have resulted in passive force compensation. The 2.5HH required almost 50% less MG fibre force generation [32.0 (18.2) N], but significantly increased its EMG activity when compared to the 4.5HH. It can therefore be suggested that the muscle moment arm was short in length and the MG muscle was not stretched or close to its optimal length position, therefore the fibres were working harder to produce that force.

Muscle force generation is also related to the velocity of muscle contraction (Delp, 1990). Another reason for offloading calf muscle whilst walking in the 4.5 cm heel test condition when compared to lower heels is that velocity of eccentric contraction was significantly increased during terminal stance as shown in the table below. The muscle length started to eccentrically contract at a good position and ended at the optimal fibre length position, which is close to the barefoot static. It allowed generating force to be more efficient when compared to all shoes. The medial gastrocnemius barefoot static position fibre length is also related to the knee flexion, therefore the barefoot static natural position might not be close to optimal fibre length positions but the soleus barefoot static is not affected by knee and therefore it shows natural position.

Another additional factor, which influenced a reduction of overall EMG activity whilst walking in the 4.5 cm heel height, is that heel height altered the external PF moment and increased the duration of it. Therefore it resulted in delaying the activation of the external ankle DF moment. It also resulted in reduction of overall calf muscle force generation. However, this effect has been seen for the 4.5HH condition, and the 5.5HH delayed the external ankle DF moment to occur. However, the muscle length was too short; which resulted in recruiting more motor units and having to work even harder. This leads to the conclusion that even a small change in muscle length may significantly result in force generation capabilities which can be altered by footwear features.

The triceps surae is formed from a combined group comprising of the gastrocnemius and soleus muscles. Table 7.1 shows that a 1.5 cm change in heel height from 3.5 to 4.5mm resulted in a reduction in the area underneath the curve for EMG activity. For the MG muscle, this reduction was 7.3% when compared to the 3.5HH condition and for soleus (SOL) this reduction was 5.8%. If both results were to be combined, it would induce significant alteration to the overall work done by the calf muscles. EMG does not show the magnitude of the force but it does show how many motor units are recruited to perform the task. It clearly indicates that muscle works harder or less hard, and therefore it is related to oxygen consumption.

The 1.5HH shoe significantly increased MG and soleus EMG activity during 5-40% of stance phase and it added to the overall work done by the muscle fibre units work and therefore would have potentially affected oxygen consumption. The reason for activation timing can be due to the premature ending of external ankle PF moment and an increase in ankle moment magnitude caused by the heel alteration.

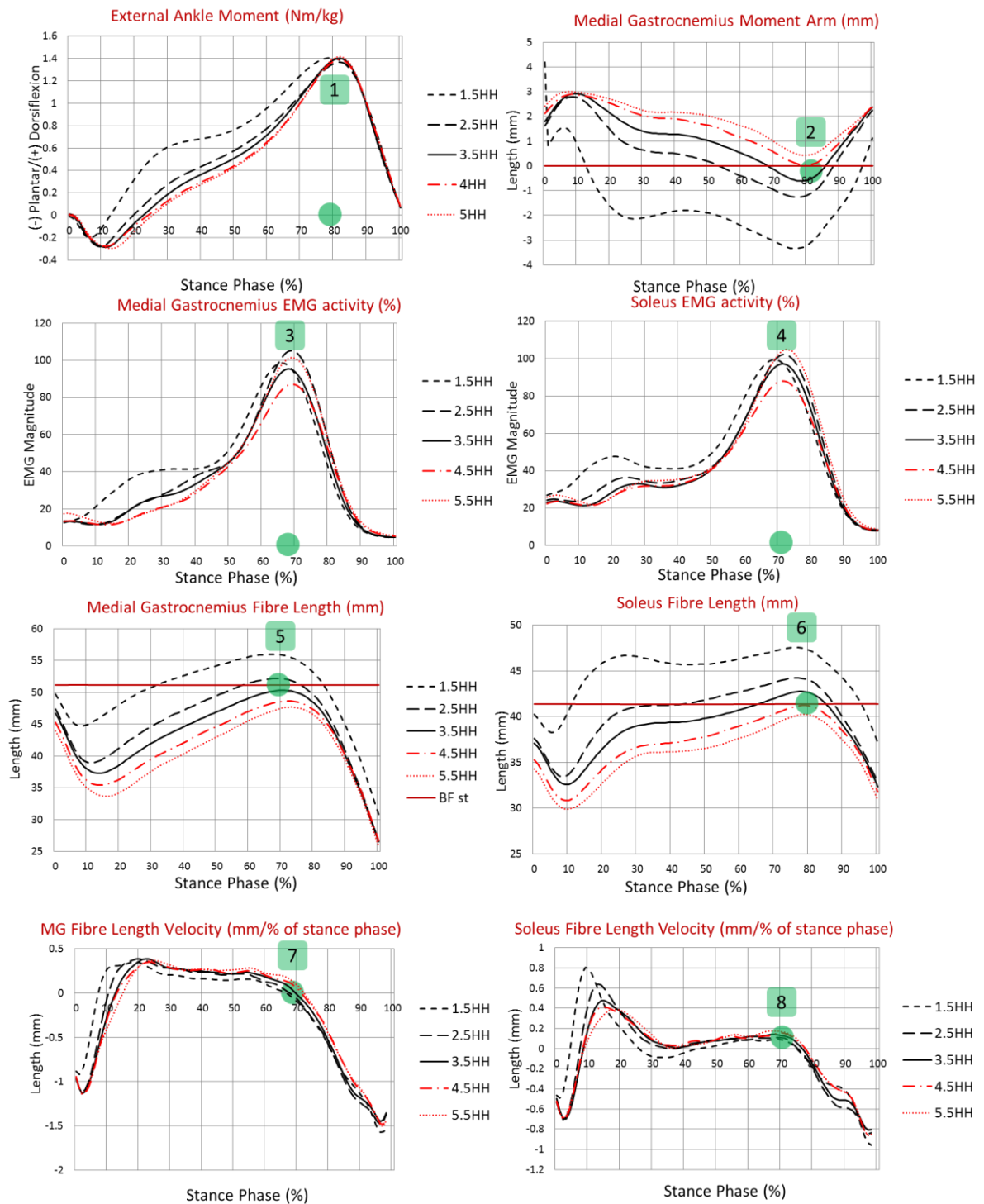


Figure 7.2: Summary of alteration to muscle function by different heel heights.

Table 7.1: Summary of comparison of factors which resulted in muscle function alteration by differing the heel heights.

	1.5 HH	2.5 HH	3.5 HH	4.5 HH	5.5 HH
Test conditions [significant when in superscript ($p < 0.05$)]	1	2	3	4	5
Medial Gastrocnemius and Soleus					
1. Max internal ankle PF moment (Nm/kg)	1.41 ^{2,3,4,5} (0.05)	1.37 ¹ (0.04)	1.41 ¹ (0.05)	1.40 ¹ (0.05)	1.42 ¹ (0.04)
1.1 Area underneath the curve for external ankle DF moment (%)	128.0 ^{2,3,4,5} (3.8)	104.7 ^{1,4,5} (5.5)	100.0 ¹ (5.9)	95.1 ^{1,2} (5.4)	95.4 ¹ (5.1)
2. Achilles tendon moment arm (mm)	40.95 ^{2,3,4,5} (0.56)	43.39 ^{1,3,4,5} (0.34)	44.11 ^{1,3,4,5} (0.30)	44.67 ^{1,2,3,5} (0.28)	44.99 ^{1,2,3,4} (0.29)
3. Max MG EMG activity (%)	104.2 (13.7)	110.1 ⁴ (11.8)	100.0 ⁵ (8.8)	93.5 ² (9.1)	108.1 ³ (9.6)
3.1 Area underneath the curve for MG EMG activity (%)	114.4 ⁴ (13.0)	107.4 ⁴ (9.1)	100.0 (10.1)	92.6 ^{1,2} (10.5)	103.6 (10.5)
4. Max soleus EMG activity (%)	104.7 (11.0)	105.8 ⁴ (9.0)	100.0 ⁴ (6.5)	91.2 ^{2,3,5} (7.3)	107.5 ⁴ (7.4)
4.1 Area underneath the curve for soleus EMG activity (%)	109.6 (8.6)	105.5 ⁴ (7.7)	100.0 ⁴ (7.3)	94.2 ^{2,3,5} (7.0)	105.8 ⁴ (7.7)
5. Max MG fibre length during TS phase (mm)	56.31 ^{2,3,4,5} (1.29)	52.45 ^{1,3,4,5} (0.88)	50.47 ^{1,3,4,5} (0.83)	48.80 ^{1,2,3,5} (0.63)	47.77 ^{1,2,3,4} (0.77)
6. Max soleus fibre length at TS phase (mm)	56.31 ^{2,3,4,5} (1.29)	52.45 ^{1,3,4,5} (0.88)	50.47 ^{1,3,4,5} (0.83)	48.80 ^{1,2,3,5} (0.63)	47.77 ^{1,2,3,4} (0.77)
7. MG fibre length velocity at 68% stance phase (mm/% stance phase)	0.001 ^{3,4,5} (0.080)	0.043 ^{3,4,5} (0.060)	0.094 ^{1,3,4,5} (0.054)	0.137 ^{1,2,3,5} (0.040)	0.185 ^{1,2,3,4} (0.054)
8. Soleus fibre length velocity at 72% stance phase (mm/% stance phase)	0.07 ^{3,4,5} (0.08)	0.09 (0.05)	0.12 ¹ (0.05)	0.14 ¹ (0.06)	0.15 ¹ (0.07)
9. MG tendon force required differences versus control shoe to produce the ankle moment (N)	61.3 (13.7)	32.0 (18.2)	0.0 (19.0)	-35.7 (15.0)	-62.7 (21.7)

There is also a gap in the understanding of how the velocity of muscle contraction would affect the force generation. For example, two different footwear conditions may only alter the velocity of muscle contraction, but the MTU lengths may be similar. Therefore, it is hard to tell if the velocity of contraction has greater impact on muscle force generation rather than its length. The results of this study suggest that the length of the muscle-tendon units are the main force factor, which influence the force generation by the muscle and it may also influence the oxygen demand. It can be seen from the summary table for heel heights that the MG and soleus muscle generate force by eccentric contraction and if it ends at the point where maximum force is required with optimal muscle-tendon length, it may guarantee an offloading the calf muscle. Overall calf muscle offloading can be achieved with

heel height alteration which resulted in a delay of the internal ankle PF moment phase as well as reduction of the ankle moment. Conversely, alteration to the heel height produced kinematic changes in the knee and hip and that gives the indication that the footwear can be altered and adjusted to compensate for that change to improve the gait pattern without altering it.

7.2.2.1 Comment

The overarching hypothesis that rocker soles (incorporating different heel heights) can significantly alter sagittal plane kinematics (at the hip, knee and ankle) is therefore accepted.

7.2.3 Conclusion

The 4.5 cm heel raise reduced the overall external ankle DF moment. It also placed the ankle at a more natural position where it could generate more force during late stance phase. However, the alteration to the heel height also produced alteration to the toe angle, and it may have resulted in resisting the ankle to plantarflex and may also have resulted in increasing the plantar pressures in the metatarsal head area. It was important to understand separate footwear features, and further research is needed to look at a combination of different footwear features to achieve desirable effects.

7.3 The effect of walking with rocker soles incorporating different apex positions

As previously stated, optimal rocker sole apex position has been the subject of numerous investigations by various authors when analysing the position to maximally offload the forefoot to relieve the symptoms associated with excessive plantar foot pressures. This becomes particularly pertinent for subjects with “at-risk” feet suffering from pathologies such as diabetic peripheral neuropathy, rheumatoid arthritis or spina bifida.

An analysis of maximal reduction in plantar foot pressures when walking in rocker-soled shoes has shown that the recommended optimal apex positions vary but most recommend a position proximal to the first metatarsal head area. Cavanagh et al (1996), demonstrated that an apex position of 55% of shoe length was the optimal position for offloading the

forefoot with an angled rocker sole; which would indicate that it may prove to also be a position that would be a natural pivot point for a solid traditionally shaped angled rocker sole. The maximum offloading of the forefoot at this position could have been due to the fact that the rocker position met “minimal resistance” to plantarflexion rotational motion at the pivot point; meaning that the posterior structures such as the ankle plantarflexors may have been offloaded by not offering so much resistance to ankle plantarflexion as other apex position. However, this is as yet unknown and is only conjecture; but this is why it was of interest for this thesis.

The results from the gait laboratory walking trials demonstrated that the shoe with a 55% apex rocker position (55AP), shifted the ankle into a more plantarflexed position during LR (1.3°) ($p=0.001$) compared to the control shoe (where the control shoe is 62.5AP) and also produced less maximum dorsiflexion during second rocker of gait (1.6°). Additionally, it placed the ankle into more plantarflexion during and at the end of third rocker of gait (1.9°) compared to both the control condition and the 70AP test condition. It therefore produced a plantarflexion shift during stance phase compared to the control shoe.

7.4 The effect of different rocker apex positions (APs) on muscle function.

The following section demonstrates the effect of altering the apex position of the rocker sole on muscle function. Figure 7.3 summarises the alterations to the MG and SOL muscles for different external parameters when walking in shoes with different apex positions.

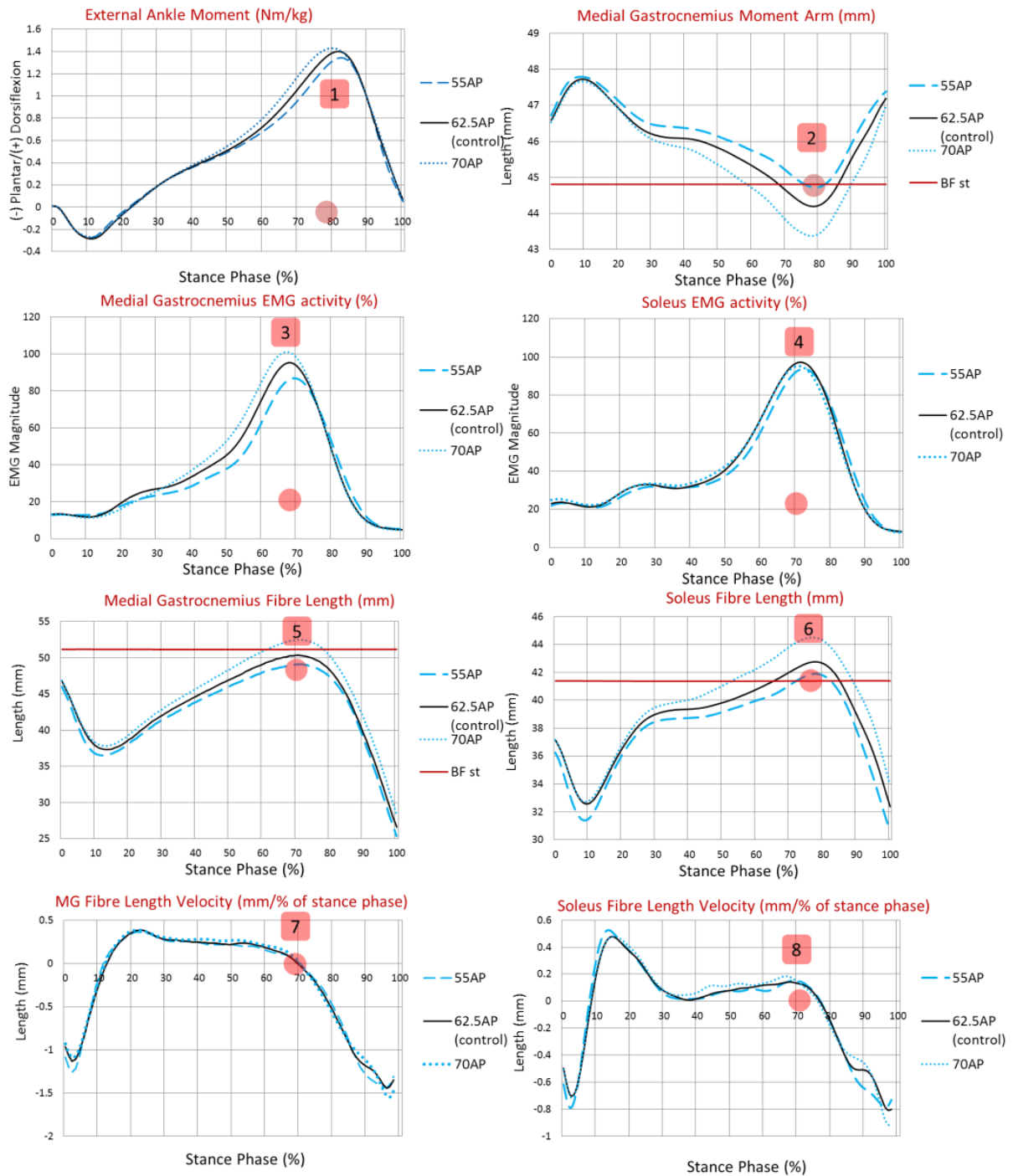


Figure 7.3: Summary of alteration to muscle function caused by alteration to the rocker sole apex position

The apex position variation produced changes in the kinematic data in the ankle but there were no significant changes demonstrated at the hip and knee. A more proximal apex position resulted in a reduction of maximum ankle DF at 50% of the gait cycle, but no

significant changes to the maximum PF angle during LR when compared to the control shoe as shown in the figure 7.4.

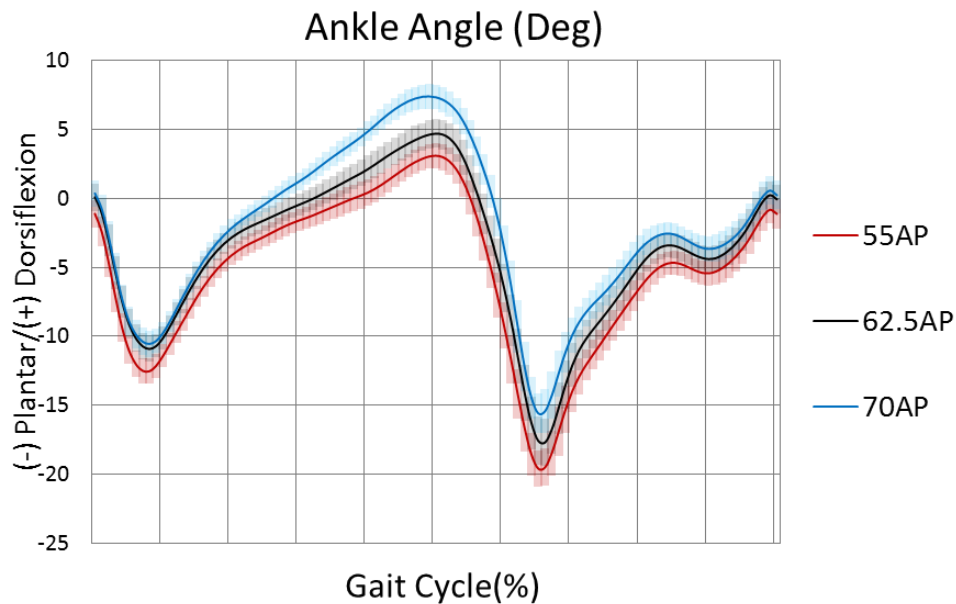


Figure 7.4: Sagittal plane ankle motion when walking with the three-apex position test conditions with standard deviation where the control shoe is 62.5AP.

From the figure above, it can be also seen that the 70AP resulted in a rapid increase ankle ROM being produced between 20-50% of the gait cycle, and therefore an increase in velocity of eccentric contraction by the calf muscle. The soleus EMG results showed that the 70AP test condition did not increase maximum EMG activity when compared to the control shoe - and even slightly reduced it. However, the Achilles tendon moment arm was significantly shorter versus the control footwear test condition (62.5AP) footwear as shown in table 7.2 and figure 7.4. The internal ankle PF moment was significantly increased which means it requires more muscle force to produce the moment about ankle. Figure 7.3 shows that soleus fibre length range was increased from 20-80% of the stance phase, which means the soleus muscle was stretched more than all footwear conditions This evidence suggests that the eccentric velocity of soleus muscle was increased, and therefore this compensation resulted in more force generation by the 70AP footwear condition.

However, there were different effects noted for the medial gastrocnemius muscle. The 70AP footwear increased maximum EMG activity by 7.1% versus control and 15.8% versus the 55AP condition. The area under the curve for MG EMG was also increased for the 70AP by 6.7% versus control and 15.6% versus the 55AP footwear. The medial gastrocnemius muscle

force generation is also related to the knee flexion position. There was a slight alteration to knee flexion for the 70AP between 10-40% of the gait cycle (figure 7.4). In figure 7.3 it is noticeable that there is less MG fibre lengthening from 20-80% of stance phase, which could have resulted in reducing the MG maximum eccentric lengthening velocity, and therefore it could have resulted in a reduction of the tension generation and more motor units were recruited to produce the required force. Thus, a significant increase in MG muscle work for the 70AP footwear test condition was produced.

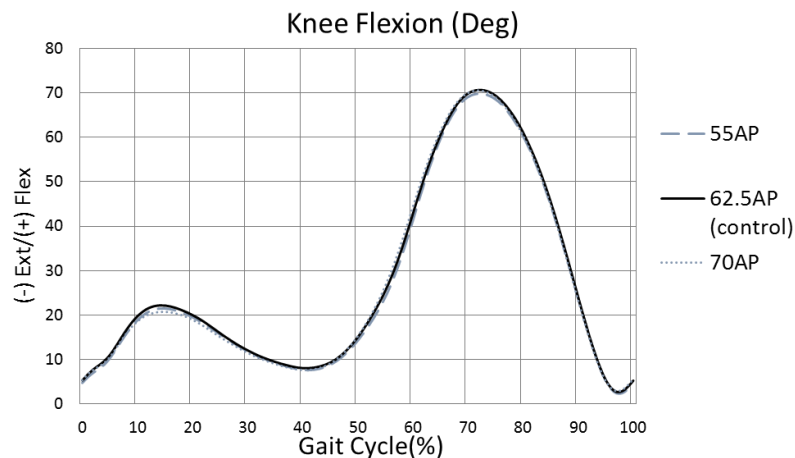


Figure 7.5: Sagittal plane knee motion during the three apex position test conditions where the control shoe is 62.5AP.

Table 7.2: Summary of alteration on muscle function produced by altering the rocker sole apex position.

	55AP	62.5AP	70AP
Test conditions [significant when in superscript (p<0.05)]	1	2	3
Medial Gastrocnemius and Soleus			
1. Max internal ankle PF moment (Nm/kg)	1.35 ^{2,3} (0.05)	1.41 ^{1,3} (0.05)	1.44 ^{1,2} (0.03)
1.1 Area underneath the curve for external ankle DF moment (%)	94.3 ^{2,3} (5.4)	100.0 ^{1,3} (5.9)	106.4 ^{1,2} (5.1)
2. Achilles tendon moment arm (mm)	44.59 ^{2,3} (0.26)	44.11 ^{1,3} (0.30)	43.26 ^{1,2} (0.33)
3. Max MG EMG activity (%)	91.3 ^{2,3} (11.3)	100.0 ¹ (8.8)	107.1 ¹ (9.3)
3.1 Area underneath the curve for MG EMG activity (%)	91.1 (12.6)	100.0 (10.1)	106.7 ¹ (9.0)
4. Max soleus EMG activity (%)	94.7 (9.4)	100.0 (6.5)	98.2 (8.3)

4.1 Area underneath the curve for soleus EMG activity (%)	97.6 (6.8)	100.0 (7.3)	99.4 (8.3)
5. Max MG fibre length during TS phase (mm)	49.15 ^{2,3} (0.74)	50.47 ^{1,3} (0.83)	52.68 ^{1,2} (0.60)
6. Max soleus fibre length at TS phase (mm)	42.03 ³ (0.73)	42.89 (0.69)	44.73 ¹ (0.74)
7. MG fibre length velocity at 68% stance phase (mm/% stance phase)	0.094 (0.059)	0.094 (0.054)	0.135 ² (0.053)
8. Soleus fibre length velocity at 72% stance phase (mm/% stance phase)	0.13 (0.08)	0.12 (0.05)	0.10 (0.07)
9. MG tendon force required differences versus control shoe to produce the ankle moment (N)	-27.5 (18.2)	0.0 (19.0)	41.4 (9.2)

7.4.1 Conclusion

There were significant increases demonstrated in MG EMG activity for the 70AP. This was due to a shorter muscle moment arm, longer fibre length (which was far from its optimal length), a reduced range of eccentric lengthening, and a greater internal ankle PF moment requirement due to the alteration of the sole.

The 55AP footwear increased the length of the Achilles tendon moment arm when more force is required, kept the fibre length closer to its optimal length (the natural position of the lower limb), reduced the force required for producing moments by the ankle, and it needed 27 N less force production when compared to the control shoe and 68.9 N less when compared to 70AP. However, the results suggest that if the 55AP increased eccentric lengthening range and kept fibres closer to optimal length, it could potentially offload calf muscle even more.

The results demonstrated that velocity of soleus contraction influenced its EMG activity.

The 55AP footwear condition is therefore perceived to be the best option for offloading calf muscle between the different apex position test conditions analysed in this research, and it may also reduce muscle oxygen demand. Patients with intermittent claudication experience pain in the gastrocnemius muscle, and therefore a 55% apex position may produce a more significant reduction in symptoms for claudicants than the other test conditions, but this is

as yet unproven. However, there were only three apex length rockers were tested and it could be possible that 50% or 52% may have greater effect rather than the 55AP footwear.

7.5 The effect of different toe apex angles on muscle function

The 20°TA significantly reduced maximum EMG activity for MG and soleus muscles when compared to the control and the 10° TA footwear condition. The results suggest that the Achilles moment arm for 20°TA was slightly increased during 75-95% of the stance phase. It may have therefore resulted in greater moments produced by the calf muscles. The results also demonstrated that the maximum internal ankle PF moment was also significantly reduced at 80% of the stance phase. The 10°TA showed a significant increase in maximum EMG activity for the MG and soleus muscles when compared to the 20°TA. The muscle moment arm was also significantly shorter at maximum EMG activity for the 10°TA, which caused more force requirement to produce the internal ankle PF moment (figure 7.6).

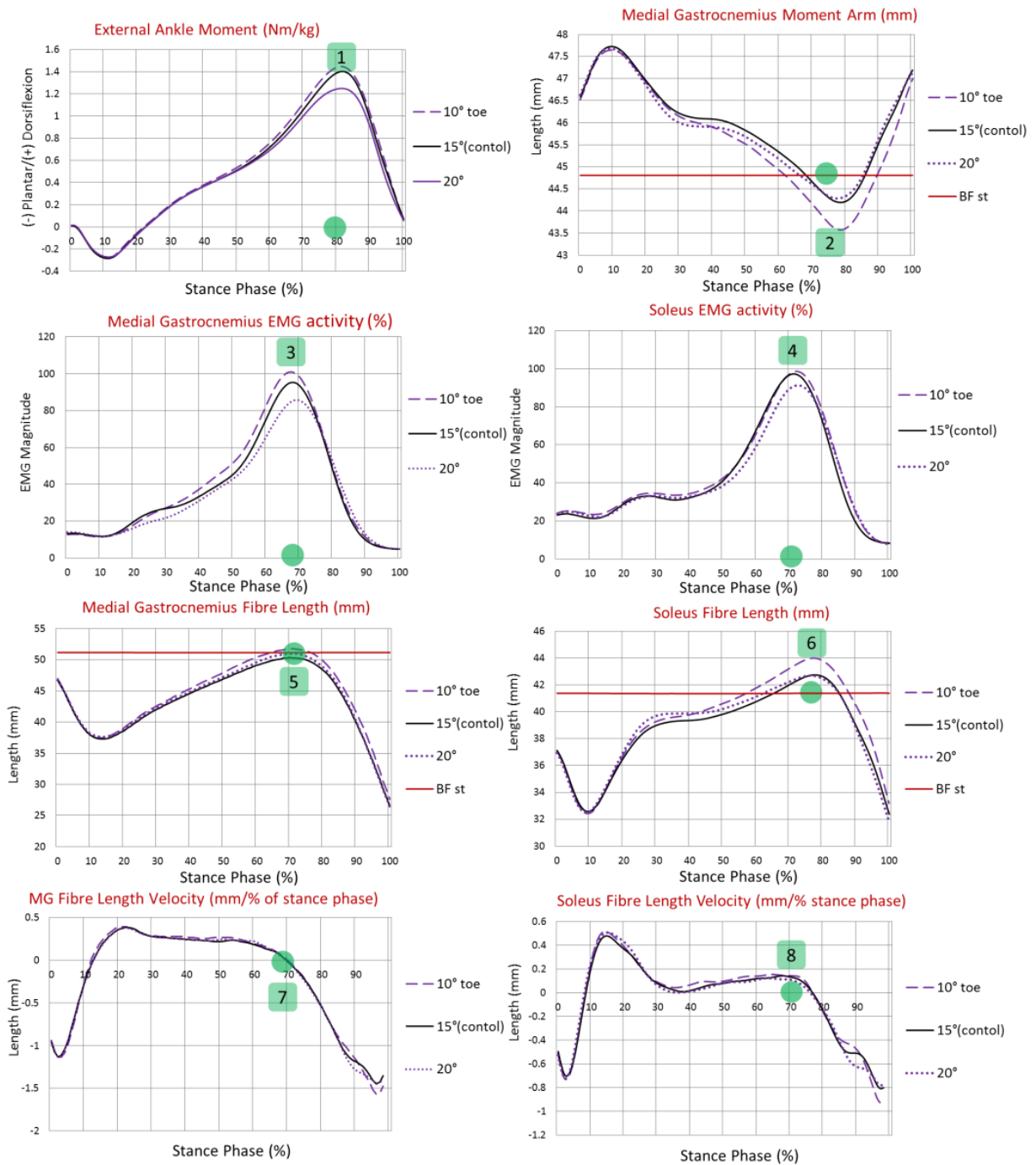


Figure 7.6: Alteration to muscle function demonstrated by altering rocker apex angle.

The 10°TA test condition did not produce any significant changes in maximum soleus EMG activity when compared to the control shoe even though the muscle tendon was far from its natural position. As previously discussed, for the 70AP position, the soleus muscle fibre lengthening range was increased and therefore so was the velocity of eccentric contraction and that was the reason for more muscle force generation.

Table 7.3: Summary comparison factors which resulted in muscle functioning alteration by the rocker apex toe angle.

	10° TA	15° TA	20° TA
Test conditions [significant when in superscript (p<0.05)]	1	2	3
Medial Gastrocnemius and Soleus			
1. Max internal ankle PF moment (Nm/kg)	1.45 ^{2,3} (0.05)	1.41 ^{1,3} (0.05)	1.26 ^{1,2} (0.04)
1.1 Area underneath the curve for external ankle DF moment (%)	105.4 ^{2,3} (5.4)	100.0 ^{1,3} (5.9)	92.5 ^{1,2} (4.1)
2. Achilles tendon moment arm (mm)	43.48 ^{2,3} (0.37)	44.11 ¹ (0.30)	44.12 ¹ (0.37)
3. Max MG EMG activity (%)	107.2 ³ (9.2)	100.0 ³ (8.8)	89.4 ^{1,2} (9.9)
3.1 Area underneath the curve for MG EMG activity (%)	108.0 ³ (11.2)	100.0 (10.1)	93.6 ¹ (10.1)
4. Max soleus EMG activity (%)	101.4 ³ (7.6)	100.0 ³ (6.5)	92.2 ^{1,2} (8.0)
4.1 Area underneath the curve for soleus EMG activity (%)	102.2 (7.7)	100.0 (7.3)	96.3 (9.1)
5. Max MG fibre length during TS phase (mm)	51.95 ² (0.65)	50.47 ¹ (0.83)	51.23 (0.81)
6. Max soleus fibre length at TS phase (mm)	44.23 ³ (0.80)	42.89 (0.69)	43.01 ¹ (0.63)
7. MG fibre length velocity at 68% stance phase (mm/% stance phase)	0.120 (0.051)	0.094 (0.054)	0.097 (0.067)
8. Soleus fibre length velocity at 72% stance phase (mm/% stance phase)	0.14 (0.08)	0.12 (0.05)	0.09 (0.07)
9. MG tendon force required differences versus control shoe to produce the ankle moment (N)	28.2 (10.5)	0.0 (19.0)	14.0 (21.7)

7.6 The effect of different curved heels on muscle function

A curvature of the heel altered the ankle kinematics and put the ankle into a more DF position throughout the entire stance phase. It therefore increased calf muscle lengthening. The full curved heel changed the point of application of the GRF and therefore caused a premature external ankle DF moment to occur and also increased the ankle moment from

20-70% of the stance phase. At 80% of stance phase the full curve heel reduced the maximum external ankle DF moment when compared to the heel without a curve. However, the full curve footwear increased the area underneath the curve for external ankle DF moment by 6% due to the premature application of the external ankle DF moment with increased magnitude within 20-70% stance phase. That also resulted in increased EMG activity from 10-65% of stance phase for medial gastrocnemius muscle and an increased EMG activity within 0-40% stance phase for soleus.

The results did not show any statistical significance for maximum EMG activity for soleus and MG muscles whilst walking in curved heels. However, the full curve heel increased EMG activity during 5-70% stance phase, which resulted in an increase of the area underneath the curve for maximum EMG activity for the medial gastrocnemius muscle when compared to the half curve test condition.

It can therefore be postulated that a greater curve may alter kinematics, kinetics, and muscle tendon length during 5-70% of the stance phase and therefore overall EMG activity. The half curve or even less should therefore be used for patients with intermittent claudication to offload the calf muscle.

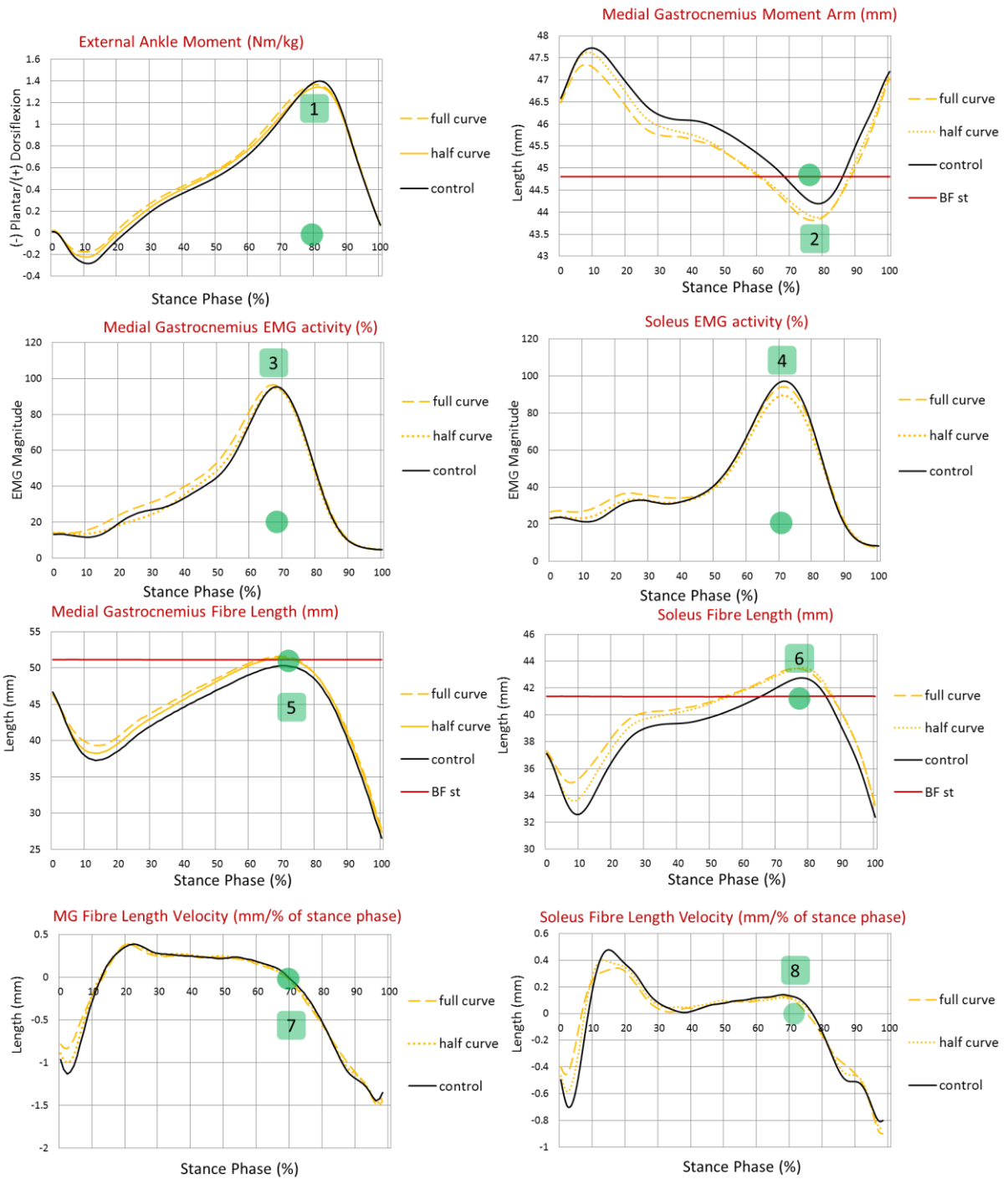


Figure 7.7: The effect of different heel curves on fibre lengths.

Table 7.4: Summary and comparison of factors which resulted in muscle function alteration by altering heel curvature.

	Full curve	Half curve	control
Test conditions [significant when in superscript ($p < 0.05$)]	1	2	3
Medial Gastrocnemius and Soleus			
1. Max internal ankle PF moment (Nm/kg)	1.37 (0.04)	1.35 ³ (0.04)	1.41 ² (0.05)
1.1 Area underneath the curve for external ankle DF moment (%)	106.0 ^{2,3} (5.3)	100.6 ¹ (5.8)	100.0 ¹ (5.9)
2. Achilles tendon moment arm (mm)	43.68 ³ (0.36)	43.77 ³ (0.38)	45.12 ^{1,2} (0.27)
3. Max MG EMG activity (%)	102.6 (11.6)	99.9 (9.8)	100.0 (8.8)
3.1 Area underneath the curve for MG EMG activity (%)	107.7 ² (10.5)	99.1 ¹ (10.4)	100.0 (10.1)
4. Max soleus EMG activity (%)	97.5 (9.8)	92.9 (7.2)	100.0 (6.5)
4.1 Area underneath the curve for soleus EMG activity (%)	100.9 (7.7)	94.9 (8.1)	100.0 (7.3)
5. Max MG fibre length during TS phase (mm)	51.90 (0.85)	51.62 (0.84)	50.47 (0.83)
6. Max soleus fibre length at TS phase (mm)	43.72 ³ (0.73)	43.72 ³ (0.81)	42.89 ^{1,2} (0.69)
7. MG fibre length velocity at 68% stance phase (mm/% stance phase)	0.060 (0.050)	0.070 (0.052)	0.048 (0.050)
8. Soleus fibre length velocity at 72% stance phase (mm/% stance phase)	0.08 (0.07)	0.09 (0.06)	0.12 (0.05)
9. MG tendon force required to produce the ankle moment (N)	21.6 (19.8)	19.8 (17.5)	0.0 (19.0)

7.7 Limitations to the methodology and the approach adopted

7.7.1 The walking trials

There were certain limitations to this study. Even though the overall test duration was kept to a minimum for each subject, the gait laboratory trials typically took a number of hours in some cases in order to ensure the quality of the data collection in the gait laboratory was at an acceptable standard to be used for subsequent analysis. This had ramifications for using

the EMG electrodes over a protracted period, as there is a possibility that electrode performance could have altered during the prolonged testing periods.

The test conditions were randomised during the testing. Due to the fact that the test subjects were all fit young males, fatigue was not deemed to be a problem. Rest periods were allowed during the test condition trials in order to ensure that fatigue was not a problem. This also allowed the researcher to check the data collected for the previous test conditions to ensure the requisite number of trials of acceptable quality were acquired prior to proceeding on to the next test condition. In addition, time was needed to alter the footwear test conditions and allow a short period of habituation prior to commencement of the walking trials for the specific rocker-soled shoe test condition. However, rocker sole carry-over effects have been shown to be insignificant in previous publications.

The fact that the walking trials speed of walking was closely controlled meant that it was possible to compare the test conditions without the complication of introducing significantly different walking speeds. The age and gender of the volunteer able-bodied subjects who performed the walking trials in this study, did not reflect that published for the general claudicant population. However, this was necessary to ensure confounding variables such as large age differences and fitness levels between the subjects, which could have affected the results and negated a direct comparison between the test conditions was kept to a minimum. It is the intention, however, to utilise the findings of this research to develop footwear for trial use by a population of volunteer claudicants in the future.

The EMG data collection equipment available was not capable of acquiring data for all the muscle groups in the lower leg. It would have been advantageous to test the activity of the hip flexors and extensors, as these have been recently shown to be weak in claudicants. Nevertheless the data quality obtained for the muscles tested was of acceptable quality to provide meaningful results.

7.7.2 Kinetic and Kinematic data

In any data collection utilising retro-reflective markers and electrodes for EMG data collection, there will have been some soft tissue artefacts occurring during ambulation;

especially on skin-mounted electrodes or those situated near joints. Whilst these could not be totally eliminated, care was taken to ensure that the leads connecting the EMG electrodes to the acquisition system and the thermoplastic plates used to mount the clusters on the anterior aspect of the thigh and shin, as well as on the pelvis, were kept to a minimum using taping and elastic strapping.

The markers used to define the first and fifth metatarsal heads and the posterior aspect of the calcaneus bilaterally, were attached directly onto the skin of the foot. This meant that during each change of shoe condition, these reflective markers had to be removed and replaced to allow the next set of shoes to be tested shoes to be donned and the previous ones taken off utilising apertures cut into the shoe uppers for the base plates of the markers to be placed through. The use of cut-outs in the shoe uppers was, however, deemed to be important, as markers placed on the uppers of the shoes cannot delineate the position of the first and fifth metatarsal heads as accurately. The anatomical position of the markers on each foot was marked on the skin by marking the position of the mounting plate for each marker concerned, and to reduce inaccuracies to a minimum.

Overall sources of error were kept to a minimum by utilising same-session testing for all subjects and using the subjects as their own control. The only variable for the gait laboratory trials for each subject was therefore the shoe condition; as walking speed was also controlled.

7.7.3 OpenSim limitation

The Gait2392 model was based on old muscle architecture data collected in 1990. There are new modern techniques to obtain that data and today there is an updated lower limb model. The new model describes muscle architecture (i.e., muscle fibre lengths, pennation angles, and physiological cross-sectional area) more precisely; based on data obtained from 21 cadavers. However, exported motion data from Visual3D cannot be used accurately with that model. Another method of marker placement should be used to scale body segments for each subject. This method was not integrated into the method of data collection used for this study, as it would require extensive investigations into the development of marker placement with different rocker profiles in order to improve the technique to be able to remove static shift effects caused by different shapes of the rocker shoes, which would

directly affect muscle-tendon properties data. OpenSim is an open source and therefore each model can be customised for subjects' demographics, muscle property data can be used according to the subjects' age, muscle architecture and anthropometric data. For example, for elderly subjects, average pennation angle of skeletal muscle such as gastrocnemius medialis muscle alters with aging (Binzoni et al., 2001).

7.7.4 The OpenSim velocity of muscle-tendon length calculation limitations

The velocity data were normalised to 100% stance phase. Therefore, it resulted in stretching the curves by time scale and it could have resulted in interpolating the data and a possible increase/decrease the muscle-tendon lengths. That could theoretically affect the velocity data. If the muscle-tendon units for each trial were not normalised to 100% time scale, in this case it would not be possible to define the same time scale points of interest during stance phase or gait cycle.

7.7.5 External foot marker placement and rigid foot model

For the purpose of the thesis foot kinematics were recorded using markers placed externally on the shoe and on the skin through windows cut in the shoe as described in method chapter. A recent study has demonstrated that there were significant differences in discrete kinematic parameters between skin and shoe mounted marker test conditions, at the midfoot-calcaneus, forefoot-midfoot and forefoot-calcaneus articulations during walking (Sinclair et al., 2013). It also showed that shoe mounted markers do not fully represent true foot movement, and should therefore be interpreted with caution during examination of multiple-segment foot kinematics. In the current PhD research markers were placed on the skin, however a rigid model of the foot was recorded. It was not practically possible to collect multisegment foot data for 16 pairs of shoes and be able to place markers on the exact same positions due to high numbers of markers needed meaning that there would have been too many holes cut in the upper of the shoes. It would also take more time to collect data for each subject and may introduce more possible errors especially within EMG data. Therefore, this was a limitation in this research and kinematic data could be affected by it. Another recent study which compared the reliability and repeatability of three

different multisegment foot models demonstrated that reliability of segmental kinematics varied, with low repeatability (Intraclass correlation coefficient <0.4) found for 14.3% of the Oxford Foot Model angles, 22.7% of 3DFoot angles and 37.6% of Kinfoot angles (Mahaffey et al., 2013). However, the literature research performed for all previous footwear studies presented in this thesis used a rigid foot model and markers were placed direct onto the shoe. It would be adventitious, if the foot was analysed as a multisegmental model. It could show more movement of the foot and can be related to plantar pressures as well as offering the possibility of investigating the effect of rocker soles on specific foot structures and articulations. However, ankle angle was the main interest in the study. All footwear conditions were inflexible in the rearfoot and midfoot areas due to the addition of the rocker soles and the shoes were fit snugly and laced properly which meant that there was limited movement in those areas.

7.7.6 The walking speed limitation

The investigation of the effect of walking speed on muscle function has been previously studied (Hof et al., 2002, den Otter et al., 2004, van Hedel et al., 2006, Byrne et al., 2007, Chiu and Wang, 2007, Stoquart et al., 2008, Chung and Wang, 2010, Sousa and Tavares, 2012) (Sousa and Tavares, 2012). The results suggest that gait speeds such as fast walking and slow walking influence not only EMG activity levels but also relative muscle activity patterns. The walking speed therefore was controlled to ensure that it would minimise the possible effect on kinematic, kinetic and EMG data. It was important to understand how footwear features change walking patterns, but not the influence of walking speed, in this study. However, different footwear test conditions produce alteration to walking speed due to the sole design. For instance, a stiff soled shoe would resist bending at the metatarsal head area which can result in reduction of step length during gait. This was one of the limitations in this research.

7.7.7 Conclusion and future work

In regards to the offloading of the calf muscles, the footwear features such as the 4.5 cm heel, the 55AP, the 20°TA demonstrated significant offloading to the calf muscle. The 55AP has a significant offloading influence on the calf muscles whilst at the same time not

significantly altering knee and hip kinematics. This would be perceived to be a viable option for individuals with intermittent claudication as one would hope with the results found in this study that this would translate to this population, and help to reduce the onset of walking pain in the posterior compartment.

Everyday walking requires to adapt to different speed of walking depending on the environment. For example, rapid stopping before the traffic light or walking accelerating when a pedestrian crosses the road or following the speed of large group of pedestrians in the city. Very stiff soles may have some limitations in being able to adapt to different levels of walking speed. The foot has more than 30 joints and it helps us to have better gait. Well-known high street footwear brands have designed comfortable shoes for running and walking by making sole of the shoe very flexible (almost as barefoot walking), and it does not limit the motion of the foot as much as a stiff-soled shoe.

Most of the footwear studies examined for this thesis did not consider the effect of walking speed on muscle changes and it not always clear whether the changes were due to sole design or walking speed. With slower walking, the calf requires less power to enable walking, and the velocity of muscle contractions is reduced, which would result in muscle function change (force generation).

A solid soled shoe may also increase chance for patients with diabetes to get blisters at the area of the heel. If there is a resistance in the metatarsals area, the heel will be forced to move up during late stance phase, if more plantaflexion power required (faster walking). Therefore, it may produce frictions. However, a flexible sole can increase pressure distribution in metatarsal area. If the sole is flexible, there will be less area of contact with a ground during foot flexion at metatarsal joint and it may apply more pressure on metatarsal region of the feet.

The figure below demonstrates one of the possible designs which may offload calf muscle during walking.



Figure 7.8: The example of estimated final design to offload the calf muscle.

The heel height was chosen to be 4.5 cm as there is strong evidence in this research that it places ankle during late stance at the position at which muscle can generate more force and therefore reduce muscle work (external DF moment, EMG activity). However, the heel height can be slightly varied for a different aged population. Older people tend to have stiffer muscles, and for this purpose, it is necessary to test older population for optimal heel pitch related to age. Healthy and young subjects were tested in this PhD to minimise age factors on the data acquired.

The small heel curve was added to the shoe to make the heel transaction smoother and slightly offload tibialis anterior muscle as the results from this research demonstrated that a curved heel reduced velocity of TA muscle contraction and significantly reduced EMG activity.

The apex position was chosen between 55% and 62.5% of the shoe length. Results demonstrated that 4.5 cm heel height significantly offloaded calf muscle work with 62.5% apex position. However, a lower heel height of 3.5 cm reduced calf work with 55% apex position as well. It helped ankle to plantarflex earlier and placed the calf fibre lengths at a more natural position (resting size) at which it can generate more efficient force. More research is also required on identifying the optimal rocker sole apex position in relation to muscle work and speed of walking.

The has addition of a flexible area at metatarsals to allow adaption of foot to any walking speed without significant sole bending resistance could potentially increase the work done by calf muscles during faster walking speeds.

The 20 degree toe angle showed a slight reduction of MG muscle activity, and therefore a different toe angle may produce the same angle, if the metatarsal area bends when it is required for adaptive walking. The flexible shoe did not show any significant increase or decrease in calf muscle work, thus there were no adverse effects on this parameter, however it may help to allow the skeletal system to adapt during walking speed changes.

There maybe be a more optimal rocker apex position and toe angle which would improve the gait kinematics and kinetics to feasibly to improve claudicant symptoms, but this needs to be explored in a future study. This could include moving the rocker apex position further forwards and back centred on your best position found in the thesis (55% apex position) plus some small alterations to the rocker angle (up to 10 degrees either side of the optimal angle in this study). The materials of the shoes can be also investigated as it can produce the shape of the shoe during the load and return some energy when person walks. There is a new material developed by Adidas to produce 'boost' shoe. This shoe has a very good cushioning system, it also mimics barefoot walking and it returns some energy by pushing the material back when it compressed.

There is a need of further work done and older population testing to understand muscle function better and then specific footwear can be designed. If it requires less pitch of the heel the apex position can help as well to place ankle into advantageous position to offload calf muscle and reduce oxygen consumption.

To the authors knowledge, there is no previous study published which has investigated the effect of different footwear features on muscle-tendon properties and EMG for the muscles action on the ankle. It is felt that when trying to identify optimal footwear features for a clinical population, muscle-tendon properties should be assessed and not only rely on kinematic and kinetic data or surface EMG data. This research demonstrated other important factors, which should be included to analyse the influence of footwear features on gait patterns in future studies.

Every single person has a different walking pattern and gait. Therefore, there is a need to expand the database of knowledge in understanding the possible effects of footwear adaption and outsole designs, which could influence gait and muscle function. However, the research presented in this thesis, is novel in that it not only investigated and interpreted kinematic and kinetic data, but also other important factors, which influence muscle force generation to more fully understand the alteration to muscle function and gait parameters, which may be expected when walking with footwear incorporating specific footwear features more clearly. The additional factors which were taken into account, which could possibly influenced the data such as: walking speed, age and previous injuries of the participants were factored out of the study so that the results were not influenced by them. Future studies are needed which should combine different footwear features based on the results of this study to achieve desirable effects and help in reducing symptoms experienced by various patient groups. There could be more future studies to understand gait alteration effects in more details by varying the apex length, heel height or toe angle of the sole, shoe weight, cushioned shoe, materials of the sole and the gait pattern changes in the footwear conditions whilst walking with different speed.

There could be potential in building up a database in the future with anthropometric data, which should be age and weight related to describe and define the effects of footwear features on gait and walking patterns for a diverse range of patient groups and ages. This would mean that it may be possible for muscle function to be accurately predicted and footwear with known desirable effects could be designed for each person to achieve maximum effects for individual patients.

REFERENCES

- ABDEL-AZIZ, Y. I. & KARARA, H. M. Direct linear transformation from comparator coordinates into object space coordinates in close-range photogrammetry. *Proceedings of the Symposium on Close-Range photogrammetry*, 1971. 18.
- ABERNETHY, B., KIPPERS, V., HANRAHAN, S. J., PANDY, M. G., MCMANUS, A. M. & MACKINNON, L. 2013. *Biophysical Foundations of Human Movement.*, the United States of America, Human Kinetics.
- AHIMASTOS, A. A., WALKER, P. J., ASKEW, C., LEICHT, A., PAPPAS, E., BLOMBERG, P., REID, C. M., GOLLEDGE, J. & KINGWELL, B. A. 2013. Effect of ramipril on walking times and quality of life among patients with peripheral artery disease and intermittent claudication: a randomized controlled trial. *Jama*, 309, 453-60.
- ALLAQABAND, S., KIRVAITIS, R., JAN, F. & BAJWA, T. 2009. Endovascular Treatment of Peripheral Vascular Disease. *Current Problems in Cardiology*, 34, 359-476.
- ALTER, M. 2004. *Science of flexibility*.
- ALZAMORA, M., FORES, R., BAENA-DIEZ, J., PERA, G., TORAN, P., SORRIBES, M., VICHETO, M., REINA, M., SANCHO, A., ALBALADEJO, C., LLUSSA, J. & GROUP, T. P. A. S. 2010. The Peripheral Arterial disease study (PERART/ARTPER): prevalence and risk factors in the general population. *BMC Public Health*, 10, 38.
- AN, H. S. & LEE, K. K. 2007. Effect of rocker heel angle of walking shoe on gait mechanics and muscle activity. *12th Annual Congress of the ECSS*, Finland.
- ANDERSEN, P. & HENRIKSSON, J. 1977. Capillary supply of the quadriceps femoris muscle of man: adaptive response to exercise. *The Journal of Physiology*, 270, 677-690.
- ANDERSON, F. C. & PANDY, M. G. 1999. A Dynamic Optimization Solution for Vertical Jumping in Three Dimensions. *Comput Methods Biomech Biomed Engin*, 2, 201-231.
- ANDRIESEN, M. P., BARENSEN, G. J., WOUDA, A. A. & DE PATER, L. 1989. Changes of walking distance in patients with intermittent claudication during six months intensive physical training. *Vasa*, 18, 63-8.
- ARAZPOUR, M., HUTCHINS, S. W., GHOMSHE, F. T., SHAKY, F., KARAMI, M. V. & AKSENOV, A. Y. 2013. Effects of the heel-to-toe rocker sole on walking in able-bodied persons. *Prosthet Orthot Int*, 37, 429-35.
- ARNOLD, A. S., ASAKAWA, D. J. & DELP, S. L. 2000. Do the hamstrings and adductors contribute to excessive internal rotation of the hip in persons with cerebral palsy? *Gait & Posture*, 11, 181-190.

- ARNOLD, A. S., LIU, M. Q., SCHWARTZ, M. H., ÖUNPUU, S. & DELP, S. L. 2006. The role of estimating muscle-tendon lengths and velocities of the hamstrings in the evaluation and treatment of crouch gait. *Gait & Posture*, 23, 273-281.
- ARNOLD, E., WARD, S., LIEBER, R. & DELP, S. 2010. A Model of the Lower Limb for Analysis of Human Movement. *Annals of Biomedical Engineering*, 38, 269-279.
- ARNOLD, E. M., HAMNER, S. R., SETH, A., MILLARD, M. & DELP, S. L. 2013. How muscle fiber lengths and velocities affect muscle force generation as humans walk and run at different speeds. *J Exp Biol*, 216, 2150-60.
- AYYAPPA, E. 1997. Normal Human Locomotion, Part 1: Basic Concepts and Terminology. *JPO Journal of Prosthetics & Orthotics Spring*, 9, 1-10.
- AYZIN ROSOKY, R. M., WOLOSKER, N., MURACO-NETTO, B. & PUECH-LEAO, P. 2000. Ground reaction force pattern in limbs with intermittent claudication. *Eur J Vasc Endovasc Surg*, 20, 254-9.
- BAKER, P. L. 1970. SACH heel improves results of ankle fusion. *Journal of Bone and Joint Surgery - Series A*, 52, 1485-1486.
- BARLETT, R. 2007. *Introduction to Sports Biomechanics: Analysing human movement patterns.*, Roger Bartlett.
- BAUMAN, J. H., GIRLING, J. P. & BRAND, P. W. 1963. PLANTAR PRESSURES AND TROPIC ULCERATION. AN EVALUATION OF FOOTWEAR. *J Bone Joint Surg Br*, 45, 652-73.
- BICK, E. M. 1961. Ageing in the connective tissues of the human musculoskeletal system. *Geriatrics*, 16(9), 448-453.
- BINNIE, A., PERKINS, J. & HANDS, L. 1999. Exercise and nursing therapy for patients with intermittent claudication. *J Clin Nurs*, 8, 190-200.
- BINZONI, T., BIANCHI, S., HANQUINET, S., KAELIN, A., SAYEGH, Y., DUMONT, M. & JEQUIER, S. 2001. Human gastrocnemius medialis pennation angle as a function of age: from newborn to the elderly. *J Physiol Anthropol Appl Human Sci*, 20, 293-8.
- BOHM, H. & HOSL, M. 2010. Effect of boot shaft stiffness on stability joint energy and muscular co-contraction during walking on uneven surface. *J Biomech*, 43, 2467-72.
- BRAND, R. A., PEDERSEN, D. R. & FRIEDERICH, J. A. 1986. The sensitivity of muscle force predictions to changes in physiologic cross-sectional area. *J Biomech*, 19, 589-96.
- BRASS, E. P. & HIATT, W. R. 2000. Acquired skeletal muscle metabolic myopathy in atherosclerotic peripheral arterial disease. *Vasc Med*, 5, 55-9.
- BREEK, J. C., HAMMING, J. F., DE VRIES, J., AQUARIUS, A. E. & VAN BERGE HENEGOUWEN, D. P. 2001. Quality of life in patients with intermittent claudication using the World Health Organisation (WHO) questionnaire. *Eur J Vasc Endovasc Surg*, 21, 118-22.

- BRONSTEIN, A. M., BRANDT, T., WOOLLACOTT, M. H. & MUTT, J. G. 2004. *Clinical Disorders of Balance, Posture and Gait*, Hodder Arnold.
- BROWN, D., WERTSCH, J. J., HARRIS, G. F., KLEIN, J. & JANISSE, D. 2004. Effect of rocker soles on plantar pressures. *Archives of Physical Medicine and Rehabilitation*, 85, 81-86.
- BRUGGEMANN, G., POTTHAST, W., BRAUNSTEIN, B. & NIEHOFF, A. 2005. Effect of increased mechanical stimuli on foot muscles functional capacity. *Proceedings of the ISB XXth Congress - ASB 29th Annual Meeting: 31 July - 5 August 2005; Cleveland*, 553.
- BYRNE, C. A., O'KEEFFE, D. T., DONNELLY, A. E. & LYONS, G. M. 2007. Effect of walking speed changes on tibialis anterior EMG during healthy gait for FES envelope design in drop foot correction. *Journal of Electromyography and Kinesiology*, 17, 605-616.
- CAPPELLO, A., CAPPOZZO, A., LA PALOMBARA, P. F., LUCCHETTI, L. & LEARDINI, A. 1997. Multiple anatomical landmark calibration for optimal bone pose estimation. *Human Movement Science*, 16, 259-274.
- CAPPOZZO, A., CATANI, F., DELLA CROCE, U. & LEARDINI, A. 1995. Position and orientation in space of bones during movement: anatomical frame definition and determination. *Clinical Biomechanics*, 10, 171-178.
- CARON, M., KRON, E. & SALTRICK, K. R. 1999. Tibiotalar joint arthrodesis for the treatment of severe ankle joint degeneration secondary to rheumatoid arthritis. *Clin Podiatr Med Surg*, 16, 337-61.
- CARTER, S. A., HAMEL, E. R., PATERSON, J. M., SNOW, C. J. & MYMIN, D. 1989. Walking ability and ankle systolic pressures: observations in patients with intermittent claudication in a short-term walking exercise program. *J Vasc Surg*, 10, 642-9.
- CAVANAGH, P. R., ULBRECHT, J. S., ZANINE, W., WELLING, R. L., LESCHINSKY, D. & VAN SCHIE, C. 1996. A method for the investigation of the effects of outsole modifications in therapeutic footwear. *Foot Ankle Int*, 17, 706-8.
- CELIS, R., PIPINOS, II, SCOTT-PANDORF, M. M., MYERS, S. A., STERGIOU, N. & JOHANNING, J. M. 2009. Peripheral arterial disease affects kinematics during walking. *J Vasc Surg*, 49, 127-32.
- CHAPMAN, J., PREECE, S., NESTER, C., BRAUNSTEIN, B., HOHNE, A. & BRUGGERMANN, G.-P. 2012. What is the best Rocker Shoe design? *Journal of Foot and Ankle Research*, 5, 06.
- CHAPMAN, J. D., PREECE, S., BRAUNSTEIN, B., HOHNE, A., NESTER, C. J., BRUEGGEMANN, P. & HUTCHINS, S. 2013. Effect of rocker shoe design features on forefoot plantar pressures in people with and without diabetes. *Clin Biomech (Bristol, Avon)*, 28, 679-85.
- CHAVATZAS, D. & JAMIESON, C. W. 1974. The doubtful place of the raised heel in patients with intermittent claudication of the leg. *British Journal of Surgery*, 61, 299-300.

- CHEN, I. H., KUO, K. N. & ANDRIACCHI, T. P. 1997. The influence of walking speed on mechanical joint power during gait. *Gait & Posture*, 6, 171-176.
- CHEN, S. J., PIPINOS, I., JOHANNING, J., RADOVIC, M., HUISINGA, J. M., MYERS, S. A. & STERGIIOU, N. 2008. Bilateral claudication results in alterations in the gait biomechanics at the hip and ankle joints. *J Biomech*, 41, 2506-14.
- CHIU, M.-C. & WANG, M.-J. 2007. The effect of gait speed and gender on perceived exertion, muscle activity, joint motion of lower extremity, ground reaction force and heart rate during normal walking. *Gait & Posture*, 25, 385-392.
- CHUNG, M.-J. & WANG, M.-J. J. 2010. The change of gait parameters during walking at different percentage of preferred walking speed for healthy adults aged 20–60 years. *Gait & Posture*, 31, 131-135.
- COLEMAN, W. C. 1985. The relief of forefoot pressures using outer shoe sole modifications. Proceedings of the International Conference on Biomechanics and Clinical Kinesiology of Hand and Foot I.I.T. Madras India, December 16-18.
- CRACCHIOLO, A. 1979. The use of shoes to treat foot disorders. *Orthopedics Review*. 8:73-83.
- CREASY, T. S., MCMILLAN, P. J., FLETCHER, E. W., COLLIN, J. & MORRIS, P. J. 1990. Is percutaneous transluminal angioplasty better than exercise for claudication? Preliminary results from a prospective randomised trial. *Eur J Vasc Surg*, 4, 135-40.
- CROWTHER, R., WARWICK, L. S., ANTHONY, S. L., KUNWARJIT, S., FRANK, Q. & JONATHAN, G. 2008. Effects of a long-term exercise program on lower limb mobility, physiological responses, walking performance, and physical activity levels in patients with peripheral arterial disease. *Journal of vascular surgery : official publication, the Society for Vascular Surgery [and] International Society for Cardiovascular Surgery, North American Chapter*, 47, 303-309.
- CROWTHER, R. G., SPINKS, W. L., LEICHT, A. S. & GOLLEDGE, J. 2009. Regarding "Gait variability is altered in patients with peripheral arterial disease". *Journal of Vascular Surgery*, 50, 976.
- CROWTHER, R. G., SPINKS, W. L., LEICHT, A. S., QUIGLEY, F. & GOLLEDGE, J. 2007. Relationship between temporal-spatial gait parameters, gait kinematics, walking performance, exercise capacity, and physical activity level in peripheral arterial disease. *J Vasc Surg*, 45, 1172-8.
- CUCCURULLO, S. 2004. Physical Medicine and Rehabilitation Board Review. Demos Medical Publishing.
- DE LUCA, C. J. 1997. The Use of Surface Electromyography in Biomechanics. *Journal of Applied Biomechanics*, 135-163.

- DEGISCHER, S., LABS, K. H., HOCHSTRASSER, J., ASCHWANDEN, M., TSCHOEPL, M. & JAEGER, K. A. 2002. Physical training for intermittent claudication: a comparison of structured rehabilitation versus home-based training. *Vasc Med*, 7, 109-15.
- DELP, S. L. 1990. *Surgery simulation: A computer graphics system to analyze and design musculoskeletal reconstructions of the lower limb*. Stanford University.
- DELP, S. L., ANDERSON, F. C., ARNOLD, A. S., LOAN, P., HABIB, A., JOHN, C. T., GUENDELMAN, E. & THELEN, D. G. 2007. OpenSim: Open-Source Software to Create and Analyze Dynamic Simulations of Movement. *Biomedical Engineering, IEEE Transactions on*, 54, 1940-1950.
- DELP, S. L. & LOAN, J. P. 1995. A graphics-based software system to develop and analyze models of musculoskeletal structures. *Computers in Biology and Medicine*, 25, 21-34.
- DELP, S. L. & MALONEY, W. 1993. Effects of hip center location on the moment-generating capacity of the muscles. *Journal of Biomechanics*, 26, 485-499.
- DELP, S. L., STATLER, K. & CARROLL, N. C. 1995. Preserving plantar flexion strength after surgical treatment for contracture of the triceps surae: a computer simulation study. *J Orthop Res*, 13, 96-104.
- DELP, S. L. & ZAJAC, F. E. 1992. Force- and moment-generating capacity of lower-extremity muscles before and after tendon lengthening. *Clin Orthop Relat Res*, 247-59.
- DEN OTTER, A. R., GEURTS, A. C. H., MULDER, T. & DUYSSENS, J. 2004. Speed related changes in muscle activity from normal to very slow walking speeds. *Gait & Posture*, 19, 270-278.
- DORLAND 1994. *Dorland's Illustrated Medical Dictionary. 28th Ed. Philadelphia, PA: W.B. Saunders Co; 1994.*
- EGGINTON, S., HUDLICKA, O., BROWN, M. D., WALTER, H., WEISS, J. B. & BATE, A. 1998. Capillary growth in relation to blood flow and performance in overloaded rat skeletal muscle. *J Appl Physiol*, 85, 2025-2032.
- EKROTH, R., DAHLLOF, A. G., GUNDEVALL, B., HOLM, J. & SCHERSTEN, T. 1978. Physical training of patients with intermittent claudication: indications, methods, and results. *Surgery*, 84, 640-3.
- ERDEMIR, A. & PIAZZA, S. J. 2004. Changes in foot loading following plantar fasciotomy: a computer modeling study. *J Biomech Eng*, 126, 237-43.
- ERNST, E. & FIALKA, V. 1993. A review of the clinical effectiveness of exercise therapy for intermittent claudication. *Arch Intern Med*, 153, 2357-60.
- ERNST, E., KOLLAR, L. & RESCH, K. L. 1992. Does pentoxifylline prolong the walking distance in exercised claudicants? A placebo-controlled double-blind trial. *Angiology*, 43, 121-5.

- ERNST, E. E. & MATRAI, A. 1987. Intermittent claudication, exercise, and blood rheology. *Circulation*, 76, 1110-4.
- ESENYEL, M., WALSH, K., WALDEN, J. G. & GITTER, A. 2003. Kinetics of high-heeled gait. *J Am Podiatr Med Assoc*, 93, 27-32.
- EVERETT, T. K. C. 2010. *Human movement : an introductory text*, Edinburgh; New York, Churchill Livingstone/Elsevier.
- FEINGLASS, J., MCCARTHY, W. J., SLAVENSKY, R., MANHEIM, L. M. & MARTIN, G. J. 1996. Effect of lower extremity blood pressure on physical functioning in patients who have intermittent claudication. The Chicago Claudication Outcomes Research Group. *J Vasc Surg*, 24, 503-11; discussion 511-2.
- FITZGERALD, P. 1985. Exercise for the elderly. *Medical Clinics of North America*, 69, 189-196.
- FOKKENROOD, H. J., BENDERMACHER, B. L., LAURET, G. J., WILLIGENDAEL, E. M., PRINS, M. H. & TEIJINK, J. A. 2013. Supervised exercise therapy versus non-supervised exercise therapy for intermittent claudication. *Cochrane Database Syst Rev*, 8, Cd005263.
- FONG, D. T., PANG, K. Y., CHUNG, M. M., HUNG, A. S. & CHAN, K. M. 2012. Evaluation of combined prescription of rocker sole shoes and custom-made foot orthoses for the treatment of plantar fasciitis. *Clin Biomech (Bristol, Avon)*, 27, 1072-7.
- FOWKES, F. G., HOUSLEY, E., CAWOOD, E. H., MACINTYRE, C. C., RUCKLEY, C. V. & PRESCOTT, R. J. 1991. Edinburgh Artery Study: prevalence of asymptomatic and symptomatic peripheral arterial disease in the general population. *Int J Epidemiol*, 20, 384-92.
- FRIEDERICH, J. A. & BRAND, R. A. 1990. Muscle fiber architecture in the human lower limb. *J Biomech*, 23, 91-5.
- FULLER, J., LIU, L. J., MURPHY, M. C. & MANN, R. W. 1997. A comparison of lower-extremity skeletal kinematics measured using skin- and pin-mounted markers. *Human Movement Science*, 16, 219-242.
- GAJDOSIK, R. November 1997. Influence of Age on Calf Muscle Length and Passive Stiffness Variables at Different Stretch Velocities. *Isokinetics and Exercise Science*, 6, 163-174.
- GAJDOSIK, R. L., VANDER LINDEN, D. W. & WILLIAMS, A. K. 1996. Influence of age on concentric isokinetic torque and passive extensibility variables of the calf muscles of women. *Eur J Appl Physiol Occup Physiol*, 74, 279-86.
- GARDNER, A. W., FORRESTER, L. & SMITH, G. V. 2001a. Altered gait profile in subjects with peripheral arterial disease. *Vascular Medicine*, 6, 31-34.
- GARDNER, A. W., KATZEL, L. I., SORKIN, J. D., BRADHAM, D. D., HOCHBERG, M. C., FLINN, W. R. & GOLDBERG, A. P. 2001b. Exercise Rehabilitation Improves Functional Outcomes and Peripheral Circulation in Patients with Intermittent Claudication: A Randomized Controlled Trial. *Journal of the American Geriatrics Society*, 49, 755-762.

- GARDNER, A. W., KATZEL, L. I., SORKIN, J. D., BRADHAM, D. D., HOCHBERG, M. C., FLINN, W. R. & GOLDBERG, A. P. 2001c. Exercise rehabilitation improves functional outcomes and peripheral circulation in patients with intermittent claudication: a randomized controlled trial. *J Am Geriatr Soc*, 49, 755-62.
- GARDNER, A. W., KATZEL, L. I., SORKIN, J. D., KILLEWICH, L. A., RYAN, A., FLINN, W. R. & GOLDBERG, A. P. 2000. Improved functional outcomes following exercise rehabilitation in patients with intermittent claudication. *J Gerontol A Biol Sci Med Sci*, 55, M570-7.
- GARDNER, A. W. & POEHLMAN, E. T. 1995. Exercise Rehabilitation Programs for the Treatment of Claudication Pain: A Meta-analysis. *Jama*, 274, 975-980.
- GEARY, N. P. & KLENERMAN, L. 1987. The insensitive foot. Northwick Park experience. *Lepr Rev*, 58, 79-84.
- GEFEN, A., MEGIDO-RAVID, M., ITZCHAK, Y. & ARCAN, M. 2002. Analysis of muscular fatigue and foot stability during high-heeled gait. *Gait & Posture*, 15, 56-63.
- GEHLSSEN, G., BRAATZ, J. S. & ASSMANN, N. 1986. Effects of heel height on knee rotation and gait. *Human Movement Science*, 5, 149-155.
- GRAF, A., JUDGE, J. O., OUNPUU, S. & THELEN, D. G. 2005. The effect of walking speed on lower-extremity joint powers among elderly adults who exhibit low physical performance. *Arch Phys Med Rehabil*, 86, 2177-83.
- GREEN, S. 2002. Haemodynamic limitations and exercise performance in peripheral arterial disease. *Clin Physiol Funct Imaging*, 22, 81-91.
- GRIMSHAW, P., LEES, A., BURDEN, A. & FOWLER, N. 2006. *Sport and Exercise Biomechanics*, Taylor and Francis,.
- GRUNDY, M., TOSH, P. A., MCLEISH, R. D. & SMIDT, L. 1975. An investigation of the centres of pressure under the foot while walking. *J Bone Joint Surg Br*, 57, 98-103.
- GUTMANN, E. 1977. *Muscle. In: handbook of the biology of aging.*, New York.
- HAMPTON, G. H. 1979. Therapeutic footwear for the insensitive foot. *Phys Ther*, 59, 23-9.
- HANSEN, A. H. & WANG, C. C. 2011. Effect of rocker shoe radius on oxygen consumption rate in young able-bodied persons. *J Biomech*, 44, 1021-4.
- HARRIS, G., KLEIN, J., JANISSE, D., PED, C., BROWN, D., SHU, Y. & WERTSCH, J. 2000. Effect of rocker-soles on lower extremity dynamic EMG patterns. *Gait & Posture*, 11, 157-158.
- HERMENS, H. J., FRERIKS, B., DISSELHORST-KLUG, C. & RAU, G. 2000. Development of recommendations for SEMG sensors and sensor placement procedures. *Journal of Electromyography and Kinesiology*, 10, 361-374.

- HIATT, W., REGENSTEINER, J., HARGARTEN, M., WOLFEL, E. & BRASS, E. 1990a. Benefit of exercise conditioning for patients with peripheral arterial disease. *Circulation*, 81, 602-609.
- HIATT, W. R. 2001. New treatment options in intermittent claudication: the US experience. *Int J Clin Pract Suppl*, 20-7.
- HIATT, W. R., REGENSTEINER, J. G., HARGARTEN, M. E., WOLFEL, E. E. & BRASS, E. P. 1990b. Benefit of exercise conditioning for patients with peripheral arterial disease. *Circulation*, 81, 602-9.
- HIATT, W. R., WOLFEL, E. E., MEIER, R. H. & REGENSTEINER, J. G. 1994. Superiority of treadmill walking exercise versus strength training for patients with peripheral arterial disease. Implications for the mechanism of the training response. *Circulation*, 90, 1866-74.
- HIGGINSON, J. S., ZAJAC, F. E., NEPTUNE, R. R., KAUTZ, S. A. & DELP, S. L. 2006. Muscle contributions to support during gait in an individual with post-stroke hemiparesis. *Journal of Biomechanics*, 39, 1769-1777.
- HOF, A. L., ELZINGA, H., GRIMMIUS, W. & HALBERTSMA, J. P. K. 2002. Speed dependence of averaged EMG profiles in walking. *Gait & Posture*, 16, 78-86.
- HOF, A. L., NAUTA, J., VAN DER KNAAP, E. R., SCHALLIG, M. A. & STRUWE, D. P. 1992. Calf muscle work and segment energy changes in human treadmill walking. *J Electromyogr Kinesiol*, 2, 203-16.
- HOLDEN, J. P., CHOU, G. & STANHOPE, S. J. 1997a. Changes in knee joint function over a wide range of walking speeds. *Clinical Biomechanics*, 12, 375-382.
- HOLDEN, J. P., ORSINI, J. A., SIEGEL, K. L., KEPPLER, T. M., GERBER, L. H. & STANHOPE, S. J. 1997b. Surface movement errors in shank kinematics and knee kinetics during gait. *Gait & Posture*, 5, 217-227.
- HOLM, J., DAHLLOF, A. G. & SCHERSTEN, T. 1975. Metabolic activity of skeletal muscle in patients with peripheral arterial insufficiency. Effect of arterial reconstructive surgery. *Scand J Clin Lab Invest*, 35, 81-6.
- HONET, J. C., STRANDNESS, D. E., JR., STOLOV, W. C. & SIMONS, B. C. 1968. Short-leg bracing for intermittent claudication of the calf. *Arch Phys Med Rehabil*, 49, 578-85.
- HONG, Y. & BARTLETT, R. 2008. *Handbook of Biomechanics and Human Movement Science*.
- HOY, M. G., ZAJAC, F. E. & GORDON, M. E. 1990a. A musculoskeletal model of the human lower extremity: the effect of muscle, tendon, and moment arm on the moment-angle relationship of musculotendon actuators at the hip, knee, and ankle. *J Biomech*, 23, 157-69.
- HOY, M. G., ZAJAC, F. E. & GORDON, M. E. 1990b. A musculoskeletal model of the human lower extremity: The effect of muscle, tendon, and moment arm on the moment-

- angle relationship of musculotendon actuators at the hip, knee, and ankle. *Journal of Biomechanics*, 23, 157-169.
- HUISINGA, J. M., PIPINOS, II, STERGIOU, N. & JOHANNING, J. M. 2010. Treatment with pharmacological agents in peripheral arterial disease patients does not result in biomechanical gait changes. *J Appl Biomech*, 26, 341-8.
- HUNT, D., LEIGHTON, M. & REED, G. 1999. Intermittent Claudication: Implementation of an Exercise Programme: Treatment report. *Physiotherapy*, 85, 149-153.
- HUTCHINS, S. 2007. The Effects of Rocker Sole Profiles on Gait: Implications for Claudicants.
- HUTCHINS, S., BOWKER, P., GEARY, N. & RICHARDS, J. 2009. The biomechanics and clinical efficacy of footwear adapted with rocker profiles--Evidence in the literature. *The Foot*, 19, 165-170.
- HUTCHINS, S. W., LAWRENCE, G., BLAIR, S., AKSENOV, A. & JONES, R. 2012. Use of a three-curved rocker sole shoe modification to improve intermittent claudication calf pain — A pilot study. *Journal of vascular nursing : official publication of the Society for Peripheral Vascular Nursing*, 30, 11-20.
- IZQUIERDO-PORRERA, A. M., GARDNER, A. W., BRADHAM, D. D., MONTGOMERY, P. S., SORKIN, J. D., POWELL, C. C. & KATZEL, L. I. 2005. Relationship between objective measures of peripheral arterial disease severity to self-reported quality of life in older adults with intermittent claudication. *J Vasc Surg*, 41, 625-30.
- JANISSE, D. J. 1995. Prescription insoles and footwear. *Clin Podiatr Med Surg*, 12, 41-61.
- JONES, P. P. P., SKINNER, J. S. P., SMITH, L. K. M. D., JOHN, F. M. M. S. & BRYANT, C. X. P. 1996. Functional Improvements Following StairMaster vs. Treadmill Exercise Training for Patients With Intermittent Claudication. *Journal of Cardiopulmonary Rehabilitation January/February*, 16, 47-55.
- JONES, R. K. 2010. *Knee valgus braces and lateral wedge insole in the threatment of medial tibiofemoral osteoarthritis.*, University of Salford.
- JONKERS, I., STEWART, C., DESLOOVERE, K., MOLENAERS, G. & SPAEPEN, A. 2006. Musculo-tendon length and lengthening velocity of rectus femoris in stiff knee gait. *Gait & Posture*, 23, 222-229.
- KARLSSON, D. & TRANBERG, R. 1999. On skin movement artefact-resonant frequencies of skin markers attached to the leg. *Human Movement Science*, 18, 627-635.
- KATCH, V. L., MCARDLE, W. D. & KATCH, F. I. 2011. *Essentials of Exercise Physiology*, Lippincott Williams & Wilkins.
- KELTIKANGAS-JARVINEN, L., LEPANTALO, M. & LINDFORS, O. 1987. Personality factors as predictors of compliance with and the outcome of supervised self-care program for patients with intermittent claudication. *Scand J Rehabil Med*, 19, 1-6.

- KEMP, G. J. 2004. Mitochondrial dysfunction in chronic ischemia and peripheral vascular disease. *Mitochondrion*, 4, 629-40.
- KERRIGAN, D. C., LEE, L. W., COLLINS, J. J., RILEY, P. O. & LIPSITZ, L. A. 2001. Reduced hip extension during walking: healthy elderly and fallers versus young adults. *Arch Phys Med Rehabil*, 82, 26-30.
- KERRIGAN, D. C., ROTH, R. S. & RILEY, P. O. 1998. The modelling of adult spastic paretic stiff-legged gait swing period based on actual kinematic data. *Gait & Posture*, 7, 117-124.
- KERSTING, U. G., JANSSEN, L., BOHM, H., MOREY-KLAPSING, G. M. & BRUGGEMANN, G. P. 2005. Modulation of mechanical and muscular load by footwear during catering. *Ergonomics*, 48, 380-98.
- KIESEWETTER, H., BLUME, J., JUNG, F., GERHARDS, M. & LEIPNITZ, G. 1987. Gehtraining und medikamentöse Therapie bei der peripheren arteriellen Verschlusskrankheit: Randomisierte, prospektive, placebo-kontrollierte Doppelblindstudie. *Deutsche Medizinische Wochenschrift - DEUT MED WOCHENSCHR* 01/1987; 112(22):873-878. DOI:10.1055/s-2008-1068157.
- KIMMEL, S. A. & SCHWARTZ, M. H. 2006. A baseline of dynamic muscle function during gait. *Gait & Posture*, 23, 211-221.
- KING, S., VANICEK, N., MOCKFORD, K. A. & COUGHLIN, P. A. 2012. The effect of a 3-month supervised exercise programme on gait parameters of patients with peripheral arterial disease and intermittent claudication. *Clin Biomech (Bristol, Avon)*, 27, 845-51.
- KIRTLEY, C. 2006. *Clinical Gait Analysis: Theory and Practice*. 1-328.
- KIRTLEY, C., WHITTLE, M. W. & JEFFERSON, R. J. 1985. Influence of walking speed on gait parameters. *Journal of Biomedical Engineering*, 7, 282-288.
- KLEVSGÅRD, R., HALLBERG, I. R., RISBERG, B. & THOMSEN, M. B. 1999. Quality of Life Associated with Varying Degrees of Chronic Lower Limb Ischaemia; Comparison with a Healthy Sample. *European journal of vascular and endovascular surgery : the official journal of the European Society for Vascular Surgery*, 17, 319-325.
- KONRAD, P. 2005. *The ABS of EMG. A practical Introduction to Kinesiological Electromyography*. Noraxon INC.USA.
- KOOPMAN, J. P., DE VRIES, A. C. & DE WEERD, A. W. 1996. Neuromuscular disorders in patients with intermittent claudication. *Eur J Surg*, 162, 443-6.
- KOUTAKIS, P., PIPINOS, I. I., MYERS, S. A., STERGIU, N., LYNCH, T. G. & JOHANNING, J. M. 2010. Joint torques and powers are reduced during ambulation for both limbs in patients with unilateral claudication. *Journal of Vascular Surgery*, 51, 80-88.

- KRUIDENIER, L. M., NICOLAÏ, S. P., HENDRIKS, E. J., BOLLEN, E. C., PRINS, M. H. & TEIJINK, J. A. W. 2009. Supervised exercise therapy for intermittent claudication in daily practice. *Journal of Vascular Surgery*, 49, 363-370.
- KUPECZ, D. 2000. Intermittent claudication treatment. *Nurse Practitioner* May 2000, 112-115.
- KURKLINSKY, A. K. & LEVY, M. 2013. Effect of ramipril on walking times and quality of life among patients with peripheral artery disease and intermittent claudication: a randomized controlled trial. *Journal of the American Medical Association* 2013; 309: 453-460. *Vasc Med*, 18, 234-6.
- KURUP, H. V., CLARK, C. I. M. & DEGA, R. K. 2012. Footwear and orthopaedics. *Foot and Ankle Surgery*, 18, 79-83.
- LARSEN, O. A. & LASSEN, N. A. 1966. Effect of daily muscular exercise in patients with intermittent claudication. *Lancet*, 2, 1093-6.
- LEARMONTH, J. & SLESSOR, A. J. 1952. Surgery in obliterative arterial disease. *British Medical Bulletin*, 8, 375-378.
- LEE, C.-M., JEONG, E.-H. & FREIVALDS, A. 2001. Biomechanical effects of wearing high-heeled shoes. *International Journal of Industrial Ergonomics*, 28, 321-326.
- LEE, K. H., SHIEH, J. C., MATTELIANO, A. & SMIEHOROWSKI, T. 1990. Electromyographic changes of leg muscles with heel lifts in women: therapeutic implications. *Archives of Physical Medicine & Rehabilitation*, 71, 31-3.
- LENG, G. C., FOWLER, B. & ERNST, E. 2000. Exercise for intermittent claudication. *Cochrane Database Syst Rev*, Cd000990.
- LI, J. X. & HONG, Y. 2007. Kinematic and Electromyographic Analysis of the Trunk and Lower Limbs During Walking in Negative-Heeled Shoes. *J Am Podiatr Med Assoc*, 97, 447-456.
- LIENGME, B. V. 2009. Preface. *A Guide to Microsoft Excel 2007 for Scientists and Engineers*. Boston: Academic Press.
- LIN, S. C., CHEN, C. P., TANG, S. F., WONG, A. M., HSIEH, J. H. & CHEN, W. P. 2013. Changes in windlass effect in response to different shoe and insole designs during walking. *Gait Posture*, 37, 235-41.
- LONG, J. T., KLEIN, J. P., SIROTA, N. M., WERTSCH, J. J., JANISSE, D. & HARRIS, G. F. 2004. Biomechanics of the double rocker sole shoe: gait kinematics and kinetics. *Journal of Biomechanics*, 40, 2882-90.
- LONG, J. T., KLEIN, J. P., SIROTA, N. M., WERTSCH, J. J., JANISSE, D. & HARRIS, G. F. 2007. Biomechanics of the double rocker sole shoe: Gait kinematics and kinetics. *Journal of Biomechanics*, 40, 2882-2890.

- LU, T. W. & O'CONNOR, J. J. 1999. Bone position estimation from skin marker co-ordinates using global optimisation with joint constraints. *J Biomech*, 32, 129-34.
- LUNDGREN, F., DAHLLOF, A. G., LUNDHOLM, K., SCHERSTEN, T. & VOLKMANN, R. 1989. Intermittent claudication--surgical reconstruction or physical training? A prospective randomized trial of treatment efficiency. *Ann Surg*, 209, 346-55.
- MAGANARIS, C., BALZOPOULOS, V. & SARGEANT, A. 1998a. Changes in Achilles tendon moment arm from rest to maximum isometric plantarflexion: in vivo observations in man. *Journal of Physiology*, 977—985.
- MAGANARIS, C. N., BALZOPOULOS, V. & SARGEANT, A. J. 1998b. In vivo measurements of the triceps surae complex architecture in man: implications for muscle function. *J Physiol*, 512 (Pt 2), 603-14.
- MAHAFFEY, R., MORRISON, S., DRECHSLER, W. & CRAMP, M. 2013. Evaluation of multi-segmental kinematic modelling in the paediatric foot using three concurrent foot models. *Journal of Foot and Ankle Research*, 6, 43.
- MANAL, K., MCCLAY, I., STANHOPE, S., RICHARDS, J. & GALINAT, B. 2000. Comparison of surface mounted markers and attachment methods in estimating tibial rotations during walking: an in vivo study. *Gait & Posture*, 11, 38-45.
- MANAL, K., ROBERTS, D. P. & BUCHANAN, T. S. 2006. Optimal pennation angle of the primary ankle plantar and dorsiflexors: variations with sex, contraction intensity, and limb. *J Appl Biomech*, 22, 255-63.
- MANNARINO, E., PASQUALINI, L., INNOCENTE, S., SCRICCILO, V., RIGNANESE, A. & CIUFFETTI, G. 1991. Physical training and antiplatelet treatment in stage II peripheral arterial occlusive disease: alone or combined? *Angiology*, 42, 513-21.
- MANZANO, L., GARCIA-DIAZ JDE, D., SUAREZ, C., MOSTAZA, J. M., CAIROLS, M., GONZALEZ-SARMIENTO, E., ROJAS, A. M., VIEITEZ, P., SANCHEZ-ZAMORANO, M. A. & ZAMORA, J. 2009. Thigh and buttock exertional pain for the diagnosis of peripheral arterial disease. *Eur J Intern Med*, 20, 429-34.
- MARBINI, A., GEMIGNANI, F., SCODITTI, U., RUSTICHELLI, P., BRAGAGLIA, M. M. & GOVONI, E. 1986. Abnormal muscle mitochondria in ischemic claudication. *Acta Neurol Belg*, 86, 304-10.
- MARZANO, R. 2002. Orthotic Considerations and Footwear Modifications Following Ankle Fusions. *Techniques in Foot & Ankle Surgery*, 1(1), 46–49.
- MCCONVILLE, J. T., CLAUSER, C. E., CHURCHILL, T. D., CUZZI, J. & KALEPS, I. 1980. Anthropometric relationships of body and body segment moment of inertia. *Technical Report AFAMRL-TR-80-119*. Wright-Patterson AFB. Ohio.: Air Force Aerospace Medical Research Laboratory.
- MCCULLY, K., LEIPER, C., SANDERS, T. & GRIFFIN, E. 1999. The effects of peripheral vascular disease on gait. *J Gerontol A Biol Sci Med Sci*, 54, B291-4.

- MCDERMOTT, M. M., FEINGLASS, J., SLAVENSKY, R. & PEARCE, W. H. 1994. The ankle-brachial index as a predictor of survival in patients with peripheral vascular disease. *J Gen Intern Med*, 9, 445-9.
- MCDERMOTT, M. M., LIU, K., GURALNIK, J. M., CRIQUI, M. H., SPRING, B., TIAN, L., DOMANCHUK, K., FERRUCCI, L., LLOYD-JONES, D., KIBBE, M., TAO, H., ZHAO, L., LIAO, Y. & REJESKI, W. J. 2013. Home-based walking exercise intervention in peripheral artery disease: a randomized clinical trial. *Jama*, 310, 57-65.
- MCDERMOTT, M. M., OHLMILLER, S. M., LIU, K., GURALNIK, J. M., MARTIN, G. J., PEARCE, W. H. & GREENLAND, P. 2001. Gait alterations associated with walking impairment in people with peripheral arterial disease with and without intermittent claudication. *J Am Geriatr Soc*, 49, 747-54.
- MCKENNA, M., WOLFSON, S. & KULLER, L. 1991. The ratio of ankle and arm arterial pressure as an independent predictor of mortality. *Atherosclerosis*, 87, 119-28.
- MEINDERS, M., GITTER, A. & CZERNIECKI, J. M. 1998. The role of ankle plantar flexor muscle work during walking. *Scand J Rehabil Med*, 30, 39-46.
- MERU, A. V., MITTRA, S., THYAGARAJAN, B. & CHUGH, A. 2006. Intermittent claudication: An overview. *Atherosclerosis*, 187, 221-237.
- MIKA, A., OLEKSY, Ł., MIKA, P., MARCHEWKA, A. & CLARK, B. C. 2012. The influence of heel height on lower extremity kinematics and leg muscle activity during gait in young and middle-aged women. *Gait & Posture*, 35, 677-680.
- MILGRAM, J. 1964. Office measures for the relief of the painful foot. *Journal Bone and Joint Surg*, 46(A), 1095-1116.
- MILLER, N. R., SHAPIRO, R. & MCLAUGHLIN, T. M. 1980. A technique for obtaining spatial kinematic parameters of segments of biomechanical systems from cinematographic data. *Journal of Biomechanics*, 13, 535-547.
- MOCKFORD, K. A., VANICEK, N., JORDAN, A., CHETTER, I. C. & COUGHLIN, P. A. 2010. Kinematic adaptations to ischemic pain in claudicants during continuous walking. *Gait and Posture*, 32, 395-399.
- MOISIO, K. C., SUMNER, D. R., SHOTT, S. & HURWITZ, D. E. 2003. Normalization of joint moments during gait: a comparison of two techniques. *Journal of Biomechanics*, 36, 599-603.
- MORGAN, D. W., MARTIN, P. E. & KRAHENBUHL, G. S. 1989. Factors affecting running economy. *Sports Med*, 7, 310-30.
- MUELLER, M. J. 1998. Invited Commentary. *Physical Therapy*, 78, 286-288.
- MUELLER, M. J., MINOR, S. D., SCHAAF, J. A., STRUBE, M. J. & SAHRMANN, S. A. 1995. Relationship of plantar-flexor peak torque and dorsiflexion range of motion to kinetic variables during walking. *Phys Ther*, 75, 684-93.

- MYERS, K. A., LONG, J. T., KLEIN, J. P., WERTSCH, J. J., JANISSE, D. & HARRIS, G. F. 2006. Biomechanical implications of the negative heel rocker sole shoe: gait kinematics and kinetics. *Gait Posture*, 24, 323-30.
- NADEAU, S., GRAVEL, D., ARSENAULT, A. B. & BOURBONNAIS, D. 1999. Plantarflexor weakness as a limiting factor of gait speed in stroke subjects and the compensating role of hip flexors. *Clin Biomech (Bristol, Avon)*, 14, 125-35.
- NAGANO, A. & KOMURA, T. 2003. Longer moment arm results in smaller joint moment development, power and work outputs in fast motions. *Journal of Biomechanics*, 36, 1675-1681.
- NARICI, M. V., BINZONI, T., HILTBRAND, E., FASEL, J., TERRIER, F. & CERRETELLI, P. 1996. In vivo human gastrocnemius architecture with changing joint angle at rest and during graded isometric contraction. *J Physiol*, 496 (Pt 1), 287-97.
- NAWOCZENSKI, D. A., BIRKE, J. A. & COLEMAN, W. C. 1988. Effect of rocker sole design on plantar forefoot pressures. *J Am Podiatr Med Assoc*, 78, 455-60.
- NEPTUNE, R. R., KAUTZ, S. A. & ZAJAC, F. E. 2001. Contributions of the individual ankle plantar flexors to support, forward progression and swing initiation during walking. *J Biomech*, 34, 1387-98.
- NEPTUNE, R. R. & SASAKI, K. 2005. Ankle plantar flexor force production is an important determinant of the preferred walk-to-run transition speed. *J Exp Biol*, 208, 799-808.
- NHS GUIDELINES 2006. Diagnosis and management of peripheral arterial disease A national clinical guideline. In: NETWORK, S. I. G. (ed.). Scotland.
- NIGG, B., HINTZEN, S. & FERBER, R. 2006. Effect of an unstable shoe construction on lower extremity gait characteristics. *Clinical Biomechanics*, 21, 82-8.
- NORDIN, M. & FRANKEL, V. 2003. *Basic Biomechanics of the Musculoskeletal System*.
- NORGREN, L., HIATT, W. R., DORMANDY, J. A., NEHLER, M. R., HARRIS, K. A. & FOWKES, F. G. 2007. Inter-Society Consensus for the Management of Peripheral Arterial Disease (TASC II). *J Vasc Surg*, 45 Suppl S, S5-67.
- ØSTERÅS, H., HOFF, J. & HELGERUD, J. 2005. Effects of High-Intensity Endurance Training on Maximal Oxygen Consumption in Healthy Elderly People. *Journal of Applied Gerontology*, 24, 377-387.
- OWEN, E. 2010. The importance of being earnest about shank and thigh kinematics especially when using ankle-foot orthoses. *Prosthet Orthot Int*, 34, 254-69.
- PALASTANGA, N. & SOAMES, R. 2012. *Anatomy and Human Movement: Structure and Function.*, Churchill Livingstone Elsevier.
- PANIZZOLO, F. A., GREEN, D. J., LLOYD, D. G., MAIORANA, A. J. & RUBENSON, J. 2013. Soleus fascicle length changes are conserved between young and old adults at their preferred walking speed. *Gait & Posture*, 38, 764-769.

- PANJABI, M. & WHITE, A. 2001. *Biomechanics in the Musculoskeletal System*, Churchill Livingstone.
- PARMENTER, B. J., RAYMOND, J., DINNEN, P. & SINGH, M. A. F. 2011. A systematic review of randomized controlled trials: Walking versus alternative exercise prescription as treatment for intermittent claudication. *Atherosclerosis*, 218, 1-12.
- PARMENTER, B. J., RAYMOND, J. & FIATARONE SINGH, M. A. 2013. The effect of exercise on fitness and performance-based tests of function in intermittent claudication: a systematic review. *Sports Med*, 43, 513-24.
- PATTERSON, R., PINTO, B., MARCUS, B., COLUCCI, A., BRAUN, T. & ROBERTS, M. 1997. Value of a supervised exercise program for the therapy of arterial claudication. *Journal of vascular surgery : official publication, the Society for Vascular Surgery [and] International Society for Cardiovascular Surgery, North American Chapter*, 25, 312-319.
- PAYTON, C. & BARTLETT, R. 2008. *BIOMECHANICAL EVALUATION OF MOVEMENT IN SPORT AND EXERCISE. The British Association of Sport and Exercise Sciences Guidelines*.
- PELL, J. P. 1995. Impact of intermittent claudication on quality of life. The Scottish Vascular Audit Group. *Eur J Vasc Endovasc Surg*, 9, 469-72.
- PERRY, J. 1992. *Gait Analysis: Normal and Pathological Function*, SLACK Incorporated.
- PIAZZA, S. J. & DELP, S. L. 1996. The influence of muscles on knee flexion during the swing phase of gait. *Journal of Biomechanics*, 29, 723-733.
- PIPINOS, II, JUDGE, A. R., ZHU, Z., SELSBY, J. T., SWANSON, S. A., JOHANNING, J. M., BAXTER, B. T., LYNCH, T. G. & DODD, S. L. 2006. Mitochondrial defects and oxidative damage in patients with peripheral arterial disease. *Free Radic Biol Med*, 41, 262-9.
- RAMOS, R., QUESADA, M., SOLANAS, P., SUBIRANA, I., SALA, J., VILA, J., MASIA, R., CEREZO, C., ELOSUA, R., GRAU, M., CORDON, F., JUVINYA, D., FITO, M., ISABEL COVAS, M., CLARA, A., ANGEL MUNOZ, M. & MARRUGAT, J. 2009. Prevalence of symptomatic and asymptomatic peripheral arterial disease and the value of the ankle-brachial index to stratify cardiovascular risk. *Eur J Vasc Endovasc Surg*, 38, 305-11.
- RAVINDRA, S. 2012. *The Science of Footwear (Human Factors and Ergonomics)*, CRC Press.
- REGENSTEINER, J. G., STEINER, J. F. & HIATT, W. R. 1996. Exercise training improves functional status in patients with peripheral arterial disease. *J Vasc Surg*, 23, 104-15.
- REICHER, M. A. 1993. MRI of the Knee. In: REICHER, M. A., CRUES, J. V. & DEUTSCH, A. L. (eds.) *An atlas of normal multiplanar anatomy of the knee joint*. Raven Press, New York.
- REINSCHMIDT, C., VAN DEN BOGERT, A. J., NIGG, B. M., LUNDBERG, A. & MURPHY, N. 1997. Effect of skin movement on the analysis of skeletal knee joint motion during running. *Journal of Biomechanics*, 30, 729-732.

- REMIJNSE-TAMERIUS, H. C., DUPREZ, D., DE BUYZERE, M., OESEBURG, B. & CLEMENT, D. L. 1999. Why is training effective in the treatment of patients with intermittent claudication? *Int Angiol*, 18, 103-12.
- RICHARDS, J. 2008. *Biomechanics in Clinic and Research*, Churchill Livingstone.
- RICHARDSON, J. 1991. Rocker-soled shoes and walking distance in patients with calf claudication. *Arch. Phys. Med. Rehabil.*, 554-558.
- RICHARDSON, J., MOON, M. & LEONARD, J. 1989. Effects of rocker bottom shoes on walking distance in patients with calf claudication (abstract) *Arch Phys Med Rehabil Vol 70(11): A48*.
- RILEY, P. O., DELLACROCE, U. & KERRIGAN, D. C. 2001. Effect of age on lower extremity joint moment contributions to gait speed. *Gait Posture*, 14, 264-70.
- ROMKES, J., RUDMANN, C. & BRUNNER, R. 2006. Changes in gait and EMG when walking with the Masai Barefoot Technique. *Clinical Biomechanics*, 21, 75-81.
- ROSE, J. & GAMBLE, J. 2006. *Human Walking.*, Lippincott Williams & Wilkins.
- SACCO, I. C. N., SARTOR, C. D., CACCIARI, L. P., ONODERA, A. N., DINATO, R. C., PANTALEÃO JR, E., MATIAS, A. B., CEZÁRIO, F. G., TONICELLI, L. M. G., MARTINS, M. C. S., YOKOTA, M., MARQUES, P. E. C. & COSTA, P. H. C. 2012. Effect of a rocker non-heeled shoe on EMG and ground reaction forces during gait without previous training. *Gait & Posture*, 36, 312-315.
- SALHIYYAH, K., SENANAYAKE, E., ABDEL-HADI, M., BOOTH, A. & MICHAELS, J. A. 2012. Pentoxifylline for intermittent claudication. *Cochrane Database Syst Rev*, 1, Cd005262.
- SAUNDERS, P. U., PYNE, D. B., TELFORD, R. D. & HAWLEY, J. A. 2004. Factors affecting running economy in trained distance runners. *Sports Med*, 34, 465-85.
- SCHAFF, P. S. & CAVANAGH, P. R. 1990. Shoes for the insensitive foot: the effect of a "rocker bottom" shoe modification on plantar pressure distribution. *Foot Ankle*, 11, 129-40.
- SCHERER, S. A., BAINBRIDGE, J. S., HIATT, W. R. & REGENSTEINER, J. G. 1998. Gait characteristics of patients with claudication. *Archives of Physical Medicine and Rehabilitation*, 79, 529-531.
- SCOTT-OKAFOR, H. R., SILVER, K. K., PARKER, J., ALMY-ALBERT, T. & GARDNER, A. W. 2001. Lower extremity strength deficits in peripheral arterial occlusive disease patients with intermittent claudication. *Angiology*, 52, 7-14.
- SCOTT-PANDORF, M. M., STERGIU, N., JOHANNING, J. M., ROBINSON, L., LYNCH, T. G. & PIPINOS, II 2007. Peripheral arterial disease affects ground reaction forces during walking. *J Vasc Surg*, 46, 491-9.

- SEIDEL, G. K., MARCHINDA, D. M., DIJKERS, M. & SOUTAS-LITTLE, R. W. 1995. Hip joint center location from palpable bony landmarks—A cadaver study. *Journal of Biomechanics*, 28, 995-998.
- SHAKOOR, N., LIDTKE, R. H., SENGUPTA, M., FOGG, L. F. & BLOCK, J. A. 2008. Effects of specialized footwear on joint loads in osteoarthritis of the knee. *Arthritis Care & Research*, 59, 1214-1220.
- SIMONSEN, E. B., SVENDSEN, M. B., NORRESLET, A., BALDVINSSON, H. K., HEILSKOV-HANSEN, T., LARSEN, P. K., ALKJAER, T. & HENRIKSEN, M. 2012. Walking on high heels changes muscle activity and the dynamics of human walking significantly. *J Appl Biomech*, 28, 20-8.
- SINCLAIR, J., GREENHALGH, A., TAYLOR PAUL, J., EDMUNDSON CHRISTOPHER, J., BROOKS, D. & HOBBS SARAH, J. 2013. Differences in Tibiocalcaneal Kinematics Measured with Skin- and Shoe-Mounted Markers. *Human Movement*.
- SOBHANI, S., HIJMANS, J., VAN DEN HEUVEL, E., ZWERVER, J., DEKKER, R. & POSTEMA, K. 2013. Biomechanics of slow running and walking with a rocker shoe. *Gait & Posture*, 38, 998-1004.
- SOUSA, A. S. & TAVARES, J. M. 2012. Effect of gait speed on muscle activity patterns and magnitude during stance. *Motor Control*, 16, 480-92.
- SQUIRES, H., SIMPSON, E., MENG, Y., HARNAN, S., STEVENS, J., WONG, R., THOMAS, S., MICHAELS, J. & STANSBY, G. 2011. A systematic review and economic evaluation of cilostazol, naftidrofuryl oxalate, pentoxifylline and inositol nicotinate for the treatment of intermittent claudication in people with peripheral arterial disease. *Health Technol Assess*, 15, 1-210.
- STACPOOLE-SHEA, S. J., SHEA, D. G., ARMSTRONG, D. G. & LAVERY, L. A. 1999. Do rocker soles reduce plantar pressure in persons at risk for diabetic neuropathic ulceration? *Am J Phys Med Rehabil* Vol.74, 93-107.
- STEFANYSHYN, D. J., NIGG, B. M., FISHER, V., O'FLYNN, B. & LIU, W. 2000. The influence of high heeled shoes on kinematics, kinetics, and muscle EMG of normal female gait. *Journal of Applied Biomechanics*, 16, 309-319.
- STEWART, A. H. R. & LAMONT, P. M. 2001. Exercise for intermittent claudication. *BMJ*. Sep 29, 2001; 323(7315): 703–704.
- STEWART, A. H. R. & LAMONT, P. M. 2007. Exercise training for claudication. *The Surgeon*, 5, 291-299.
- STEWART, K. J., HIATT, W. R., REGENSTEINER, J. G. & HIRSCH, A. T. 2002. Exercise Training for Claudication. *N Engl J Med*, 347, 1941-1951.
- STOQUART, G., DETREMBLEUR, C. & LEJEUNE, T. 2008. Effect of speed on kinematic, kinetic, electromyographic and energetic reference values during treadmill walking. *Neurophysiologie Clinique/Clinical Neurophysiology*, 38, 105-116.

- STREDNEY, D. L. 1982. *The representation of anatomical structures through computer animation for scientific, educational and artistic applications.*
- SUTHERLAND, D. H., COOPER, L. & DANIEL, D. 1980. The role of the ankle plantar flexors in normal walking. *J Bone Joint Surg Am*, 62, 354-63.
- TÖZEREN, A. 2000. *Human Body Dynamics: Classical Mechanics and Human Movement*, Springer.
- TREPMAN, E. & YEO, S. J. 1995. Nonoperative treatment of metatarsophalangeal joint synovitis. *Foot Ankle Int*, 16, 771-7.
- TREW, M. & EVERETT, T. 2005. *Human Movement - An Introductory Text.*
- TYRRELL, W. & CARTER, G. 2008. *Therapeutic Footwear: A Comprehensive Guide, 1e*, Churchill Livingstone.
- VAN BOGART, J. J., LONG, J. T., KLEIN, J. P., WERTSCH, J. J., JANISSE, D. J. & HARRIS, G. F. 2005. Effects of the toe-only rocker on gait kinematics and kinetics in able-bodied persons. *IEEE Transactions on Neural Systems and Rehabilitation Engineering*, 13, 542-550.
- VAN HEDEL, H. J. A., TOMATIS, L. & MÜLLER, R. 2006. Modulation of leg muscle activity and gait kinematics by walking speed and bodyweight unloading. *Gait & Posture*, 24, 35-45.
- VAN SCHIE, C., ULBRECHT, J. S., BECKER, M. B. & CAVANAGH, P. R. 2000. Design criteria for rigid rocker shoes. *Foot and Ankle International*, 21, 833-44.
- VISWANATHAN, V., MADHAVAN, S., GNANASUNDARAM, S., GOPALAKRISHNA, G., DAS, B. N., RAJASEKAR, S. & RAMACHANDRAN, A. 2004. Effectiveness of different types of footwear insoles for the diabetic neuropathic foot: a follow-up study. *Diabetes Care*, 27, 474-7.
- WANG, C. C. & HANSEN, A. H. 2010. Response of able-bodied persons to changes in shoe rocker radius during walking: changes in ankle kinematics to maintain a consistent roll-over shape. *J Biomech*, 43, 2288-93.
- WANG, J. C., CRIQUI, M. H., DENENBERG, J. O., MCDERMOTT, M. M., GOLOMB, B. A. & FRONEK, A. 2005. Exertional leg pain in patients with and without peripheral arterial disease. *Circulation*, 112, 3501-8.
- WATERS, R. L. & MULROY, S. 1999. The energy expenditure of normal and pathologic gait. *Gait & Posture*, 9, 207-231.
- WATSON, L., ELLIS, B. & LENG, G. C. 2008. Exercise for intermittent claudication. *Cochrane Database Syst Rev*, Cd000990.
- WEBER, F. & ZIEGLER, A. 2002. Axonal neuropathy in chronic peripheral arterial occlusive disease. *Muscle Nerve*, 26, 471-6.

- WERTSCH, J. J., HARRIS, G. F., JANISSE, D. J., KLEIN, J. P. & BROWN, D. W. 2000. Effect of Double Rocker, Toe-Only, and Heel Rocker Soles. *American Journal of Physical Medicine & Rehabilitation*, 79, 218.
- WESSLER, S. 1955. Intermittent Claudication. *Circulation*, 11, 806-818.
- WHITTLE, M. 2007. *Gait Analysis: An Introduction*. , Butterworth-Heinemann.
- WHITTLE, M. W. 1982. Calibration and performance of a 3-dimensional television system for kinematic analysis. *Journal of Biomechanics*, 15, 185-196.
- WHITTLE, M. W. 2003. *Gait Analysis an introduction*.
- WICKIEWICZ, T. L., ROY, R. R., POWELL, P. L. & EDGERTON, V. R. 1983. Muscle architecture of the human lower limb. *Clin Orthop Relat Res*, 275-83.
- WILLIAMS, K. R. & CAVANAGH, P. R. 1987. Relationship between distance running mechanics, running economy, and performance. *J Appl Physiol (1985)*, 63, 1236-45.
- WINTER, D. 1987. *The biomechanics and motor control of human gait*, University of Waterloo Press.
- WINTER, D. 2009. *Biomechanics and Motor Control of Human Movment*, John Wiley and Sons.
- WINTER, D. A. 1983. Energy generation and absorption at the ankle and knee during fast, natural, and slow cadences. *Clin Orthop Relat Res*, 147-54.
- WINTER, D. A. & SCOTT, S. H. 1991. Technique for interpretation of electromyography for concentric and eccentric contractions in gait. *Journal of Electromyography and Kinesiology*, 1, 263-269.
- WULLINK, M., STOFFERS, H. E. & KUIPERS, H. 2001. A primary care walking exercise program for patients with intermittent claudication. *Med Sci Sports Exerc*, 33, 1629-34.
- WURDEMAN, S. R., KOUTAKIS, P., MYERS, S. A., JOHANNING, J. M., PIPINOS, II & STERGIU, N. 2012. Patients with peripheral arterial disease exhibit reduced joint powers compared to velocity-matched controls. *Gait Posture*, 36, 506-9.
- YAMAMOTO, T., OHKUWA, T., ITOH, H., YAMAZAKI, Y. & SATO, Y. 2000. Walking at Moderate Speed with Heel-Less Shoes Increases Calf Blood Flow. *Archives Of Physiology And Biochemistry: Formerly Archives Internationales de Physiologie, de Biochimie et de Biophysique, founded in 1904*, 108, 398 - 404.
- YENTES, J. M., HUISINGA, J. M., MYERS, S. A., PIPINOS, II, JOHANNING, J. M. & STERGIU, N. 2012. Pharmacological treatment of intermittent claudication does not have a significant effect on gait impairments during claudication pain. *J Appl Biomech*, 28, 184-91.

- YUNG-HUI, L. & WEI-HSIEN, H. 2005. Effects of shoe inserts and heel height on foot pressure, impact force, and perceived comfort during walking. *Applied Ergonomics*, 36, 355-362.
- ZAJAC, F. E. 1989. Muscle and tendon: properties, models, scaling, and application to biomechanics and motor control. *Crit Rev Biomed Eng*, 17, 359-411.
- ZAMOSKY, I. 1964. Shoe modifications in lower-extremity orthotics. *Bull Prosthet Res*;10(2):54-95.
- ZHOU, Y., LI, J. Z., ZHOU, G. & ZHENG, Y. P. 2012. Dynamic measurement of pennation angle of gastrocnemius muscles during contractions based on ultrasound imaging. *Biomed Eng Online*, 11, 63.
- ZWIERSKA, I., WALKER, R., CHOKSY, S., MALE, J. & SAXTON, J. 2005. Upper- vs lower-limb aerobic exercise rehabilitation in patients with symptomatic peripheral arterial disease: A randomized controlled trial. *Journal of vascular surgery : official publication, the Society for Vascular Surgery [and] International Society for Cardiovascular Surgery, North American Chapter*, 42, 1122-1130.

APENDICES

**APPENDIX ONE
CONSENT FORM**

Rocker shoe study: Consent form

Title of Research study:

The effects of different footwear features on walking biomechanics and muscles.

Name of Researchers: **Andrey Aksenov**

Identification Number for this trial: Subject.....

Date of Birth Weight..... Height..... Shoe size.....

Please initial box

1 I confirm that I have read and understand the information sheet for the above study and have had the opportunity to ask questions and have been given 24 hours to decide on participation in the study after reading the information.

2 I understand that my participation is voluntary and that I am free to withdraw at any time, without giving any reason, without my medical care or legal rights being affected.

I agree to take part in the above study.

Name of Participant Date Signature

Name of Person taking consent
(if different from researcher) Date Signature

Researcher Date Signature

APPENDIX TWO

PATIENT INFORMATION SHEET

Rocker shoe study: Information sheet

The study

This current research is aimed at systematically understanding the precise effects of different footwear profiles on kinematics, kinetics linked to muscle activity changes in the lower limbs (especially for the calf group of muscles and anterior leg muscles)

What is involved?

Your part in the study will involve just one 3-4 hours visit to the University of Salford Podiatry gait laboratory. The researcher and an academic member of staff will also be present. Feel free to withdraw from the study whenever you want.

In the laboratory movement analysis (kinematic, kinetic) and muscle activity will be recorded wearing 13 different footwear conditions.

Measurements to be taken:

Anthropometry - height, weight. These are standard measurements and will not cause any discomfort.

Movement analysis

Your walking will be analysed by computer in a similar way to how human movement is reproduced in computer games. You will be required to wear retro-reflective markers placed on landmarks of the lower limb. These are attached to the skin using double sided tape picture 1. This procedure will not cause any discomfort. Special infrared cameras see these markers as you move in front of the cameras. The computer then produces a special 3D image of your movement and tells us how your joints moved. You'll have to wear short shorts to be able to attach marker and EMG electrodes on your legs.



Figure 1.

Ground reaction force

You will be asked to walk over two force plates secured in a walkway on the floor.

Muscle activity

The activity of muscles that work the foot will also be recorded by computer; this is called Electromyography (EMG). This is done by attaching small electrodes to the skin on the back of your calf muscles, tibialis anterior, Rectus femoris and Biceps Femoris and lower back muscles. Electrodes would be attached only to the right leg. To achieve low impedance of the skin, it will be cleaned, hair will be shaved if necessary (with a new shaver for every subjects) in the small are of the electrodes which will be placed on the muscle according to the SENIAM guidelines.

These are the same electrodes that are used to monitor heart beats in hospital. The electrodes detect electrical activity in muscles which is produced whenever they contract. This will indicate which muscles are working when you are walking, and how your muscle activity might relate to the movements we have recorded. Wires from the electrodes connected to your skin are attached to a box that is worn on your waist figure 2. There is no danger from electrical shock because the electrodes only measure electrical activity and do not themselves have any electricity in them.

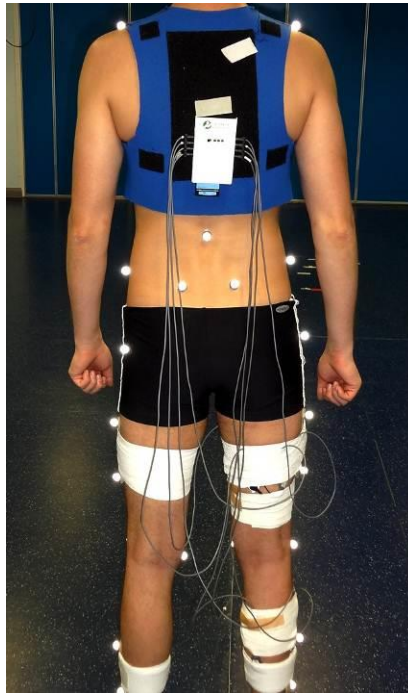


Figure 2.

Marker arrangement

Reflective markers of 14.5 mm diameter will be used in the data collection in the gate lab. The markers will be attached to the skin using standard double sealer tape which is commonly used in the gate lab.

Markers will be attached to the following anatomical locations for the left and right sides: heel, 5th metatarsal, 1st metatarsal, ankle lateral, ankle medial, knee lateral, knee medial, ASIS, PSIS, ILI, hip, spine, sternum, acromium figure 3. There will be 3 additional marker clusters attached to thigh and shank for each leg figure 3.

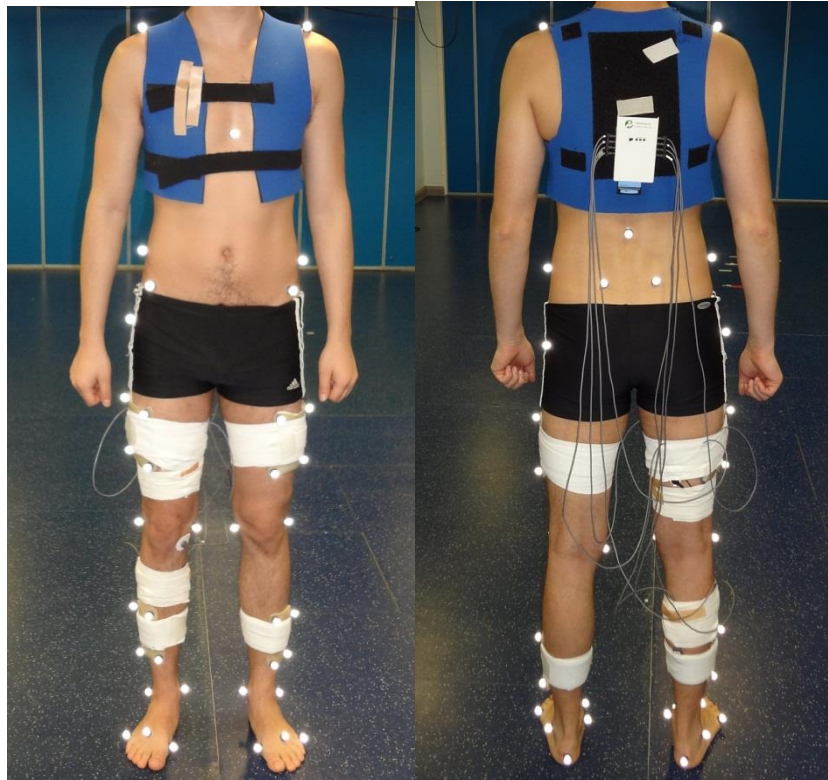


Figure 3.

What will you be asked to do?

You will be asked to walk along a 10 metre walkway wearing 13 different types of shoes which we will be provided. For each pair of shoes you will be asked to walk 10 metres approximately 10 times, and you will be able to take a break at any time. At the end you will be asked to give your opinion on each type of shoe after you have walked with them. We value your opinion as it will help us with future shoe designs.

Please be aware markers and electrodes need to be attached to your lower legs therefore your legs need to be exposed from the knee down, so wearing shorts (which we can provide) will be ideal for the study.

These tests will take approximately three to four hours to complete.

You will be required to wear tight fitting garments such as lycra shorts or swimwear so that there is a limited amount of movement caused by the clothing which may bring inaccuracies into the results of the study

Withdrawal from the study

You can withdraw from the study at any time without explanation.

Confidentiality

All your personal details will be confidential and the data collected will be totally anonymous.

Results from the study

The results from the study will be used to help the researchers in understanding how these rocker soled shoes have on normal walking . Findings of the study will be published in scientific journals and may be used in press releases to newspapers and magazines. All participants will remain anonymous.

Consent

If you are happy to take part, and understand all the information provided, please sign the attached consent form. This shows that you have read and understood this information sheet and agree to take part in the study.

Thank you for your time it is greatly appreciated.

Researcher contact details

Andrey Aksenov

University of Salford

1 Runnymede

Salford

M6 7PJ

Tel : +447818250960

E-mail : andreynet83@hotmail.com